THESE DE DOCTORAT EN COTUTELLE

Pour obtenir le grade de Docteur délivré par

Université de Lille

Ecole Doctorale Sciences de la Matière, du Rayonnement et de l'environnement

Université Libanaise

Ecole Doctorale des Sciences et Technologie

Spécialités : Chimie Théorique, Physique, Analytique

Chimie Organique, Chimie Analytique

Identification, décryptage de la composition chimique et de la structure, des polymères et microplastiques insolubles par dépolymérisation chimique & spectrométrie de masse avancée

Presentée et soutenue publiquement par

Bayan ALMASRI

Le 28 Mai 2025 devant le jury composé de

Pr. Brice BOUYSSIÈRE	Professeur, Université de Pau et des Pays de l'Adour	Rapporteur
Dr. Laurence DE VIGUERIE	Chargée de recherche, HDR, Sorbonne Université	Rapportrice
Pr. Rachid AMARA	Professeur, Université du littoral et Côte d'Opale	Examinateur, président du jury
Dr. Julia CHAMOT-ROOKE	Directeur de recherche, Institut Pasteur Paris	Examinatrice
Pr. Carine ABI GHANEM	Professeur, Université Libanaise	Examinatrice
Dr. Christian ROLANDO	Directeur de recherche émérite au CNRS, Université de Lille	Co-encadrant de thèse et référent scientifique
Pr. Ahmed MAZZAH	Professeur, Université de Lille	Directeur de thèse, France
Pr. Youssef BAKKOUR	Professeur, Université Libanaise	Directeur de thèse, Liban

DOCTORAL THESIS IN JOINT DIPLOMAS

To obtain the degree of Doctor of Philosophy (PhD) issued by

University of Lille

Doctoral School of Matter, Radiation and Environmental Sciences

Lebanese University

Doctoral School of Sciences and Technology

Disciplines: Theoretical, Physical, Analytical Chemistry

Organic Chemistry, Analytical Chemistry

Identifying, deciphering the chemical composition and the structure, of insoluble polymers and microplastics by chemical depolymerization & advanced mass spectrometry

Presented and publicly supported by

Bayan ALMASRI

On May 28, 2025 in front of the jury composed of

Prof. Brice BOUYSSIÈRE	Professor, University of Pau and the Adour Region	Reviewer
Dr. Laurence DE VIGUERIE	Research Fellow, HDR, Sorbonne University	Reviewer
Prof. Rachid AMARA	Professor, University of the Littoral Opal Coast	Examiner, president of jury
Dr. Julia CHAMOT-ROOKE	Research Director, Institut Pasteur Paris	Examiner
Prof. Carine ABI GHANEM	Professor, Lebanese University	Examiner
Dr. Christian ROLANDO	Emeritus Research Director at CNRS, University of Lille	Co-supervisor of PhD thesis & scientific advisor
Prof. Ahmed MAZZAH	Professor, University of Lille	Supervisor of PhD thesis, France
Prof. Youssef BAKKOUR	Professor, Lebanese University	Supervisor of PhD thesis, Lebanon

AKNOWLEDGMENTS

This thesis in the frame of PhD joint diploma was carried out in the Miniaturization for Synthesis, Analysis and Proteomics laboratory (UAR CNRS 3290, MSAP) at the University of Lille, Faculty of Sciences and Technologies under the supervision of Dr. Christian Rolando and Pr. Ahmed MAZZAH and the Laboratory of Applied Chemistry (LAC) at Lebanese University under the supervision of Pr. Youssef BAKKOUR.

Here we start with the emotional part in this long report. First, talking about my little academic trip. I am Syrian student. I was always at the first rank in the Syrian schools and I obtained the third rank over Syria in my “Brevet”. I left my country after the war and moved to Lebanon where I spent more than 10 years. I am really lucky to have my parents, my mom who is a history teacher passioned with sciences and my Dad who was a dentist. Both, they turned the impossible into possible to be able to complete my academic passion in the way of sciences. Thanks God, I was lucky to have such supporting and caring Mom and Dad who saved my professional life in the time where many other Syrian still surviving colleagues could not be able to complete their studies; this was an extra motivation for me to complete my way in sciences achieving my dreams. Graduating was not enough for me to meet my parents’ best expectations. Working hard, being successful and being the best among my colleagues is always my path to make them happy that’s how they may see their fruitful efforts. So, in Lebanon I got my Baccalaureate and my Bachelor from Lebanese University with the best ranks. Then, I achieved my Master 1 in Analytical Chemistry and got my Master 2 diploma in petrochemistry and polymers “Raffinage et technologies des hydrocarbures” in 2020, the year of Covid-19. At the end of 2021, Dr. Christian ROLANDO welcomed me to have my PhD studies in Lille. So, I started to initiate my brain for this relatively long journey in which I was missing my family all the time.

And here comes another lecture of my academic life where I started my PhD. In 2022, I had the official acceptance from the doctoral school in Lille to start the new adventure of PhD studies between University of Lille and Lebanese University. From May 2022 until May 2025, I lived unforgettable moments; they were 3 years of PhD research decorated by challenges, stress, emotions of laugh and cry, and finally success.

I am really thankful for all people who supported me on all levels during my 3-years’ PhD journey.

First of all, I would like to thank my co-supervisor **Dr. Christian ROLANDO** for all his encouragements, support, kindness and all his efforts during these challenging years. I am really proud that I am achieving this success after learning from an expert like you! I am grateful for every moment discussing about my scientific work and my plans, for all the conferences I participated in, and for all the experiences I gained

after teaching and supervising students and technical trainees or after the participation at the EU FTICR_MS project as provider of short course and practical trainings for European researchers. Under your wise supervision, I am really proud that my thesis work allowed us to collaborate with other teams, institutions, start-ups and industries in the field of environment, textiles, resins, plastics, nano-plastics, etc. Integrating the world of analysis especially mass spectrometry (MS) in MSAP laboratory allowed me to have an excellent expertise in MS techniques especially the ultra-high resolution ones as FTICR and Orbitrap. In addition, I am glad that I gained the CJSM elections to be a member of the office of Youth Club of the French Society of Mass Spectrometry (CJSM) as industrial and academic partner relations manager in which I participated and still participating in the organization of conferences, workshops, webinars, and other activities in France. Despite the fact that this is an additional responsibility that needs a big investment, it is very enriching experience that I managed with my PhD. Thanks for your encouragement to be a candidate for the CJSM office. I am really happy and thankful for the confidence you showed in me and for your support on all levels not only the scientific; but also when I was motivated to do other activities within the past 3 years such as MT180s, "fête de la science", workshops, CJSM community work, etc. Your precious advices will accompany me while stepping to the beginning of my career and sure always!

I would like also to thank my thesis supervisor, the director of MSAP laboratory in France, **Pr. Ahmed MAZZAH** for his kindness, his administrative work and all his efforts during my PhD journey.

To my supervisor in Lebanon, **Pr. Youssef BAKKOUR** who trusted me since my master studies in Lebanon: Thank you for your confidence in me that led to this fruitful PhD between Lebanon and France.

Special thanks and appreciations go to **PAUSE « Programme national d'Accueil en Urgence des Scientifiques et des Artistes en Exil » funding** with **all their kind members**. This funding allowed me to rescue my PhD at my third year by their support after 2 years of tough challenges! Thanks also for inviting me to be a speaker in one of the amazing workshops of Inspireurope+ Stakeholder Forum 2025.

I am deeply grateful for my both thesis reviewers, **Pr. Brice BOUYSSIÈRE** from "Institut des Sciences Analytiques et de Physico-Chimie pour l'Environnement et les Matériaux (IPREM), Université de Pau et des Pays de l'Adour'' and **Dr. Laurence DE VIGUERIE** from "Laboratoire d'Archéologie Moléculaire et Structurale (LAMS) de Sorbonne Université'' for their precious time while evaluating my thesis work.

Big thanks to my three thesis examiners for their kindness and time accepting being members of my PhD thesis jury: **Pr. Rachid AMARA** from "Laboratoire d'Océanographie et Géosciences (LOG) UMR CNRS 8187, Université du littoral et Côte d'Opale'' who was the president of my PhD defense's jury, **Dr. Julia CHAMOT-ROOKE** from "Laboratoire de Spectrométrie de Masse pour la Biologie (UTechS MSBio), Institut Pasteur Paris'' and **Pr. Carine ABI GHANEM** from Lebanese University.

I am very glad to have five brilliant scientists from different domains as members of my dissertation committee.

Special thanks go to the research engineer in MSAP, **Dr. Fabrice BRAY**, for his technical support while using mass spectrometry, for his good vibes and advices which are very appreciated. Thank you, Fabrice!

I cannot forget to thank the technical engineer **Stéphanie Flament** for her help while struggling together to fix the Orbitrap. I would like to thank as well **Françoise PRETE,** the MSAP administrative responsible for her kindness, advices and good vibes during my 3 last years.

Big thanks to all the **MSAP team**, to all my colleagues and friends for the good atmosphere, the nice vibes in the laboratory and the good moments we spent together.

It was a pleasure for me to create a new collaboration basing on my PET depolymerization work with an environmental team of the Université Littoral, Pr. Rachid AMARA's team in which Florence LAVALETTE provided some environmental PET samples. Your kindness **Pr. Rachid AMARA** is always appreciated!

I would like to thank **all teams' members of institutions, universities, start-ups and industries** for trusting me to conduct their mass spectrometry analyses: Fleurine AKOUESON and Perine DOYEN from Pr. Rachid AMARA's team of the Université Littoral and the ANSES, Séverine LE GAC from the University of Twente - Netherlands, Milda LEBEDYTE and Antoine COSNE from Refact-textile company, Mathilde BODY-MALAPEL from the faculty of medicine of University of Lille and CHU Lille, and MADER group team. Big thanks to **BASF** company - Germany for providing their PBAT flakes for MS analyses and being interested in my research work 😊.

I would like also to thank all the national and international masters (Erasmus programs or not), bachelor and engineering **students** and **technical trainees** who I supervised and had the chance to work with during the last 3 years: Chloé, Zoé, Elena, Assia, Safaa, Mathieu, Giulia, Lisa, Elias, Juliette and finally Eros who was under my supervision two times during his "BTS" then bachelor! I appreciate our good moments spent together with you all!

To all my **friends in France, Lebanon and everywhere in this big world** without citing to not forget anyone, I spent my quality time with you and shared my best moments. Thank you so much!

My sincere gratitude goes to my family, the most lovely and brave family ever. My sisters and brother in Lebanon and France: My lovely sister **Batool**, my crazy sister **Afnan**, our little angel **Jenan**, and our prince **Abdul Noor**. Thank you for your care, love, support and interest. I am the first to be a Doctor. Waiting for you in the next few years! For Jenan, you still have a long journey! 😊

Finally, to my parents who believed in me and are the support and motivation in my life, thank you for every advice, for your love, and for all your sacrifices. I really cannot express by words my feelings toward you. **Dad**, the greatest father and dentist, you left me only physically at my second year of PhD but your words, advices, love and all our souvenirs together are accompanying me, you are still with me and you will stay forever. You are not sharing with me this moment as you did before; it's really sad but at the same time I am very satisfied that I achieved this because of you as you wanted me to be! **Mom**, my best friend and the most person caring ever, my life idol, you are the source of my power and motivation in this tough life. Mom, thanks alot for your patience with me. You shared with me all the moments of crying, laughing, and success. Hope for you a long life full of happiness and health. Mom, you are a great history teacher passioned with sciences, I will inform you that I worked on cultural heritage samples analysis during my PhD. And finally, I am a Doctor in chemistry!

Mom and Dad, you are the unique example of unconditional love so thanks for everything, love you so much!

TABLE OF CONTENTS

AKNOWLEDGMENTS ..... **i**

TABLE OF CONTENTS ..... **v**

OUTLINE ..... **ix**

Vulgarized subject with my oil painting and my fable (in French) xii

ABSTRACT ..... **xiii**

RESUME ..... **xv**

PART I **1**

Synthetic polyesters and co-polyesters 1

Chapter 1: Introduction part I **3**

Polyethylene terephthalates (PET) 3

Statistics 4

PET microplastics: Pollution source 4

PET additives in bottled water 4

PET analytical methods 5

PET degradation mechanisms 5

Our PET analytical method used in Part I articles 6

PET nanoplastics: Health and environmental issues, synthesis pathways 6

References 8

Vulgarized image of part I 10

Chapter 2: Identification and quantification of PET polyesters and microplastics **11**

Introduction: Analysis of PET terephthalic acid part 11

1. Original methodology 11
2. Improved methodology 11
3. Quantification: Internal standard synthesis 13

Article 1 ..... **15**

Identification and quantification of polyethylene terephthalate (PET) polyesters and microplastics by combining mild chemical depolymerization with dimethylaminopropylamine (DMAPA) and MALDI FTICR & LC ESI Orbitrap mass spectrometry analysis 15

Supporting information 27

Chapter 3: PET diols structural deciphering 57

Introduction: Analysis of diols and polyols 57

Article 2 59

New approach for polyethylene terephthalate (PET) diols deciphering: Application on PET daily life packaging objects paving their structural modifications 59

Supporting information 68

Chapter 4: Additives and enchased products in PET 75

Introduction: Additives 75

Article 3 77

Discovering the secrets of PET-labeled food packaging objects and bottles including their oligomers, additives and possible enchased products 77

Supporting information 89

Annex: Additives verification 103

Chapter 5: Ageing and environmental PET 105

Introduction: Degradation products 105

Article 4 107

Ageing of PET polyesters & deciphering the secrets of environmental PET for better assessment of their origin and future fate in ecosystems 107

Supporting information 116

Chapter 6: Related works 125

1. Co-polyesters and marine objects structural deciphering 125

1.1. Experimental work 125

1.2. Results and discussions 127

1.3. Conclusions and perspectives 133

2. Synthesis of PET nanoparticles 134

2.1. Literature's protocol miniaturized 134

2.2. First protocol 135

2.3. Test with solvents 135

DLS measurements 138

3. Analysis and quantification of terephthalic acid (TPA) using LC-MS 143

Conclusions and perspectives: Part I 147

Conclusions 147
Perspectives 147
PART II 149
Oil and alkyd paints 149
Chapter 7: Introduction part II 151
Introduction 151
Binders: Siccativity of oils 151
Pigments & driers 152
Analytical challenges: Our new methods 153
Siccativation (autoxidation) mechanism 154
Chapter 8: Oil binders' effect on siccativation 157
Introduction 157
Article 5 159
Siccative vegetable oils and their mock-up for oil-based paints applications: Oil differentiation and ageing for drying process assessment using a new methodology of soft chemical depolymerization with advanced mass spectrometry analysis 159
Supporting information 168
Chapter 9: Driers & pigments effect on siccativation 177
Introduction 177
Article 6 179
Oil artists' paints structural deciphering & study of the parameters affecting oil polymerization mechanisms including transition metal driers and pigments for better conservation of artistic works in museums 179
Supporting information 190
Annex: First trials before finding the best methodology 201
1. Experimental work 201
2. Results and discussions 206
Chapter 10: Alkyd paints and industrial resins 213
Introduction 213
Article 7 215
Structural deciphering of alkyd paints and industrial resins 215
Supporting information 223

Chapter 11: Related works **227**

Oil pastel analysis 227

Experimental work 227

1. First innovative approach: With and without HFIP 227
2. Second innovative approach: With TFA 229

Results and discussions 231

Annex 235

1. Extraction of vintage oil paints' pots 235
2. Column chromatography of polymerized binders 237
3. Adjusting solvents for the liquid-liquid extractions 240
4. Metal driers complexation 241
5. Reduction conditions: Aldehydes? 244
6. Analysis by ^{1}H NMR spectroscopy 245
7. ESI analysis on Orbitrap 251

Conclusions and perspectives: Part II **253**

Conclusions 253

Perspectives 253

GENERAL CONCLUSIONS & PERSPECTIVES **255**

OUTLINE

The aim of this thesis is to develop a new innovative method for the analysis of insoluble natural and synthetic polymers especially polyesters for the follow-up of their structural modifications at molecular level over time before and after weathering by different phenomena, which are data still debated among researchers.

I developed a soft chemical depolymerization strategies in which the depolymerized products were identified by ultra-high resolution mass spectrometry using a 9.4 Tesla FTICR MS and an Orbitrap MS hyphenated to liquid chromatography.

I wrote my **PhD thesis mainly as articles**. My work includes two big parts as described below, the first linked to environment and health and the second to cultural heritage and museums. My work during this PhD includes methodological development, organic chemistry, structural elucidation, data analysis and creation of new databases and miniaturization.

The **first part** deals with synthetic polyesters and co-polyesters and their micro- and nano-plastics. Indeed, I studied polyethylene terephthalate (PET) formed initially of terephthalic acid and ethylene glycol units in details to know its degradation pathways leading to the formation of micro- and nano-plastics found in our environment and bodies to assess their lifetime and fate.

Indeed, I depolymerized this polymer widely used in bottles, containers and textiles and I determined the structural modifications of its aromatic acid and diol parts before and after accelerated ageing by UV and temperature. Additives characterization and their structural modifications with ageing were also studied. I compared various bottles and containers of different contents, types and manufacturing countries and determined a specific chemical signature for each PET; and I extended my study on environmental PET samples from sea and river. Miniaturization attempts of analysis were done to achieve microplastics analysis. Nano-plastics of PET were also manufactured. I applied my work on co-polyesters such as poly(ethylene glycol-co-1,4-cyclohexanedimethanol) terephthalate (PETG) and the biodegradable co-polymer polybutylene adipate terephthalate (PBAT) and I characterized successfully some biodegradable marine objects.

The **second part** deals with oil paints, alkyd paints and industrial resins. Oil paints are formed of fatty acids but alkyd paints contain polyols and polyaromatic acids in addition. I derivatized all these constitutive parts and analyzed them. Indeed, I studied the polymeric 3D-crosslinked films formation which is the result of a complex siccativation mechanism to follow-up the drying process of these paints and to determine the type of oil used in artworks. In a first step, I prepared mock-up samples by formulating different siccative oils with different types and ratios of transition metal driers and artistic

pigments. Then, I studied their ageing on short and long-term under natural conditions and accelerated ageing to mimic the museum oil painting drying. I differentiated oils and pigments and determined their important effect on the drying of films. At final step, this methodology was miniaturized and applied to museum-size historical samples and industrial resins.

Two different parts related to cultural heritage & environmental and biological studies, what is the common point that led me to study them during my PhD?

Both oil paints and polyethylene terephthalates are "polyesters" of chemical point of view, containing or not alcoholic parts. I developed a new, innovative and sensitive methodology for the depolymerization and analysis of polyester chains. This original method is applicable in the same time to museum samples of oil and alkyd paints as well as to polyethylene terephthalate and their micro- and nano-plastics and co-polyesters. The methodology was optimized for each studied polyester. For instance, a depolymerization of ester bonds using direct transamidation with 3-(dimethylamino)-1-propylamine (DMAPA) was efficient on oil and alkyd paints at room temperature. This methodology worked on synthetic polyesters and co-polyesters but necessitated a heating at 70 °C and a transamidation for longer time. Thus, it was improved by adding a step of pre-solubilization using the fluorinated solvent 1, 1, 1, 3, 3, 3-hexafluoro-2-propanol (HFIP) that allowed to work at softer conditions even at room temperature providing extra advantages on the yield of depolymerized products. Furthermore, I developed another new method to analyze diols and polyols parts in alkyd paints and synthetic polymers in which they were transesterified after swelling in THF then benzoylated with 4-dimethylaminobenzoyl chloride (DMABC).

In addition to the common methodologies used for their full analysis basing on their same chemical family "polyesters", one another similarity is the study of their structural modifications induced by environmental phenomena of ageing (UV-irradiation, temperature, etc.).

My new and promising results in these different fields allowed me to share them in oral presentations and posters in many national, European and international conferences: Oral at RCJSM2025, Toulouse; 2 orals & 1 poster at SMAP 2024, Lille; 3 orals & 1 poster at JNOEJC2024, Rouen; poster at ASMS2024, Anaheim-United States; oral at RCJSM2024, Metz, talk of 30 minutes at EFTMS2024, Prague-Czech Republic; poster at Formula XI, Lille; 2 Posters at JFSM2023, Marseille; and orals at the following conferences: ASMS2023, Houston-United States; IMMS2023, Paris; Club jeune SFSM2023, Marseille; JNOEJC2023,Villeneuve d'Ascq; EU-FTICR MS, Lille; FTMS2022, Ambleteuse…

A collaboration with environmental teams led to two orals at Micro 2024 - Plastic Pollution from Macro to Nano conference, Spain and "Rencontres 2024 du GDR Plastiques Environnement Santé", Marseille.

I presented also a part of my work as speaker at the event "Journée des utilisateur.ices d'Infranalytics 2025" in Orléans and at the Graduate Program SCP 2023 "Science for a Changing Planet".

I participated in public events vulgarizing my works for the “Grand public”, for example MT180s competition or Science Festival 2024 with the workshop I organized and animated “Les micro-plastiques, c’est dramatique!”.

This full manuscript including all its articles is written by Bayan ALMASRI. It is divided in two parts and will contain the following chapters, in which references, annexes, figures and tables will be numerated for each chapter separately:

- PART I: Synthetic polyesters and co-polyesters
    1. Chapter 1: Introduction of part I
    2. Chapter 2: Identification and quantification of PET polyesters and microplastics
    3. Chapter 3: PET diols structural deciphering
    4. Chapter 4: Additives and enchased products in PET
    5. Chapter 5: Ageing and environmental PET
    6. Chapter 6: Related works: Nano-plastics generation, co-polyesters deciphering, etc.
- PART II: Oil and alkyd paints
    7. Chapter 7: Introduction of part II
    8. Chapter 8: Oil binders’ effect on siccativation
    9. Chapter 9: Driers and pigments effect on siccativation
    10. Chapter 10: Alkyd paints and industrial resins
    11. Chapter 11: Related works: Oil pastels

Vulgarized subject with my oil painting and my fable (in French)



Il était une fois un pays appelé polymère où dominait un royaume nommé polyester composé de tribus qui vivaient ensemble en harmonie. Dans chaque tribu les habitants formaient de longue, longue chaine. Le royaume était sous contrôle royal des tribus des arts et des plastiques et était entouré par des magiciens aux pouvoirs mystérieux.

La reine Oliana de la lignée des peintures à l'huile était une très belle femme avec son sceptre, sa fine brosse à poils délicats, sa robe chamarrée d'huile et ses bijoux incrustés de perles aux couleurs éclatantes.

Le roi PET de la lignée des polyéthylène téréphtalates avait fière allure avec sa couronne en bouteilles recyclées, et ses amples vêtements en fourrure synthétiques.

Le roi et la reine partagèrent leur point de vue sur l'existence et les inquiétudes de leur peuple. En effet, la population se sentait menacés par une vague de dégradation environnementale et étaient touchés par le vieillissement.

Le couple royal invita au palais une énorme machine magique qui s'appelle spectromètre de masse à très haute résolution.

La reine consulta la machine pour déchiffrer les secrets artistiques qui sont restés mystérieux depuis des siècles entre les habitants et lui demanda comment conserver sa beauté. Mais le roi était plus intéressé par la réputation des plastiques et leur influence sur la santé humaine et sur l'environnement, car ses sujets avait dit que des milliers des micro- et nano-plastiques étaient présents dans le sang humain et qu'en 2050, il y aurait plus de bouteille que de poisson dans l'océan.

La machine répondit sagement : « oui tout est possible mais mes pouvoirs visuels magiques restent limités car vous avez une structure bien complexe comme un puzzle et il me faut l'aide d'une chercheuse qui s'appelle Bayan. Elle a développé une nouvelle méthode chimique douce basée sur la séparation de vos pièces du puzzle en vue de leurs analyses. Grâce à elle et avec mes pouvoirs visuels magiques, la base de données créé répondra à vos attentes. Bayan a déjà analysé des peintures à l'huile du 18ème au 20ème siècle ainsi que des bouteilles de différents pays et marques. Pour chacun, elle a déterminé une empreinte spécifique ».

Le roi et la reine furent contents car grâce à ses initiatives, le royaume des polyesters put documenter ses anciennes générations d'œuvre d'art. Mais pas seulement ! Il put aussi concevoir de nouvelles générations de PET et ainsi contribuer à un futur radieux plus propre.

C'est l'histoire de ma thèse racontée à ma petite sœur qui m'a dit : Cette histoire est un véritable enchantement ! Ta chimie, c'est de la magie !

ABSTRACT

Natural or synthetic organic polymers are omnipresent in our daily life. Most are insoluble due to their high molecular weight or cross-linked structure. They are most often used in blends of several polymers with additives such as plasticizers to improve their mechanical properties and anti-UV agents. The characterization of these polymers highlighting their ageing, crosslinking and degradation pathways remains a significant analytical challenge. Enhanced knowledge in the field of polymers analysis addresses not only scientific issues but also other concerns (environment, economic and health) and will pave the way for advancements in industrial manufacturing and recycling practices of synthetic polymers.

There is no analytical method that satisfies the most elementary molecular elements of their structures: The patterns of initiation and termination, the chemical nature of monomers and crosslinking units, and their modifications due to ageing or exposure to the environment (light, micro-organisms, etc.). In this project, two complementary techniques: The chemical depolymerization of polymers and the advanced ultra-high resolution mass spectrometry (Fourier Transform Ion Cyclotron Resonance Mass Spectrometry (FTICR MS) and Orbitrap MS) are reunited to develop a radically new approach for the characterization of polymers especially polyesters. Indeed, several methods have been proposed for the recycling of polyesters but they are not suitable for analytical purposes because they use very harsh conditions.

The aim was to develop soft chemical depolymerization techniques that preserve the important characteristics of these polymers. In a practical part, the developed methodologies were applied to concrete cases of analysis: (i) The industrial oil and alkyd paints; (ii) the polyethylene terephthalates (PET) polyesters from different daily life sources; (iii) samples of ancient art paints based on oil paints and modern art paints based on alkyd paints available in small quantities; and (iv) the identification of microplastics and their chemical modifications due to environmental ageing.

First of all, an organic catalysis for the depolymerization of insoluble polyesters breaking their ester bonds was developed. This chemical depolymerization was optimized on soft conditions and for better yield. In parallel, diols and polyols in polyesters were derivatized for better deciphering using another combined organic reaction. The depolymerized samples were analyzed by FTICR MS and LC Orbitrap MS. These methodologies have been applied on industrial, environmental and cultural heritage samples. These samples were studied after ageing (UV, temperature, siccativation, etc.) and after exposure to the environment. This strategy allowed the analysis of complex mixtures of polyesters and co-polyesters and afforded a new database of depolymerized products, dimers, oligomers, additives and crosslinking compounds identified with high accuracy. Finally, it allowed the miniaturization of analysis on microplastics and museum-size samples while preserving good sensitivity and accuracy.

© Copyright by Bayan ALMASRI
All rights reserved

RESUME

Les polymères organiques naturels ou synthétiques sont omniprésents dans notre vie quotidienne. La plupart sont insolubles en raison de leur poids moléculaire élevé ou de leur structure réticulée. Ils sont le plus souvent utilisés dans des mélanges de plusieurs polymères avec des additifs tels que des plastifiants pour améliorer leurs propriétés mécaniques et des agents anti-UV. La caractérisation de ces polymères mettant en évidence leurs voies de vieillissement, de réticulation et de dégradation reste un défi analytique important. L'amélioration des connaissances dans le domaine de l'analyse des polymères répond non seulement à des questions scientifiques mais également à d'autres préoccupations (environnementales, économiques et sanitaires) et ouvrira la voie à des avancées dans la fabrication industrielle et les pratiques de recyclage des polymères synthétiques. Il n'existe pas de méthode analytique satisfaisante les éléments moléculaires les plus élémentaires de leur structure : les motifs d'initiation et de terminaison, la nature chimique des monomères et des unités de réticulation, et leurs modifications dues au vieillissement ou à l'exposition à l'environnement (lumière, micro-organismes, etc.). Dans ce projet, deux techniques complémentaires : la dépolymérisation chimique des polymères et la spectrométrie de masse à ultra haute résolution (Spectrométrie de Masse à Résonance Cyclotronique Ionique à Transformée de Fourier (FTICR MS) et Orbitrap MS) sont réunies pour développer une approche radicalement nouvelle de la caractérisation des polymères, en particulier des polyesters. En effet, plusieurs méthodes ont été proposées pour le recyclage des polyesters mais elles ne conviennent pas à des fins analytiques car elles utilisent des conditions trop rudes. Le but était de développer des techniques de dépolymérisation chimique douce qui préservent les caractéristiques importantes de ces polymères. Dans une partie pratique, les méthodologies développées ont été appliquées à des cas concrets d'analyse : (i) les peintures à l'huile et glycérophtaliques industrielles; (ii) les polyesters en polyéthylène téréphtalates (PET) de différentes sources de notre vie quotidienne; (iii) des échantillons de peintures d'art anciennes à base de peintures à l'huile et modernes à base de peintures glycérophtaliques disponibles en faible quantité; et (iv) l'identification de microplastiques et de leurs modifications chimiques dues au vieillissement environnemental. Tout d'abord, une catalyse organique pour la dépolymérisation de polyesters insolubles cassant leurs liaisons esters a été développée. Cette dépolymérisation chimique a été optimisée dans des conditions douces et pour un meilleur rendement. En parallèle, les diols et polyols des polyesters ont été dérivatisés pour un meilleur décryptage à l'aide d'une autre réaction organique combinée. Les échantillons dépolymérisés ont été analysés par FTICR MS et LC Orbitrap MS. Ces méthodologies ont été appliquées sur des échantillons industriels, environnementaux et du patrimoine culturel. Ces échantillons ont été étudiés après vieillissement (UV, température, siccativation, etc.) et après exposition à l'environnement. Cette stratégie a permis l'analyse de mélanges complexes des polyesters et co-polyesters et a permis d'obtenir une nouvelle base de données de produits dépolymérisés, dimères, oligomères, additifs et composés réticulants identifiés avec une grande précision. Enfin, elle a permis la miniaturisation des analyses sur des microplastiques et des échantillons de taille musée tout en préservant une bonne sensibilité et précision.

© Copyright par Bayan ALMASRI
Tous droits réservés

PART I

Synthetic polyesters and co-polyesters

Chapter 1: Introduction part I

Polyethylene terephthalates (PET)

Polyethylene terephthalate is thermoplastic polyester formed of terephthalic acid and ethylene glycol units. This polyester is synthesized industrially by different processes, either by elimination of water molecule after polycondensation between terephthalic acid and ethylene glycol (Figure 1) or by elimination of methanol after transesterification between dimethyl terephthalate and ethylene glycol. However, PET in laboratory may be synthesized using terephthaloyl chloride and ethylene glycol units which is easier reaction but much more expensive and need more security prevention as this chloride is more dangerous than terephthalic acid, so the reaction is not compatible for industries.

The degradation of PET in the environment by physical and chemical phenomena (photodegradation, mechanical stress, hydrolysis by water…) led to the formation of small particles, microplastics (1 micrometer to 5 millimeters in size) and nanoplastics (less than 1 micrometer to few nanometers), the lifetime and fate of which are unknown. PET-microplastics are a major source of pollution especially for marine ecosystems. Their effects on marine organisms and human health and their long-term impact on ecosystems are subjects of researchers' interests.

PET is difficult to decompose biologically, it has a slow rate of natural decomposition made by complex and expensive procedure with very specific requirements for PET (viscosity, flake size, melting temperature, metal content, etc).

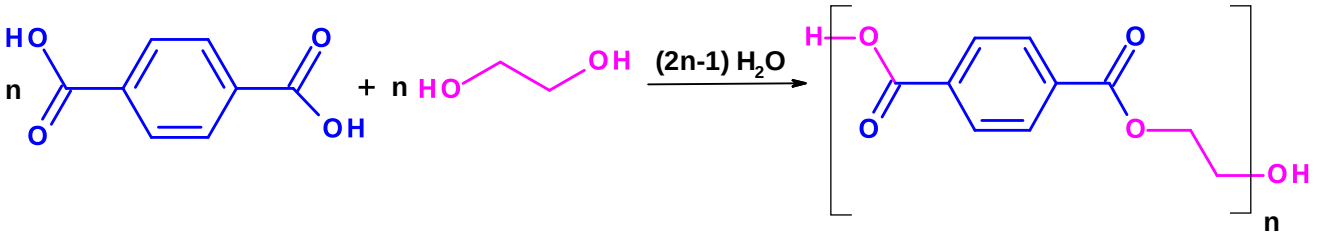


Figure 1. Production of PET by polycondensation between terephthalic acid and ethylene glycol units.

Statistics

PET has been used in the textile field since the mid-1940s, and in drinking bottles since the 1980s. PET is also used for the fabrication of films, containers, and molded products.[1] The overall world plastics production reached 390.7 million tons in 2021 after a stagnation period in 2020 due to covid-19 pandemic. The plastic European demand is increased from 48.9 to 50.3 million tons between 2020 and 2021. PET alone constitutes around 7.9% of the European plastics demand for the year 2021.[2]

PET microplastics: Pollution source

The degradation of PET in the environment by physical and chemical phenomena (photodegradation, mechanical stress, hydrolysis by water…) lead to the formation of small particles ranging from 1 micrometer to 5 millimeters in size called microplastics which their lifetime and fate are unknown.[3-5]

Microplastics are a major source of pollution especially for marine ecosystems;[6] it is estimated that 8 to 12 million of tons of plastics enter the aquatic environment each year.[7]

PET additives in bottled water

PET has many additives to improve its chemical and mechanical properties in addition to traces of metals remaining that can be used as catalysts during the fabrication process. These additives may be released to the bottled water after different degradation phenomena.

- **Plasticizers:** Phthalates (and DEHA) are the most used plasticizers in PET industry; they are used to improve PET flexibility. The release of PET plasticizers in bottled water is related to the type of water (phthalate levels detected in still mineral water are slightly higher than in sparkling water), sunlight exposure, pH, storage conditions…. Plasticizers may come from bottling lines, cap-sealing resins, water facilities or from PET itself (PhA, DMP, DEP, DiBP, DBP and DEHP).[8-13]
- **Metal traces:** PET typically contains Sb levels in the range of 170-300 mg/kg due to antimony trioxide (Sb_2O_3).[14-15] Fortunately, only a small fraction of the Sb contained in PET is released into the bottled water.[16] Other metals traces such as Co, Cr, Fe and Mn, with 27 mg/kg, 0.1 mg/kg, 1.3 mg/kg and 0.3 mg/kg respectively have been found in PET bottles.[14]
- **Carbonyl compounds:** Formaldehyde and acetaldehyde are the most relevant carbonyl compounds migrating from PET bottles after thermo-mechanical and thermo-oxidative degradation.[17] The amount of these compounds depends on the chemical quality of the raw material, the technology used and the difference in formulations and in packaging production.[18-21] The monitoring of a production line of carbonated water showed the appearance of the main two aldehydes in addition to propanal, nonanal, glyoxal, and methylglyoxal in ozonated water used for disinfecting bottles. It is necessary to mention that other parameters like contact time, temperature,

sunlight exposure, pH, and CO_2 of bottled water affect the release of these carbonyl compounds.[22-23]

- **Other additives:** UV-stabilizers such as benzotriazoles are used in the production of PET packaging in some markets.[24] Lubricants like erucamide and oleamide are used for the manufacturing of food-contact packaging.[25] Another compound, bisphenol A (BPA) is found in bottled water. The source of BPA in PET-bottled water is not clear, it may come from bottle closures,[26] the water itself (polluted prior to bottling),[27] or the use of recycled PET.[28]

PET analytical methods

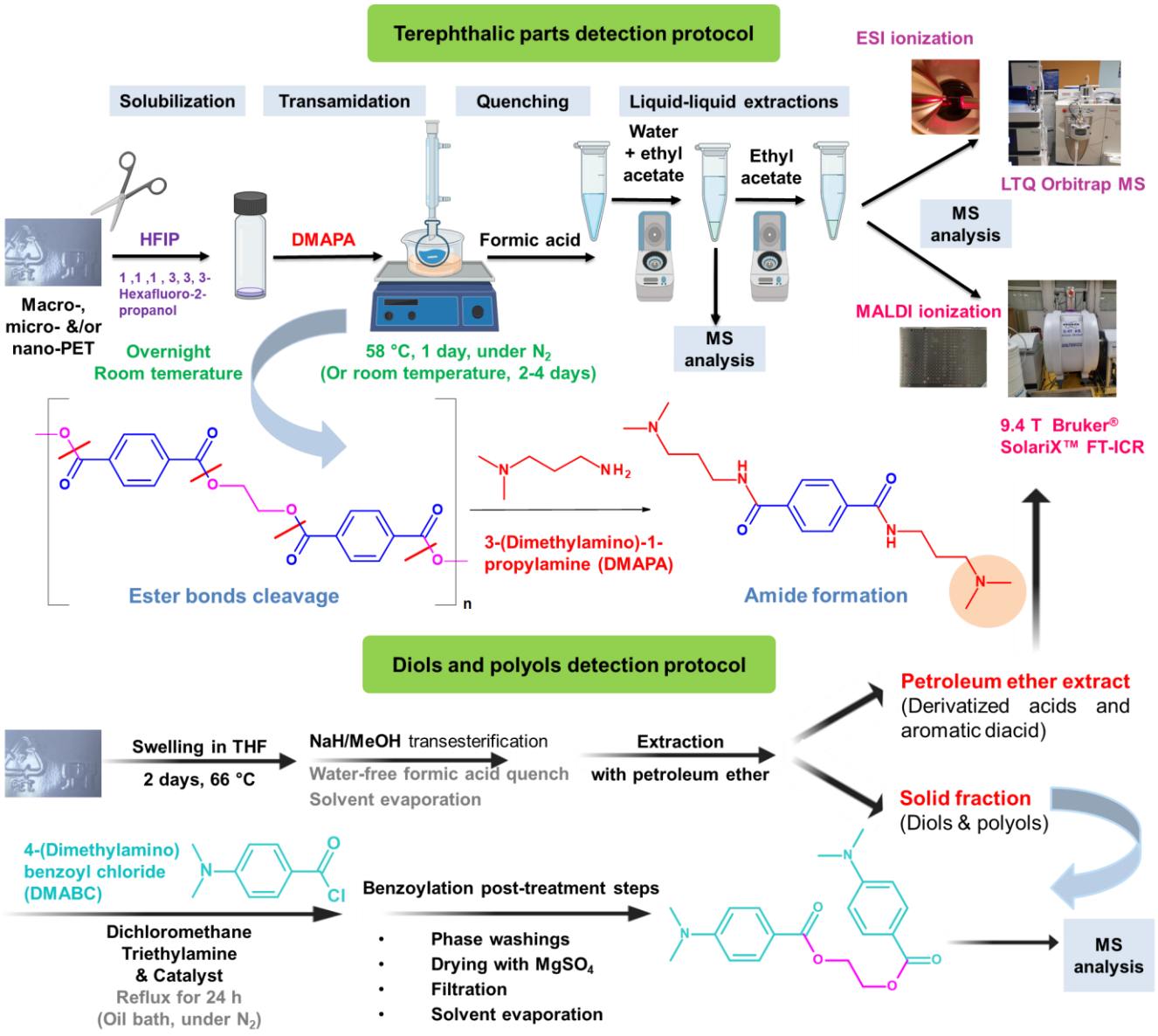
Py-GC/MS analysis was used to detect the degradation products after PET recycling and their possible contamination, it showed that virgin PET decomposition products at 400 °C are mainly carbon dioxide, acetaldehyde, benzoic acid and their derivatives. The variation of these products' concentration depends on the type of PET and may be a sign of contamination in recycled PET samples.[29] Reactive Py-GC/MS in the presence of alkaline medium (Thermally assisted Hydrolysis and Methylation (THM)) such as tetramethyl ammonium hydroxide (TMAH) provides insight of thermal decomposition and condensation type of PET at lower temperature.[29-30] Solid NMR is mainly used for the microscopic structural elucidation of the insoluble polymers. Concerning PET polyesters, zero quantum magic-angle spinning solid state NMR was used to identify and quantify the amorphous *trans* conformers in the doubly ^{13}C labelled PET which is easily combined with double quantum spectroscopy of isotropic chemical shifts showing different results according to the crystallinity of PET material.[31-32] Some vibrational analysis studies using Raman and X-ray photoelectron spectroscopy were also reported.[33-34] A recent study shows a fast identification of microplastics using simulated Raman scattering microscopy without molecular characterization of them.[35]

PET degradation mechanisms

The degradation of PET provides different products after UV exposure for which crosslinking was found and demonstrated by a reduction in UV transmission and oxygen permeability of the PET material.[36] Two main mechanisms were mentioned as a result of PET chain scission: Norrish type I mechanism that forms mainly radicals after photolysis and ester bond cleavage, and Norrish type II reactions resulting in the formation of polymer chains with vinyl and carboxylic acid end groups explained by abstraction of hydrogen atoms via intramolecular reactions or by oxidation reactions. The formation of carboxylic acid end-groups, aldehydes and hydroxyl terephthalate was also explained differently via radical mechanisms.[37-39] Some studies suggested the formation of quinone-type structures after formation of peroxides and release of hydroxy radical after thermo-oxidative PET degradation.[40-41]

The aim of my further studies is to develop fast and reliable method for the characterization of polyethylene terephthalate that may be used to facilitate recycling procedures and to a better assessment of their pollution as microplastics in the environment.

Our PET analytical method used in Part I articles



PET nanoplastics: Health and environmental issues, synthesis pathways

Nanoplastics could be found accumulated in aquatic organisms (marine mammals, marine turtles, birds, and fish). They are also vehicles for several other pollutants, such as pesticides, heavy metals or polychlorinated biphenyls which are strongly adsorbed on the surface of different polymers.

Nanoplastics may enter the food chain through multiple routes, in which ingestion is the most common. The ingestion of micro- or nano-plastics could induce behavioral variations, fertility changes, liver damage, weakened immune responses, and at high concentrations, lethal damage. In recent years, *in vitro*

studies have been carried out with human cells to address the toxicological impact of nanoplastics especially for polystyrene nanoplastics.[42]

Nano-PET were recently detected in the water of PET bottles with an average mean size of ~88.2 nm using Surface-Enhanced Raman Spectroscopy (SERS). The estimated annual nanoplastics consumption of human beings through bottled drinking water is about 1014 particles, assuming water consumption of 2 L/day for adults.[43]

Very few articles mentioned the synthesis of PET. PET nanoparticles were synthesized by laser ablation but producing very small amounts of chemically-modified nanoparticles due to high temperatures.[44] Another study reported another approach for PET nanoparticles synthesis, they were produced using the following steps starting from 1 gram of sample then analyzed by TEM microscopy:

- Dissolution of PET in 10 mL of concentrated trifluoroacetic acid (solution of TFA 90%) under magnetic stirring at 50 °C (2h)
- Precipitation in TFA 20%, stirring for 2 hours
- Centrifugation of the suspension at 2500 g/h, discharge of supernatant
- Stabilization of nanoparticles in 100 mL of 0.5% sodium dodecyl sulfate (SDS), vigorously stirred and ultrasonicated.[42]

Another method using a modified-low speed hand blender to breakdown plastics was performed. The supernatant was centrifuged many times to obtain different size of nano-PET. The nano-PET were dispersed in 0.05% BSA solution or 0.01% SDS solution.[45] This method is high time-consuming and necessitates a mechanical modification of the blender. If the speed of the blender is not well adjusted, this may bring thermal modification to the produced nano-PET.

I will show in this report our easy and simple method of production of PET-nanoparticles that they will be used for further *in vitro* and *in vivo* studies.

References

1. Rogers, M. E.; Long, T. E.; Turner, S. R., Introduction to synthetic methods in step-growth polymers. *Synthetic Methods in Step-Growth Polymers* **2003**, 1-16.
2. Europe, P. *Plastics- The facts 2022, analysis of the latest data related to plastics production, demand, conversion and waste management in Europe*; 2022.
3. Andrady, A. L., Microplastics in the marine environment. *Marine pollution bulletin* **2011,** *62* (8), 1596-1605.
4. Rochman, C. M.; Browne, M. A.; Underwood, A. J.; Van Franeker, J. A.; Thompson, R. C.; Amaral-Zettler, L. A., The ecological impacts of marine debris: unraveling the demonstrated evidence from what is perceived. *Ecology* **2016,** *97* (2), 302-312.
5. Geyer, R.; Jambeck, J. R.; Law, K. L., Production, use, and fate of all plastics ever made. *Science advances* **2017,** *3* (7), e1700782.
6. Barboza, L. G. A.; Vethaak, A. D.; Lavorante, B. R.; Lundebye, A.-K.; Guilhermino, L., Marine microplastic debris: An emerging issue for food security, food safety and human health. *Marine pollution bulletin* **2018,** *133*, 336-348.
7. Jambeck, J. R.; Geyer, R.; Wilcox, C.; Siegler, T. R.; Perryman, M.; Andrady, A.; Narayan, R.; Law, K. L., Plastic waste inputs from land into the ocean. *Science* **2015,** *347* (6223), 768-771.
8. Higuchi, A.; Yoon, B. O.; Kaneko, T.; Hara, M.; Maekawa, M.; Nohmi, T., Separation of endocrine disruptors from aqueous solutions by pervaporation: dioctylphthalate and butylated hydroxytoluene in mineral water. *Journal of applied polymer science* **2004,** *94* (4), 1737-1742.
9. Hirayama, K.; Tanaka, H.; Kawana, K.; Nakazawa, H., Analysis of plasticizers in cap-sealing resins for bottled foods. *Food Additives & Contaminants* **2001,** *18* (4), 357-362.
10. Leivadara, S. V.; Nikolaou, A. D.; Lekkas, T. D., Determination of organic compounds in bottled waters. *Food chemistry* **2008,** *108* (1), 277-286.
11. Montuori, P.; Jover, E.; Morgantini, M.; Bayona, J. M.; Triassi, M., Assessing human exposure to phthalic acid and phthalate esters from mineral water stored in polyethylene terephthalate and glass bottles. *Food Additives and Contaminants* **2008,** *25* (4), 511-518.
12. Penalver, A.; Pocurull, E.; Borrull, F.; Marce, R., Determination of phthalate esters in water samples by solid-phase microextraction and gas chromatography with mass spectrometric detection. *Journal of Chromatography A* **2000,** *872* (1-2), 191-201.
13. Kayali, N.; Tamayo, F. G.; Polo-Díez, L. M., Determination of diethylhexyl phtalate in water by solid phase microextraction coupled to high performance liquid chromatography. *Talanta* **2006,** *69* (5), 1095-1099.
14. Westerhoff, P.; Prapaipong, P.; Shock, E.; Hillaireau, A., Antimony leaching from polyethylene terephthalate (PET) plastic used for bottled drinking water. *Water Research* **2008,** *42* (3), 551-556.
15. Keresztes, S.; Tatár, E.; Mihucz, V. G.; Virág, I.; Majdik, C.; Záray, G., Leaching of antimony from polyethylene terephthalate (PET) bottles into mineral water. *Science of the Total Environment* **2009,** *407* (16), 4731-4735.
16. Welle, F.; Franz, R., Migration of antimony from PET bottles into beverages: determination of the activation energy of diffusion and migration modelling compared with literature data. *Food Additives & Contaminants: Part A* **2011,** *28* (1), 115-126.
17. Romao, W.; Franco, M. F.; Corilo, Y. E.; Eberlin, M. N.; Spinace, M. A.; De Paoli, M.-A., Poly (ethylene terephthalate) thermo-mechanical and thermo-oxidative degradation mechanisms. *Polymer Degradation and Stability* **2009,** *94* (10), 1849-1859.
18. Sugaya, N.; Nakagawa, T.; Sakurai, K.; Morita, M.; Onodera, S., Analysis of aldehydes in water by head space-GC/MS. *Journal of health science* **2001,** *47* (1), 21-27.
19. Mutsuga, M.; Kawamura, Y.; Sugita-Konishi, Y.; Hara-Kudo, Y.; Takatori, K.; Tanamoto, K., Migration of formaldehyde and acetaldehyde into mineral water in polyethylene terephthalate (PET) bottles. *Food additives and contaminants* **2006,** *23* (2), 212-218.
20. Choodum, A.; Thavarungkul, P.; Kanatharana, P., Acetaldehyde residue in polyethylene terephthalate (PET) bottles. *Journal of Environmental Science and Health, Part B* **2007,** *42* (5), 577-583.
21. Pinto, B.; Reali, D., Screening of estrogen-like activity of mineral water stored in PET bottles. *International Journal of Hygiene and Environmental Health* **2009,** *212* (2), 228-232.
22. Dąrowska, A.; Borcz, A.; Nawrocki, J., Aldehyde contamination of mineral water stored in PET bottles. *Food additives and contaminants* **2003,** *20* (12), 1170-1177.
23. Nawrocki, J.; Dąbrowska, A.; Borcz, A., Investigation of carbonyl compounds in bottled waters from Poland. *Water Research* **2002,** *36* (19), 4893-4901.
24. Laboratory, C. S.; Bradley, E.; Coulier, L. In *An investigation into the reaction and breakdown products from starting substances used to produce food contact plastics*, CSL: 2007.
25. Strube, A.; Buettner, A.; Groetzinger, C., Characterization and identification of a plastic-like off-odor in mineral water. *Water science and technology: water supply* **2009,** *9* (3), 299-309.

26. Guart, A.; Bono-Blay, F.; Borrell, A.; Lacorte, S., Migration of plasticizersphthalates, bisphenol A and alkylphenols from plastic containers and evaluation of risk. *Food additives and contaminants* **2011,** *28* (5), 676-685.
27. Li, X.; Ying, G.-G.; Su, H.-C.; Yang, X.-B.; Wang, L., Simultaneous determination and assessment of 4-nonylphenol, bisphenol A and triclosan in tap water, bottled water and baby bottles. *Environment international* **2010,** *36* (6), 557-562.
28. Sax, L., Polyethylene terephthalate may yield endocrine disruptors. *Environmental health perspectives* **2010,** *118* (4), 445-448.
29. Dimitrov, N.; Krehula, L. K.; Siročić, A. P.; Hrnjak-Murgić, Z., Analysis of recycled PET bottles products by pyrolysis-gas chromatography. *Polymer degradation and stability* **2013,** *98* (5), 972-979.
30. Wampler, T. P., *Applied pyrolysis handbook*. CRC press: 2006.
31. Kaji, H.; Schmidt-Rohr, K., Selective observation and quantification of amorphous trans conformers in doubly 13C-labeled poly (ethylene terephthalate), PET, by zero-quantum magic-angle-spinning solid-state NMR. *Macromolecules* **2002,** *35* (21), 7993-8004.
32. Müller, L., Mapping of spin-spin coupling via zero-quantum coherence. *Journal of Magnetic Resonance (1969)* **1984,** *59* (2), 326-331.
33. Boerio, F.; Bahl, S.; McGraw, G., Vibrational analysis of polyethylene terephthalate and its deuterated derivatives. *Journal of Polymer Science: Polymer Physics Edition* **1976,** *14* (6), 1029-1046.
34. Lippert, T.; Zimmermann, F.; Wokaun, A., Surface analysis of excimer-laser-treated polyethylene-terephthalate by surface-enhanced Raman scattering and x-ray photoelectron spectroscopy. *Applied spectroscopy* **1993,** *47* (11), 1931-1942.
35. Zada, L.; Leslie, H. A.; Vethaak, A. D.; Tinnevelt, G. H.; Jansen, J. J.; de Boer, J. F.; Ariese, F., Fast microplastics identification with stimulated Raman scattering microscopy. *Journal of Raman spectroscopy* **2018,** *49* (7), 1136-1144.
36. Gardette, J.-L.; Colin, A.; Trivis, S.; German, S.; Therias, S., Impact of photooxidative degradation on the oxygen permeability of poly (ethyleneterephthalate). *Polymer degradation and stability* **2014,** *103*, 35-41.
37. Sang, T.; Wallis, C. J.; Hill, G.; Britovsek, G. J., Polyethylene terephthalate degradation under natural and accelerated weathering conditions. *European polymer journal* **2020,** *136*, 109873.
38. Lu, J.; Chen, N.; Ji, S.; Sun, Z.; Ding, M.; Zhu, X., Polymerization of benzoguanamine and pyromellitic dianhydride under microwave radiation and its third-order optical nonlinearities. *Journal of applied polymer science* **2001,** *82* (6), 1356-1363.
39. Hurley, C. R.; Leggett, G. J., Quantitative investigation of the photodegradation of polyethylene terephthalate film by friction force microscopy, contact-angle goniometry, and X-ray photoelectron spectroscopy. *ACS applied materials & interfaces* **2009,** *1* (8), 1688-1697.
40. Chamas, A.; Moon, H.; Zheng, J.; Qiu, Y.; Tabassum, T.; Jang, J. H.; Abu-Omar, M.; Scott, S. L.; Suh, S., Degradation rates of plastics in the environment. *ACS Sustainable Chemistry & Engineering* **2020,** *8* (9), 3494-3511.
41. MacDonald, W. A., New advances in poly (ethylene terephthalate) polymerization and degradation. *Polymer international* **2002,** *51* (10), 923-930.
42. Rodríguez-Hernández, A. G.; Muñoz-Tabares, J. A.; Aguilar-Guzmán, J. C.; Vazquez-Duhalt, R., A novel and simple method for polyethylene terephthalate (PET) nanoparticle production. *Environmental Science: Nano* **2019,** *6* (7), 2031-2036.
43. Zhang, J.; Peng, M.; Lian, E.; Xia, L.; Asimakopoulos, A. G.; Luo, S.; Wang, L., Identification of poly (ethylene terephthalate) nanoplastics in commercially bottled drinking water using surface-enhanced Raman spectroscopy. *Environmental Science & Technology* **2023,** *57* (22), 8365-8372.
44. Magrì, D.; Sánchez-Moreno, P.; Caputo, G.; Gatto, F.; Veronesi, M.; Bardi, G.; Catelani, T.; Guarnieri, D.; Athanassiou, A.; Pompa, P. P., Laser ablation as a versatile tool to mimic polyethylene terephthalate nanoplastic pollutants: characterization and toxicology assessment. *ACS nano* **2018,** *12* (8), 7690-7700.
45. Ji, Y.; Wang, C.; Wang, Y.; Fu, L.; Man, M.; Chen, L., Realistic polyethylene terephthalate nanoplastics and the size-and surface coating-dependent toxicological impacts on zebrafish embryos. *Environmental Science: Nano* **2020,** *7* (8), 2313-2324.

Vulgarized image of part I



French Version

Chapter 2: Identification and quantification of PET polyesters and microplastics

Introduction: Analysis of PET terephthalic acid part

The terephthalic acid part of PET was analyzed by an innovative transamidation reaction. The described methodology used is improved with the addition of 1, 1, 1, 3, 3, 3-hexafluoro-2-propanol (HFIP) solvent prior to the transamidation.

1. Original methodology

100 mg of the mini-fragments of PET were transamidated for 2-6 days at 70 °C with 1 mL of *N*,*N*-dimethyl-1,3-propanediamine under magnetic stirring and N_2 inert atmosphere to avoid the hydrolysis by water (Figure 1). After cooling at room temperature, the mixture cooled with an ice bath was quenched with 100 µL of formic acid (caution: exothermic reaction) then transferred to a 5 mL Falcon™ conical tube, extracted two times with 2 mL of acidified ultrapure water (20 µL of formic acid) and 2 mL of petroleum ether by centrifugation at 10,000 rpm during 5 minutes at room temperature. The remaining aqueous phase was reextracted four times with 2 mL of ethyl acetate under the same centrifugation conditions. After each centrifugation, the organic phase was transferred to a 2-mL clear glass tube using a glass pipette. The obtained phases were then evaporated under nitrogen at room temperature, solubilized in methanol or dichloromethane, diluted then analyzed by mass spectrometry.

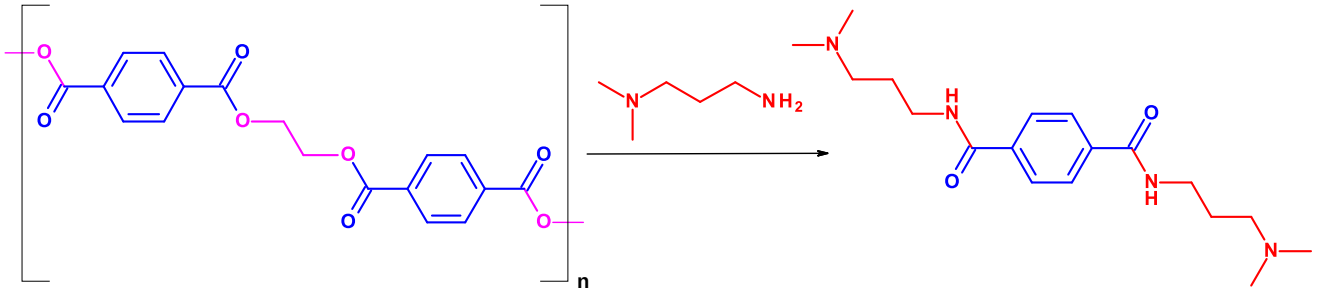


Figure 1. Transamidation reaction of PET using 3-(dimethylamino)-1-propylamine (DMAPA).

2. Improved methodology

In order to improve the extraction yield and work at softer conditions, the already described methodology was developed. I tried to pre-solubilize PET samples in 1, 1, 1, 3, 3, 3-hexafluoro-2-propanol (HFIP).[1] PET samples were perfectly soluble in HFIP, but different aspects were observed after the addition of DMAPA. I optimized the new protocol by variation of PET/HFIP/DMAPA ratios as described in Table 1.

HFIP is relatively acidic (pKa = 9.3) alcohol, more acidic than the standard alcohols and equivalent to phenol, but it has relatively high dielectric constant so it is supposed to be a good solvent for ion pairs. The formation of white fibers or precipitates after DMAPA addition maybe due to the formation of the ion pair $[HFIP\text{-}H]^-$ $[DMAPA\text{-}H]^+$.

The volume of HFIP added depends also on the type of PET sample. Two different samples have been tested: A simple PET polyester from a French fruit container and a rigid film of PETG co-polyester, poly(ethylene glycol-co-1,4-cyclohexanedimethanol terephthalate).

Table 1. Experimental conditions optimization for PET solubilization in HFIP followed by its transamidation at room temperature.

PET weight (mg)	**PET type**	**HFIP weight (mg)**	**Solubility in HFIP after 1 day of stirring**	**DMAPA volume (µL)**	**Solubility with DMAPA**	**Solubility with DMAPA after days of stirring**
25	Fruit container	400	☑	250	A little solubilization with a huge white cloud	☒
25	PETG					
25	Fruit container	400	☑	33	Gel (transparent white) + white fibers	☒
25	PETG				☑	☑
25	Fruit container	40	☒	-	-	-
25	Fruit container	**400**	☑	**1000 Fast addition**	☒ **PET cloud of agglomerated nanoparticles**	☑ **Soluble after 4 days**
25				**1000 Slow addition**	☒ **PET fibers of nanoparticles**	

The best condition is found to be the pre-solubilization of 25 mg of PET samples in 400 mg of HFIP solvent for one day at room temperature followed by addition of 1 mL of DMAPA at room temperature for 4 days or at the temperature of reflux of HFIP (58 °C) for 1 day. Both products at room temperature and at 58 °C will be compared and analyzed afterwards.

Here, an excess of formic acid (400 µL) was added and the liquid-liquid extractions by centrifugation were simplified: After the introduction of 2 mL of ultrapure water, the depolymerized products were extracted four times only by ethyl acetate. The step of extraction by petroleum ether is eliminated as very low extraction yield in this organic phase was observed.

The full improved methodology is given in Figure 2.

This methodology was used for the depolymerization of many PET containers and bottles of different countries, contents and brands as well as of environmental PET samples and other co-polyesters.

Despite the fact that HFIP is liquid, HFIP is sampled only by glass pipette as it dissolves plastics and the measurements of HFIP are always done in mg in this report.

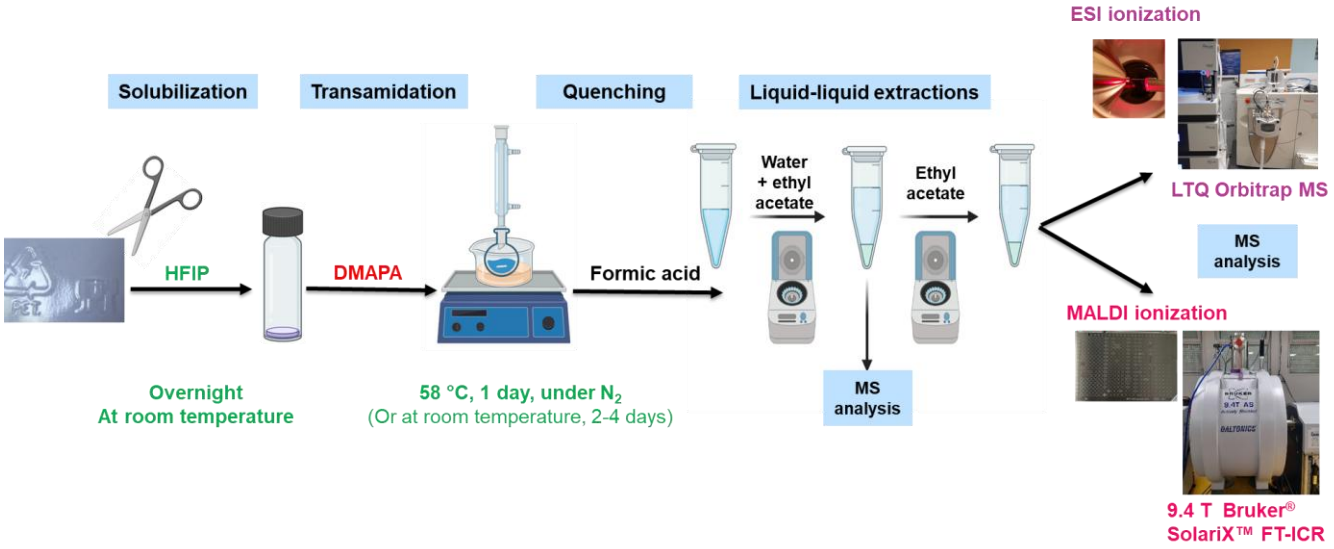


Figure 2. Full methodology steps of PET depolymerization.

3. Quantification: Internal standard synthesis

An internal standard made from terephthaloyl chloride with another amine was tested, first starting from 200 mg of terephthaloyl chloride. The successful synthesis allowed the production of bigger quantity of products to quantify PET samples starting from 2 g of the starting material. Indeed, 2 g of terephthaloyl chloride were added to 20 mL of *N*,*N*-dimethylethylenediamine. This mixture was left at 70 °C under magnetic stirring and N_2 inert atmosphere for 2 days, the corresponding reaction is shown in Figure 3. After cooling at room temperature, the mixture cooled with an ice bath was quenched with 2 mL of formic

acid. Then, this mixture was divided into two equal-volume parts then each 10 mL was transferred to a 15 mL Falcon™ conical tube, extracted two times with 20 mL of ultrapure water acidified with 400 µL of formic acid and 20 mL of petroleum ether by centrifugation at 10,000 rpm during 5 minutes at room temperature. The remaining aqueous phase in each tube was reextracted four times with 20 mL of ethyl acetate under the same centrifugation conditions. After each centrifugation, the organic phases were collected in 7-mL clear glass tube using a glass pipette. The obtained phases were then evaporated, solubilized and used on PET samples as internal standard. The total extraction yield was 21.70% (434.2 mg).

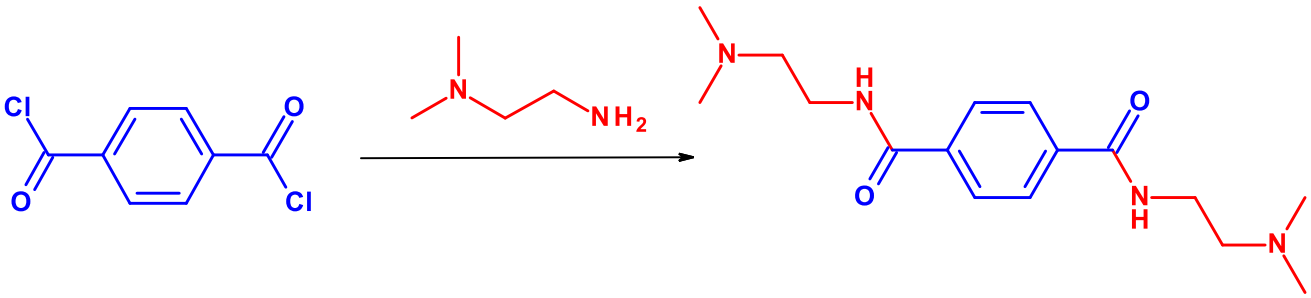


Figure 3. Synthesis of internal standard of polyethylene terephthalate using terephthaloyl chloride and *N*,*N*-dimethylethylenediamine.

Reference

1- Moroni, A.; Havard, T., Characterization of polyesters and polyamides through sec and light scattering using 1, 1, 1, 3, 3, 3-hexafluoro-2-propanol as eluent. ACS Publications: **1999**.

Article 1

Identification and quantification of polyethylene terephthalate (PET) polyesters and microplastics by combining mild chemical depolymerization with dimethylaminopropylamine (DMAPA) and MALDI FTICR & LC ESI Orbitrap mass spectrometry analysis

Bayan Almasri[1,2], Christian Rolando[1,3,*]

[1] Univ. Lille, CNRS, UAR 3290, MSAP, Miniaturisation pour la Synthèse l'Analyse et la Protéomique, F-59 000 Lille, France

[2] Laboratoire de Chimie Appliquée, Faculté des Sciences III, Université Libanaise, Ras Maska, Tripoli, Liban

[3] Shrieking Sixties, 1-3 Allée Lavoisier, 59650, Villeneuve-d'Ascq, France

Corresponding author's email: christian.rolando@univ-lille.fr

ABSTRACT: Polyethylene terephthalate polyesters (PET) formed of terephthalic acid and ethylene glycol units are one of the most commonly found plastics in our daily life and environment. Micro- and nano-PET occurs since their fabrication as they have been detected in water of PET-bottles and in marine ecosystems due to weathering degradation. The identification of PET microplastics modification is still very challenging. They are principally identified by optical spectroscopy and by Py-GC-MS. Unfortunately, these techniques are not efficient for identifying and quantifying PET at molecular level and they provide very few structural information on their modifications. In this work, PET was depolymerized in soft conditions combined and analyzed by complementary mass spectrometry approaches. After pre-solubilization with 1,1,1,3,3,3-hexafluoro-2-propanol (HFIP), a direct transamidation using *N,N*-dimethyl-1,3-propanediamine (DMAPA) at soft temperature was performed to break ester bonds and improve MS ionization allowing the detection of acids and aromatic di- and poly-acids. The resulting products were analyzed by ultra-high resolution mass spectrometry using MALDI ionization on a 9.4 Tesla FTICR MS and ESI ionization on an Orbitrap MS hyphenated to liquid chromatography. Daily life PET samples from different countries, brands and contents were studied and their depolymerized products were identified and quantified. A specific fingerprinting for each sample was attributed. Dimers, oligomers, scission products, oxygenated species, crosslinking structures and additives were successfully identified with high accuracy and resolution. This strategy can be applied to other polyesters and co-polyesters.

Keywords: PET, microplastics, depolymerization, transamidation, crosslinking, additives, oligomers, MALDI FTICR MS, LC ESI Orbitrap-MS.

Polyethylene terephthalate (PET) has been used in the textile field since the mid-1940s, and in drinking bottles since the 1980s.[1] Around 30% of PET production is intended for bottles manufacturing field.[2] This polyester is also used for the fabrication of films, containers, and molded products.[3] PET alone constitutes around 8% of the worldwide plastics demand, with consumption reaching 57 million metric tons in the US in 2019 and 50 million metric tons in Europe in 2021.[4,5] For improving its mechanical properties, PET is often used in blend with random co-polymers made from terephthalic acid, ethylene glycol and other diols.[6,7] The thermal condensation of terephthalic acid and ethylene glycol may lead to the formation of diethylene glycol (DEG) also incorporated in PET.[8] Heating even at moderate temperature, exposure to sun and mechanical stress induce the degradation of PET and the formation of new species.[9] The use of recycled PET (rPET) is increasing worldwide.[10-13] In Europe starting from this year 2025, it is mandatory to have at least 25% of rPET in all fabricated packaging objects.[14] As a result, new PET bottles will have more complex composition compared to those made exclusively from virgin PET.[11] Furthermore, PET micro- and nano-plastics are widely found in environment,[15] and even in human body.[16] So, there is a strong need for a sensitive analytical technique which will be able to decipher the precise composition of the PET plastics and their chemical modifications caused by weathering and/or living organisms.

There are two approches for analyzing PET by mass spectrometry, the first one performs the analysis on the bulk polymer itself; whereas the second one starts by liberating the monomers. The first approach includes Py-GC-MS and MALDI-MS and more recently ASAP-MS and DART-MS. Py-GC-MS may be performed at high temperature around 600 °C affording a bunch of small molecules characteristic of PET, that allows nevertheless to disinguish between PET and recycled PET.[17] More informative Py-GC-MS is obtained by performing the pyrolysis at a lower temperature around 400 °C in the presence of an alkaline methylating reagent such as tetramethylammonium acetate or hydroxyde.[17,18] In addition, thermal desorption/pyrolysis-DART-MS and ASAP-MS or DIP-MS during which a slow pyrolysis is

performed allowing the following of the PET degradation by MS have been recently introduced.[19,20] With all these MS techniques, it is still difficult to determine the chemical changes in the polymer due to the complex reactions occuring during pyrolysis.

Analysis of the bulk PET polymer may be performed also by MALDI-MS affording *m/z* as high as 80 kDa in linear mode but without monomer identification.[21] The identification here is done after solubilization of the polymer at the lower *m/z* fraction allowing to distinguish bottles made from PET or recycled PET.[22] A mixture of protonated and sodiated species is obtained precluding the identification of thermo-mechanical or UV degradation mechanisms.[23-25]

The analysis of PET monomers after hydrolysis has a long tradition.[26] After hydrolysis with KOH, terephtalic acid and diol can be recovered and analyzed by GC-MS after derivatization or by LC-MS.[27,28] It has been used recently to detect PET in human feces.[16] The PET sample's hydrolysis can be performed *in situ* on the MALDI plate.[29] However, the relatively harsh hydrolysis precludes the detection of fragile modifications.

None of the above techniques is able to determine the precise composition of PET samples which contain small amount of other polyesters or the PET modifications. We present here a fast, sensitive and reliable method for the characterization of polyethylene terephthalate plastics based on their transamidation by 3-(dimethylamino)-1-propylamine (DMAPA) as shown in Figure 1 and high-resolution MALDI FTICR and LC ESI Orbitrap-MS. The tertiary amine of DMAPA increases the ionization yield so the MS sensitivity and affords good chromatographic properties. We analyzed different brands and contents of commercial PET bottles from different countries and degraded PET samples to show the analytical potential of our method on everyday life PET samples.

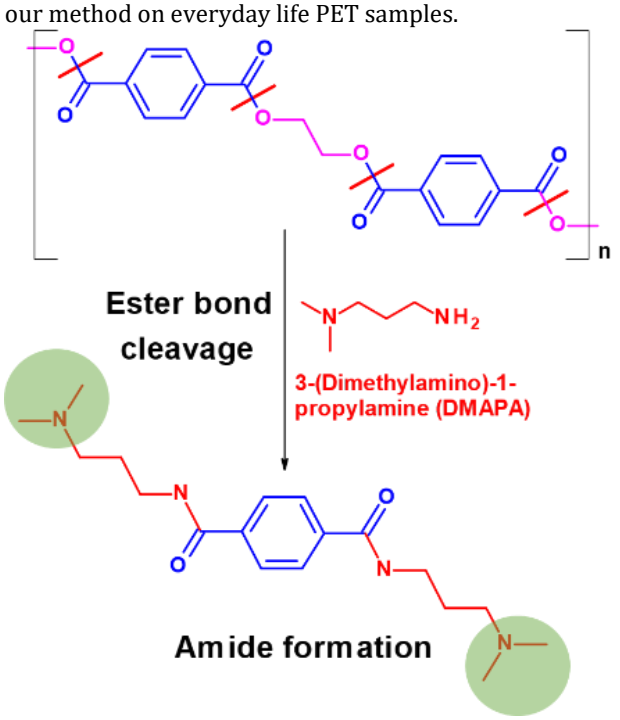


Figure 1. Transamidation reaction of PET using DMAPA.

EXPERIMENTAL SECTION

Chemicals. All aqueous solutions were prepared from ultrapure grade water obtained by water filtration with a two stages Millipore system (Milli-Q® Academic with a cartouches Q-Gard 1 and Progard 2, Merck Millipore, Burlington, Massachusetts, United States). All solvents were MS analytical grade. All solvents and chemicals were purchased from Merck (Merck KGaA, Darmstadt, Germany) and used without further purification. 3-(Dimethylamino)-1-propylamine also called *N,N*-dimethyl-1,3-propanediamine (DMAPA) 99%, 2-(dimethylamino)ethylamine also called *N,N*-dimethylethylenediamine (DMEN) 95% and 1,1,1,3,3,3-hexafluoro-2-propanol (HFIP) ≥ 99%, were used as received. Terephthaloyl chloride > 99% was the only chemical purchased from TCI Europe (TCI Co. Ltd, Tokyo, Japan) and used without further purification.

Samples. Polyethylene terephthalate samples were daily life containers and bottles naturally aged. French fruit containers of different colors were studied: Recyclable transparent container; 100% recyclable black container of recycled PET (rPET) and recyclable blue container 100% rPET. Three types of bottles were also studied: Still water, sparkling water and soft drinks' bottles from different brands and countries (France, Germany, Switzerland, Spain and United States). The description of these bottles including data, as given in their labels, on their fabrication from raw or recycled PET and their recyclability (if given) is shown in Table 1. Poly(ethyleneglycol-co-1,4-cyclohexanedimethanol terephthalate) (PETG) films, 750 micron thickness were purchased from Alt-Intech (Neresheim, Germany).

Table 1. Studied PET bottles.

Bottle name[a]	Country	Volume	PET type[b]
Water FRA1	France	1.5 L	-
Water FRA2	France	50 cL	100% recyclable
Water GER	Germany	500 mL	100% rPET
Water SP	Spain	1.5 L	50% rPET
Water US1	United States	500 mL	Recyclable
Water US2	United States	240 mL	-
Water-S FRA1	France	50 cL	25% rPET
Water-S FRA2	France	1.25 L	-
Water-S GER	Germany	0.5 L	100% rPET
Water-S CH	Switzerland	50 cL	100% rPET
Water-S SP	Spain	1.0 L	-
Cola-1 FRA[c,d]	France	1.5 L	100% rPET

Cola-1 GER[c,d]	Germany	0.5 L	100% rPET
Cola-1 CH[c,d]	Switzerland	500 mL	-
Cola-1 SP[c,d]	Spain	1.75 L	Recyclable 100% rPET
Cola-1 US[c]	United States	20.0 oz (591 mL)	-
Cola-2 FRA[c]	France	1.25 L	100% recyclable
Cola-2 US[c,d]	United States	20.0 oz (591 mL)	100% rPET

[a]Water: Still water bottles; Water-S: Sparkling water bottles; and Cola: Carbonated cola bottles.

[b]Volume and PET type as given in bottles' labels.

[c]For Cola, the number referrers to a given brand across countries.

[d]Zero sugar.

Sample preparation. PET and PETG samples were washed four times with ultrapure water to remove impurities. After that, they were left to dry at room temperature then cut with scissors in pieces of around 2.5 mm × 2.5 mm size.

Direct transamidation. In a 50-mL flask, 100 mg of PET microplastics were transamidated for 2-6 days at 70 °C with 1 mL (7.93 mmol) of 3-(dimethylamino)-1-propylamine (DMAPA) under magnetic stirring and N_2 inert atmosphere to avoid spurious hydrolysis by water. After cooling at room temperature, the mixture cooled with an ice bath was quenched with 100 µL of formic acid (2.65 mmol) (caution: exothermic reaction) then transferred to a 5 mL Falcon™ conical tube (Corning, NY, USA), added to 2 mL of acidified ultrapure water (20 µL of formic acid) and extracted two times with 2 mL of petroleum ether by centrifugation at 10,000 rpm during 5 minutes at room temperature using Beckman-Coulter (Brea, CA, USA) Allegra® X-30R centrifuge with the corresponding C1015 fixed angle conical tube rotor. The remaining aqueous phase was reextracted four times with 2 mL of ethyl acetate under the same centrifugation conditions. After each centrifugation, the organic phase was transferred to a 2-mL clear glass tube using a glass pipette. The obtained organic phases were evaporated under nitrogen at room temperature and stored in 2-mL glass tube.

Dissolution in HFIP before transamidation. As HFIP dissolves plastics, glass materials have been used to avoid contamination of PET samples. In a 2-mL glass vial fitted Teflon caps (Merck), 25 mg of PET microplastics were pre-solubilized in 400 mg (2.38 mmol, 250 µL) of HFIP overnight by stirring at room temperature using a vortex-Genie® 2. The content of the tube was transferred to a 50-mL flask then 1 mL (7.93 mmol) of DMAPA was added. The solution was left at room temperature for 2-4 days or at HFIP reflux's temperature (58 °C) under N_2 for only 1 day. After quenching by 400 µL of formic acid (10.6 mmol, in excess), a simplified liquid-liquid extraction protocol by centrifugation was followed. After the addition of 2 mL of ultrapure water, the depolymerized products were extracted four times only with ethyl acetate using centrifugation as previously.

Miniaturization. In a 1-mL glass hydrolysis tube (ThermoFisher Scientific, Rockford, USA), 1 mg of PET microplastics (roughly 4 pieces of 1 mm × 1 mm) was solubilized with 50 mg (0.3 mmol, 80 µL) of HFIP after 1 hour of stirring. After that, 250 µL of DMAPA was added and left at 58 °C under N_2 overnight. After stopping the reaction with 16 µL of formic acid, the content was transferred to a 1.5 mL microcentrifuge tube (Sarstedt, Nümbrecht, Germany). The liquid-liquid extractions by centrifugation under the same previous conditions were performed but with the corresponding F2402H fixed angle conical tube rotor. The depolymerized products were extracted four times with 500 µL of ethyl acetate after addition of 500 µL of ultrapure water. To avoid any possible leaching from the micro tube plastics, the required quantity of water was added before adding the transamidation products.

Quantification. The synthesized internal standard *N1,N4*-bis[2-(dimethylamino)ethyl] terephthalamide was added to PET products which were already solubilized in HFIP and transamidated just before stopping the reaction, stirred for one minute then the extraction steps were performed as before. The internal standard was added to PET in a ratio of 50/100 (w/w). Details about internal standard synthesis are given in the supporting information.

Analytical method. For MS analysis, the ethyl acetate fractions were solubilized in methanol at 1 mg/10 µL then diluted 100 times in acetonitrile/water/formic acid 5/95/0.1 (v/v/v).

1. MALDI FTICR MS analysis. The analyses were performed on a SolariX XR instrument with a 9.4 Tesla actively shielded superconducting magnet fitted with a dynamically harmonized cell (Bruker Daltonics, Bremen, Germany) and controlled by FTMS Control software. MALDI FTICR mass spectra were acquired in positive ion mode using a MTP 384 ground steel MALDI plate (Bruker Daltonics). The matrix was α-cyano-4-hydroxycinnamic acid (10 mg/mL in acetonitrile/water/trifluoroacetic acid 70/30/0.1 (v/v/v)). 1 µL of the diluted sample at 1 mg/1 mL was mixed with 1 µL of matrix. Then 1 µL of this binary mixture was spotted on the MALDI plate and dried at room temperature. Spectra were acquired using broadband detection, 8 M points, 32 scans accumulation for a better signal-to-noise ratio with a mass range from *m/z* 100 to 1,500. These parameters led to a transient time of 2.936 s and resulted in a theoretical resolution of 530,000 at *m/z* 400 in magnitude mode. Instrument calibration was achieved using red phosphorous as external calibrant and a quadratic calibration[30]. No internal calibration was performed. The obtained spectra were processed using Data Analysis software version 5.0 (Bruker Daltonics, Bremen, Germany).

2. LC ESI MS analysis. LC-MS analyses were performed on an Orbitrap LTQ XL mass spectrometer hyphenated to a Dionex Ultimate 3000 HPLC System (ThermoFisher Scientific, Bremen, Germany). The analysis was performed using a 60 min gradient at a flow rate of 0.50 $mL.min^{-1}$ on a Zorbax RRHD SB-C18 column (2.1 µm i.d. × 150 mm) packed with 1.8 µm beads pores with 80 Å pore size from Agilent Technologies (Santa Clara, CA, USA) placed in an oven at a temperature of 50 °C. The depolymerized PET products were separated using a

multi-step gradient with a mobile phase of 5% acetonitrile in acidified water, 0.1% formic acid (solution A) and 75% acetonitrile in acidified water, 0.1% formic acid (solution B). The gradient started by 100% of solution A for 5 min then increased to 30% A, 70% B until 35 min. It increased more to 100% of solution B at 40 min holding this mobile phase until 50 min then it returned to the initial conditions at 55 min holding 100% of solution A for the remaining 5 min. The LC runs were acquired in positive ion mode using ESI ionization with a non-heated source (spray voltage 4.50 kV, sheath gas flow 22 $mL.min^{-1}$, auxiliary gas flow 12 $mL.min^{-1}$). The MS scans were acquired from *m/z* 200 to 1,000 with a 60,000 resolution at *m/z* 200 leading to a scan duration of 30 ms. Data acquisition and interpretation were performed using Xcalibur™ 4.21 SP1 software (Thermo Fisher Scientific).

RESULTS AND DISCUSSIONS

The composition of PET daily life containers and bottles from different countries was investigated. For this aim, we developed an analytical protocol for PET soft depolymerization by transamidation after HFIP solubilization at low temperature (58 °C) using 3-(dimethylamino)-1-propylamine (DMAPA) as transamidation agent compatible with MS ionization. This new method allowed us to constitute a database for PET depolymerization products, oligomers, crosslinked structures, oxygenated species and additives of more than 120 structures.

PET may be transamidated by piperidine at high temperature before analysis by FAB-MS.[31] However, DMAPA is by far a better reagent for transamidation reactions as it bears a primary amine. On the one hand, it has been used for removing the acetate protecting group during sugar synthesis.[32] On the other hand, several studies have shown that derivatizing organic acid with DMAPA in the presence of a coupling reagent such as HOBt leads to very sensitive LC-MS analyses.[33,34] So, in this study, DMAPA was chosen as a reagent for the transamidation of polyethylene terephthalate because it cleaves efficiently the ester bonds of PET to form amides containing side chain(s) incorporating tertiary amine that improves mass spectrometry ionization. Furthermore, the transamidated aromatic acids have good chromatographic properties. Finally, the easy neutral loss of dimethyl amine (- 45.048 *m/z*) from the side chain affords a characteristic signature of the transamidated molecules.[33,35]

Protocol optimization. In a first step, direct transamidation of 25 mg of PET microplastics was performed using 1 mL of DMAPA for 2-6 days at 70 °C under N_2 inert atmosphere. After stopping the reaction by formic acid and adding 2 mL of acidified ultrapure water, 2 extractions by petroleum ether then 4 extractions by ethyl acetate were performed using high speed centrifugation. The collected organic phases were dried, resolubilized in other solvents, diluted then analyzed by mass spectrometry. However, the yield after total extraction was only moderate in all cases, up to 27% at maximum. This yield was different according to the type, recyclability and purity of the studied PET. In order to improve the extraction yield and work under softer conditions, PET samples were pre-solubilized in 1,1,1,3,3,3-hexafluoro-2-propanol (HFIP).[36] All samples were perfectly soluble in HFIP after at least 2 hours of stirring, but different aspects were observed after the addition of DMAPA. The PET/HFIP/DMAPA ratio was optimized for the different PET sources. The best ratio was found to be 25/400/810 (w/w/w) for which white fibers were formed. HFIP is relatively acidic alcohol (pKa = 9.3), more acidic than the standard alcohols almost equivalent to phenol, but it has relatively high polarity (ε = 15.7) favorizing the stabilization of ion pairs.[37] The formation of white fibers or precipitates after DMAPA addition to the solution of PET in HFIP maybe due to the formation of the ion pair $[HFIP\text{-}H]^-[DMAPA\text{-}H]^+$. The tertiary amine group of DMAPA is deactivated by HFIP yielding stable H-bond adducts.[38] With HFIP, a simple one-day heating at the temperature of reflux of HFIP or a transamidation of more days at room temperature was necessary to resolubilize the fibers. Products depolymerized at room temperature and at 58 °C were compared showing no major effects on the formation of main PET depolymerization products. However, important minor depolymerized products appeared only after HFIP addition (SI, Figure S1). Consequently, the depolymerization at the temperature of reflux of HFIP has been used to speed-up the reaction time. The extraction step by petroleum ether used before was omitted because very low extraction yield in this organic phase was observed. So, by using HFIP, the extraction yield was improved reaching 93% for some PET bottles, the reaction time was reduced and softer temperature has been used. This depolymerization method with HFIP has been used for all data in this work.

The extraction yield was calculated using the following formula where IS represents the internal standard if added.

$$\%\ Extraction\ yield = \frac{Weight\ of\ dried\ products}{PET\ weight + IS\ weight} \times 100$$

Different extraction yields for each type of PET bottles were obtained upon depolymerization. This yield is varying even for the same brand; it may depend on many parameters that affect PET recycling capacity such as PET manufacturing country, its starting material (rPET or not) and the purity of rPET if present. For instance, the extraction yield of bottles in the presence of internal standard was the highest for Swiss sparkling bottle (93%) which is made from 100% of rPET easily recyclable. For Cola-1 bottles, the yield was 79% for French bottle which is higher than German and Swiss Cola-1 bottles (59% and 36% respectively); this confirms the effect of starting PET origin because Cola-1 bottles from France and Germany were indicated as 100% rPET. Concerning the other soft drinks' bottles, the American Cola-1 and Cola-2 bottles had almost the same extraction yield (~85%) and the French Cola-2 bottle yielded 68% of depolymerization products. For French still water bottles, Water FRA2 had higher extraction yield than the other one Water FRA1 with 91% and 59% respectively (SI, Table S1).

MALDI FTICR MS analysis. As the reaction yields a complex mixture of depolymerized products with plastic additives, the use of high-resolution FTICR MS of resolving power of 530,000 at *m/z* 400 was efficient to separate the very close peaks in the complex MS spectra. 2,000 to ten-thousands of peaks were present per each spectrum; this

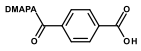
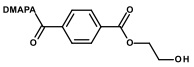
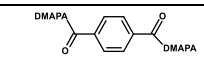
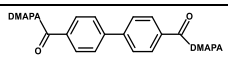
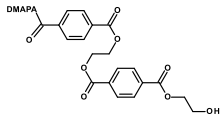
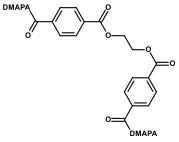
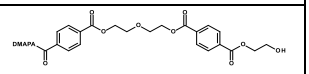
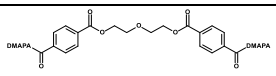
number was different for each PET bottle revealing different composition. The soft ionization technique MALDI was used to identify very fast in almost 3 min each PET depolymerization products. MALDI FTICR MS spectra determined with high accuracy (errors in the sub ppm range) the *m/z* ratios of each compound. The main PET depolymerization marker's peak appearing at *m/z* 335.2442 that corresponds to terephthalic acid bearing two DMAPA molecules was present in all PET products. This monoisotopic peak was registered with high accuracy, very high resolution (~600,000 at *m/z* 335.2442) and accurate isotopic ratio after simulation with the theoretical parameters in Bruker Data Analysis software; the isotopes containing ^{15}N, ^{13}C and deuterium were clearly present when enlarging the first isotopic peak (SI, Figure S2).

MALDI FTICR MS analysis of PET bottles in positive mode showed two main families of products between *m/z* 100 and *m/z* 1,500 separated by the monomeric unit $C_{10}H_8O_4$. The first family starts by the major depolymerization peak of di-derivatized terephthalic acid [$C_{18}H_{30}N_4O_2$ + H^+] appearing at *m/z* 335.2442 (theoretical *m/z* 335.24415) with very high accuracy; the distribution of errors of this peak in all studied PET bottles considering 5 digits is given in SI, Table S2. Its dimer [$C_{28}H_{38}N_4O_2$ + H^+] corresponding to ethylene glycol with two terminal groups of derivatized terephthalic acids appeared at *m/z* 527.2864 (Table 2). Its oligomers including trimer [$C_{38}H_{46}N_4O_{10}$ + H^+], tetramer [$C_{48}H_{54}N_4O_{14}$ + H^+], and pentamer [$C_{58}H_{62}N_4O_{18}$ + H^+] had been detected at *m/z* 719.3287, 911.3709 and 1103.4132 respectively. The second family starts by the mono-derivatized PET monomer [$C_{15}H_{22}N_2O_4$ + H^+] at *m/z* 295.1652 (Table 2). Its oligomers up to 5 units [$C_{25}H_{30}N_2O_8$ + H^+], [$C_{35}H_{38}N_2O_{12}$ + H^+], [$C_{45}H_{46}N_2O_{16}$ + H^+] and [$C_{55}H_{54}N_2O_{20}$ + H^+] appeared at *m/z* 487.2075, 679.2498, 871.2920 and 1063.3343 respectively were detected with high accuracy. An elimination of terminal C_2H_4O group from the trimer resulted in the formation of its corresponding mono-acidic compound [$C_{33}H_{34}N_2O_{11}$ + H^+] represented by the peak at *m/z* 635.2235. This second series may occur from the hydrolysis of PET cyclic oligomers.

PET plastics are well known to contain both cyclic and linear oligomers, the most abundant are the cyclic dimers and trimers.[39] The minority linear oligomers cannot be distinguished by our approach as they give the same products as the bulk polymer, whereas the cyclic oligomers afford the mono-derivatized PET oligomers. This difference in origin is highlighted by the plot of the logarithm of oligomers' relative intensities versus the number of terephthalic units. While the intensities of the di-derivatized PET oligomers decrease linearly with their sizes as expected,[40] the mono-derivatized PET oligomers display a sharp maximum corresponding to the cyclic trimer (Figure S3, 4, & 5). The mono-derivatized PET monomer (*m/z* 295.1652) was detected in its acidic form at *m/z* 251.1390 after the loss of its ethylene glycol unit. This acidic form appeared in lower intensity than the mono-derivatized PET monomer.

An interesting compound [$C_{30}H_{42}N_4O_7$ + H^+] corresponding to diethylene glycol (DEG) with two terminal groups of derivatized terephthalic acids was detected at *m/z* 571.3126. This compound was found mono-transamidated with its ethylene glycol terminal group [$C_{27}H_{34}N_2O_9$ + H^+] at *m/z* 531.2337 and mono-oxygenated at *m/z* 587.3075. Other depolymerization compounds, crosslinked products, additives, oxygenated compounds, dimers and oligomers have been also identified (SI, Table S3).

Table 2. Example of structures identified in the transamidated PET bottles and containers with their corresponding chemical formula and theoretical *m/z*.

Theoretical *m/z*	$[M+H]^+$ Formula	Identified structures
251.1390	$C_{13}H_{19}N_2O_3$	
295.1652	$C_{15}H_{23}N_2O_4$	
335.2442	$C_{18}H_{31}N_4O_2$	
411.2755	$C_{24}H_{35}N_4O_2$	
487.2075	$C_{25}H_{31}N_2O_8$	
527.2864	$C_{28}H_{39}N_4O_2$	
531.2337	$C_{27}H_{35}N_2O_9$	
571.3126	$C_{30}H_{43}N_4O_7$	

The compound with DEG appearing at *m/z* 571.3126 was found crosslinked with one PET monomer [$C_{40}H_{50}N_4O_{11}$ + H^+], 2 PET monomers [$C_{50}H_{58}N_4O_{15}$ + H^+] and 3 PET units [$C_{60}H_{66}N_4O_{19}$ + H^+]; these products were detected at *m/z* 763.3549, 955.3971 and 1147.4394 respectively (SI, Table S3). Di-benzylic compounds have been also detected, they were represented by the di-derivatized compound [$C_{24}H_{34}N_4O_2$ + H^+] appearing at *m/z* 411.2755 (Table 2). Oxygenated compounds in the depolymerized PET mixtures have been identified. For example, we detected the oxidation of the major peak [$C_{18}H_{30}N_4O_3$ + H^+], the first dimer of the family with one ethylene glycol [$C_{28}H_{38}N_4O_7$ + H^+], the mono-derivatized PET monomer [$C_{15}H_{22}N_2O_5$ + H^+] appearing at *m/z* 351.2391, 543.2813 and 311.1602 respectively (SI, Table S3).

Differentiation of PET bottles: MALDI FTICR MS. To compare the different depolymerized PET bottles, the percentage of the main depolymerization compound will be calculated in comparison to the sum of relative intensities of the major composition formed by the 24 compounds present in SI, Table S4, as given in the following formula:

$$\%\ Main\ depolymerization\ marker = \frac{RI\ of\ the\ main\ depolymerization\ marker}{RI\ of\ the\ major\ composition\ peaks} \times 100$$

RI represents the relative intensity of a given peak.

The percentage of oxygenated compounds, dimers and oligomers in each mixture will be calculated as previously.

Table 3. Abundances (in %) of the depolymerization marker, oxygenated compounds, dimers and oligomers in each depolymerized PET bottle.

Bottle name	% Marker (*m/z* 335.2442)	% Dimers & oligomers	% Oxygenated products
Water FRA1	80	8.5	0.8
Water FRA2	35	58	0.2
Water GER	43	53	1.0
Water SP	68	18	6.0
Water US1	82	4	6.0
Water US2	40	41	5.6
Water-S FRA1	26	68	0.1
Water-S FRA2	49	44	0.4
Water-S GER	72	18	1.0
Water-S CH	60	30	1.8
Water-S SP	36	47	2.5
Cola-1 FRA	40	48	2.0
Cola-1 GER	54	34	1.0
Cola-1 CH	25	68	0.3
Cola-1 SP	67	26	0.3
Cola-1 US	48	45	0.2
Cola-2 FRA	27	66	0.1
Cola-2 US	34	59	0.2

MALDI FTICR MS spectra of the depolymerized still water bottles showed that the main depolymerization peak appearing at *m/z* 335.2242 was highly intense in Water US1 and Water FRA1 followed by Water SP, Water GER, Water US2 then Water FRA2 bottles with 82%, 80%, 68%, 43%, 40% and 35% respectively. In Water FRA1, Water US1 and Water US2 still water bottles, the intensities of the first family's oligomers were higher than the second one. Water SP and Water US1 had the highest intensity of oxygenated compounds with 60‰. The oxygenated mono-transamidated monomer appearing at *m/z* 311.1602 was the main oxygenated compound in the American bottle Water US1 (Table 3).

Despite the similarity in chemical composition of these still water bottles, the difference in intensity of their common compounds and the presence of other specific depolymerization products and additives in each bottle may differentiate them. For example, the American still water bottles contain more structures with diethylene glycol in their backbone such as [$C_{30}H_{42}N_4O_7$+ H^+] (*m/z* 571.3126) than the two French still water bottles. The intensity of this last compound was the highest in Water US2 with ~38‰ (SI, Table S4).

For all sparkling water bottles, the intensity of the main depolymerization peak did not exceed the 73% showing differences in their depolymerization yield; the lowest was registered for Water-S FRA1 with 26%. All these bottles have relatively high intensity of dimers and oligomers in which the first family was more prominent. Water-S FRA1 having the highest intensity of oligomers (~68%) was very resistant to oxidation reactions (oxygenated compounds represented only 0.1%). No traces of the oxygenated mono-transamidated monomer at *m/z* 311.1602 have been detected in the two French bottles (SI, Table S5).

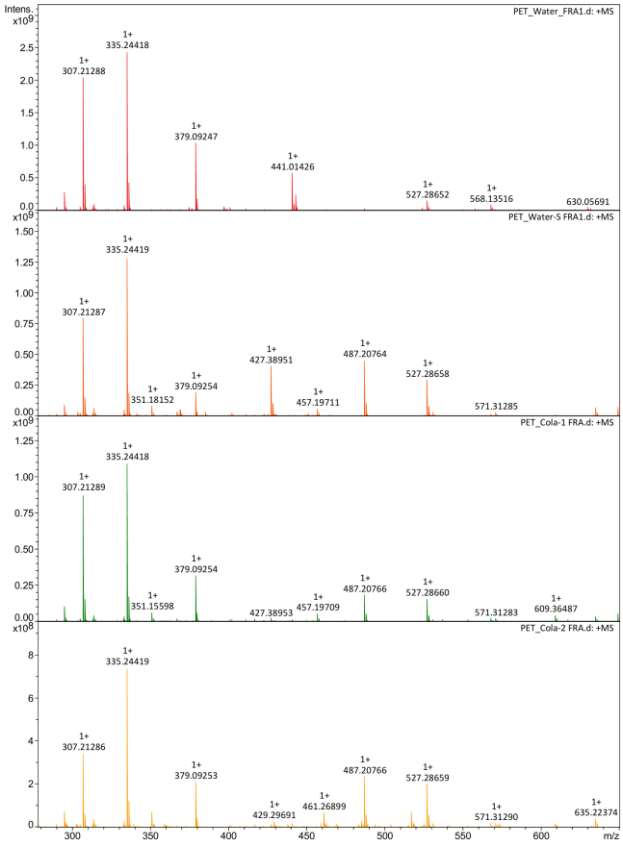


Figure 2. MALDI FTICR MS spectra (*m/z* 280-650) for Water FRA1, Water-S FRA1, Cola-1 FRA and Cola-2 FRA respectively. (The peak at *m/z* 379.092 is the main peak of HCCA matrix).

The sparkling water bottles are relatively similar concerning their major chemical composition but they may be differentiated by their major compounds' abundances and their minor composition. However, sparkling water bottles had additional compounds than still water bottles from same countries. Indeed, MALDI FTICR MS spectra of German sparkling water bottle showed the presence of dioctyl adipate (DOA) additive appearing in its initial form [$C_{22}H_{42}O_4$ + H^+] at *m/z* 371.3156 and its mono-transamidated form [$C_{19}H_{38}N_2O_3$ + H^+] at *m/z* 343.2955. This additive was absent in still

water bottle from Germany (SI, Table S3). DOA is commonly used as plasticizer in PVC and PS blends but not in PET.[41,42] It is found in high quantity in glue label. So, the traces of DOA in PET water bottles may due to a contamination or a possible migration.[43,44]

The soft drinks' bottles from the first studied brand Cola-1 showed less depolymerization yield than the previous bottles. Indeed, the depolymerization marker's abundance had a range between 25% for the Swiss Cola-1 and 67% for the Spanish one. The German bottle had 54% of this marker. The American bottle was depolymerized 8% more than the French one. The dimers and oligomers' abundances were also significant here especially for the Swiss Cola-1 bottle with 68%. The oxygenated compounds appeared in traces (less than 1%) in Swiss, American and Spanish Cola-1 bottles. However, French and German Cola-1 bottles were relatively oxidized with 2% and 1% of each bottle's major composition (SI, Table S6).

Cola-2 bottles had lower depolymerization yield than Cola-1 bottles. Hence, Cola-2 bottles from France and US contained 27% and 34% of the main peak at *m/z* 335.2442 in comparison to 40% and 48% respectively for their homologous from Cola-1 brand (SI, Table S6).

The depolymerization rate and PET composition in dimers and oligomers were different for Cola-1 bottles according to their manufacturing countries. The same trend has been found for Cola-2 bottles. The lower intensity of the depolymerization marker in Cola-2 bottles had been compensated by the presence of dimers and oligomers in the mixtures. The French Cola-2 bottle was more resistant to oxidations than the French Cola-1 bottle with only 0.1% (vs 2%) of oxygenated products. The same trend has been found for the American Cola-1 and Cola-2 bottles (Table 3 & SI, Table S6).

All the spectra of soft drinks' PET bottles, Cola-1 and Cola-2, showed the presence of two additional relatively intense peaks at *m/z* 377.2435 and *m/z* 609.3647 (Figure 2). Among the known industrial terephthalic co-polyesters, poly(ethyleneglycol-co-1,4-cyclohexanedimethanol terephthalate (PETG) appears to be a good candidate to afford these peaks after depolymerization by DMAPA.[45,46] PETG films display good mechanical properties, they are chemically more resistant than PET polyesters with their slow crystallization and good clarity properties.[47] PETG modifies also the surface properties of PET films and affects their ability to support microflora growth.[48]

To decipher the structure of these two compounds, our depolymerization methodology was applied to PETG authentic polymer. PETG was perfectly depolymerized with an extraction yield of 90% leading to two abundant compounds: The first one representing the main peak [$C_{34}H_{48}N_4O_6$ + H^+] appearing at *m/z* 609.3647 corresponds to cyclohexanedimethanol with two di-derivatized terephthalic acid terminal groups (74% of PETG major composition) and the second one [$C_{21}H_{32}N_2O_4$ + H^+] appearing at *m/z* 377.2435 corresponds to the mono-transamidated terephthalic acid with cyclohexanedimethanol (13% of PETG major composition) (Table 4 & SI Table S7).

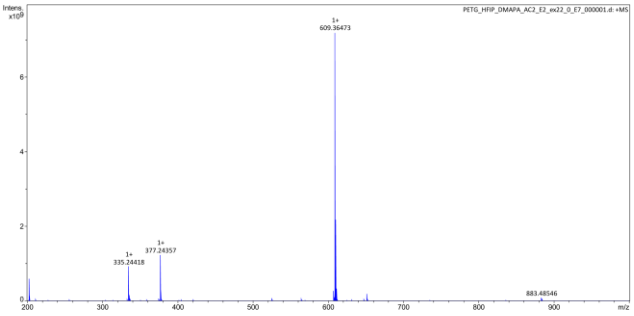
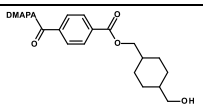
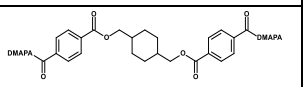


Figure 3. MALDI FTICR MS spectrum of the depolymerized PETG film*; m/z* 200-1,000.

Table 4. The two main identified structures in the transamidated PETG with their corresponding chemical formula and theoretical *m/z.*

Theoretical *m/z*	$[M+H]^+$ Formula	Identified structures
377.2435	$C_{21}H_{33}N_2O_4$	
609.3647	$C_{34}H_{49}N_4O_6$	

MALDI FTICR MS spectrum of PETG films (Figure 3) showed the presence of almost 3,033 peaks, including the major depolymerization compounds found in water bottles' PET. However, some PET compounds disappeared in the depolymerized PETG. For example, no traces were detected for the oxygenated compounds of mono- and di-transamidated PET monomer or for the product [$C_{30}H_{42}N_4O_7$ + H^+] having diethylene glycol with all its associated compounds. Specific compounds having terephthalic acid and cyclohexanedimethanol crosslinks were revealed only in PETG films. Indeed, the dimer [$C_{50}H_{66}N_4O_{10}$ + H^+] and trimer [$C_{66}H_{84}N_4O_{14}$ + H^+] of PETG's main peak separated by $C_{16}H_{18}O_4$ unit appearing at *m/z* 883.4852 and 1157.6057 respectively were detected only in PETG. The mono-transamidated 4-(4-carboxyphenyl)benzoic acid with cyclohexanedimethanol [$C_{27}H_{36}N_2O_4$ + H^+] was identified at *m/z* 453.2748. The mixed di-transamidated trimer combining two cyclohexanedimethanol units and one ethylene glycol unit [$C_{60}H_{74}N_4O_{14}$ + H^+] was found at *m/z* 1075.5274.

[4-[[4(Hydroxymethyl)cyclohexyl]methoxymethyl] cyclohexyl] methanol was crosslinked to the mono- and di-transamidated terephthalic acid(s); these 2 compounds [$C_{29}H_{46}N_2O_5$ + H^+], [$C_{42}H_{62}N_4O_7$ + H^+] were appeared at *m/z* 503.3479 and *m/z* 735.4691 respectively. The identified peaks in PETG are shown in SI, Table S7.

The two main compounds (Table 4) have been existed in the two studied brands, Cola-1 and Cola-2 of soft drinks' bottles from different manufacturing countries. They are a clear chemical signature of this type of bottles. MALDI FTICR MS spectra displayed almost 1.7% and 0.6% of PETG main peak (at *m/z* 609.3647) in Cola-1 bottles from France and US respectively. This peak was less abundant in French Cola-2 bottle (0.6%) and much more presented

in the American Cola-2 bottle (2.6%) as shown in SI, Table S6.

Some sparkling water bottles contained either one or both PETG main compounds. Still and sparkling Spanish water bottles showed the presence of pure PET that does not contain any PETG co-polyester. However, still and sparkling water bottles from Germany are consisting of PETG with its two main compounds. This may due to the differences in recycling policies among countries especially in Germany which is known as the first PET recycling market in Europe.[49,50] This same tendency is found for Swiss sparkling water bottles (SI, Tables S4 & S5). Indeed, Germany and Switzerland may use all types of PET recyclable bottles including Cola bottles without doing additional sorting for the fabrication of their new bottles.

Reverting to Cola soft drinks' bottles differentiated by the presence of PETG, their composition was not identical according to the popular two manufacturing brands referring to a specific database for each brand and each country. Despite the presence of common peaks, their intensities were not the same in each depolymerized mixture. Indeed, the depolymerized compound having ethylene glycol and DEG [$C_{37}H_{42}N_2O_{13} + H^+$] has appeared at *m/z* 723.2759 in all bottles but with different intensities; the highest was found for the Swiss Cola-1 bottle. To the best of our knowledge, this is the first time that PETG has been identified in commercial bottles.

According to their manufacturing country and brands, the soft drinks' bottles were also different. For instance, the French Cola-1 and Cola-2 bottles showed the presence of di-transamidated terephthalic parts with butanediol alone [$C_{30}H_{42}N_4O_6 + H^+$] at *m/z* 555.3177; this compound was absent in both American Cola bottles. For the same brand Cola-1, the French bottle revealed the presence of 4-[4-(4-carboxyphenyl)phenyl]benzoic acid di-derivatized [$C_{30}H_{38}N_4O_2 + H^+$] at *m/z* 487.3068; which was absent in the American Cola-1 bottle. Comparing all Cola soft drinks' bottles, French Cola-1 bottle was differentiated by the presence of the peak at *m/z* 453.2748 already described in PETG and the compound bearing 4-(hydroxymethyl)cyclohexanol [$C_{20}H_{30}N_2O_4 + H^+$] at *m/z* 363.2278. The mono-oxidized PETG main compound [$C_{34}H_{48}N_4O_7 + H^+$] appearing at *m/z* 625.3596 was only detected in the American Cola-2 bottle as in the depolymerized PETG. The corresponding identified structures are shown in SI, Table S3.

Comparison of LC-MS and MALDI FTICR MS results. PET depolymerization products were analyzed using another source of ionization ESI but this time with an Orbitrap LTQ-XL coupled to liquid chromatography fitted with a C18 column using a water/acetonitrile gradient. A complex mixture of products has been identified by LC-MS with good resolution at 1 mg/mL (Figure 4).

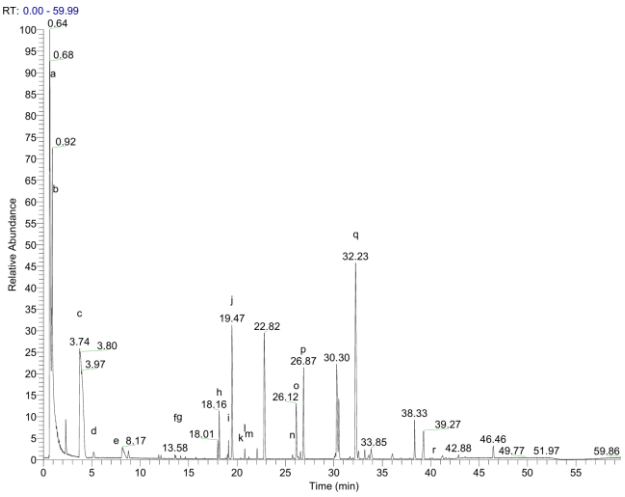


Figure 4. LC chromatogram of the depolymerized French Cola-1 bottle, at 1 mg/mL. LC peaks indicated by letters are described in SI, Table S8.

The depolymerization products including oligomers and additives identified in MALDI FTICR MS were compared to LC-MS results (*m/z* 200-1,000). The intensities of the common peaks were comparable but not identical showing a performance difference of ionization mode and instrument used on the identification of compounds according to their chemical nature. LC-MS identified the depolymerization products with good accuracy for an Orbitrap (0-3 ppm). The sensitivity of LC-MS was very good to confirm the presence of traces already identified by MALDI FTICR MS such as the oxygenated main depolymerization compound at *m/z* 351.2391. This last peak constituted 1.9% of major composition of the French Cola-1 bottle in MALDI FTICR MS and 0.1% in LC ESI Orbitrap-MS as shown in SI, Table S8.

The correlation of the identified data between LC-MS and MALDI FTICR MS has been attributed showing an excellent correlation after using these 2 methods of ionization on two analytical devices (SI, Figure S6).

Furthermore, LC-MS detected the presence of additional peaks not revealed in MALDI FTICR MS. Indeed, LC-MS revealed the presence of the mono-transamidated 4-(4-carboxyphenyl)benzoic crosslinked with ethylene glycol [$C_{21}H_{26}N_2O_4 + H^+$] (*m/z* 371.197) at 15.80 min, and with both diols ethylene glycol and cyclohexanedimethanol detected oxygenated [$C_{29}H_{40}N_2O_6 + H^+$] (*m/z* 513.296) at 1.05 min (SI, Table S3; entries 29 & 78 respectively). Other products were identified: The mono-transamidated additive bis(2-ethylhexyl) sebacate [$C_{23}H_{46}N_2O_3 + H^+$] was detected by both instruments at *m/z* 399.3581 in the French Cola-1 bottle; but its oxygenated compound [$C_{23}H_{46}N_2O_4 + H^+$] of *m/z* 415.353 has appeared only in LC-MS using electrospray ionization at 21.27 min (SI, Table S3; entries 36 & 40 respectively).

Miniaturization. The depolymerization methodology worked after scaling-down the initial quantity of PET material from 25 mg to only 1 mg. The steps of solubilization, transamidation and liquid-liquid extractions were carefully followed using less volumes of reagents and solvents. MALDI FTICR MS remained sensitive and resulted in the formation of PET depolymerization marker (*m/z* 335.2442) at high resolution and accuracy. Unlike all previous microplastics

collected mainly from the body of bottles, two areas of the same bottle will be studied here, the base and the body of Water FRA2 bottle. As it is known that the PET has different crystallinity according to the part of the bottle, this crystallinity has a strong influence on PET enzymatic degradation.[51] Indeed, a lower depolymerization yield of the base part, which has a higher crystallinity, was registered comparing to the bottle's body (decrease of 50%). In addition, the analysis of these two parts showed similar chemical composition but with observable different intensities of some minor peaks as shown in SI, Figure S7. For instance, PETG main marker appearing at *m/z* 609.3647 was more intense in the base part of the bottle which is more rigid than its body. These observations demonstrate the effect of PET crystallinity on its depolymerization efficiency.

Quantification. PET bottles and containers were quantified using the synthesized internal standard *N1,N4*-bis[2-(dimethylamino)ethyl] terephthalamide. This product [$C_{16}H_{26}N_4O_2 + H^+$] was successfully produced and analyzed before using it for PET quantification. It appeared as intense peak at *m/z* 307.2129 in MALDI FTICR MS with very high accuracy (error = 170 ppb). It was also confirmed in LC-MS by an intense peak at 0.73 min with its corresponding expected *m/z* and by a fragmentation yielding *m/z* 262.156 resulting of the neutral loss of dimethyl amine group (SI, Figure S8 & S9).

Among the 3 tested concentrations for LC-MS, 0.1 mg/mL was the best for PET quantification. The peaks area of depolymerization marker and internal standard was used for better precision, and the depolymerization marker/IS ratio was calculated to confirm the depolymerization yield in each mixture. Indeed, this ratio was 0.7 and 0.5 for Cola-1 FRA and Cola-1 GER respectively, and it was higher having 1.4, 1.5 and 1.5 for Cola-1 US, Cola-2 FRA and Cola-2 US respectively. These results almost matched the relative intensities in MALDI FTICR MS where the ratios were 3 and 2 for Cola-1 FRA and Cola-1 GER respectively, and 5.1, 8 and 8 for Cola-1 US, Cola-2 FRA and Cola-2 US respectively. LC-MS results were more quantitative than MALDI FTICR MS without a matrix presence. Using the same calculations, each compound may be quantified in comparison to the added internal standard.

CONCLUSIONS AND PERSPECTIVES

A new methodology of chemical depolymerization of polyesters and co-polyesters by transamidation was developed. Its first application was applied to PET polyesters, their microplastics and PETG co-polyesters. The transamidation by DMAPA amine occurred at soft conditions capturing carboxylic acids and aromatic di- and poly-acids associated with diols and polyols. Using HFIP before transamidation was excellent choice for improving the extraction yield of depolymerized products and for working at softer conditions for less reaction duration. Combining this soft chemical depolymerization with ultra-high resolution mass spectrometry techniques, FTICR and Orbitrap, was a powerful tool for PET structural identification at molecular level and for their quantification. Thus, the utilization of both ionization mode MALDI and ESI on two different analytical devices enhanced reliability of the complementary data on the full composition of PET bottles and containers allowing to create a large database for their depolymerization compounds including dimers, oligomers, oxygenated species, crosslinking products and additives. This approach enabled recognizing a specific chemical signature for each PET containers and bottles from different countries, brands and contents especially water and carbonated liquids with high resolution and high accuracy. For the same PET object, our approach affords also information about the crystallinity of its different parts. This analysis was scaled-down to 1 mg of microplastics. In conclusion, this is a unique novel study for the differentiation of PET packaging objects especially bottles after soft chemical depolymerization using advanced mass spectrometry. The additives of these bottles and others of different contents will be further investigated. This method can be used on other polyesters and co-polyesters. It is very promising strategy to determine the pollution source by PET bottles and their micro- and nano-plastics in the environment. PET ageing and environmental PET samples analysis will be investigated and other attempts for the follow-up of diols and polyols structural modifications will be developed.

ASSOCIATED CONTENT

Supporting Information

Mass spectrometry and analytical data for PET depolymerized products. Additional experimental details and characterization data.
This material is available free of charge on the ACS Publications website http://pubs.acs.org.

AUTHOR INFORMATION

Corresponding Author

*Christian Rolando - Univ. Lille, CNRS, UAR 3290, MSAP, Miniaturisation pour la Synthèse l'Analyse et la Protéomique, F-59000 Lille, France ; Shrieking Sixties, 1-3 Allée Lavoisier, 59650, Villeneuve-d'Ascq, France ; Email : christian.rolando@univ-lille.fr; orcid.org/0000-0002-3266-8860.

Authors

Bayan Almasri - Univ. Lille, CNRS, UAR 3290, MSAP, Miniaturisation pour la Synthèse l'Analyse et la Protéomique, F-59000 Lille, France ; Laboratoire de Chimie Appliquée, Faculté des Sciences III, Université Libanaise, Ras Maska, Tripoli, Liban ; orcid.org/0009-0001-9467-5716.

Author Contributions

The manuscript was written through contributions of all authors and all authors have given approval to the final version of the manuscript.

Note

The authors declare no competing financial interest.

ACKNOWLEDGMENT

Bayan ALMASRI gratefully acknowledges the funding of her joint PhD between University of Lille and Lebanese University by the PAUSE funding program. The mass spectrometers were funded by University of Lille, CNRS, Région Hauts-de-France and the European Regional Development Fund (ERDF). The authors gratefully acknowledge the financial support of the FTICR MS facility from the IR INFRANALYTICS FR2054 CNRS and of the

EU_FTICR _MS project Grant Agreement 731077 funded by EU Horizon 2020 Research and Innovation Program.

REFERENCES

(1) Lepoittevin, B.; Roger, P. In *Handbook of engineering and speciality thermoplastics*, Sabu, T.; Visakh, P. M., Eds., 2011, pp 97-126. http://doi.org/10.1002/9781118104729.ch4

(2) Tsironi, T. N.; Chatzidakis, S. M.; Stoforos, N. G. *The future of polyethylene terephthalate bottles: Challenges and sustainability*. *Packaging Technology and Science* **2022**, *35*, 317-325. http://doi.org/10.1002/pts.2632

(3) Nisticò, R. *Polyethylene terephthalate (PET) in the packaging industry*. *Polymer Testing* **2020**, *90*, 106707. http://doi.org/10.1016/j.polymertesting.2020.106707

(4) Hendrickson, T. P.; Bose, B.; Vora, N.; Huntington, T.; Nordahl, S. L.; Helms, B. A.; Scown, C. D. *Paths to circularity for plastics in the United States*. *One Earth* **2024**, *7*, 520-531. http://doi.org/10.1016/j.oneear.2024.02.005

(5) *Plastics- The facts 2022, analysis of the latest data related to plastics production, demand, conversion and waste management in Europe*. Plastics Europe, 2022. https://plasticseurope.org/wp-content/uploads/2022/12/PE-plastics-the-facts_final_digital.pdf. Accessed:11 May 2025

(6) Turner, S.; Seymour, R.; Dombroski, J. In *Modern polyesters: Chemistry and technology of polyesters and copolyesters*, Scheirs, J.; Long, T. E., Eds.; John Wiley & Sons: Chichester, United Kingdom, 2004, pp 267-292. http://doi.org/10.1002/0470090685.ch7

(7) Fiorillo, C.; Trossaert, L.; Bezeraj, E.; Debrie, S.; Ohnmacht, H.; Van Steenberge, P. H.; D'hooge, D. R.; Edeleva, M. *Molecular and material property variations during the ideal degradation and mechanical recycling of PET*. *RSC Sustainability* **2024**, *2*, 3596-3637. http://doi.org/10.1039/D4SU00485J

(8) Hovenkamp, S.; Munting, p. J. *Formation of diethylene glycol as a side reaction during production of polyethylene terephthalate*. *Journal of Polymer Science Part A-1: Polymer Chemistry* **1970**, *8*, 679-682. http://doi.org/10.1002/pol.1970.150080310

(9) Sang, T.; Wallis, C. J.; Hill, G.; Britovsek, G. J. *Polyethylene terephthalate degradation under natural and accelerated weathering conditions*. *Eur. Polym. J.* **2020**, *136*, 109873. http://doi.org/10.1016/j.eurpolymj.2020.109873

(10) Andreasi Bassi, S.; Tonini, D.; Saveyn, H.; Astrup, T. F. *Environmental and socioeconomic impacts of poly (ethylene terephthalate)(PET) packaging management strategies in the EU*. *Environmental Science & Technology* **2021**, *56*, 501-511. http://doi.org/10.1021/acs.est.1c00761

(11) Smith, R. L.; Takkellapati, S.; Riegerix, R. C. *Recycling of plastics in the United States: plastic material flows and polyethylene terephthalate (PET) recycling processes*. *ACS Sustain. Chem. Eng.* **2022**, *10*, 2084-2096. http://doi.org/10.1021/acssuschemeng.1c06845

(12) Chu, J.; Zhou, Y.; Cai, Y.; Wang, X.; Li, C.; Liu, Q. *Flows and waste reduction strategies of PE, PP, and PET plastics under plastic limit order in China*. *Resour. conserv. recycl.* **2023**, *188*, 106668. http://doi.org/10.1016/j.resconrec.2022.106668

(13) Lee, C.; Jang, Y.-C.; Choi, K.; Kim, B.; Song, H.; Kwon, Y. *Recycling, material flow, and recycled content demands of polyethylene terephthalate (PET) bottles towards a circular economy in Korea*. *Environments* **2024**, *11*, 25. http://doi.org/10.3390/environments11020025

(14) Lambré, C.; Barat Baviera, J. M.; Bolognesi, C.; Chesson, A.; Cocconcelli, P. S.; Crebelli, R.; Gott, D. M.; Grob, K.; Mengelers, M. *Scientific Guidance on the criteria for the evaluation and on the preparation of applications for the safety assessment of post-consumer mechanical PET recycling processes intended to be used for manufacture of materials and articles in contact with food*. *EFSA Journal* **2024**, *22*, e8879. http://doi.org/10.2903/j.efsa.2024.8879

(15) Alaraby, M.; Abass, D.; Velázquez, A.; Hernández, A.; Marcos, R. *Occurrence, analysis, and toxicity of polyethylene terephthalate microplastics: a review*. *Environmental Chemistry Letters* **2025**, 1-35. http://doi.org/10.1007/s10311-025-01841-8

(16) Zhang, J.; Wang, L.; Trasande, L.; Kannan, K. *Occurrence of polyethylene terephthalate and polycarbonate microplastics in infant and adult feces*. *Environmental Science & Technology Letters* **2021**, *8*, 989-994. http://doi.org/10.1021/acs.estlett.1c00559

(17) Dimitrov, N.; Krehula, L. K.; Siročić, A. P.; Hrnjak-Murgić, Z. *Analysis of recycled PET bottles products by pyrolysis-gas chromatography*. *Polym. Degrad. Stab.* **2013**, *98*, 972-979. http://doi.org/10.1016/j.polymdegradstab.2013.02.013

(18) Dziwiński, E. J.; Iłowska, J.; Gniady, J. *Py-GC/MS analyses of poly (ethylene terephthalate) film without and with the presence of tetramethylammonium acetate reagent. Comparative study*. *Polymer Testing* **2018**, *65*, 111-115. http://doi.org/10.1016/j.polymertesting.2017.11.009

(19) Liang, J.; Frazier, J.; Benefield, V.; Chong, N. S.; Zhang, M. *Forensic fiber analysis by thermal desorption/pyrolysis-direct analysis in real time-mass spectrometry*. *Anal. Chem.* **2019**, *92*, 1925-1933. http://doi.org/10.1021/acs.analchem.9b04167

(20) Vitali, C.; Janssen, H.-G.; Ruggeri, F. S.; Nielen, M. W. *Rapid single particle atmospheric solids analysis probe-mass spectrometry for multimodal analysis of microplastics*. *Anal. Chem.* **2022**, *95*, 1395-1401. http://doi.org/acs.analchem.2c04345

(21) Wu, T.; Hu, H. L.; Du, Y. P.; Jiang, D.; Yu, B. H. *Discrimination of thermoplastic polyesters by MALDI-TOF MS and Py-GC/MS*. *International Journal of Polymer Analysis and Characterization* **2014**, *19*, 441-452. http://doi.org/10.1080/1023666X.2014.920126

(22) Romão, W.; Franco, M. F.; Iglesias, A. H.; Sanvido, G. B.; Maretto, D. A.; Gozzo, F. C.; Poppi, R. J.; Eberlin, M. N.; De Paoli, M.-A. *Fingerprinting of bottle-grade poly (ethylene terephthalate) via matrix-assisted laser desorption/ionization mass spectrometry*. *Polym. Degrad. Stab.* **2010**, *95*, 666-671. http://doi.org/10.1016/j.polymdegradstab.2009.11.046

(23) Romao, W.; Franco, M. F.; Corilo, Y. E.; Eberlin, M. N.; Spinace, M. A.; De Paoli, M.-A. *Poly (ethylene terephthalate) thermo-mechanical and thermo-oxidative degradation mechanisms*. *Polym. Degrad. Stab.* **2009**, *94*, 1849-1859. http://doi.org/10.1016/j.polymdegradstab.2009.05.017

(24) Badía, J.; Strömberg, E.; Ribes-Greus, A.; Karlsson, S. *A statistical design of experiments for optimizing the MALDI-TOF-MS sample preparation of polymers. An application in the assessment of the thermo-mechanical degradation mechanisms of poly (ethylene terephthalate)*. *Anal. Chim. Acta* **2011**, *692*, 85-95. http://doi.org/10.1016/j.aca.2011.02.063

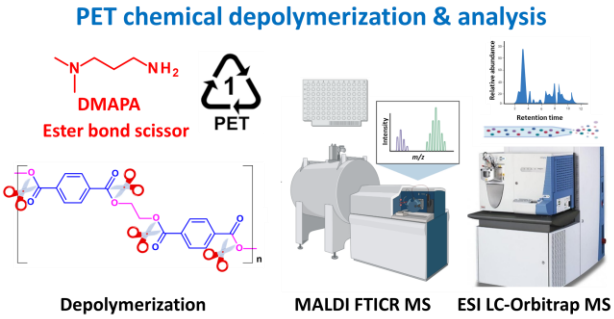
(25) Watanabe, R.; Sugahara, A.; Shinzawa, H.; Yamane, S.; Nakamura, S.; Sato, H.; Hagihara, H.; Oishi, A.; Mizukado, J.; Ueda, Y. *Photodegradation behavior of polyethylene terephthalate analyzed by MALDI-TOFMS and ATR-FTIR microscopic analysis in combination with two-trace two-dimensional (2T2D) correlation mapping*. *Polym. Degrad. Stab.* **2023**, *208*, 110246. http://doi.org/10.1016/j.polymdegradstab.2022.110246

(26) Fouquet, T. N.; Cody, R. B.; Charles, L. *Degradation strategies for structural characterization of insoluble synthetic polymers by mass spectrometry*. *Mass Spectrom. Rev.* **2024**. http://doi.org/10.1002/mas.21903

(27) Allen, B.; Elsea, G.; Keller, K.; Kinder, H. *Quantitative hydrolysis-gas chromatographic methods for the*

determination of selected acids and glycols in polyesters. *Anal. Chem.* **1977**, *49*, 741-743. http://doi.org/10.1021/ac50014a019
(28) Wang, L.; Zhang, J.; Hou, S.; Sun, H. *A simple method for quantifying polycarbonate and polyethylene terephthalate microplastics in environmental samples by liquid chromatography-tandem mass spectrometry*. *Environmental Science & Technology Letters* **2017**, *4*, 530-534. http://doi.org/10.1021/acs.estlett.7b00454
(29) Nakamura, S.; Fouquet, T.; Sato, H. *Molecular characterization of high molecular weight polyesters by matrix-assisted laser desorption/ionization high-resolution time-of-flight mass spectrometry combined with on-plate alkaline degradation and mass defect analysis*. *J. Am. Soc. Mass Spectrom.* **2018**, *30*, 355-367. http://doi.org/10.1007/s13361-018-2092-x
(30) Sládková, K.; Houška, J.; Havel, J. *Laser desorption ionization of red phosphorus clusters and their use for mass calibration in time-of-flight mass spectrometry*. *Rapid Commun. Mass Spectrom.* **2009**, *23*, 3114-3118. http://doi.org/10.1002/rcm.4230
(31) Montaudo, G.; Scamporrino, E.; Vitalini, D. *Structural characterization of copolyesters by fast atom bombardment mass spectrometry analysis of the partial ammonolysis products*. *Makromol. Chem. Rapid Commun.* **1989**, *10*, 411-417. http://doi.org/10.1002/marc.1989.030100806
(32) Andersen, S. M.; Heuckendorff, M.; Jensen, H. H. *3-(Dimethylamino)-1-propylamine: a cheap and versatile reagent for removal of byproducts in carbohydrate chemistry*. *Org. Lett.* **2015**, *17*, 944-947. http://doi.org/10.1021/acs.orglett.5b00041
(33) Huang, Y.-Q.; Wang, Q.-Y.; Liu, J.-Q.; Hao, Y.-H.; Yuan, B.-F.; Feng, Y.-Q. *Isotope labelling-paired homologous double neutral loss scan-mass spectrometry for profiling of metabolites with a carboxyl group*. *Analyst* **2014**, *139*, 3446-3454. http://doi.org/10.1039/C4AN00312H
(34) Yuan, B.; Li, X.; Xu, S.; Sun, H.; Shen, C.; Ji, J.; Lin, L.; Xu, W.; Shan, J.; Tong, W. *Discovery of N-Acyl Amino Acids and Novel Related N-, O-Acyl Lipids by Integrating Molecular Networking and an Extended In Silico Spectral Library*. *Anal. Chem.* **2023**. http://doi.org/10.1021/acs.analchem.2c04822
(35) Zhu, Q.-F.; Zhang, Z.; Liu, P.; Zheng, S.-J.; Peng, K.; Deng, Q.-Y.; Zheng, F.; Yuan, B.-F.; Feng, Y.-Q. *Analysis of liposoluble carboxylic acids metabolome in human serum by stable isotope labeling coupled with liquid chromatography-mass spectrometry*. *J. Chromatogr. A* **2016**, *1460*, 100-109. http://doi.org/10.1016/j.chroma.2016.07.017
(36) Moroni, A.; Havard, T. In *Chromatography of Polymers*; American Chemical Society, 1999, pp 249-262. http://doi.org/10.1021/bk-1999-0731.ch018
(37) Pozhydaiev, V.; Power, M.; Gandon, V.; Moran, J.; Lebœuf, D. *Exploiting hexafluoroisopropanol (HFIP) in Lewis and Brønsted acid-catalyzed reactions*. *Chem. Commun.* **2020**, *56*, 11548-11564. http://doi.org/10.1039/D0CC05194B
(38) Lebleu, T.; Ma, X.; Maddaluno, J.; Legros, J. *Selective monomethylation of primary amines with simple electrophiles*. *Chem. Commun.* **2014**, *50*, 1836-1838. http://doi.org/10.1039/C3CC48997C
(39) Ubeda, S.; Aznar, M.; Nerín, C. *Determination of oligomers in virgin and recycled polyethylene terephthalate (PET) samples by UPLC-MS-QTOF*. *Anal. Bioanal. Chem.* **2018**, *410*, 2377-2384. http://doi.org//10.1007/s00216-018-0902-4
(40) Nishida, H.; Yamashita, M.; Nagashima, M.; Hattori, N.; Endo, T.; Tokiwa, Y. *Theoretical prediction of molecular weight on autocatalytic random hydrolysis of aliphatic polyesters*. *Macromolecules* **2000**, *33*, 6595-6601. http://doi.org/10.1021/ma992102j
(41) Howick, C. J. In *Kirk-Othmer Encyclopedia of Chemical Technology*, 2000, pp 1-36. http://doi.org/10.1002/0471238961.1612011903010415.a01.pub2
(42) Wypych, G. In *Handbook of plasticizers*, Wypych, G., Ed.; ChemTec Publishing: Toronto, Canada, 2004, p 273.
(43) Badeka, A. B.; Pappa, K.; Kontominas, M. G. *Effect of microwave versus conventional heating on the migration of dioctyl adipate and acetyltributyl citrate plasticizers from food grade PVC and P (VDC/VC) films into fatty foodstuffs*. *Zeitschrift Für Lebensmitteluntersuchung und-Forschung A* **1999**, *208*, 429-433. http://doi.org/10.1007/s002170050442
(44) Shin, U.-S.; Ahn, H.-S.; Shin, H.-S. *Quantitation of phthalate and adipate in natural mineral water and PET container*. *Anal. Sci. Technol.* **2002**, *15*, 475-481.
(45) Turner, S. R. *Development of amorphous copolyesters based on 1, 4-cyclohexanedimethanol*. *J. Polym. Sci. Part A: Polym. Chem.* **2004**, *42*, 5847-5852. http://doi.org/10.1002/pola.20460
(46) Liu, Y.; Turner, S. R. *Synthesis and properties of cyclic diester based aliphatic copolyesters*. *J. Polym. Sci. Part A: Polym. Chem.* **2010**, *48*, 2162-2169. http://doi.org/10.1002/pola.23985
(47) Arangdad, K.; Detwiler, A.; Cleven, C. D.; Burk, C.; Shamey, R.; Pasquinelli, M. A.; Freeman, H.; El-Shafei, A. *Photodegradation of copolyester films: A mechanistic study*. *J. Appl. Polym. Sci.* **2019**, *136*, 47148. http://doi.org/10.1002/app.47148
(48) Jones, C.; Adams, M.; Zhdan, P.; Chamberlain, A. *The role of surface physicochemical properties in determining the distribution of the autochthonous microflora in mineral water bottles*. *Journal of applied microbiology* **1999**, *86*, 917-927. http://doi.org/10.1046/j.1365-2672.1999.00768.x
(49) Žmak, I.; Hartmann, C. *Current state of the plastic waste recycling system in the European Union and in Germany*. *Teh. Glas.* **2017**, *11*, 138-142.
(50) Patel, M.; von Thienen, N.; Jochem, E.; Worrell, E. *Recycling of plastics in Germany*. *Resour. conserv. recycl.* **2000**, *29*, 65-90. http://doi.org/10.1016/S0921-3449(99)00058-0
(51) Thomsen, T. B.; Hunt, C. J.; Meyer, A. S. *Influence of substrate crystallinity and glass transition temperature on enzymatic degradation of polyethylene terephthalate (PET)*. *New Biotechnology* **2022**, *69*, 28-35. http://doi.org/10.1016/j.nbt.2022.02.006

Table of Contents artwork: Abstract



Submitted article to *ACS Analytical Chemistry*

ChemRxiv® link: https://chemrxiv.org/engage/chemrxiv/article-details/686e2fad43bc52e4ec01c3d3

DOI: 10.26434/chemrxiv-2025-88b1d

Supporting information

Identification and quantification of polyethylene terephthalate (PET) polyesters and microplastics by combining mild chemical depolymerization with dimethylaminopropylamine (DMAPA) and MALDI FTICR & LC ESI Orbitrap mass spectrometry analysis

Bayan Almasri[1,2], Christian Rolando[1,3,*]

[1] Univ. Lille, CNRS, UAR 3290, MSAP, Miniaturisation pour la Synthèse l'Analyse et la Protéomique, F-59 000 Lille, France

[2] Laboratoire de Chimie Appliquée, Faculté des Sciences III, Université Libanaise, Ras Maska, Tripoli, Liban

[3] Shrieking Sixties, 1-3 Allée Lavoisier, 59650, Villeneuve-d'Ascq, France

Corresponding author's email: christian.rolando@univ-lille.fr

EXPERIMENTAL SECTION

Internal standard synthesis. For PET quantification, an internal standard (IS) has been synthesized from terephthaloyl chloride and 2-(dimethylamino)ethylamine (DMEN).

In 100-mL flask, 20 mL (183 mmol) of DMEN was added to 2 g (10.1 mmol) of terephthaloyl chloride (exothermic reaction). This mixture was left at 70 °C under magnetic stirring and N_2 inert atmosphere for 2 days. After cooling at room temperature, the mixture was quenched with 2 mL of formic acid in an ice bath. Then, the mixture was divided into two equal-volume parts then each 10 mL was transferred to a 15 mL Falcon™ conical tube, added to 20 mL of ultrapure water acidified with 400 µL of formic acid, extracted four times with 20 mL of ethyl acetate by centrifugation at 10,000 rpm during 5 minutes at room temperature. After each centrifugation, the organic phase was collected using a glass pipette. The obtained phases were then evaporated, collected and restored in 7-mL glass tube. An amber-colored crystal has been formed.

FIGURES AND TABLES

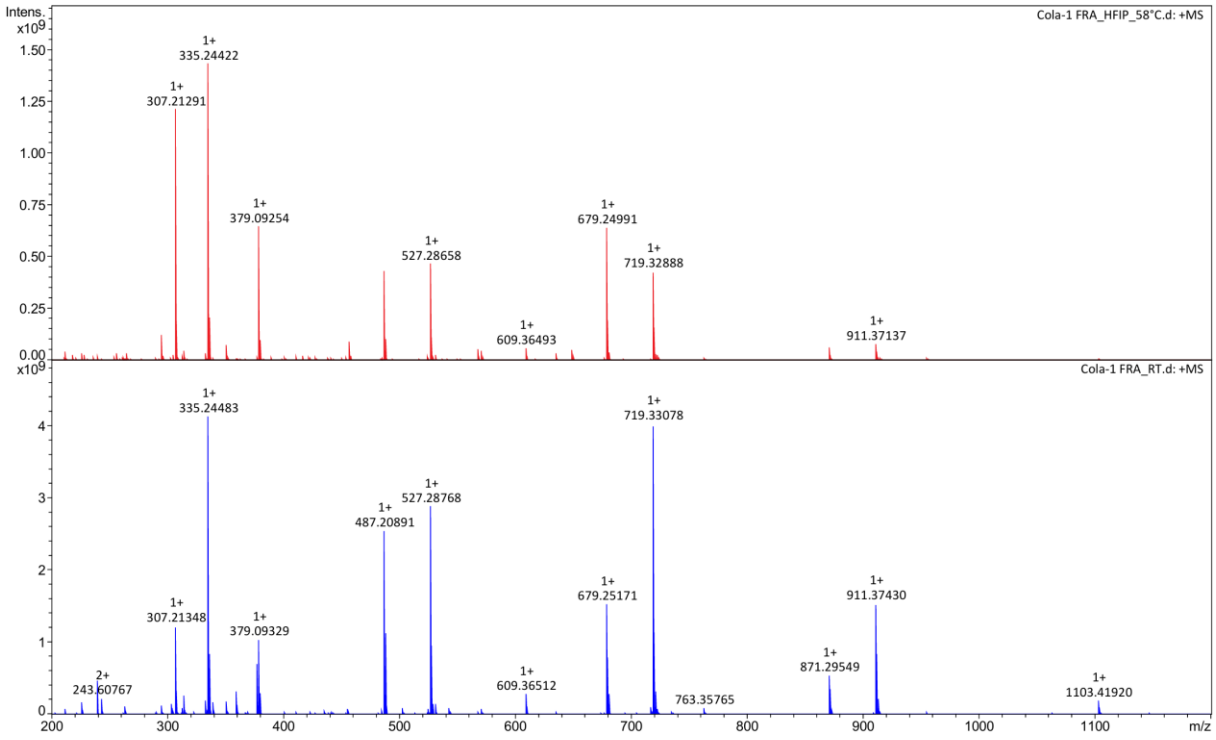


Figure S 1. MALDI FTICR MS spectra of French Cola-1 bottle, depolymerized by transamidation in the presence of IS. In red: Transamidation for 1 day at the temperature of reflux of HFIP (58 °C); in blue: Transamidation for 6 days at room temperature without HFIP.

Table S 1. Extraction yield of the analyzed PET bottles.

Bottle name	Extraction yield with IS (%)
Water FRA1	59%
Water FRA2	91%
Water GER	77%
Water-S FRA1	75%
Water-S FRA2	66%
Water-S GER	63%
Water-S CH	93%
Cola-1 FRA	79%
Cola-1 GER	59%
Cola-1 CH	36%
Cola-1 US	86%
Cola-2 FRA	68%
Cola-2 US	85%

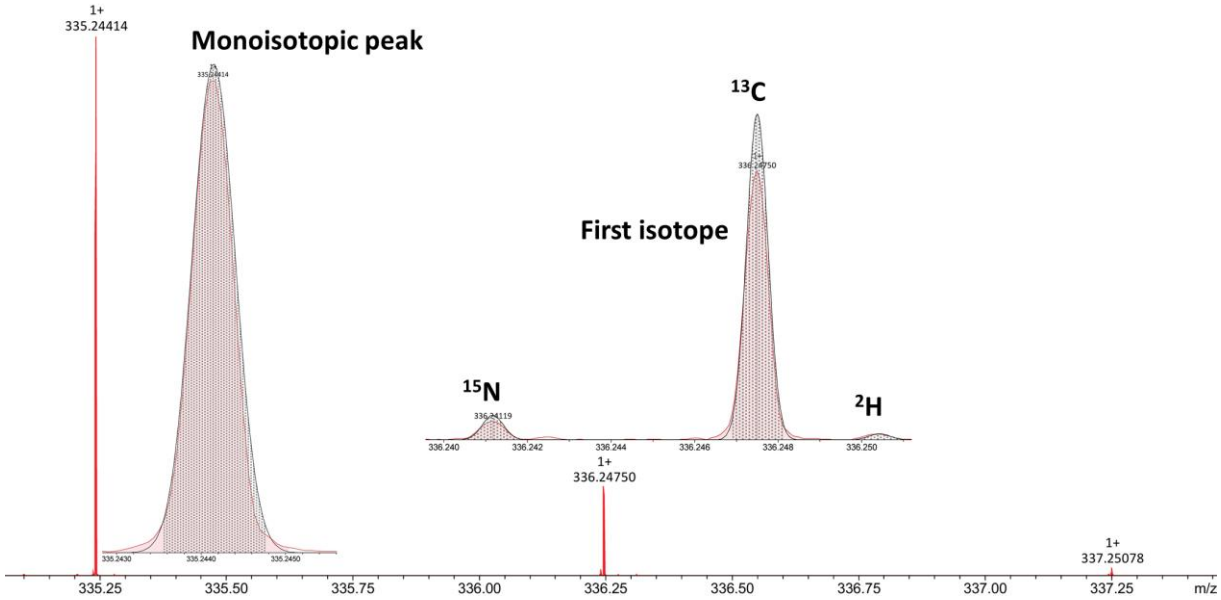
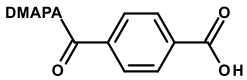
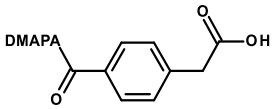
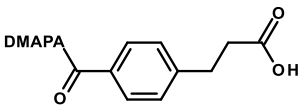
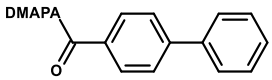
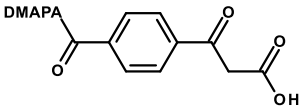
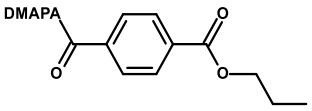
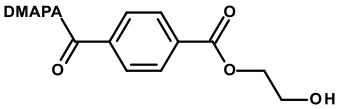
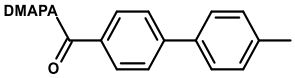
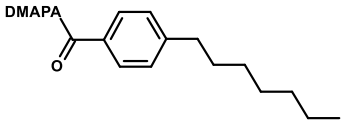
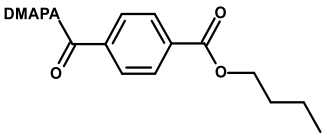
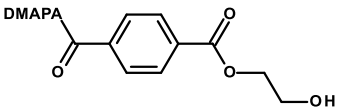
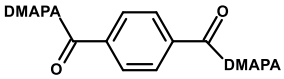
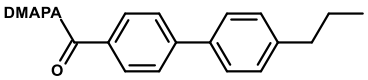
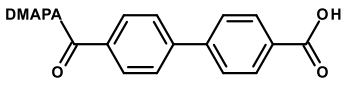


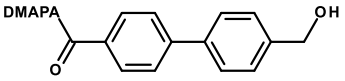
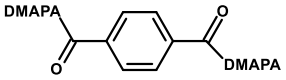
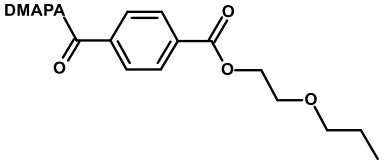
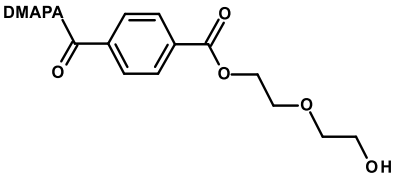
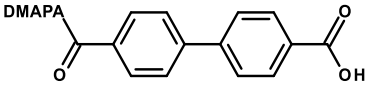
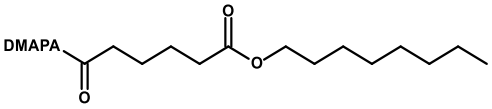
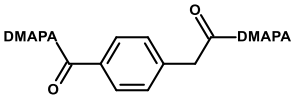
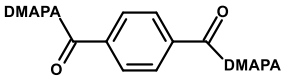
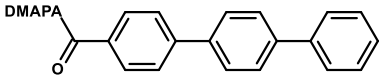
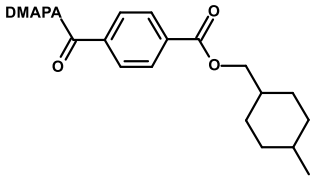
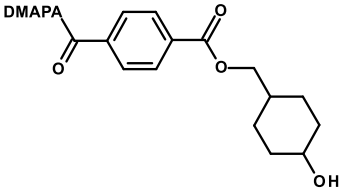
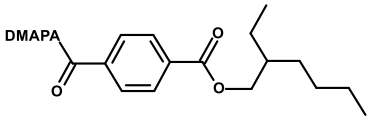
Figure S 2. Isotopic distribution of the main depolymerization peak and enlargement of the simulated monoisotopic peak and its first isotope; PET Water-S GER sample (red: Experimental results and black: Theoretical simulation).

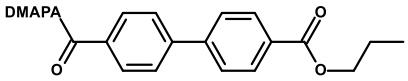
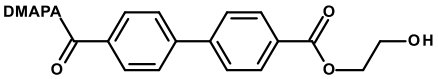
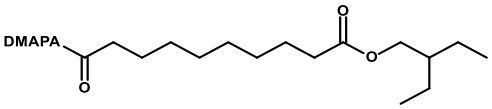
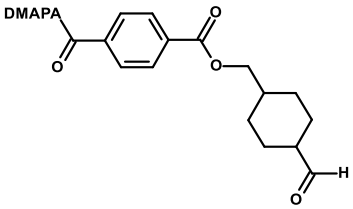
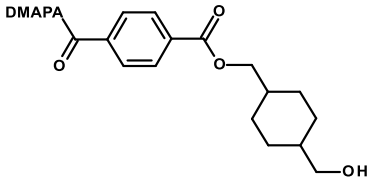
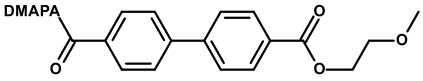
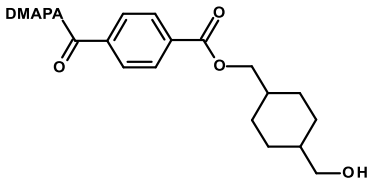
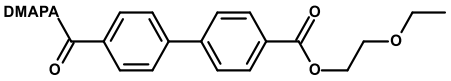
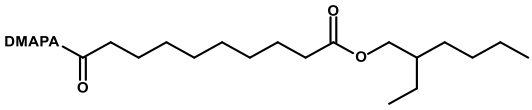
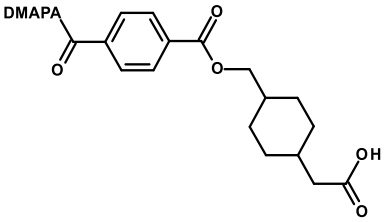
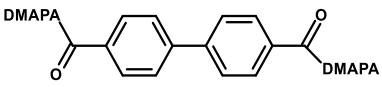
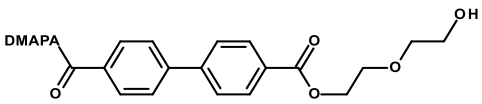
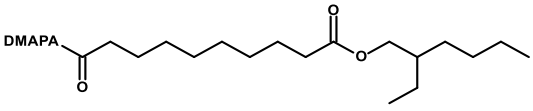
Table S 2. Errors distribution of the main depolymerization marker in the analyzed bottles and containers.

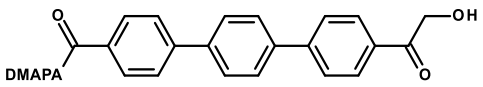
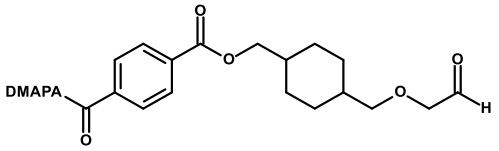
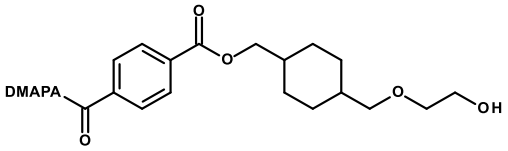
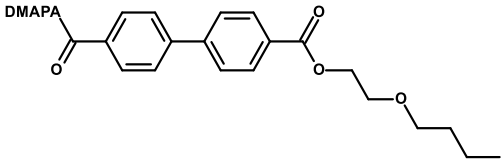
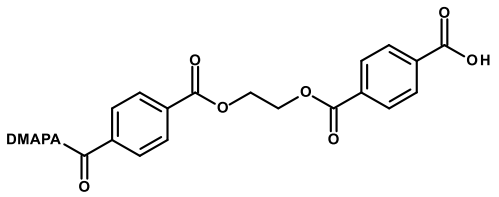
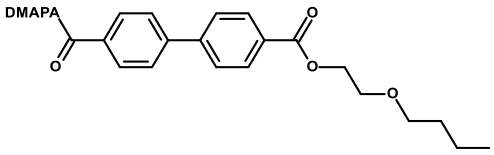
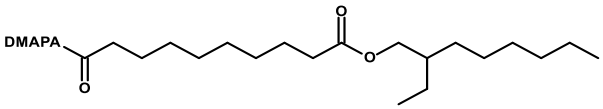
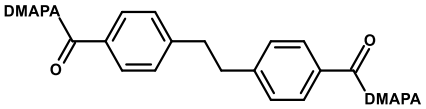
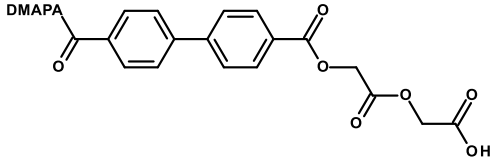
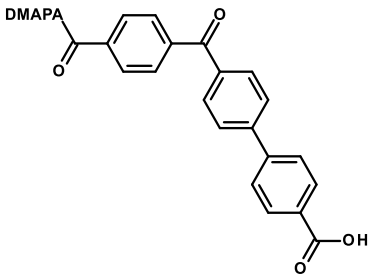
PET packaging object name	Theoretical *m/z*	Experimental *m/z*	Delta *m/z*	*m/z* error (ppm)
Transparent container	335.24415	335.24422	7E-05	0.21
Black container	335.24415	335.24425	1E-4	0.3
Blue container	335.24415	335.24425	1E-4	0.3
Water FRA1	335.24415	335.24418	3E-05	0.09
Water FRA2	335.24415	335.24414	-1E-05	-0.03
Water GER	335.24415	335.24416	1E-05	0.03
Water SP	335.24415	335.24414	-1E-05	-0.03
Water US1	335.24415	335.24414	-1E-05	-0.03
Water US2	335.24415	335.24419	4E-05	0.12
Water-S FRA1	335.24415	335.24412	-3E-05	-0.09
Water-S FRA2	335.24415	335.24412	-3E-05	-0.09
Water-S GER	335.24415	335.24413	-2E-05	-0.06
Water-S CH	335.24415	335.24413	-2E-05	-0.06
Water-S SP	335.24415	335.24419	4E-05	0.12
Cola-1 FRA	335.24415	335.24422	7E-05	0.21
Cola-1 GER	335.24415	335.24415	0.00	0.00
Cola-1 CH	335.24415	335.24417	2E-05	0.06
Cola-1 SP	335.24415	335.24419	4E-05	0.12
Cola-1 US	335.24415	335.24418	3E-05	0.09
Cola-2 FRA	335.24415	335.24424	9E-05	0.27
Cola-2 US	335.24415	335.24419	4E-05	0.12

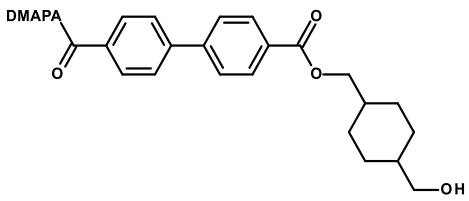
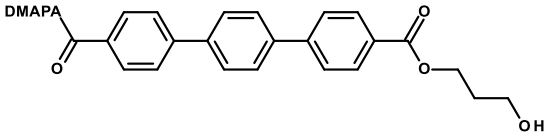
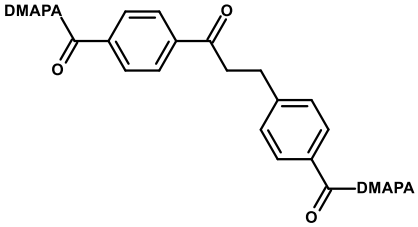
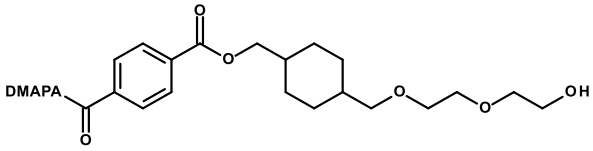
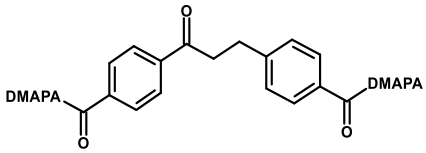
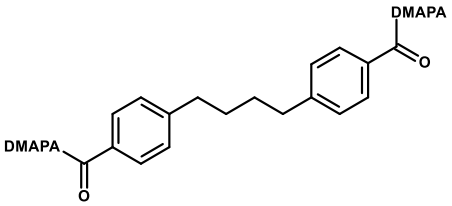
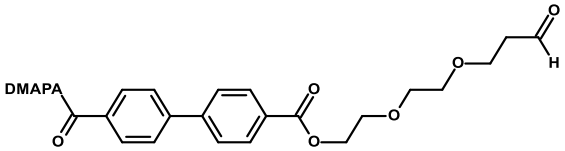
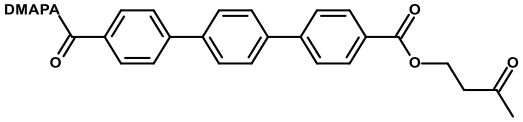
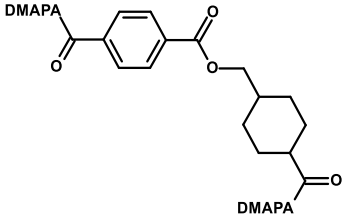
Table S 3. Peaks present in all the depolymerized PET bottles and containers & PETG film with their corresponding chemical formula, theoretical *m/z* and their probable structures.

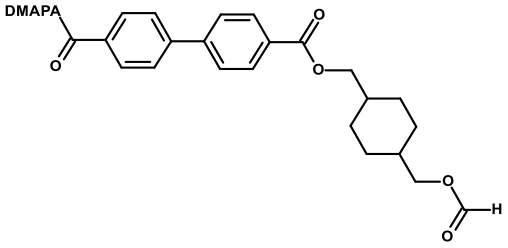
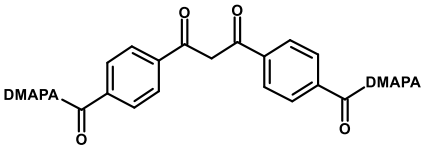
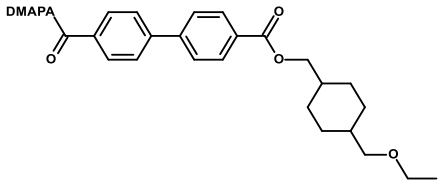
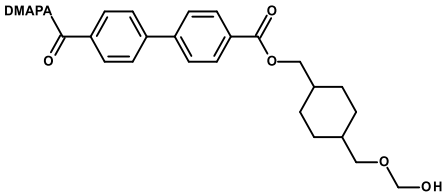
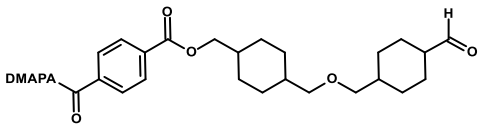
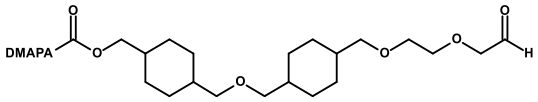
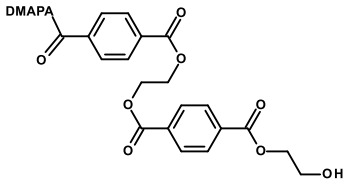
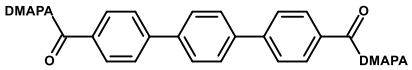
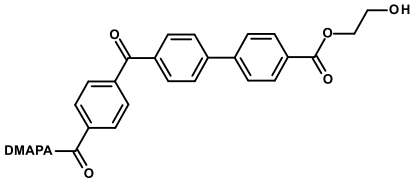
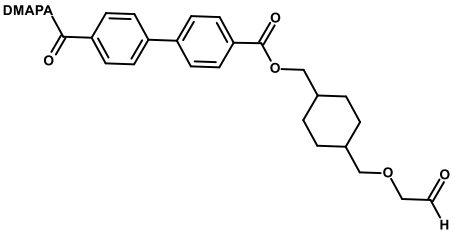
Entry	Theoretical *m/z*	Formula $[M+H]^+$	Structure
1	251.1390	$C_{13}H_{19}N_2O_3$	
2	265.1547	$C_{14}H_{21}N_2O_3$	
3	267.2067	$C_{15}H_{27}N_2O_2$	
4	283.1805	$C_{18}H_{23}N_2O$	
5	293.1496	$C_{15}H_{21}N_2O_4$	
6	293.18597	$C_{16}H_{25}N_2O_3$	
7	295.1652	$C_{15}H_{23}N_2O_4$	
8	297.1961	$C_{19}H_{25}N_2O$	
9	303.2431	$C_{19}H_{31}N_2O$	 Minus H_2
10	305.18597	$C_{17}H_{25}N_2O_3$	 Minus H_2
11	311.1602	$C_{15}H_{23}N_2O_5$	 Plus 1 O
12	321.2285	$C_{17}H_{29}N_4O_2$	 Minus CH_2
13	325.2274	$C_{21}H_{29}N_2O$	
14	327.1703	$C_{19}H_{23}N_2O_3$	

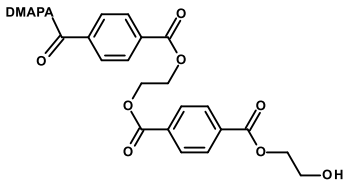
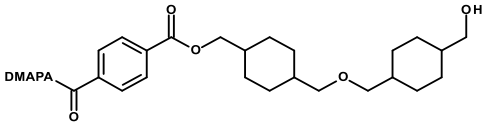
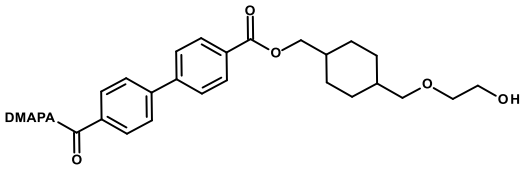
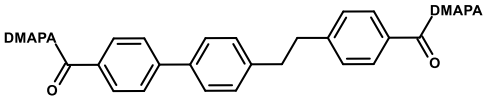
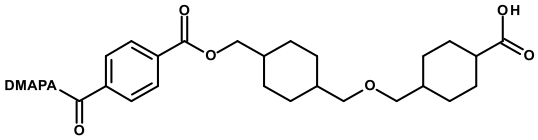
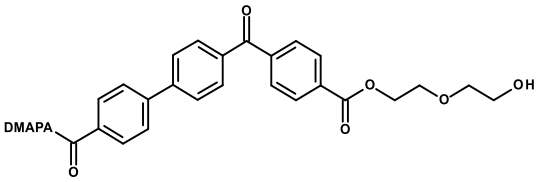
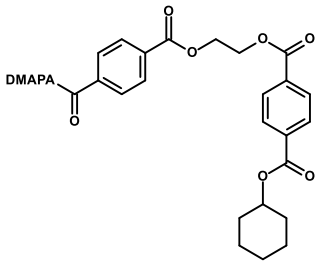
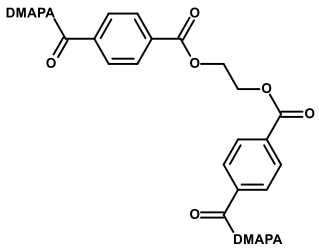
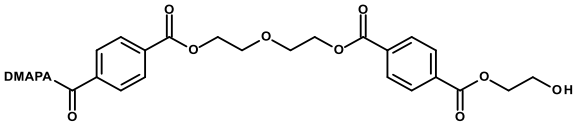
15	329.18597	$C_{19}H_{25}N_2O_3$	 Plus 1 O
16	335.2442	$C_{18}H_{31}N_4O_2$	
17	337.2122	$C_{18}H_{29}N_2O_4$	
18	339.1915	$C_{17}H_{27}N_2O_5$	
19	341.18597	$C_{20}H_{25}N_2O_3$	 Plus CH_2
20	343.2955	$C_{19}H_{39}N_2O_3$	 Dioctyl adipate (DOA) additive
21	347.2442	$C_{19}H_{31}N_4O_2$	-
22	349.2598	$C_{19}H_{33}N_4O_2$	
23	351.2391	$C_{18}H_{31}N_4O_3$	 Plus 1 O
24	359.2118	$C_{24}H_{27}N_2O$	
25	359.2329	$C_{21}H_{31}N_2O_3$	 Minus H_2
26	363.2278	$C_{20}H_{31}N_2O_4$	
27	363.2642	$C_{21}H_{35}N_2O_3$	 Bis(2-ethylhexyl) phthalate Or dioctyl phthalate (DOP)

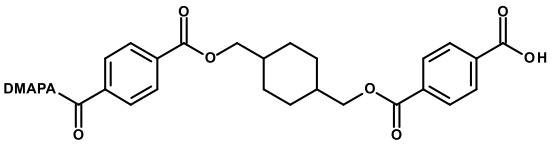
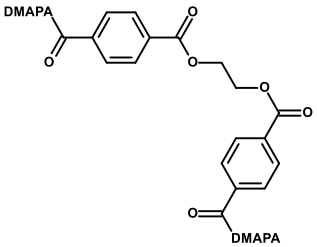
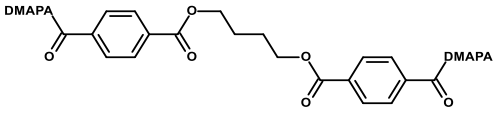
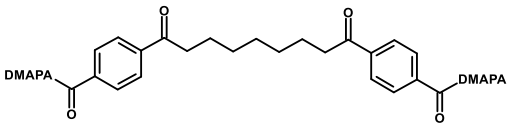
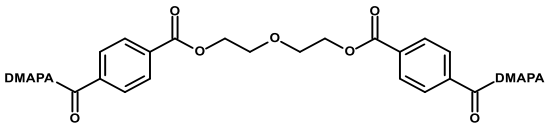
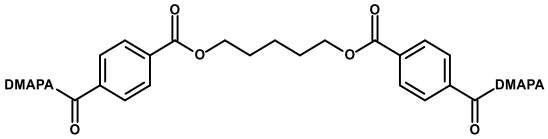
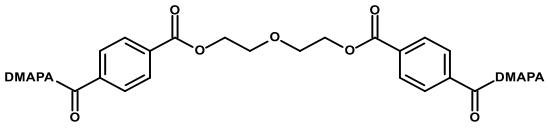
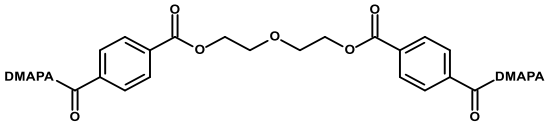
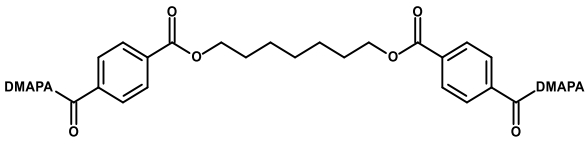
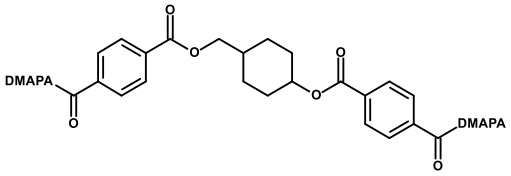
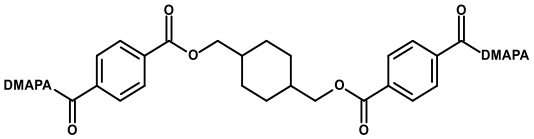
28	369.2173	$C_{22}H_{29}N_2O_3$	
29	371.1965	$C_{21}H_{27}N_2O_4$	
30	371.3268	$C_{21}H_{43}N_2O_3$	 Dioctyl suberate additive
31	375.2278	$C_{21}H_{31}N_2O_4$	
32	377.2435	$C_{21}H_{33}N_2O_4$	
33	385.2122	$C_{22}H_{29}N_2O_4$	
34	393.2384	$C_{21}H_{33}N_2O_5$	 Plus 1 O
35	399.2278	$C_{23}H_{31}N_2O_4$	
36	399.3581	$C_{23}H_{47}N_2O_3$	 Bis(2-ethylhexyl)/Dioctyl sebacate additive
37	405.2384	$C_{22}H_{33}N_2O_5$	
38	411.2755	$C_{24}H_{35}N_4O_2$	
39	415.2228	$C_{23}H_{31}N_2O_5$	
40	415.3530	$C_{23}H_{47}N_2O_4$	 Plus 1 O

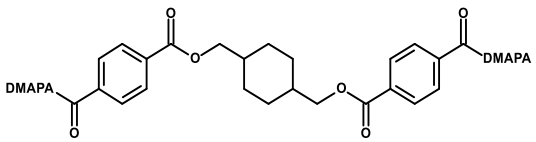
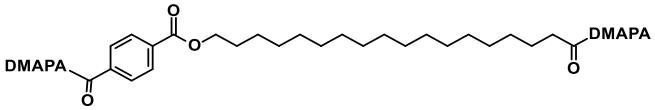
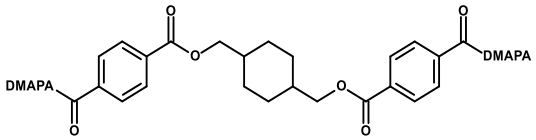
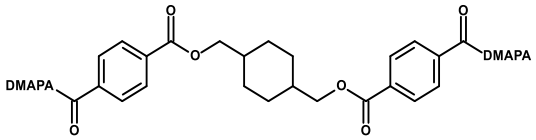
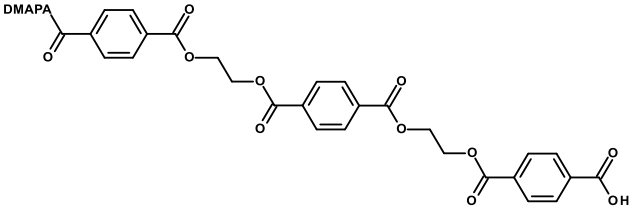
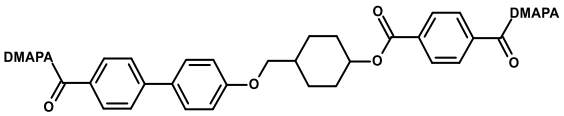
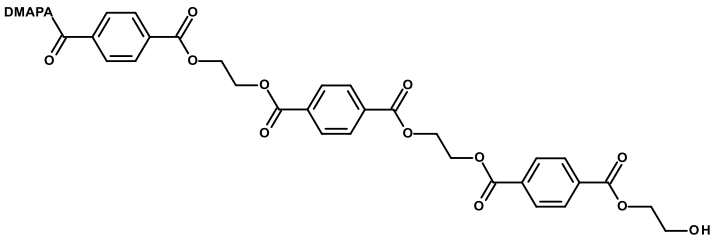
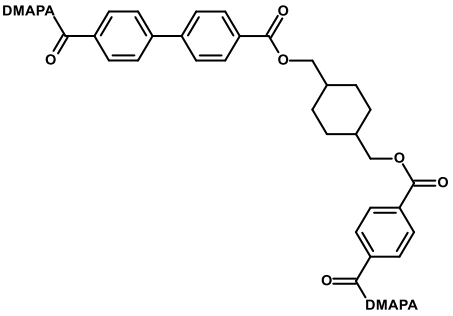
41	417.2173	$C_{26}H_{29}N_2O_3$	
42	419.2540	$C_{23}H_{35}N_2O_5$	
43	421.2697	$C_{23}H_{37}N_2O_5$	
44	423.2755	$C_{25}H_{35}N_4O_2$	-
45	425.2435	$C_{25}H_{33}N_2O_4$	 Minus H_2
46	427.1864	$C_{23}H_{27}N_2O_6$	
47	427.2591	$C_{25}H_{35}N_2O_4$	
48	427.3894	$C_{25}H_{51}N_2O_3$	 Dioctyl dodecanoate additive
49	439.3068	$C_{26}H_{39}N_4O_2$	
50	443.1814	$C_{23}H_{27}N_2O_7$	
51	447.1915	$C_{26}H_{27}N_2O_5$	 Plus 1 O

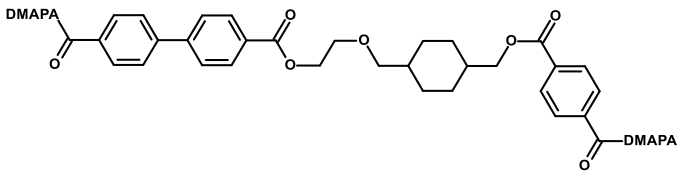
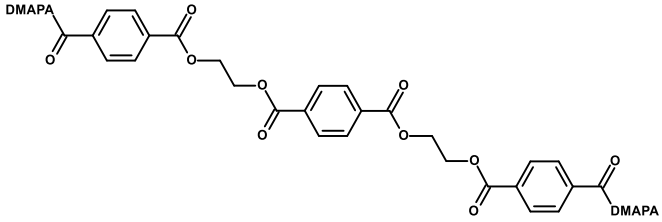
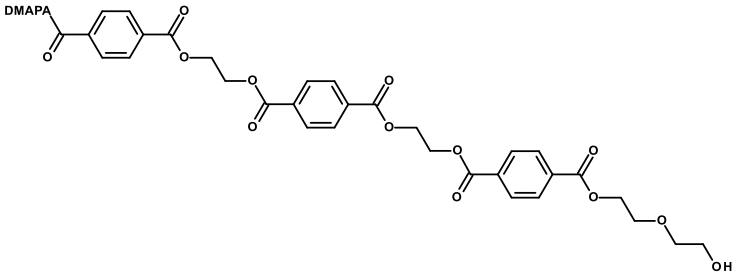
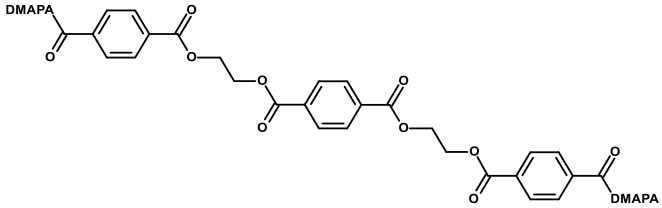
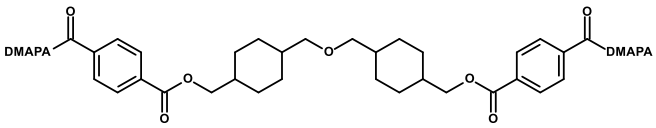
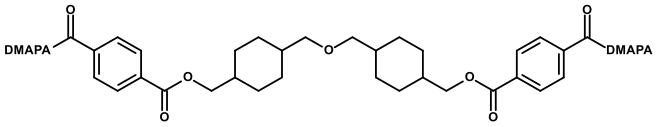
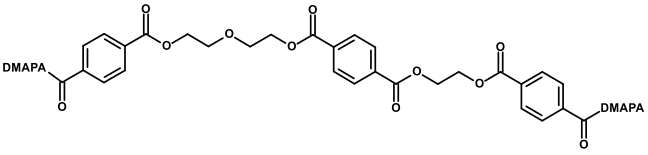
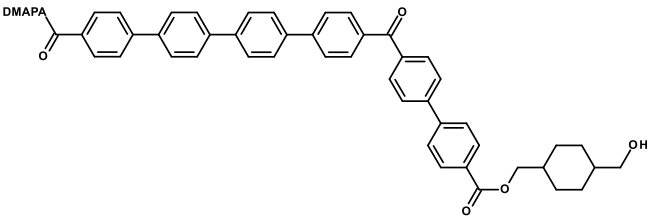
52	453.2748	$C_{27}H_{37}N_2O_4$	
53	455.3381	$C_{27}H_{43}N_4O_2$	-
54	461.2435	$C_{28}H_{33}N_2O_4$	
55	465.2860	$C_{27}H_{37}N_4O_3$	 Minus H_2
56	465.2959	$C_{25}H_{41}N_2O_6$	
57	467.3017	$C_{27}H_{39}N_4O_3$	
58	467.3381	$C_{28}H_{43}N_4O_2$	
59	471.24896	$C_{26}H_{35}N_2O_6$	
60	473.2435	$C_{29}H_{33}N_2O_4$	
61	475.3279	$C_{26}H_{43}N_4O_4$	
62	477.2860	$C_{28}H_{37}N_4O_3$	-

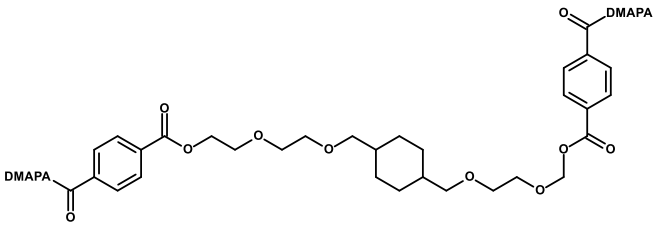
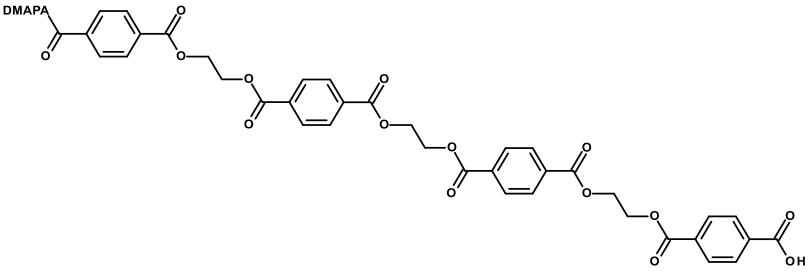
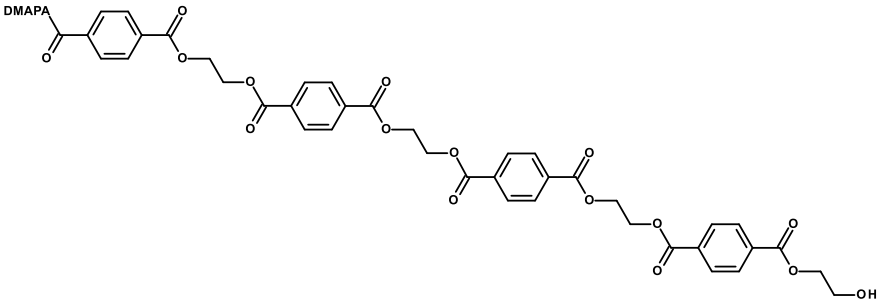
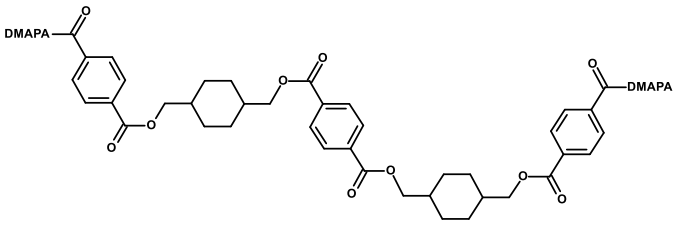
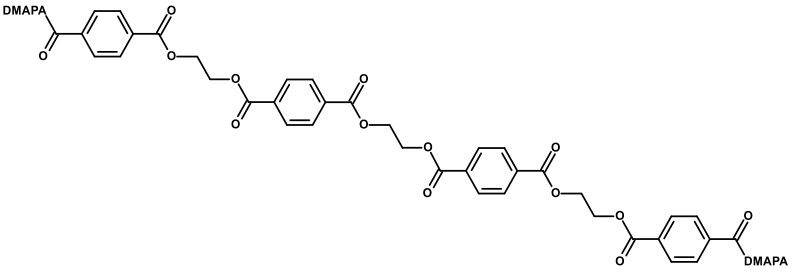
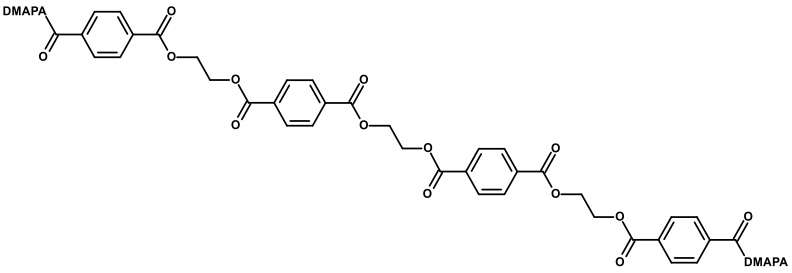
63	481.2697	$C_{28}H_{37}N_2O_5$	
64	481.2809	$C_{27}H_{37}N_4O_4$	
65	481.3061	$C_{29}H_{41}N_2O_4$	
66	483.2854	$C_{28}H_{39}N_2O_5$	
67	485.2911	$C_{30}H_{37}N_4O_2$	-
68	485.3374	$C_{29}H_{45}N_2O_4$	
69	485.3585	$C_{26}H_{49}N_2O_6$	
70	487.2075	$C_{25}H_{31}N_2O_8$	
71	487.3068	$C_{30}H_{39}N_4O_2$	
72	491.2177	$C_{28}H_{31}N_2O_6$	 Plus 1 O
73	495.2854	$C_{29}H_{39}N_2O_5$	

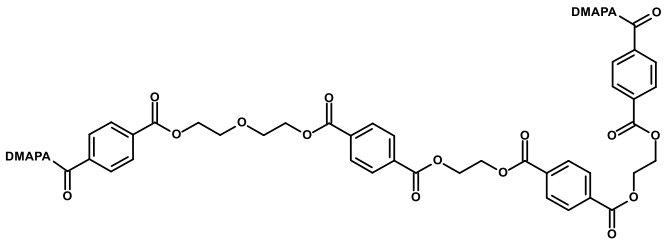
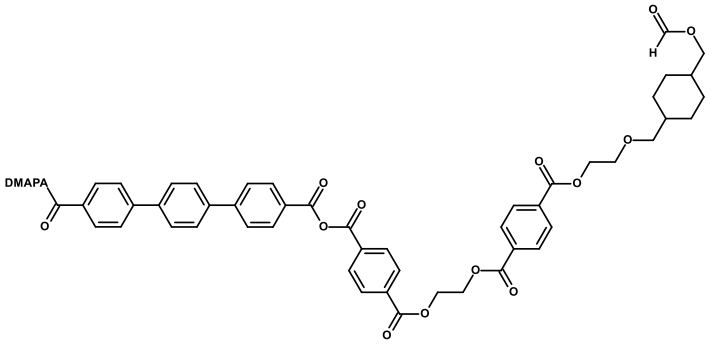
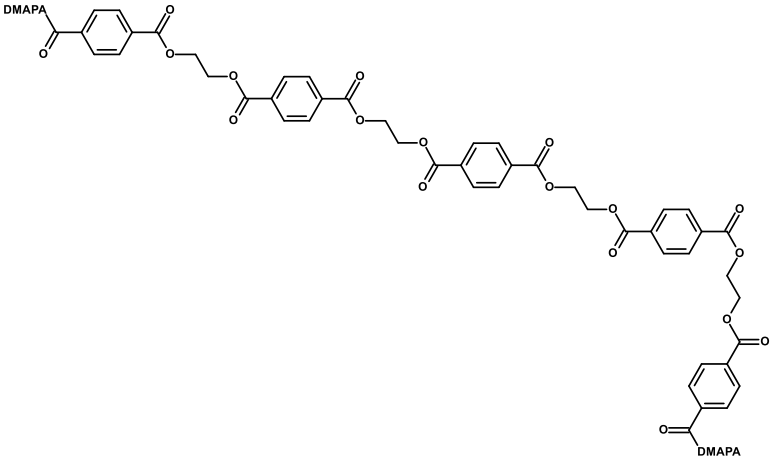
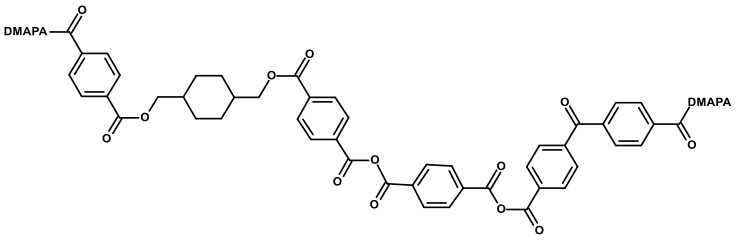
74	499.3068	$C_{31}H_{39}N_4O_2$	-
75	503.2024	$C_{25}H_{31}N_2O_9$	 Plus 1 O
76	503.34795	$C_{29}H_{47}N_2O_5$	
77	513.2860	$C_{31}H_{37}N_4O_3$	-
78	513.2959	$C_{29}H_{41}N_2O_6$	 Plus 1 O
79	513.3224	$C_{32}H_{41}N_4O_2$	 Minus H_2
80	517.3272	$C_{29}H_{45}N_2O_6$	
81	519.24896	$C_{30}H_{35}N_2O_6$	
82	525.2595	$C_{29}H_{37}N_2O_7$	
83	527.2864	$C_{28}H_{39}N_4O_6$	
84	531.2337	$C_{27}H_{35}N_2O_9$	
85	537.2595	$C_{30}H_{37}N_2O_7$	-

86	539.2752	$C_{30}H_{39}N_2O_7$	 Plus CH_2
87	543.2813	$C_{28}H_{39}N_4O_7$	 Plus 1 O
88	555.3177	$C_{30}H_{43}N_4O_6$	
89	565.3748	$C_{33}H_{49}N_4O_4$	
90	569.29697	$C_{30}H_{41}N_4O_7$	 Minus H_2
91	569.3334	$C_{31}H_{45}N_4O_6$	
92	571.3126	$C_{30}H_{43}N_4O_7$	
93	587.3075	$C_{30}H_{43}N_4O_8$	 Plus 1 O
94	593.3334	$C_{33}H_{45}N_4O_6$	 Minus H_4
95	595.3490	$C_{33}H_{47}N_4O_6$	
96	607.3490	$C_{34}H_{47}N_4O_6$	 Minus H_2

97	609.3647	$C_{34}H_{49}N_4O_6$	
98	617.5000	$C_{36}H_{65}N_4O_4$	
99	623.3442	$C_{34}H_{47}N_4O_7$	 Minus H_2 plus 1 O
100	625.3596	$C_{34}H_{49}N_4O_7$	 Plus 1 O
101	633.3534	$C_{37}H_{49}N_2O_7$	-
102	635.2235	$C_{33}H_{35}N_2O_{11}$	
103	643.3857	$C_{38}H_{51}N_4O_5$	
104	649.3483	$C_{37}H_{49}N_2O_8$	-
105	651.36399	$C_{37}H_{51}N_2O_8$	-
106	679.2498	$C_{35}H_{39}N_2O_{12}$	
107	685.39596	$C_{40}H_{53}N_4O_6$	
108	695.3902	$C_{39}H_{55}N_2O_9$	-
109	701.4102	$C_{49}H_{53}N_2O_2$	-
110	713.3299	$C_{25}H_{53}N_4O_{19}$	-

111	713.4273	$C_{42}H_{57}N_4O_6$	
112	719.3287	$C_{38}H_{47}N_4O_{10}$	
113	723.27596	$C_{37}H_{43}N_2O_{13}$	
114	735.3236	$C_{38}H_{47}N_4O_{11}$	 Plus 1 O
115	735.4691	$C_{42}H_{63}N_4O_7$	
116	749.4484	$C_{42}H_{61}N_4O_8$	 Minus H_2
117	753.4051	$C_{52}H_{53}N_2O_3$	-
118	755.4207	$C_{52}H_{55}N_2O_3$	-
119	763.3549	$C_{40}H_{51}N_4O_{11}$	
120	799.4106	$C_{53}H_{55}N_2O_5$	

121	799.4124	$C_{41}H_{59}N_4O_{12}$	 Plus 2 O
122	827.2658	$C_{43}H_{43}N_2O_{15}$	
123	843.4063	$C_{47}H_{59}N_2O_{12}$	-
124	871.2920	$C_{45}H_{47}N_2O_{16}$	
125	883.4852	$C_{50}H_{67}N_4O_{10}$	
126	885.4949	$C_{57}H_{65}N_4O_5$	-
127	909.3553	$C_{48}H_{53}N_4O_{14}$	 Minus H_2
128	911.3709	$C_{48}H_{55}N_4O_{14}$	
129	915.3182	$C_{47}H_{51}N_2O_{17}$	-

130	955.3971	$C_{50}H_{59}N_4O_{15}$	
131	955.4012	$C_{55}H_{59}N_2O_{13}$	
132	987.4579	$C_{64}H_{63}N_2O_8$	-
133	989.4601	$C_{48}H_{69}N_4O_{18}$	-
134	1103.4132	$C_{58}H_{63}N_4O_{18}$	
135	1025.3968	$C_{60}H_{57}N_4O_{12}$	-
136	1057.4077	$C_{57}H_{61}N_4O_{16}$	 Plus 3 O

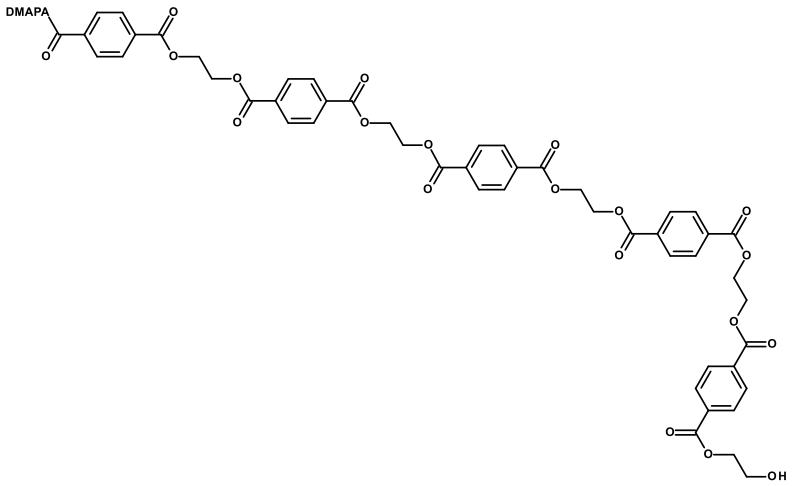
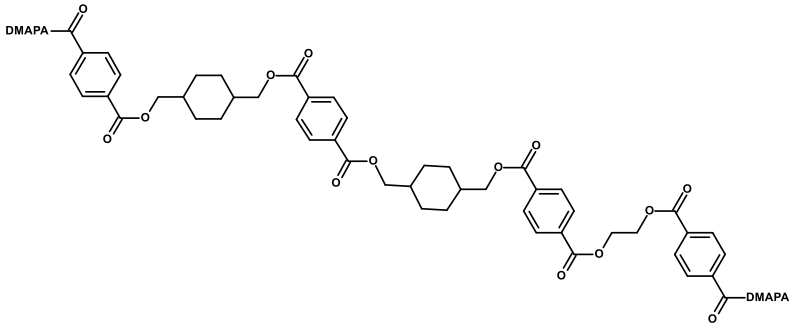
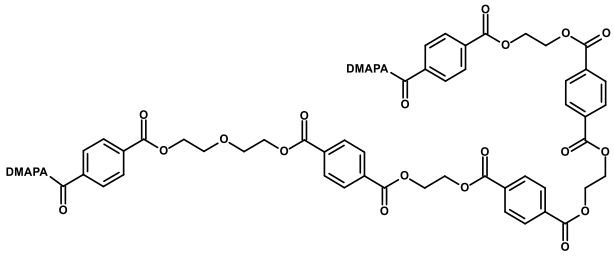
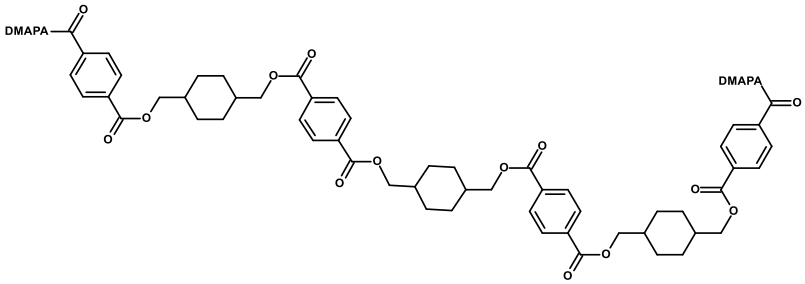
137	1063.3343	$C_{55}H_{55}N_2O_{20}$	
138	1075.5274	$C_{60}H_{75}N_4O_{14}$	
139	1147.4394	$C_{60}H_{67}N_4O_{19}$	
140	1157.6057	$C_{66}H_{85}N_4O_{14}$	

Table S 4. MALDI FTICR MS relative intensities of the major composition's peaks in the analyzed still water bottles.

Theoretical *m/z*	Water FRA1	Water FRA2	Water GER	Water SP	Water US1	Water US2
251.1390	1.31E+07	1.58E+06	4.99E+06	4.79E+07	3.13E+07	1.67E+07
295.1652	2.86E+08	1.53E+08	7.15E+07	1.08E+07	1.58E+08	3.12E+08
311.1602	3.43E+06	1.02E+06	1.16E+06	0.00E+00	1.09E+07	2.34E+07
335.2442	2.45E+09	9.42E+08	1.35E+09	8.56E+08	2.07E+09	1.55E+09
351.2391	1.72E+07	2.03E+06	2.34E+07	6.15E+06	1.37E+08	1.37E+08
377.2435	0.00E+00	1.42E+06	4.17E+06	2.19E+07	0.00E+00	0.00E+00
411.2755	2.09E+07	3.28E+06	8.40E+06	2.66E+06	7.05E+06	3.25E+07
487.2075	2.58E+07	2.74E+08	3.82E+08	1.65E+08	1.53E+07	3.78E+08
527.2864	1.50E+08	2.15E+08	3.60E+08	5.49E+06	4.10E+07	1.03E+09
531.2337	0.00E+00	1.31E+07	1.42E+07	9.04E+06	1.85E+06	3.31E+07
543.2813	2.60E+06	9.14E+05	5.05E+06	6.97E+07	2.32E+06	5.13E+07
571.3126	1.22E+07	1.94E+07	4.17E+07	1.23E+06	1.17E+07	1.47E+08
587.3075	0.00E+00	0.00E+00	1.07E+06	0.00E+00	1.06E+06	8.80E+06
609.3647	0.00E+00	1.17E+07	1.57E+07	2.76E+06	0.00E+00	1.71E+06
635.2235	3.84E+06	3.41E+07	3.68E+07	0.00E+00	8.81E+05	1.32E+06
679.2498	2.19E+07	4.95E+08	4.63E+08	4.34E+07	1.53E+07	4.84E+07
719.3287	1.74E+07	4.14E+08	3.36E+08	1.36E+07	4.67E+06	9.70E+07
763.3549	0.00E+00	1.02E+07	1.46E+07	2.07E+06	0.00E+00	1.20E+07
871.2920	2.14E+07	3.39E+07	6.83E+07	1.60E+06	7.81E+06	1.10E+07
911.3709	1.82E+07	1.29E+08	5.63E+07	0.00E+00	9.48E+06	6.65E+06
955.3971	0.00E+00	1.07E+07	3.17E+06	1.20E+06	0.00E+00	0.00E+00
1063.3343	2.07E+06	1.62E+06	4.10E+06	0.00E+00	9.09E+05	1.61E+06
1103.4132	3.70E+06	6.86E+06	9.00E+06	0.00E+00	3.71E+06	4.45E+06
1147.4394	0.00E+00	5.82E+06	1.69E+06	0.00E+00	8.77E+05	0.00E+00

Table S 5. MALDI FTICR MS relative intensities of the major composition's peaks in the analyzed sparkling water bottles.

Theoretical *m/z*	Water-S FRA1	Water-S FRA2	Water-S GER	Water-S CH	Water-S SP
251.1390	2.31E+06	9.05E+05	1.12E+06	1.77E+07	1.09E+08
295.1652	9.32E+07	3.61E+07	7.51E+07	7.72E+07	7.76E+08
311.1602	0.00E+00	0.00E+00	7.64E+08	2.09E+06	5.22E+07
335.2442	1.30E+09	4.54E+08	2.96E+06	9.58E+08	3.23E+09
351.2391	3.65E+06	2.57E+06	6.47E+06	2.26E+07	6.87E+07
377.2435	1.13E+06	7.59E+06	1.32E+06	1.31E+06	0.00E+00
411.2755	1.21E+07	1.68E+06	2.25E+06	1.63E+06	5.72E+07
487.2075	4.56E+08	5.54E+07	2.97E+07	1.51E+08	9.34E+08
527.2864	2.89E+08	4.80E+07	3.62E+07	1.25E+08	2.04E+09
531.2337	2.17E+07	2.06E+06	1.55E+06	6.07E+06	8.34E+07
543.2813	1.63E+06	1.07E+06	9.85E+05	2.43E+06	9.44E+07
571.3126	3.20E+07	4.39E+06	4.53E+06	1.26E+07	2.43E+08
587.3075	0.00E+00	0.00E+00	0.00E+00	7.49E+05	9.61E+06
609.3647	5.98E+06	0.00E+00	5.79E+06	3.82E+06	0.00E+00
635.2235	7.22E+07	7.93E+06	3.01E+06	6.13E+06	6.81E+06
679.2498	1.15E+09	1.15E+08	5.00E+07	9.13E+07	3.47E+08
719.3287	9.07E+08	1.09E+08	4.54E+07	7.80E+07	5.24E+08
763.3549	1.88E+07	1.75E+06	9.41E+05	3.38E+06	3.80E+07
871.2920	1.25E+08	1.82E+07	9.87E+06	1.63E+07	1.36E+08
911.3709	5.08E+08	5.31E+07	1.69E+07	1.16E+07	1.74E+08
955.3971	1.94E+07	1.82E+06	1.02E+06	0.00E+00	1.37E+07
1063.3343	5.41E+06	0.00E+00	0.00E+00	1.50E+06	7.28E+06
1103.4132	2.70E+07	5.61E+06	0.00E+00	2.71E+06	6.15E+07
1147.4394	2.54E+07	1.21E+06	0.00E+00	9.66E+05	1.57E+07

Table S 6. MALDI FTICR MS relative intensities of the major composition's peaks in the analyzed Cola soft drinks bottles.

Theoretical *m/z*	Cola-1 FRA	Cola-2 FRA	Cola-1 GER	Cola-1 CH	Cola-1 SP	Cola-1 US	Cola-2 US
251.1390	1.96E+06	1.20E+06	4.29E+06	2.47E+07	1.67E+07	1.54E+06	2.00E+06
295.1652	1.23E+08	6.57E+07	1.82E+08	3.95E+08	3.00E+08	7.80E+07	9.48E+07
311.1602	0.00E+00	0.00E+00	1.27E+09	7.53E+06	3.28E+06	1.07E+06	1.86E+06
335.2442	1.42E+09	7.42E+08	4.63E+06	3.25E+09	1.02E+10	1.21E+09	1.62E+09
351.2391	6.72E+07	1.01E+06	1.44E+07	1.43E+07	3.34E+07	3.03E+06	4.35E+06
377.2435	1.26E+07	2.10E+06	2.16E+06	4.09E+06	8.21E+07	2.94E+06	1.74E+07
411.2755	1.76E+07	5.32E+06	5.72E+06	2.31E+07	3.43E+08	3.44E+06	0.00E+00
487.2075	7.75E+06	2.36E+08	1.22E+08	1.62E+09	6.85E+08	2.14E+08	4.81E+08
527.2864	4.66E+08	2.01E+08	1.57E+08	1.47E+09	1.87E+09	1.62E+08	3.14E+08
531.2337	2.48E+07	1.17E+07	7.87E+06	5.91E+07	4.24E+07	1.09E+07	1.70E+07
543.2813	1.35E+06	8.61E+05	3.42E+06	1.67E+07	1.18E+07	1.68E+06	3.76E+06
571.3126	4.60E+07	1.59E+07	2.17E+07	1.18E+08	9.99E+07	1.45E+07	2.35E+07
587.3075	0.00E+00	7.28E+05	7.40E+05	1.89E+06	0.00E+00	0.00E+00	0.00E+00
609.3647	5.85E+07	1.70E+07	1.58E+07	1.89E+07	3.65E+07	1.48E+07	1.24E+08
635.2235	3.25E+07	3.99E+07	1.05E+07	1.23E+08	3.55E+06	1.18E+07	2.89E+07
679.2498	6.37E+08	6.33E+08	2.06E+08	2.10E+09	3.37E+08	3.58E+08	9.89E+08
719.3287	4.29E+08	5.44E+08	1.87E+08	2.70E+09	5.89E+08	2.89E+08	8.36E+08
763.3549	1.13E+07	8.24E+06	6.07E+06	4.83E+07	1.64E+07	8.65E+06	1.79E+07
871.2920	6.09E+07	3.81E+07	5.00E+07	2.25E+08	1.08E+08	3.82E+07	4.76E+07
911.3709	7.78E+07	1.33E+08	6.40E+07	4.67E+08	2.76E+08	7.17E+07	1.81E+08
955.3971	9.80E+06	1.10E+07	2.69E+06	2.45E+07	6.78E+06	6.79E+06	1.24E+07
1063.3343	3.08E+06	1.59E+06	2.56E+06	8.64E+06	8.97E+06	2.22E+06	2.44E+06
1103.4132	7.75E+06	5.72E+06	8.40E+06	5.43E+07	8.53E+07	3.77E+06	6.65E+06
1147.4394	3.71E+06	5.23E+06	2.23E+06	1.08E+07	7.31E+06	3.24E+06	6.41E+06

Table S 7. Compounds found in the depolymerized PETG films with their corresponding *m/z*, chemical formula and relative intensities in MALDI FTICR MS spectrum. The entry of each identified compound in Table S3 will be mentioned here.

Theoretical *m/z*	Formula $[M+H]^+$	Entry Table S3	Relative intensity
251.1390	$C_{13}H_{19}N_2O_3$	1	3.11E+06
295.1652	$C_{15}H_{23}N_2O_4$	7	2.21E+06
335.2442	$C_{18}H_{31}N_4O_2$	16	9.31E+08
337.2122	$C_{18}H_{29}N_2O_4$	17	4.35E+07
359.2329	$C_{21}H_{31}N_2O_3$	25	3.01E+07
375.2278	$C_{21}H_{31}N_2O_4$	31	6.54E+07
377.2435	$C_{21}H_{33}N_2O_4$	32	1.24E+09
393.2384	$C_{21}H_{33}N_2O_5$	34	3.69E+06
405.2384	$C_{22}H_{33}N_2O_5$	37	3.20E+07
411.2755	$C_{24}H_{35}N_4O_2$	38	1.16E+06
419.2540	$C_{23}H_{35}N_2O_5$	42	1.96E+06
421.2697	$C_{23}H_{37}N_2O_5$	43	2.42E+07
453.2748	$C27H_{37}N_2O_4$	52	1.26E+06
465.2959	$C_{25}H_{41}N_2O_6$	56	1.56E+06
475.3279	$C_{26}H_{43}N_4O_4$	61	2.21E+06
481.2697	$C_{28}H_{37}N_2O_5$	63	5.14E+06
485.3374	$C_{29}H_{45}N_2O_4$	68	1.36E+06
487.2075	$C_{25}H_{31}N_2O_8$	70	1.18E+06
495.2854	$C_{29}H_{39}N_2O_5$	73	3.14E+06
503.34795	$C_{29}H_{47}N_2O_5$	76	4.79E+06
517.3272	$C_{29}H_{45}N_2O_6$	80	5.04E+06
519.24896	$C_{30}H_{35}N_2O_6$	81	2.52E+06
525.2595	$C_{29}H_{37}N_2O_7$	82	7.26E+07
565.3748	$C_{33}H_{49}N_4O_4$	89	7.08E+06
569.3334	$C_{31}H_{45}N_4O_6$	91	2.20E+07
593.3334	$C_{33}H_{45}N_4O_6$	94	3.51E+06
609.3647	$C_{34}H_{49}N_4O_6$	97	7.21E+09
623.3442	$C_{34}H_{47}N_4O_7$	99	3.57E+06
625.3596	$C_{34}H_{49}N_4O_7$	100	1.70E+07
633.3534	$C_{37}H_{49}N_2O_7$	101	2.51E+06
643.3857	$C_{38}H_{51}N_4O_5$	103	1.95E+06
649.3483	$C_{37}H_{49}N_2O_8$	104	8.35E+06

651.36399	$C_{37}H_{51}N_2O_8$	105	1.85E+08
679.2498	$C_{35}H_{39}N_2O_{12}$	106	3.25E+06
685.39596	$C_{40}H_{53}N_4O_6$	107	5.22E+06
695.3904	$C_{39}H_{55}N_2O_9$	108	3.50E+06
701.4102	$C_{49}H_{53}N_2O_2$	109	3.55E+06
713.4273	$C_{42}H_{57}N_4O_6$	110	1.61E+06
719.3287	$C_{38}H_{47}N_4O_{10}$	112	2.73E+06
723.27596	$C_{37}H_{43}N_2O_{13}$	113	1.02E+06
735.4691	$C_{42}H_{63}N_4O_7$	115	1.81E+07
749.4484	$C_{42}H_{61}N_4O_8$	116	8.14E+06
753.4051	$C_{52}H_{53}N_2O_3$	117	1.51E+06
755.4207	$C_{52}H_{55}N_2O_3$	118	3.09E+06
799.4124	$C_{41}H_{59}N_4O_{12}$	121	2.06E+06
843.4063	$C_{47}H_{59}N_2O_{12}$	123	4.14E+06
871.2920	$C_{45}H_{47}N_2O_{16}$	124	2.04E+06
883.4852	$C_{50}H_{67}N_4O_{10}$	125	2.04E+06
911.3709	$C_{48}H_{55}N_4O_{14}$	128	3.22E+06
1025.3968	$C_{60}H_{57}N_4O_{12}$	135	6.17E+06
1057.4077	$C_{57}H_{61}N_4O_{16}$	136	1.51E+06
1075.5274	$C_{60}H_{75}N_4O_{14}$	138	1.40E+06
1157.6057	$C_{66}H_{85}N_4O_{14}$	140	7.75E+06

Table S 8. Comparison of MALDI FTICR MS and LC-MS dynamics for the major composition of Cola-1 FRA bottle (*m/z* 200-1,000), at 1 mg/mL. The percentages given here for each peak are calculated in comparison to the sum of intensities of the major composition (*m/z* 200-1,000) represented by the 23 compounds mentioned here. The letters put next to the retention time in increasing order are indicated on Figure 4 of the paper.

Theoretical *m/z*	**LC-MS data**				**FTICR MS data**		
	RT (min)	**Intensity**	**Percentage % major composition**	**Error (ppm)**	**Intensity**	**Percentage % major composition**	**Error (ppm)**
251.1390	0.68 (a)	1.02E+05	0.78%	0.00	1.96E+06	0.06%	0.40
251.1390	0.9	9.11E+04	0.70%	0.00			
295.1652	3.74 (c)	1.13E+06	8.67%	3.39	1.23E+08	3.51%	0.34
311.1602	5.64 (d)	3.82E+03	0.03%	3.21	0.00E+00	0.00%	0.00
335.2442	0.68 (a)	4.13E+06	31.69%	2.98	1.42E+09	40.53%	0.00
335.2442	0.92 (b)	3.24E+06	24.86%	2.98			
351.2391	0.92 (b)	1.76E+04	0.14%	0.00	6.72E+07	1.92%	0.28
377.2435	18.16 (h)	4.99E+05	3.83%	2.65	1.26E+07	0.36%	0.53
411.2755	7.5 (e)	4.11E+03	0.03%	2.43	1.76E+07	0.50%	0.24
487.2075	19.47 (j)	1.26E+06	9.67%	2.05	7.75E+06	0.22%	0.41
527.2864	13.58 (f)	5.59E+04	0.43%	0.00	4.66E+08	13.30%	0.38
531.2337	19.12 (i)	2.05E+05	1.57%	1.88	2.48E+07	0.71%	0.56
543.2813	40.31 (r)	4.28E+02	0.00%	0.00	1.35E+06	0.04%	0.55
571.3126	13.65 (g)	4.17E+04	0.32%	-1.75	4.60E+07	1.31%	0.53
587.3075	0.00	0.00E+00	0.00%	0.00	0.00E+00	0.00%	0.00
609.3647	21.21 (m)	1.58E+04	0.12%	-1.64	5.85E+07	1.67%	0.33
635.2235	26.54	8.66E+04	0.66%	-1.57	3.25E+07	0.93%	0.47
679.2498	26.81 (p)	8.94E+04	0.69%	-1.47	6.37E+08	18.16%	0.15
719.3287	20.79 (l)	2.26E+04	0.17%	-1.39	4.29E+08	12.24%	0.28
763.3549	20.25 (k)	1.08E+03	0.01%	-2.62	1.13E+07	0.32%	0.26
871.2920	32.23 (q)	2.02E+06	15.50%	1.15	6.09E+07	1.74%	0.57
911.3709	26.16 (o)	1.69E+04	0.13%	0.00	7.78E+07	2.22%	0.55
955.3971	25.81 (n)	1.21E+03	0.01%	1.05	9.80E+06	0.28%	0.42

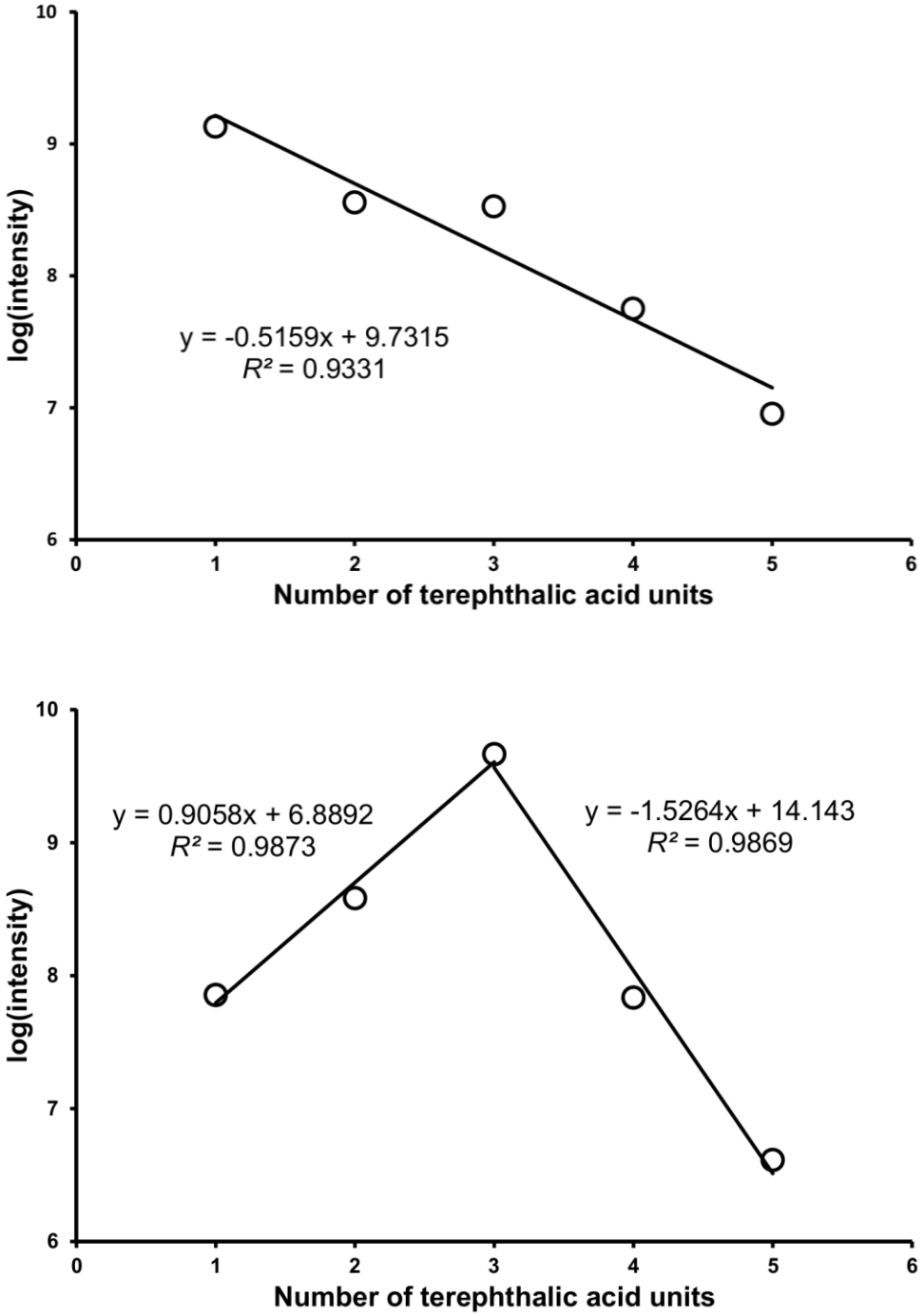


Figure S 3. MALDI FTICR MS both families' oligomers correlation of the German still water bottle, Water GER. First series oligomers: Di-derivatized having the structure nT + (n-1)E + 2D; second series oligomers: Mono-derivatized having the structure nT + nE + D. T: Terephthalic part(s), E: Ethylene glycol unit(s), D: DMAPA molecule(s), n: Integer number from 1 to 5.

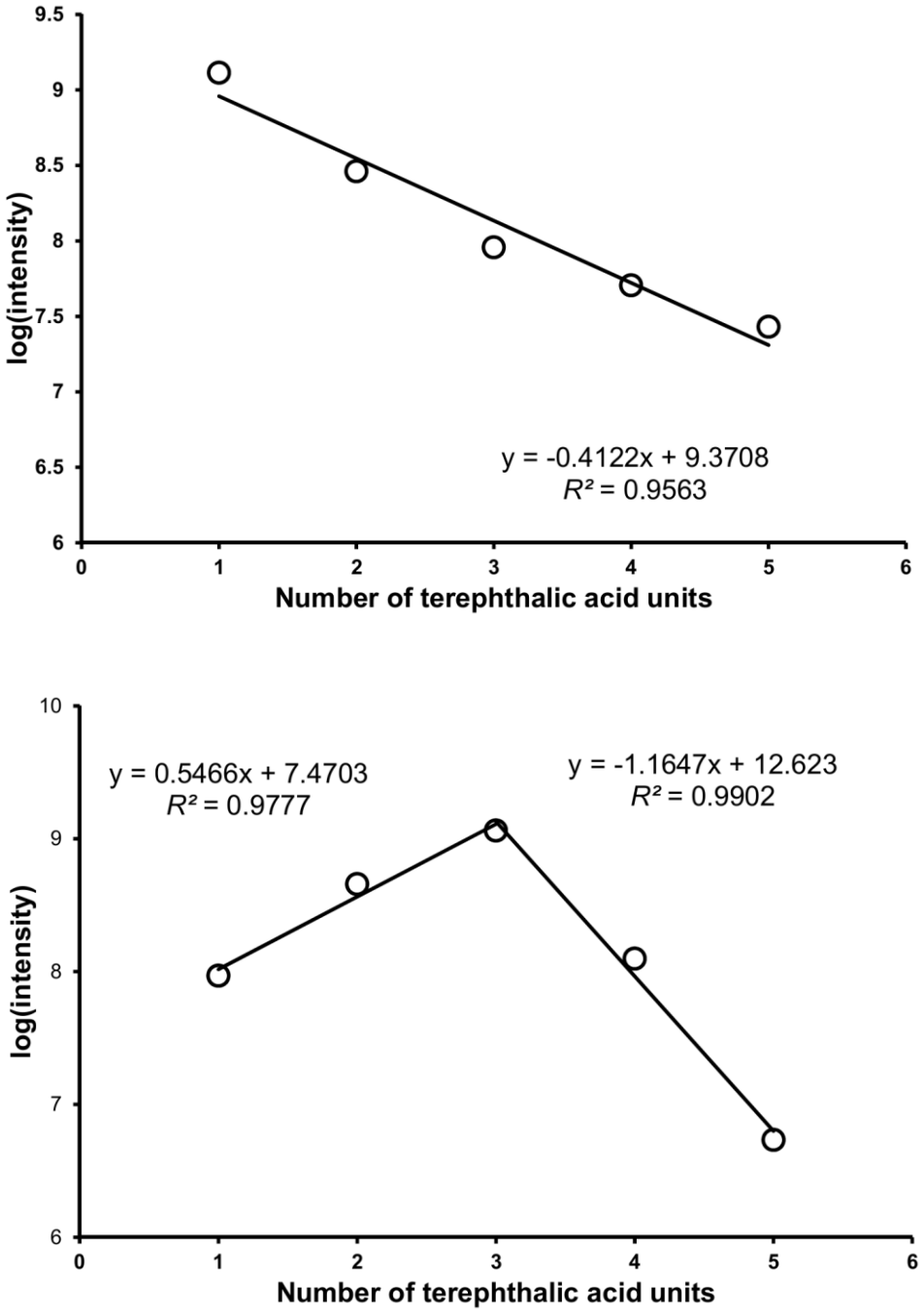


Figure S 4. MALDI FTICR MS both families' oligomers correlation of the French sparkling water bottle, Water-S FRA1. First series oligomers: Di-derivatized having the structure nT + (n-1)E + 2D; second series oligomers: Mono-derivatized having the structure nT + nE + D. T: Terephthalic part(s), E: Ethylene glycol unit(s), D: DMAPA molecule(s), n: Integer number from 1 to 5.

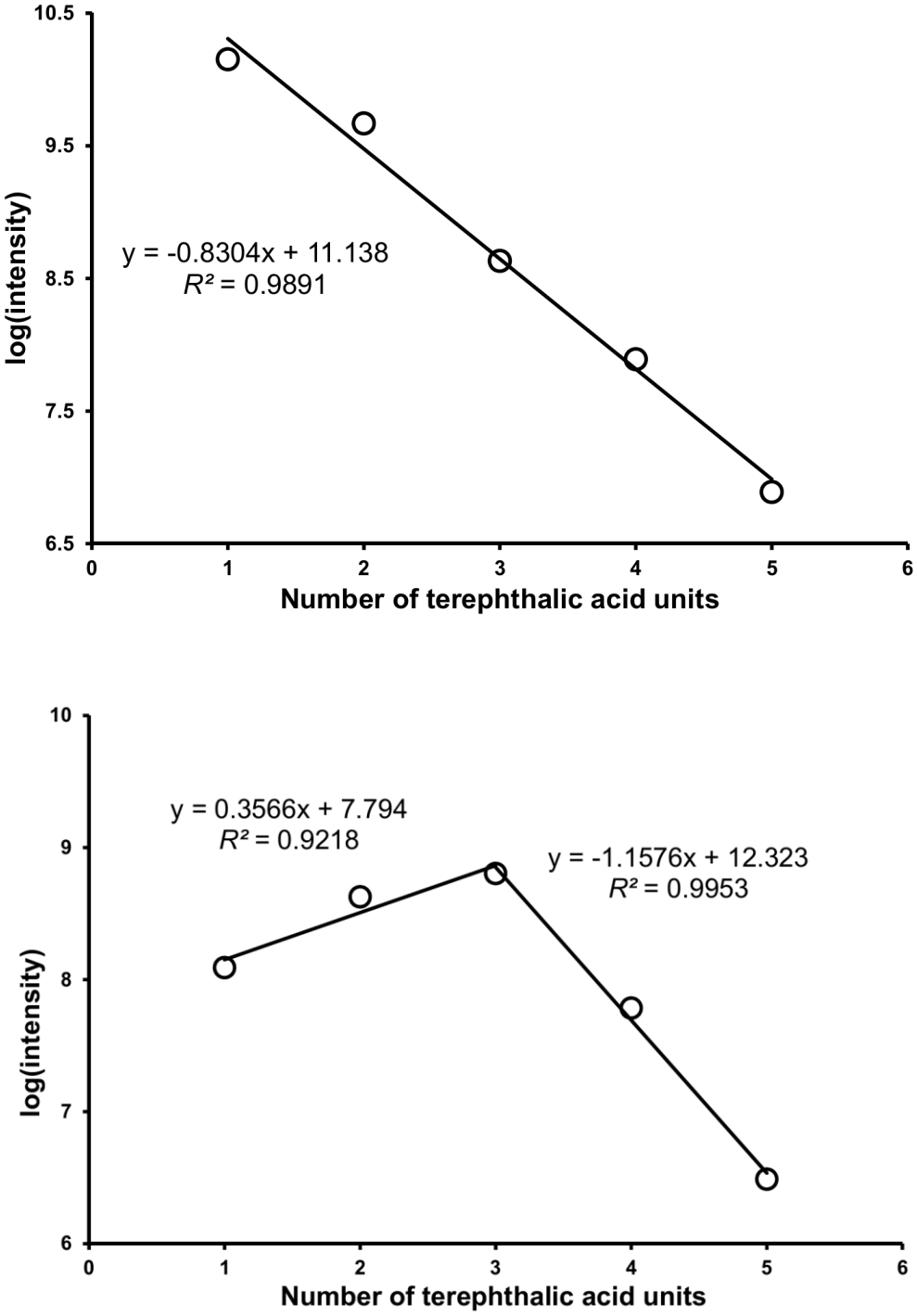


Figure S 5. MALDI FTICR MS both families' oligomers correlation of the French Cola-1 bottle, Cola-1 FRA. First series oligomers: Di-derivatized having the structure nT + (n-1)E + 2D; second series oligomers: Mono-derivatized having the structure nT + nE + D. T: Terephthalic part(s), E: Ethylene glycol unit(s), D: DMAPA molecule(s), n: Integer number from 1 to 5.

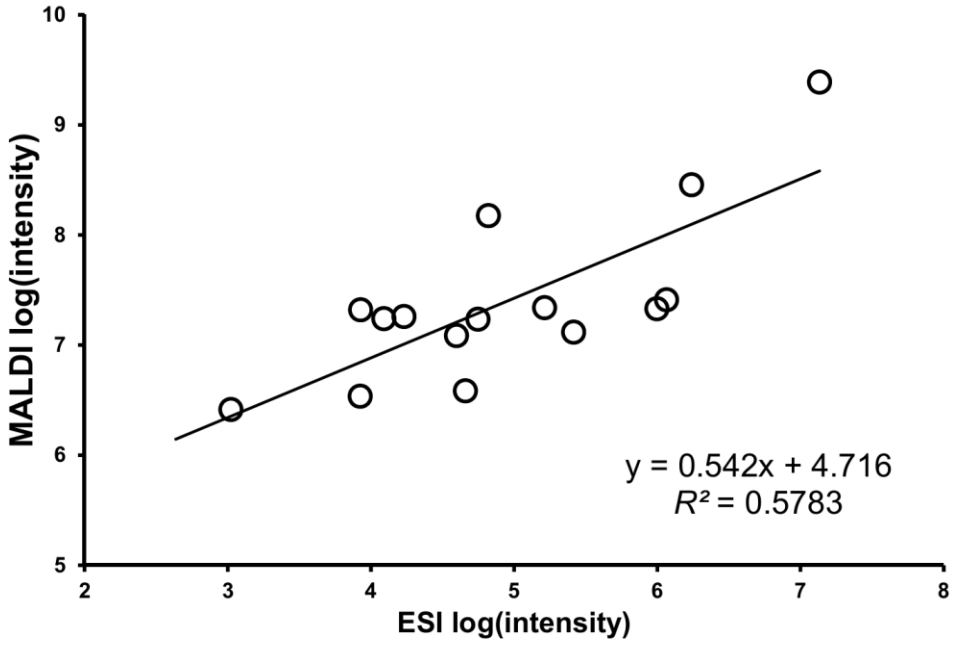


Figure S 6. MALDI FTICR MS vs ESI LC-MS comparison of Water FRA1 spectral data.

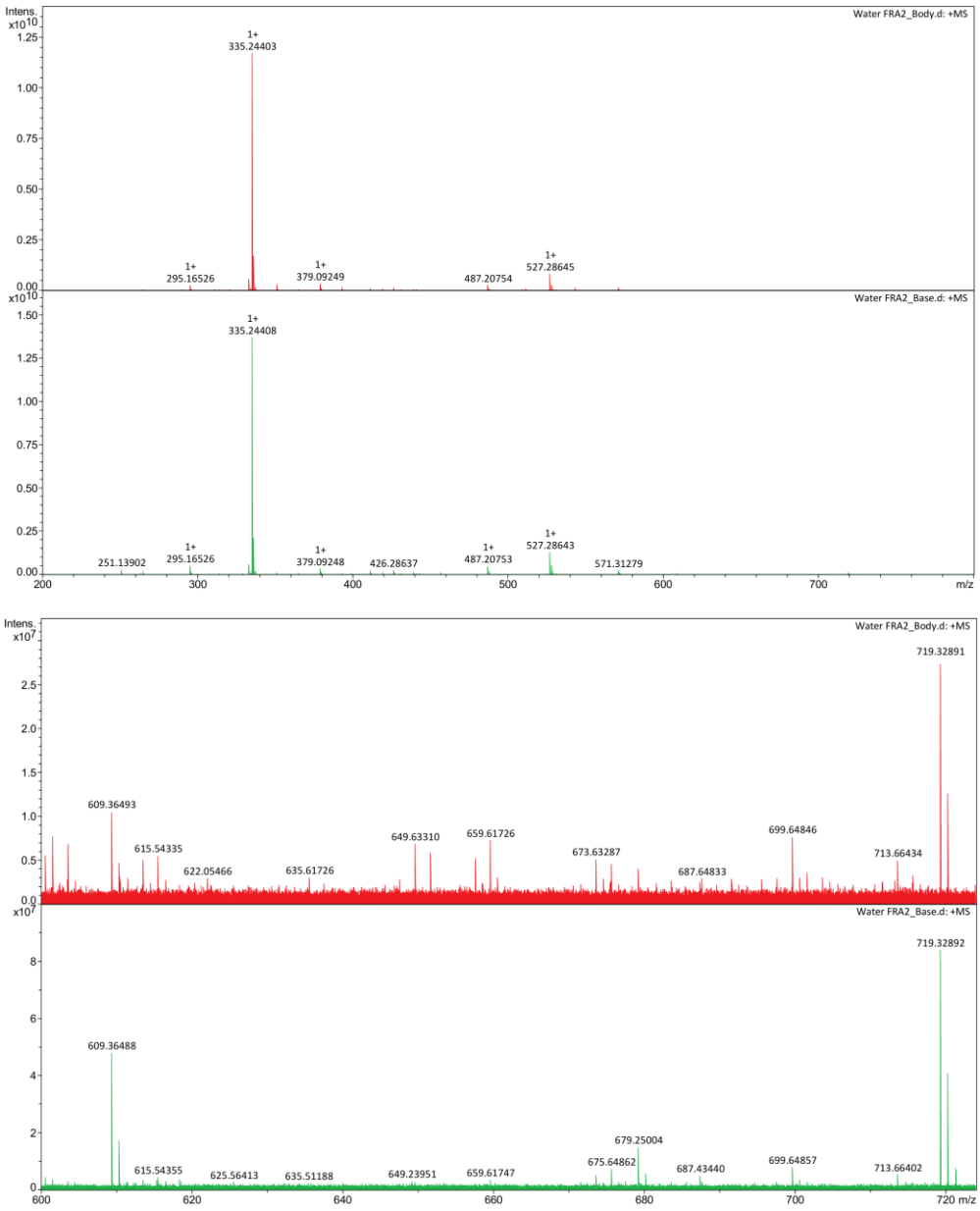


Figure S 7. MALDI FTICR MS spectra of both parts of Water FRA2 microplastics collecting from its body (in red) and its base (in green). First two spectra: *m/z* 200-800; Second two spectra: *m/z* 600-724.

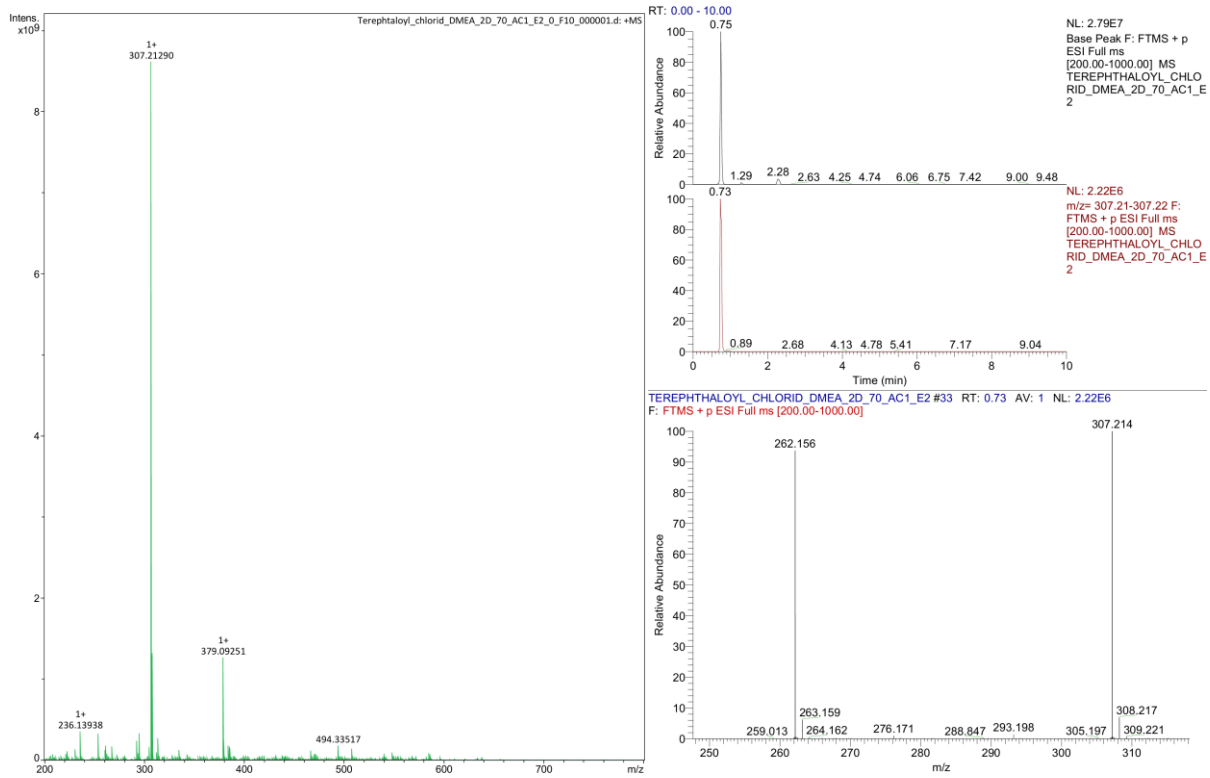


Figure S 8. MALDI FTICR MS (left) and LC-MS (right) results of the synthesized internal standard.

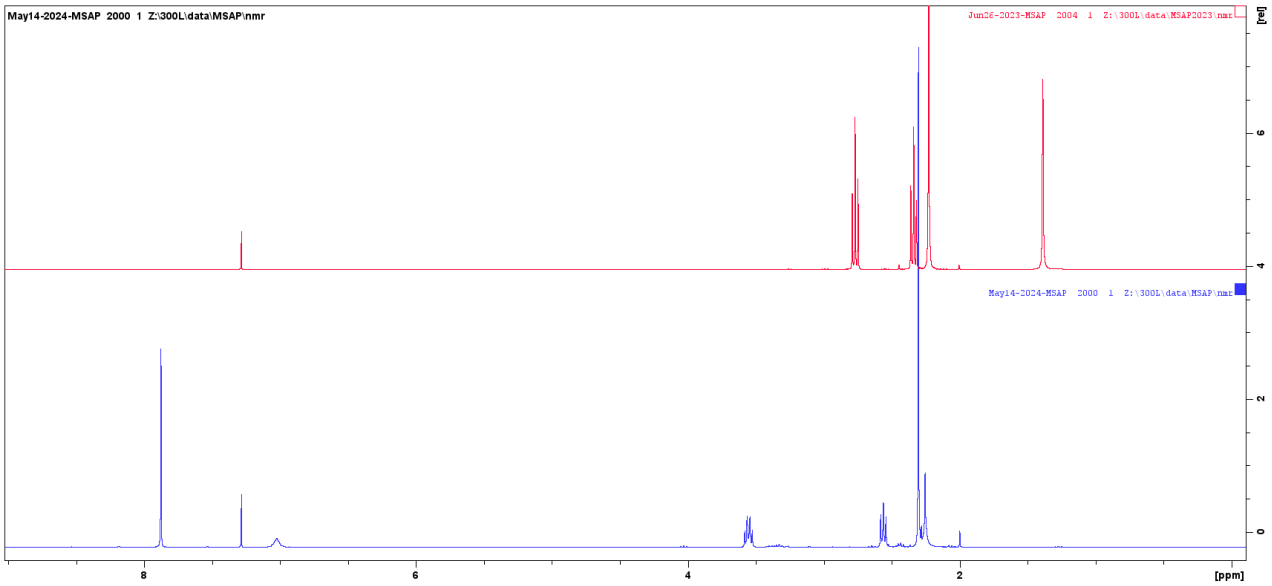


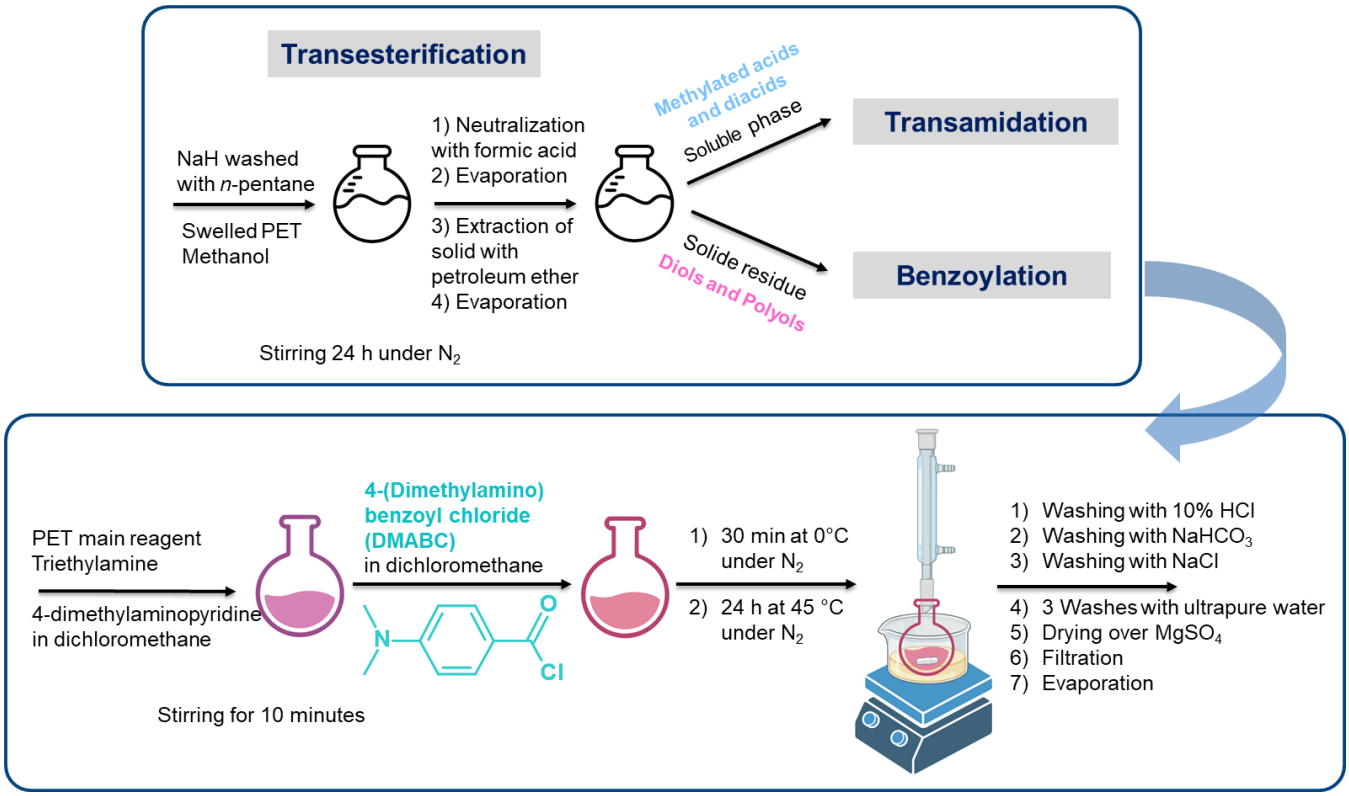
Figure S 9. ^{1}H NMR spectra of 2-(dimethylamino)ethylamine (DMEN) alone and PET synthesized internal standard respectively.

Chapter 3: PET diols structural deciphering

Introduction: Analysis of diols and polyols

Free polyols and diols maybe lost during the already described method of transamidation because they are soluble in water and may stay in the aqueous phase during the liquid-liquid extractions. So, for analyzing this part, diols and polyols were separated of the acidic part after a transesterification with methanol. The diols part was derivatized by benzoylation using 4-(dimethylamino)benzoyl chloride chosen specifically to increase the mass spectrometry detection of the final product due to its tertiary amine function. The remaining phase after methanolysis can be transamidated as previously.

The detailed strategy is shown in the following figure.



In 50-mL flask, 250 mg of PET were swelled in THF under N_2 at 66 °C for two days to facilitate PET solubilization during the reaction of transesterification. In another 50-mL flask, 165 mg (2.41 mmol) of NaH 60% were washed five times with 5 mL of pentane, then 5 mL (0.123 mol) of pure methanol were added and stirred for 1 minute. The content of the two flasks were mixed and left under magnetic stirring under N_2 for 24 hours. The mixture was cooled by an ice bath then neutralized with 123 µL (3.26 mmol) of formic acid, evaporated using rotary evaporation then vacuum pump. The solid was crushed with a spatula then extracted twice with 30 mL of petroleum ether. The soluble part was transferred using a glass pipette to another flask for transamidation with DMAPA as described previously but without heating. The

remaining solid residue contains polyols which are insoluble in petroleum ether. To the solid residue cooled with an ice bath, 1 mg of the catalyst 4-dimethylaminopyridine in 5 ml of dichloromethane and 0.7 mL (5 mmol) of triethylamine were added. The mixture was stirred under N_2 during 10 minutes. Then, 370 mg (1.54 mmol) of 4-(dimethylamino)benzoyl chloride dissolved in 5 mL of dichloromethane were added to the mixture cooled with an ice bath. After stirring for 30 minutes with an ice bath cooling, the mixture was heated at gentle solvent reflux by an oil bath set at 45 °C for 24 h under N_2. The mixture was allowed to cool at room temperature and by an ice bath then almost 1 mL of 10% HCl was added to neutralize the excess of triethylamine. This mixture was washed successively with saturated $NaHCO_3$ solution to neutralize the excess of hydrochloric acid, with saturated aqueous sodium chloride solution, and 3 times with ultrapure water. This solution was then dried over $MgSO_4$, filtrated and evaporated. A white or pinkish white solid was finally obtained and analyzed by mass spectrometry LC-MS.

The **internal standards** made of ethylene glycol and 1,4-butanediol were synthesized after direct benzoylation with DMABC then analyzed as well by LC-MS.

Article 2

New approach for polyethylene terephthalate (PET) diols deciphering: Application on PET daily life packaging objects paving their structural modifications

ABSTRACT: Polyethylene terephthalate (PET) is a thermoplastic polyester that includes diols and/or polyols part, especially ethylene glycol which is the main diol constituting this polyester, in addition to their terephthalic acids' parts. Given PET prominence in the bottle manufacturing industry, a detailed study of this polymer is of utmost importance. The identification of the initial diols and/or polyols constituting PET manufactured bottles and containers and their structural modifications is a challenging research field. In this study, PET diols and/or polyols were derivatized using a new approach combining an innovative methanolysis-benzoylation methodology with the analysis by Orbitrap-MS. First, a transesterification with methanol for freeing diols and polyols was performed followed by a derivatization with 4-dimethylaminobenzoyl chloride (DMABC) as benzoylation agent under specific conditions. After reaction post-treatment, the derivatized products were analyzed using ESI ionization on an Orbitrap-MS hyphenated to liquid chromatography LC-MS. This method was applied to PET daily life bottles in comparison to authentic diols and co-polyesters used as references showing extra data on their diols' composition that may be affected by recycling, manufacturing procedures and/or natural weathering. Other polyesters and co-polyesters' diols and polyols can be studied using this new strategy.

Keywords: PET, diols, structural modification, recycling, derivatization, transesterification, methanolysis, benzoylation, ESI, LC Orbitrap-MS.

Polyethylene terephthalate (PET) is a thermoplastic polyester that governs bottles production field. Chemically, it is formed of two parts forming its ester bonds. This polyester is synthesized industrially by different processes, either by elimination of water molecule after polycondensation between terephthalic acid and ethylene glycol[1] or by elimination of methanol after transesterification between dimethyl terephthalate and ethylene glycol. However, PET in laboratory may be synthesized using terephthaloyl chloride and ethylene glycol units which is easier method but more expensive and needs more security prevention than the other PET synthesis approaches**,** as this chloride is more dangerous than its acid homologous**,** so this last reaction is not compatible for industries. In all cases, ethylene glycol is the initial diol constituting mainly PET.[1-3] During PET polymerization reactions, diethylene glycol (DEG) maybe formed as a side reaction by-product.[3]

Many analytical methods were used to characterize PET polyesters and their microplastics but without affording satisfying identification at molecular level.[4-5] Extended research in this field is necessary for environmental[6-7] and health[8-9] reasons.

Recently, our new approach combining soft chemical depolymerization by transamidation using *N,N*-dimethyl-1,3-propanediamine (DMAPA) and advanced mass spectrometry has revealed new data on PET structural composition, its crosslinking and additives. Despite the wide use of PET in bottles' manufacturing sector, this study allowed the chemical differentiation among water, sparkling water and soft drinks' PET bottles for the first time. It showed that a plastic bottle contain not only ethylene glycol but also other diols such as cyclohexanedimethanol added to improve pet final strength especially in carbonated liquid-containing bottles.[10] However, this approach containing a liquid-liquid extraction step may lead to the loss of some diols and polyols of polyesters because they are aqua-soluble. For this reason, another new approach to study diols and/or polyols of PET plastics will be described here in order to identify the original diols constituting PET bottles. This study will allow to provide extra data on the full structural composition of PET for better recycling and prediction of its microplastics and nanoplastics' fate and of their impacts on our health and environment.

First, combined organic reactions for diols and polyols derivatization were developed to reveal diols present in PET since its fabrication from raw or recycled materials or after structural modifications by natural weathering. Then, the analysis of the derivatized products was performed using advanced mass spectrometry LC-ESI Orbitrap MS allowing the deciphering of diols; that may differentiate PET bottles. A comparison with diols obtained inside the monomeric, crosslinked and oligomeric backbone of depolymerized PET after transamidation[10] will be mentioned here. Furthermore, this strategy will be applied mainly on three daily life PET samples aged naturally: French sparkling water bottle, French cola bottle and French transparent fruit container. Indeed, a free-water methanolysis reaction and isolation of PET diols followed by their benzoylation using 4-dimethylaminobenzoyl chloride (DMABC) will be described here. The reaction of PET benzoylation is shown in Figure 1.

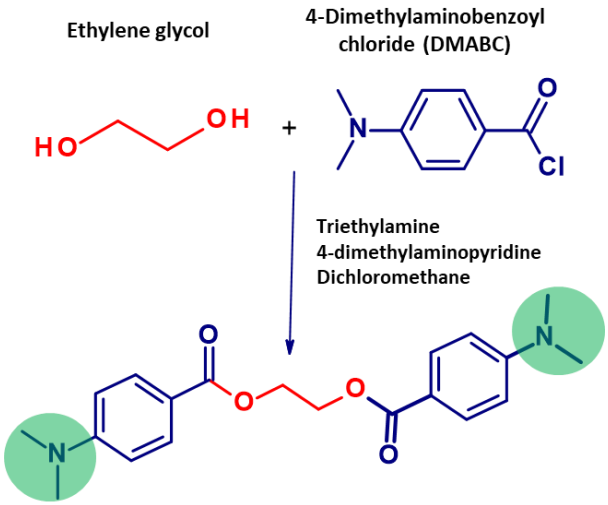


Figure 1. Benzoylation reaction of ethylene glycol, main PET diol, using 4-dimethylaminobenzoyl chloride (DMABC).

EXPERIMENTAL SECTION

Chemicals. All aqueous solutions were prepared from ultrapure grade water obtained by water filtration with a two stages Millipore system (Milli-Q® Academic with a cartouches Q-Gard 1 and Progard 2, Merck Millipore, Burlington, Massachusetts, United States). All solvents were MS analytical grade and were purchased from Merck (Merck KGaA, Darmstadt, Germany) and used as received.

All chemicals were MS analytical grade: 1,2-ethanediol Reagent Plus® ≥ 99% (ethylene glycol, EG), 1,4-butanediol 99%, 4-dimethylaminobenzoyl chloride (DMABC) 97%, 4-dimethylaminopyridine 99%, triethylamine ≥ 99.5% and 3-(dimethylamino)-1-propylamine also called *N,N*-dimethyl-1,3-propanediamine (DMAPA) 99%. All these chemicals were purchased from Merck (Merck KGaA, Darmstadt, Germany) and used without further purification. Additional chemical was purchased from Merck also: Sodium hydride (NaH) 60% dispersion in mineral oil but it was washed in pentane under N_2 inert atmosphere before utilization.

Other chemicals were used for post-reactional treatment: Sodium bicarbonate ($NaHCO_3$) ≥ 99.7%, hydrochloric acid (HCl) 37% and magnesium sulfate ($MgSO_4$) anhydrous, Reagent Plus® ≥ 99.5%. They were purchased from Merck (Merck KGaA, Darmstadt, Germany). Only sodium chloride NaCl ≥ 99.5% was purchased from Fischer Scientific (Fischer Scientific, Loughborough, UK).

Samples and samples preparation. Polyethylene terephthalate samples studied here were daily life samples aged in nature: French sparkling water bottle and French soft drink cola bottle in addition to a transparent fruit container from France.

Poly(ethylene glycol-co-1,4-cyclohexanedimethanol terephthalate) (PETG) films, 750 micron thickness were purchased from Alt-Intech (Neresheim, Germany).

These samples were cut into microplastics of 2.5 mm × 2.5 mm size after washing with ultrapure water then they have been used after drying.

Protocol of derivatization of PET diols and polyols: Transesterification-benzoylation. In 50-mL flask, 250 mg of PET microplastics were swelled in THF under N_2 inert atmosphere at 66 °C for two days to facilitate PET solubilization during the further reaction of transesterification. In another 50-mL flask, 165 mg (2.41 mmol) of sodium hydride NaH 60% were washed five times with 5 mL of pentane under N_2, then 5 mL (0.123 mol) of pure methanol were added and stirred for 1 minute. The content of the two flasks were mixed and left under magnetic stirring under N_2 atmosphere for 24 hours. The obtained mixture was cooled by an ice bath then neutralized with 123 µL (3.26 mmol) of formic acid then evaporated until total dryness using rotary evaporation followed by vacuum pump use. The obtained solid at this step was crushed with a spatula then extracted twice with 30 mL of petroleum ether resulting in the formation of two distinct phases. The soluble phase was transferred using a glass pipette to another flask for direct transamidation at room temperature as described in Almasri et al. publication.[10] The remaining solid residue contains diols and polyols, insoluble in petroleum ether, was evaporated. To the solid residue cooled with an ice bath, 1 mg (0.006 mmol) of the catalyst 4-dimethy-laminopyridine in 5 mL of dichloromethane and 0.7 mL (5 mmol) of triethylamine were added. The mixture was stirred under N_2 during 10 minutes. Then 370 mg (1.54 mmol) of 4-(dimethylamino)benzoyl chloride (DMABC) dissolved in 5 mL of dichloromethane were added to the mixture cooled with an ice bath. After stirring for 30 minutes with an ice bath cooling, the mixture was heated at gentle solvent reflux by an oil bath set at 45 °C for 24 h under N_2 inert atmosphere. For post-benzoylation treatment, the obtained mixture was cooled at room temperature, then by an ice bath, then almost 1 mL of 10% HCl aqueous solution was added to neutralize the excess of triethylamine. After that, this mixture was washed successively with saturated $NaHCO_3$ solution to neutralize the excess of hydrochloric acid, with Brine solution of aqueous sodium chloride NaCl, and three times by ultrapure water. This last obtained solution was then dried over $MgSO_4$, filtrated and evaporated using rotary evaporation. A white or pinkish white solid was formed and analyzed by LC-MS.

Authentic samples preparation. The authentic samples of two diols, ethylene glycol and 1,4-butanediol, were synthesized without any methanolysis after direct benzoylation with 4-dimethylaminobenzoyl chloride (DMABC) according to the protocol of PET benzoylation previously described.

LC-ESI MS analysis. LC-MS analyses were performed on an Orbitrap LTQ XL mass spectrometer hyphenated to a Dionex Ultimate 3000 HPLC System (ThermoFisher Scientific, Bremen, Germany). The analysis was performed using a 60 min gradient at a flow rate of 0.50 mL.min^{-1} on a Hypersil Gold™ C18 column (2.1 µm i.d. × 150 mm) packed with 1.9 µm beads pores with 175 Å pore size from ThermoFisher Scientific (Bremen, Germany) placed in an oven at a temperature of 50 °C. The derivatized PET products were analyzed using a multi-step gradient with a mobile phase of 5% acetonitrile in acidified water, 0.1% formic acid (solution A) and 75% acetonitrile in acidified water, 0.1% formic acid (solution B). The gradient started with full composition of solution A at the first 5 min followed by a gradual shift to 30% A, 70% B by 35 min. It then increased until 100% of solution B at 40 min and was held at this composition until 50 min then finally returned

to the initial conditions at 55 min which were maintained until 60 min. The LC runs were acquired in positive ion mode using ESI ionization with a non-heated source (spray voltage 4.50 kV, sheath gas flow 22 mL.min^{-1}, auxiliary gas flow 12 mL.min^{-1}). The MS scans were acquired from *m/z* 150 to 1,000 with a 60,000 resolution at *m/z* 400. Xcalibur™ 4.21 SP1 software (Thermo Fisher Scientific) was used for data acquisition and interpretation.

Analytical method. For LC-MS analysis, the obtained derivatized products were solubilized at 0.1 mg/µL in 75/25 (v/v) of dichloromethane/methanol then diluted until 1 mg/mL in acetonitrile/water/formic acid 75/25/0.1 (v/v/v).

RESULTS AND DISCUSSIONS

Methodology. Transesterification in PET field was used as depolymerization step in its recycling procedure. PET glycolysis with ethylene glycol (EG) afforded bis(2-hydroxyethyl terephthalate) (BHET), a prepolymer in PET recycling process.[11] The catalytic transesterification of dimethyl terephthalate with EG at high temperature (150-200 °C) has been also reported.[12] This reaction may be occurred in the presence of glycol (EG, DEG, glycerol) with or without catalyst[11] and lead to the formation of new polymers and polyols.[13] After depolymerization and formation of prepolymer, a polycondensation reaction was necessary for recycling.[12]

In our methodology, transesterification with methanol in the presence of sodium hydride was used to liberate diols and polyols for further derivatization. This methanolysis was performed under N_2 inert atmosphere as this reaction is water-sensitive, to prevent hydrolysis of esters. PET microplastics were previously swelled in THF to facilitate their solubilization. PET methanolysis was performed after stirring at room temperature for 24 h. After stopping the reaction with formic acid and solvent evaporation, the obtained products were extracted with petroleum ether to separate methylated acids and aromatic diacids that remain soluble in petroleum ether of PET diols and polyols remaining insoluble. The first part containing terephthalic acids was transamidated at room temperature affording similar data on PET after MS analysis as in the case of direct transamidation reported recently.[10] The free diols and polyols were evaporated then benzoylated.

Benzoylation reaction was mentioned to be effective with some PVC plasticizers bio-based alcohols as 3,5-dihydroxybenzoic acid using benzoyl chloride as benzoylation agent.[14] In general, this reagent has been reported widely for benzoylation reactions as it is cheap and commercially available. For example, it was used to derivatize alcohols and phenols in water,[15] lipids,[16] sugars and glycosides,[17] and biogenic amines.[18]

Here, an innovative benzoylation involves the usage in specific conditions of another benzoylation agent, 4-dimethylaminobenzoyl chloride (DMABC) that will be used for the first time on PET plastics. This last reagent having good properties for ESI ionization was not reported for benzoylation reactions at our best knowledge.[19-20] DMABC is commercially available and can improve the mass spectrometry response due to the presence of its tertiary amine terminal group. This benzoylation has been occurred in alkaline medium in dichloromethane using dimethylaminopyridine in catalytic amount. This reaction heated at 45°C has been performed under N_2 atmosphere for 24 h. The steps of addition of each reagent were previously described. After reaction quenching, the steps of neutralization, washing, drying and evaporation were achieved before LC-MS analysis.

In practical order, the authentic samples ethylene glycol and 1,4-butanediol were first benzoylated directly as described previously to test this new method on pure diols before its application to more complex mixtures, polyesters and co-polyesters. After that, PET bottles & container and PETG films were transesterified with methanol then benzoylated.

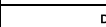
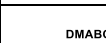
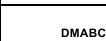
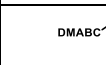
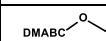
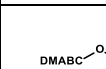
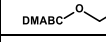
LC-MS analysis. The relative intensity of each peak will be represented as percentage and calculated in comparison to the sum of relative intensities of the major composition in each sample's mixture according to the following formula:

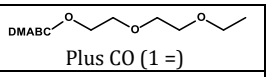
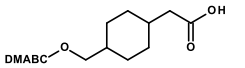
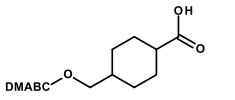
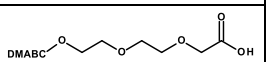
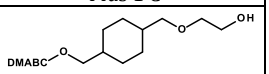
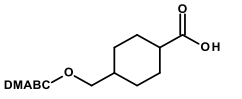
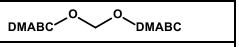
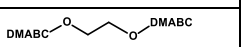
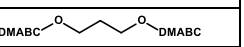
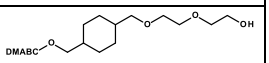
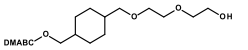
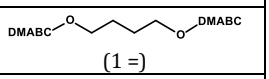
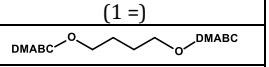
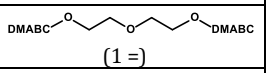
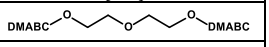
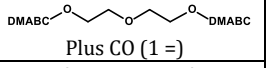
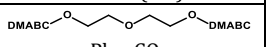
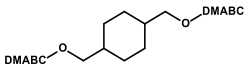
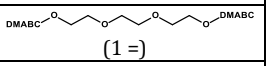
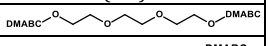
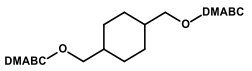
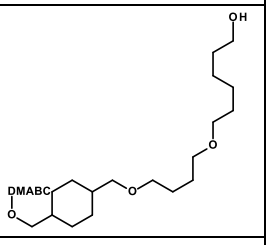
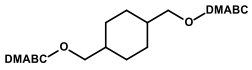
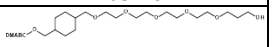
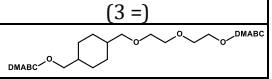
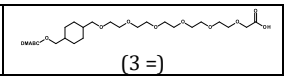
$$\%\ Identified\ peak = \frac{RI\ of\ this\ identified\ peak}{RI\ of\ the\ major\ composition\ peaks} \times 100$$

RI represents the relative intensity of a given peak.

A new database composed of 44 structures in all benzoylated samples has been identified with high accuracy (0-5 ppm). These structures and their corresponding chemical formula are shown in Table 1.

Table 1. Structures of benzoylated compounds identified with LC-MS with their corresponding *m/z* and protonated chemical formula ((=) is unsaturation in the chain backbone).

Entry	*m/z*	$[M+H]^+$	Structure
1	166.086	$C_9H_{12}NO_2$	
2	180.102	$C_{10}H_{14}NO_2$	
3	192.102	$C_{11}H_{14}NO_2$	
4	194.118	$C_{11}H_{16}NO_2$	
5	206.118	$C_{12}H_{16}NO_2$	(1 =)
6	210.113	$C_{11}H_{16}NO_3$	
7	220.133	$C_{13}H_{18}NO_2$	 (1 =)
8	224.128	$C_{12}H_{18}NO_3$	
9	238.107	$C_{12}H_{16}NO_4$	
10	238.144	$C_{13}H_{20}NO_3$	
11	252.123	$C_{13}H_{18}NO_4$	 (1 =)
12	254.139	$C_{13}H_{20}NO_4$	
13	266.139	$C_{14}H_{20}NO_4$	 (1 =)
14	280.154	$C_{15}H_{22}NO_4$	 (1 =)
15	292.191	$C_{17}H_{26}NO_3$	
16	298.165	$C_{15}H_{24}NO_5$	
17	306.167	$C_{17}H_{24}NO_4$	

18	308.149	$C_{16}H_{22}NO_5$	 Plus CO (1 =)
19	313.155	$C_{18}H_{21}N_2O_3$	
20	320.186	$C_{18}H_{26}NO_4$	
21	322.165	$C_{17}H_{24}NO_5$	 Plus 1 O
22	324.144	$C_{16}H_{22}NO_6$	 Plus 1 C
23	336.217	$C_{19}H_{30}NO_4$	
24	338.159	$C_{17}H_{24}NO_6$	 Plus 2 O
25	343.165	$C_{19}H_{23}N_2O_4$	
26	357.181	$C_{20}H_{25}N_2O_4$	
27	371.197	$C_{21}H_{27}N_2O_4$	
28	378.228	$C_{21}H_{32}NO_5$	 (1 =)
29	381.251	$C_{21}H_{34}NO_5$	
30	383.197	$C_{22}H_{27}N_2O_4$	 (1 =)
31	385.212	$C_{22}H_{29}N_2O_4$	
32	399.192	$C_{22}H_{27}N_2O_5$	 (1 =)
33	401.207	$C_{22}H_{29}N_2O_5$	
34	427.186	$C_{23}H_{27}N_2O_6$	 Plus CO (1 =)
35	429.202	$C_{23}H_{29}N_2O_6$	 Plus CO
36	439.259	$C_{26}H_{35}N_2O_4$	
37	443.218	$C_{24}H_{31}N_2O_6$	 (1 =)
38	445.233	$C_{24}H_{33}N_2O_6$	
39	455.254	$C_{26}H_{35}N_2O_5$	 Plus1 O
40	463.329	$C_{27}H_{45}NO_5$	
41	471.249	$C_{26}H_{35}N_2O_6$	 Plus 2 O
42	520.291	$C_{28}H_{42}NO_8$	 (3 =)
43	527.312	$C_{30}H_{43}N_2O_6$	
44	548.285	$C_{29}H_{42}NO_9$	 (3 =)

Common composition. LC-MS results of all samples (authentic, PET and PETG) showed a common composition with different intensities indicating the presence of common diols. Indeed, the mono-benzoylated ethylene glycol [$C_{11}H_{15}NO_3$ + H^+] appearing at *m/z* 210.113 constituted 31%, 21%, 14% and 10% of the major composition of the French sparkling water and cola bottles, EG authentic sample and PET container respectively. In PETG sample, it appeared with 16% of the major composition but in trace (less than 0.01%) in the butanediol sample (Entry 6, Table 2 & 3). The di-benzoylated ethylene glycol [$C_{20}H_{24}N_2O_4$ + H^+] appearing at *m/z* 357.181 constituted the main compound in EG authentic sample as expected with 41% of its major composition. This peak constituted 14% of the French container composition. But it appeared in traces less than 0.01% in the other remaining samples and was absent in the butanediol authentic sample (Entry 26, Table 2 & 3).

Diethylene glycol (DEG) and triethylene glycol (TEG) have been identified in all samples. Indeed, DEG has been appeared mono-derivatized [$C_{13}H_{19}NO_4$ + H^+] at *m/z* 254.139 with 3% and 2% in sparkling water and cola bottles respectively and in traces 0.02%, 0.03% and 0.95% in the authentic samples and the container respectively, it was present with the same relative abundance in PETG as cola bottle (3% of their major composition) (Entry 12, Table 2 & 3). DEG was detected di-derivatized [$C_{22}H_{28}N_2O_5$ + H^+] at *m/z* 401.207 in traces < 0.2% in all PET samples and butanediol reference (Entry 33, Table 2 & 3). Furthermore, triethylene glycol (TEG) has been identified mono-derivatized [$C_{15}H_{23}NO_5$ + H^+] at *m/z* 298.165 in all benzoylated samples except the authentic diols' samples in traces (< 0.1%) (Entry 16, Table 2 & 3) and di-derivatized [$C_{24}H_{32}N_2O_6$ + H^+] at *m/z* 445.233 in traces (less than 0.1%) in all benzoylated samples except PETG (Entry 38, Table 2 & 3). The presence of DEG and TEG may due to the PET manufacturing process itself.[3,11]

In addition, 1,4-butanediol has been identified in all samples (except PETG reference) in its mono-benzoylated form [$C_{13}H_{19}NO_3$ + H^+] at *m/z* 238.144 appearing with 15% of the major composition in the French fruit container and 29% in butanediol authentic sample but in traces (≤ 0.01%) in the other benzoylated samples (Entry 10, Table 2 & 3).

Another diol has been also identified, propane-1,3-diol which was found di-derivatized [$C_{21}H_{26}N_2O_4$ + H^+] at *m/z* 371.197 in traces less than 0.2% of the major composition in all samples (Entry 27, Table 2 & 3), and mono-derivatized [$C_{12}H_{17}NO_3$ + H^+] at *m/z* 224.128. This last compound has been detected in all samples except EG authentic sample and constituted almost 2% in cola bottle as in butanediol and PETG references; it appeared in traces less than 1% in the other PET packaging objects (Entry 8, Table 2 & 3). In addition, propane-1,3-diol was identified in its carboxylic acid form, 3-hydroxypropanoic acid mono-benzoylated [$C_{12}H_{15}NO_4$ + H^+] for *m/z* 238.107 in all samples except the butanediol reference (Entry 9, Table 2 & 3).

Another new diol was detected in all PET packaging objects after benzoylation: 1,6-Hexanediol. This diol was linked to both 1,4-butanediol and 1,4-cyclohexanedimethanol (the principle diol present in PETG co-polyester) found

benzoylated with 1 molecule of DMABC [$C_{27}H_{44}NO_5$ + H^+], *m/z* 463.329 where it was present in traces (< 0.1% of the major composition) (Entry 40, Table 2 & 3). The formation of these diols may due to the recycling procedures of PET that may form not very pure blends after PET molding.

Despite the identified diols, other structures containing the remaining DMABC benzoylation agent, already introduced in excess, were identified. For instance, the acidic form of DMABC [$C_9H_{11}NO_2$ + H^+] appearing at *m/z* 166.086 constituted 10% of the major composition.in both authentic samples. However, it constituted 37%, 35 % and 20% in the French container and cola then sparkling water bottles respectively. In PETG, it appeared with 46% of its major composition formed of 33 structures (Entry 1, Table 2 & 3). This indicates that further steps of washing may be performed in alkaline media. The compound having DMABC with O-CH_3 terminal group [$C_{10}H_{13}NO_2$ + H^+] for *m/z* 180.102 has been also identified in all the benzoylated samples (Entry 2, Table 2 & 3).

Table 2. Relative intensities of authentic diols' samples and PETG reference after benzoylation and analysis by LC-MS.

Entry (Table 1)	1,2-Ethanediol	1,4-Butanediol	PETG co-polyester
1	9.82E+06	3.69E+07	2.08E+07
2	6.38E+05	3.04E+07	7.56E+05
3	3.10E+07	3.84E+04	2.56E+04
4	9.49E+03	7.79E+05	1.29E+04
5	0.00E+00	6.83E+04	4.34E+03
6	1.46E+07	2.70E+04	7.28E+06
7	1.03E+04	2.83E+06	0.00E+00
8	0.00E+00	5.46E+06	1.01E+06
9	7.45E+03	0.00E+00	1.13E+06
10	4.81E+05	1.09E+08	0.00E+00
11	1.04E+06	1.86E+06	9.20E+06
12	1.55E+04	1.24E+05	1.45E+06
13	1.94E+03	7.65E+03	2.84E+04
14	1.54E+03	7.64E+06	2.68E+04
15	0.00E+00	0.00E+00	1.73E+06
16	0.00E+00	0.00E+00	1.65E+04
17	0.00E+00	6.21E+03	8.15E+05
18	0.00E+00	0.00E+00	1.85E+04
19	2.19E+06	2.37E+06	1.38E+03
20	0.00E+00	0.00E+00	1.89E+04
21	0.00E+00	0.00E+00	2.60E+05
22	0.00E+00	6.73E+04	4.98E+03
23	0.00E+00	0.00E+00	1.59E+04
24	0.00E+00	0.00E+00	7.30 E+03
25	4.95E+05	1.12E+06	4.51E+03
26	4.28E+07	0.00E+00	7.91E+02
27	8.53E+03	3.76E+05	1.34E+03
28	0.00E+00	0.00E+00	4.75E+03
29	0.00E+00	0.00E+00	0.00E+00
30	0.00E+00	3.04E+05	0.00E+00
31	1.23E+05	1.70E+08	6.35E+02
32	2.83E+03	1.58E+06	1.64E+03
33	0.00E+00	4.53E+04	0.00E+00
34	0.00E+00	2.55E+03	1.56E+03
35	2.65E+03	4.82E+03	0.00E+00
36	0.00E+00	1.25E+04	2.47E+03
37	0.00E+00	8.03E+03	0.00E+00
38	1.47E+03	8.76E+03	0.00E+00
39	0.00E+00	1.06E+04	0.00E+00
40	9.49E+03	0.00E+00	1.77E+04
41	0.00E+00	7.05E+04	0.00E+00
42	2.29E+03	0.00E+00	1.96E+05
43	0.00E+00	9.23E+03	0.00E+00
44	0.00E+00	0.00E+00	9.72E+03

Main peaks in each benzoylated sample. To decipher the detailed alcoholic composition of each PET sample, the number of peaks and the main peak's abundance in each blend will be discussed, followed by a comparison between all samples in order to differentiate the diols found. For authentic samples, LC-MS results of the EG authentic sample showed the presence of 22 structures in which the main peak was the expected di-benzoylated ethylene glycol [$C_{20}H_{24}N_2O_4$ + H^+] appearing at *m/z* 357.181 constituting 41% of the major composition. In addition, the benzoylated butanediol authentic sample contained 31 structures in which the expected 1,4-butanediol di-derivatized [$C_{22}H_{28}N_2O_4$ + H^+] appearing at *m/z* 385.212 was the main peak constituting 46% of its major composition (Entry 31, Table 2).

Concerning PET container, 33 structures have been identified. This blend was very acidic. Indeed, the two main peaks were found to be acidic compounds: The first one was the remaining DMABC carboxylic acid (37%) and the second one was 3-hydroxypropanoic acid mono-benzoylated [$C_{12}H_{15}NO_4$ + H^+] appearing at *m/z* 238.107 constituting 14.5% of the major composition. However, the third peak was the di-derivatized ethylene glycol appearing also with high intensity (14%) as shown in Table 3.

For French carbonated bottles, the sparkling water bottle had 38 structures in which the mono-benzoylated ethylene glycol was the main peak (31%) after the remaining DMABC carboxylic acid compound. However, the main peak in cola bottle was the mono-benzoylated diethylene glycol (unsaturated) [$C_{13}H_{17}NO_4$ + H^+] which appeared at *m/z* 252.123 constituting 46% of the major composition composed of 34 compounds. This peak appeared as main peak in the benzoylated PETG with 20% of its major composition after the remaining DMABC carboxylic acid compound (Entry 11, Table 2 & 3).

There were differences in ratios of DMABC acidic compounds over main peaks in the benzoylated mixtures. Indeed, in authentic samples, the benzoylation agent DMABC was introduced in stoichiometric ratio and the benzoylation reaction was directly performed on diols generating the expected compounds as main peaks. However, in PET samples and PETG co-polyester which are complex mixtures, a transesterification with methanol was performed before benzoylation. This methanolysis resulted

in two fractions: The first containing the free diols and polyols was benzoylated with DMABC and the second fraction containing the terephthalic acid parts, that may still trap diols, was transamidated with DMAPA.[10] This procedure may affect the intensities of main peaks after benzoylation due to the loss of some diols in the transesterified and/or transamidated parts. To confirm this hypothesis, both transesterified and transamidated fractions were analyzed by LC-MS for PET from the simplest mixture, the French fruit container.

The transesterified PET fraction revealed the presence of terephthalic acid either with one methanol [$C_9H_9O_4$ + H^+] which appeared at *m/z* 181.049 with a relative intensity of 1.50E+04 or with two molecules of methanol [$C_{10}H_{10}O_4$ + H^+] which appeared at *m/z* 181.049 with a relative intensity of 3.69E+04. No compounds having diols in their monomeric or oligomeric backbone have been found in this fraction. On the other, the transamidated PET fraction obtained after methanolysis contained, in addition to the mono- and di-transamidated terephthalic acids as main peaks, some traces of mono-transamidated PET monomer having ethylene glycol [$C_{15}H_{22}N_2O_4$+ H^+] which appeared at *m/z* 295.165 with a relative intensity of 1.70E+03. So, as expected some diols remained in the other fractions before benzoylation. Hence, this new multi-approach provides the full identification of PET diols including the free diols and those trapped inside PET backbone with their further possible quantification by considering all the obtained fractions.

Table 3. LC-MS relative intensities of compounds found in the French PET packaging objects after benzoylation.

Entry (Table 1)	Fruit Container	Sparkling water bottle	Cola bottle
1	1.22E+07	1.67E+07	2.09E+07
2	5.21E+05	1.26E+06	2.53E+06
3	2.82E+06	5.13E+04	6.78E+04
4	2.06E+04	5.36E+04	3.94E+04
5	5.22E+04	7.10E+03	2.48E+03
6	3.34E+06	1.52E+07	2.16E+07
7	3.96E+02	0.00E+00	0.00E+00
8	8.60E+04	3.66E+05	1.67E+06
9	4.73E+06	4.75E+06	2.61E+06
10	3.11E+03	2.40E+03	2.10E+03
11	2.32E+06	7.67E+06	4.81E+07
12	3.09E+05	1.42E+06	2.02E+06
13	6.17E+05	6.31E+05	3.49E+06
14	3.84E+05	4.81E+03	1.15E+05
15	7.37E+02	1.54E+04	9.43E+03
16	8.92E+03	1.38E+04	2.17E+04
17	1.80E+05	7.17E+03	1.96E+04
18	7.13E+03	2.71E+04	1.28E+05
19	8.09E+04	9.17E+03	1.27E+04
20	0.00E+00	3.58E+03	6.15E+02
21	4.81E+04	9.62E+03	2.93E+04
22	8.22E+04	5.66E+04	2.54E+04
23	0.00E+00	0.00E+00	4.20E+03
24	2.74E+03	8.73E+03	2.68E+05
25	2.59E+05	1.46E+04	9.34E+03
26	4.39E+06	6.94E+02	6.58E+02
27	5.41E+04	2.95E+04	2.06E+03
28	0.00E+00	2.92E+03	0.00E+00
29	4.10E+02	0.00E+00	0.00E+00
30	0.00E+00	2.10E+03	0.00E+00
31	0.00E+00	6.71E+02	0.00E+00
32	0.00E+00	0.00E+00	0.00E+00
33	3.44E+04	3.57E+03	2.40E+03
34	0.00E+00	0.00E+00	0.00E+00
35	4.23E+02	1.62E+04	2.73E+04
36	0.00E+00	2.50E+03	5.89E+03
37	3.84E+04	2.80E+03	4.32E+03
38	2.63E+03	9.42E+02	1.06E+03
39	1.64E+03	5.49E+02	0.00E+00
40	1.13E+04	2.77E+04	3.69E+04
41	0.00E+00	3.97E+02	0.00E+00
42	3.08E+03	4.34E+02	1.39E+04
43	0.00E+00	4.01E+02	4.43E+02
44	7.46E+02	0.00E+00	0.00E+00

Specific composition. Moving to the differentiating diols in polymers' blends, some structures were specific for some PET packaging or for each object in comparison to the authentic samples and PETG references. For example, French sparkling water and cola bottles contained 1,4-cyclohexanedimethanol. This diol has been found mono-benzoylated [$C_{17}H_{25}NO_3$ + H^+] at *m/z* 292.191 with 0.03% and 0.01% of the major composition in French sparkling water and cola bottles respectively compared to 4% in PETG reference (Entry 15, Table 2 & 3); and di-benzoylated [$C_{26}H_{34}N_2O_4$ + H^+] at *m/z* 439.259 with 0.01% of the major composition in both French sparkling water and cola bottles & PETG reference (Entry 36, Table 2 & 3).

The two carbonated bottles contained also the compound having 1,4-cyclohexanedimethanol crosslinked to diethylene glycol. It was found di-benzoylated [$C_{30}H_{42}N_2O_6$ + H^+] at *m/z* 527.312 in the benzoylated sparkling water bottle and cola bottle in tiny traces (0.0008% and 0.0004% of their major composition respectively) (Entry 43, Table 2 & 3). The mono-benzoylated 2-[4-(hydroxymethyl)cyclohexyl]acetic acid [$C_{18}H_{25}NO_4$ + H^+] was also detected in carbonated bottles at *m/z* 320.186 (Entry 20, Table 1).

In addition, some compounds appeared to be differentiating between these two bottles. Indeed, a crosslinking of 1,4-cyclohexanedimethanol with ethylene glycol was found only in cola bottle (as in PETG reference) mono-benzoylated [$C_{19}H_{29}NO_4$ + H^+] at *m/z* 336.217 with 0.004% of its major composition (Entry 23, Table 2 & 3).

However, sparkling water bottle was more oxygenated. Hence, 1,4-cyclohexanedimethanol was detected dibenzoylated with 2 oxygen atoms [$C_{26}H_{34}N_2O_6$ + H^+] at *m/z* 471.249 with 0.001% of its major composition (Entry 41, Table 2 & 3). With the same abundance, the di-benzoylated

1,4-butanediol was found only in this bottle (Entry 31, Table 2 & 3).

These data confirm that the carbonated bottles contain the specific diol 1,4-cyclohexanedimethanol which is the main diol in PETG as mentioned by Almasri et al. recently[10]. This diol has been modified during manufacturing procedures and natural ageing resulting in its crosslinking with other diols present initially during PET fabrication.

CONCLUSIONS AND PERSPECTIVES

A new methodology for analyzing diols and polyols of polyesters has been developed. In this work, it was successfully applied to PET polyesters and PETG co-polyester to follow-up their diols' structural modifications. A methanolysis reaction was performed followed by separation of the two parts of polyester by extraction with petroleum ether. After that, a benzoylation reaction using DMABC was performed on the diols part that were analyzed by LC-MS. Three daily life PET packaging objects were studied and compared to authentic samples of diols and to PETG co-polyester as reference. In addition to ethylene glycol (the main diol of PET), this method confirmed the presence of various diols such as diethylene glycol, triethylene glycol, 1,4-butanediol, 1,4-cyclohexanedimethanol, 1,6-hexanol and 1,3-propanol. These diols not clearly labeled on PET packaging were identified with high accuracy for an Orbitrap. This approach revealed the possible crosslinking among diols present in PET containers and bottles that may differentiate them. These structural modifications may due to the source of fabrication of PET especially after recycling or to the natural ageing of PET. Combining this approach with our recently developed method of transamidation will allow the full characterization and quantification of all diols present in PET plastics. This strategy will be applied to PET after controlled ageing to assess the source of their structural modifications and will be applied to other polyesters and industrial resins.

ASSOCIATED CONTENT

Supporting Information

Mass spectrometry and analytical data for PET benzoylated products. Additional experimental details and characterization data.

AUTHOR INFORMATION

First author

Bayan Almasri - Univ. Lille, CNRS, UAR 3290, MSAP, Miniaturisation pour la Synthèse l'Analyse et la Protéomique, F-59000 Lille, France ; Laboratoire de Chimie Appliquée, Faculté des Sciences III, Université Libanaise, Ras Maska, Tripoli, Liban ; orcid.org/0009-0001-9467-5716.

Note

The authors declare no competing financial interest.

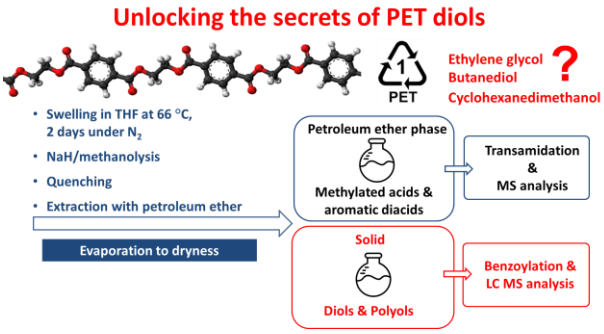
AKNOWLEDGMENT

Bayan ALMASRI gratefully acknowledges the funding of her joint PhD between University of Lille and Lebanese University by the PAUSE funding program. The mass spectrometer was funded by University of Lille, CNRS, Région Hauts-de-France and the European Regional Development Fund (ERDF). The authors gratefully acknowledge the financial support of the FTICR MS facility from the IR INFRANALYTICS FR2054 CNRS and of the EU_FTICR _MS project Grant Agreement 731077 funded by EU Horizon 2020 Research and Innovation Program.

REFERENCES

1. Das, S. K.; Eshkalak, S. K.; Chinnappan, A.; Ghosh, R.; Jayathilaka, W.; Baskar, C.; Ramakrishna, S., Plastic recycling of polyethylene terephthalate (PET) and polyhydroxybutyrate (PHB)—A comprehensive review. *Materials Circular Economy* **2021,** *3* (1), 9.
2. Al-Sabagh, A.; Yehia, F.; Eshaq, G.; Rabie, A.; ElMetwally, A., Greener routes for recycling of polyethylene terephthalate. *Egyptian Journal of Petroleum* **2016,** *25* (1), 53-64.
3. Pang, K.; Kotek, R.; Tonelli, A., Review of conventional and novel polymerization processes for polyesters. *Progress in polymer science* **2006,** *31* (11), 1009-1037.
4. Dziwiński, E. J.; Iłowska, J.; Gniady, J., Py-GC/MS analyses of poly (ethylene terephthalate) film without and with the presence of tetramethylammonium acetate reagent. Comparative study. *Polymer Testing* **2018,** *65*, 111-115.
5. Peez, N.; Becker, J.; Ehlers, S. M.; Fritz, M.; Fischer, C. B.; Koop, J. H.; Winkelmann, C.; Imhof, W., Quantitative analysis of PET microplastics in environmental model samples using quantitative 1 H-NMR spectroscopy: validation of an optimized and consistent sample clean-up method. *Analytical and bioanalytical chemistry* **2019,** *411*, 7409-7418.
6. Thomas, D.; Schütze, B.; Heinze, W. M.; Steinmetz, Z., Sample preparation techniques for the analysis of microplastics in soil—a review. *Sustainability* **2020,** *12* (21), 9074.
7. Müller, A.; Goedecke, C.; Eisentraut, P.; Piechotta, C.; Braun, U., Microplastic analysis using chemical extraction followed by LC-UV analysis: a straightforward approach to determine PET content in environmental samples. *Environmental Sciences Europe* **2020,** *32*, 1-10.
8. Piccardo, M.; Provenza, F.; Grazioli, E.; Cavallo, A.; Terlizzi, A.; Renzi, M., PET microplastics toxicity on marine key species is influenced by pH, particle size and food variations. *Science of the Total Environment* **2020,** *715*, 136947.
9. Stock, V.; Laurisch, C.; Franke, J.; Dönmez, M. H.; Voss, L.; Böhmert, L.; Braeuning, A.; Sieg, H., Uptake and cellular effects of PE, PP, PET and PVC microplastic particles. *Toxicology in vitro* **2021,** *70*, 105021.
10. Almasri, B.; Rolando, C., Identification and quantification of polyethylene terephthalate (PET) polyesters and microplastics combining soft chemical depolymerization by dimethylaminopropylamine (DMAPA) and analysis by MALDI FTICR & LC ESI Orbitrap mass spectrometry. *ChemRxiv®*, **2025**, submitted to *ACS Analytical Chemistry.*
11. Wang, L.; Nelson, G. A.; Toland, J.; Holbrey, J. D., Glycolysis of PET using 1, 3-dimethylimidazolium-2-carboxylate as an organocatalyst. *ACS Sustainable Chemistry & Engineering* **2020,** *8* (35), 13362-13368.
12. Di Serio, M.; Tesser, R.; Ferrara, A.; Santacesaria, E., Heterogeneous basic catalysts for the transesterification and the polycondensation reactions in PET production from DMT. *Journal of Molecular Catalysis A: Chemical* **2004,** *212* (1-2), 251-257.
13. Pardal, F.; Tersac, G., Comparative reactivity of glycols in PET glycolysis. *Polymer degradation and stability* **2006,** *91* (11), 2567-2578.
14. Howell, B. A.; Alrubayyi, A.; Ostrander, E. A., Thermal properties of charring plasticizers from the biobased alcohols, pentaerythritol and 3, 5-dihydroxybenzoic acid. *Journal of Thermal Analysis and Calorimetry* **2019,** *138*, 2661-2668.

15. Asan, A.; Isildak, I., Determination of major phenolic compounds in water by reversed-phase liquid chromatography after pre-column derivatization with benzoyl chloride. *Journal of Chromatography A* **2003,** *988* (1), 145-149.
16. Peterka, O. e.; Jirásko, R.; Vaňková, Z.; Chocholoušková, M.; Wolrab, D.; Kulhanek, J.; Bureš, F.; Holčapek, M., Simple and Reproducible Derivatization with Benzoyl Chloride: Improvement of Sensitivity for Multiple Lipid Classes in RP-UHPLC/MS. *Analytical Chemistry* **2021,** *93* (41), 13835-13843.
17. Porter, J.; Roberts, J.; Miller, G. J., Benzoylation of Tetrols: A Comparison of Regioselectivity Patterns for O-and S-Glycosides of d-Galactose. *The Journal of Organic Chemistry* **2024,** *89* (19), 14090-14097.
18. Jain, A.; Verma, K. K., Strategies in liquid chromatographic methods for the analysis of biogenic amines without and with derivatization. *TrAC Trends in Analytical Chemistry* **2018,** *109*, 62-82.
19. Qi, B.-L.; Liu, P.; Wang, Q.-Y.; Cai, W.-J.; Yuan, B.-F.; Feng, Y.-Q., Derivatization for liquid chromatography-mass spectrometry. *TrAC Trends in Analytical Chemistry* **2014,** *59*, 121-132.
20. Cardinael, P.; Casabianca, H.; Peulon-Agasse, V.; Berthod, A., Sample derivatization in separation science. Wiley-VCH Verlag GmbH & Co: 2015; pp 1725-1756.


Unlocking the secrets of PET diols
PET
Ethylene glycol
Butanediol
Cyclohexanedimethanol
?
• Swelling in THF at 66 °C, 2 days under N2
• NaH/methanolysis
• Quenching
• Extraction with petroleum ether
Evaporation to dryness
Petroleum ether phase
Methylated acids & aromatic diacids
Transamidation & MS analysis
Solid
Diols & Polyols
Benzoylation & LC MS analysis

Supporting information

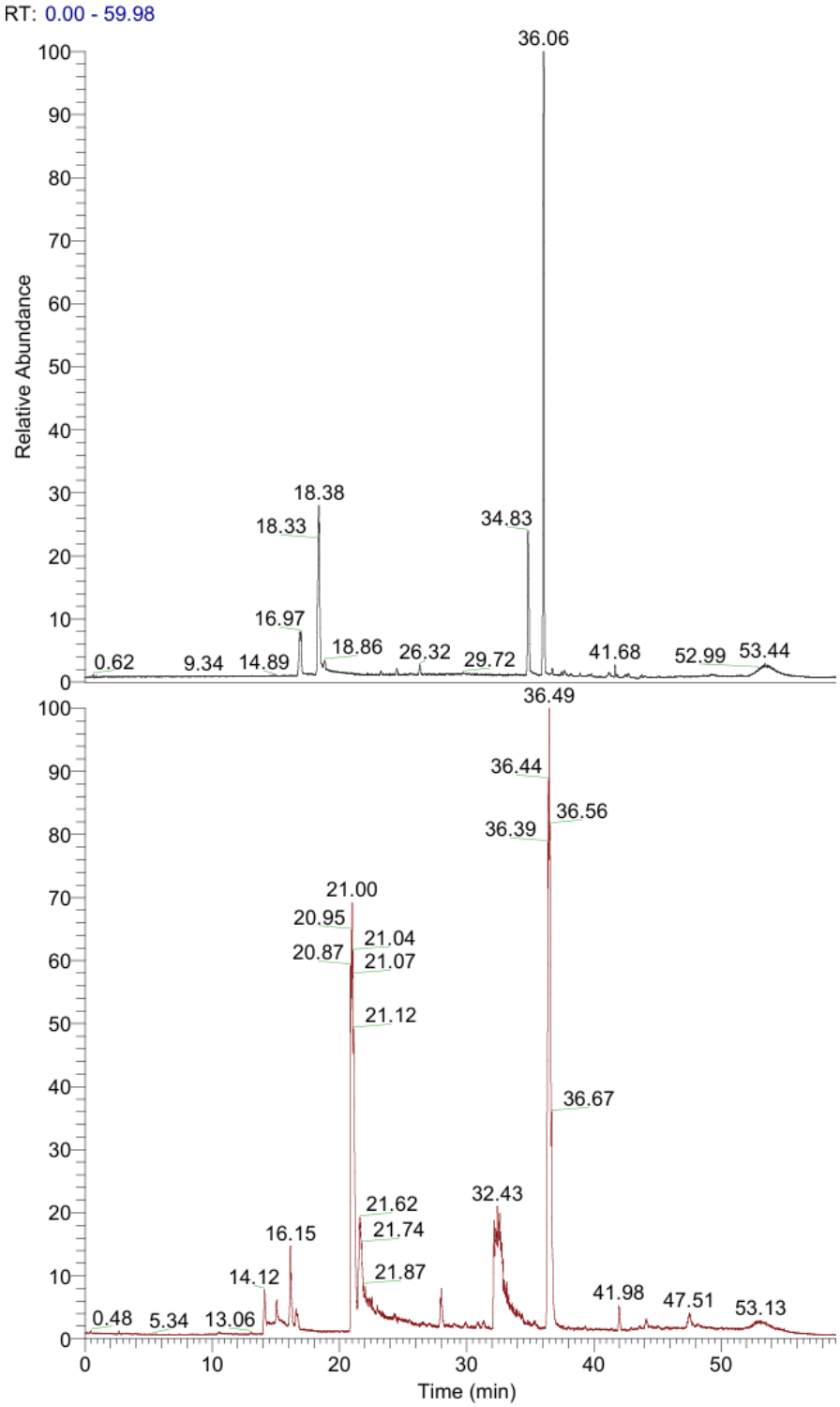


Figure S 1. LC chromatograms of ethylene glycol and 1,4-butanediol authentic samples respectively after benzoylation at 1 mg/mL (0-60 min).

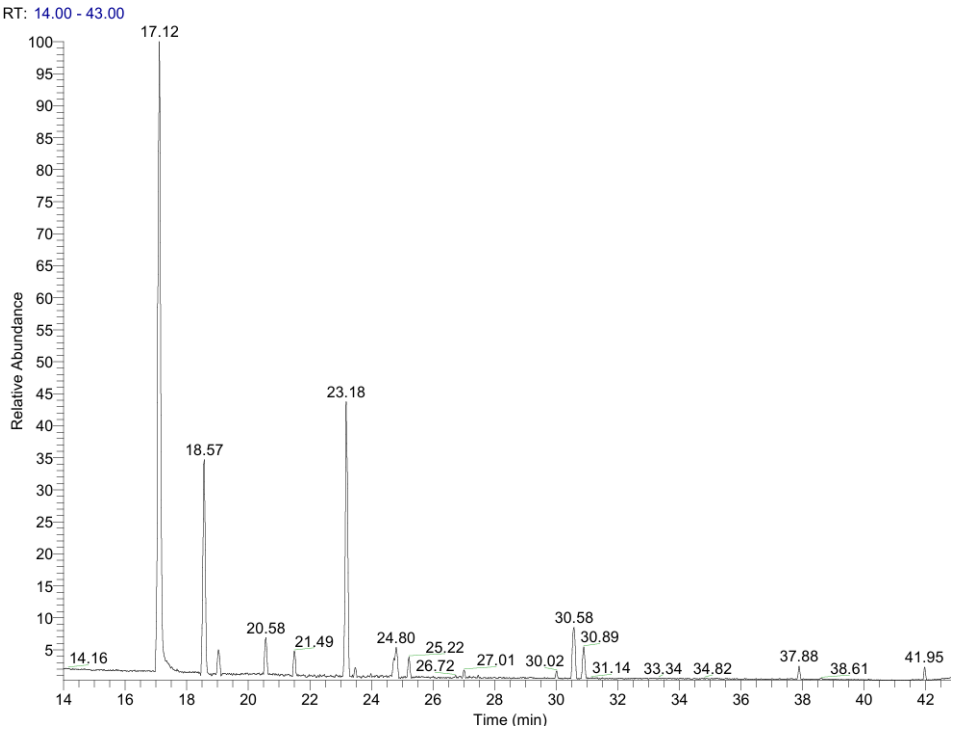


Figure S 2. LC chromatogram of PETG reference after benzoylation at 1 mg/mL (14-43 min).

Table S 1. LC-MS dynamics for the benzoylated authentic diols' samples (1 mg/mL).

Entry	*m/z*	Ethylene glycol			Butanediol		
		RT (min)	Error (ppm)	Intensity	RT (min)	Error (ppm)	Intensity
1	166.08626	34.83	-1.45	9.82E+06	32.43	-2.65	3.69E+07
2	180.10191	24.51	-1.05	6.38E+05	21.62	-1.05	3.04E+07
3	192.10191	36.06	-2.03	3.10E+07	33.53	0.05	3.84E+04
4	194.11756	28.43	0.31	9.49E+03	25.51	-1.75	7.79E+05
5	206.11756	0.00	0.00	0.00E+00	33.29	-0.68	6.83E+04
6	210.11247	18.38	-2.05	1.46E+07	15.99	0.33	2.70E+04
7	220.13321	38.93	0.50	1.03E+04	36.46	1.41	2.83E+06
8	224.12812	0.00	0.00	0.00E+00	16.59	-1.25	5.46E+06
9	238.10738	24.59	0.34	7.45E+03	0.00	0.00	0.00E+00
10	238.14377	23.28	-1.39	4.81E+05	21	1.13	1.09E+08
11	252.12303	26.32	-1.86	1.04E+06	15.03	-1.86	1.86E+06
12	254.13868	20.38	0.31	1.55E+04	20.94	1.10	1.24E+05
13	266.13868	29.66	-1.20	1.94E+03	26.55	-1.58	7.65E+03
14	280.15433	30.58	0.46	1.54E+03	28.02	-2.03	7.64E+06
15	292.19072	0.00	0.00	0.00E+00	31.1	-0.62	2.00E+04
16	298.164899	0.00	0.00	0.00E+00	0.00	0.00	0.00E+00

17	306.16998	0.00	0.00	0.00E+00	16.15	-0.39	6.21E+03
18	308.14925	0.00	0.00	0.00E+00	0.00	0.00	0.00E+00
19	313.15467	34.85	-2.01	2.19E+06	32.56	-0.42	2.37E+06
20	320.18563	0.00	0.00	0.00E+00	0.00	0.00	0.00E+00
21	322.1649	0.00	0.00	0.00E+00	0.00	0.00	0.00E+00
22	324.14416	0.00	0.00	0.00E+00	36.46	-3.52	6.73E+04
23	336.21693	0.00	0.00	0.00E+00	0.00	0.00	0.00E+00
24	338.15981	0.00	0.00	0.00E+00	0.00	0.00	0.00E+00
25	343.16523	36.74	-1.08	4.95E+05	34.17	-2.24	1.12E+06
26	357.18088	36.05	-1.18	4.28E+07	0.00	0.00	0.00E+00
27	371.19653	37.95	-1.00	8.53E+03	33.28	-0.46	3.76E+05
28	378.2275	0.00	0.00	0.00E+00	0.00	0.00	0.00E+00
29	381.250975	0.00	0.00	0.00E+00	0.00	0.00	0.00E+00
30	383.19656	0.00	0.00	0.00E+00	36.49	0.16	3.04E+05
31	385.21218	38.93	-0.83	1.23E+05	36.49	-0.57	1.70E+08
32	399.19145	40.83	0.63	2.83E+03	30.91	-1.13	1.58E+06
33	401.207098	0.00	0.00	0.00E+00	30.8	-1.25	4.53E+04
34	427.18636	0.00	0.00	0.00E+00	16.58	0.14	2.55E+03
35	429.20201	34.92	5.15	2.65E+03	20.25	-0.91	4.82E+03
36	439.25913	0.00	0.00	0.00E+00	47.58	-3.35	1.25E+04
37	443.21766	0.00	0.00	0.00E+00	35.98	-0.54	8.03E+03
38	445.23331	16.94	-4.24	1.47E+03	16.58	-1.10	8.76E+03
39	455.254049	0.00	0.00	0.00E+00	42.42	-1.87	1.06E+04
40	463.32922	29.7	3.93	9.49E+03	0.00	0.00	0.00E+00
41	471.24896	0.00	0.00	0.00E+00	37.43	-0.08	7.05E+04
42	520.29049	32.73	1.13	2.29E+03	0.00	0.00	0.00E+00
43	527.31156	0.00	0.00	0.00E+00	47.12	-2.54	9.23E+03
44	548.28541	0.00	0.00	0.00E+00	0.00	0.00	0.00E+00

Table S 2. LC-MS dynamics for the benzoylated PETG reference and PET fruit container (1 mg/mL).

Entry	*m/z*	PETG			PET fruit container		
		RT (min)	Error (ppm)	Intensity	RT (min)	Error (ppm)	Intensity
1	166.08626	17.12	-2.05	2.08E+07	16.91	-1.45	1.22E+07
2	180.10191	24.74	-1.05	7.56E+05	24.46	-1.61	5.21E+05
3	192.10191	18.56	-0.47	2.56E+04	36.06	-1.51	2.82E+06
4	194.11756	28.7	1.34	1.29E+04	28.83	0.31	2.06E+04
5	206.11756	27.01	1.75	4.34E+03	37.11	-0.19	5.22E+04
6	210.11247	18.57	-2.52	7.28E+06	18.35	-2.52	3.34E+06
7	220.13321	0.00	0.00	0.00E+00	24.94	5.50	3.96E+02
8	224.12812	21.49	-0.36	1.01E+06	21.25	0.09	8.60E+04
9	238.10738	24.8	-1.76	1.13E+06	24.54	-2.18	4.73E+06
10	238.14377	0.00	0.00	0.00E+00	24.54	0.71	3.11E+03
11	252.12303	23.18	-2.66	9.20E+06	22.92	-1.86	2.32E+06
12	254.13868	20.58	-1.65	1.45E+06	20.33	-0.87	3.09E+05
13	266.13868	28.68	0.68	2.84E+04	28.36	-1.20	6.17E+05
14	280.15433	32.5	0.82	2.68E+04	28.15	-1.32	3.84E+05
15	292.19072	30.58	-1.99	1.73E+06	0.00	0.00	0.00E+00
16	298.164899	21.76	1.00	1.65E+04	21.5	0.00	8.92E+03
17	306.16998	25.22	-0.72	8.15E+05	24.92	-1.37	1.80E+05
18	308.14925	21.14	-0.16	1.85E+04	20.88	0.16	7.13E+03
19	313.15467	37.18	-0.10	1.38E+03	36.74	-0.73	8.09E+04
20	320.18563	36.9	0.41	1.89E+04	0.00	0.00	0.00E+00
21	322.1649	23.99	-0.62	2.60E+05	25.81	0.00	4.81E+04
22	324.14416	28.41	0.49	4.98E+03	28.09	-0.74	8.22E+04
23	336.21693	30.73	0.39	1.59E+04	0.00	0.00	0.00E+00
24	338.15981	26.74	1.80	7.30E+03	26.4	-0.27	2.74E+03
25	343.16523	37.18	-0.20	4.51E+03	36.74	-0.79	2.59E+05
26	357.18088	36.55	3.86	7.91E+02	36.05	-1.18	4.39E+06
27	371.19653	20.18	0.08	1.34E+03	37.13	-0.19	5.41E+04
28	378.2275	32.21	0.00	4.75E+03	0.00	0.00	0.00E+00
29	381.250975	0.00	0.00	0.00E+00	46.69	0.20	4.10E+02
30	383.19656	0.00	0.00	0.00E+00	0.00	0.00	0.00E+00
31	385.21218	15.93	-1.09	6.35E+02	0.00	0.00	0.00E+00
32	399.19145	23.36	4.38	1.64E+03	0.00	0.00	0.00E+00

33	401.207098	0.00	0.00	0.00E+00	34.62	0.49	3.44E+04
34	427.18636	18.29	1.54	1.56E+03	0.00	0.00	0.00E+00
35	429.20201	0.00	0.00	0.00E+00	34.47	-1.61	4.23E+02
36	439.25913	24.84	0.75	2.47E+03	0.00	0.00	0.00E+00
37	443.21766	0.00	0.00	0.00E+00	37.13	0.59	3.84E+04
38	445.23331	0.00	0.00	0.00E+00	35.24	0.70	2.63E+03
39	455.254049	0.00	0.00	0.00E+00	39.66	-2.09	1.64E+03
40	463.32922	30.02	3.71	1.77E+04	29.65	2.85	1.13E+04
41	471.24896	0.00	0.00	0.00E+00	0.00	0.00	0.00E+00
42	520.29049	26.74	1.13	1.96E+05	32.7	1.71	3.08E+03
43	527.31156	0.00	0.00	0.00E+00	0.00	0.00	0.00E+00
44	548.28541	29.85	0.38	9.72E+03	30.05	1.48	7.46E+02

Table S 3. LC-MS dynamics for the benzoylated French carbonated bottles (1 mg/mL).

Entry	*m/z*	Sparkling water bottle			Cola bottle		
		RT (min)	Error (ppm)	Intensity	RT (min)	Error (ppm)	Intensity
1	166.08626	17.1	-4.46	1.67E+07	17.1	-2.05	2.09E+07
2	180.10191	24.73	-1.61	1.26E+06	24.74	-1.61	2.53E+06
3	192.10191	18.54	-0.47	5.13E+04	18.55	-0.99	6.78E+04
4	194.11756	28.7	0.31	5.36E+04	28.71	0.31	3.94E+04
5	206.11756	20.19	2.72	7.10E+03	21.51	2.23	2.48E+03
6	210.11247	18.57	-2.52	1.52E+07	18.55	-3.00	2.16E+07
7	220.13321	0.00	0.00	0.00E+00	0.00	0.00	0.00E+00
8	224.12812	21.5	-0.80	3.66E+05	21.51	-1.25	1.67E+06
9	238.10738	24.81	-2.18	4.75E+06	24.8	-1.34	2.61E+06
10	238.14377	24.81	2.39	2.40E+03	24.8	3.23	2.10E+03
11	252.12303	23.18	-2.66	7.67E+06	23.17	-2.66	4.81E+07
12	254.13868	20.56	-0.87	1.42E+06	20.57	-1.65	2.02E+06
13	266.13868	28.7	-1.20	6.31E+05	28.69	-2.33	3.49E+06
14	280.15433	28.47	-0.25	4.81E+03	28.46	-0.61	1.15E+05
15	292.19072	8.38	1.10	1.54E+04	30.56	0.41	9.43E+03
16	298.164899	21.75	0.33	1.38E+04	21.75	0.00	2.17E+04
17	306.16998	25.21	0.91	7.17E+03	25.23	0.26	1.96E+04
18	308.14925	21.13	0.49	2.71E+04	21.14	0.16	1.28E+05
19	313.15467	35.27	-0.73	9.17E+03	35.24	-0.73	1.27E+04
20	320.18563	13.83	1.03	3.58E+03	14.97	-1.16	6.15E+02
21	322.1649	23.98	-0.93	9.62E+03	23.99	0.00	2.93E+04
22	324.14416	28.43	0.19	5.66E+04	28.42	0.19	2.54E+04
23	336.21693	0.00	0.00	0.00E+00	15.6	0.98	4.20E+03
24	338.15981	26.74	0.33	8.73E+03	26.73	0.03	2.68E+05
25	343.16523	37.19	-0.50	1.46E+04	37.18	-0.20	9.34E+03
26	357.18088	17.92	3.30	6.94E+02	36.6	3.02	6.58E+02
27	371.19653	20.19	1.70	2.95E+04	37.6	-0.46	2.06E+03
28	378.2275	17.15	-0.26	2.92E+03	0.00	0.00	0.00E+00
29	381.250975	0.00	0.00	0.00E+00	0.00	0.00	0.00E+00
30	383.19656	19.14	-1.67	2.10E+03	0.00	0.00	0.00E+00
31	385.21218	21.31	-2.39	6.71E+02	0.00	0.00	0.00E+00
32	399.19145	0.00	0.00	0.00E+00	0.00	0.00	0.00E+00

33	401.207098	35.06	-1.50	3.57E+03	35.07	1.24	2.40E+03
34	427.18636	0.00	0.00	0.00E+00	0.00	0.00	0.00E+00
35	429.20201	20.23	-0.68	1.62E+04	20.22	1.42	2.73E+04
36	439.25913	26.61	2.12	2.50E+03	25.75	-0.39	5.89E+03
37	443.21766	37.57	-1.90	2.80E+03	37.58	-1.67	4.32E+03
38	445.23331	29.01	0.02	9.42E+02	25.94	4.96	1.06E+03
39	455.254049	20.63	1.43	5.49E+02	0.00	0.00	0.00E+00
40	463.32922	30.01	3.93	2.77E+04	30	3.50	3.69E+04
41	471.24896	50	-2.84	3.97E+02	0.00	0.00	0.00E+00
42	520.29049	33.1	-1.94	4.34E+02	33.07	1.52	1.39E+04
43	527.31156	53.9	2.77	4.01E+02	48.53	4.10	4.43E+02
44	548.28541	0.00	0.00	0.00E+00	0.00	0.00	0.00E+00

Chapter 4: Additives and enchased products in PET

Introduction: Additives

Additives are intentionally added substances (IAS), incorporated in plastics to improve their properties and increase their lifetime against the external possible degradation phenomena.

Additives are classified in many categories:

1- Plasticizers are added to improve the mechanical properties of polymers; the most common ones are phthalates and adipates.[1]
2- Thermal stabilizers are used to reduce the degrading effects of heating.[2]
3- Antioxidants are used to protect plastics against oxidation reactions.[3]
4- UV stabilizers are used to protect plastic films against UV irradiation especially sunlight.[4]
5- Flame retardants are added to avoid the ignition and burning of plastics.[5]
6- Dyes are added to provide a specific coloration of plastics.[6]
7- Coupling agents are incorporated in plastics to improve its bonding to inorganic filler materials or fibers.[7]
8- Slip agents are used to reduce friction between plastic films or films with other materials; to minimize adhesion between the mold and injection molded polymer.[8]
9- Crosslinking agents are usually used to enhance the formation of covalent bonding between adjacent polymer backbones. It may create an interconnected three-dimensional structure.[9]
10- Others

Once plastics are degraded by weathering, the additives can be migrated from food packaging objects (food containers, water bottles, etc.) directly into the alimentation or beverages leading to their consumption at the end by humans.

Some additives are harmful for our health after ingestion such as Bisphenol A which is an endocrine-disrupting chemical and already found in water bottles. And others are constituting pollution source such as benzotriazole UV stabilizers.[1,10]

The following table shows some low-weight additives identified in beverages.

Additive name	Information	Formula [M]	*m/z* $[M+H]^+$	Reference
Thiodiethylene glycol	Plasticizer in beer bottles	$C_4H_{10}O_2S$	123.0474	[11]
2-Aminobenzamide/ anthranilamide	Acetaldehyde scavenger	$C_7H_8N_2O$	137.07094	[12, 13, 14]
2-Carboxyethyl(methyl) phosphinic acid	Flame retardant	$C_4H_9O_4P$	153.0311	[15]
Ethyl-4-ethoxybenzoate	Polymer modifier/ fatty acid derivative	$C_{11}H_{14}O_3$	195.1016	[16]

The aim of this work here is to detect a large number of additives present in PET films after depolymerization to predict their possible migration. This work has been performed on different types of packaging objects with many contents such as water, carbonated liquids, oils, juices, milk, beer, alcohol, wine, etc. The enchased products remaining in PET films were also successfully identified.

References

1- Higuchi, A.; Yoon, B. O.; Kaneko, T.; Hara, M.; Maekawa, M.; Nohmi, T., Separation of endocrine disruptors from aqueous solutions by pervaporation: dioctylphthalate and butylated hydroxytoluene in mineral water. *Journal of applied polymer science* 2004**,** *94* (4), 1737-1742.

2- Allen, N. S., Edge, M., Corrales, T., Childs, A., Liauw, C. M., Catalina, F., ... & Aldcroft, D. (1998). Ageing and stabilisation of filled polymers: an overview. *Polymer Degradation and Stability*, *61*(2), 183-199.

3- Halliwell, B. (1996). Antioxidants: the basics-what they are and how to evaluate them. *Advances in pharmacology*, *38*, 3-20.

4- Wypych, A., & Wypych, G. (2025). *Databook of UV stabilizers*. Elsevier.

5- Taib, M. N. A. M., Antov, P., Savov, V., Fatriasari, W., Madyaratri, E. W., Wirawan, R., ... & Hussin, M. H. (2022). Current progress of biopolymer-based flame retardant. *Polymer Degradation and Stability*, *205*, 110153.

6- Kühlborn, J., Danner, A. K., Frey, H., Iyer, R., Arduengo, A. J., & Opatz, T. (2017). Examples of xylochemistry: colorants and polymers. *Green Chemistry*, *19*(16), 3780-3786.

7- Xie, Y., Hill, C. A., Xiao, Z., Militz, H., & Mai, C. (2010). Silane coupling agents used for natural fiber/polymer composites: A review. *Composites Part A: Applied Science and Manufacturing*, *41*(7), 806-819.

8- Minami, I. (2017). Molecular science of lubricant additives. *Applied sciences*, *7*(5), 445.

9- Tillet, G., Boutevin, B., & Ameduri, B. (2011). Chemical reactions of polymer crosslinking and post-crosslinking at room and medium temperature. *Progress in polymer science*, *36*(2), 191-217.

10- Khare, A., Jadhao, P., Vaidya, A. N., & Kumar, A. R. (2023). Benzotriazole UV stabilizers (BUVs) as an emerging contaminant of concern: a review. *Environmental Science and Pollution Research*, *30*(58), 121370-121392.

11- Habschied, K.; Mastanjević, K.; Šibalić, M.; Krstanović, V.; Galić, V., A Survey on Detection of Plastic-Related Chemicals in Beer Packaged in PET Using FT-IR Technology. Beverages 2022, 8 (4), 73.

12- Yilmaz, M. A.; Temel, H., Screening of Polymer Additives in Drinking Water Stored in PET Bottles by UHPLC-ESI-IT-TOF MS. J Environ Sci Eng A 2016, 5, 59-64.

13- Welle, F., The facts about PET. URL: https://www. petcore-europe. org/images/news/pdf/factsheet_the_facts_about_pet_dr_frank_welle_2018. pdf (Accessed June 13, 2021) 2018.

14- Franz, R.; Welle, F. In Investigation of non-intentionally added substances (NIAS) in PET bottles and closures, Poster Presentation at the 4th International Symposium on Food Packaging, 19e21 November, Prague, Czech Republic, 2008.

15- Levchik, S. V.; Weil, E. D., Flame retardancy of thermoplastic polyesters—a review of the recent literature. Polymer International 2005, 54 (1), 11-35.

16- Bach, C.; Dauchy, X.; Severin, I.; Munoz, J.-F.; Etienne, S.; Chagnon, M.-C., Effect of temperature on the release of intentionally and non-intentionally added substances from polyethylene terephthalate (PET) bottles into water: chemical analysis and potential toxicity. Food Chemistry 2013, 139 (1-4), 672-680.

Article 3

Discovering the secrets of PET-labeled food packaging objects and bottles including their oligomers, additives and possible enchased products

ABSTRACT: Additives are widely present in plastics. They are used to improve plastics' properties such as plasticizers to improve their mechanical properties or anti-UV agents to extend the lifetime of plastics. Upon degradation of plastics in our environment due to ageing factors, additives may leachate from food packaging into beverages constituting a sanitary problem or from container into ecosystems affecting water sources such as rivers and seas so the life of their fauna and flora. Most of food packaging objects including different bottles and containers with various contents are made of polyethylene terephthalate (PET). So, it is crucial to identify the additives in PET objects and classify them according to bottle's content and additives type to predict their possible migration into human bodies and ecosystems. This work responds to these concerns by using an innovative depolymerization method on PET combined with the analysis by liquid chromatography coupled to mass spectrometry LC-MS. Many PET bottles of different contents (oil, juice, milk, beer, alcohol, wine, liqueur, etc.) and fruit containers of different colors have been studied. Their content in oligomers and diols have been described and their additives present in traces or not were detected and classified: Plasticizers, thermal stabilizers, antioxidants and UV stabilizers, flame retardants, dyes, coupling agents, lubricants/slip agents, crosslinking agents, etc. Furthermore, the enchased products in PET films were identified enabling bottles differentiation according to their remaining content inside the amorphous pores of plastics. This methodology can be used on other plastics in blends with polyesters or co-polyesters.

Keywords: PET, additives, bisphenol, PFAS, FCC, IAS, NIAS, depolymerization, LC-MS.

Polyethylene terephthalate (PET) polyester is widely used in food packaging because of its attractive properties such as its lightweight, possible colorless nature to see through, gas hindrance properties against CO_2 and moisture, short shelf life and single-use nature. PET is easily blended with other polymers and more recycled than other plastics.[1-2] PET packaging objects found transparent or colored are numerous covering a wide range of contents such as water, carbonated drinks, juice, milk, tea,[2-3] beer,[4] wine,[5] alcohol,[6] fruits and vegetables, etc.[7]

The manufacturing of PET necessitates the intentional addition of food contact chemicals (FCCs) that includes the monomers forming its polymeric chain, mainly terephthalic acid and ethylene glycol, as well as catalysts and additives.[2] These intentionally added substances (IAS) maybe accompanied by the presence of non-intentionally added substances (NIAS) that includes PET degradation products and modified additives after weathering or metal traces remaining from catalysts and other contaminants.[8-10] These compounds may migrate to the bottled content after degradation of PET packaging by natural weathering or misuse of packaging.[2,11-12]. For example, carbonyl compounds such as formaldehyde and acetaldehyde may migrate from PET bottles after thermo-mechanical and thermo-oxidative degradation.[13] So, the use of recycled PET (rPET) in food packaging industry adds more concerns than raw PET in term of quality and safety of the final manufactured product.[2] In fact, PET typically contains Sb levels in the range of 170-300 mg/kg due to antimony trioxide (Sb_2O_3).[14-15] Fortunately, only a small fraction of the Sb contained in PET is released into the bottled water.[16] Other metals' traces such as Co, Cr, Fe and Mn, with 27 mg/kg, 0.1 mg/kg, 1.3 mg/kg and 0.3 mg/kg respectively, have been found in PET bottles.[14] Initially, many additives maybe introduced to improve PET chemical, physical and mechanical properties. For instance, plasticizers are used to improve polymer's flexibility and are constituted mainly of phthalates (and DEHA). Their release in bottled water is related to sunlight exposure, pH, storage conditions and the type of water as phthalate levels detected in still mineral water were slightly higher than those in sparkling water. Plasticizers may come from bottling lines, cap-sealing resins, water facilities or from PET itself including PhA, DMP, DEP, DiBP, DBP and DEHP.[17-22] Other additives may be used such as stabilizers,[23] anti-UV agents,[24] antistatic agents,[25] slip and anti-blocks additives,[26] flame retardants (halogen-, phosphorus-halogen-, phosphorous-, sulfur-containing additives and inorganic flame retardants),[27-28] antibacterial additives[29] or biocides,[30] colorants (azo-dyes and pigments)[31-32], etc. The structures of some PET additives are shown in Figure 1. Some studies have been performed on certain packaging objects for assigning specific additives leaching from PET in only some drinks. From safety concerns related to PET & rPET, this work aims to characterize for the first time a package of PET degradation products focusing on oligomers, additives and enchased products in different colored or transparent packaging objects from various contents (oil, juice, milk, beer, alcohol, wine, etc.) and manufacturing countries. This will be done using our recent analytical approach combining soft chemical depolymerization with advanced mass spectrometry.[33] These data will allow the prediction of health impacts resulting from leaching of these compounds into food and drinks.

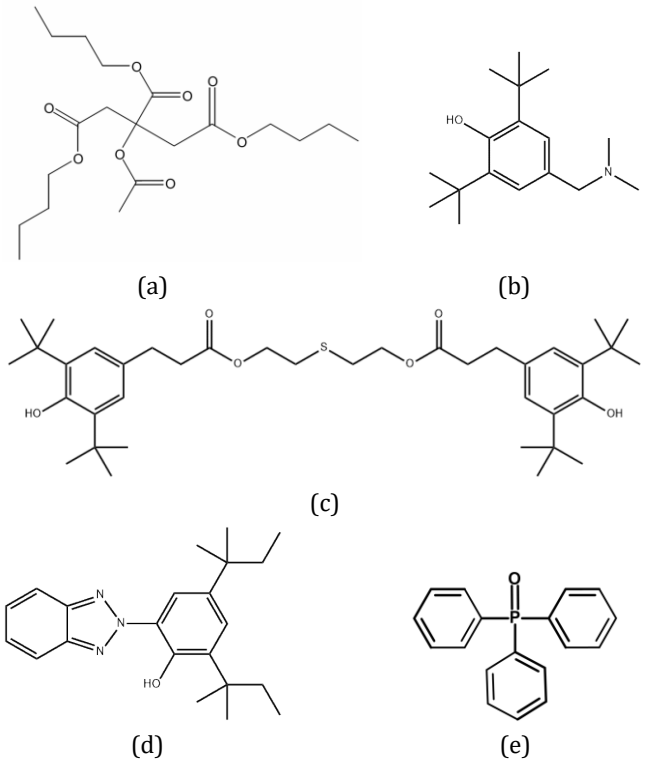


Figure 1. Chemical structure of some additives found in PET packaging objects. (a): Acetyl tributylcitrate plasticizer (Citroflex A-4), (b): Ethanox 703 antioxidant, (c): Irganox 1035 antioxidant, (d): Tinuvin 328 UV absorbing agent, and (e): Triphenylphosphine oxide (TPPO) flame retardant.

EXPERIMENTAL SECTION

Chemicals. All aqueous solutions were prepared from ultrapure grade water obtained by water filtration with a two stages Millipore system (Milli-Q® Academic with a cartouches Q-Gard 1 and Progard 2, Merck Millipore, Burlington, Massachusetts, United States). All solvents were MS analytical grade. All solvents and chemicals were purchased from Merck (Merck KGaA, Darmstadt, Germany) and used without further purification. 3-(Dimethylamino)-1-propylamine (DMAPA) 99%, 1,1,1,3,3,3-hexafluoro-2-propanol (HFIP) ≥ 99%, dimethyl terephthalate ≥ 99%, dimethyl phthalate ≥ 99% and dimethyl isophthalate 99% were used as received.

Samples. Polyethylene terephthalate samples were packaging objects, containers and bottles, naturally aged. The studied containers were French fruit containers of three different colors: Recyclable transparent container (FC transparent); 100% recyclable black container of recycled PET or rPET (FC black) and recyclable blue container 100% rPET (FC blue).

The studied bottles were collected from many countries and contained different contents such as water, sparkling water, sparkling drinks, juices, milk, oils, liqueur, alcohol, wine and beer. The details of these bottles are shown in Table 1.

Table 1. Studied PET bottles collected from different countries with different contents and brands. The description of bottles including their volume and PET recyclability are given as written on each bottle label.

Bottle name indicating its content	Country	Volume	PET type & other content description
Water SP	Spain	75 cL	100% r-PET
Water QA	Qatar	330 mL	-
Water-S FRA	France	1.25 L	-
Water-S SP	Spain	1.0 L	-
Cola-1 FRA	France	1.5 L	100% rPET
Cola-2 FRA	France	1.25 L	100% recyclable
Cola-1 US	United States	20.0 oz (591 mL)	-
Juice FRA1	France	900 mL	50% rPET at least; juice %: 86% Orange & 14% mango
Juice FRA2	France	330 mL	- ; fruits juice
Juice SP	Spain	750 mL	100%rPET, 100% recyclable
Milk SP	Spain	1 L	-
Oil FRA1	France	1 L	- ; olive oil
Oil FRA2	France	1 L	- ; content : 80% Rapeseed & 20% olive oils
Liqueur FRA	France	30 mL	-
Alcohol FRA	France	3 cL	-
Beer AUT	Austria	33 cL	-
Wine FRA1	France	18.7 cL	-
Wine FRA2	France	18.7 cL	-

Samples preparation. PET samples were washed 8 times with ultrapure water to remove bottle's content traces and other superficial impurities. Only oil bottles were washed with petroleum ether. PET fragments were then left to dry and cut into small pieces of around 2.5 mm × 2.5 mm size. Three bottles were constituted of 3 different layers of plastics which are the beer and wine bottles indicated as internal: Separating the bottle content of the other layer, central: Between 2 layers, and external: In contact with air.

PET depolymerization. In a 2-mL glass tube, 25 mg of PET microplastics were solubilized in 400 mg of HFIP overnight. The content of the tube was transferred to a 50-mL flask then 1 mL of 3-(dimethylamino)-1-propylamine (DMAPA) was added. The solution was left at 58 °C under N_2 for 1 day. The mixture was quenched by 400 µL of formic acid then transferred to a 5 mL Falcon™ conical tube (Corning, NY, USA), added to 2 mL of ultrapure water and extracted four times with 2 mL of ethyl acetate. This liquid-liquid extraction was performed by centrifugation. at 10,000 rpm during 5 minutes at room temperature using Beckman-Coulter (Brea, CA, USA) Allegra® X-30R centrifuge with the corresponding C1015 fixed angle conical tube rotor. The

obtained ethyl acetate phases were evaporated under nitrogen at room temperature and stored.[33]

Analytical method. For MS analysis, the organic fractions were solubilized in methanol at 1 mg/10 µL then diluted 100 times in acetonitrile/water/formic acid 5/95/0.1 (v/v/v). For better visualization of additives in some samples, the prepared solution at 1 mg/10 µL was directly used for analysis.

LC-ESI MS analysis. LC-MS analyses were performed on an Orbitrap LTQ XL mass spectrometer hyphenated to a Dionex Ultimate 3000 HPLC System (ThermoFisher Scientific, Bremen, Germany). The analysis was performed using a 60 min gradient at a flow rate of 0.50 mL.min^{-1} on a Zorbax RRHD SB-C18 column (2.1 µm i.d. × 150 mm) packed with 1.8 µm beads pores with 80 Å pore size from Agilent Technologies (Santa Clara, CA, USA) placed in an oven at a temperature of 50 °C. The depolymerized PET products were separated using a multi-step gradient with a mobile phase of 5% acetonitrile in acidified water, 0.1% formic acid (solution A) and 75% acetonitrile in acidified water, 0.1% formic acid (solution B). The gradient started by 100% of solution A for 5 min then increased to 30% A, 70% B until 35 min. It increased more to 100% of solution B at 40 min holding this mobile phase until 50 min then it returned to the initial conditions at 55 min holding 100% of solution A for the remaining 5 min. The LC runs were acquired in positive ion mode using ESI ionization with a non-heated source (spray voltage 4.50 kV, sheath gas flow 22 mL.min^{-1}, auxiliary gas flow 12 mL.min^{-1}). The MS scans were acquired from *m/z* 200 to 1,000 with a 60,000 resolution at *m/z* 200. Data acquisition and interpretation were performed using FreeStyle™ 1.8SP2 QF1 software (Thermo Fisher Scientific).

RESULTS AND DISCUSSIONS

PET daily life bottles and containers of different contents have been studied using soft chemical depolymerization combined to LC-MS. This method has been first used to differentiate water, sparkling water and soft drinks bottles without detailed investigation of their additives.[33] In this work, PET additives and minor compounds will be further studied not only for water and soft drinks bottles but also for oils, juices, milk, liqueur and alcoholic PET bottles (beer, wine and alcohol). Indeed, PET fragments pre-solubilized in HFIP were transamidated by DMAPA for derivatization then analyzed by LC Orbitrap-MS using ESI ionization suitable for analyzing traces of compounds.

The elution gradient used with the two solvents acetonitrile 5%, 0.1% formic acid (solvent A) and acetonitrile 75%, 0.1% formic acid (solvent B) was efficient to separate in 1 hour the peaks in the complex mixture of PET depolymerized products. LC-MS results were detected with high accuracy (0-5 ppm) and high resolution (~60,000 at *m/z* 200) while validating the isotopic ratios of all detected peaks even the traces of additives. An example of this correct isotopic LC-MS ratio is given in SI, Figure S1 for an accuracy of 3.6 ppm.

As expected, all depolymerized samples showed the presence of the main depolymerization marker [$C_{18}H_{30}N_4O_2$ + H^+] at *m/z* 335.244 corresponding to the di-derivatized terephthalic acid. Only the central layer of Wine FRA2 bottle did not contain this marker indicating a different chemical composition of this plastic. This main peak was the most intense in Water-S SP bottle with 97% of its major composition (SI, Table S1).

This *m/z* appeared in some bottles at only around 0.9 min such as Water-S FRA, Juice SP, Milk SP, Beer AUT-central and both oil bottles. However, it appeared under two retention times around 0.68 min and 0.9 min in the other remaining bottles. Around 0.9 min, the main depolymerization marker was the most intense in the Water SP bottle made of 100% recycled PET with 5.51E+06 of relative intensity. At around 0.68 min, it was the most intense in liqueur FRA and Wine FRA2-external with 1.15E+07 and 1.20E+07 of relative intensities respectively.

To decipher the chemical nature of these peaks having same *m/z* 335.244, three dimethyl esters' isomers were depolymerized: Dimethyl phthalate, isophthalate and terephthalate. The LC-MS runs for each dimethyl ester were performed to determine their exact retention time. Injected separately, dimethyl phthalate, dimethyl isophthalate and dimethyl terephthalate appeared di-derivatized at 0.66 min, 0.70 and 0.72 min respectively. An additional peak at 1.41 min for *m/z* 251.139 appeared in the depolymerized dimethyl phthalate. Injected simultaneously at 1 mg/mL in an isochoric mixture after depolymerization, a wide peak has been appeared at 0.73 min corresponding to *m/z* 335.244. This last sample was diluted 10 and 100 times as the isomers were not separated: At 0.1 mg/mL, the phthalic peak at 0.66 min was well separated but 2 maximums at 0.81 and 0.85 min of an overlapping peak remained. At 0.01 mg/mL, only 2 peaks remained at 0.66 and 0.85 min for phthalic and terephthalic dimethyl esters respectively (SI, Figure S2). This shows that some studied bottles contain simultaneously terephthalic and phthalic acid isomers, this last may be due either to the use of PET modified by *O*-phthalic acid units,[34] or to the presence of di-derivatized phthalic additives, or even to the type of recycling process used with PET melting and molding procedures.[35-36]

Oligomers of the main depolymerization marker have been appeared in all bottles with different intensities. Taking to account the percentage of relative intensities' sum of its dimer, trimer and tetramer appearing at *m/z* 527.286, 719.329, 911.371 around 14 min, 21.4 min and 26.9 min respectively, these oligomers constituted only 0.01% of Water-S SP bottle's major composition (SI, Table S1).

The terephthalic acid was found mono-derivatized with its ethylene glycol unit [$C_{15}H_{22}N_2O_4$ + H^+] (*m/z* 295.165) around 3.9 min in all bottles confirming the depolymerization efficiency. Its abundance registered 0.02% of Water SP bottle's major composition.

The rate of depolymerization of each packaging object was estimated by the sum of abundances of both peaks: Mono- and di-derivatized PET monomers' peaks according to the following equation:

$$Depolymerization\ rate = \sum_{n\,(DMAPA)=1}^{n\,(DMAPA)=2} PET\ derivatized\ monomers\ abundance$$

Where the abundance of PET derivatized monomers is calculated considering the sum of relative intensities of the mono- and di-derivatized monomers in comparison to the major composition of the depolymerized mixture according to the following formula:

$$PET\ derivatized\ monomers\ abundance = \frac{\sum_{n\,(DMAPA)=1}^{n\,(DMAPA)=2} PET\ derivatized\ monomers\ relative\ intensities}{Major\ composition\ peaks\ relative\ intensities} \times 100$$

All other compounds abundances are calculated by this same formula.

This rate reflected the efficiency of our depolymerization methodology on the different studied bottles. This depolymerization was very efficient reaching 97% on Spanish water and milk bottles as well as Qatar water bottle as shown in Table 2. The Spanish water bottle was commercialized as 100% rPET, but no indication of manufacturing PET material was indicated for the two other bottles suggesting that they were made of 100% rPET. However, two other bottles, Cola-1 FRA and Juice SP, were made also of total recycled PET but their depolymerization rate was 60% and 49% respectively. This is due to the high abundance of total dimers and oligomers present in their mixtures; they constituted 37% and 42% of the major composition of Cola-1 FRA and Juice SP respectively (SI, Table S1).

Among the studied packaging objects, most of them revealed the presence of cyclohexanedimethanol presented by the sum of both mono- [$C_{21}H_{32}N_2O_4$ + H^+] and di-transamidated terephthalic acid [$C_{34}H_{48}N_4O_6$ + H^+] with cyclohexanedimethanol at *m/z* 377.243 (18.5 min) and *m/z* 609.365 (21.7 min) respectively. Indeed, the three fruit containers contained this diol in high intensity, up to 11% for the black container's major composition. This diol was intense in soft drinks and juice bottles, up to 4% of their major composition. It was present in traces in the other PET bottles. However, this diol was totally absent in the central layers of Beer AUT and Wine FRA1, the internal layer of the beer bottle in addition to the Spanish sparkling water bottle and the Qatar water bottles.

Diethylene glycol (DEG) was also presented by the di-derivatized product [$C_{30}H_{42}N_4O_7$+ H^+] at almost 13.9 min (*m/z* 571.313). It has been detected in all bottles except the both central wine layers and the Spanish sparkling water bottle. This confirms the composition's difference according to PET manufacturing country and brand (SI, Table S1).

Table 2: Depolymerization rate of bottles in order.

Bottle	Depolymerization rate (%)
Water-S SP	96.62
Water QA	95.76
Milk SP	95.40
Wine FRA2-external	79.69
Liqueur FRA	77.48
Wine FRA2-internal	77.37
Wine FRA1-internal	67.35
Cola-1 FRA	59.48
Cola-2 FRA	58.20
Wine FRA1-external	51.59
FC black	50.81
Cola-1 US	50.37
Juice SP	49.41
Juice FRA2	49.30
Wine FRA1-central	45.08
Water SP	44.86
Juice FRA1	44.04
FC transparent	40.11
FC blue	37.56
Beer AUT-external	36.52
Water-S FRA	36.36
Olive FRA1	36.02
Rapeseed FRA2	30.12
Alcohol FRA	28.41
Beer AUT-internal	28.21
Beer AUT-central	11.11
Wine FRA2-central	0.00

Moving into the deciphering of wine and beer bottles' layers, the external beer layer showed higher extraction yield than the other layers. For beer and wine bottles, the internal layer was less extracted than the corresponding external and central layers (Figure 2). The analysis of chromatograms of the external layers confirmed their constitution of PET as indicated on the label of wine and beer bottles. Indeed, the depolymerization rate was 37%, 52% and 80% for Beer AUT, Wine FRA1 and Wine FRA2 external layers respectively and they contained cyclohexanedimethanol and diethylene glycol diols.

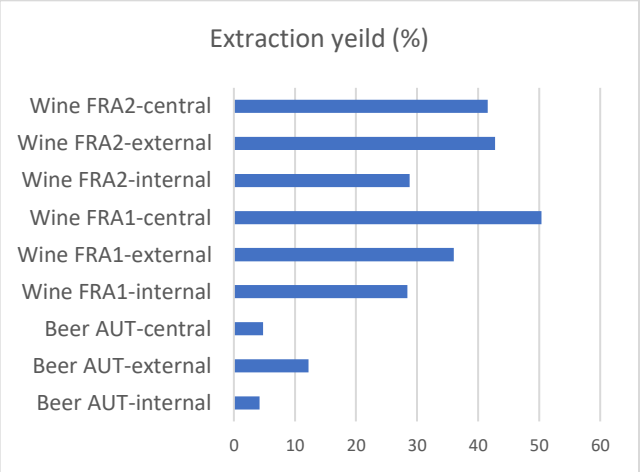


Figure 2. Extraction yield of the 3 layers of wine and beer bottles (in %).

Both internal layers of wine bottles had similar extraction yield of 28%. They were constituted also of PET with traces of cyclohexanedimethanol and diethylene glycol. However, the internal layer of beer was formed of PET with diethylene glycol compounds.

The central layers of these bottles were very different in composition. Indeed, Wine FRA2 contained both diols but Wine FRA1 have not contained any additional diols. The beer central layer was exempt of cyclohexanedimethanol.

A comparison of the chromatograms of the 3 layers of bottles has been achieved (Figure 3). Indeed, the central layers of wine and beer bottles having low depolymerization rate were differentiated by the presence

of some common peaks that were absent in the two other layers. For instance, hexaethylene glycol with 2 terephthalic acids was detected di-transamidated and oxygenated [$C_{38}H_{56}N_4O_{12}$+ H^+] at 21.45 min (*m/z* 761.398) only in the central layers of these bottles.

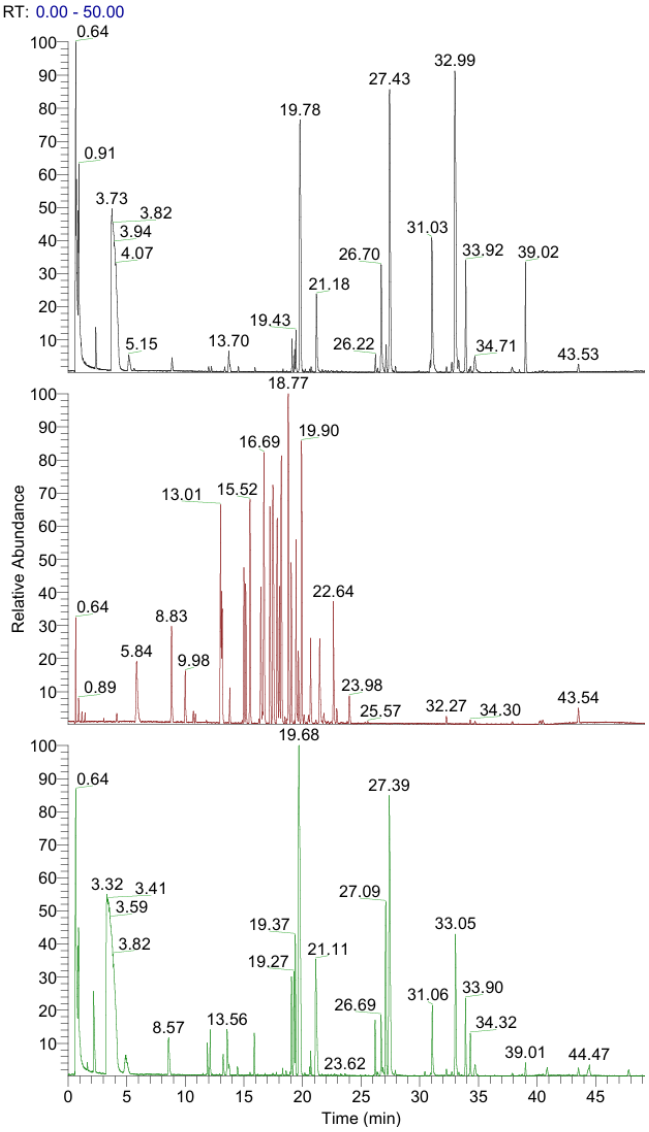


Figure 3. LC chromatograms of external, central and internal layers respectively of Beer AUT bottle (0-50 min).

Deciphering the total composition of bottles and containers means detecting their minor compounds in addition to the polymeric and oligomeric nature and diols already described.

More than 350 additives have been detected with high accuracy (0-5 ppm) even when they were present in traces in LC chromatograms. Their presence was confirmed like previously and after direct derivatization of esters compounds with DMAPA. The detected additives were classified in many categories: Plasticizers, thermal stabilizers, antioxidants and UV stabilizers, flame retardants, retarders, dyes, coupling agents, lubricants/slip agents, crosslinking agents, etc. Some of these additives are shown in Table S2.

Some additives were present in all bottles. For example, acetyl tributylcitrate (Citroflex A-4) of chemical formula $C_{20}H_{34}O_8$ appeared at *m/z* 403.233, 43 min in all bottles and containers (Figure 1, (a)). This compound is known as plasticizer for food contact materials.[37,38] This tetra-ester has been also confirmed by its two forms di-derivatized at *m/z* 459.318 and tri-derivatized at *m/z* 487.360.

An oxygen scavenger known as MXD6 ($C_{14}H_{20}N_2O_4$) from poly(hexamethylene adipamide) and poly(meta-xylene adipamide)[39-41] has been found in all packaging objects at *m/z* 281.1495.

The degraded oxygenated product of the antioxidant Irgafos®168 oxide/tris[2,4-bis(2-methyl-2-propanyl) phenyl] phosphate ($C_{42}H_{63}O_4P$)[37, 42] was detected in all studied PET objects at *m/z* 663.454. Traces of the original antioxidant ($C_{42}H_{63}O_3P$) before degradation remained resistant only in the external layer of beer bottle, internal layer of Wine FRA1 bottle and Water-S bottle.

Another antioxidant Ethanox 703 ($C_{17}H_{29}NO$) was present in all bottles except cola bottles at *m/z* 264.232 but it was absent in all containers (Figure 1, (b)).

Triphenylphosphine oxide (TPPO) of chemical formula $C_{18}H_{15}OP$ was present in all packaging objects except the transparent fruit container (Figure 1, (e)). This flame retardant[28] appeared at *m/z* 279.093.

So, according to PET manufacturer and the policies of countries concerning its fabrication and to the content of the final bottle, additives were different in bottles and containers. Some additives were specific for some packaging objects such as dicyclohexyl phthalate/Morflex 150 ($C_{20}H_{26}O_4$) which is a plasticizer; it was appeared at *m/z* 331.190 only in the external beer layer.

The UV absorbing agent 2-(2H-benzotriazol-2-yl)-4,6-ditertpentylphenol commercially known as Tinuvin 328 ($C_{22}H_{29}N_3O$) appeared at *m/z* 352.238 only in Oil FRA1 bottle and Wine FRA2-central layer (Figure 1, (d)). However, another antioxidant was specific for Oil FRA2 bottle and Wine FRA2-external: 2,2'-Methylenebis(4-methyl-6-tert-butylphenol) purchased as Intioxidant 2246 or Cyanox 2246 of chemical formula $C_{23}H_{32}O_2$ (*m/z* 341.248).[42] The Oil FRA1 bottle of olive oil content had also another specific compound: The sulfonated antioxidant Irganox 1035 (3,5-bis(1,1-dimethylethyl)-4-hydroxybenzenepropanoic acid thiodi-2,1-ethanediyl ester) of chemical formula $C_{38}H_{58}O_6S$ (*m/z* 643.403) (Figure 1, (c)).

Wine FRA2-central layer contained alpha-tocopherol (vitamin E), $C_{29}H_{50}O_2$ (*m/z* 431.389) which is a natural antioxidant in polymer extrusion since 1990s,[29] it was absent in the other bottles.

Wine FRA2-internal layer with Cola-2 FRA had a specific antioxidant trisnonylphenyl phosphite commercialized as Weston 399 or Naugard PHR[42] ($C_{45}H_{69}O_3P$) for *m/z* 689.506.

Tinuvin 234 or (2 (2H-benzotriazol-2-yl)-4,6-bis(1-methyl-1-phenylethyl) phenol,[38, 42-44] ($C_{30}H_{29}N_3O$), a UV absorbing agent or UV stabilizer was detected only in the black fruit container at *m/z* 448.238.

The Alcohol FRA bottle was differentiated by the presence of the slip agent or anti-blocking agent: 2,3-Di(octanoyloxy)propyl octanoate/tricaprylin ($C_{27}H_{50}O_6$) appearing at *m/z* 471.368. However, its transamidated form [$C_{13}H_{28}N_2O$+H^+] at *m/z* 229.22744 (18.08 min) appeared in this bottle and in Water SP bottle with higher intensity.

Unfortunately, despite the recalling of tris-(2,3-dibromopropyl) phosphate known as TRIS ($C_9H_{15}Br_6O_4P$)

from the market due to its mutagenicity, this brominated retarder already used in polyesters' manufacturing[28] was detected in one bottle at *m/z* 692.588: Milk SP.

Concerning the juice bottles, all bottles contain 2,4-di-tert-butylphenol ($C_{14}H_{22}O$), a thermal stabilizer and by-product of an antioxidant[37-38, 45] at *m/z* 207.174. This compound is present also in liqueur, external and central layer of beer; internal layer of Wine FRA2, central layer of Wine FRA1, oil, Cola-1 US, Cola-2 FRA and Water-S SP bottles as well as transparent and black fruit containers.

Both French juice bottles contain exclusively the antioxidant dibenzylhydroxylamine ($C_{14}H_{15}NO$), appeared at *m/z* 214.123. They contain also Naugard PANA antioxidant ($C_{16}H_{13}N$) of *m/z* 220.112 which is also present in Alcohol FRA, liqueur, internal beer layer, external and central Wine FRA2, oil, Cola-1 US, Cola-2 FRA and both Water-S bottles as well as transparent and black fruit containers. Tinuvin® P: 2-(Benzotriazol-2-yl) 4-methylphenol/(2-(2H-benzotriazol-2-yl)-p-cresol)/ drometrizole which is used as an Azo dye (chromophore) or UV absorber and stabilizer[37, 44, 46] of chemical formula $C_{13}H_{11}N_3O$ (*m/z* 226.097) was detected in French juice bottles and liqueur, internal and central beer layer, central Wine FRA2 layer, Oil FRA2, Cola-1 US and both Spanish water bottles in addition to the blue container.

Both Juice FRA1 and Juice SP bottles contained the antioxidant Isonox 132 ($C_{18}H_{30}O$) appearing at 263.237 which was also present in Alcohol FRA, Cola-1 FRA, and Water-S SP bottles and in the external layer of Wine FRA2. They were containing in common the UV absorbing agent methanone, 2-hydroxy-4-(octyloxy)-phenyl/2-hydroxy-4-*n*-octoxybenzophenone ($C_{21}H_{26}O_3$) known commercially as Chimassorb 81, UV 531 or Uvinul 3008,[42] it was present in these 2 bottles and in Cola-1 FRA at *m/z* 327.195.

Furthermore, the Spanish orange juice bottle had common compounds with Juice FRA2 such as the plasticizer Santicizer 148 ($C_{22}H_{31}O_4P$) for *m/z* 391.203 present also in Wine FRA2 external layer and the depolymerized transparent and blue containers. The UV stabilizer Uvinul 3040 ($C_{14}H_{12}O_3$) was present in Juice FRA2 and Juice SP bottles at *m/z* 229.086 in addition to milk, central layers of beer and Wine FRA2, external layer of Wine FRA1 & 2, internal layer of Wine FRA1, Oil FRA1 and Water-S FRA bottles with the black FC.

Juice FRA1 was differentiated of the other juice bottles by the presence of the flame retardant tripropyl phosphate ($C_9H_{21}O_4P$)[28] appearing at *m/z* 225.125. It contained also the plasticizer tributyl phosphate ($C_{12}H_{27}O_4P$) appearing at *m/z* 267.172 which was also present in all layers of Wine FRA1, the internal layer of Wine FRA2, the external and internal layers of Beer AUT, both oil bottles, Water Qatar and Water-S FRA bottles in addition to the transparent and black fruit containers. The primary phenolic antioxidant Irganox MD 1024: 2',3-Bis[[3-[3,5-di-tert.-butyl-4-hydroxyphenyl] propionyl]] propionohydrazide[38, 42] was found in Juice FRA1 bottle. This metal deactivator $C_{34}H_{52}N_2O$ has been detected at *m/z* 505.415 in this bottle in addition to Alcohol FRA, internal layers of both wine bottles, central layer of beer bottle, Water-FRA and Oil FRA2 bottles. However, Juice FRA2 was differentiated by the presence of the plasticizer glycerol triacetate ($C_9H_{14}O_6$) at *m/z* 219.086. This additive was also present in milk, liqueur, external beer layer, central layers of Wine FRA 1 & 2, Oil FRA1, Cola-1 US, Cola-2 FRA and Water-S SP bottles. Juice FRA2 bottle contained also the Tinuvin 326 ($C_{17}H_{18}N_3OCl$): Phenol, 2-(5-chloro-2H-benzotriazol-2-yl)-6-(1,1-dimethylethyl)-4-methyl/2-(2′-Hydroxy-3′-tert-butyl-5′-methylphenyl)-5-chlorobenzortriazole which is a UV absorbing agent[42, 44] appeared at *m/z* 316.121, detected also in Water Qatar bottle. Irganox 3125 antioxidant ($C_{60}H_{87}O_2S$) appeared in Juice FRA2 bottle at *m/z* 872.649 in addition to Alcohol FRA, Liqueur FRA, Water-Qatar, Cola-1 US, Cola-2 FRA and Oil FRA1 bottles with the central layers of beer and Wine FRA1 bottles and the internal layer of Wine FRA1.

The orange juice bottle from Spain was differentiated by the presence of the antioxidant tris(3,5-di-tert-butyl-4-hydroxybenzyl) isocyanurate ($C_{48}H_{69}N_3O_6$) known as Irganox 3114 or Ethanox 314[42] (*m/z* 784.526) present also in Oil FRA2 bottle.

This detailed analysis of juice bottles showed that the Spanish bottle had fewer remaining antioxidants after PET depolymerization than the other bottles. This may due either to the degradation of antioxidants after using or more probably to the differences of manufacturing policies of this kind of PET bottles between France and Spain.

Concerning plasticizers in the PET depolymerized packaging objects, ester compounds such as phthalates, adipates, sebacates and maleates have been detected (Table 3).

Table 3. Some detected plasticizers in PET packaging objects. n is the number of DMAPA molecules of the derivatized compounds.

Plasticizer name	[M]	*m/z*	[M]	*m/z*
Dimethyl phthalate (DMP)	$C_{10}H_{10}O_4$	195.065	n=1 $C_{14}H_{20}N_2O_3$	265.155
Diethyl phthalate (DEP)	$C_{12}H_{14}O_4$	223.096	n=1 $C_{15}H_{22}N_2O_3$	279.170
Diallyl phthalate	$C_{14}H_{14}O_4$	247.096	n=1 $C_{16}H_{22}N_2O_3$	291.170
Diisopropyl phthalate	$C_{14}H_{18}O_4$	251.128	n=1 $C_{16}H_{24}N_2O_3$	293.186
Bis(2-methoxy-ethyl)-phthalate	$C_{14}H_{18}O_6$	283.118	n=1 $C_{16}H_{24}N_2O$	309.181
Dibutyl phthalate (DBP)	$C_{16}H_{22}O_4$	279.159	n=1 $C_{17}H_{26}N_2O_3$	307.202
Benzyl butyl phthalate (BBP)	$C_{19}H_{20}O_4$	313.143	n=1 $C_{17}H_{26}N_2O_3$ n=1′ $C_{20}H_{24}N_2O_3$	307.202 341.186
Diphenyl isophthalate	$C_{20}H_{14}O_4$	319.096	n=1 $C_{19}H_{22}N_2O_3$	327.170
Diamyl phthalate	$C_{18}H_{26}O_4$	307.190	n=1 $C_{18}H_{28}N_2O_3$	321.217
Dicyclohexyl phthalate	$C_{20}H_{26}O_4$	331.190	n=1 $C_{20}H_{28}N_2O_2$	329.222
Di-*n*-heptyl phthalate	$C_{22}H_{34}O_4$	363.253	n=1 $C_{20}H_{32}N_2O_3$	349.249
Bis (2-*n*-butoxyethyl) phthalate	$C_{20}H_{30}O_6$	367.212	n=1 $C_{19}H_{30}N_2O_4$	351.228

Di(2-ethylhexyl) phthalate (DEHP)	$C_{24}H_{38}O_4$	391.284	n=1 $C_{21}H_{34}N_2O_3$	363.264
Di-isononyl phthalate	$C_{26}H_{42}O_4$	419.316	n=1 $C_{22}H_{36}N_2O_3$	377.279
Diisodecyl phthalate	$C_{28}H_{46}O_4$	447.349	n=1 $C_{23}H_{38}N_2O_3$	391.296
Diundecyl phthalate	$C_{30}H_{50}O_4$	475.378	n=1 $C_{24}H_{40}N_2O_3$	405.311
Didodecyl phthalate	$C_{32}H_{54}O_4$	503.409	n=1 $C_{25}H_{42}N_2O_3$	419.327
Diethyl adipate	$C_{10}H_{18}O_4$	203.1278	n=1 $C_{13}H_{26}N_2O_3$ n=2 $C_{16}H_{34}N_4O_2$	259.202 315.275
Bis(2-ethylhexyl) adipate (DEHA)	$C_{22}H_{42}O_4$	371.316	n=1 $C_{19}H_{38}N_2O_3$ n=2 $C_{16}H_{34}N_4O_2$	343.296 315.275
Diisodecyl adipate	$C_{26}H_{50}O_4$	427.378	n=1 $C_{21}H_{42}N_2O_3$	371.327
Dimethyl sebacate	$C_{12}H_{22}O_4$	231.159	n=1 $C_{16}H_{32}N_2O_3$ n=2 $C_{20}H_{42}N_4O_2$	301.249 371.338
Dibutyl sebacate	$C_{18}H_{34}O_4$	315.2523	n=1 $C_{19}H_{38}N_2O_3$ n=2 $C_{20}H_{42}N_4O_2$	343.296 371.338
Di(2-ethylhexyl) maleate	$C_{20}H_{36}O_4$	341.269	n=1 $C_{17}H_{32}N_2O_3$ n=2 $C_{14}H_{28}N_4O_2$	313.249 285.228

First, concerning the phthalates found, diethyl phthalate (DEP)[37, 42, 44] of chemical formula $C_{12}H_{14}O_4$ appeared at *m/z* 223.096 in French Cola-2, Juice FRA1, Oil FRA2, Cola-2 US, external and internal layers of both wine bottles and transparent container. Diallyl phthalate ($C_{14}H_{14}O_4$) has been detected at *m/z* 247.096 in the external layers of beer and Wine FRA1 bottles, Water Qatar bottle and the blue and black fruit containers. Diisopropyl phthalate ($C_{14}H_{18}O_4$) was also detected at *m/z* 251.128 in Oil FRA2 bottle, internal and central layers of Wine FRA1 and internal and external layers of Wine FRA2. Bis (2-methoxyethyl) phthalate ($C_{14}H_{18}O_6$) appeared at *m/z* 283.118 in Spanish milk, sparkling water and juice bottles and liqueur FRA bottle. Furthermore, dibutyl phthalate (DBP)[38, 42, 46] of chemical formula $C_{16}H_{22}O_4$ was also detected at *m/z* 279.159 in Juice FRA2, liqueur FRA, Water-S FRA, internal layers of Wine FRA2 and beer bottles and the blue FC. Benzyl butyl phthalate (BBP) known commercially as Santicizer 160[42] appeared at *m/z* 313.143 in the Spanish milk, sparkling water and juice bottles and liqueur FRA, Cola-1 FRA, Oil FRA2 and Water Qatar bottles, external and central layers of Wine FRA2 and Beer AUT and the blue and black fruit containers.

Diphenyl isophthalate($C_{20}H_{14}O_4$) appeared in liqueur and Spanish orange juice bottle and Wine FRA1-internal only at *m/z* 319.096. Bis(2-*n*-butoxyethyl) phthalate ($C_{20}H_{30}O_6$) appeared at *m/z* 367.212 in Milk SP, Water Qatar, Water-S FRA, Cola-1 US, external and central layers of beer bottle and external and internal layers of Wine FRA1 and black fruit container. Di(2-ethylhexyl) phthalate (DEHP)[37, 42, 46] ($C_{24}H_{38}O_4$) appeared at *m/z* 391.284 in Juice FRA1, Alcohol and Liqueur FRA, oil bottles, both French cola bottles and the four analyzed water bottles in addition to the external layers of beer and wine bottles, internal layers of both wine bottles and Wine FRA2-central.

Di-isononyl phthalate[37-38] ($C_{26}H_{42}O_4$) was detected at *m/z* 419.316 in Spanish milk, sparkling water and juice bottles and liqueur FRA, Cola-1 US, Cola-2 FRA, Oil FRA2 and Water-S FRA bottles, external and internal layers of Wine FRA1 and central and internal layers of beer bottles and transparent fruit container.

The plasticizer diisodecyl phthalate of chemical formula $C_{28}H_{46}O_4$ was detected at *m/z* 447.347 in Juice FRA1 and Cola-1 FRA bottles, blue and black fruit containers and central layers of beer and Wine FRA1, and external layer of Wine FRA2. Diundecyl phthalate (Jayflex L11 P-E) ($C_{30}H_{50}O_4$) was found at *m/z* 475.378 in the three containers, Juice FRA, Liqueur FRA, Water-S FRA, Cola-1 US, Milk SP, Beer AUT-external and Wine FRA1-central.

Didodecyl phthalate ($C_{32}H_{54}O_4$) has been detected at *m/z* 503.409 in Spanish sparkling water bottle, French sparkling water, juice, liqueur, cola and oils bottles, blue and black fruit containers, external and internal layers of Wine FRA1 and Beer AUT and central layer of Wine FRA2 bottle.

All bottles and containers contained phthalates plasticizers; even Water SP made of 100% rPET contained the mentioned plasticizers but only under their transamidated form. Indeed, diamyl and di-*n*-heptyl phthalates absent in all depolymerized PET objects under their not derivatized form were also detected under their mono- and di-derivatized forms $C_{18}H_{28}N_2O_3$ (*m/z* 321.217) and $C_{20}H_{32}N_2O_3$ (*m/z* 349.249) respectively. Water SP contained the diisodecyl phthalate $C_{23}H_{39}N_2O_3$ mono-derivatized at 36.62 min (*m/z* 391.296) at relatively high intensity (1.48E+03). The same trend was observed for dimethyl phthalate, diethyl phthalate, DEHP, bis (2-methoxyethyl) phthalate, diisopropyl phthalate all mono-derivatized at 9.28 min, 13.7 min, 31.5 min, 9.4 min and 10.4 respectively (Table 3).

Unfortunately, bisphenolic compounds and their analogous were also detected in the depolymerized bottles (SI, Table S3). Indeed, Bisphenol A (BPA)[42] ($C_{15}H_{16}O_2$) has been detected at *m/z* 229.122 in the following bottles: Juice FRA2, Milk SP, both Cola-1 bottles, Water Qatar, central beer layer, internal Wine FRA2 and external Wine FRA1 layers. In addition, Bisphenol A diglycidyl ether (BADGE)[38] of chemical formula $C_{21}H_{24}O_4$ have appeared in both Alcohol FRA and Oil FRA2 bottles at *m/z* 341.175.

It is well known that phthalate esters and Bisphenol A are endocrine-disrupting chemicals.[47] In fact, BPA is a monomer in the fabrication of polycarbonate and epoxy resins and many studies determined the migration of BPA from PET bottles into beverages.[42, 46]

Secondly, for adipate additives: The detection of the di-derivatized adipic acid (*m/z* 315.275) is an indication of the presence of adipate plasticizers which are numerous such as bis(2-ethylhexyl) adipate (DEHA), diethyl adipate, diisobutyl adipate, di(tridecyl) adipate, etc. So, the detection of the mono-derivatized form and the additive molecule traces before derivatization are necessary.

Indeed, bis(2-ethylhexyl) adipate (DEHA)[37-38, 46] of chemical formula $C_{22}H_{42}O_4$ has been detected at *m/z* 371.316 in both French juice bottles, oil bottles, both Cola-1 bottles, all

water bottles except Water-S SP, transparent fruit container and central layers of Wine FRA1 & 2 and internal layer of Wine FRA1 bottle. Diethyl adipate ($C_{10}H_{18}O_4$) has been also detected at *m/z* 203.128 in the French liqueur and Water-S bottles, Water SP, Water Qatar, Cola-1 US and the internal layer of Wine FRA2 bottle. Diisodecyl adipate plasticizer was also found in Juice FRA2 and Juice SP, all layers of beer bottle, Cola-1 & 2 FRA, Water-S FRA, central and internal layers of Wine FRA1.

For maleate plasticizers, dibutyl maleate was detected in all French bottles except oil and juices, the 3 containers, both Spanish water and Water Qatar bottles. But, the di(2-ethylhexyl) maleate was detected in all juice bottles, Oil FRA1, Spanish water bottles and Alcohol FRA in addition to the internal layer of Beer AUT. For sebacate plasticizers, the dimethyl sebacate was detected in all internal layers of wine and beer bottles, all containers, both French Cola bottles, Juice FRA1 and Water Qatar bottles (Table 3).

Moving into some rare additives like whitening agents (FWAs), 3 compounds have been detected. Indeed, 1,2-bis (5-methyl-2-benzoxazole) ethylene (FWA135)[48-49] of chemical formula $C_{18}H_{14}N_2O_2$ has been detected only in the central layer of Wine FRA2 bottle at *m/z* 291.113. In the other wine bottle (Wine FRA1), 4,4'-bis (2-benzoxazolyl) stilbene (FWA393),[49,50,51] of chemical formula $C_{28}H_{18}N_2O_2$ was found in both the internal layer of wine bottle and the external beer's bottle layer at *m/z* 415.144. The French sparkling water and Cola-2 bottles contained FWA184: 2,5-Bis(5-tert-butyl-2-benzoxazolyl) thiophene ($C_{26}H_{26}N_2O_2S$)[48-51] appearing at *m/z* 431.179 only in these two bottles. However, no traces of 1,4-bis-(2-benzoxazolyl)-naphthalene (FWA 367)[48-49] were found in any analyzed PET packaging object.

A detailed search was extended to perfluoroalkyl carboxylic acids (PFAS) from C4-C12 that may be present[52] in the analyzed samples. Indeed, perfluoroheptanoic acid (PFHpA) was absent in all bottles and containers. However, perfluorobutanoic acid (PFBA), perfluorobutanesulfonate (PFBS), perfluorohexanesulfonate (PFHxS), perfluorooctanesulfonate (PFOS) and perfluorodecanesulfonate (PFDS) were detected in different bottles and containers as shown in Table 4.

Table 4. Perfluoroalkyl carboxylic acids (PFAS) detected in PET packaging objects.

PFAS	[M]	*m/z*	Presence in
Perfluorobutanoic acid (PFBA)	$C_3F_7CO_2H$	214.994	Juice SP Transparent FC Black FC Cola-2 FRA Liqueur FRA Beer AUT-external & internal Wine FRA1-external & internal
Perfluorobutane sulfonate (PFBS)	$C_4HF_9O_3S$	300.958	Juice FRA Juice SP Liqueur FRA Cola-1 FRA Oil FRA1
			Water SP Beer AUT-central Wine FRA1-central Blue FC
Perfluorohexane sulfonate (PFHxS)	$C_6H_1F_{13}O_3S$	400.951	Juice FRA1 Cola-1 US Transparent FC
Perfluorooctane sulfonate (PFOS)	$C_8HF_{17}O_3S$	500.945	Juice FRA1 Juice SP Milk SP Liqueur FRA Water QA Wine FRA1-external Wine FRA2-external & central Blue FC
Perfluorodecane sulfonate (PFDS)	$C_{10}HF_{21}O_3S$	600.938	Juice SP Juice FRA2 Beer AUT-external Cola-2 FRA Water QA

After this detailed discussion about additives in each bottle and container, bottles can be classified according to similarities in terms of additives. Indeed, Spanish bottles were very similar. However, Cola-1 US and Cola-2 FRA were very similar despite the difference of the brand.

This methodology was useful also to detect the enchased remaining products inside the pores of PET film from its content. Indeed, French oil bottles had remaining oil compounds in form of free fatty acids after depolymerization of PET; they were found under their mono-transamidated forms. For instance, the mono-derivatized fatty acids: Palmitic (*m/z* 341.352), oleic (*m/z* 367.367) and stearic (*m/z* 369.381) acids have been detected at 40.65 min, 41.67 min and 44.19 min respectively. This confirms also the presence of some compounds already found in literature in oil bottles such as octadecanoic acid, 2,3-bis(acetoxy)propyl ester $C_{25}H_{46}O_6$ (*m/z* 443.337) and 12- (acetoxy)-stearic acid 2,3-bis(acetoxy)propyl ester $C_{27}H_{48}O_8$ (*m/z* 501.342).[53]

The three studied juice bottles from France and Spain showed the presence of remaining nootkatone [$C_{15}H_{21}O_4$ + H^+], a volatile flavor component of orange juice,[54] at 40.1 min (*m/z* 219.174). In the Spanish milk bottle, two vitamins were detected: Vitamin B presented by riboflavin[55-57] [$C_{17}H_{19}N_4O_6$ + H^+] (*m/z* 377.144) and vitamin A presented by retinol[56-57] [$C_{20}H_{29}O$+ H^+] at 7.4 min (*m/z* 287.237). The internal layers of both wine bottles contained the three compounds: Diethyl tartrate[58] $C_8H_{14}O_6$ (*m/z* 207.086, 1.6 min), ethyl 3-methyl butyl butanedioate[58] $C_{11}H_{20}O_4$ (*m/z* 217.143) and butyl cyclohexyl phthalate (BcEP) $C_{18}H_{25}O_4$ (*m/z* 306.183, 1.56 min); these compounds were also confirmed by their mono-transamidated forms. However, beer bottle's internal layer had the encapsulating materials alpha-cyclodextrin[47] of chemical formula $C_{36}H_{60}O_{30}$ appearing at *m/z* 973.324.

CONCLUSIONS AND PERSPECTIVES

The innovative methodology of depolymerization of polyesters and co-polyesters by transamidation after HFIP solubilization was very efficient while combining it with LC-MS analysis in order to determine the full composition in additives of PET packaging objects. Many additives have been described such as plasticizers, antioxidants, flame retardant, crosslinking agents and other additives present in traces or not in a wide range of PET bottles and containers differentiated by their contents, brands and manufacturing countries. The presence of esters in PET films of different types such as phthalates, adipates and fatty acids were doubly checked by searching their mono- and/or di-derivatized forms in addition to their remaining form without derivatization.

All the detailed data about additives maybe used for the prediction of their migration from food packaging into beverages to study their toxicity.

Furthermore, using this methodology, it was also possible to define the content of unknown bottles by finding the enchased products inside PET films which were remaining after depolymerization. This will help to determine the pollution source by PET wastes in all polluted ecosystems especially sea and oceans.

ASSOCIATED CONTENT

Supporting Information

Additional experimental details and characterization data.

AUTHOR INFORMATION

First Author

Bayan Almasri - Univ. Lille, CNRS, UAR 3290, MSAP, Miniaturisation pour la Synthèse l'Analyse et la Protéomique, F-59000 Lille, France ; Laboratoire de Chimie Appliquée, Faculté des Sciences III, Université Libanaise, Ras Maska, Tripoli, Liban ; orcid.org/0009-0001-9467-5716.

Note

The authors declare no competing financial interest.

AKNOWLEDGMENT

Bayan ALMASRI gratefully acknowledges the funding of her joint PhD between University of Lille and Lebanese University by the PAUSE funding program. The mass spectrometer was funded by University of Lille, CNRS, Région Hauts-de-France and the European Regional Development Fund (ERDF). The authors gratefully acknowledge the financial support of the FTICR MS facility from the IR INFRANALYTICS FR2054 CNRS and of the EU_FTICR _MS project Grant Agreement 731077 funded by EU Horizon 2020 Research and Innovation Program.

REFERENCES

1. Nisticò, R., Polyethylene terephthalate (PET) in the packaging industry. *Polymer Testing* **2020,** *90*, 106707.
2. Gerassimidou, S.; Lanska, P.; Hahladakis, J. N.; Lovat, E.; Vanzetto, S.; Geueke, B.; Groh, K. J.; Muncke, J.; Maffini, M.; Martin, O. V., Unpacking the complexity of the PET drink bottles value chain: A chemicals perspective. *Journal of Hazardous Materials* **2022,** *430*, 128410.
3. Malik, N.; Kumar, P.; Shrivastava, S.; Ghosh, S. B., An overview on PET waste recycling for application in packaging. *International Journal of Plastics Technology* **2017,** *21*, 1-24.
4. Habschied, K.; Mastanjević, K.; Šibalić, M.; Krstanović, V.; Galić, V., A Survey on Detection of Plastic-Related Chemicals in Beer Packaged in PET Using FT-IR Technology. *Beverages* **2022,** *8* (4), 73.
5. Baude, C. K., *A preliminary analysis of PET barrier technologies and mechanical performance related to a 3L PET wine bottle*. Rochester Institute of Technology: 2008.
6. Ioannidou, M. D.; Samouris, G.; Achilias, D. S., Acetaldehyde contamination of water, alcoholic, and non-alcoholic beverages stored in glass or plastic bottles. *Toxicological & Environmental Chemistry* **2016,** *98* (10), 1183-1190.
7. Auras, R.; Singh, S. P.; Singh, J., Performance evaluation of PLA against existing PET and PS containers. *Journal of testing and Evaluation* **2006,** *34* (6), 530-536.
8. Colombo, G.; Corredig, M.; Ünalan, I. U.; Tsochatzis, E., Untargeted screening of NIAS and cyclic oligomers migrating from virgin and recycled polyethylene terephthalate (PET) food trays. *Food Packaging and Shelf Life* **2024,** *41*, 101227.
9. Franz, R.; Welle, F. In *Investigation of non-intentionally added substances (NIAS) in PET bottles and closures*, Poster Presentation at the 4th International Symposium on Food Packaging, 19e21 November, Prague, Czech Republic, 2008.
10. Cincotta, F.; Verzera, A.; Tripodi, G.; Condurso, C., Non-intentionally added substances in PET bottled mineral water during the shelf-life. *European Food Research and Technology* **2018,** *244*, 433-439.
11. Schmid, P.; Welle, F., Chemical migration from beverage packaging materials—A review. *Beverages* **2020,** *6* (2), 37.
12. Orabi, S. A.; Abd-ElRazic, T. A.; Elsayed, H. H., Migration of Plasticizers from Polyethylene Terephthalate Bottles to Vinegar and Water via different Temperature and Storage Periods. *Bulletin of the National Nutrition Institute of the Arab Republic of Egypt* **2021,** *58* (2), 91-108.
13. Romao, W.; Franco, M. F.; Corilo, Y. E.; Eberlin, M. N.; Spinace, M. A.; De Paoli, M.-A., Poly (ethylene terephthalate) thermo-mechanical and thermo-oxidative degradation mechanisms. *Polymer Degradation and Stability* **2009,** *94* (10), 1849-1859.
14. Westerhoff, P.; Prapaipong, P.; Shock, E.; Hillaireau, A., Antimony leaching from polyethylene terephthalate (PET) plastic used for bottled drinking water. *Water Research* **2008,** *42* (3), 551-556.
15. Keresztes, S.; Tatár, E.; Mihucz, V. G.; Virág, I.; Majdik, C.; Záray, G., Leaching of antimony from polyethylene terephthalate (PET) bottles into mineral water. *Science of the Total Environment* **2009,** *407* (16), 4731-4735.
16. Welle, F.; Franz, R., Migration of antimony from PET bottles into beverages: determination of the activation energy of diffusion and migration modelling compared with literature data. *Food Additives & Contaminants: Part A* **2011,** *28* (1), 115-126.
17. Higuchi, A.; Yoon, B. O.; Kaneko, T.; Hara, M.; Maekawa, M.; Nohmi, T., Separation of endocrine disruptors from aqueous solutions by pervaporation: dioctylphthalate and butylated hydroxytoluene in mineral water. *Journal of applied polymer science* **2004,** *94* (4), 1737-1742.
18. Hirayama, K.; Tanaka, H.; Kawana, K.; Nakazawa, H., Analysis of plasticizers in cap-sealing resins for bottled foods. *Food Additives & Contaminants* **2001,** *18* (4), 357-362.
19. Leivadara, S. V.; Nikolaou, A. D.; Lekkas, T. D., Determination of organic compounds in bottled waters. *Food chemistry* **2008,** *108* (1), 277-286.
20. Montuori, P.; Jover, E.; Morgantini, M.; Bayona, J. M.; Triassi, M., Assessing human exposure to phthalic acid and phthalate esters from mineral water stored in polyethylene

terephthalate and glass bottles. *Food Additives and Contaminants* **2008,** *25* (4), 511-518.
21. Penalver, A.; Pocurull, E.; Borrull, F.; Marce, R., Determination of phthalate esters in water samples by solid-phase microextraction and gas chromatography with mass spectrometric detection. *Journal of Chromatography A* **2000,** *872* (1-2), 191-201.
22. Kayali, N.; Tamayo, F. G.; Polo-Díez, L. M., Determination of diethylhexyl phtalate in water by solid phase microextraction coupled to high performance liquid chromatography. *Talanta* **2006,** *69* (5), 1095-1099.
23. Bi, T.-T.; Shuai, M.-K.; Gong, Y.; Ding, Q.; Sun, K.-Y.; Tang, X.-F.; Yang, Z.-G.; Zhang, Z.-Z., Effect of hydrolysis stabilizers on anti-aging performance of PET under pressure cooker test. *Polymer Degradation and Stability* **2024,** *225*, 110816.
24. Fechine, G.; Rabello, M.; Souto-Maior, R., The effect of ultraviolet stabilizers on the photodegradation of poly (ethylene terephthalate). *Polymer Degradation and Stability* **2002,** *75* (1), 153-159.
25. Kobayashi, T.; Wood, B. A.; Takemura, A.; Ono, H., Antistatic performance and morphological observation of ternary blends of poly (ethylene terephthalate), poly (ether esteramide), and Na-neutralized poly (ethylene-co-methacrylic acid) copolymers. *Journal of Electrostatics* **2006,** *64* (6), 377-385.
26. Markarian, J., Slip and antiblock additives: surface medication for film and sheet. *Plastics, Additives and Compounding* **2007,** *9* (6), 32-35.
27. Gooneie, A.; Simonetti, P.; Salmeia, K. A.; Gaan, S.; Hufenus, R.; Heuberger, M. P., Enhanced PET processing with organophosphorus additive: Flame retardant products with added-value for recycling. *Polymer degradation and stability* **2019,** *160*, 218-228.
28. Levchik, S. V.; Weil, E. D., Flame retardancy of thermoplastic polyesters—a review of the recent literature. *Polymer International* **2005,** *54* (1), 11-35.
29. Stanley, J.; John, A.; Pušnik Črešnar, K.; Fras Zemljič, L.; Lambropoulou, D. A.; Bikiaris, D. N., Active agents incorporated in polymeric substrates to enhance antibacterial and antioxidant properties in food packaging applications. *Macromol* **2022,** *3* (1), 1-27.
30. Nichols, D., *Biocides in plastics*. iSmithers Rapra Publishing: 2004; Vol. 15.
31. Cardozo-Filho, L.; Mazzer, H. R.; Santos, J. C.; Andreaus, J.; Feihrmann, A. C.; Beninca, C.; Cabral, V. F.; Zanoelo, E. F., Dyeing of polyethylene terephthalate fibers with a disperse dye in supercritical carbon dioxide. *Textile Research Journal* **2014,** *84* (12), 1279-1287.
32. Chudgar, R. J., Azo dyes. *Kirk-Othmer Encyclopedia of Chemical Technology* **2000**.
33. Almasri, B.; Rolando, C., Identification and quantification of polyethylene terephthalate (PET) polyesters and microplastics combining soft chemical depolymerization by dimethylaminopropylamine (DMAPA) and analysis by MALDI FTICR & LC ESI Orbitrap mass spectrometry. *ChemRxiv®*, **2025**, submitted to *ACS Analytical Chemistry.*
34. Wiegner, J.-P.; Voerckel, V.; Munjal, S., Process for preparation of polyethylene terephthalate modified by o-phthalic acid units. Google Patents: 2003.
35. Cosimbescu, L.; Merkel, D. R.; Darsell, J.; Petrossian, G., Simple but tricky: investigations of terephthalic acid purity obtained from mixed PET waste. *Industrial & Engineering Chemistry Research* **2021,** *60* (35), 12792-12797.
36. Joseph, T. M.; Azat, S.; Ahmadi, Z.; Jazani, O. M.; Esmaeili, A.; Kianfar, E.; Haponiuk, J.; Thomas, S., Polyethylene terephthalate (PET) recycling: a review. *Case Studies in Chemical and Environmental Engineering* **2024**, 100673.
37. Singh, N.; Mann, B.; Sharma, R.; Verma, A.; Panjagari, N. R.; Gandhi, K., Identification of polymer additives from multilayer milk packaging materials by liquid-solid extraction coupled with GC-MS. *Food Packaging and Shelf Life* **2022,** *34*, 100975.
38. Buchalla, R.; Begley, T. H., Characterization of gamma-irradiated polyethylene terephthalate by liquid-chromatography–mass-spectrometry (LC–MS) with atmospheric-pressure chemical ionization (APCI). *Radiation Physics and Chemistry* **2006,** *75* (1), 129-137.
39. Sängerlaub, S.; Müller, K., Long-time performance of bottles made of PET blended with various concentrations of oxygen scavenger additive stored at different temperatures. *Packaging Technology and Science* **2017,** *30* (1-2), 45-58.
40. Mrozinski, B. A., *Acetaldehyde scavengers for poly (ethylene terephthalate): chemistry of reactions, capacity, and modeling of interactions*. The University of Toledo: 2010.
41. Dattilo, S.; Gugliuzzo, C.; Mirabella, E. F.; Puglisi, C.; Scamporrino, A. A.; Zampino, D. C.; Samperi, F., Characterization of VOCs and additives in Italian PET bottles and studies on potential functional aldehydes scavengers. *European Food Research and Technology* **2022,** *248* (5), 1407-1420.
42. Yilmaz, M. A.; Temel, H., Screening of Polymer Additives in Drinking Water Stored in PET Bottles by UHPLC-ESI-IT-TOF MS. *J Environ Sci Eng A* **2016,** *5*, 59-64.
43. Begley*, T.; Biles, J.; Cunningham, C.; Piringer, O., Migration of a UV stabilizer from polyethylene terephthalate (PET) into food simulants. *Food additives and contaminants* **2004,** *21* (10), 1007-1014.
44. Li, B.; Wang, Z.-W.; Lin, Q.-B.; Hu, C.-Y., Study of the migration of stabilizer and plasticizer from polyethylene terephthalate into food simulants. *Journal of Chromatographic Science* **2016,** *54* (6), 939-951.
45. Bach, C.; Dauchy, X.; Severin, I.; Munoz, J.-F.; Etienne, S.; Chagnon, M.-C., Effect of temperature on the release of intentionally and non-intentionally added substances from polyethylene terephthalate (PET) bottles into water: chemical analysis and potential toxicity. *Food Chemistry* **2013,** *139* (1-4), 672-680.
46. Bach, C.; Dauchy, X.; Chagnon, M.-C.; Etienne, S., Chemical migration in drinking water stored in polyethylene terephthalate (PET) bottles: a source of controversy reviewed. *Water Research* **2012,** *46* (3), pp. 571-583.
47. Habschied, K.; Kartalović, B.; Lazić, D.; Krstanović, V.; Mastanjević, K., Survey on phthalates in beer packaged in aluminum cans, PET and glass bottles. *Fermentation* **2023,** *9* (2), 125.
48. Wu, Q.; He, B.; Guo, R.; Cui, J.; Yan, S.; Liu, D.; Yao, B., Fluorescent whitening agents in Baiyangdian Lake in North China: Analysis, occurrence, distribution and ecological risk assessment. *Environmental Pollution* **2021,** *291*, 118235.
49. Alberto Lopes, J. F.; Tsochatzis, E. D.; Emons, H.; Hoekstra, E., Development and validation of an HPLC method with fluorescence detection for the determination of fluorescent whitening agents migrating from plastic beverage cups. *Food Additives & Contaminants: Part A* **2018,** *35* (7), 1438-1446.
50. Wu, Z.; Xu, Y.; Li, M.; Guo, X.; Xian, Y.; Dong, H., Determination of three fluorescent whitening agents (FWAs) and their migration research in food contact plastic packaging containers and food simulants by UPLC-MS/MS method. *RSC advances* **2016,** *6* (22), 17941-17946.
51. Guo, R.; Liang, X.; Su, M.; Yao, B.; Yan, S.; Han, Y.; Cui, J., Occurrence, migration and health risks of fluorescent whitening agents and phthalates in bottled water. *Journal of Hazardous Materials* **2024**, 134631.

52. Chinthakindi, S.; Zhu, H.; Kannan, K., An exploratory analysis of poly-and per-fluoroalkyl substances in pet food packaging from the United States. *Environmental Technology & Innovation* **2021,** *21*, 101247.
53. Beraza-Gómez, I.; Gómez-Ramos, M. J.; Díaz-Galiano, F. J.; Alba, A. R. F., Identification of colourant-carrier migrants from polyethylene terephthalate bottles into vegetable oils. *Journal of Food Composition and Analysis* **2023,** *123*, 105587.
54. Bacigalupi, C.; Lemaistre, M. H.; Boutroy, N.; Bunel, C.; Peyron, S.; Guillard, V.; Chalier, P., Changes in nutritional and sensory properties of orange juice packed in PET bottles: An experimental and modelling approach. *Food chemistry* **2013,** *141* (4), 3827-3836.
55. Limbo, S.; Pellegrino, L.; D'Incecco, P.; Gobbi, S.; Rosi, V.; Fracassetti, D., Storage of pasteurized milk in clear PET bottles combined with light exposure on a retail display case: A possible strategy to define the shelf life and support a recyclable packaging. *Food chemistry* **2020,** *329*, 127116.
56. Mestdagh, F.; De Meulenaer, B.; De Clippeleer, J.; Devlieghere, F.; Huyghebaert, A., Protective influence of several packaging materials on light oxidation of milk. *Journal of Dairy Science* **2005,** *88* (2), 499-510.
57. Moyssiadi, T.; Badeka, A.; Kondyli, E.; Vakirtzi, T.; Savvaidis, I.; Kontominas, M. G., Effect of light transmittance and oxygen permeability of various packaging materials on keeping quality of low fat pasteurized milk: chemical and sensorial aspects. *International dairy journal* **2004,** *14* (5), 429-436.
58. Dombre, C.; Rigou, P.; Wirth, J.; Chalier, P., Aromatic evolution of wine packed in virgin and recycled PET bottles. *Food chemistry* **2015,** *176*, 376-387.


Structural deciphering of PET secrets
• Fruit containers
• Water bottles
• Soft drinks bottles
• Juice bottles
• Milk bottles
• Oil bottles
• Vinegar bottles
• Spirituel drinks bottles
1
PET
Oligomers
Additives
Enchased products
One method !

Supporting information

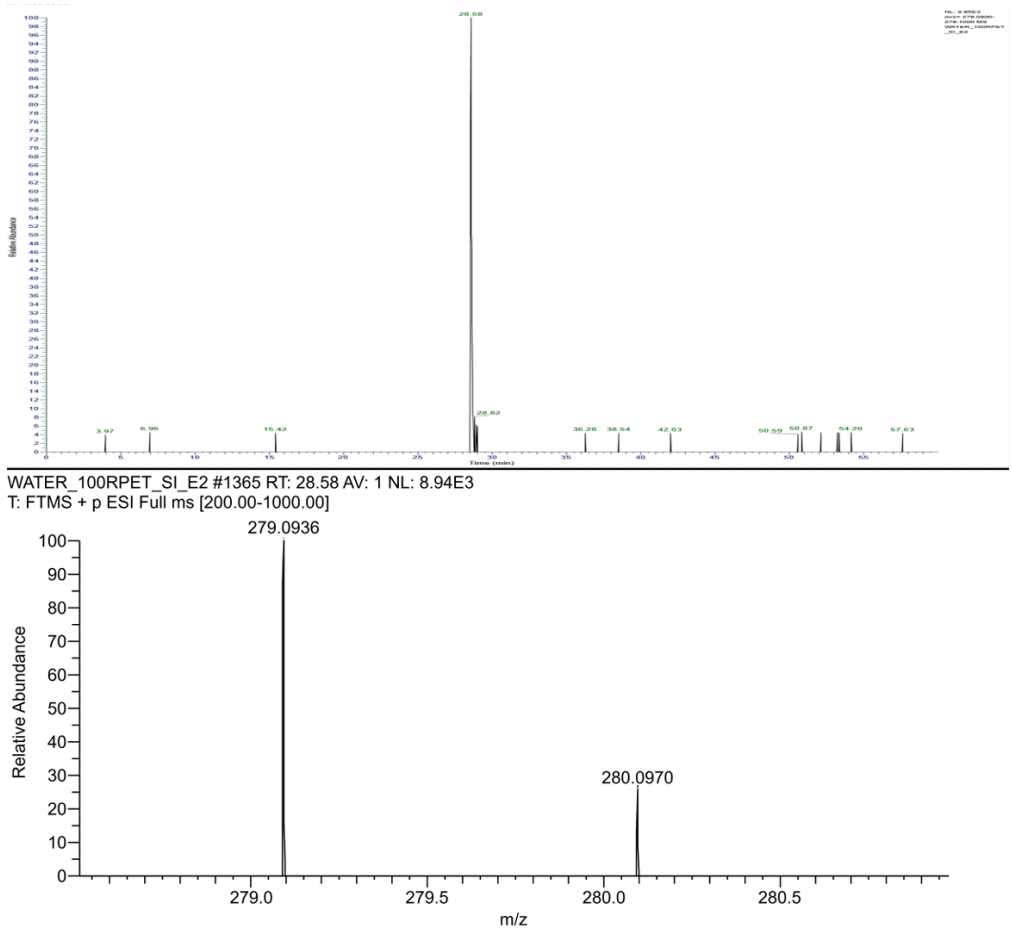


Figure S 1. An example of the correct isotopic ratio of one additive present as traces in the Water SP bottle, LC-MS. The additive present here is triphenylphosphine oxide $C_{18}H_{15}OP$ (TPPO), a flame retardant in PET at 28.58 min (*m/z* 279.093).

Table S 1. Relative abundance (in %) of the following LC-MS peaks present in all the studied containers and bottles: Both depolymerization markers at *m/z* 335.244 and *m/z* 295.165 respectively, their dimers and oligomers, DEG markers' product at *m/z* 571.313 with its oligomers, and cyclohexanedimethanol markers presented by the sum of mono- and di-derivatized products appearing at *m/z* 377.243 and *m/z* 609.365.

Packaging objects	% Di-derivatized depolymerization marker	% Oligomers' sum of di-derivatized depolymerization marker	% Mono-derivatized depolymerization marker	% Oligomers' sum of mono-derivatized depolymerization marker	% DEG marker product	% Oligomers sum of DEG marker's products	% Cyclo-hexane-dimethanol
FC transparent	32.70	1.56	7.41	47.61	0.27	0.09	3.76
FC black	36.38	0.68	14.43	33.41	0.60	0.01	10.58
FC blue	28.61	1.45	8.95	47.52	0.35	0.08	9.70
Water SP	38.25	1.06	6.61	44.03	0.20	0.07	3.09
Water QA	85.50	0.08	10.26	0.32	0.23	0.01	0.00
Water-S FRA	28.27	2.18	8.09	56.15	0.34	0.21	0.01
Water-S SP	96.60	0.01	0.02	0.05	0.00	0.00	0.00
Cola-1 FRA	51.93	0.95	7.55	36.16	0.27	0.03	0.57
Cola-1 US	46.14	0.63	4.23	18.24	0.17	0.03	3.60
Cola-2 FRA	49.80	0.91	8.39	33.80	0.31	0.02	3.95
Juice FRA1	36.46	2.03	7.58	44.16	0.43	0.12	3.70
Juice FRA2	38.97	1.17	10.32	46.08	0.19	0.05	0.16
Juice SP	36.13	1.71	13.28	40.34	0.71	0.04	1.37
Milk SP	88.22	0.10	7.18	0.29	0.48	0.00	0.01
Oil FRA1	29.09	2.33	6.93	58.35	0.40	0.09	0.31
Oil FRA2	22.00	2.54	8.12	62.06	0.37	0.11	0.02
Liqueur FRA	73.03	0.16	4.45	3.85	0.04	0.00	0.01
Alcohol FRA	22.83	1.27	5.58	61.30	0.18	0.14	0.002
Wine FRA2-external	74.68	0.63	5.01	13.97	0.16	0.00	0.40
Wine FRA2-internal	69.65	0.86	7.72	13.86	0.23	0.01	0.59
Wine FRA2-central	0.00	0.00	0.00	0.00	0.00	0.00	24.99
Wine FRA1-external	32.21	3.42	19.38	7.67	0.75	0.39	2.00
Wine FRA1-internal	59.92	2.37	7.44	24.53	0.20	0.00	0.16
Wine FRA1-central	36.76	4.17	8.32	23.57	0.00	0.00	0.00
Beer AUT-external	25.93	2.53	10.59	54.02	0.54	0.09	0.01
Beer AUT-internal	17.04	3.92	11.16	46.17	0.72	0.19	0.00
Beer AUT-central	3.92	14.66	7.19	16.78	7.03	0.00	0.00

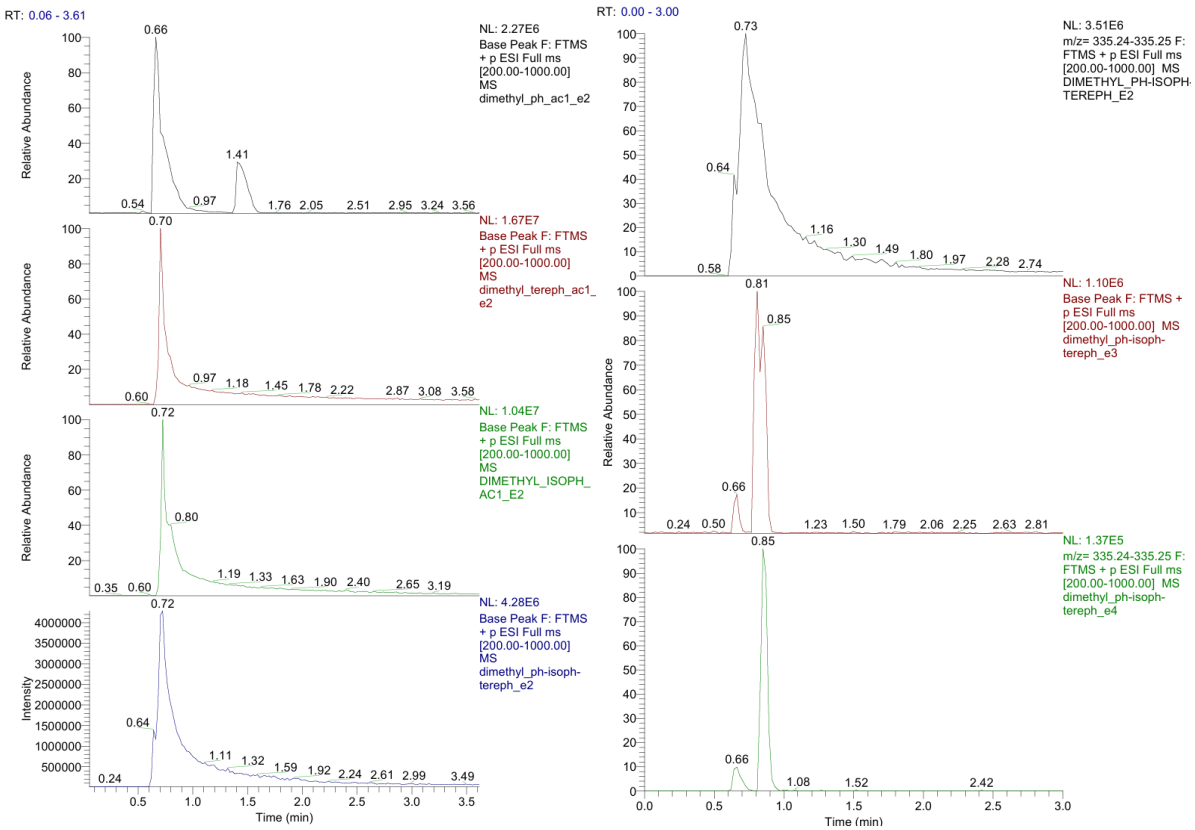


Figure S 2. LC chromatograms. Left panel: The depolymerized dimethyl phthalate, dimethyl terephthalate, dimethyl isophthalate and their ternary isochoric mixture respectively at 1 mg/mL; right panel: The depolymerized dimethyl ester's ternary isochoric mixture at 1, 0.1 and 0.01 mg/mL respectively.

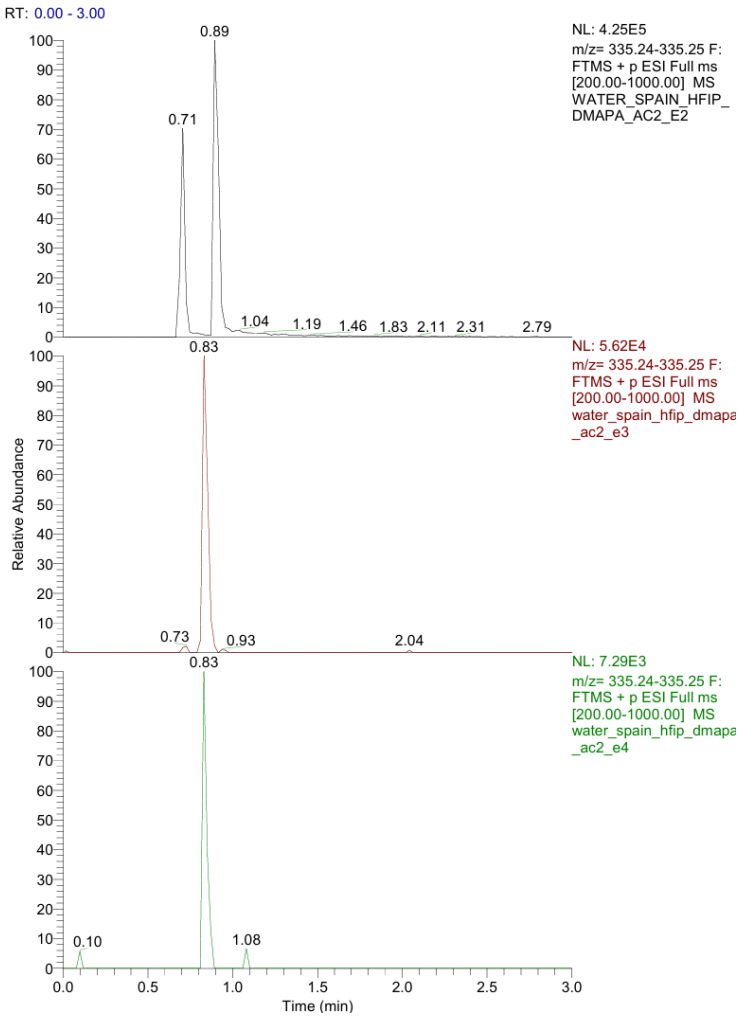


Figure S 3. LC chromatograms for Water SP (0-3 min) at 1, 0.1 and 0.01 mg/mL respectively.

Table S 2. Additives detected in PET bottles and containers with their corresponding chemical formula, theoretical *m/z*, and derivatization with DMAPA.

Additive name	Additive type/ information	Formula [M]	*m/z*	[M] n DMAPA (n = 1-4)	*m/z* with DMAPA
Dimethyl phthalate (DMP)	NIAS (impurity)	$C_{10}H_{10}O_4$	195.065	n=1 $C_{14}H_{20}N_2O_3$	265.155
Diethyl adipate	Plasticizer	$C_{10}H_{18}O_4$	203.128	n=1 $C_{13}H_{26}N_2O_3$ n=2 $C_{16}H_{34}N_4O_2$	259.202 315.275
2,4-Di-tert-butylphenol	Thermal stabiliser/ by-product of antioxidant	$C_{14}H_{22}O$	207.174	-	-
Monohydroxyethyl terephthalate	NIAS (oligomer)	$C_{10}H_{10}O_5$	211.060	n=1 $C_{13}H_{18}N_2O_3$	251.139
Propyl gallate	Antioxidant	$C_{10}H_{12}O_5$	213.076	n=1 $C_{12}H_{17}N_2O_4$	254.126
Dibenzylhydroxylamine	Antioxidant	$C_{14}H_{15}NO$	214.123	-	-
Perfluorobutanoic acid (PFBA)	PFAS: Perfluoroalkyl carboxylic acids (PFCA; C4-C12) and Perfluoroalkyl acids (PFAA)	$C_3F_7CO_2H$	214.994	-	-
Uvinul 3000	UV stabilizer	$C_{13}H_{10}O_3$	215.070	-	-
Bisphenol E	Bisphenol analog	$C_{14}H_{14}O_2$	215.107	-	-
9,10-Dihydro-9-oxa-10-phosphaphenanthrene-10 oxide (DOPO)	Flame retardant in polyesters fibers & in PET	$C_{12}H_9O_2P$	217.041	-	-
Dimethyl azelate	Plasticizer	$C_{11}H_{20}O_4$	217.143	n=1 $C_{15}H_{31}N_2O_3$ n=2 $C_{19}H_{45}N_4O_3$	287.233 377.349
Glycerol triacetate	Plasticizer	$C_9H_{14}O_6$	219.086		
3,5-Di-tert-butyl-4-hydroxybenzaldehyde (BHT-CHO)	NIAS	$C_{15}H_{22}O$	219.174	-	-
Naugard PANA	Antioxidant	$C_{16}H_{13}N$	220.112	-	-
Butylated hydroxytoluene (BHT)	Additive (antioxidant)	$C_{15}H_{24}O$	221.189	-	-
2,6-Ditert-butyl-4-methylphenol	Antioxidant/ thermal stabilizer in hot-melt adhesives	$C_{15}H_{24}O$	221.189	-	-
2-Cyano-2-propyl benzodithioate	Retarder	$C_{11}H_{11}NS_2$	222.041	-	-
Silquest A-1102	Coupling agent	$C_9H_{23}NO_3Si$	222.152	-	-
Silquest A-1100	Coupling agent	$C_9H_{23}NO_3Si$	222.152	-	-
Diethyl phthalate (DEP)/ diethyl	NIAS (impurity)	$C_{12}H_{14}O_4$	223.096	n=1 $C_{15}H_{22}N_2O_3$	279.170

benzene-1,2-dicarboxylate					
Hexyl 2-hydroxybenzoate/ 1-hexyl salicylate	UV Stabilizer	$C_{13}H_{18}O_3$	223.133	n=1 $C_{12}H_{19}N_2O_2$	223.144
Tripropyl phosphate	Flame retardant	$C_9H_{21}O_4P$	225.125	-	-
Tinuvin® P: 2-(Benzotriazol-2-yl) 4- methylphenol/ (2-(2H-benzotriazol-2-yl)-p-cresol)/ drometrizole	Azo dyes (chromophore)/ UV absorbers and stabilizers	$C_{13}H_{11}N_3O$	226.097	-	-
Santoflex IPPD	Antidegradant	$C_{15}H_{18}N_2$	227.154	-	-
Hexadecane	Alkane Hydrocarbon	$C_{16}H_{34}$	227.273	-	-
Uvinul 3040	UV stabilizer	$C_{14}H_{12}O_3$	229.086	-	-
Dibutyl fumarate or dibutyl maleate	Plasticizer	$C_{12}H_{20}O_4$	229.143	n=1 $C_{13}H_{24}N_2O_3$ n=2 $C_{14}H_{28}N_4O_2$	257.186
Dimethyl sebacate	Plasticizer	$C_{12}H_{22}O_4$	231.159	n=1 $C_{16}H_{32}N_2O_3$ n=2 $C_{20}H_{42}N_4O_2$	301.249 371.338
1,3-Di-o-tolylguanidine	Antioxidant	$C_{15}H_{17}N_3$	240.149	-	-
Heptadecane	Alkane Hydrocarbon	$C_{17}H_{36}$	241.289	-	-
2-(2 Hydroxy-benzotriazol-2-yl) 4-methylphenol	Azo dyes (chromophore)/ UV absorbers	$C_{13}H_{11}N_3O_2$	242.092	-	-
Markstat®51	Plasticizer	$(C_2H_4O)nC_{12}H_{24}O_2$	245.211 (n=1)	-	-
Diallyl phthalate	NIAS	$C_{14}H_{14}O_4$	247.096	n=1 $C_{16}H_{22}N_2O_3$	291.170
Diisopropyl phthalate	NIAS	$C_{14}H_{18}O_4$	251.128	n=1 $C_{16}H_{24}N_2O_3$	293.186
Lowinox AH25	Antioxidant	$C_{16}H_{26}O_2$	251.201	-	-
Diisobutyl adipate	Plasticizer	$C_{14}H_{26}O_4$	259.190		
Naugard J	Antioxidant	$C_{18}H_{16}N_2$	261.139	-	-
Triphenylphosphine	Flame retardant	$P(C_6H_5)_3$	263.098	-	-
3,3,5-Trimethylcyclohexyl 2-hydroxybenzoate	Antioxidant/UV stabilizer	$C_{16}H_{22}O_3$	263.164	n=1 $C_{12}H_{18}N_2O_2$	223.144
Isonox 132	Antioxidant	$C_{18}H_{30}O$	263.237	-	-
Ethanox 703	Antioxidant	$C_{17}H_{29}NO$	264.232	-	-
2-(2H-benzotriazol-2-yl)-4-methyl,-6-(2-propenyl)phenol	UV stabilizer	$C_{16}H_{15}N_3O$	266.129	-	-
Tributyl phosphate	Plasticizer	$C_{12}H_{27}O_4P$	267.172	-	-
Uvinul 3049	UV stabilizer	$C_{15}H_{14}O_5$	275.091	-	-
Triphenylphosphine oxide (TPPO)	Flame retardant in PET	$C_{18}H_{15}OP$	279.093	-	-

Dibutyl phthalate (DBP)/ di-isobutyl phthalate (DiBP)	NIAS (impurity)	$C_{16}H_{22}O_4$	279.159	n=1 $C_{17}H_{26}N_2O_3$	307.202
MXD6: Poly(hexamethylene adipamide) and poly(meta-xylene adipamide)	Oxygen scavenger	$C_{14}H_{20}N_2O_4$	281.149	-	-
Oleamide or octadec-9-enamide	Stabilizers or slip agent/ lubricant/ fatty acid derivative	$C_{18}H_{35}NO$	282.279	-	-
Bis(2-Methoxyethyl) phthalate	NIAS	$C_{14}H_{18}O_6$	283.118	n=1 $C_{16}H_{24}N_2O_4$	309.181
Octadecanamide/ stearamide	Lubricants/ thermal stabilizers	$C_{18}H_{37}NO$	284.295	-	-
Stearic acid	Crosslinking agent	$C_{18}H_{36}O_2$	285.279	-	-
FWA135: 1,2-Bis (5-methyl-2-benzoxazole)ethylene	Whitening agents (FWAs)	$C_{18}H_{14}N_2O_2$	291.113	-	-
4-[1-(4-Hydroxy-3-methylphenyl) cyclohexyl] 2-methylphenol	Thermal stabilizer/ antioxidant	$C_{20}H_{24}O_2$	297.185	-	-
Methyl oleate	Plasticizer	$C_{19}H_{36}O_2$	297.279	n=1 $C_{23}H_{46}N_2O$	367.368
Propan-2-yl hexadecanoate/ isopropyl palmitate	Lubricant/ emulsifiers/ stabilizers, resins/ plasticizers/ fatty acid derivatives	$C_{19}H_{38}O_2$	299.294	n=1 $C_{21}H_{44}N_2O$	341.353
Methyl *n*-octadecanoate/ methyl stearate	Lubricant/ thermal stabilizers	$C_{19}H_{38}O_2$	299.294	n=1 $C_{23}H_{48}N_2O$	369.384
Perfluorobutanesulfonate (PFBS)	PFAS: Perfluoroalkyl sulfonic acids (PFSA; C4-C10).	$C_4HF_9O_3S$	300.958	-	-
Diamyl phthalate	NIAS	$C_{18}H_{26}O_4$	307.190	n=1 $C_{18}H_{28}N_2O_3$	321.217
Benzyl butyl phthalate (BBP) = Santicizer 160	NIAS (impurity)/ plasticizer	$C_{19}H_{20}O_4$	313.143	n=1 $C_{17}H_{26}N_2O_3$ n=1' $C_{20}H_{24}N_2O_3$	307.202 341.186
Perfluorohexanoic acid (PFHxA)	PFAS: Perfluoroalkyl carboxylic acids (PFCA; C4-C12)	$C_6HF_{11}O_2$	314.987	-	-
Dibutyl sebacate	Plasticizer	$C_{18}H_{34}O_4$	315.253	n=1 $C_{19}H_{38}N_2O_3$ n=2 $C_{20}H_{42}N_4O_2$	343.296 371.338
Tinuvin 326: Phenol, 2-(5-chloro-2H-benzotriazol-2-yl)-6-(1,1-	UV absorbing agents	$C_{17}H_{18}N_3OCl$	316.121	-	-

dimethylethyl)-4-methyl/ 2-(2′-Hydroxy-3′-tert-butyl-5′-methylphenyl)-5-chlorobenzortriazole					
Diphenyl isophthalate	NIAS	$C_{20}H_{14}O_4$	319.096	n=1 $C_{19}H_{22}N_2O_3$	327.170
Chimassorb 81/ UV 531: Methanone, 2-hydroxy-4-(octyloxy)-phenyl/ 2-hydroxy-4-*n*-octoxybenzophenone (Uvinul 3008 in Tech Lab)	UV absorbing agents	$C_{21}H_{26}O_3$	327.195	-	-
Dicyclohexyl phthalate = Morflex 150	NIAS/ plasticizer	$C_{20}H_{26}O_4$	331.190	n=1 $C_{19}H_{28}N_2O_3$	333.217
2-Palmitoylglycerol/ 1,3-dihydroxypropan-2-yl hexadecanoate	Anti-fogging agent/fatty acid derivatives	$C_{19}H_{38}O_4$	331.284	n=1 $C_{21}H_{44}N_2O$	341.353
Bis(4-methylpentyl) phthalate	NIAS	$C_{20}H_{30}O_4$	335.222	n=1 $C_{19}H_{30}N_2O_3$	335.233
Erucamide epoxidized soybean oil (ESBO) or docos-13-enamide (erucamide = Kemamide® E Ultra; processing aid agent in Tech Lab)	Stabilizers lubricant/ plasticizer additives or anti-blocking agent/Slip agent	$C_{22}H_{43}NO$	338.342		
Intioxidant 2246: 2,2'-Methylenebis(4-methyl-6-tert-butylphenol)/ Cyanox 2246 (Tech Lab)	Antioxidant agents	$C_{23}H_{32}O_2$	341.248	-	-
Di(2-ethylhexyl) maleate	Plasticizer	$C_{20}H_{36}O_4$	341.269	n=1 $C_{17}H_{32}N_2O_3$ n=2 $C_{14}H_{28}N_4O_2$	313.249 285.229
n-Butyl stearate	Plasticizer	$C_{22}H_{44}O_2$	341.341	n=1 $C_{23}H_{48}N_2O$	369.384
Dibenzyl phthalate	NIAS	$C_{22}H_{18}O_4$	347.128	n=1 $C_{20}H_{24}N_2O_3$	341.186
Tinuvin 328: 2-(2H-benzotriazol-2-yl)-4,6-ditertpentylphenol	UV absorbing agents	$C_{22}H_{29}N_3O$	352.238	-	-
Tetracosan-1-ol	Fatty acyl /alcohol	$C_{24}H_{50}O$	355.393	-	-
Tinuvin 327: 2,4-Di tertbutyl-6-(5-chlorobenzotriazole-2-yl)phenol	UV absorbing agent/ UV stabilizer	$C_{20}H_{24}N_3OCl$	358.168	-	-

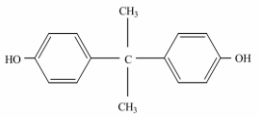
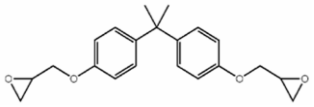
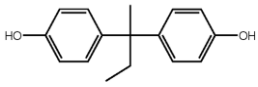
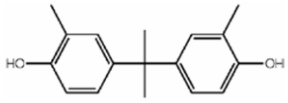
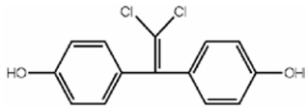
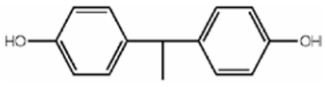
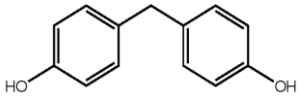
Irganox 1081:6,6'-Thiobis(2-(tert-butyl)-4-methylphenol)	Antioxidant agents	$C_{22}H_{30}O_2S$	359.204	-	-
Lowinox TBM-6	Antioxidant	$C_{22}H_{30}O_2S$	359.204	-	-
FWA 367: 1,4-Bis-(2-benzoxazolyl)-naphthalene	Whitening agents (FWAs)	$C_{24}H_{14}N_2O_2$	363.113	-	-
Di-*n*-heptyl phthalate Or Jayflex; diisoheptyl phthalate	NIAS/ plasticizer	$C_{22}H_{34}O_4$	363.253	n=1 $C_{20}H_{32}N_2O_3$	349.249
Perfluoroheptanoic acid (PFHpA)	PFAS: Perfluoroalkyl carboxylic acids (PFCA; C4-C12)	$C_7HF_{13}O_2$	364.984	-	-
Bis (2-*n*-butoxyethyl) phthalate	NIAS/ plasticizer	$C_{20}H_{30}O_6$	367.212	n=1 $C_{19}H_{30}N_2O_4$	351.228
Santicizer 261	Plasticizer	$C_{23}H_{28}O_4$	369.206	-	-
Cyanox 425	Antioxidant	$C_{25}H_{36}O_2$	369.279	-	-
Bis(2-ethylhexyl) adipate (DEHA) hexanedioic acid, bis(2-ethylhexyl) ester/ dioctyladipate (DOP)	NIAS/ plasticizer	$C_{22}H_{42}O_4$	371.316	n=1 $C_{19}H_{38}N_2O_3$ n=2 $C_{16}H_{34}N_4O_2$	343.296 315.275
Santicizer 148	Plasticizer	$C_{22}H_{31}O_4P$	391.203	-	-
Resimene 3520	Crosslinking agent	$C_{15}H_{30}N_6O_6$	391.229	-	-
Di-*n*-octyl phthalate (DnOP) or di(2-ethylhexyl) phthalate (DEHP) or diisooctyl phthalate	NIAS (impurity) or DEHP = Plasticizer/ solvent for paints/ vehicles for pigment dispersions	$C_{24}H_{38}O_4$	391.284	n=1 $C_{21}H_{34}N_2O_3$	363.264
DOPO-PEPA	Flame retardant	$C_{17}H_{16}O_7P_2$	395.044	-	-
Diisononyl adipate	NIAS/ plasticizer	$C_{24}H_{46}O_4$	399.347	n=1 $C_{20}H_{40}N_2O_3$ n=2 $C_{16}H_{34}N_4O_2$	357.311 315.275
Perfluorohexanesulfonate (PFHxS)	PFAS: Perfluoroalkyl sulfonic acids (PFSA; C4-C10).	$C_6H_1F_{13}O_3S$	400.951	-	-
Tributyl 2-(acetyloxy) propane- 1,2,3-tricarboxylate/ acetyl tributylcitrate/ Citroflex A-4	Plasticizer for both food contact materials and for inks, adhesives	$C_{20}H_{34}O_8$	403.233	n=1 $C_{21}H_{38}N_2O_7$ n=2 $C_{22}H_{42}N_4O_6$ n=3 $C_{23}H_{46}N_6O_5$	431.275 459.318 487.360
[(2r) 2-[(2r,3r,4 s) 3,4-Dihydroxyoxolan-2-yl] 2-hydroxyethyl] hexadecanoate/ sorbitan palmitate	Sealants/ intermediate for detergents, emulsifiers, stabilizers	$C_{22}H_{42}O_6$	403.305	n=1 $C_{21}H_{44}N_2O$	341.353

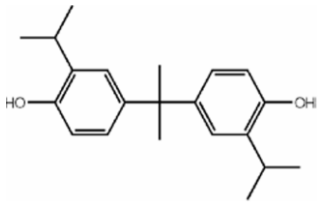
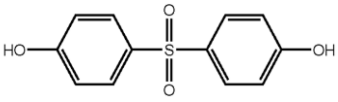
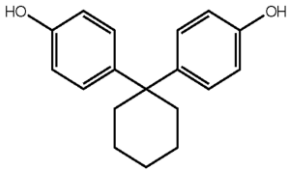
Squalene/ (6e,10e,14e,18e) 2,6,10,15,19,23-hexamethyltetracosa- 2,6,10,14,18,22-hexaene	Substituted hydrocarbon/ plasticizer and oxygen scavenger	$C_{30}H_{50}$	411.399	-	-
Perfluorooctanoic acid (PFOA)	PFAS: Perfluoroalkyl carboxylic acids (PFCA; C4-C12)	$C_8HF_{15}O_2$	414.981	-	-
FWA393: 4,4'-Bis (2-benzoxazolyl) stilbene	Whitening agents (FWAs)	$C_{28}H_{18}N_2O_2$	415.144	-	-
Di-isononyl phthalate/ nonyl 2-(nonyloxycarbony) benzoate = Jayflex DINP (Tech Lab)	Plasticizer/ solvent for paints/ vehicles for pigment dispersions	$C_{26}H_{42}O_4$	419.316	n=1 $C_{22}H_{36}O_3N_2$	377.279
Ethanox 702	Antioxidant	$C_{29}H_{44}O_2$	425.341	-	-
Tinuvin 1577: 2-(4,6-Diphenyl-1-3,5 triazin-2-yl)-5-hexyloxy-phenol,	UV absorbing agent/UV stabilizer	$C_{27}H_{27}N_3O_2$	426.218	-	-
Diisodecyl adipate or 2-ethylhexyl sebacate	Plasticizer	$C_{26}H_{50}O_4$	427.378	n=1 $C_{21}H_{42}N_2O_3$ n=2 $C_{16}H_{34}N_4O_2$	371.327 315.275
FWA368: 4-(2-Benzoxazolyl)-4'-(5-methyl-2-benzoxazolyl) stilbene	Whitening agents (FWAs)	$C_{29}H_{20}N_2O_2$	429.159	-	-
FWA184: 2,5-Bis(5-tert-butyl-2-benzoxazolyl) thiophene	Whitening agents (FWAs)	$C_{26}H_{26}N_2O_2S$	431.179	-	-
Alpha-tocopherol (vitamin E)/ Irganox E201	Natural antioxidant in polymer extrusion since 1990s.	$C_{29}H_{50}O_2$	431.389	-	-
Diisodecyl phthalate Jayflex DIDP	Plasticizer	$C_{28}H_{46}O_4$	447.347	n=1 $C_{23}H_{39}N_2O_3$	391.296
Tinuvin 234: (2 (2H-benzotriazol-2-yl)-4,6-bis(1-methyl-1-phenylethyl) phenol	UV absorbing agent/ UV stabilizer	$C_{30}H_{29}N_3O$	448.238	-	-
Sanitizer 278	Antioxidant and plasticizer	$C_{27}H_{34}O_6$	455.243	-	-
Akrochem NIBUD	Antiozonant	$C_{18}H_{36}N_2NiS_4$	467.119	-	-
Perkacit NDBC	Crosslinking agent	$C_{18}H_{36}N_2NiS_4$	467.119	-	-
Diisodecyl azelate	Plasticizer	$C_{29}H_{56}O_4$	469.425	n=1 $C_{23}H_{47}N_2O_3$	399.358
2,3-Di(octanoyloxy)propyl octanoate/ tricaprylin	Slip agent/ anti-blocking agent	$C_{27}H_{50}O_6$	471.368	n=1 $C_{13}H_{28}N_2O$ with 3 fragments	229.227

Anthraquinone (SB 104) solvent blue 104	Colorant	$C_{32}H_{30}N_2O_2$	475.238	-	-
Diundecyl phthalate = Jayflex L11 P-E	Plasticizer	$C_{30}H_{50}O_4$	475.378	n=1 $C_{24}H_{40}N_2O_3$	405.311
2,2',4,4'-Tetrabromodiphenyl ether	Flame retardant	$C_{12}H_6Br_4O$	482.723	-	-
Naugard 635	Antioxidant	$C_{38}H_{27}N$	498.222	-	-
Perfluorooctanesulfonate (PFOS)	PFAS: Perfluoroalkyl sulfonic acids (PFSA; C4-C10).	$C_8HF_{17}O_3S$	500.945	-	-
Didodecyl phthalate	NIAS/ plasticizer	$C_{32}H_{54}O_4$	503.409	n=1 $C_{25}H_{42}N_2O_3$	419.327
Irganox MD 1024: 2',3-Bis[[3-[3,5-di-tert.-butyl-4-hydroxyphenyl]propionyl]]propionohydrazide	Antioxidant agents (a metal deactivator and primary (phenolic) antioxidant)	$C_{34}H_{52}N_2O$	505.415	-	-
Di(tridecyl) adipate	Plasticizer	$C_{32}H_{62}O_4$	511.472	n=1 $C_{24}H_{48}N_2O_3$ n=2 $C_{16}H_{34}N_4O_2$	413.374 315.275
Ditridecyl benzene-1,2- dicarboxylate = Jayflex DTDP or Morflex X-1125	Plasticizer	$C_{34}H_{58}O_4$	531.441	n=1 $C_{26}H_{44}N_2O_3$	433.342
Irganox MD 1024	Antioxidant	$C_{35}H_{52}N_2O_4$	565.399	-	-
Perfluorodecanesulfonate (PFDS)	PFAS: Perfluoroalkyl sulfonic acids (PFSA; C4-C10).	$C_{10}HF_{21}O_3S$	600.938	-	-
Ultranox 626/ Irgafos 126: 3,9-Bis(2,4-di-tert-butylphenoxy)-2,4,8,10-tetraoxa-3,9-diphosphaspiro[5.5]undecane/ Ultranox 626	Antioxidant agents	$C_{33}H_{50}O_6P_2$	605.316	-	-
Irganox 1098	Antioxidant	$C_{40}H_{64}N_2O_4$	637.494	-	-
Irganox 259	Antioxidant	$C_{40}H_{62}O_6$	639.462	-	-
Irganox 1035: 3,5-Bis(1,1-dimethylethyl)-4-hydroxybenzenepropanoic acid thiodi-2,1-ethanediyl ester	Antioxidant agents	$C_{38}H_{58}O_6S$	643.403		
Irgafos®168: Phenol, 2,4-bis(1,1-dimethy lethyl)-, phosphite/ Ethaphos 368	Phenolic Antioxidant	$C_{42}H_{63}O_3P$	647.459	-	-
Naugarde XL-1	Antioxidant	$C_{40}H_{60}N_2O_5$	649.457	-	-

Irgafos®168 oxide: Tris[2,4-bis(2-methyl-2-propanyl) phenyl] phosphate	Oxidized/ degradation product of antioxidant Irgafos®168	$C_{42}H_{63}O_4P$	663.454	-	-
Weston 399: Trisnonylphenyl Phosphite/ Naugard PHR (Tech Lab)	Antioxidant agents	$C_{45}H_{69}O_3P$	689.506	-	-
Tris-(2,3-dibromopropyl) phosphate known as TRIS	Very efficient fire-retardant additive for polyester fibers but recalled from the market due to its mutagenicity.	$C_9H_{15}Br_6O_4P$	692.588	-	-
Irganox 1330: 1,3,5-Trimethyl-2,4,6-tris(3,5-di-tert-butyl-4-hydroxybenzyl)benzene/ Ethanox 330	Antioxidant agents	$C_{54}H_{78}O_3$	775.602	-	-
Irganox 3114: Tris(3,5-di-tert-butyl-4-hydroxybenzyl) isocyanurate	Antioxidant agents	$C_{48}H_{69}N_3O_6$	784.526		
3,9-Bis(2,4-dicumylphenoxy)-2,4,8,10-tetraoxa-3,9-dipjosphaspiro [5,5]undecane	Antioxidant	$C_{53}H_{58}O_2P_2$	789.398	-	-
Irganox 3125	Antioxidant	$C_{60}H_{87}O_2S$	872.649	-	-

Table S 3. Bisphenolic compounds and their analogous detected in the analyzed PET packaging objects with their corresponding chemical formula, *m/z*, structure and exact presence.

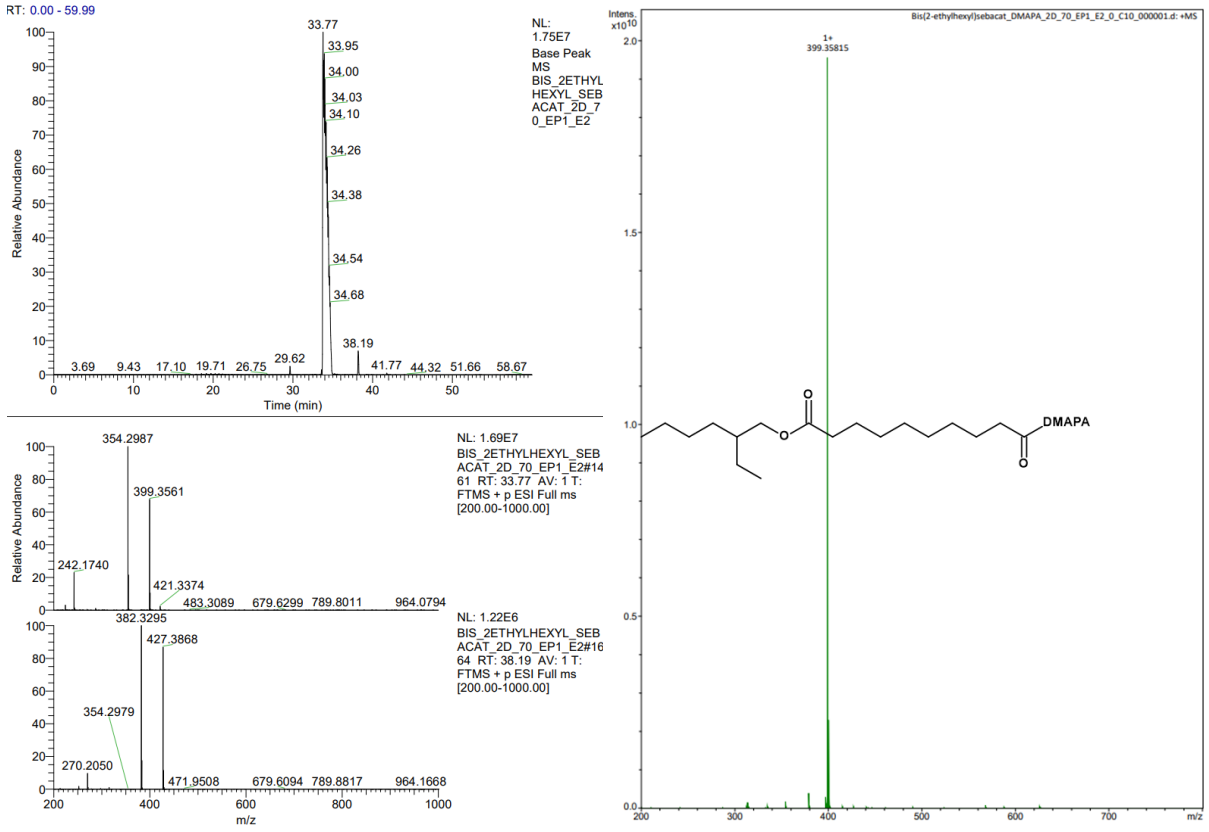
Bisphenol compound	$[M+H]^+$	*m/z*	Presence in
Bisphenol A (BPA) 	$C_{15}H_{16}O_2$	229.122	Juice FRA2 Milk SP Cola-1 FRA Cola-1 US Water QA Beer AUT-central Wine FRA1-external Wine FRA2-internal
Bisphenol A diglycidyl ether (BADGE) 	$C_{21}H_{24}O_4$	341.175	Alcohol FRA Oil FRA2
Bisphenol B: Bisphenol analog 	$C_{16}H_{18}O_2$	243.138	Juice FRA1 Juice FRA2 Milk SP Water SP Cola-1 US Beer AUT-internal Wine FRA1-internal Wine FRA2-internal & central Black FC
Bisphenol C: Bisphenol analog 	$C_{17}H_{20}O_2$	257.153	Alcohol FRA Oil FRA2 Cola-2 FRA Juice SP Water QA Transparent & black FC Beer AUT-external
Bisphenol C-dichloride: Bisphenol analog 	$C_{14}H_{10}Cl_2O_2$	281.013	Juice SP Water-S SP Water-S FRA Beer AUT-internal Wine FRA1-central Blue FC
Bisphenol E 	$C_{14}H_{14}O_2$	215.107	Juice FRA2 Cola-1 FRA Cola-1 US Black FC Beer AUT-external & internal Wine FRA2-external & internal Wine FRA1-external
Bisphenol F: Bisphenol analog 	$C_{13}H_{12}O_2$	201.091	Water SP Water-S FRA Cola-1 US Cola-2 FRA Alcohol FRA Beer AUT-external

			Wine FRA1-external Wine FRA2-internal
Bisphenol G: Bisphenol analog  	$C_{21}H_{28}O_2$	313.216	Juice FRA1 Wine FRA2-central
Bisphenol S: Bisphenol analog  	$C_{12}H_{10}O_4$	251.037	Alcohol FRA Juice FRA2 Milk SP Water SP Water-S SP Liqueur FRA Wine FRA1-central Wine FRA2-external & internal
Bisphenol Z: Bisphenol analog  	$C_{18}H_{20}O_2$	269.154	Liqueur FRA Oil FRA1 & 2 Cola-2 FRA Water SP Water QA Water-S SP Water-S FRA Beer AUT-external Wine FRA1 & 2-central

Annex: Additives verification

After the successful identification of additives in PET samples, these additives were validated after depolymerization of authentic additives, such as dihexhyl phthalate, dihexyl isophthalate, diisopropyl phthalate, bis(2-ethylhexyl)phthalate, bis(2-ethylhexyl)isophthalate, bis(2-ethylhexyl)sebacate, bis(2-methoxyethyl)phthalate, phthalic acid bis (2-butoxyethyl)ester, dibutyl phthalate, diamyl phthalate, di-*n*-octyl phthalate, butylphthalyl butylglycolate, polyethylenglycomononolaurate (n = approx. 10), butyl stearate…

One example will be showed here for the additive bis(2-ethylhexyl)sebacate after analysis by MALDI FTICR MS and LC-MS. In these both analytical methods (Annex 1), the predicted structure of the mono-derivatized additive of chemical formula $C_{23}H_{47}N_2O_3$ has been found at *m/z* 399.3581. In LC-MS, the loss of 45 units (part of DMAPA) was also identified.



Annex 1. LC-MS (right panel) and MALDI FTICR MS (left panel) spectra of the depolymerized additive bis(2-ethylhexyl) sebacate.

Chapter 5: Ageing and environmental PET

Introduction: Degradation products

Polyethylene terephthalate polyesters are major source of marine pollution. In environmental studies, they are principally identified by optical spectroscopy and few by Py-GC-MS. Unfortunately, these techniques are not efficient for identifying and quantifying PET,[1] they provide very few structural information on their modifications. It is crucial to study the modifications of environmental PET after weathering (UV, microorganisms, salinity, etc.) to understand their origin and compare the degree of modifications between macro-PET and micro- or nano-PET.

This work will answer the following open chemical and environmental questions:

- Can we distinguish between PET bottles damped in river versus PET bottles directly damped in seawater?
  This point is important for understanding the origin of the PET polymer from cost or from rivers in order to decrease the quantity damped in the sea;
- What are the chemical modifications of PET induced by weathering?
  For long term the cocktail sun, UV and water may form oxidized phenols from terephthalic acids which are potentially toxic to wildlife marine ecosystems. Even worse, sun, UV and chloride from sea water may form chlorinated aromatics from terephthalic acids which are known to be very toxic;
- What are the chemical modifications of PET induced by microorganisms growing on their surface in the environment?
  It will be interesting also to determine which microorganisms are able to grow on PET in the environment;
- What products are leaching from PET during their ageing?
  These products may be the plasticizers and antioxidants added to the PET polyester or products formed during the PET environmental degradation.

Reference

1- Ivleva, N.P. Chemical analysis of microplastics and nanoplastics: challenges, advanced methods, and perspectives. Chem. Rev. **2021**, 121, 1188611936. http://doi.org/10.1021/acs.chemrev.1c00178

Article 4

Ageing of PET polyesters & deciphering the secrets of environmental PET for better assessment of their origin and future fate in ecosystems

ABSTRACT: Pollution by plastics is an important issue in our environment especially for aquatic ecosystems. An important part of these plastics is constituted by disposables bottles and fabrics microplastics which are made mainly from polyethylene terephthalate (PET). This polyester is degraded by physical phenomena, chemical weathering due to sunlight, temperature and sea water, and/or biological procedures due to microorganisms. In environmental studies, there was no robust method for the identification of structural modifications of PET after natural ageing so the information about the possible source of PET waste that constitutes one of the striking ecosystems pollution problems is still very challenging. More chemical data about PET degradation pathways are still to reveal. In this work, our recent developed methodology combining soft chemical depolymerization by transamidation using *N,N*-dimethyl-1,3-propanediamine (DMAPA) with the analysis by ultra-high resolution mass spectrometry (FTICR and Orbitrap) was applied to three different types of PET samples. Indeed, PET ageing was first studied after short and long-term UV-irradiation at a wavelength of 365 nm and after thermo-ageing at 75 °C. After that, aquatic PET samples from well-known natural and/or semi-natural conditions were studied to clarify the origin of PET in environment (sea water or river) and to determine the exact PET packaging object's content (still water or carbonated liquid bottles). Finally, environmental marine samples from the English Channel were studied to assess the possible effect of microorganisms on their degradation. In fact, many physical and chemical modifications were observed after artificial, natural and semi-natural ageing concerning oxidation reactions, additives abundance and C-C coupling inside PET backbone. PET microplastics were well differentiated according to their aquatic origin and packaging type; and the marine PET samples showed a specific signature due to the presence of microorganisms. All these data will allow us to get a global understanding of the parameters affecting PET degradation mechanisms and to attribute the possible origin of pollution by PET microplastics in order to predict their fate in the ecosystems.

Keywords: PET, microplastics, structural modifications, ageing, UV-irradiation, thermo-ageing, depolymerization, transamidation, environmental PET, microorganisms, pollution, MALDI FTICR MS, ESI LC-Orbitrap-MS.

Polyethylene terephthalate (PET) is a polyester formed by polycondensation reaction between terephthalic acid and ethylene glycol. PET may be blended with other diols such as 1,4-cyclohexanedimethanol, present in poly(ethylene glycol-co-1,4-cyclohexanedimethanol) terephthalate co-polymers, in order to increase the final polymer strength.[1-2] The degradation of PET in the environment by physical and chemical phenomena (photodegradation, mechanical stress, hydrolysis by water…) leads to the formation of small particles ranging from 1 micrometer to 5 millimeters in size called microplastics which their lifetime and fate in the environment are still unknown.[3-5] Microplastics are still a major source of pollution for soils[6] and other ecosystems especially aquatic ecosystems[7-8] such as rivers[9] or sea[10-11] and oceans[12-13] that affect aquatic fauna.[14] The degradation of PET provides different products after UV exposure for which crosslinking were found and demonstrated by a reduction in UV transmission and oxygen permeability of PET material.[15] Two main mechanisms were mentioned as a result of PET chain scission: Norrish type I mechanism that forms mainly radicals after photolysis and ester bond cleavage, and Norrish type II reactions resulting in the formation of polymer chains with vinyl and carboxylic acid end groups explained by the abstraction of hydrogen atoms via intramolecular reactions or by oxidation reactions. The formation of carboxylic acid end-groups, aldehydes and hydroxyl terephthalate was also explained differently via radical mechanisms (Figure 1).[16-18] Some studies suggested the formation of quinone-type structures after formation of peroxides and release of hydroxy radical after thermo-oxidative PET degradation.[16, 19] In parallel, these microplastics may be degraded more by specific microorganisms especially after UV treatment.[20] Indeed, microbial degradation by the bacteria *Nocardia* was very slow even in the presence of esterase.[21] Other fungi species may contribute to PET biological degradation such as the filamentous fungi *Fusarium oxysporum and F. Solani.*[22-23] In addition, enzymatic degradation may be occurred resulting in the erosion of the surface of PET using enzymes such as petase,[24] hydrolase from the actinomycete *Thermobifida fusca*[25] *or* cutinase from *Thermobifida alba.*[26] This enzymatic degradation is strongly dependent on PET physical properties especially crystallinity; for example, cutinase from *F. Solani pisi* degrades only the amorphoeous areas of PET.[27] Polyethylene terephthalate may be also contaminated by a high quantity of non-intentionally added substances (NIAS) such as acrylate adhesive.[28-29] In fact, nothing is known about the structural modifications of PET which may be induced in the marine environment[30] except their hydrolysis.[31] Our recent methodology allowed the study of the structural modification and quantification of PET microplastics[1] and it will be used here to assess PET ageing and to study aquatic samples. Here, the aim is to study PET ageing mechanisms after UV-exposure and heating and to characterize the structural modifications of their microplastics from different environmental origins

that yield complex and crosslinked degradation products. This strategy will be used to determine PET pollution sources and to discover more data about its degradation mechanisms after natural and accelerated ageing.

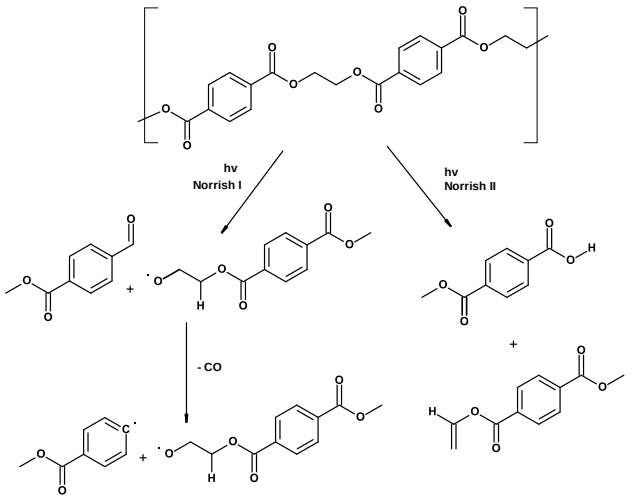


Figure 1. Formation of CO and COOH end-groups after PET photodegradation: Norrish type I and Norrish type II reactions.

EXPERIMENTAL SECTION

Chemicals. All aqueous solutions were prepared from ultrapure grade water obtained by water filtration with a two stages Millipore system (Milli-Q® academic with a cartouches Q-Gard 1 and Progard 2, Merck Millipore, Burlington, Massachusetts, United States). All solvents were MS analytical grade. All solvents and chemicals were purchased from Merck (Merck KGaA, Darmstadt, Germany) and used without further purification. 3-(Dimethylamino)-1-propylamine also called *N,N*-dimethyl-1,3-propanediamine (DMAPA) 99% and 1,1,1,3,3,3-hexafluoro-2-propanol (HFIP) ≥ 99% were used as received.

Samples. For both artificial ageing experiments, polyethylene terephthalate was a French transparent fruit container film.

For natural and semi-natural experiments, two French bottles were used: Water bottle (330 ml) and cola bottle (250 ml).

Ten other random marine samples of different bottles and containers were collected from the English channel numerated from 1 to 10 (Envi-number).

One another sample (Envi-11) which is visually more contaminated was collected from the North French beach.

Only a piece of 3 cm × 3 cm was received for MS analysis for all samples.

The original photos of these environmental marine samples are shown in Figure 2.



Figure 2. Random marine PET samples: First ten from the English channel and the last one from the North French beach.

Ageing experiments.

(a). PET UV-irradiation: A French fruit container film (7 cm × 7 cm) was irradiated for short period (48 hours) and for long period (6 months) at room temperature using a led lamp emitting UVA at wavelength of 365 nm, specifically using HP UV LEDs-B [365 nm, irradiance of 150 mW.cm^{-2}, Omnicure® AC475 equipped with an optical adaptor, Excelitas technologies, Waltham, MA, USA] as light source.

Samples were abbreviated as FC ref for the fruit container before ageing and FC UV-6M for the corresponding fruit container after UV-ageing of 6 months.

(b). PET thermo-oxidation: A French fruit container film (7 cm × 7 cm) was placed horizontally in GC oven set at a temperature of 75 °C during 48 hours. The aged sample by heating was abbreviated as FC 2D-75 °C.

Natural and semi-natural experiments. The two bottles of water and cola were washed with ultrapure water. They were then dried under air and immersed partially in Fontainebleau sand. Each type of PET bottle was placed in an aquatic environment in rural sweet water in Liane river (Figure 3 & 4) and exposed to natural temperature and light for 2 months.



Figure 3. Natural deposit of PET bottles in Liane river.



Figure 4. Exact position of PET bottles in Liane river deposited from 17th December 2023 until 17th February 2024.

A direct trial in sea was performed at the same period, but unfortunately it was very hard to keep bottles in the sea during these 2 months because of strong tides, so a semi-natural experiment was performed in which two water and cola bottles from the same brands as previously were introduced in a tank of galvanized steel to not interfere with the natural light intensity. The seawater agitation was maintained with a water pump at a flow rate of 300 L/h. Sea water was taken from the natural environment and partially changed every 15 days (Figure 5).

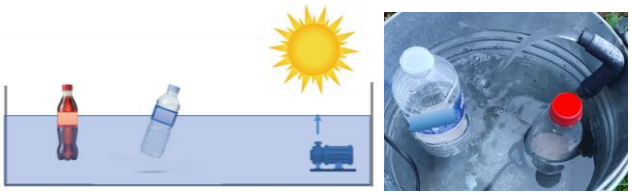


Figure 5. Semi-natural sea water experiment, PET bottles deposited from 14th February 2024 until 14th April 2024.

For facilitating the coming discussion, the samples mentioned in this section will be abbreviated as present in the following table, Table 1.

Table 1. Abbreviation of PET samples used for the natural and semi-natural experiments.

PET abbreviation	Description
Ref-water	Water bottle before ageing
Sea-water	Water bottle in sea water experiment (semi-natural conditions)
Liane-water	Water bottle in rural sweet water in Liane river (natural conditions)
Ref-cola	Cola bottle before ageing
Sea-cola	Cola bottle in sea water experiment (semi-natural conditions)
Liane-cola	Cola bottle in rural sweet water in Liane river (natural conditions)

Samples preparation. PET environmental samples were washed eight times with ultrapure water to remove sands, impurities and other possible superficial contaminants. Some samples were dirtier than others and necessitate more washing steps. After drying at room temperature, they were cut in pieces of around 2.5 mm × 2.5 mm size.

Depolymerization of environmental PET samples. The innovative methodology of Almasri et al. has been performed on environmental PET samples. Indeed, 25 mg of PET microplastics were solubilized in 400 mg of 1,1,1,3,3,3-hexafluoro-2-propanol (HFIP) overnight; then they were added to 1 mL of 3-(dimethylamino)-1-propylamine (DMAPA) and left under N_2 at 58 °C for 1 day. The reaction was then quenched by 400 µL of formic acid and the mixture was extracted with ethyl acetate after ultrapure water addition by high-speed centrifugation. The obtained organic phases were evaporated and stored.[1]

Environmental PET samples' MS analysis. Before MS analysis, PET samples were solubilized in methanol at 1 mg/10 µL then diluted 100 times in acetonitrile/water/formic acid 5/95/0.1 (v/v/v). Environmental PET samples were analyzed using first a MALDI ionization on SolariX XR instrument with a 9.4 Tesla actively shielded superconducting magnet fitted with a dynamically harmonized cell (Bruker Daltonics, Bremen, Germany) and controlled by FTMS Control software. The matrix used here was α-cyano-4-hydroxycinnamic acid. MALDI FTICR MS spectra were acquired in positive mode using broadband detection, 8 M points; 32 scans accumulation with a mass range from *m/z* 100 to 1,500. Only an external calibration was achieved using red phosphorous and data were processed using Data Analysis software version 5.0 (Bruker Daltonics, Bremen, Germany). PET samples were analyzed also using an Orbitrap LTQ XL mass spectrometer hyphenated to a Dionex Ultimate 3000 HPLC System (ThermoFisher Scientific, Bremen, Germany). The analysis was performed using a 60 min multi-step gradient at a flow rate of 0.50 mL.min^{-1} on a Zorbax RRHD SB-C18 column (2.1 µm i.d. × 150 mm) packed with 1.8 µm beads pores with 80 Å pore size from Agilent Technologies (Santa Clara, CA, USA) placed in an oven at a temperature of 50 °C. The mobile phases used were solution A of 5% acetonitrile in acidified water, 0.1% formic acid and solution B of 75% acetonitrile in acidified water, 0.1% formic acid.[1] Data were processed using FreeStyle™ 1.8SP2 QF1 software (Thermo Fisher Scientific).

RESULTS AND DISCUSSIONS

The depolymerization by transamidation using 3-(dimethylamino)-1-propylamine (DMAPA) after HFIP solubilization was performed on all environmental samples except the ten random samples of English Channel. The last samples were transamidated directly without HFIP utilization. All samples were analyzed both by LC-MS and MALDI FTICR MS.

Accelerated ageing has been performed to compare the thermo-oxidative and photolytic degradation processes on PET. For this aim, a film of the same fruit container was divided into two fragments, one of them was heated for 2 days at the temperature of 75 °C and the second was irradiated at 365 nm for 6 months. As a result, a deformation of the shape of PET film after heating was observed without any color changing. The UV-irradiated PET has remained transparent after one week of irradiation indicating that it contains anti-UV additives still resistant, not degraded yet. But it changed its color to become yellowish and brownish after 6 months of UV-exposure (Figure S1) as most of additives and polymers absorb light at wavelengths below 400 nm resulting in the degradation of polymeric films.[32] This suggested evidently that the increase of UV-exposure time enhances the degradation of PET polyester due to the degradation of its additives in function of time.

Environmental experiments in sea water and Liane river were performed on water and cola bottles. Both environmental bottles provided less extraction yield than their corresponding references. Indeed, the extraction yield of water bottle decreased drastically from 45% and 43% to 10% for Liane-water, Sea-water and Ref-water bottles respectively. This decrease was less violent in the case of

cola bottle with 59%, 49% and 33% for Liane-cola, Sea-cola and Ref-cola bottles respectively. This observation was the first sign of degradation of PET films in natural and semi-natural conditions during two months of ageing. The PET in the natural river conditions seems to be more degraded than the semi-natural conditions in seawater. Concerning the effect of heating at 75 °C of 2 days and UV-irradiation of 6 months on the yield of extraction, the heating yielded 80% vs 73% for the 6-months of irradiation; both were higher than the yield of the reference fruit container sample (34%).

All depolymerization reactions were successful providing the expected depolymerization marker [$C_{18}H_{30}N_4O_2$ + H^+] formed of the terephthalic acid di-transamidated at *m/z* 335.2442. The relative abundance of this marker and the other peaks were calculated in comparison to the major composition of each depolymerized mixture.

The following data will be given according to LC-MS dynamics.

In the environmental experiments, this marker was the highest in Liane-cola bottle then Liane-water bottle with abundances of 49% and 36% of their major composition respectively confirming the extraction yields' trend of these experiments. The depolymerization rates of these bottles taking to account, in addition to the main depolymerization marker, the mono-derivatized PET monomer [$C_{15}H_{22}N_2O_4$ + H^+] at *m/z* 295.1652 were 59% and 42% respectively. However, for the accelerated ageing experiments, the depolymerization marker was the most intense after 6 months of UV-exposure with an abundance of 82% versus 39% after heating at 75 °C for 2 days and 33% without accelerated ageing. The rate of depolymerization of these aged samples was in accordance with the main depolymerization marker results. Indeed, this rate diminished from 82% to 45% then 40% for FC UV-6M, FC 2D-75 °C and FC ref respectively (Table S1).

The content of dimers and oligomers of the previous two peaks in the environmental experiments was the most intense in Liane-water bottle and Sea-cola bottle registering 50% and 61% respectively. However, it was very similar in the case of FC and FC 2D-75 °C with almost 49% but negligible after UV-exposure for FC UV-6M with only 0.58% of the major composition (Table S1).

Polyols present in the environmental and accelerated aged experiments were cycohexanedimethanol marked by the presence of both mono- and di-derivatized compounds containing this diol [$C_{21}H_{32}N_2O_4$ + H^+] (*m/z* 377.244) and [$C_{34}H_{48}N_4O_6$ + H^+] (*m/z* 609.365) (Figure 6, (d)); and diethylene glycol (DEG) marked by the presence of this diol bearing two terminal groups of derivatized terephthalic acids [$C_{30}H_{42}N_4O_7$ + H^+] at *m/z* 571.313 with its dimer and trimer.[1] The content of the cyclohexanedimethanol derivatized compounds decreased from 4% to only 0.15% and 0.08% for FC ref, FC 2D-75 °C and FC UV-6M respectively.

On the other hand, four main oxygenated compounds were detected: The main depolymerization marker with one oxygen molecule [$C_{18}H_{30}N_4O_3$ + H^+] at *m/z* 351.239, the PET monomer mono-derivatized with one oxygen molecule [$C_{15}H_{22}N_2O_5$ + H^+] at *m/z* 311.16, the dimer of the main depolymerization marker with one oxygen molecule [$C_{28}H_{38}N_4O_7$ + H^+] at *m/z* 543.281 and the main marker of DEG diol with one oxygen molecule [$C_{27}H_{34}N_2O_9$ + H^+] at *m/z* 587.308. Indeed, the sum of these oxygenated compounds' abundances was the most intense in Sea-cola and Liane-cola in comparison to Ref-cola with almost 0.02%, 0.01% and 0.004% respectively confirming the degradation of cola bottle in seawater and river. However, it was the most intense in Ref-water followed by Sea-water then Liane-water with 0.05%, 0.02% and 0.01% of their major composition respectively suggesting the possible presence of other intense oxygenated compounds in the blend to justify this unexpected profile of oxygenated species.

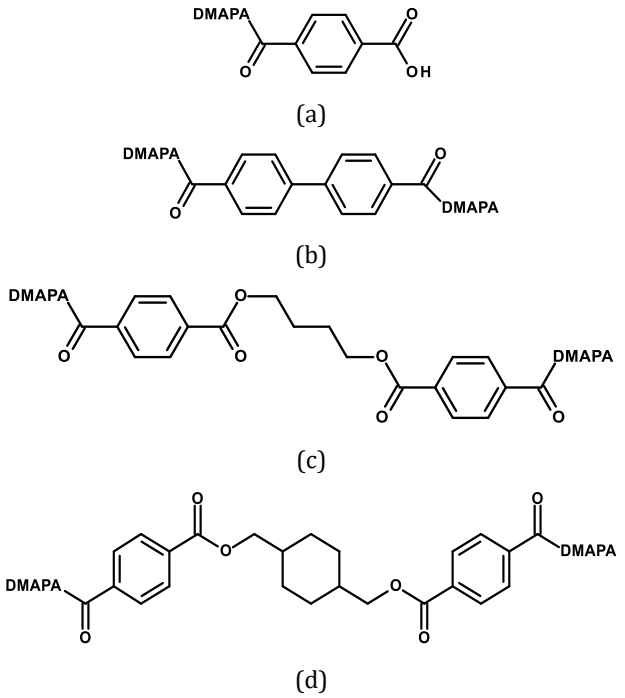


Figure 6. Structures of degradation products detected in the aged and environmental samples with the following *m/z*: (a) 251.139, (b) 411.275, (c) 555.318 and (d) 609.365.

The degradation product appearing at *m/z* 251.139 (Figure 6, (a)) has been detected in all PET samples under two separated retention times around 0.9 min and 1.7 min suggesting the presence of two sources; first, the degradation of PET polymer itself and second, the derivatization of non-intentionally added substances (NIAS) or the intentionally added substances (IAS) like additives or monomers/oligomers used during manufacturing such as mono-hydroxyethyl terephthalate present at *m/z* 211.060 (Table S 2). An interesting profile of the di-derivatized di-benzylic compound [$C_{24}H_{34}N_4O_2$ + H^+] appearing at *m/z* 411.275 was identified (Figure 6, (b)). Indeed, a remarkable growth of this last compound's abundance was detected. The percentage of growth in comparison to FC ref was 0.13% after thermo-treatment (FC 2D-75 °C) and 1.6% after UV-irradiation during 6 months (FC UV-6M). This confirms that heating and UV-exposure can easily enhance the C-C coupling. This observation was also confirmed in the natural and semi-natural conditions in seawater and Liane river where sun, emitting light and temperature, is present.

Another compound was detected, it was formed of di-transamidated terephthalic parts with butanediol diol[2] [$C_{30}H_{42}N_4O_6$ + H^+] at *m/z* 555.318 (Figure 6, (c)). This compound was surprisingly detected in traces (less than 0.1%) in only FC UV-6M, Liane-water and Sea-cola. It was absent in the FC before ageing as well as the water and cola bottles of reference. This may confirm that accelerated and

natural ageing procedures can form new compounds after degradation. The heating at 75°C for 2 days was not enough to generate this compound as it was absent in the corresponding sample. This degradation compound may be explained by the dissociation of the compound having cyclohexanedimethanol (*m/z* 609.365) (Figure 6, (d)) by intramolecular reactions enhanced by light. In fact, the content in cyclohexanedimethanol decreased 4% after UV-ageing of the fruit container.

All the previous data suggest that the difference of degradation ways between water and cola bottles in Liane river and seawater is related to the PET type/crystallinity and to the salinity of water.

These samples have been analyzed by stereomicroscopy and macro-Raman, the two analytical techniques used commonly in environmental studies, without providing any additional data (Figure S2 & 3)

Concerning the additives present in PET artificially aged samples, a screening of almost 46 additives will be described after LC-MS analysis (Table S2). Indeed, some additives were present in all aged samples but with different abundances. For instance, the antioxidant propyl gallate of chemical formula $C_{10}H_{12}O_5$ was present in all samples at *m/z* 213.075 but it was more deteriorated after thermo-treatment. However, despite the presence of the antioxidant Irganox MD 1024: 2',3-Bis[[3-[3,5-di-tert-butyl-4-hydroxy-phe-nyl]propionyl]] propionohydrazide of chemical formula $C_{30}H_{58}O_4S$ (*m/z* 515.413) in all samples, it was more deteriorated after 6 months of UV-exposure (Table S2).

Some additives were very sensitive to temperature. For example, the flame retardant 9,10-dihydro-9-oxa-10-phosphaphenanthrene-10 oxide (DOPO) of chemical formula $C_{12}H_9O_2P$ and *m/z* 217.041 was resistant to UV-exposure but it was absent totally after heating; as the case of the antioxidant 1,3-diphenyl-2-thiourea ($C_{13}H_{12}N_2S$) appeared at *m/z* 229.079 in FC ref and FC UV-6M only. However, others were very sensitive to UV irradiation. For instance, the antioxidant butylated hydroxytoluene (BHT) of *m/z* 221.189 was detected before ageing and after heating only. The same evolution was observed for the retarder cyanomethyl methyl (phenyl)carbodithioate ($C_{10}H_{10}N_2S_2$) and the antioxidant 1,3-di-o-tolylguanidine ($C_{15}H_{17}N_3$) appearing at *m/z* 223.036 and 240.149 respectively (Table S2).

On the other hand, some additives were very sensitive to temperature and UV irradiation. The antioxidant Naugard PANA ($C_{16}H_{13}N$) of *m/z* 220.112 was detected before ageing but it disappeared totally after both ageing experiments. The same observation was registered for the UV stabilizer hexyl 2-hydroxybenzoate $C_{13}H_{18}O_3$ (*m/z* 223.133). Same observation was registered for some NIAS or intermediates such as bis(4-methylpentyl) phthalate $C_{20}H_{30}O_4$ and docosanoic acid $C_{22}H_{44}O_2$ appearing at *m/z* 335.222 and 341.341 respectively (Table S2).

Some additives and degradation products have been also studied in the case of the environmental experiments, natural and semi-natural conditions, for both water and cola bottles. Indeed, the monohydroxyethyl terephthalate was detected in all samples at *m/z* 211.060 with its derivatized form at *m/z* 251.139. Furthermore, the antioxidant butylated hydroxytoluene (BHT) have been detected in all PET films at *m/z* 219.174. However, the plasticizer tributyl phosphate ($C_{12}H_{27}O_4P$) have been detected at *m/z* 267.172 only in the water bottle before and after environmental weathering. The oxidized or degradation product of antioxidant Irgafos®168 ($C_{42}H_{63}O_4P$) appearing at *m/z* 663.454 was found only in Water-ref, Water-Liane and Cola-ref bottles.

The ten random environmental samples from the English Channel, which were transamidated directly with DMAPA, have been studied. It was possible to predict their content after attributing some specific markers of these bottles after PET depolymerization. Indeed, a specific composition for each PET sample was found (Figure S4) except PET Envi-6 sample which was not soluble in DMAPA even after 4 days; it stayed intact. This plastic was definitely not a polyester or co-polyester. PET Envi-1, 2, 4, 5, 8 & 9 have contained the marker peaks of cyclohexanedimethanol diol appearing at *m/z* 377.243 and *m/z* 609.365. This observation was in accordance to our previous data of depolymerized bottles. [1, 33] PET environmental samples 1 and 5 were very similar in composition to cola bottles and samples 4 and 8 were more simulated to oil bottles. The possible prediction of the content of bottles differentiated by structural composition after depolymerization was confirmed through the source of bottles (Figure 2). The relative abundances of the mono-derivatized PET monomer, the main depolymerization peak and the marker peaks of cyclohexanedimethanol/PETG co-polyester presence in MALDI FTICR MS are described in Table 2.

Table 2. MALDI FTICR MS relative abundances of PET and PETG markers present in environmental PET samples.

PET Envi-n (n = 1-11)	First PET marker *m/z* 335.244	Second PET marker *m/z* 295.165	First PETG marker *m/z* 377.243	Second PETG marker *m/z* 609.365
Envi-1	1.74E+10	1.68E+08	2.99E+08	3.30E+09
Envi-2	1.13E+10	3.90E+08	3.27E+08	1.60E+09
Envi-3	3.75E+09	5.77E+07	0.00E+00	0.00E+00
Envi-4	8.02E+09	2.78E+08	2.52E+06	1.89E+07
Envi-5	1.40E+10	3.09E+08	1.23E+08	6.68E+08
Envi-6	Not PET	Not PET	Not PET	Not PET
Envi-7	1.01E+10	2.62E+08	0.00E+00	0.00E+00
Envi-8	7.46E+09	8.62E+07	1.12E+08	2.82E+08
Envi-9	4.69E+09	1.04E+08	2.68E+06	1.64E+07
Envi-10	7.38E+09	6.69E+07	0.00E+00	0.00E+00
Envi-11	9.43E+08	1.59E+08	0.00E+00	0.00E+00

A transamidation after solubilization in HFIP of the Envi-11 sample collected from the beach, the more degraded sample, was performed. The results of analysis were registered after addition of an internal standard (peak at *m/z* 307.213).[1] Dimers and oligomers in this environmental sample were very intense in comparison to the other marine samples. This is due to its higher deterioration by weathering and mechanical degradation on the beach as

well as maybe the unknown time of this natural weathering which is longer than the other samples (Figure S5).

A detailed MALDI FTICR MS data treatment was achieved on the marine PET samples. For example, PET Envi-2 (originally a container) contained more oxidized PET products in comparison to its similar daily life PET before ageing. Two oxidized products of the main depolymerization peak with one [$C_{18}H_{30}N_4O_3 + H^+$] and two oxygen atoms [$C_{18}H_{30}N_4O_4 + H^+$] appearing at *m/z* 351.2391 and *m/z* 367.2339 respectively were detected. The compound having 2 oxygen atoms was not found previously in the bottles and containers before ageing.

In addition, mono-derivatized saturated fatty acids such as palmitic acid (C16:0) [$C_{21}H_{44}N_2O + H^+$] appearing at *m/z* 341.3526 with its corresponding oxygenated product [$C_{21}H_{44}N_2O_2 + H^+$] appearing at *m/z* 357.3476 and stearic acid (C18:0) [$C_{23}H_{48}N_2O + H^+$] appearing at *m/z* 369.3839 have been detected. Other unsaturated mono-derivatized fatty acids were also identified such as linoleic acid (C18:2) [$C_{23}H_{44}N_2O + H^+$] at *m/z* 365.3526 and oleic acid (C18:1) [$C_{23}H_{46}N_2O + H^+$] at *m/z* 367.3683 as shown in Figure 7.

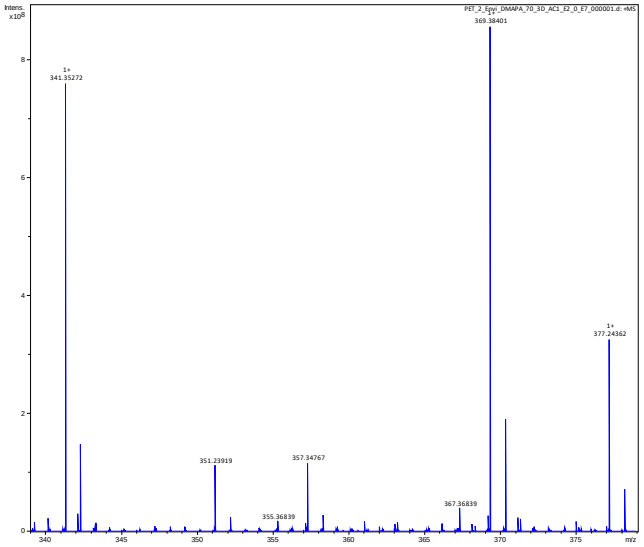


Figure 7. MALDI FTICR MS spectrum of PET Envi-2 (*m/z* 339-*m/z* 379).

It is interesting to find all these fatty acids in this sample but they may have many sources. They maybe enchased in the films of PET or coming from additives depolymerization.[33] An external contamination by the used solvent or even other sources are also possible. As fatty acids appeared in MALDI FTICR MS spectrum with relatively high intensity so the contamination and additives hypothesis are excluded. To investigate their origin, the analysis results of environmental PET were compared to a depolymerized oil bottle. A specific family of compounds were detected only in the environmental marine sample. Indeed, odd fatty acids such as the derivatized margaric acid (C17:0) [$C_{22}H_{46}N_2O + H^+$] appearing at *m/z* 355.3683 with its oxygenated compound [$C_{22}H_{46}N_2O_2 + H^+$] appearing at *m/z* 371.3632 were found in addition to other odd fatty acids such as C15:0 [$C_{20}H_{42}N_2O + H^+$] at *m/z* 327.3369 and C19:0 [$C_{24}H_{50}N_2O + H^+$] at *m/z* 383.3996. These odd fatty acids, which were absent in the depolymerized oil bottle, are a signature of the presence of microorganisms (biological signature). This confirms that environmental PET samples have been affected by bacteria and/or marine planktons.

CONCLUSIONS AND PERSPECTIVES

The strategy of depolymerization by transamidation combined to mass spectrometry analysis by LC-MS and MALDI FTICR MS was used for the first time to study ageing by weathering on molecular level. In fact, accelerated ageing by heating and UV irradiation was studied and the difference of these ageing parameters on PET degradation products was described. In addition, natural experiments in Liane river and semi-natural experiments in seawater have been performed on water and cola bottles indicating the effect of salinity and type of bottle on the degradation products. In conclusion, it was found generally that the accelerated and natural weathering enhances the formation of phthalates NIAS, favorizes the C-C coupling of degradation products, forms more oxidized species and diminishes or even disappears some additives especially antioxidants and plasticizers. Random plastic wastes purchased from English Channel and beach were also studied. Our methodology was useful to predict the content of these pollutants' wastes after excluding the plastics of other polymeric nature from polyesters and co-polyesters. Not only chemical signatures have been found in the studied samples but also a biological signature was determined after the detection of microorganisms' effect. It will be possible with this strategy to estimate the time of degradation of plastic wastes in polyesters and co-polyesters in order to know more data about their lifetime and fate in the environment.

ASSOCIATED CONTENT

Supporting Information

Additional experimental details and characterization data.

AUTHOR INFORMATION

First author

Bayan Almasri - Univ. Lille, CNRS, UAR 3290, MSAP, Miniaturisation pour la Synthèse l'Analyse et la Protéomique, F-59000 Lille, France ; Laboratoire de Chimie Appliquée, Faculté des Sciences III, Université Libanaise, Ras Maska, Tripoli, Liban ; orcid.org/0009-0001-9467-5716.

Note

The authors declare no competing financial interest.

AKNOWLEDGMENT

Bayan ALMASRI gratefully acknowledges the funding of her joint PhD between University of Lille and Lebanese University by the PAUSE funding program. The mass spectrometer was funded by University of Lille, CNRS, Région Hauts-de-France and the European Regional Development Fund (ERDF). The authors gratefully acknowledge the financial support of the FTICR MS facility from the IR INFRANALYTICS FR2054 CNRS and of the EU_FTICR _MS project Grant Agreement 731077 funded by EU Horizon 2020 Research and Innovation Program.

REFERENCES

1. Almasri, B.; Rolando, C., Identification and quantification of polyethylene terephthalate (PET) polyesters and microplastics combining soft chemical depolymerization by dimethylaminopropylamine (DMAPA) and analysis by MALDI FTICR & LC ESI Orbitrap mass spectrometry. *ChemRxiv*®, **2025**, submitted to *ACS Analytical Chemistry.*
2. Almasri, B.; Rolando, C., New approach for polyethylene terephthalate (PET) diols deciphering: Application on PET bottles paving their structural modification. Submitted, **2025.**
3. Andrady, A. L., Microplastics in the marine environment. *Marine pollution bulletin* **2011,** *62* (8), 1596-1605.
4. Rochman, C. M.; Browne, M. A.; Underwood, A. J.; Van Franeker, J. A.; Thompson, R. C.; Amaral-Zettler, L. A., The ecological impacts of marine debris: unraveling the demonstrated evidence from what is perceived. *Ecology* **2016,** *97* (2), 302-312.
5. Geyer, R.; Jambeck, J. R.; Law, K. L., Production, use, and fate of all plastics ever made. *Science advances* **2017,** *3* (7), e1700782.
6. Ng, E. L.; Lin, S. Y.; Dungan, A. M.; Colwell, J. M.; Ede, S.; Lwanga, E. H.; Meng, K.; Geissen, V.; Blackall, L. L.; Chen, D., Microplastic pollution alters forest soil microbiome. *Journal of hazardous materials* **2021,** *409*, 124606.
7. Barboza, L. G. A.; Vethaak, A. D.; Lavorante, B. R.; Lundebye, A.-K.; Guilhermino, L., Marine microplastic debris: An emerging issue for food security, food safety and human health. *Marine pollution bulletin* **2018,** *133*, 336-348.
8. Zhang, B.; Wu, D.; Yang, X.; Teng, J.; Liu, Y.; Zhang, C.; Zhao, J.; Yin, X.; You, L.; Liu, Y., Microplastic pollution in the surface sediments collected from Sishili Bay, North Yellow Sea, China. *Marine Pollution Bulletin* **2019,** *141*, 9-15.
9. He, B.; Smith, M.; Egodawatta, P.; Ayoko, G. A.; Rintoul, L.; Goonetilleke, A., Dispersal and transport of microplastics in river sediments. *Environmental pollution* **2021,** *279*, 116884.
10. Van Cauwenberghe, L.; Vanreusel, A.; Mees, J.; Janssen, C. R., Microplastic pollution in deep-sea sediments. *Environmental pollution* **2013,** *182*, 495-499.
11. Zhao, J.; Ran, W.; Teng, J.; Liu, Y.; Liu, H.; Yin, X.; Cao, R.; Wang, Q., Microplastic pollution in sediments from the Bohai Sea and the Yellow Sea, China. *Science of the Total Environment* **2018,** *640*, 637-645.
12. Lusher, A. L.; Burke, A.; O'Connor, I.; Officer, R., Microplastic pollution in the Northeast Atlantic Ocean: validated and opportunistic sampling. *Marine pollution bulletin* **2014,** *88* (1-2), 325-333.
13. Zhang, D.; Liu, X.; Huang, W.; Li, J.; Wang, C.; Zhang, D.; Zhang, C., Microplastic pollution in deep-sea sediments and organisms of the Western Pacific Ocean. *Environmental Pollution* **2020,** *259*, 113948.
14. Courtene-Jones, W.; Quinn, B.; Gary, S. F.; Mogg, A. O.; Narayanaswamy, B. E., Microplastic pollution identified in deep-sea water and ingested by benthic invertebrates in the Rockall Trough, North Atlantic Ocean. *Environmental pollution* **2017,** *231*, 271-280.
15. Gardette, J.-L.; Colin, A.; Trivis, S.; German, S.; Therias, S., Impact of photooxidative degradation on the oxygen permeability of poly (ethyleneterephthalate). *Polymer degradation and stability* **2014,** *103*, 35-41.
16. Chamas, A.; Moon, H.; Zheng, J.; Qiu, Y.; Tabassum, T.; Jang, J. H.; Abu-Omar, M.; Scott, S. L.; Suh, S., Degradation rates of plastics in the environment. *ACS Sustainable Chemistry & Engineering* **2020,** *8* (9), 3494-3511.
17. Lu, J.; Chen, N.; Ji, S.; Sun, Z.; Ding, M.; Zhu, X., Polymerization of benzoguanamine and pyromellitic dianhydride under microwave radiation and its third-order optical nonlinearities. *Journal of applied polymer science* **2001,** *82* (6), 1356-1363.
18. Hurley, C. R.; Leggett, G. J., Quantitative investigation of the photodegradation of polyethylene terephthalate film by friction force microscopy, contact-angle goniometry, and X-ray photoelectron spectroscopy. *ACS applied materials & interfaces* **2009,** *1* (8), 1688-1697.
19. MacDonald, W. A., New advances in poly (ethylene terephthalate) polymerization and degradation. *Polymer international* **2002,** *51* (10), 923-930.
20. Falkenstein, P.; Gräsing, D.; Bielytskyi, P.; Zimmermann, W.; Matysik, J.; Wei, R.; Song, C., UV pretreatment impairs the enzymatic degradation of polyethylene terephthalate. *Frontiers in Microbiology* **2020,** *11*, 689.
21. Sharon, C.; Sharon, M., Studies on biodegradation of polyethylene terephthalate: a synthetic polymer. *J. Microbiol. Biotechnol. Res* **2012,** *2* (2), 248-257.
22. Nimchua, T.; Punnapayak, H.; Zimmermann, W., Comparison of the hydrolysis of polyethylene terephthalate fibers by a hydrolase from Fusarium oxysporum LCH I and Fusarium solani f. sp. pisi. *Biotechnology Journal: Healthcare Nutrition Technology* **2007,** *2* (3), 361-364.
23. Nimchua, T.; Eveleigh, D. E.; Sangwatanaroj, U.; Punnapayak, H., Screening of tropical fungi producing polyethylene terephthalate-hydrolyzing enzyme for fabric modification. *Journal of Industrial Microbiology and Biotechnology* **2008,** *35* (8), 843.
24. Pirillo, V.; Pollegioni, L.; Molla, G., Analytical methods for the investigation of enzyme-catalyzed degradation of polyethylene terephthalate. *The FEBS Journal* **2021,** *288* (16), 4730-4745.
25. Müller, R. J.; Schrader, H.; Profe, J.; Dresler, K.; Deckwer, W. D., Enzymatic degradation of poly (ethylene terephthalate): rapid hydrolyse using a hydrolase from T. fusca. *Macromolecular rapid communications* **2005,** *26* (17), 1400-1405.
26. Ribitsch, D.; Acero, E. H.; Greimel, K.; Eiteljoerg, I.; Trotscha, E.; Freddi, G.; Schwab, H.; Guebitz, G. M., Characterization of a new cutinase from Thermobifida alba for PET-surface hydrolysis. *Biocatalysis and Biotransformation* **2012,** *30* (1), 2-9.
27. Vertommen, M.; Nierstrasz, V.; Van Der Veer, M.; Warmoeskerken, M., Enzymatic surface modification of poly (ethylene terephthalate). *Journal of biotechnology* **2005,** *120* (4), 376-386.
28. Otoukesh, M.; Nerín, C.; Aznar, M.; Kabir, A.; Furton, K. G.; Es' haghi, Z., Determination of adhesive acrylates in recycled polyethylene terephthalate by fabric phase sorptive extraction coupled to ultra performance liquid chromatography-mass spectrometry. *Journal of Chromatography A* **2019,** *1602*, 56-63.
29. Franz, R.; Welle, F., Contamination levels in recollected PET bottles from non-food applications and their impact on the safety of recycled PET for food contact. *Molecules* **2020,** *25* (21), 4998.
30. Sang, T.; Wallis, C. J.; Hill, G.; Britovsek, G. J., Polyethylene terephthalate degradation under natural and accelerated weathering conditions. *European polymer journal* **2020,** *136*, 109873.
31. Stanica-Ezeanu, D.; Matei, D., Natural depolymerization of waste poly (ethylene terephthalate) by neutral hydrolysis in marine water. *Scientific reports* **2021,** *11* (1), 4431.
32. Funabashi, M.; Ninomiya, F.; Oishi, A.; Ouchi, A.; Hagihara, H.; Suda, H.; Kunioka, M., Highly accelerated aging method for poly (ethylene terephthalate) film using xenon lamp with heating system. *Journal of Polymers* **2016,** *2016*.

33. Almasri, B. ; Rolando, C., Discovering the secrets of PET-labeled food packaging objects and bottles including their oligomers, additives and possible enchased products. Submitted.

Degradation pathways of PET



1- Accelerated ageing:
- UV-irradiation
- Thermo-oxidation

2-Environmental experiments:
- Seawater (semi-natural)
- River (natural)

3- Natural weathering:
- Marine wastes

Chemical and biological signatures

Supporting information

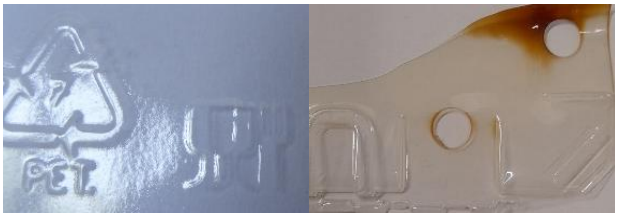


Figure S 1. PET film before and after UV-irradiation at 365 nm for 6 months respectively.

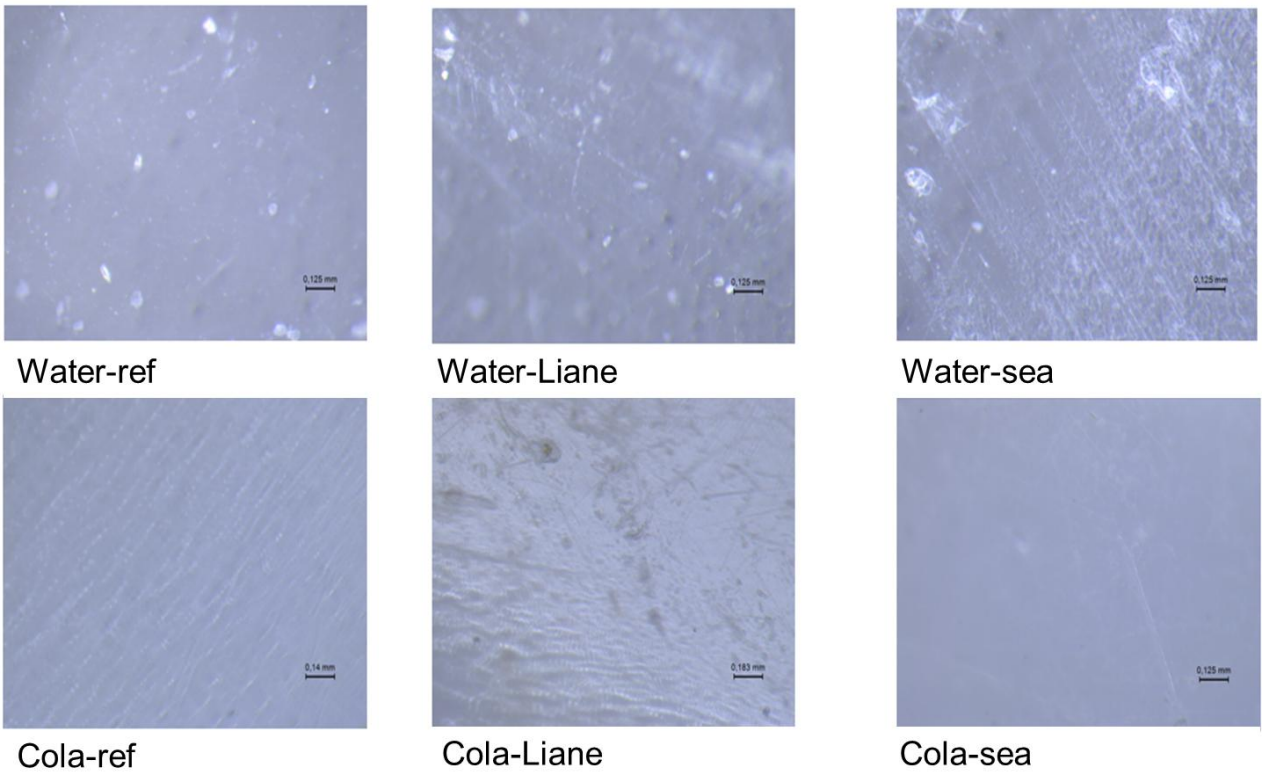
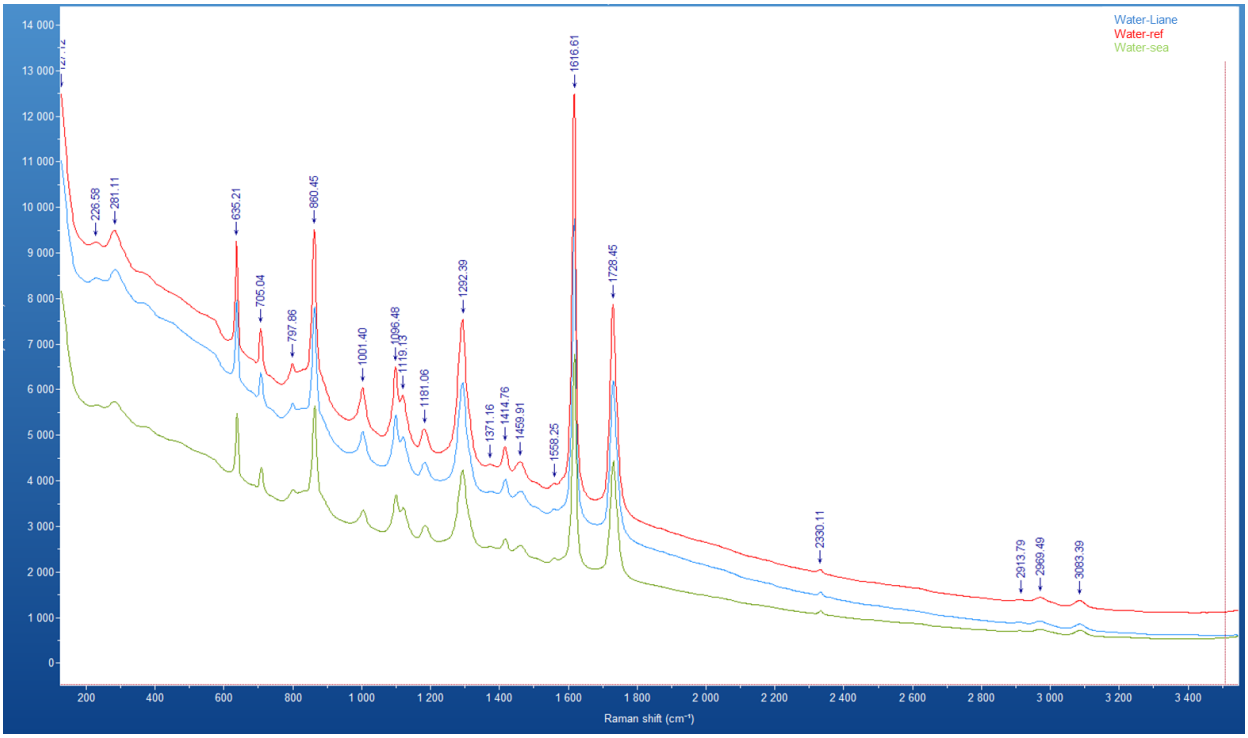


Figure S 2. Stereomicroscopy of 2-months' aged PET bottles in natural and semi-natural conditions compared to their references (stereomicroscope Leica 165C).

Little modification of the PET surface was noticeable and a few additional crystallites have been seen in the PET of water bottle. A biofilm mainly present in Liane sweet water river was visualized.



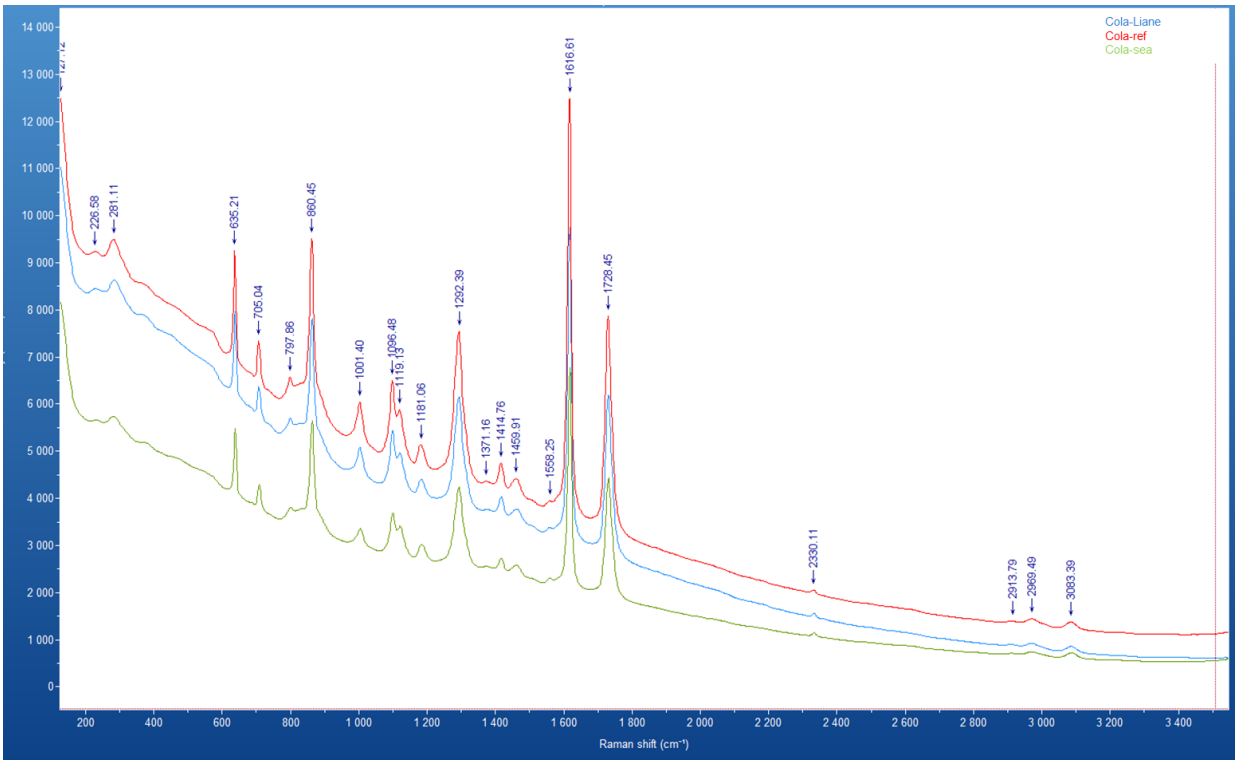


Figure S 3. Macro-Raman spectra (macro-Raman spectroscopy Horiba) of 2-months' aged PET bottles in natural and semi-natural conditions compared to their references: Water and cola bottles respectively. Red: Reference, bleu: Liane river and green: Seawater.

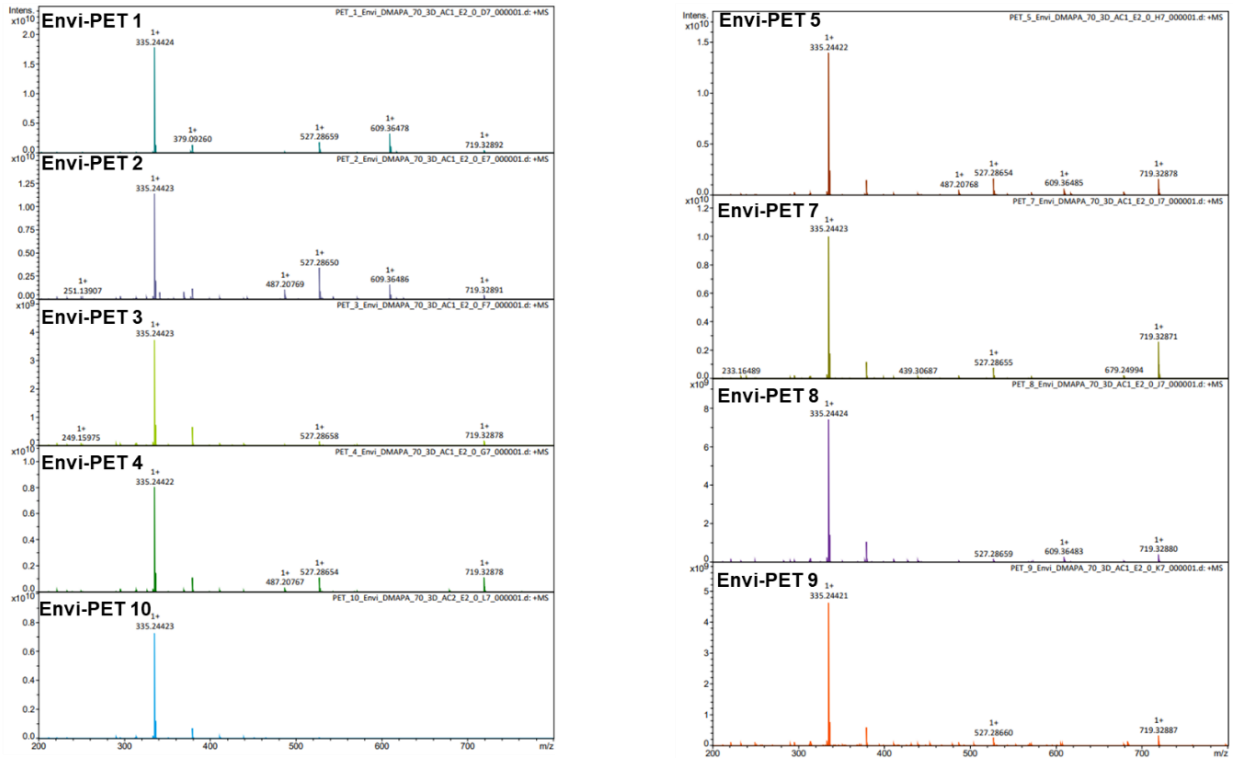


Figure S 4. MALDI FTICR MS of the random environmental PET samples from the English Channel after direct transamidation by DMAPA (*m/z* 200-800).

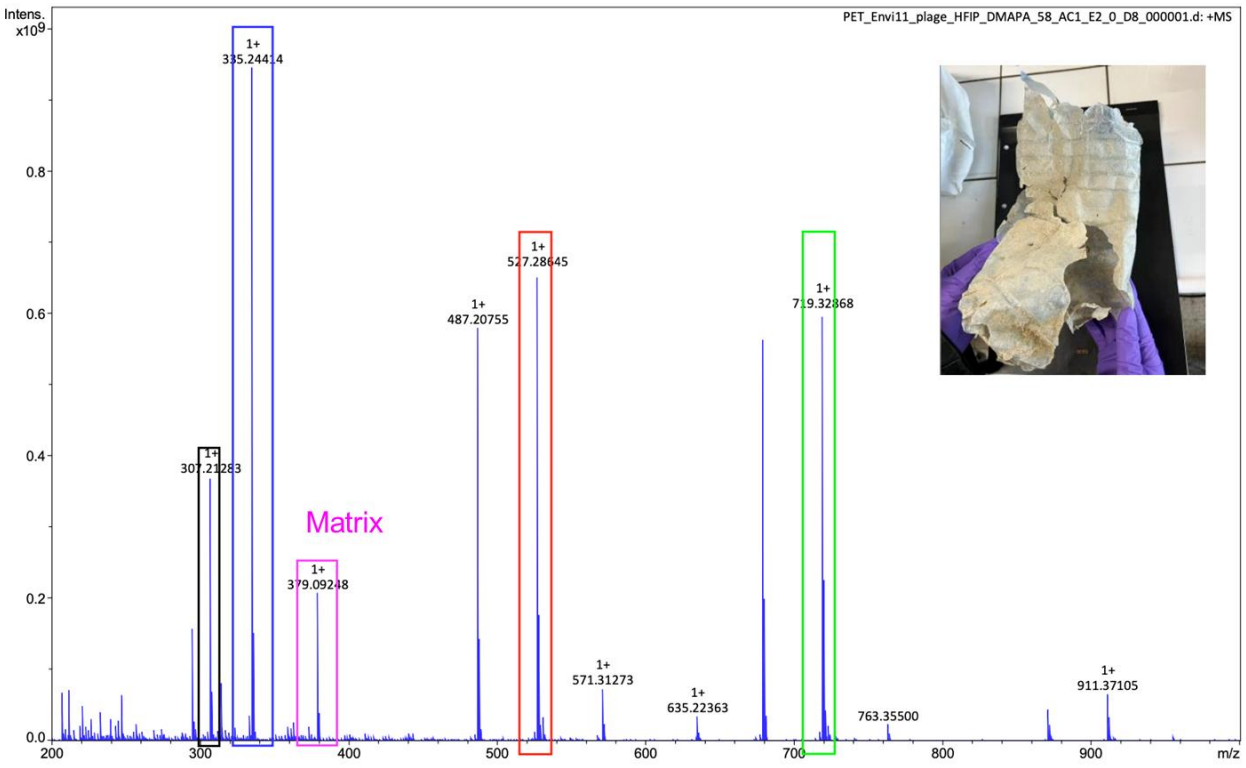


Figure S 5. MALDI FTICR MS spectrum of the depolymerized environmental PET sample found degraded on the beach (PET Envi-11); in the presence of internal standard.

Table S 1. Relative abundance (in %) of the following LC-MS peaks present in all the studied PET samples: Both depolymerization markers at *m/z* 335.244 and *m/z* 295.165 respectively, their dimers and oligomers, DEG product at *m/z* 571.313 with its oligomers, and cyclohexanedimethanol markers presented by the sum of mono- and di-derivatized products at *m/z* 377.243 and *m/z* 609.365.

PET sample	% Di-derivatized depolymerization marker	% Oligomers' sum of di-derivatized depolymerization marker	% Mono-derivatized depolymerization marker	% Oligomers' sum of mono-derivatized depolymerization marker	% DEG marking products	% Oligomers' sum of DEG marking products	% Cyclohexane dimethanol
Ref-water	19.54	2.73	17.87	42.99	0.80	0.09	4.73
Sea-water	32.09	1.98	16.94	44.07	0.49	0.02	0.38
Liane-water	35.53	1.90	6.24	48.39	0.32	0.10	3.04
Ref-cola	48.62	1.71	5.93	39.85	0.32	0.09	3.48
Sea-cola	13.26	2.22	8.23	58.66	0.42	0.11	5.07
Liane-cola	49.21	1.35	10.02	35.72	0.27	0.02	0.56
FC ref	32.70	1.56	7.40	47.61	0.27	0.09	3.76
FC 2D-75 °C	38.47	1.88	6.11	47.47	0.34	0.10	0.15
FC UV-6M	82.34	0.02	0.10	0.56	0.00	0.01	0.08

Table S 2. LC-MS relative intensity of some additives and degradation products present in both artificial aged samples with their FC reference.

Additive/ degradation product	Function	[M]	*m/z*	If ester: n DMAPA *m/z* with DMAPA	FC ref		FC UV-6M		FC 2D-75 °C	
					RT	Intensity	RT	Intensity	RT	Intensity
2,4-Di-tert-butylphenol	Thermal stabiliser/ by-product of antioxidant	$C_{14}H_{22}O$	207.174	-	58.35	3.83E+02	53.95	3.37E+02	51.20	3.73E+02
Mono-hydroxyethyl terephthalate	NIAS (oligomer)	$C_{10}H_{10}O_5$	211.060	-	3.78	4.50E+02	8.93	3.57E+02	3.62	6.41E+02
				n=1 251.139	0.92	8.88E+04	0.90	1.23E+05	0.68	7.95E+04
				n=1 251.139	1.74	2.86E+03	1.81	5.16E+04	1.70	1.59E+04
Perkacit DPG	Crosslinking agent	$C_{13}H_{13}N_3$	212.118	-	41.90	3.98E+02	24.82	3.24E+02	36.06	3.69E+02
Propyl gallate	Antioxidant	$C_{10}H_{12}O_5$	213.078	-	20.88	3.25E+03	13.92	4.20E+02	21.15	2.86E+03
Perfluorobutanoic acid (PFBA)	PFAS	$C_3F_7CO_2H$	214.994	-	0.58	4.09E+02	0.92	1.21E+03	0.52	3.55E+02
9,10-Dihydro-9-oxa-10-phosphaphenanthrene-10 oxide (DOPO)	Flame retardant in polyesters fibers & in PET	$C_{17}H_{15}O_6P$	217.041	-	7.65	3.78E+02	5.36	3.24E+02	0.00	0.00E+00
3,5-Di-tert-butyl-4-hydroxybenzaldehyde (BHT-CHO)	NIAS	$C_{15}H_{22}O$	219.174	-	39.57	1.20E+03	40.16	1.41E+03	40.01	1.47E+03
Naugard PANA	Antioxidant	$C_{16}H_{13}N$	220.112	-	2.36	5.48E+02	0.00	0.00E+00	0.00	0.00E+00
Butylated hydroxytoluene (BHT)	Antioxidant	$C_{15}H_{24}O$	221.189	-	50.35	3.71E+02	0.00	0.00E+00	55.54	3.69E+02
Cyanomethyl methyl (phenyl)carbodithioate	Retarder	$C_{10}H_{10}N_2S_2$	223.036	-	5.96	4.64E+02	0.00	0.00E+00	12.54	3.86E+02
Diethyl phthalate (DEP)	NIAS (impurity)	$C_{12}H_{14}O_4$	223.096	-	48.77	3.82E+02	49.19	3.81E+02	33.73	3.70E+02
				n=1 279.170	13.27	9.24E+04	13.49	5.42E+05	13.34	6.35E+04
Hexyl 2-hydroxybenzoate	UV Stabilizer	$C_{13}H_{18}O_3$	223.133	-	51.92	4.27E+02	0.00	0.00E+00	0.00	0.00E+00
				n=1 223.144	28.90	4.53E+02	3.89	1.21E+04	41.21	3.97E+02
1,3-Diphenyl-2-thiourea	Antioxidant	$C_{13}H_{12}N_2S$	229.079	-	42.50	3.89E+02	46.18	3.66E+02	0.00	0.00E+00
Dibutyl maleate	Plasticizer	$C_{12}H_{20}O_4$	229.143	-	47.89	4.21E+02	39.89	4.25E+02	44.70	4.17E+02
				n=1 257.186	34.60	4.11E+02	0.00	0.00E+00	0.00	0.00E+00
Silquest A-187	Coupling agent	$C_9H_{20}O_5Si$	237.115	-	20.94	3.86E+02	0.00	0.00E+00	24.03	3.79E+02
1,3-Di-o-tolylguanidine	Antioxidant	$C_{15}H_{17}N_3$	240.149	-	18.20	3.51E+02	0.00	0.00E+00	6.30	3.54E+02
Bisphenol C	Bisphenol analog	$C_{17}H_{20}O_2$	257.154	-	49.07	3.58E+02	33.29	3.58E+02	0.00	0.00E+00

Naugard J	Antioxidant	$C_{18}H_{16}N_2$	261.139	-	40.38	3.83E+02	40.95	3.69E+02	0.00	0.00E+00
3,3,5-Trimethylcyclohexyl 2-hydroxybenzoate	Antioxidant/ UV stabilizer	$C_{16}H_{22}O_3$	263.164	n=1 223.144104 (like before)	8.36	4.09E+02	10.48	3.75E+02	0.00	0.00E+00
Tributyl phosphate	Plasticizer	$C_{12}H_{27}O_4P$	267.172	-	7.63	3.99E+02	4.04	7.05E+03	0.00	0.00E+00
MXD6	Oxygen scavenger	$C_{14}H_{20}N_2O_4$	281.149	-	3.68	2.27E+03	1.35	1.33E+05	3.56	1.78E+04
Oleamide	Stabilizers or slip agent/ lubricant/ fatty acid derivative	$C_{18}H_{35}NO$	282.279	-	46.90	1.67E+05	48.14	2.27E+03	47.78	1.38E+04
Stearamide	Lubricants/ thermal stabilizers	$C_{18}H_{37}NO$	284.295	-	51.25	6.42E+02	42.66	5.56E+03	34.35	3.61E+02
Cyanomethyl dodecyl trithiocarbonate	Retarder	$C_{15}H_{27}NS_3$	318.138	-	0.04	4.19E+02	20.09	9.77E+02	28.46	4.19E+02
Bis(4-methylpentyl) phthalate	NIAS	$C_{20}H_{30}O_4$	335.222	-	0.92	9.30E+03	0.00	0.00E+00	0.00	0.00E+00
Docosanoic acid	Intermediate/ fatty alcohol, lubricant	$C_{22}H_{44}O_2$	341.341	-	40.33	4.24E+03	0.00	0.00E+00	0.00	0.00E+00
n-Butyl stearate	Plasticizer	$C_{22}H_{44}O_2$	341.341	n=1 369.384	43.78	4.06E+05	44.81	1.63E+04	44.35	5.63E+05
Citroflex 4	Plasticizer	$C_{18}H_{32}O_7$	361.222	-	43.06	3.72E+03	43.68	3.42E+03	0.00	0.00E+00
Santicizer 261	Plasticizer	$C_{23}H_{28}O_4$	369.206	-	37.08	4.01E+02	0.00	0.00E+00	33.04	3.90E+02
Cyanox 425	Antioxidant	$C_{25}H_{36}O_2$	369.279	-	43.80	1.96E+03	26.51	4.89E+02	0.00	0.00E+00
Bis(2-ethylhexyl) adipate (DEHA)	Plasticizer/ NIAS	$C_{22}H_{42}O_4$	371.316	-	8.78	1.12E+03	18.60	1.45E+03	0.00	0.00E+00
				n=1 343.296	29.74	6.26E+02	30.62	8.05E+02	30.38	5.13E+02
				n=2 315.275	11.12	4.61E+02	0.54	4.91E+02	0.00	0.00E+00
Dipentamethylenethiuuram tetrasulfide	Antioxidant	$C_{12}H_{20}N_2S_6$	385.002	-	13.12	4.34E+02	14.45	4.14E+02	0.00	0.00E+00
Santicizer 148	Plasticizer	$C_{22}H_{31}O_4P$	391.203	-	45.00	4.77E+02	32.30	3.50E+02	0.00	0.00E+00
Di-*n*-octyl phthalate (DnOP)/ di(2-ethylhexyl) phthalate (DEHP)	NIAS (impurity) or DEHP = Plasticizer	$C_{24}H_{38}O_4$	391.284	-	21.67	2.07E+03	31.17	2.01E+03	29.04	1.65E+03
			-	n=1 363.264	30.63	2.54E+03	31.03	5.96E+02	31.24	4.63E+02
Perfluorohexanesulfonate (PFHxS)	PFAS	$C_6H_1F_{13}O_3S$	400.951	-	24.22	4.19E+02	0.00	0.00E+00	25.60	4.28E+02
Di-isononyl phthalate	Plasticizer/ solvent for paints/ vehicles for pigment dispersions	$C_{26}H_{42}O_4$	419.316	-	44.01	1.65E+03	0.00	0.00E+00	0.00	0.00E+00
Tinuvin 1577: (2-(4,6-Diphenyl-1-3,5 triazin-2-yl)-5-hexyloxy-phenol	UV absorbing agent/ UV stabilizer	$C_{27}H_{27}N_3O_2$	426.218	-	43.06	9.24E+03	43.68	3.05E+04	43.54	1.12E+04
BNX1077	Antioxidant	$C_{30}H_{52}O_3$	461.399	-	50.58	5.29E+02	0.00	0.00E+00	48.31	4.44E+02

2,2',4,4'-Tetrabromo diphenyl ether	Flame retardant	$C_{12}H_6Br_4O$	482.722	-	38.72	4.33E+02	0.00	0.00E+00	30.00	4.59E+02
Irganox MD 1024: 2',3-Bis[[3-[3,5-di-tert.-butyl-4-hydroxyphenyl]propionyl]]propionohydrazide	Antioxidant	$C_{30}H_{58}O_4S$	515.415	-	45.58	3.51E+04	46.39	8.73E+02	45.47	6.62E+03
Poly(tetrabromobisphenolAcarbonate)/ Firemaster BP4A	High-performance flame retardants used in polyesters	$C_{15}H_{12}Br_4O_2$	540.764	-	17.70	9.03E+02	44.72	2.96E+03	32.94	9.67E+02
Irgafos®168 oxide: Tris[2,4-bis(2-methyl-2-propanyl) phenyl] phosphate	Oxidized/ degradation product of antioxidant Irgafos®168	$C_{42}H_{63}O_4P$	663.454	-	43.94	4.67E+03	26.49	5.23E+02	51.13	5.96E+03
Irganox 3125	Antioxidant	$C_{60}H_{87}O_2S$	872.649	-	32.35	7.82E+02	35.76	4.78E+02	0.00	0.00E+00
Decabromodiphenyl ether	Flame retardant	$C_{12}Br_{10}O$	950.186	-	27.26	7.64E+02	35.76	4.78E+02	0.00	0.00E+00
Saytex 8010	Flame retardant	$C_{14}H_4Br_{10}$	962.222	-	45.14	1.19E+03	41.27	1.56E+03	0.00	0.00E+00

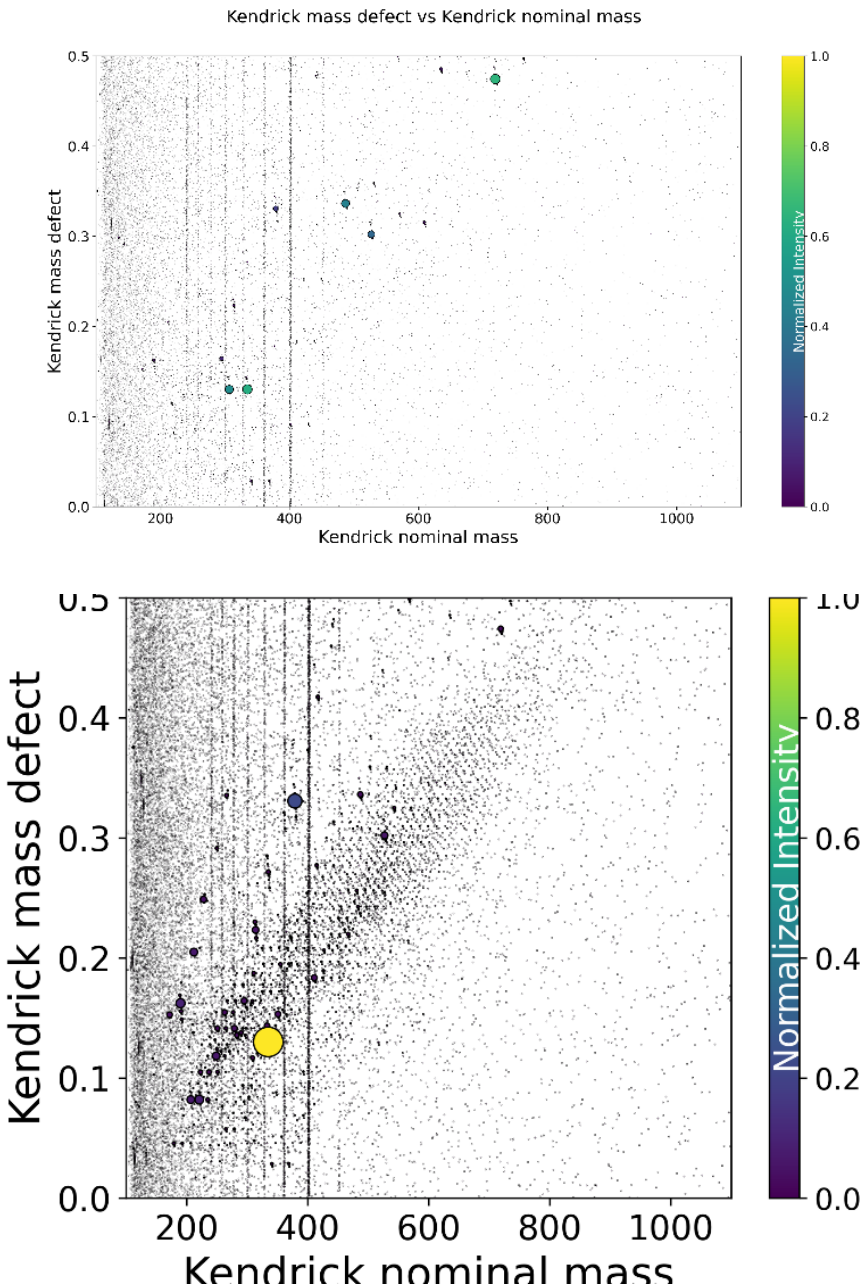


Figure S 6. Kendrick mass defect vs Kendrick nominal mass for FC UV-6M and FC respectively.

Chapter 6: Related works

1. Co-polyesters and marine objects structural deciphering

The developed methodology of depolymerization combined with advanced high-resolution mass spectrometry was applied on co-polyesters and marine objects such as the biodegradable mussel nets.

1.1. Experimental work

1.1.1. The studied co-polyesters

Two co-polyesters were depolymerized according to the final protocol with HFIP solvent. These polyesters were PBT (Polybutylene adipate) purchased from Merck and PBAT (Polybutylene adipate terephthalate). PBAT is a new biodegradable polymer received from BASF company (Figure 1).



Figure 1. PBT and PBAT granules respectively.

1.1.1.1. Ageing of PBAT

PBAT was aged at 395 nm for 48 hours. The industrial PBAT granules were received as white granules so it was necessary to solubilize them in a solvent which was HFIP overnight. The obtained solution was then spread on a microscopic glass slide on which HFIP evaporates very fast and the slide was put directly on the corresponding UV LED (Figure 2).

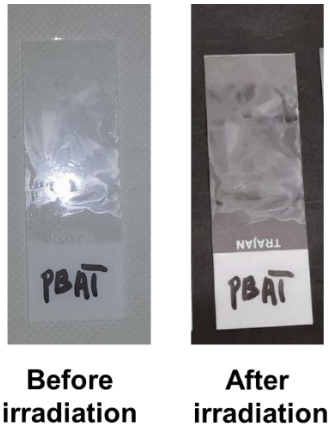


Figure 2. PBAT aspect on the glass slide before and after UV-irradiation.

After 2 days, a step of PBAT collecting was performed using a clean single-use scalpel then a re-solubilization of the aged PBAT in HFIP was achieved before transamidation. The same UV-ageing technique was performed on PET granules.

1.1.2. Identification of biodegradable mussel nets

Mussel farming has traditionally relied on conventional plastic nets, which, if broken and unintentionally dispersed, can wash up on beaches and contribute to marine litter.[1] Additionally, recycling these nets is often challenging and expensive. Unlike conventional nets covered by various marine organisms, the biodegradable nets will present a viable alternative to be composted directly after use. Furthermore, for environmental and sanitary point of view, the petroleum-based plastics are probably more toxic than the biodegradable alternatives. However, the bio-based-biodegradable mussel nets are still in the early stages of market introduction. As a result, there is limited data on their chemical composition, their behavior in the environment, and their potential impacts on organisms, ecosystems, and human health.[2,3]

It's necessary to identify at molecular level their degradation products releasing microplastics and additives in the aquatic systems. The received biodegradable nets were two of green colors, dark green and light green as shown in Figure 3.



Figure 3. Biodegradable mussel nets.

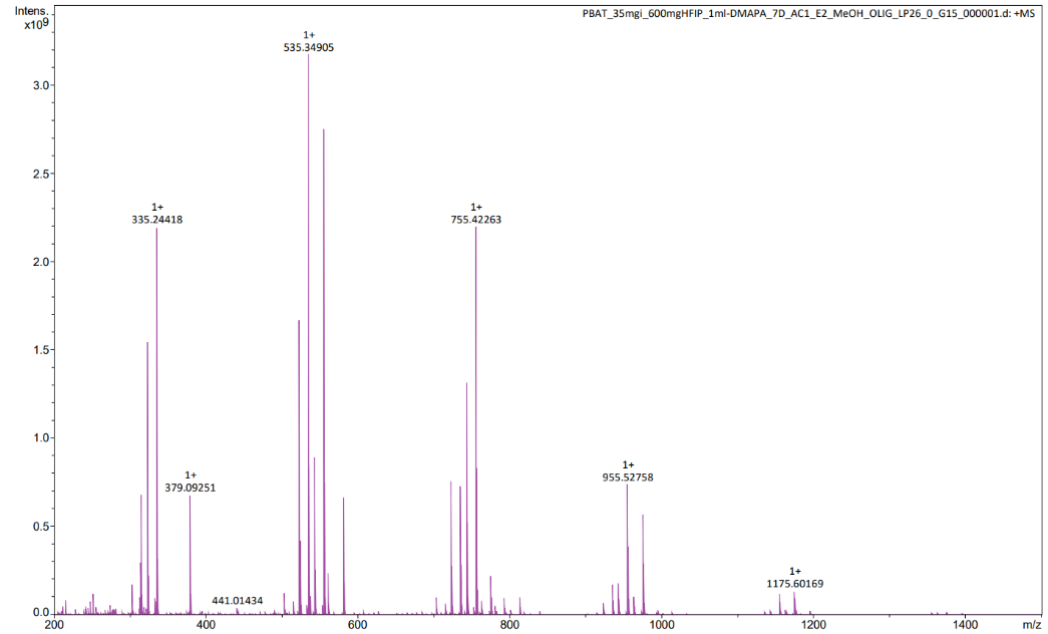
The type of polymers and additives used for the fabrication of these new nets were unknown.

Indeed, 25 mg of net samples were solubilized overnight with HFIP, then transamidated at room temperature with 1 mL of DMAPA. After reaction's post-treatment as described previously, the depolymerized products were analyzed by MALDI FTICR MS and Orbitrap ESI MS (LC-MS & LC-MS/MS).

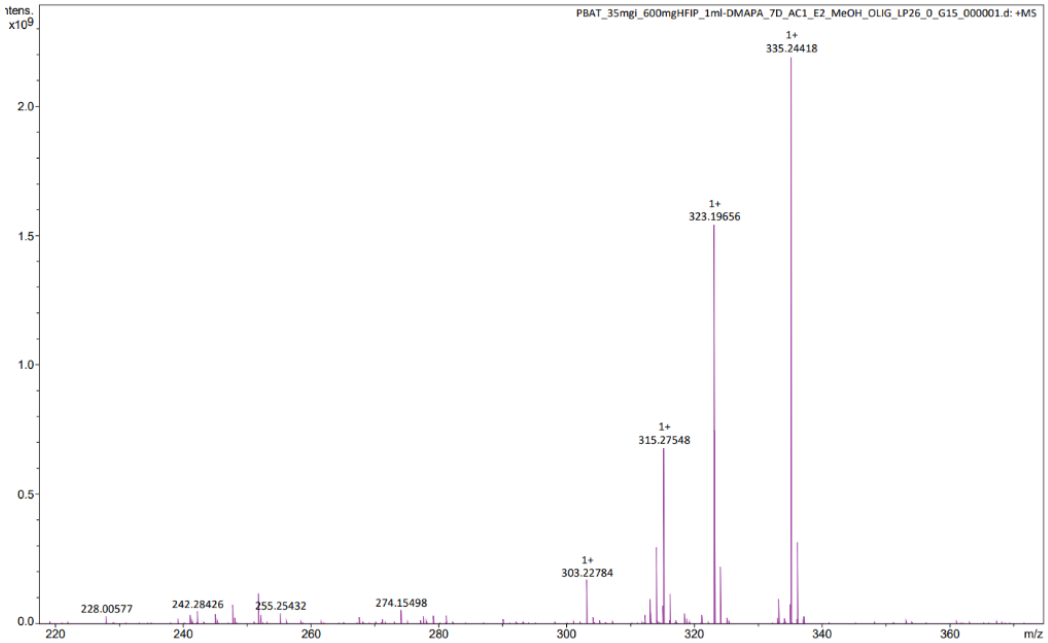
The degradation products of the biodegradable mussel nets were compared to the already depolymerized PET polyesters, PBAT and PBT co-polyesters as well as to the authentic dimethyl adipate in order to have information about their polymeric composition (blends, co-polymers, etc.) then to identify them in detail with the three analytical methods already mentioned.

1.2. Results and discussions

The biodegradable PBAT co-polyester purchased from BASF company was successfully depolymerized according to our innovative methodology. The 3 degradation markers of PBAT were detected with high accuracy: Adipic acid with 2 molecules of DMAPA [$C_{16}H_{34}N_4O_2$ + H^+] appearing at *m/z* 315.2755, butanediol with terephthalic acid and 1 molecule of DMAPA [$C_{17}H_{26}N_2O_4$ + H^+] appearing at *m/z* 323.1965 and the di-transamidated terephthalic acid with 2 molecules of DMAPA [$C_{18}H_{30}N_4O_2$ + H^+] appearing at *m/z* 335.2442 as shown in the following MALDI FTICR MS spectrum of the depolymerized PBAT (Figure 4).



(a)



(b)

Figure 4. MALDI FTICR MS spectrum of depolymerized PBAT BASF. (a): Full spectrum; (b): Spectrum from *m/z* 215 to *m/z* 370.

The UV ageing of PBAT under 395 nm for 2 days showed some differences in the minority products as shown in Figure 5.

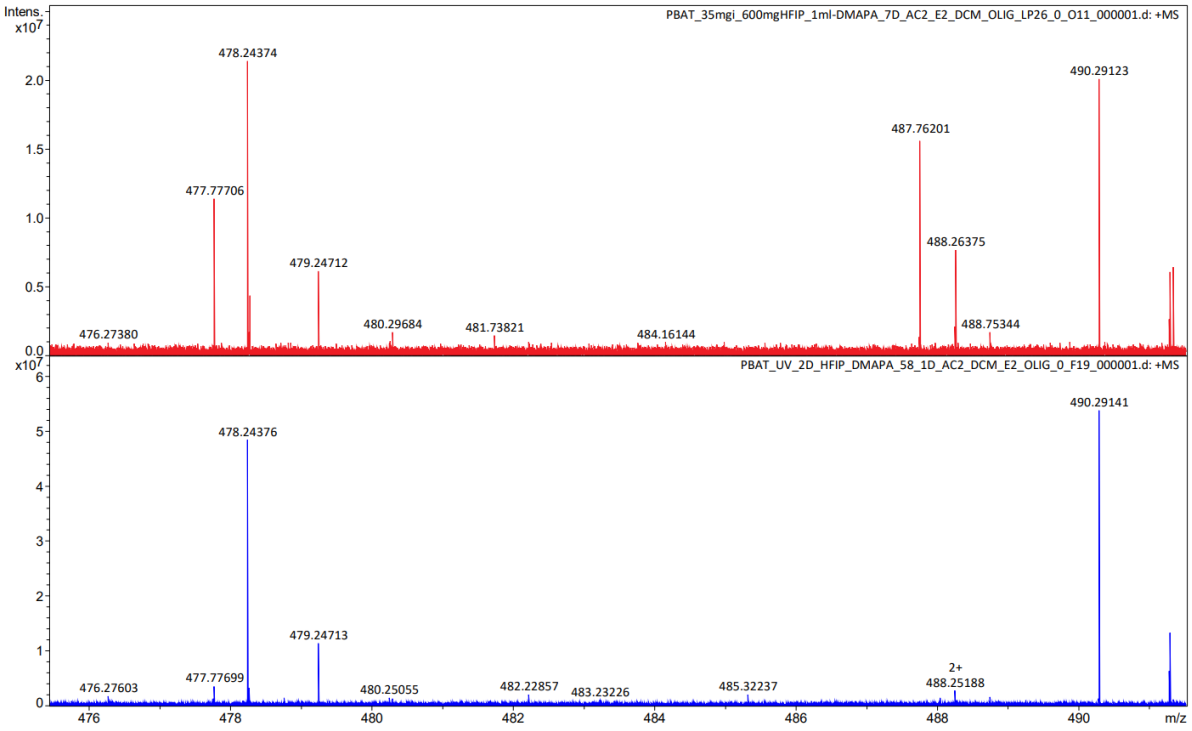


Figure 5. MALDI FTICR MS spectra of the depolymerized PBAT before and after UV-irradiation (2 days) respectively.

The depolymerized mussel nets were compared to the depolymerized PBAT BASF, PBT and dimethyl adipate to search polymers similarity. The results were analyzed by MALDI FTICR MS.

First, the clear green mussels were compared to these co-polymers. They contained the same degradation markers already found in PBAT BASF. So, these clear green mussels are almost made from PBAT as shown in Figure 6.

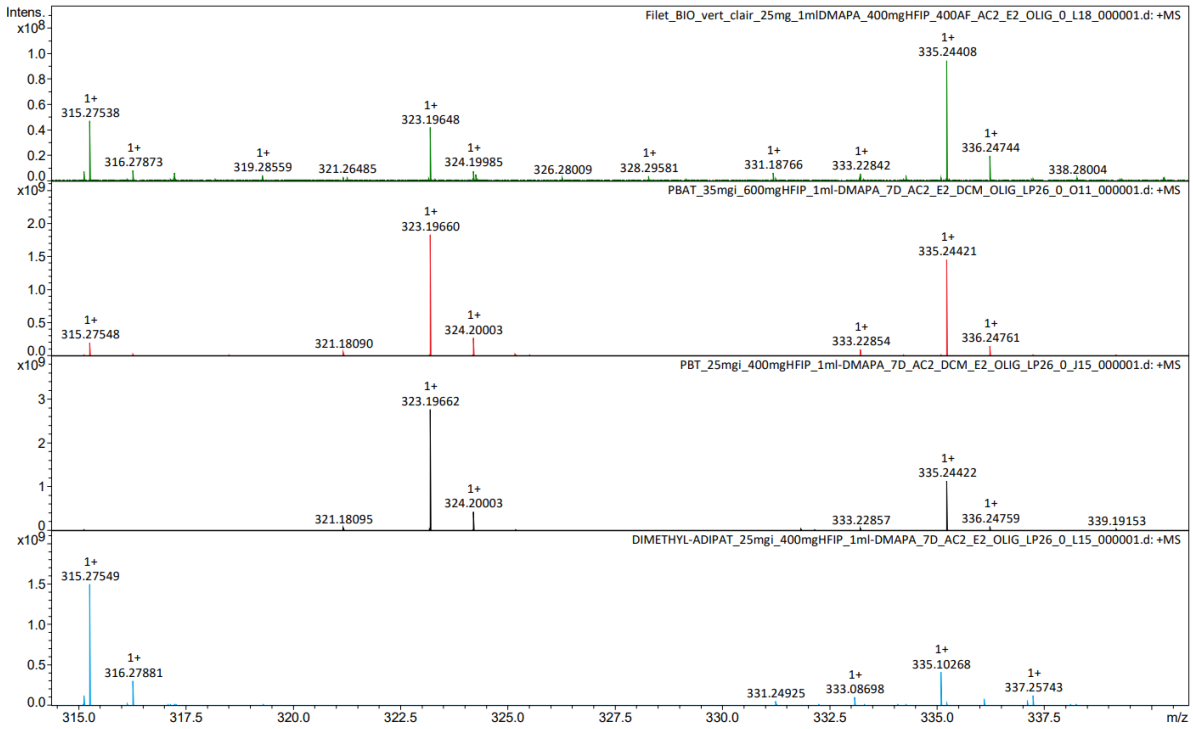


Figure 6. MALDI FTICR MS spectra of the depolymerized green clear mussel nets, PBAT, PBT & dimethyl adipate respectively.

After determination of the possible polymeric nature constituting the clear green mussel nets, the results were compared to the dark green mussel nets and PBAT in MALDI FTICR MS.

The results showed perfect similarities in structural composition and intensities of peaks between the two analyzed mussel nets as shown in Figure 7. These mussel nets had many peaks in common with PBAT BASF showing that they are composed of PBAT co-polymer but maybe not very similar to the industrial BASF manufacturing company. 25 structures have been successfully identified. Minority products not belonging to PBAT BASF remain to be identified.

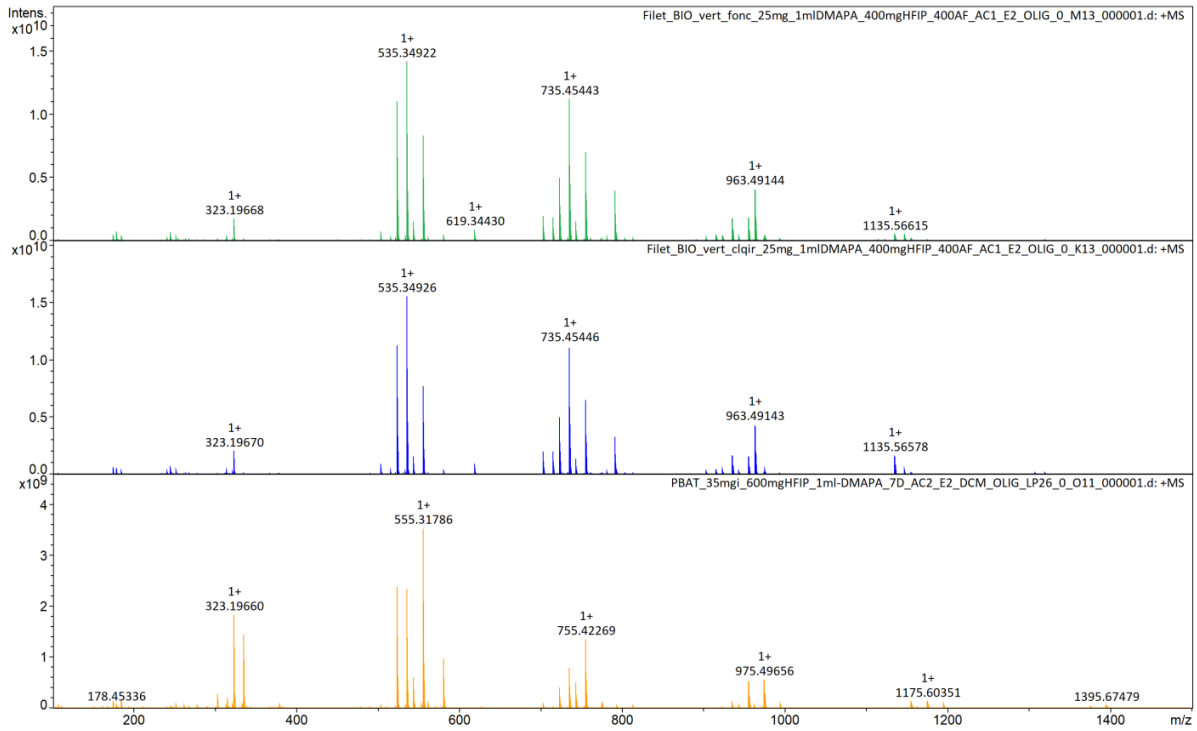


Figure 7. MALDI FTICR MS spectra of the depolymerized dark and clear green mussel nets and PBAT BASF respectively.

A peak appearing in the three samples at *m/z* 523.3014 of chemical formula [$C_{27}H_{42}N_2O_8$ + H^+] was characteristic for the 3 analyzed samples. To determine its structure, these samples were analyzed by LC-MS/MS to study the fragmentation of this peak (Figure 8). The fragmentation of this peak is demonstrated in Table 1 with the prediction of the fragment's structures.

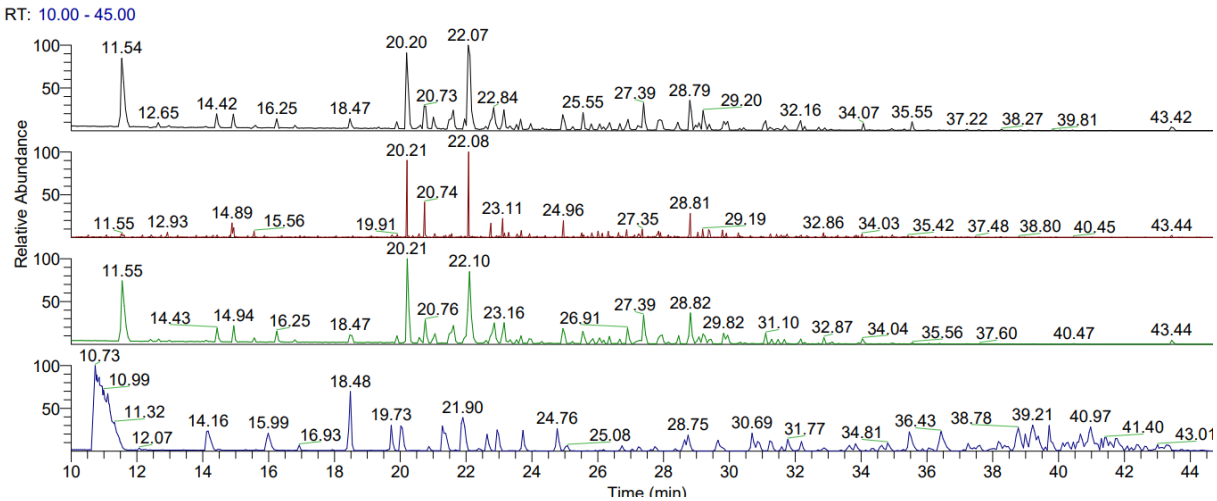
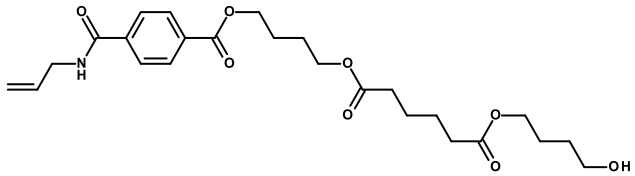
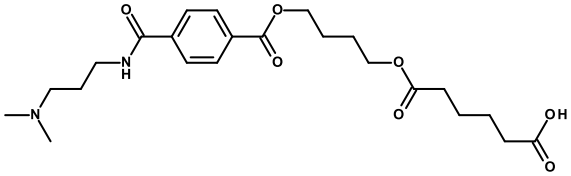
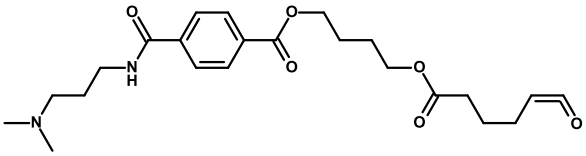
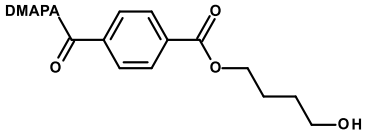
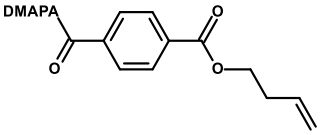
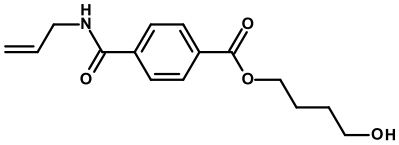


Figure 8. LC-MS/MS chromatograms of the depolymerized dark (MS and MS/MS) and clear green mussel nets and PBAT BASF respectively.

Table 1. PBAT LC-MS/MS interpretation of the fragmentation of the peak at *m/z* 523.301.

Theoretical *m/z* of fragment	**Fragment $[M+H]^+$**	**Loss from $C_{27}H_{43}N_2O_8$**	**Neutral fragment**
478.244	$C_{25}H_{37}NO_8$	$HN(CH_3)_2$	
451.244	$C_{23}H_{36}N_2O_7$	C_4H_8O	
433.233	$C_{23}H_{34}N_2O_6$	$C_4H_{10}O_2$	
323.197	$C_{17}H_{28}N_2O_4$	$C_{10}H_{16}O_4$	
305.186	$C_{17}H_{26}N_2O_3$	$C_{10}H_{18}O_5$	
278.139	$C_{15}H_{21}NO_4$	$C_{12}H_{23}NO_4$	

The interpretation of the fragments of the peak at *m/z* 535.301 confirms that it is the structure of one block of the co-polyester PBAT as shown in Figure 9 below.

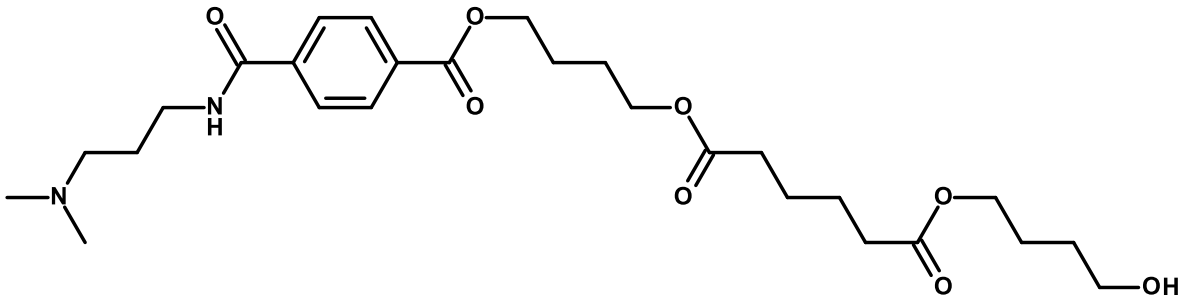


Figure 9. Structure of one block of PBAT.

There is no available data about additives present in the analyzed biodegradable mussel nets. The developed methodology of soft chemical depolymerization combined with LC-MS allowed their identification. The already created database for PET was used to decipher the additives of these marine objects. Indeed, 23 additives of different categories (plasticizers, antioxidants and flame retarders) have been attributed with high accuracy, the esters compounds were doubly checked after derivatization with DMAPA as shown in Table 2.

Table 2. Identified additives in the clear green mussel nets after LC-MS analysis, *m/z* 200-1,000.

	Identifiied additives	**Abbreviation**	**Chemical Formula [M]**	***m/z***	***m/z* and identified additive (+ 1 or 2 DMAPA) if ester**
1	Butylated Hydroxytoluene	BHT	$C_{15}H_{24}O$	221.1899	-
2	Dibutyl phthalate/ diisobutyl phthalate	DBP/DIBP	$C_{16}H_{22}O_4$	279.1591	$C_{17}H_{26}N_2O_3$ (1 DMAPA); 307.2016
3	Bis(2-ethylhexyl)adipate	DEHA	$C_{22}H_{42}O_4$	371.3156	$C_{19}H_{38}N_2O_3$ (1 DMAPA); 343.2955
4	Bis(2-ethylhexyl)phthalate	DEHP	$C_{24}H_{38}O_4$	391.2843	$C_{21}H_{34}N_2O_3$ (1 DMAPA); 363.2642
5	Diethyl phthalate	DEP	$C_{12}H_{14}O_4$	223.0965	$C_{15}H_{24}N_2O_2$ (1 DMAPA); 265,1911
6	Dimethyl phthalate	DMP	$C_{10}H_{10}O_4$	195.065185	$C_{14}H_{20}N_2O_4$ (1 DMAPA); 281,1496
7	Tris(2-chloroethyl) phosphate	TCEP	$C_6H_{12}Cl_3O_4P$	284.9612	$C_{11}H_{25}N_2O_4Cl_2P$ (1 DMAPA); 351.1002
8	Tri(2-ethylhexyl)phosphate	TEHPA	$C_{24}H_{51}O_4P$	435.3598	-
9	2-(2H-benzotriazol-2-yl)-4,6-bis(1-methyl-1-phenylethyl)phenol	UV-328	$C_{22}H_{29}N_3O$	352.2384	-
10	6,6'-Di-tert-butyl-2,2'-thiodi-p-crésol	Irganox 1081	$C_{22}H_{30}O_2S$	359.2039	-
11	2.4-Di-tert-butylphenol	2,4-Di-TBP	$C_{14}H_{22}O$	207.1743	-
12	Diallyl phthalate	DAP	$C_{14}H_{14}O_4$	247.0965	$C_{16}H_{22}N_2O_3$ (1 DMAPA); 291.1703
13	Dihexyl phthalate	-	$C_{20}H_{30}O_4$	335.2217	$C_{19}H_{30}N_2O_3$ (1 DMAPA); 335.2329
14	Markstat®51 (Poly(ethylene glycol) monolaurate)	Markstat®51	-	-	$C_{17}H_{36}N_2O$ (1 DMAPA); 285.2900
15	Diisopropyl phthalate	-	$C_{14}H_{18}O_4$	251.1278	$C_{16}H_{24}N_2O_3$ (1 DMAPA); 293.1859
16	Bis(2-methoxyethyl) phthalate	-	$C_{14}H_{18}O_6$	283.1176	$C_{16}H_{24}N_2O_4$ (1 DMAPA); 309.1809
17	Di-*n*-pentyl phthalate	DnPP	$C_{18}H_{26}O_4$	307.1904	$C_{18}H_{28}N_2O_3$ (1 DMAPA); 321.2173

18	Di-*n*-octyl phthalate	-	$C_{24}H_{38}O_4$	391.2843	$C_{20}H_{34}N_2O_2$ (1 DMAPA); 335.2693
19	Bis(2-*n*-butoxyethyl) phthalate	-	$C_{20}H_{30}O_6$	367.2115	$C_{18}H_{28}N_2O_4$ (1 DMAPA); 337.2122
20	Bis(2-ethylhexyl)sebacate	-	$C_{26}H_{50}O_4$	427.3782	$C_{23}H_{46}N_2O_3$ (1 DMAPA); 399.3581
21	Didodecyl phthalate	-	$C_{32}H_{54}O_4$	503.4095	$C_{25}H_{42}N_2O_3$ (1 DMAPA); 419.3268
22	Tris(chloropropyl) phosphate	TCPP	$C_9H_{18}Cl_3O_4P$	327.0081	$C_{14}H_{31}N_2O_4Cl_2P$ (1 DMAPA); 393.1471
23	Triphenyl phosphate	TPP	$C_{18}H_{15}O_4P$	327.0781	-

1.3. Conclusions and perspectives

Both biodegradable green mussel nets had a common chemical composition. They are made of PBAT, a biodegradable polymer. For the clear green mussel nets, an investigation of the present additives had been performed after LC-MS analysis showing the presence of some common additives with PET's additives especially plasticizers transamidated with DMAPA. Flame retardants such as TCPP and TPP were identified in addition to plasticizers of phthalate, adipate, laurate and sebacate. These mussel nets contain also antioxidants such as UV-328.[5]

A further characterization in details will be performed taking to account their polyols part and their leaching additives.

References

1- Bringer, A, *et al.* Coastal ecosystem inventory with characterization and identification of plastic contamination and additives from aquaculture materials. *Mar. Pollut. Bull.* **2021**, *167*, 112286. https://doi.org/10.1016/j.marpolbul.2021.112286

2- Bringer, A, *et al.* Intergenerational effects of environmentally-aged microplastics on the *Crassostrea gigas*. *Environ. Pollut.* **2022**, *294*, 118600. https://doi.org/10.1016/j.envpol.2021.118600

3- Dusacre, E, *et al.* Distinct toxicity profiles of conventional and biodegradable fishing nets' leachates after artificial aging. *J. Hazard. Mater.* **2025**, 137609. https://doi.org/10.1016/j.jhazmat.2025.137609

4- Akoueson, F., et al. Evaluation of the emission potential (microplastics & organic additives) by conventional or biodegradable mussel nets. *Micro2024*, **2024** https://anses.hal.science/anses-04761265v1

2. Synthesis of PET nanoparticles

The plastics that our society uses intensively in daily life are susceptible to the release of plastic fragments, microplastiques, for size less than 5 mm, and nanoplastics, for size less than 1 µm. Polyethylene terephthalate (PET) is the polymer used in plastic bottles for alimentation. Part of the recycled plastic in these bottles is stored, under the pressure of European reglementation (25% minimum by 2025) and consumer volume.

47% of French people drink bottled water daily (source CITEAU, Kantar 2022, Les français et l'eau, https://www.debatpublic.fr/sites/default/files/202304/BarometreCIEAU2022_GLOBALChiffres.pdf).
PET microplastics have been repeatedly found in human stools worldwide, as well as in arteries,[1] providing evidence of human ingestion and contamination by these small plastics. These PET microplastics are likely to fragment into PET nanoplastics, as it has been shown that digestion[2] and microbiota[3] degrade them. It has also been shown that PET bottles release nano-PET with an average size of 88 nm.[4] It is therefore crucial to better understand the health impacts of human exposure to PET nanoplastics.

The aim of this part is the creation of non-denaturated PET nanoplastics for biological purposes, more precisely for the further study of their immunotoxicity *in vivo* and *in vitro* by scientific teams of the medicine Faculty of the University of Lille and CHU Lille. Any type of PET may be used but PET from French fruit container was used here to create nano-PET.

For biological applications, these nanoplastics must be stabilized in not toxic solvent, ideally in water with a good dispersant agent for cells. The different trials for PET nanoplastics synthesis will be resumed.

2.1. Literature's protocol miniaturized

According to literature, starting from 1 g of PET and after many steps, nanoplastics may be formed by precipitation in trifluoroacetic acid (TFA), two solutions of decreased concentration.[6] It contains the following steps starting from 1 g of PET:

- Dissolution of PET in 10 mL of concentrated trifluoroacetic acid (solution of TFA 90%) under magnetic stirring at 50 °C (2h);
- Precipitation in TFA 20%, stirring for 2 hours;
- Centrifugation of the suspension at 2500g/h, discharge of supernatant.
- Stabilization of nanoparticles in 100 mL of 0.5% sodium dodecyl sulfate (SDS), vigorously stirred and ultrasonicated.[6]

I miniaturized the method. So, 100 mg of PET were dissolved in 5 mL of TFA 90%, then heated at 50 °C under N_2 for 1 day. After cooling at room temperature, 5 mL of TFA 20% was added. A white precipitate has been formed. After stirring for 2 hours at room temperature, a sonication for 1 hour at room temperature was performed resulting into the formation of suspension. A first centrifugation at 2800g/h was done in a glass tube of 15 mL in order to eliminate the acid phase. Then 5 mL of ultrapure water was added and the suspension was centrifuged under the same conditions, macro-PETs were observed stuck on the wall of tube, the aqueous phase was collected and two other centrifugations with water were performed. A stabilization of the formed nano-PET was achieved with 25 mg of SDS (Sodium Dodecyl Sulfate) and 25 mg of NaCl salts used as dispersants. They were left under stirring overnight, the sedimentation/precipitation speed was 2 hours. A little volume of the solution was spread on microscope glass slide and put under UV LED 365 nm to study the degradation of nanoplastics. Unfortunately, very low nano-PET yield was observed.

2.2. First protocol

A trial was done to increase the dissolution of PET and to work at softer conditions in order to improve the yield of nano-PET. Indeed, 5 mg of PET was dissolved in 800 mg of HFIP (10 mg/mL) overnight at room temperature, a perfect solubilization was obtained. The obtained solution was precipitated with TFA 20%, then the steps of centrifugation were identical to the previous protocol using this time only 1 mg of dispersant salts to maintain the critical concentration of micellar SDS which is between 8-8.5 mM because the dispersant concentration must be higher than the solubility. Unfortunately, also very low nano-PET yield was observed.

2.3. Test with solvents

2.3.1. Test with methanol/HFIP

5 mg of PET was solubilized in 1 mL of HFIP (5 mg/mL) for one day. Tests with the following ratios of solvents were performed (the aspects of the obtained solutions are shown in Figure 1):

- 250 µL methanol and 750 µL HFIP: No special observations.
- 500 µL methanol and 500 µL HFIP: PET filaments formation.
- 500 µL methanol and 500 µL HFIP stabilized with 2.5 mg NaCl: PET filaments formation.
- 750 µL methanol and 250 µL HFIP: PET filaments formation.
- 750 µL methanol and 250 µL HFIP stabilized with 2.5 mg NaCl: Instantaneous suspension but PET filaments were formed after stirring.
- 1 mL methanol: PET gel formation.
- 1 mL methanol stabilized with 2.5 mg NaCl: PET gel/filaments formation.

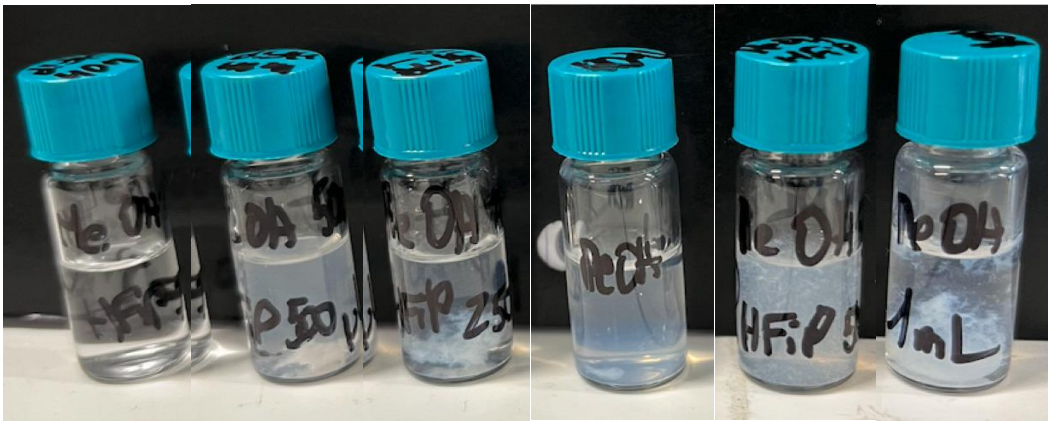


Figure 1. Aspects of solutions in methanol/HFIP with the following (v/v) ratios respectively: 250/750; 500/500; 750/250; 100/0; 500/500 with NaCl then 100/0 with NaCl.

These tests with different ratios of methanol and HFIP resulted in the formation of PET gels more than nano-PETs.

2.3.2. Test with other organic solvents and co-solvents

A concentrated solution of PET in HFIP was prepared (25 mg in 800 mg HFIP); then using a glass pipette 5 drops of this solution were added to 5 mL of the following solvents (Figure 2):

- Isopropanol: Strong PET precipitation was observed.
- Pentane: A solution was remained.
- Dichloromethane: A solution was remained.

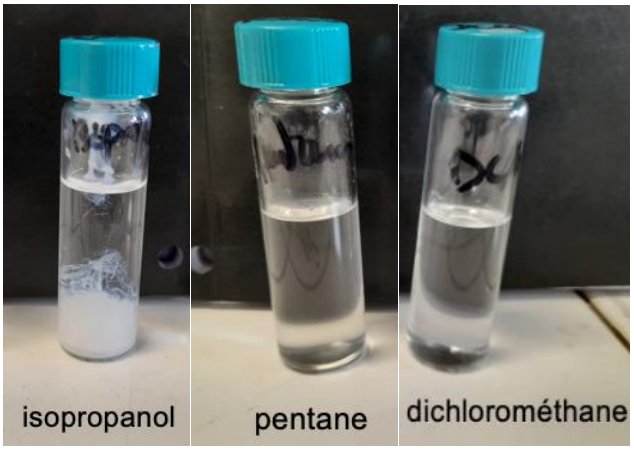


Figure 2. PET solutions aspect in isopropanol, pentane and dichloromethane respectively.

So, a precipitation with isopropanol alone was observed. We tried to add to the same solutions some drops of ethyl acetate as co-solvent: With isopropanol, the formation of more complicated PET filaments was observed. With pentane, a PET agglomerate was precipitated directly. However, a direct suspension was observed in dichloromethane followed by precipitation after a few minutes (Figure 3). So, the results with dichloromethane were promising to do further specific microfluidic tests to determine precisely the concentration of solutions and to stabilize the formed nano-PET in water.

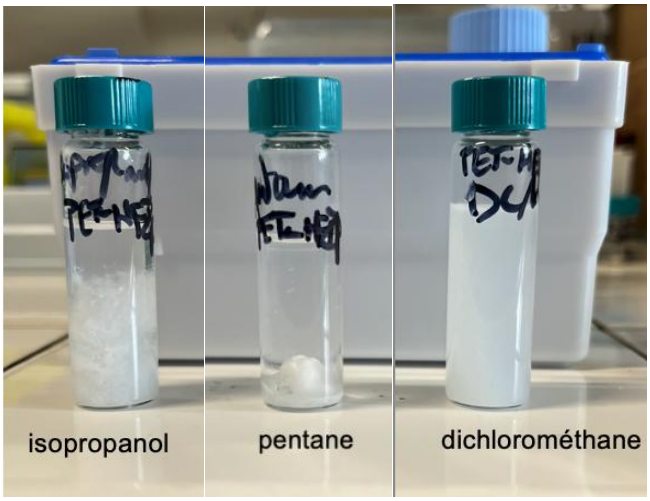


Figure 3. PET solutions aspect in isopropanol, pentane and dichloromethane respectively after adding ethyl acetate as co-solvent.

2.3.3. Microfluidic test

5 mg PET/800 mg HFIP were added to 5 mL of dichloromethane. This first step will give the mother solution on which two trials were performed:

- 1 mL of the mother solution was added to a solution of 4 mL dichloromethane and 1 mL of ethyl acetate, no suspension was observed that is why adjusting the quantity of ethyl acetate was necessary.
- 1 mL of the mother solution was added to a solution of 2.5 mL dichloromethane and 2.5 mL of ethyl acetate, the formation of micro-PET was observed.

Another more concentrated mother solution was prepared starting from 25 mg PET/800 mg HFIP in 5 mL of dichloromethane. 1 mL of the last solution was added to a solution of 2.5 mL of dichloromethane and 2.5 mL of ethyl acetate, micro-PETs were also obtained but they were bigger than the ones in the diluted solution. After that, 0.6 mL of water have been added resulting in the formation of agglomeration followed by 5 mg of SDS for stabilization (the critical micellar concentration of SDS was less than the solubility as we added high weight of SDS/0.6mL). 1.6 mL of water was added and the solution was then left under stirring all the night but it was very difficult to reobtain the suspension after the precipitation.

The same steps of this last experiment were repeated to adjust the dispersion in SDS by adding 1 mg of SDS in water, but unfortunately an agglomerate has been remaining even after stirring all the night. A trial of solvent evaporation followed by addition of water was also performed but it was useless.

These experiments confirmed the good ratios of dichloromethane/ethyl acetate but it was not possible to stabilize nano-PET in water.

2.3.4. Pre-final promising protocol

This time, nanoparticles will be stabilized with BSA solution (2.5 mg/5mL of water). BSA (Bovine Serum Albumin) is a monomeric protein of molecular weight of 66.5 kDa. Indeed, 25 mg PET/800 mg HFIP in 5 mL of dichloromethane were prepared and constituted the mother solution. 1 mL of the last solution was added to a solution of 2.5 mL of dichloromethane and 2.5 mL of ethyl acetate. From the final solution, 0.5 mL was added to the 5 mL of BSA in water. Fortunately, the nano-PETs have remained in suspension this time but they were in the bottom of the tube; it was not easy to evaporate the dichloromethane phase under air.

2.3.5. Final protocol: New and efficient

Here, a not chlorinated organic solvent have been used. So, pentane has replaced dichloromethane to obtain PET nanoparticles in the upper phase that facilitates solvent evaporation and avoid the precipitation problem. Two experiments were performed with simplification of steps:

- Concentrated solution of nano-PETs: 25 mg PET/800 mg HFIP in 5 mL of pentane were prepared as mother solution. 0.5 mL of this solution was added to the 5 mL of BSA in water (2.5 mg).
- Diluted solution of nano-PETs: 25 mg PET/400 mg HFIP in 1 mL of pentane were prepared as mother solution. 0.5 mL of this solution was added to the 5 mL of BSA in water (2.5 mg).

The PET nanoparticles remained in the upper phase. They left to dry under air while shaking the two phases each 10 minutes for better dispersion. After evaporation, the nano-PETs stabilized in water were centrifuged and then analyzed by DLS (Dynamic Light Scattering) to measure their size. DLS measurements were performed on both concentrated and diluted fruit container nano-PETs and on both solutions of environmental PET. The size of BSA alone was also measured.

DLS measurements

DLS measurements were done on the nano-PETs from the fruit container after centrifugation at 2800g during 10 minutes. The measurements were repeated twice for ensuring the reproducibility of results. The results of the first measurement showed the presence of huge nanoparticles (microplastics) around 7 µm. However, the second trial showed smaller particles that may due to the precipitation of microplastics that allow the detection of the nanoparticles stayed in suspension (Figure 4 & 5).

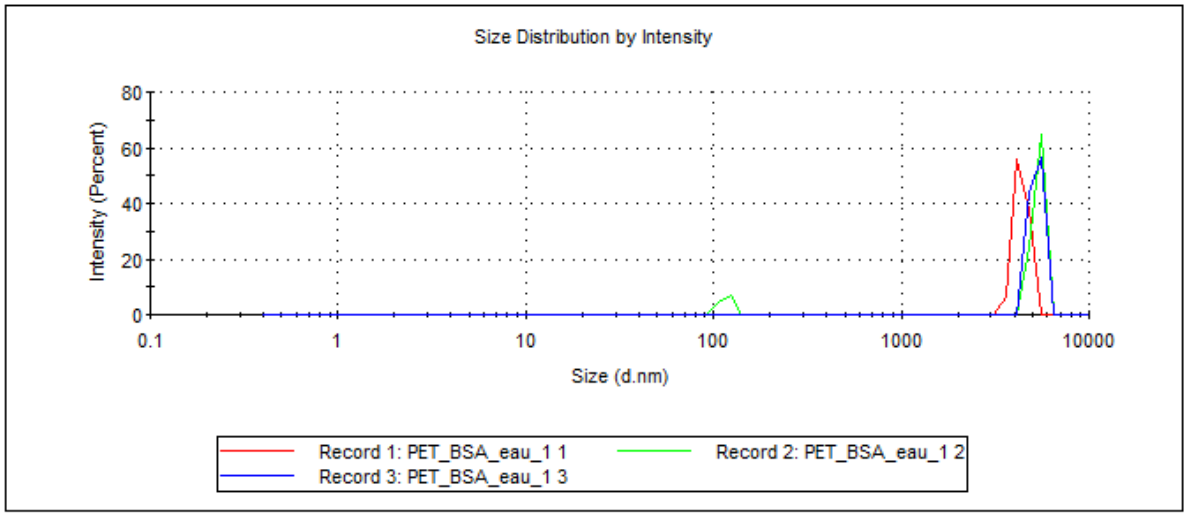


Figure 4. Diluted nano-PETs solution DLS measurement after centrifugation at 2800g during 10 minutes: 1st DLS trial.

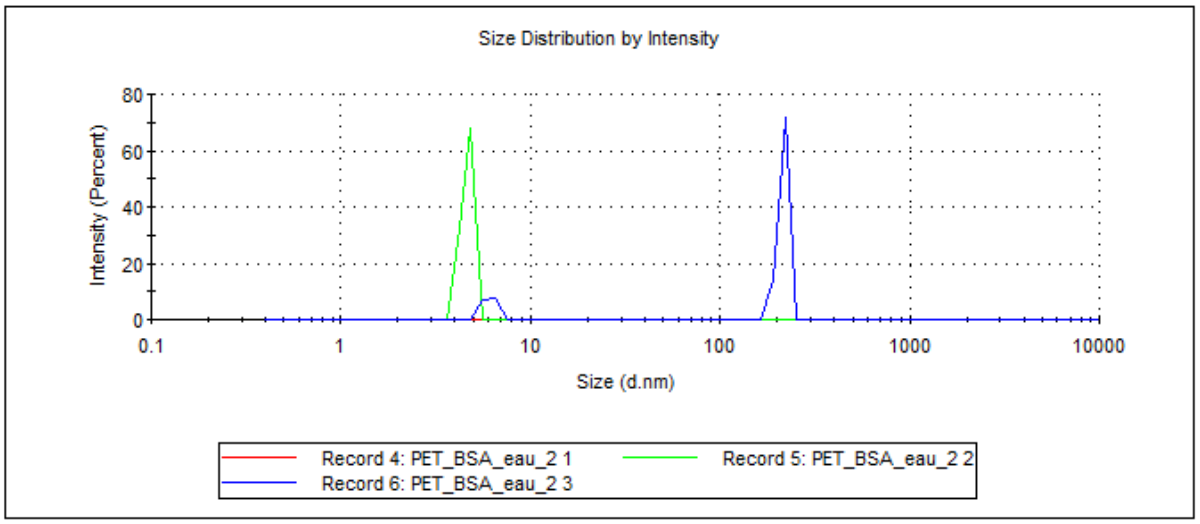


Figure 5. Diluted nano-PET solution DLS measurement after centrifugation at 2800g during 10 minutes: 2d DLS trial.

The previous DLS results showed non-homogeneity in size of the formed PET particles. So, another centrifugation for this sample for longer time was performed to eliminate more microplastics, at 2800g during 30 minutes. And it was necessary to check the size of BSA solution alone.

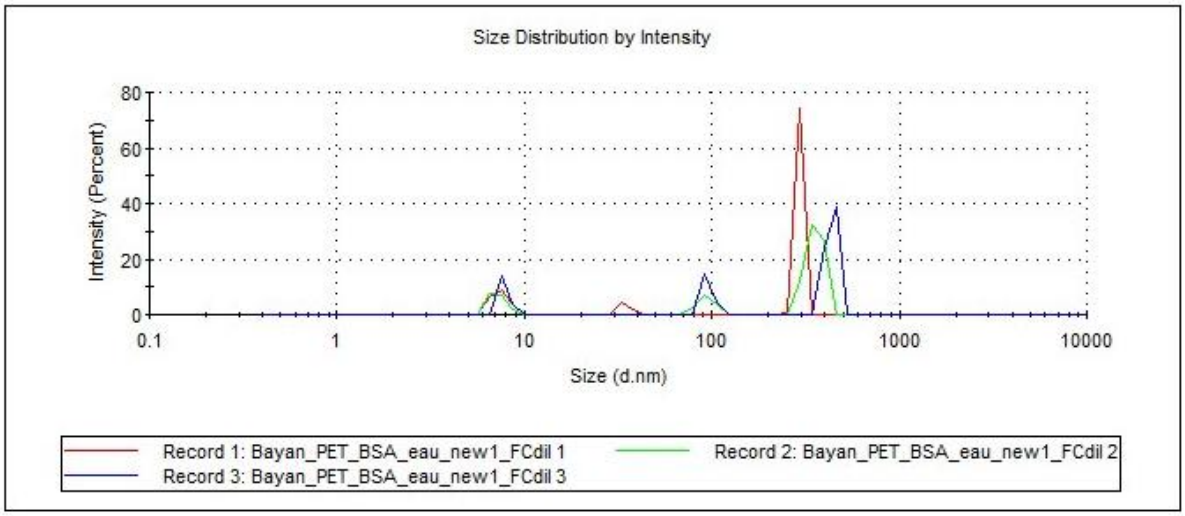


Figure 6. Diluted nano-PETs solution DLS measurement after centrifugation at 2800g during 30 minutes.

DLS measurements of the same nano-PETs solution confirmed our hypothesis and showed the importance of centrifugation on adjusting the size of nano-PETs. As shown in Figure 6, the biggest particles disappeared after longer centrifugation and low intense particles around 10 nm remained.

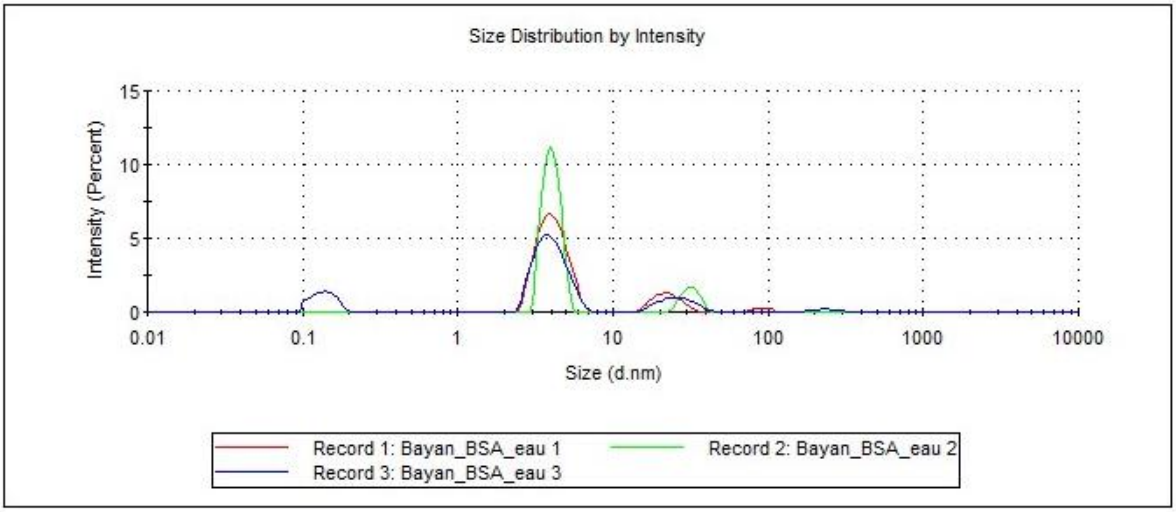


Figure 7. DLS measurement of BSA solution.

DLS measurement of BSA alone confirmed the presence of low intensity BSA particles between 1-10 nm (Figure 7). So, the effect of centrifugation duration was important: 2800g/10 minutes and 2800g/30 minutes gave different sized-nanoparticles.

In addition, trials to improve the quality of these measurements were done using this time purer BSA powder in addition to filtration of the BSA solution with a filter of 0.02 µm. The results showed cleaner DLS measurements of two types of particles: PET+BSA around 100 nm and BSA alone around 10 nm (Figure 8 & 9).

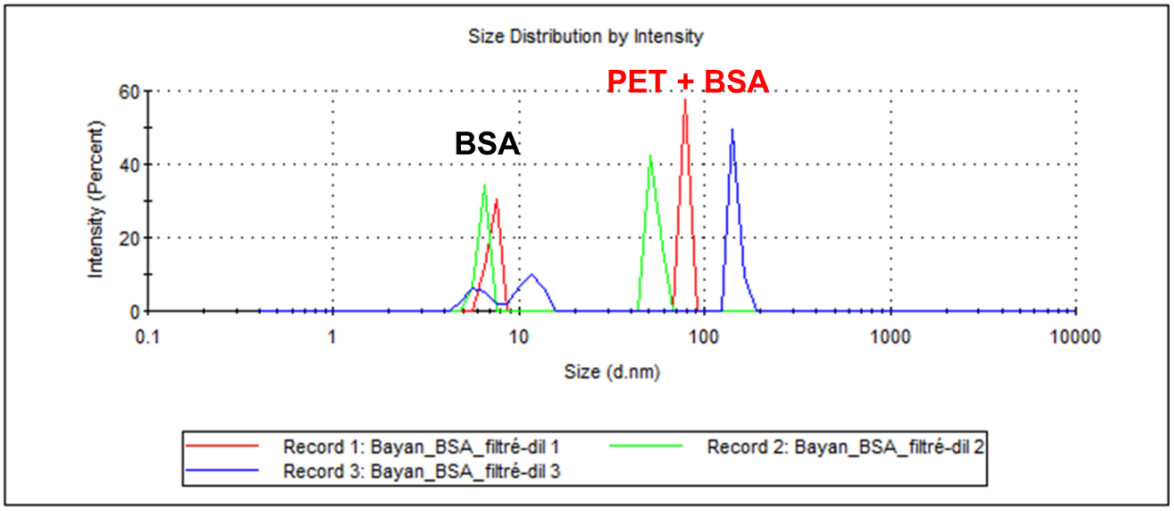


Figure 8. Diluted nano-PETs solution DLS measurement after centrifugation at 2800g during 30 minutes and after filtration of BSA.

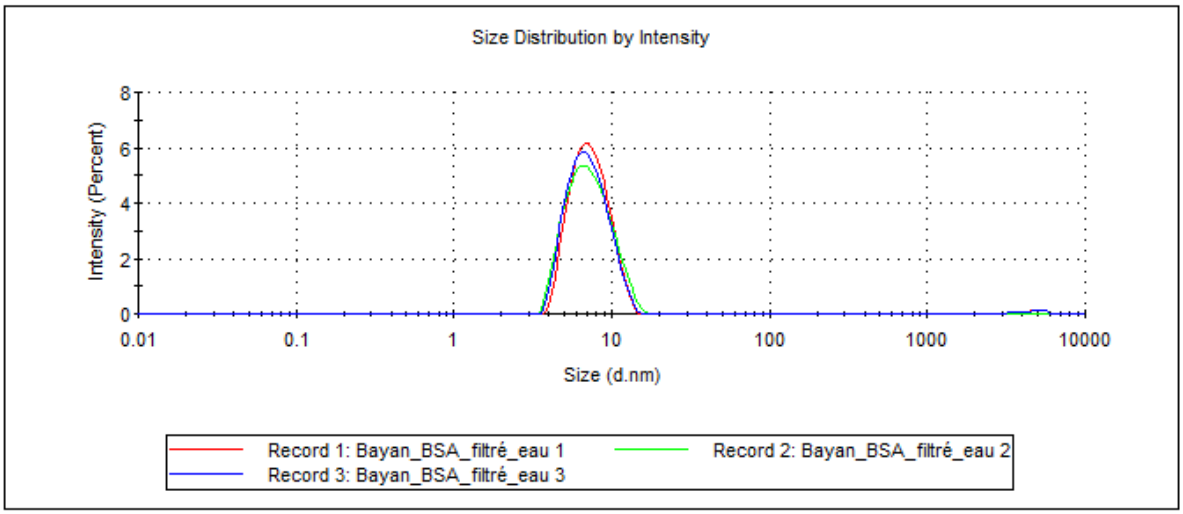


Figure 9. DLS measurement of BSA solution after filtration.

As conclusion, the type of BSA and the duration of centrifugation are important parameters that can affect the size of nano-PETs in this new protocol. The best results were obtained with a centrifugation at 2800g/30 minutes using pure analytical BSA and after filtration of BSA solution at 0.02 µm.

References

1- Liu, S.; Wang, C.; Yang, Y.; Du, Z.; Li, L.; Zhang, M.; Ni, S.; Yue, Z.; Yang, K.; Wang, Y., Microplastics in three types of human arteries detected by pyrolysis-gas chromatography/mass spectrometry (Py-GC/MS). *Journal of Hazardous Materials* **2024,** *469*, 133855.

2- Tamargo, A.; Molinero, N.; Reinosa, J. J.; Alcolea-Rodriguez, V.; Portela, R.; Bañares, M. A.; Fernández, J. F.; Moreno-Arribas, M. V., PET microplastics affect human gut microbiota communities during simulated gastrointestinal digestion, first evidence of plausible polymer biodegradation during human digestion. *Scientific Reports* **2022,** *12* (1), 528.

3- Zhou, H.; Shi, S.; You, Q.; Zhang, K.; Chen, Y.; Zheng, D.; Sun, J., Polyethylene terephthalate hydrolases in human gut microbiota and their implications for human health. *Microorganisms* **2024,** *12* (1), 138.

4- Zhang, J.; Peng, M.; Lian, E.; Xia, L.; Asimakopoulos, A. G.; Luo, S.; Wang, L., Identification of poly (ethylene terephthalate) nanoplastics in commercially bottled drinking water using surface-enhanced Raman spectroscopy. *Environmental Science & Technology* **2023,** *57* (22), 8365-8372.

5- Rodríguez-Hernández, A. G.; Muñoz-Tabares, J. A.; Aguilar-Guzmán, J. C.; Vazquez-Duhalt, R., A novel and simple method for polyethylene terephthalate (PET) nanoparticle production. *Environmental Science: Nano* **2019,** *6* (7), 2031-2036.

3. Analysis and quantification of terephthalic acid (TPA) using LC-MS

The aim here is to perform the analysis by LC-MS of regenerated terephthalic acid (rTPA) sample purchased from the SME company “Induo”.

First, solubility issues appeared for the pure TPA, when 1 mg was solubilized in 1 mL of:

- 10% DMSO + 90% of solvent B (75% acetonitrile, 0.1% formic acid).
- Solvent B after sonication 30 minutes.
- 75% MeOH + 0.1% formic acid after sonication 30 minutes.
- Concentrated NaOH (30%).

So, the solubilization solvent has been changed by adding 1 mg of TPA in 1 mL of solvent in which 10 µL of trimethylamine was introduced in the presence of 90% of one of those solvents: Pure acetonitrile, solvent A (5% acetonitrile, 0.1% formic acid) and solvent B (75% acetonitrile, 0.1% formic acid). The solubility was not enough using the pure acetonitrile but was better using solvent A and B.

For the analysis, the same gradient as described in chapter 2 (article 1) with the elution solvents A and B (normal gradient & positive mode) was achieved. However, chromatography problems appeared so a flat gradient in positive mode was used instead for which a better intensity of TPA was obtained. Indeed, TPA relative intensity was 1.84 E+03 at *m/z* 167.034 (theoretical *m/z* 167.0338) as shown in Figure 1 using solvent B for solubilization; as the chromatography was better with the solubilization solvent B in the presence of formic acid than in A or B without formic acid. The chromatography properties depend on ionization (in acidic or alkaline medium) but unfortunately, chromatography problems remained.

The LC performances were compared by changing the elution solvents to A` (5% ammonium formiate 10 Mm) and B` (75% ammonium formiate 10Mm), but the results were not better than A & B with acetonitrile.

So, to improve the quality of analysis, we stayed on the elution solvents A and B, but the analysis was performed in negative mode using the flat gradient and the results were quite satisfying as we obtained real peak shape at the retention time of 4.71 minutes with higher intensity 1.64 E+06 as shown in Figure 2 in which the TPA appeared at *m/z* 165.019 (theoretical *m/z* 165.018).

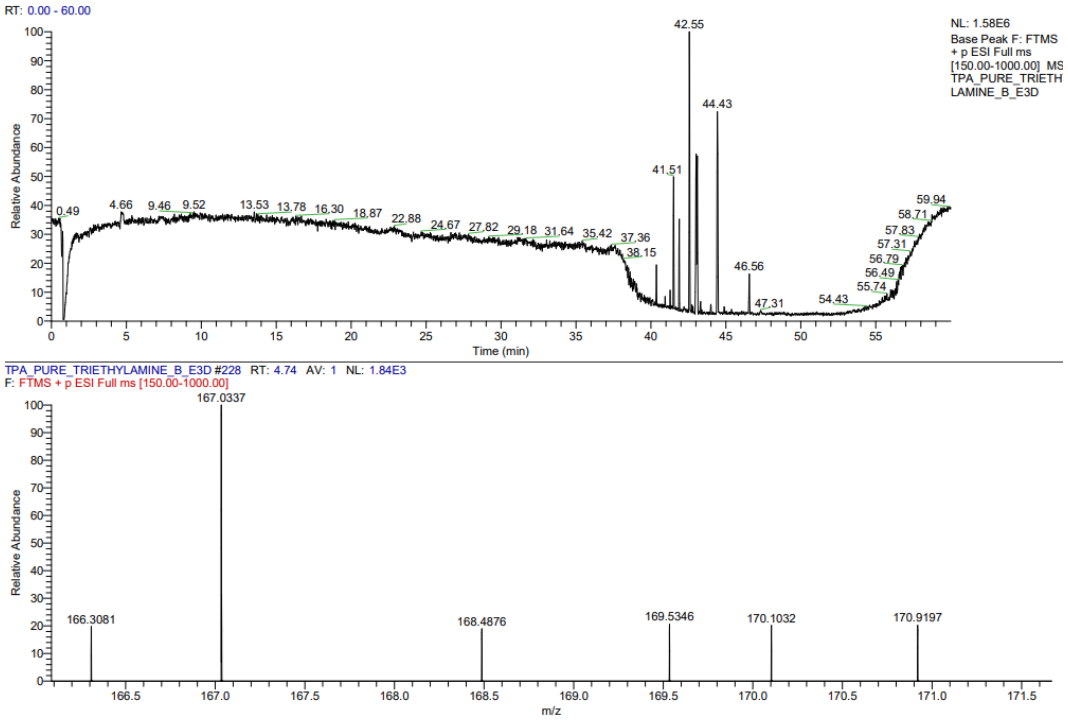


Figure 1. LC chromatogram and MS associated spectrum of pure TPA using 10% triethylamine + solvent B (0.1% formic acid) as solubilizing solvent, analysis in positive mode, flat gradient.

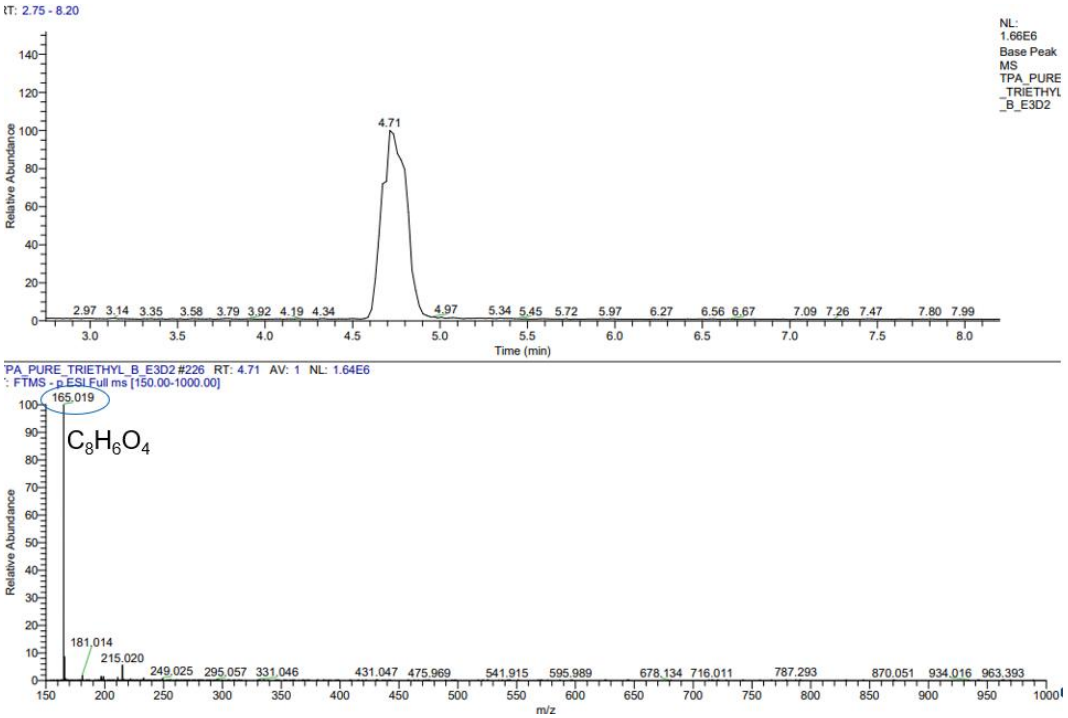


Figure 2. LC chromatogram and MS associated spectrum of pure TPA using 10% triethylamine + solvent B (0.1% formic acid) as solubilizing solvent, analysis in negative mode, flat gradient.

Our best results until now is solubilizing 1 mg of TPA in 10 mL of acidified methanol (+ 0.1% formic acid) after 20-30 minutes of sonication, using the elution solvents A and B performing the analysis in negative mode with the flat gradient.

Thus, different mixtures of pure TPA and 4-deuterated TPA were analyzed and compared to a mixture of rTPA with 4-deuterated TPA where each sample was analyzed three times by LC-MS then the average of these three acquisitions was used for quantification.

The experimental weights are shown in Table 1. In sample 1, the 4-dTPA was appeared at *m/z* 169.043 (theoretical *m/z* 169.0433) with high intensity (7.59E+04) as shown in Figure 3.

Table 1. Experimental weights of pure TPA and deuterated TPA (sample 6 contains the regenerated TPA).

Sample number	Pure TPA experimental weight (mg)	Deuterated TPA experimental weight (mg)
1	1.00	0.80
2	0.99	0.92
3	1.01	1.02
4	0.91	1.00
5	0.80	1.10
6 “rTPA”	1.01	1.04

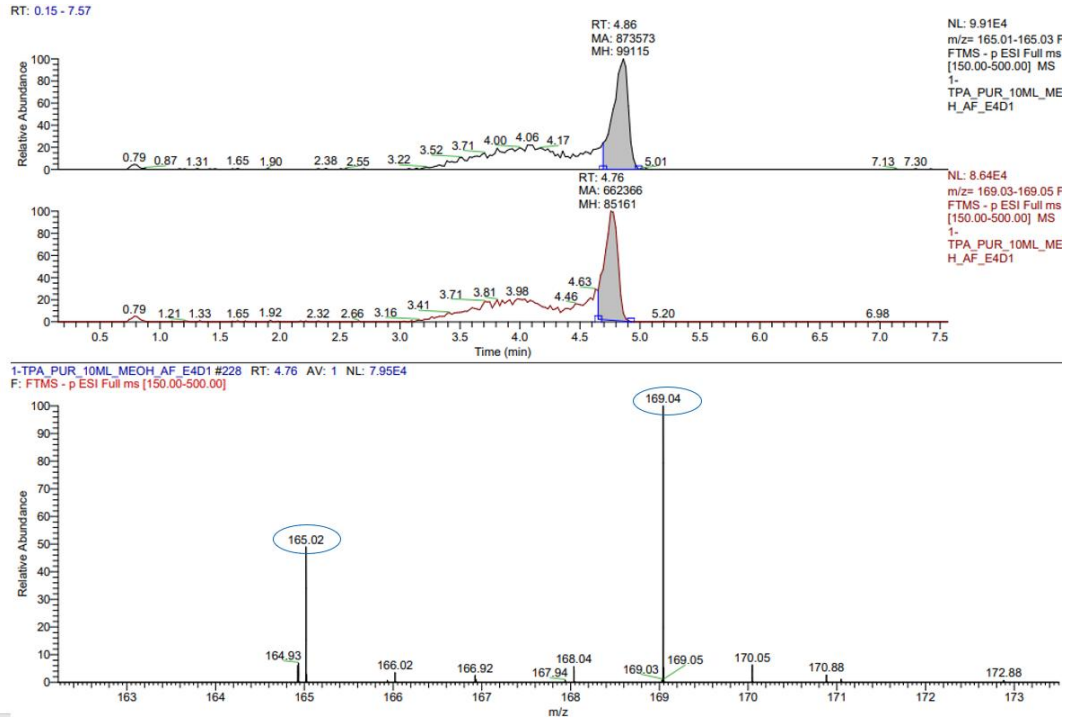


Figure 3. LC chromatogram and MS associated spectrum of sample 1 analyzed in negative mode & flat gradient.

As shown in Figure 4, only three mixtures were used to draw the calibration curve as the results were dispersed. For the calibration curve, the slope was 1.27145952 and the intercept was -0.1407016. The intensity was calculated through the following formula:

$$\text{Intensity} = \text{weight_ratio} \times \text{slope} + \text{intercept}$$

So, weight_ratio = (intensity - intercept)/slope = 0.979492.

This allowed us to determine the Induo TPA calculated weight which was 1.01867168; and the ratio Induo TPA calculated/introduced % which is 100.9%; above 100% as the LC-MS sensitivity was not perfect, so we have to improve the quality of this quantification by changing LC column and the solubilization solvent.

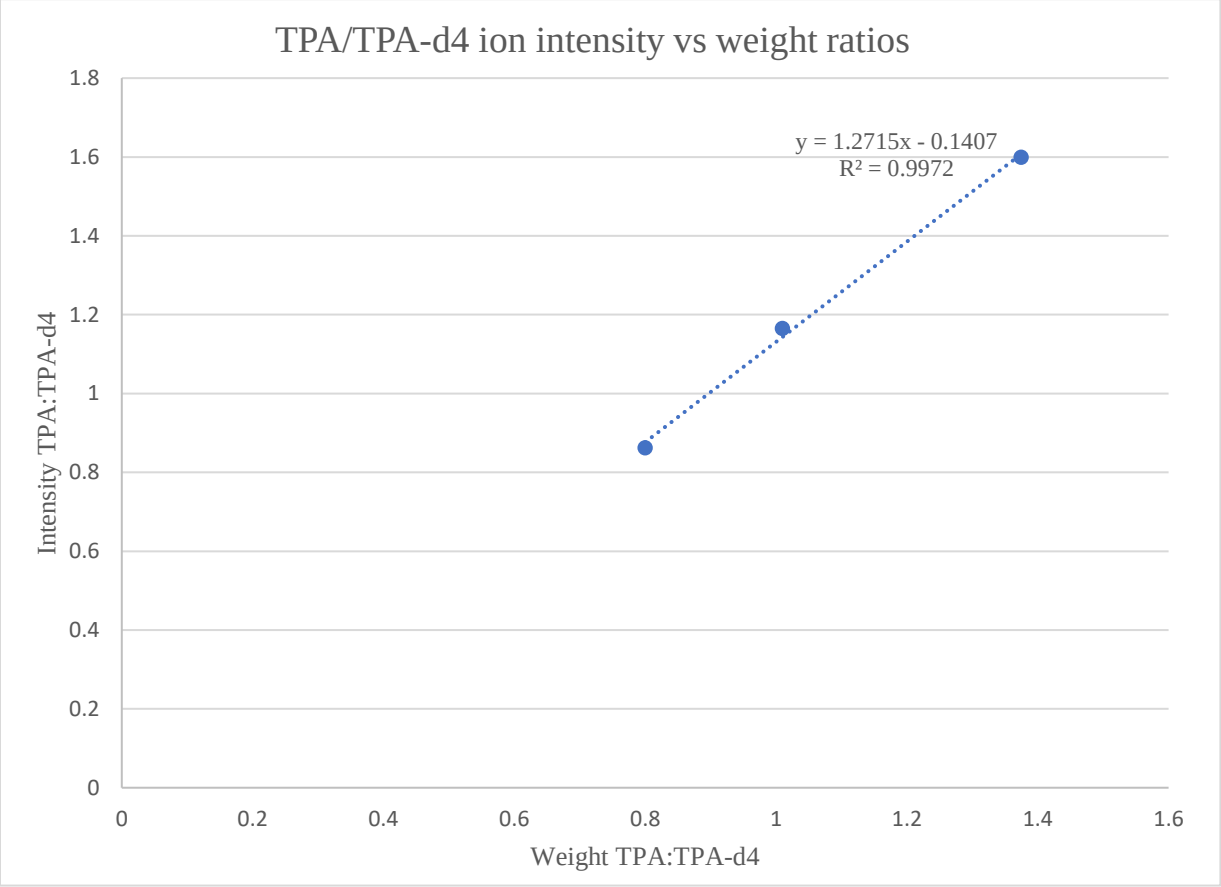


Figure 4. Calibration curve, TPA/TPA-d4 ion intensity vs weight ratios.

Conclusions and perspectives: Part I

Conclusions

- A new, original and sensitive method for the depolymerization of polyesters and co-polyesters was developed under soft conditions.
- Both acids and polyols were identified and quantified by MALDI FTICR and LC ESI Orbitrap.
- Polyols modifications were followed-up.
- The extraction yield of transamidation was improved after solubilization in HFIP.
- Polyethylene terephthalate (PET) dimers, oligomers, degradation products, oxygenated species and additives were studied in details.
- Enchased products in PET films were detected.
- UV-ageing was studied for short and long-term irradiation and compared to thermo-ageing.
- PET packaging objects from different day life sources, contents and manufacturing countries were compared and differentiated.
- PET bottles treated under natural and semi-natural conditions were compared (river and seawater).
- The degradation of environmental marine PET bottles was studied and the effect of microorganisms on this degradation was detected.
- Biodegradable co-polyesters and marine objects (PBAT and biodegradable mussel nets) were studied.
- The main structure of biodegradable mussel nets was found.
- A new protocol for the synthesis of not denatured PET nanoparticles was developed.
- Solubilization of PET nanoparticles in water with BSA for biological assays was performed.

Perspectives

- Ascertaining the structure of the remaining minority products.
- Studying the degradation of environmental PET nanoparticles.
- Adjusting the size of the created nanoparticles and developing another protocol by grinding PET.
- Studying the structural modifications of PET exposed to cell culture.
- Detailed study of mussel nets with their additives and nanoparticles.
- Application of the developed methodologies on other PET microplastics and environmental samples.

PART II

Oil and alkyd paints

Chapter 7: Introduction part II

Introduction

Oil paint binders are made from triacylglycerol of polyunsaturated fatty acids which crosslink by exposition to light and atmosphere by a mechanism named siccativation. Despite their wide use as binders in artworks for centuries; little is known about the structure of the 3D-crosslinked polymeric film of oil paints, and the mechanism of their siccativation is still under debate. Three oils were used: Walnut, linseed and poppy oils which differ only by the number of double bonds of their fatty acids. Until now there is no robust method to identify which oil was used from a painting sample, which is an important information for historians of arts and restorers. To solve this problem, we developed a new methodology for the analysis of insoluble paint films starting by an innovative soft chemical depolymerization protocol which is a transamidation reaction using dimethylaminopropylamine (DMAPA) which breaks the ester bonds. This catalyst was selected also to improve the mass spectrometry ionization and to enhance the cleavage by participation.

The resulting depolymerized paint films were then analyzed using MALDI ionization on an ultra-high resolution Fourier Transform Ion Cyclotron Resonance Mass Spectrometry (FTICR MS) 9.4 Tesla. In a first step, we made mock-up samples using different oils, pigments, driers and ageing conditions as temperature or UV exposure. We identified successfully the remaining traces of polyunsaturated fatty acids of the original paint, their modifications induced by the siccativation process and the crosslinking dimers, linked by C-C or C-O-C bonds and oligomers. The products obtained were shown to be very dependent and characteristic of the initial oil. The distribution of products in the 3D reticulated network depends also on the pigment. In a second step, this sensitive method was applied to museum size samples on historical paintings from XX^{th} century to predict the oil used by the artist according to the period but also to the pigments which bring the desired colour.

We will show that this methodology works for other polyester polymers such as alkyd paints which are formed of phthalic or isophthalic part, polyols and unsaturated fatty acids.

For identifying the diols or polyols which are water soluble, we modified slightly the above protocol starting by a free-water transesterification with methanol and derivatization of the alcohols by benzoylation with dimethylaminobenzoyl chloride.

Binders: Siccativity of oils

Siccativity, which is the ability of oils to form a polymeric film, (drying oils) is closely related to the types of fatty acids composing triacylglycerols. The ability of polymerization is determined by the presence of

(poly)unsaturated fatty acids (> 60%). Depending on the percentage of unsaturated fatty acids, drying, semi-drying and non-drying oils are present.[1] Table 1 shows the composition of some siccative oils, and Figure 1 the possible structure of linseed oil.

Table 1. Composition of siccative oils in terms of fatty acids.

	Palmitic acid (C16:0)	**Stearic acid (C18:0)**	**Oleic acid (C18:1)**	**Linoleic acid (C18:2)**	**Linolenic acid (C18:3)**
Linseed oil	4-7%	2-5%	12-34%	17-24%	35-60%
Safflower oil	3-6%	1-4%	13-21%	73-79%	In traces
Poppy oil	10%	2%	11%	72%	5%
Walnut oil	11%	5%	28%	51%	5%
Soybean oil	7-11%	2-6%	22-34%	43-56%	5-11%

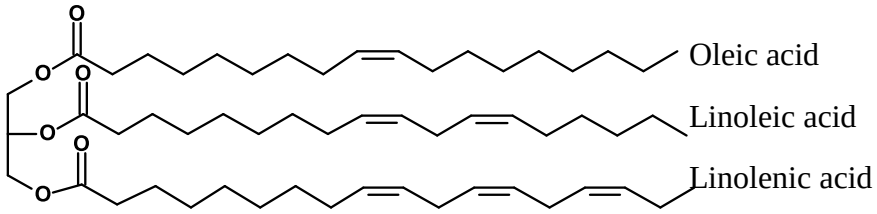


Figure 1. A possible structure of linseed oil.

Pigments & driers

Multiple studies highlighted the central role that play transition metals contained in pigments, such as manganese and lead and the well-known traditional metal: Cobalt, that accelerate the drying rate, simply named driers. There are different types of driers: Primary, secondary and auxiliary driers. In historical paints, the driers were lead salts or the pigments their selves.

Cobalt(II) 2-ethylhexanoate (2-ethyl-hexanoic acid, cobalt(2+) salt (2:1)) is powerful and well-known drier. There are other used driers such as cobalt(II) acetylacetonate (2,4-pentanedione cobalt(II) derivative), manganese(II) 2-ethylhexanoate (2-ethyl-hexanoic acid, manganese(2+) salt (2:1)), manganese(III) acetylacetonate (2,4-pentanedione manganese(III) derivative) [$Mn(acac)_3$], manganese(II) carboxylates treated with various *N*,*N*-chelating ligands, iron(III) 2-ethylhexanoate, Iron(II) complexes bearing polydentate ligands of 5 nitrogen donors, benzoylferrocene, oxovanadium(IV) acetylacetonate, and oxovanadium(IV) acetylacetonate modified with ligands.[2]

Analytical challenges: Our new methods

Oil paints are typically composed of two major phases: Organic (binders, adhesives and varnishes) and inorganic (pigments). Previous studies on oil paints using non-invasive state-of-the-art techniques provide a comprehensive characterization of the pigment only (e.g., XRF mapping) without giving information on the nature of the binder. Several techniques of characterizing oil paint binders are reported in literature. But, the harsh conditions (for example, the temperature for Py-GC-MS) limit the reproducibility of these experiments, impede quantification and cause the complete neglecting of several classes of compounds (hydroperoxides, epoxides, oxidized fatty acids, …).[3,4] Degradation studies on oil paints employing IR and NMR spectroscopies have also been reported. Therefore, our aim is the full characterization of oil-based paint binders by the methodology described below.

Our analytical methodology to analyze fatty acids and carboxylic acids is shown in Figure 2.

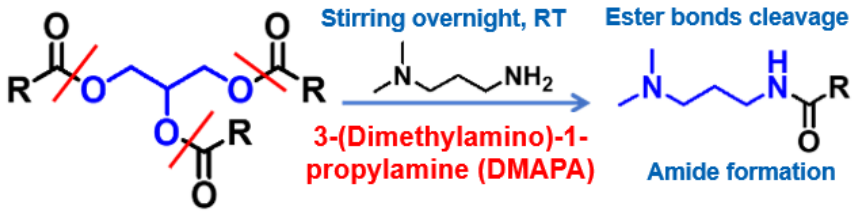


Figure 2. The new transamidation reaction of triglycerides.

To analyze at the same time polyols and carboxylic acids, our full analytical strategy is shown in Figure 3.

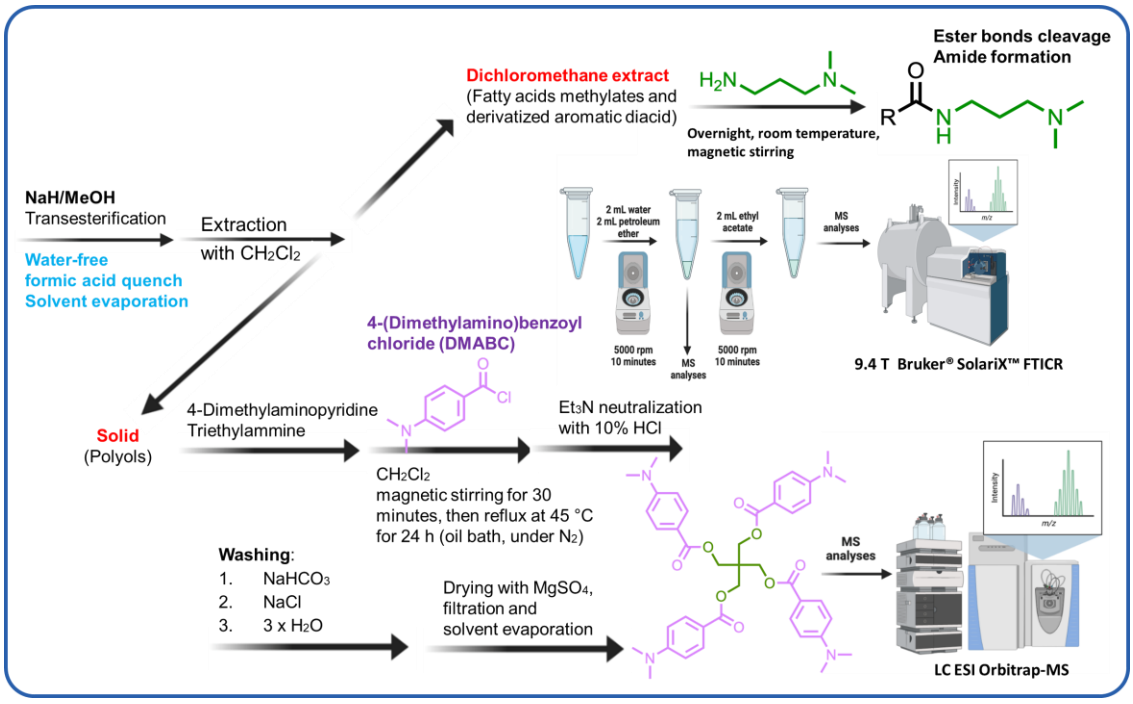


Figure 3. The new analytical methodology combining polyols and carboxylic acids derivatization.

Siccativation (autoxidation) mechanism

The polymeric paint film starts its formation as soon as paint starts drying via free radical-chain reactions. The exact polymerization mechanism is still debated. But, many researchers suggest some possible mechanisms.

Polymerization extent and rate are mainly affected by the presence of (poly)unsaturated fatty acids, oxygen, light, humidity, temperature, metals (transition metals from pigments), and other additives in paint formulations.[5]

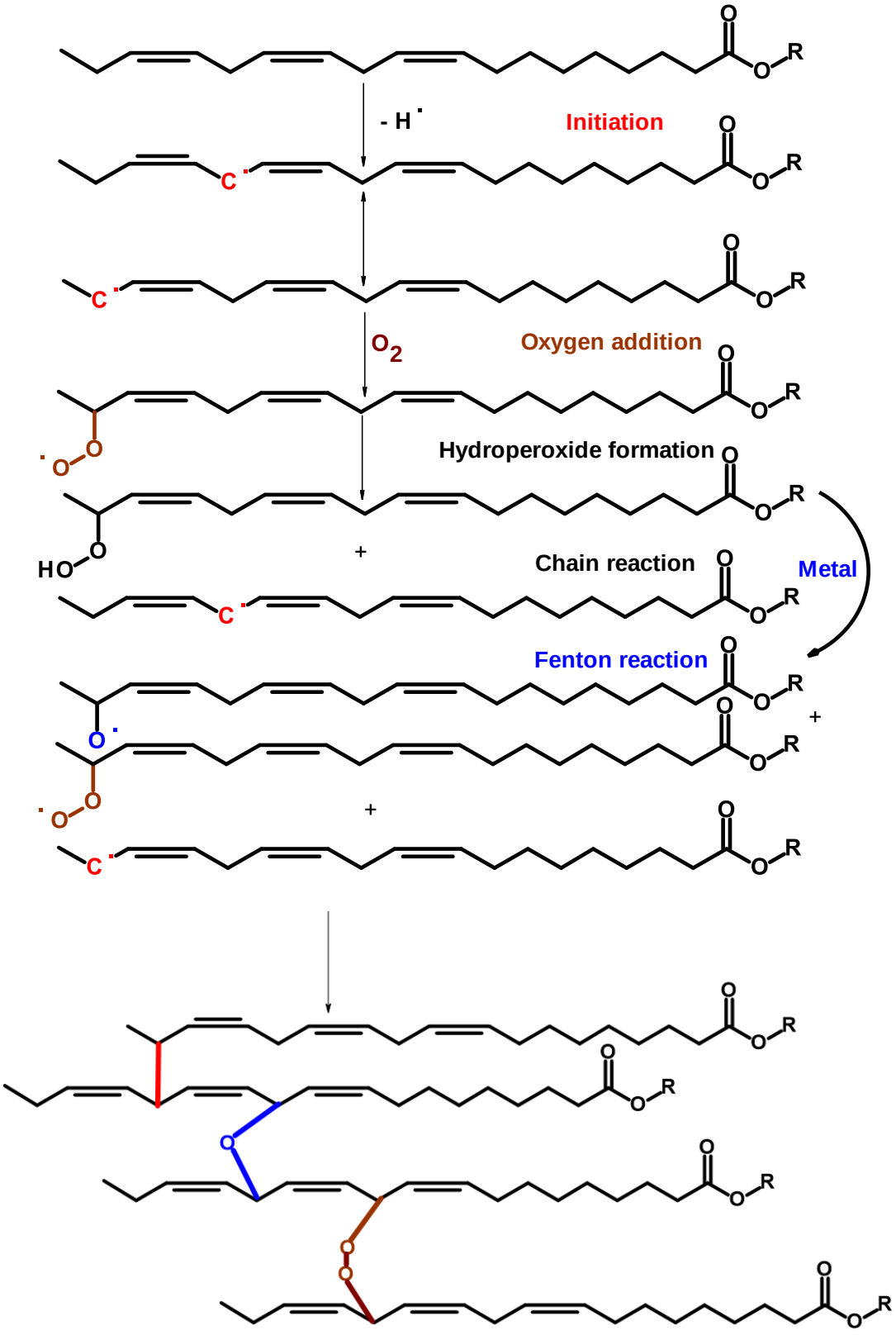
The siccativation process proceeds via a spontaneous, radical autoxidation of the double bonds in the carbon chains of fatty acids, normally composed of initiation, propagation and finally chain termination following these steps, as shown in Scheme 1:

- Abstraction of a bis-allylic proton by a reactive radical initiator leading to a carbon centered free radical.
- Formation of peroxy-radicals by oxygen capture of the initial radical.
- A chain reaction of the peroxy-radicals with a bis-allylic proton of an unsaturated fatty acid leading to the formation of hydroperoxide and a new carbon centered free radical.
- A Fenton reaction of two hydroperoxides' fatty acids leading to the formation of a hydroxy radical and a new carbon centered free radical.
- Formation of high molecular weight three-dimensional cross-linked product, combination of the formed free radicals.
- Formation of low molecular weight oxidation products as volatile organic compounds (VOCs), responsible for the typical smell of paint, by decomposition of peroxides and hydroxides, being both very reactive, and leading to the formation of aldehydes (hexanal, pentanal), ketones and alcohols.
- The same family of reactions lead to the formation of oxidation products such as dicarboxylic acids, carboxylic acids and their hydroxylated homologues.

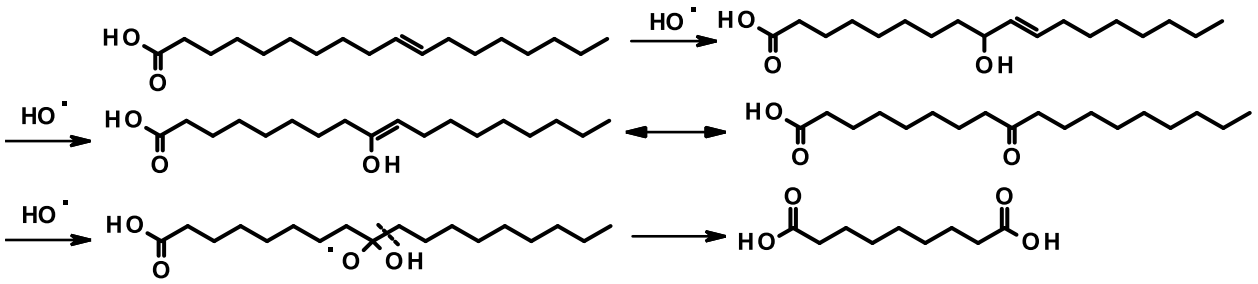
The termination step can be occurred via Russel and Baeyer Villiger reactions or other disproportionation reactions or by photooxidation reactions leading to the formation of epoxy-, oxo- and hydroxyl- by-products.[6,7]

As the reaction may be catalyzed by pigments, their transition metals may decompose rapidly the hydroperoxides formed to dry the final films faster. There are also β-scission degradation reactions that compete with autoxidation reactions and yield organic acids such as azelaic, suberic and sebacic acids.

Scheme 2 shows our proposed mechanism for the formation of azelaic acid (C9:0) detected in some degraded samples.



Scheme 1. Proposed possible mechanism of oil siccativation.



Scheme 2. Proposed mechanism of the formation of azelaic acid by β-scission reaction.

References

1- Koleske, J. V., *Paint and coating testing manual: of the Gardner-Sward handbook*. ASTM international: 2012.
2- Honzicek, J., Curing of air-drying paints: a critical review. *Industrial & engineering chemistry research* **2019,** *58* (28), 12485-12505.
3- Pitthard, V.; Stanek, S.; Griesser, M.; Muxeneder, T., Gas chromatography–mass spectrometry of binding media from early 20th century paint samples from Arnold Schönberg's Palette. *Chromatographia* **2005,** *62*, 175-182.
4- Oyman, Z.; Ming, W.; Van der Linde, R., Oxidation of drying oils containing non-conjugated and conjugated double bonds catalyzed by a cobalt catalyst. *Progress in organic coatings* **2005,** *54* (3), 198-204.
5- Zovi, O.; Lecamp, L.; Loutelier-Bourhis, C.; Lange, C. M.; Bunel, C., Stand reaction of linseed oil. *European Journal of Lipid Science and Technology* **2011,** *113* (5), 616-626.
6- Y. Orlova, R. E. Harmon, L. J. Broadbelt, and P. D. Iedema, "Review of the kinetics and simulations of linseed oil autoxidation," *Progress in Organic Coatings*, vol. 151. Elsevier B.V., Feb. 01, 2021. doi: 10.1016/j.porgcoat.2020.106041.
7- M. D. Soucek, T. Khattab, and J. Wu, "Review of autoxidation and driers," *Prog Org Coat*, vol. 73, no. 4, pp. 435–454, Apr. 2012, doi: 10.1016/j.porgcoat.2011.08.021.

Chapter 8: Oil binders' effect on siccativation

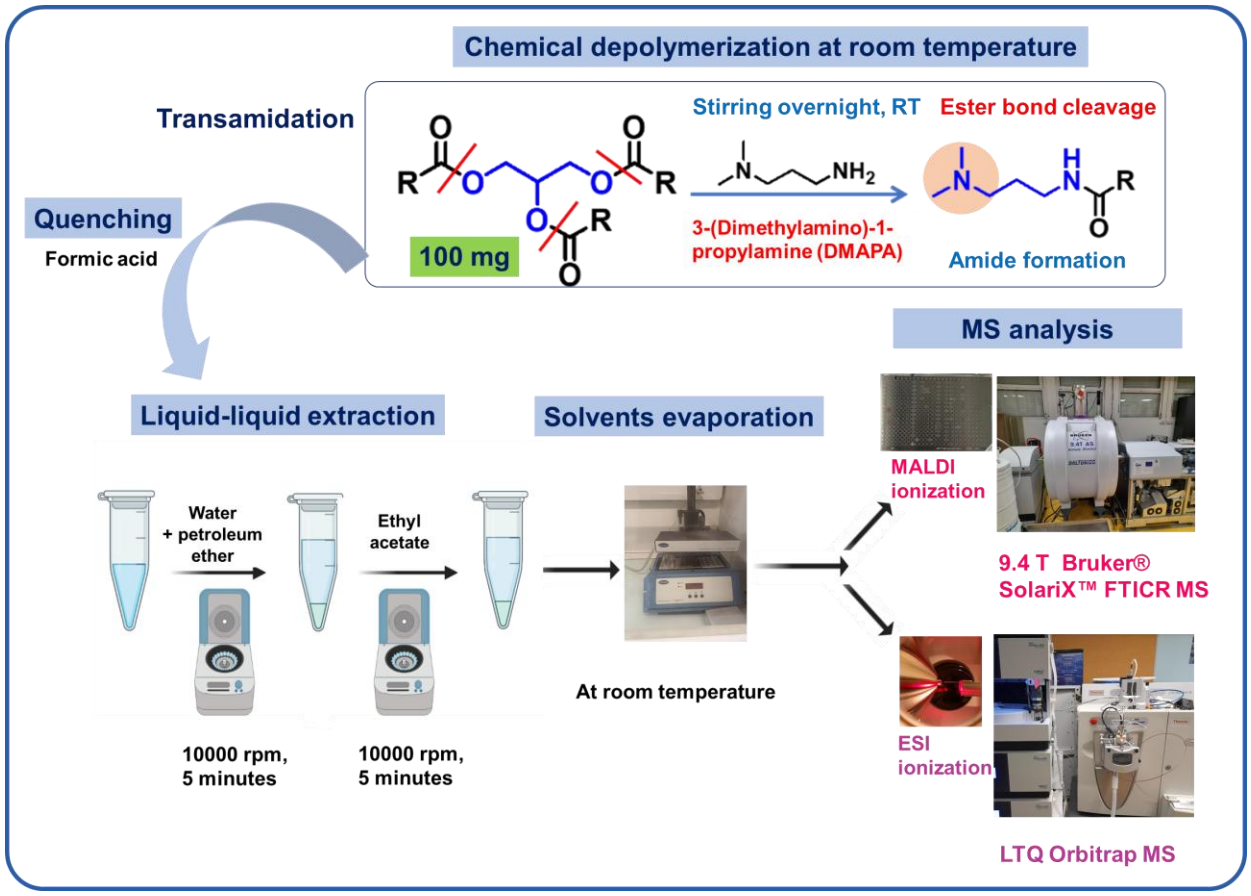
Introduction

Oil Paintings are invaluable cultural heritage objects known since centuries. Oil paints are formed mainly of inorganic pigments and vegetable siccative oils as binder. The most common binders historically used are linseed, poppy and walnut oils, which their siccativation mechanism is still debated.

The aim of the work here is to respond to these open questions:

- Can the 3-D crosslinked oil film be fully characterized at molecular level?
- Does the type of oil binders affect siccativation?
- Can the structural modifications induced by ageing be detected?
- Is it possible to predict the oil binder used in oil paintings according to full structural characterization by advanced mass spectrometry techniques?

The analytical methodology, starting from 100 mg of oil or oil paints, which is used in article 5 is shown in the following figure.


Chemical depolymerization at room temperature
Transamidation
Stirring overnight, RT
Ester bond cleavage
Quenching
Formic acid
100 mg
3-(Dimethylamino)-1-propylamine (DMAPA)
Amide formation
MS analysis
Liquid-liquid extraction
Solvents evaporation
MALDI ionization
Water + petroleum ether
Ethyl acetate
9.4 T Bruker® SolariX™ FTICR MS
At room temperature
ESI ionization
10000 rpm, 5 minutes
10000 rpm, 5 minutes
LTQ Orbitrap MS

Article 5

Siccative vegetable oils and their mock-up for oil-based paints applications: Oil differentiation and ageing for drying process assessment using a new methodology of soft chemical depolymerization with advanced mass spectrometry analysis

ABSTRACT: Oil paints are made from triacylglycerol of polyunsaturated fatty acids which crosslink by exposition to light and atmosphere by a mechanism named siccativation. Despite their wide use as binders in artwork for centuries, little is known about the structure of the 3D-crosslinked polymeric film after siccativation, and the mechanism of this reaction is still under debate. Three oils were commonly used: Linseed, walnut and poppy oils which differ only by the number of unsaturations of their fatty acids. Until now there is no robust method to identify which oil was used from a painting sample, which is an important information for historians of arts and restorers. To solve this problem, a new methodology for the analysis of insoluble paint films was developed starting by an innovative soft chemical depolymerization protocol which is a transamidation reaction using 3-(dimethylamino)-1-propylamine (DMAPA) that cleaves the ester bonds. This catalyst was selected also to improve the mass spectrometry ionization and to enhance the cleavage by participation. The resulting depolymerized paint films were then analyzed using MALDI ionization on an ultra-high resolution Fourier transform ion cyclotron resonance mass spectrometry (FTICR MS) 9.4 Tesla and an ESI ionization on an Orbitrap LTQ hyphenated with liquid chromatography (LC-MS). For this, mock-up samples using different oils were made and ageing conditions as temperature or UV exposure were applied. Polymerization process was followed during one week of oil film drying. After depolymerization, the remaining traces of polyunsaturated fatty acids of the original paint, their modifications induced by the siccativation process and the crosslinking dimers and oligomers were identified. The products obtained were shown to be very dependent and characteristic of the initial oil. This will allow to create a new database in order to differentiate oils used in museum oil paintings.

Keywords: Oil, oil paints, fatty acids, siccativation/polymerization, oil drying, ageing, depolymerization, transamidation, MALDI FTICR MS, ESI LC-Orbitrap-MS.

Vegetable oils are triacylglycerols (TAGs), tri-esters of three fatty acids with glycerol comprising three aliphatic chains or olefinic fatty acids of variable length (12-24 carbon atoms). Minor components are represented by diacylglycerols (DAGs), monoacylglycerols (MAGs), free fatty acids and a non-saponifiable fraction.[1]

For centuries, oils have been the most used binding medium in artworks. Vegetable oils are able to form solid films and fix pigments due to their siccative properties. The traditional oils used as oil paint binders were linseed, poppy and walnut oils. The invention of metal tubes which were introduced for the first time in the art market in 1841 by the British company *Winsor & Newton* had a great influence on the fabrication of oil paints. Modern paint formulations were manufactured, and constituted an affordable alternative to ancient drying oils. These alternatives are safflower, sunflower, castor and cotton-seed oils.[2] All these oils are called siccative oils or drying oils. Indeed, siccativity is the ability of oils to form a polymeric film upon exposure to light and air which is closely related to the types of fatty acids composing their triacylglycerols. The ability of this polymerization or autoxidation is determined by the presence of (poly)unsaturated fatty acids in percentage higher than 60%. Table 1 shows the composition of some siccative oils in terms of fatty acids. Depending on their percentages, siccative oils were classified into drying, semi-drying and non-drying oils. The siccativity can be determined by two factors: The first one is the drying index given by the following formula: DI = (% linoleic acid) + 2 (% linolenic acid), and the second one is the iodine value (IV) defined as the quantity in grams of iodine required for the saturation of the double bonds in the fatty acid chain. In general, DI > 70 and IV > 140 for drying oils.[3-4] The drying process of siccative oil which is a free radical chain mechanism starts by an induction period due to a consequence of antioxidants, and lack of singlet oxygen concentration. Then, an oxygen uptake step may be done which is related to the hydroperoxide formation. Peroxides may be then formed during the propagation step that finally decomposes leading to crosslinking during the termination step.[5]

In artworks, oil paints are typically composed of two major phases: Organic including binders, adhesives and varnishes and inorganic including pigments. Previous studies on oil paints using non-invasive state-of-the-art techniques provided a comprehensive characterization of the pigment only (e.g., XRF mapping) without giving information on the nature of the binder or oil siccativation.[6] Several techniques of characterizing oil paint binders are reported in literature. But, the harsh conditions (for example, the temperature for Py-GC-MS) limit the reproducibility of these experiments, impede quantification and cause the complete neglecting of several classes of compounds such as hydroperoxides, epoxides, oxidized fatty acids, ….

Degradation studies on oil paints employing IR and NMR spectroscopies have also been reported.[7-14] Therefore, the aim of this study is the full characterization of oil-based paint binders and the assessment of their siccativation mechanism which is under debate; by a new methodology applied on native oils and oil films after ageing. This strategy combines soft chemical depolymerization by transamidation reaction (Figure 1) with ultra-high resolution mass spectrometry analysis.

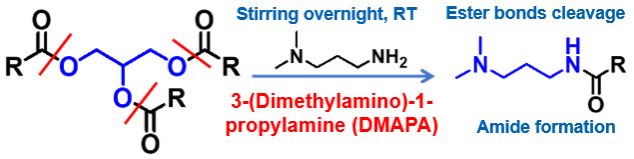


Figure 1. Transamidation reaction of a triglyceride.

Table 1. Composition in fatty acids of some siccative oils.

	Palmitic acid C16:0	Stearic acid C18:0	Oleic acid C18:1	Linoleic acid C18:2	Linolenic acid C18:3
Linseed	4-7%	2-5%	12-34%	17-24%	35-60%
Walnut	11%	5%	28%	51%	5%
Poppy	10%	2%	11%	72%	5%
Safflower	3-6%	1-4%	13-21%	73-79%	Traces

EXPERIMENTAL SECTION

Chemicals. All aqueous solutions were prepared from ultrapure grade water obtained by water filtration with a two stages Millipore system (Milli-Q® Academic with a cartouches Q-Gard 1 and Progard 2, Merck Millipore, Burlington, MA, USA). All solvents were MS analytical grade. All solvents and chemicals were purchased from Merck (Merck KGaA, Darmstadt, Germany) and used without further purification. 3-(Dimethylamino)-1-propylamine also called *N,N*-dimethyl-1,3-propanediamine (DMAPA) 99% was used as received.

Samples. Linseed oil, castor oil and tung oil were purchased from Merck (Merck KGaA, Darmstadt, Germany). Poppy oil and safflower oil were purchased from *Gamblin* brand (Portland, OR, USA). Walnut oil was *M. Graham & Co.* brand (Hubbard, OR, USA). Another linseed oil type, linseed stand oil was *Sennelier* brand (Paris, France).

Mock-up samples preparation.

Ageing at room temperature for one week. Linseed oil and poppy oil were each spread homogeneously over glass slide (thickness was almost 0.04 mm). 50 mg of each oil was put and left under natural conditions for one week.

Ageing accelerated by heating. 50 mg of linseed oil was spread homogeneously over glass slide and left under natural conditions for one week to fix oil on the slide. After that, the slide was put in GC oven at the temperature of 80 °C for one week.

Ageing accelerated by UV-irradiation. 50 mg of linseed oil was spread homogeneously over glass slide and put directly over UV-LED at 395 nm for 44 days. UV LEDs-B (395 nm, irradiance of 14 W.cm^{-2}, Omnicure® AC9150, from Excelitas Technologies Corp., Pittsburgh, PA, USA) was used as light source.

All oil films were collected carefully using clean scalpel blades before depolymerization.

Depolymerization by direct transamidation. In a 2-mL transparent tube, 100 mg of the collected films or native oils were transamidated overnight at room temperature with 1 mL (7.93 mmol) of 3-(dimethylamino)-1-propylamine (DMAPA) under stirring using a vortex-Genie® 2. The mixture was quenched with 100 µL of formic acid (2.65 mmol) (caution: exothermic reaction) then transferred to a 5 mL Falcon™ conical tube (Corning, NY, USA), added to 2 mL of ultrapure water acidified with 20 µL of formic acid and extracted two times with 2 mL of petroleum ether by centrifugation at 10,000 rpm during 5 minutes at room temperature using Beckman-Coulter (Brea, CA, USA) Allegra® X-30R centrifuge with the corresponding C1015 fixed angle conical tube rotor. The remaining aqueous phase was reextracted two times with 2 mL of ethyl acetate under the same centrifugation conditions. After each centrifugation, the organic phase was transferred to a 2-mL clear glass tube using a glass pipette. The obtained organic phases were evaporated under nitrogen at room temperature and stored in 2-mL glass tube.

Analytical method. For MS samples preparation, the petroleum ether fractions were solubilized in dichloromethane at 1 mg/10 µL. However, the ethyl acetate fractions were solubilized in methanol at 1 mg/10 µL. After solubilization, they were diluted in methanol/water/formic acid 30/70/0.1 (v/v/v); 100 times for MALDI FTICR MS analysis and 1000 times for LC-MS analysis.

1. MALDI FTICR MS analysis. The analyses were performed on a SolariX XR instrument with a 9.4 Tesla actively shielded superconducting magnet fitted with a dynamically harmonized cell (Bruker Daltonics, Bremen, Germany) and controlled by FTMS Control software. MALDI FTICR mass spectra were acquired in positive ion mode using a MTP 384 ground steel MALDI plate (Bruker Daltonics). The matrix was α-cyano-4-hydroxycinnamic acid (10 mg/mL in acetonitrile/water/trifluoroacetic acid 70/30/0.1 (v/v/v)). 1 µL of the diluted sample at 1 mg/1 mL was mixed with 1 µL of matrix. Then 1 µL of this binary mixture was spotted on the MALDI plate and dried at room temperature. Spectra were acquired using broadband detection, 8 M points; 32 scans accumulation for a better signal-to-noise ratio with a mass range from *m/z* 100 to 1,500. The transient time was 2.936 s and resulted in a theoretical resolution of 530,000 at *m/z* 400 in magnitude mode. Instrument calibration was achieved using red phosphorous as external calibrant and a quadratic calibration. Internal calibration using derivatized fatty acids list was performed. The obtained spectra were processed using Data Analysis software version 5.0 (Bruker Daltonics, Bremen, Germany).

2. LC-ESI MS analysis. LC-MS analyses were performed on an Orbitrap LTQ XL mass spectrometer hyphenated to a Dionex Ultimate 3000 HPLC System (ThermoFisher Scientific, Bremen, Germany). The analysis was performed using a 40 min gradient at a flow rate of 0.50 mL.min^{-1} on a Hypersil GOLD™ C18 column (2.1 µm i.d. × 150 mm) packed with 3 µm beads pores from ThermoFisher Scientific, Bremen, Germany; placed in an oven at a temperature of 50 °C. The depolymerized products were separated using a

multi-step gradient with a mobile phase of 30% methanol in acidified water, 0.1% formic acid (solution A) and 50% methanol, 50% 2-propanol in acidified water, 0.1% formic acid (solution B). The gradient started by 100% of solution A for 5 min then increased to 30% A, 70% B until 20 min. It increased more to 100% of solution B at 25 min holding this mobile phase until 30 min then it returned to the initial conditions at 35 min holding 100% of solution A for the remaining 5 min. The LC runs were acquired in positive ion mode using ESI ionization with a non-heated source (spray voltage 4.50 kV, sheath gas flow 22 mL.min^{-1}, auxiliary gas flow 12 mL.min^{-1}). After testing many injections at different concentrations to have a good peak shape, the concentration of 1 mg/10 mL was found to be the best. The MS scans were acquired from *m/z* 200 to 1,000 with a 60,000 resolution at *m/z* 200 leading to a scan duration of 30 ms. Data acquisition and interpretation were performed using Xcalibur™ 4.21 SP1 software (Thermo Fisher Scientific).

RESULTS AND DISCUSSIONS

The study of different oils and oil films aged differently (natural drying, heating and UV-exposure) have been achieved after soft chemical depolymerization and analysis by mass spectrometry high resolution LC-MS and MALDI FTICR MS.

The MALDI FTICR MS analyses have been done on all native oils and polymerized oil films. A list of more than 300 peaks was identified and used for internal calibration of MS spectra. 58 peaks were considered as major composition in all spectra constituted of the main saturated and unsaturated fatty acids with their dimers and oxidized compounds. All MALDI FTICR MS spectra were registered with very high accuracy (0-2 ppm) as shown in SI, Figure S1. In addition, all LC-MS results were registered for an accuracy less than 5 ppm.

Mock-up oil films' preparation. In a first step, mock-up samples of linseed, poppy, walnut, safflower and castor oils have been prepared after one week of polymerization at natural conditions. The drying process of oil films has been followed over 5 days on each slide containing initially 50 mg by the measurement of oil weight each 2 hours in the first day of spreading oil over the slide then each 4 hours for the rest of the week, no measurements have been performed at night.

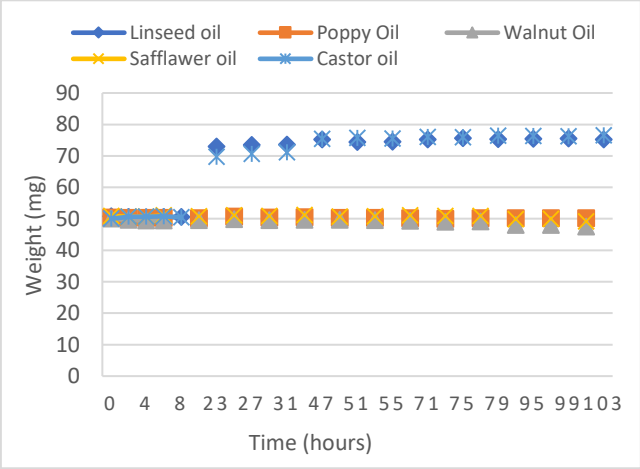


Figure 2. Evolution of polymerized oil films' weight during 5 days of polymerization at room temperature. All these measurements were done in relatively cold days, from January to February 2025 in Lille, France.

The measurement of the weight of all oil polymerized films for one week under natural conditions will provide an idea about volatile organic compounds (VOC) that may be lost during drying process and the evolution of the siccativation mechanism. The films of linseed oil and castor oil had an increase of weight up to 5% during the first 23 hours then their weight has been stabilized over the remaining days (Figure 2). The results obtained for linseed oil drying was in accordance to Fjällström et al. that confirmed a weight increase up to a maximum of 7% after 20 hours of treatment under air flow at a constant temperature of 80 °C.[15] However, the weight remained relatively constant over time after 1 day. There was no formation of real polymeric film of poppy oil even after three weeks of natural polymerization without pigments or driers.

Linseed oil contains normally 35% to 60% of linolenic acid ($C_{18}H_{30}O_2$), a C18 fatty acid with 3 unsaturations and castor oil is very rich in ricinoleic acid ($C_{18}H_{34}O_3$), a C18 fatty acid with 1 unsaturation and additional oxygen atom in its chain (85-94%).[16] However, poppy, walnut and safflower oils contain lower percentages of unsaturated fatty acids but still have relatively high percentages of linoleic acid ($C_{18}H_{32}O_2$) with 2 unsaturations (Table 1). This explains why the drying of linseed and castor oils were faster than the other oils even without driers or pigments. On the other hand, tung oil contains high percentages of the tri-unsaturated compound α-eleostearic acid ($C_{18}H_{30}O_2$).[17] In the cases of linseed and castor oils, the oxygen uptake was found after an induction period within the first day resulting in the weight gain of oil films. Some of this weight gain will be then lost due to decomposition and loss of volatile compounds (VOC) as a result of oxidation reactions during the lifetime of the film.

In fact, the siccativation process proceeds via a spontaneous, radical autoxidation of the double bonds in the carbon chains of fatty acids, normally composed of initiation, propagation and finally chain termination following these steps, as shown in Figure 3:

(i). Abstraction of a bis-allylic proton by a reactive radical initiator leading to the formation of a carbon centered free radical;

(ii) Formation of peroxy-radicals by oxygen capture of the initial radical;

(iii) A chain reaction of the peroxy-radicals with a bis-allylic proton of an unsaturated fatty acid leading to the formation of a hydroperoxide and a new carbon centered free radical;

(iv) A Fenton reaction of two hydroperoxides of fatty acids leading to the formation of a hydroxy radical and a new carbon centered free radical;

(v) Formation of high molecular weight three-dimensional cross-linked product by the combination of the formed free radicals;

(vi) Formation of low molecular weight oxidation products as volatile organic compounds (VOCs), responsible for the

typical smell of paint, by decomposition of peroxides and hydroxides, being both very reactive, and leading to the formation of aldehydes (hexanal, pentanal), ketones and alcohols; and (vii) the same family of reactions can form oxidation products such as dicarboxylic acids, carboxylic acids and their hydroxylated homologues.

A termination by photooxidation reactions can also lead to the formation of epoxy-, oxo- and hydroxyl- by-products.[5, 17-20]

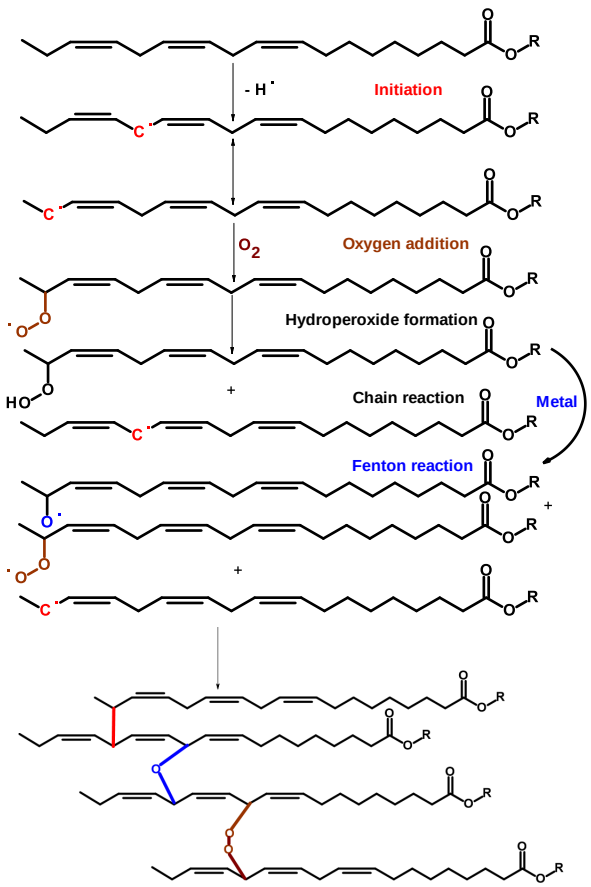


Figure 3. Proposed siccativation mechanism of oil films.

Depolymerization of oils and oil siccativated films. The depolymerization method was transamidation overnight using 3-(*N*,*N*-dimethylamino)-1-propylamine (DMAPA) at room temperature, followed by addition of acidified water then liquid-liquid extractions for the transamidated products were performed first with petroleum ether then with ethyl acetate. The order of the solvents was necessary here to extract first the more apolar compounds in petroleum ether then the more polar and apolar remaining compounds in ethyl acetate. The addition of 20 µL of formic acid with water improved a little bit the extraction yield in petroleum ether. The extracted phases were finally dried, resolubilized in methanol or dichloromethane, diluted and then analyzed by LC-MS and MALDI FTICR MS.

The extraction yield, measured based on the recovered weight, was different not only according to oil type but also according to polymerization rate. Indeed, the poppy and linseed oil films polymerized for one week had extraction yields of 97% and 72% respectively. For linseed oil film, the extraction yield went from 72% to 29% then 19 % after its natural polymerization of 1 week, heating at 80 °C and irradiation for 44 days respectively (Figure 4). Native oils have always higher extraction yields than their corresponding films.

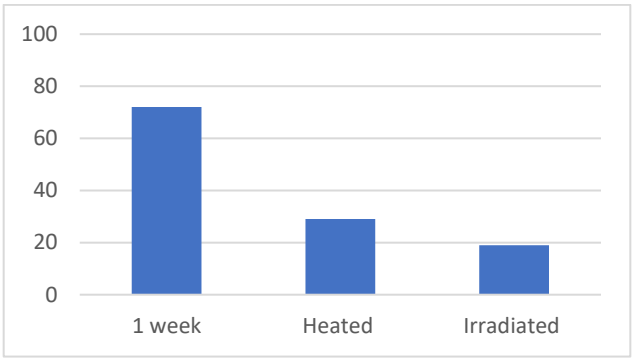


Figure 4. Extraction yield of linseed oil films after ageing.

Analysis of native oils. LC-MS results of petroleum ether fractions showed the presence of the main unsaturated fatty acids: Oleic (C18:1), linoleic (C18:2) and linolenic (C18:3) acids and the main saturated fatty acids: Stearic (C18:0) and palmitic (C16:0) acids mono-derivatized with DMAPA.

The abundance of each fatty acid's peak in the mixture will be given in comparison to its major composition, according to the following formula:

$$\text{Abundance of a fatty acid's peak} = \frac{\textit{Relative intensity of the}\ \text{fatty acid's peak}}{\textit{Relative intensity of the major composition peaks}} \times 100$$

Indeed, the native linseed oil first major three peaks were the mono-derivatized fatty acids: Linolenic [$C_{23}H_{42}N_2O$ + H^+], oleic [$C_{23}H_{46}N_2O$ + H^+] and linoleic [$C_{23}H_{44}N_2O$ + H^+] acids with 38%, 22% and 15% respectively of the major composition (SI, Table S1).

The MALDI FTICR MS analyses of both native linseed oils, the stand oil from *Sennelier* brand and the linseed oil from Merck, showed the presence of linolenic acid (C18:3) as main peak appearing at *m/z* 363.3369 under its mono-derivatized form with 19% and 38% respectively. The lower percentage of linolenic acid in the stand oil is explained by the preparation mode of this oil by heating at high temperature for increasing its drying index.[21]

Native castor oil had a main peak appearing at *m/z* 383.3632 with 15% of its major composition. This peak corresponds to [$C_{23}H_{46}N_2O_2$ + H^+] formed of $C_{18}H_{34}O_3$ with 1 DMAPA molecule showing the presence of ricinoleic acid as main compound. The native poppy, safflower and walnut oils had a common main peak appearing at *m/z* 320.2947 appearing with 86%, 62% and 64% of their major composition respectively. This last detected peak [$C_{21}H_{37}NO$ + H^+] is formed of linoleic acid ($C_{18}H_{34}O_2$) but with $N(CH_3)_2$ terminal group obtained after DMAPA fragmentation. The native tung oil was rich in α-eleostearic acid with $N(CH_3)_2$ terminal group [$C_{21}H_{35}NO$ + H^+] appearing at *m/z* 318.2791 with 62% of its major composition. All MALDI FTICR MS

relative intensities of the native siccative oils are shown in SI, Table S2.

Analysis of oil films siccativated for one week. Moving to the study of ageing effect on fatty acids composition in LC-MS. The polymerized linseed oil film after one week of natural polymerization showed the consuming of its starting main linolenic acid peak (*m/z* 363.3369) from 37% to only 7% of its major composition. The abundance of oleic acid at *m/z* 367.3683 decreased drastically from 20% to 1% but linoleic acid abundance (*m/z* 365.3526) diminished only from 11% to 8% of the major composition. The brutal consuming of oleic acid was due to the apparition of its oxygenated form [$C_{23}H_{46}N_2O_3 + H^+$] at *m/z* 383.3632 with high intensity (17%). However, the saturated mono-derivatized palmitic acid [$C_{21}H_{44}N_2O + H^+$] (*m/z* 341.3526) was the main peak after this one week's polymerization constituting 29% of this mixture's major composition. It constituted only 9% of the native linseed oil composition. The mono-derivatized stearic acid [$C_{23}H_{48}N_2O + H^+$] (*m/z* 369.3839) abundance was doubled to 12% after this polymerization (SI, Table S1).

The ratio of a given unsaturated fatty acid versus saturated fatty acids, defined as the sum of abundances of mono- and di-derivatized forms of this unsaturated fatty acid in comparison to the sum of abundances of both main saturated fatty acids, has been calculated according to the following formula:

$$\text{Ratio of unsaturared fatty acid vs saturated fatty acids} = \frac{\sum unsaturated\ fatty\ acid\ abundances}{\sum C16{:}\,0\ abundances + \sum C18{:}\,0\ abundances}$$

As shown in Table 2, the abundances of each unsaturated fatty acid vs saturated fatty acid was lower after one week of autoxidation.

Table 2. LC-MS data: Ratio of main unsaturated fatty acids in comparison to saturated fatty acids present in the native linseed oil and its polymerized film, petroleum ether fraction.

Ratio	Native linseed oil	Polymerized linseed oil, 1 week
C18:1 vs saturated	2.23	0.19
C18:2 vs saturated	0.90	0.24
C18:3 vs saturated	1.30	0.88

The abundance of all detected oxygenated compounds increased from 2% to 10% after one week of polymerization confirming the oxygen diffusion inside linseed oil film during the siccativation mechanism. The oxygenated species found were palmitoleic (C16:1), palmitic, stearic and C18 unsaturated fatty acids with one oxygen, C18 saturated and unsaturated fatty acids with two oxygen atoms and C18 unsaturated fatty acids with three oxygen atoms (SI, Table S1).

In MALDI FTICR MS, after one week of natural drying, many dimers containing or not several oxygen atoms have been detected with two DMAPA molecules constituting almost 1.22% of its major composition (Table 3). Indeed, the C-C dimers of linoleic acid [$C_{46}H_{86}N_4O_2 + H^+$] and linolenic, linoleic [$C_{46}H_{84}N_4O_2 + H^+$] acids appeared at *m/z* 727.6823 and *m/z* 725.6667 with 0.07% and 0.06% of the major composition respectively. The linoleic [$C_{46}H_{86}N_4O_3 + H^+$] and linoleic, oleic [$C_{46}H_{88}N_4O_3 + H^+$] acids' dimers with 1 oxygen atom appearing at *m/z* 743.6773 and *m/z* 745.6934 respectively constituted 0.2% of the major composition. The dimers with 2 oxygen atoms of linolenic, linoleic [$C_{46}H_{84}N_4O_4 + H^+$], linoleic [$C_{46}H_{86}N_4O_4 + H^+$] and linoleic, oleic [$C_{46}H_{88}N_4O_4 + H^+$] fatty acids appearing at *m/z* 757.6565, *m/z* 759.6722 and *m/z* 761.6875 respectively have been also detected with 0.3% abundance. Their dimers with 3 oxygen atoms [$C_{46}H_{84}N_4O_5 + H^+$], [$C_{46}H_{86}N_4O_5 + H^+$] and [$C_{46}H_{88}N_4O_5 + H^+$] were detected at *m/z* 773.6515, *m/z* 775.6617 and *m/z* 777.6828 respectively. These compounds constituted also 0.3% of the major composition. Even the dimers with 4 oxygen atoms of C18:2 [$C_{46}H_{86}N_4O_6 + H^+$] and C18:2, C18:1 [$C_{46}H_{88}N_4O_6 + H^+$] have been detected at *m/z* 791.6621 and *m/z* 793.6776 respectively. The dimers with 5 oxygen atoms appeared only for linoleic, oleic acid mixed dimer [$C_{46}H_{88}N_4O_7 + H^+$] at *m/z* 809.6727 (SI, Table S3). Unfortunately, MALDI alone affords no clue to identify the precise structure of the dimers. They may have C-OC, or C-O-OC bridges or C-C dimer bearing oxygen. Furthermore, it should be pointed out that the ketone -CH_2-CH_2C=O- is isobaric with the unsaturated alcohol-CH=CHCH(-OH)-.

Table 3. Comparison of percentages of the main fatty acids (mono- and di-derivatized forms) and their dimers and oxygenated compounds in the polymerized oil films, petroleum ether fractions analyzed by MALDI FTICR MS.

	Linseed oil, 1 week	Linseed oil 1 week + heating 1week at 80 °C	Linseed oil irradiated at 395 nm for 44 days	Poppy oil 1 week
% All dimers	1.22%	1.17%	0.46%	0.13%
% C18:3	7.74%	1.27%	0.89%	0.75%
% C18:2	8.75%	5.40%	1.72%	0.65%
% C18:1	1.23%	6.77%	16.65%	0.27%
% C16:0	29.14%	16.31%	30.92%	0.05%
% C18:0	12.30%	5.48%	27.70%	0.08%
% Saturated	41.44%	21.79%	58.61%	0.13%
Ratio C18:3 vs saturated	0.19	0.06	0.02	5.75
Ratio C18:2 vs saturated	0.21	0.25	0.03	4.99
Ratio C18:1 vs saturated	0.03	0.31	0.28	2.09
% O	34.92%	55.57%	17.87%	0.33%

Moving to poppy oil, comparing poppy oil before and after one week of natural polymerization, the main peak remained the linoleic acid [$C_{21}H_{37}NO + H^+$] with $N(CH_3)_2$ terminal group but with lower intensity going from 86% to 58% of the major composition. After 1 week, only 0.33% of oxygenated species were detected in MALDI FTICR MS spectrum (Table 3). Despite the presence of common peaks between poppy and linseed oils' films polymerized for one week, poppy oil showed unique compounds that were not found in linseed oil. For example, this oil contained the mono-derivatized compounds [$C_{18}H_{32}N_2O_2 + H^+$] and [$C_{18}H_{32}N_2O_3 + H^+$] appearing at *m/z* 309.2537 and *m/z* 325.2486 respectively. Contrary to linseed oil, the abundances of the main unsaturated and saturated fatty acids in poppy oil before and after one week of polymerization were very similar. This shows that poppy oil needs more time to be dry and that pigments are necessary for its rapid drying during short time in comparison to linseed oil. This last was more siccative and very fast to dry alone.

Comparison of oils, films and aged films. In petroleum ether fraction, the number of peaks per spectrum was very high up to 48,000 peaks. The native oil spectra showed lower number of peaks per spectrum. For instance, the native poppy oil spectrum had 492 peaks but its polymerized film's spectrum had 45,989 peaks. This number was increasing with polymerization rate from 41,330 to 44,880 then 47,624 for the aged linseed oil film for 1 week, heated at 80 °C and irradiated at 395 nm for 44 days respectively (Figure 5).

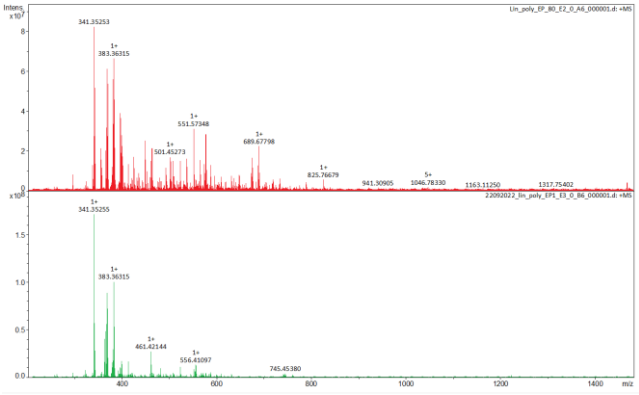


Figure 5. MALDI FTICR MS spectra (*m/z* 200- *m/z* 1,500) of heated linseed oil at 80 °C after drying one week (upper panel) and linseed oil naturally polymerized for one week (lower panel).

For linseed oil films comparing the full natural polymerization of one week to the drying by heating at 80 °C after one week of natural drying, a stronger consuming of linolenic acid was observed in the MALDI FTICR MS spectrum. Only 1.3% of this fatty acid remained after heating. The percentage of the oxygenated C16 and C18 saturated and unsaturated fatty acids with oxygen atoms up to 3 have been increased after heating from 35% to 56% of the major composition (Table 3 & SI, Table S3). More peaks were identified in the heated linseed oil that were not present in the polymerized linseed oil for one week. Among these additional peaks, the first more intense peak in petroleum ether fraction was the di-derivatized compound [$C_{30}H_{58}N_4O_2 + H^+$] appearing at *m/z* 507.4633 with 12% of the minor unique composition (SI, Table S4). This compound may be a dimer with degraded fatty acids chain. It constituted only 0.5% of the corresponding ethyl acetate fraction showing difference of the lipidic composition according to the polarity of derivatized compounds and of the extraction solvents (Figure 6 & SI, Table S4). However, the ethyl acetate fraction had two main peaks appearing with 14% and 7% of the minor composition. The first main compound was the di-derivatized oxygenated compound with 3 oxygen atoms [$C_{37}H_{72}N_4O_5 + H^+$] appearing at *m/z* 653.5576 and the second was the di-derivatized dimer also oxygenated with 3 oxygen atoms [$C_{40}H_{74}N_4O_5+H^+$] appearing at *m/z* 691.5732 (SI, Table S4).

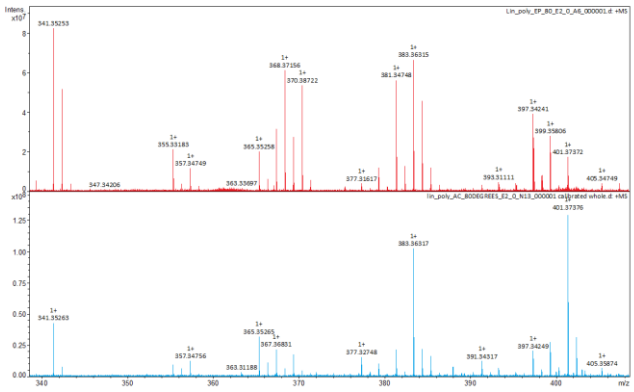


Figure 6. MALDI FTICR MS spectra (*m/z* 338-*m/z* 408) of heated linseed oil film at 80 °C after drying one week. Upper panel: Petroleum ether fraction; lower panel: Ethyl acetate fraction.

Ageing of oil film by UV-irradiation. Moving into the most aged linseed oil film that underwent an irradiation for 44 days at 395 nm. The most intense peaks in this petroleum ether sample were the mono-derivatized palmitic and stearic acids appearing at *m/z* 341.3526 and *m/z* 369.3839 with 31% and 28% of the major composition respectively. Oxygenated products decreased until 18% showing that maybe the full formation of crosslinking is still not complete in comparison to the native oil having 10% of oxygenated species. Going back to the proposed siccativation mechanism (Figure 3), some volatile compounds (VOC) can be lost during all the life of film due to oxidation procedures and crosslinking formation.

Degradation marker's formation. The azelaic acid di-derivatized [$C_{19}H_{41}N_4O_2 + H^+$] have been detected only in the linseed oil after heating at *m/z* 357.3224 in trace (error= 0 ppm) showing that β-scission degradation reaction competed with the siccativation reactions in this sample[22](Figure 7).

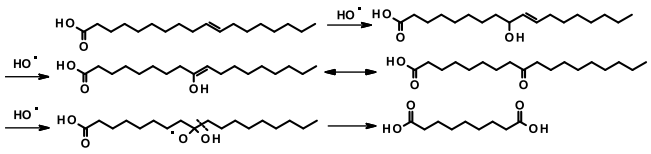


Figure 7. Proposed mechanism of the formation of azelaic acid by β-scission reaction.

All these data confirm that the siccativation mechanism affording the 3D-crosslinked films depends on oil type and ageing time and rate in the presence of light and oxygen.

CONCLUSIONS AND PERSPECTIVES

A new and original methodology was developed for the analysis of oils and oil paints. Chemical depolymerization by transamidation with DMAPA at room temperature, combined to advanced mass spectrometry (MALDI FTICR MS and LC-MS) was used. Mock-up samples of oils and different ageing procedures were studied after the follow-up of their drying over 5 days. This method allowed the full characterization with high accuracy of fatty acids, their oxygenated species and crosslinked dimers as well as the differentiation of oils in function of their structural composition and polymerization rate. The siccativation mechanism has been approved according to the identified compounds. A wide database of depolymerized compounds has been attributed. These results will allow the determination of the type of binder used in the museum oil paintings in order to conserve these artworks for long-term. Our method will be used soon to assess the effect of driers and pigments on the formation of the final polymeric film of oils.

ASSOCIATED CONTENT

Supporting Information

Additional experimental details and characterization data.

AUTHOR INFORMATION

First author

Bayan Almasri - Univ. Lille, CNRS, UAR 3290, MSAP, Miniaturisation pour la Synthèse l'Analyse et la Protéomique, F-59000 Lille, France ; Laboratoire de Chimie Appliquée, Faculté des Sciences III, Université Libanaise, Ras Maska, Tripoli, Liban ; orcid.org/0009-0001-9467-5716.

Note

The authors declare no competing financial interest.

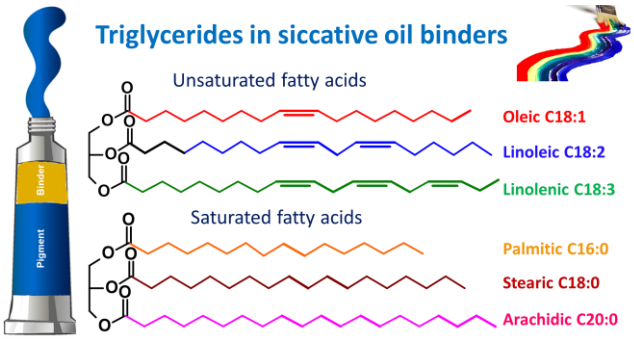
AKNOWLEDGMENT

Bayan ALMASRI gratefully acknowledges the funding of her joint PhD between University of Lille and Lebanese University by the PAUSE funding program. The mass spectrometer was funded by University of Lille, CNRS, Région Hauts-de-France and the European Regional Development Fund (ERDF). The authors gratefully acknowledge the financial support of the FTICR MS facility from the IR INFRANALYTICS FR2054 CNRS and of the EU_FTICR _MS project Grant Agreement 731077 funded by EU Horizon 2020 Research and Innovation Program.

REFERENCES

1. ALMASRI, B., Préparation de nouveaux catalyseurs hétérogènes basiques pour la production de biocarburant. Master thesis, Université Libanaise, 2020.
2. Izzo, F. C.; Berg, K. J. v. d.; Keulen, H. v.; Ferriani, B.; Zendri, E., Modern oil paints–formulations, organic additives and degradation: some case studies. In Issues in contemporary oil paint, Springer: 2014; pp 75-104.
3. Wexler, H., Polymerization of drying oils. Chemical reviews 1964, 64 (6), 591-611.
4. Ahmad, Z., Drying oils. In Principles of Corrosion Engineering and Corrosion Control,, Ahmad, Z., Ed. Butterworth-Heinemann, 2006; pp 382-437.
5. Soucek, M.; Khattab, T.; Wu, J., Review of autoxidation and driers. Progress in Organic Coatings 2012, 73 (4), 435-454.
6. Walter, P.; de Viguerie, L., Materials science challenges in paintings. Nature materials 2018, 17 (2), 106-109.
7. Spyros, A.; Anglos, D., Study of aging in oil paintings by 1D and 2D NMR spectroscopy. Analytical chemistry 2004, 76 (17), 4929-4936.
8. Spyros, A.; Anglos, D., Studies of organic paint binders by NMR spectroscopy. Applied Physics A 2006, 83, 705-708.
9. Catalano, J.; Di Tullio, V.; Wagner, M.; Zumbulyadis, N.; Centeno, S. A.; Dybowski, C., Review of the use of NMR spectroscopy to investigate structure, reactivity, and dynamics of lead soap formation in paintings. Magnetic Resonance in Chemistry 2020, 58 (9), 798-811.
10. Bonaduce, I.; Andreotti, A., Py-GC/MS of organic paint binders. Organic mass spectrometry in art and archaeology 2009, 304-326.
11. Van der Weerd, J., Microspectroscopic analysis of traditional oil paint. Universiteit van Amsterdam: 2002.
12. Schönemann, A.; Edwards, H. G., Raman and FTIR microspectroscopic study of the alteration of Chinese tung oil and related drying oils during ageing. Analytical and bioanalytical chemistry 2011, 400, 1173-1180.
13. Tammekivi, E., Vahur, S., Vilbaste, M., & Leito, I. (2021). Quantitative GC–MS analysis of artificially aged paints with variable pigment and linseed oil ratios. Molecules, 26(8), 2218.
14. Nardelli, F., Martini, F., Lee, J., Lluvears-Tenorio, A., La Nasa, J., Duce, C., ... & Bonaduce, I. (2021). The stability of paintings and the molecular structure of the oil paint polymeric network. Scientific Reports, 11(1), 14202.
15. Fjällström, P.; Andersson, B.; Nilsson, C.; Andersson, K., Drying of linseed oil paints: a laboratory study of aldehyde emissions. Industrial Crops and Products 2002, 16 (3), 173-184.
16. Sen, B.; Gupta, M. K.; Mia, M.; Pimenov, D. Y.; Mikołajczyk, T., Performance assessment of minimum quantity castor-palm oil mixtures in hard-milling operation. Materials 2021, 14 (1), 198.
17. Samadzadeh, M.; Boura, S. H.; Peikari, M.; Ashrafi, A.; Kasiriha, M., Tung oil: An autonomous repairing agent for self-healing epoxy coatings. Progress in Organic Coatings 2011, 70 (4), 383-387.
18. Oyman, Z.; Ming, W.; Van der Linde, R., Oxidation of drying oils containing non-conjugated and conjugated double bonds catalyzed by a cobalt catalyst. Progress in organic coatings 2005, 54 (3), 198-204.

19. Lazzari, M.; Chiantore, O., Drying and oxidative degradation of linseed oil. Polymer degradation and stability 1999, 65 (2), 303-313.
20. Frankel, E., Volatile lipid oxidation products. Progress in lipid research 1983, 22 (1), 1-33.
21. Juita; Dlugogorski, B. Z.; Kennedy, E. M.; Mackie, J. C., Low temperature oxidation of linseed oil: a review. Fire science reviews 2012, 1, 1-36.
22. Orlova, Y.; Harmon, R. E.; Broadbelt, L. J.; Iedema, P. D., Review of the kinetics and simulations of linseed oil autoxidation. Progress in Organic Coatings 2021, 151, 106041.


Triglycerides in siccative oil binders
Unsaturated fatty acids
Oleic C18:1
Linoleic C18:2
Linolenic C18:3
Saturated fatty acids
Palmitic C16:0
Stearic C18:0
Arachidic C20:0
Binder
Pigment

Supporting information

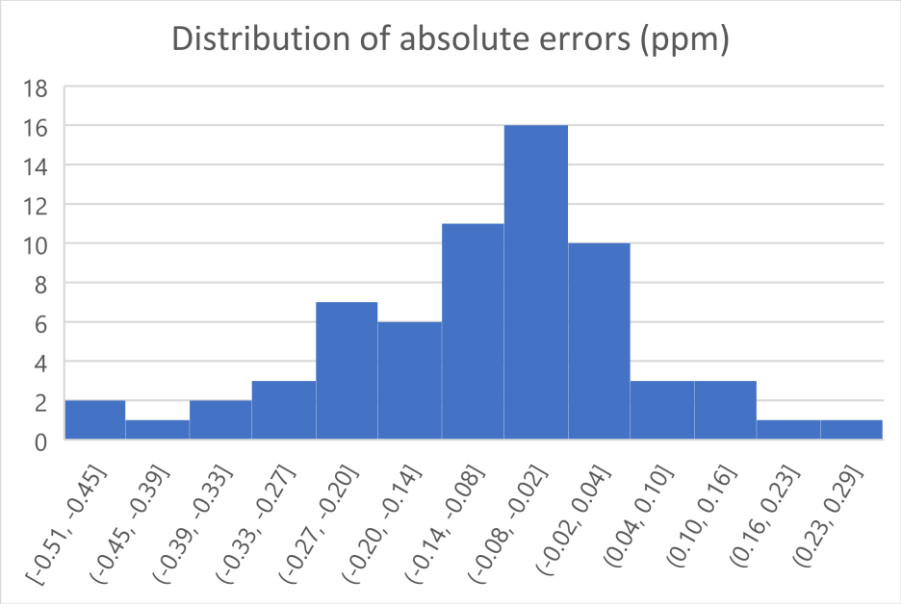


Figure S 1. MALDI FTICR MS absolute errors distribution of the identified peaks of poppy oil polymerized for one week. The errors were distributed around 0.13 ppm.

Table S 1. LC-MS dynamics for the native and polymerized linseed oil for one week at 1 mg/10 mL, petroleum ether fractions. The name of the fatty acids refers to the number of unsaturation. One unsaturation may be either a double bond or for oxygenated compound a carbonyl function. The errors are calculated considering the digits numbers put here.

Theoretical *m/z*	**$[M+H]^+$**	**Attribution**	**Native linseed oil**				**Polymerized linseed oil for 1 week**			
			RT (min)	Intensity	*m/z* exp	error (ppm)	RT (min)	Intensity	*m/z* exp	error (ppm)
296.2948	$C_{19}H_{38}NO$	Palmitic with $N(CH_3)_2$ of 1 DMAPA	16.11	1.96E+03	296.2952	-1.38	16.55	2.15E+06	296.2953	-1.72
320.29472	$C_{21}H_{38}NO$	Linoleic with $N(CH_3)_2$ of 1 DMAPA	15.45	3.89E+06	320.2954	-2.14	16.02	4.75E+05	320.2953	-1.82
322.31044	$C_{21}H_{40}NO$	Oleic with $N(CH_3)_2$ of 1 DMAPA	16.62	4.65E+06	322.3111	-2.04	17.11	3.33E+06	322.3109	-1.42
324.32609	$C_{21}H_{42}NO$	Stearic with $N(CH_3)_2$ of 1 DMAPA	18	8.25E+05	324.3266	-1.57	18.47	1.07E+06	324.3268	-2.19
339.33699	$C_{21}H_{43}N_2O$	Palmitoleic- 1 DMAPA	14.69	1.45E+05	339.3368	0.56	15.26	1.37E+05	339.3371	-0.32
341.3526	$C_{21}H_{45}N_2O$	Palmitic- 1 DMAPA	16.13	1.30E+07	341.3531	-1.46	16.55	1.44E+07	341.3532	-1.76
355.3319	$C_{21}H_{43}N_2O_2$	Palmitoleic- 1 DMAPA- 1 O	10.78	6.79E+03	355.3324	-1.41	10.02	4.29E+04	355.3316	0.84
357.3476	$C_{21}H_{45}N_2O_2$	Palmitic- 1 DMAPA- 1 O	16.32	6.71E+04	357.3471	1.40	16.8	1.01E+05	357.3476	0.00
363.33699	$C_{23}H_{43}N_2O$	Linolenic- 1 DMAPA	14.17	5.22E+07	363.3377	-1.95	14.93	4.99E+06	363.3372	-0.58
365.3526	$C_{23}H_{45}N_2O$	Linoleic- 1 DMAPA	15.46	2.11E+07	365.3532	-1.64	16.02	6.27E+06	365.3531	-1.37
367.3683	$C_{23}H_{47}N_2O$	Oleic- 1 DMAPA	16.62	3.05E+07	367.3689	-1.63	17.14	2.31E+07	367.3689	-1.63
369.3839	$C_{23}H_{49}N_2O$	Stearic – 1 DMAPA	18	1.04E+07	369.3843	-1.08	18.47	1.19E+07	369.3844	-1.35
379.3319	$C_{23}H_{43}N_2O_2$	Linolenic- 1 DMAPA- 1 O	9.94	1.03E+03	379.3327	-2.10	11.23	2.67E+05	379.3322	-0.78
381.3476	$C_{23}H_{45}N_2O_2$	Linoleic- 1 DMAPA- 1 O	10.49	2.18E+06	381.3473	0.79	12.3	1.23E+01	381.3476	0.00

383.3632	$C_{23}H_{47}N_2O_2$	Oleic- 1 DMAPA- 1 O	16.85	1.52E+05	383.3628	1.04	14.02	3.02E+06	383.3634	-0.52
385.37886	$C_{23}H_{49}N_2O_2$	Stearic- 1 DMAPA- 1 O	18.16	4.36E+04	385.3782	1.70	18.62	4.20E+06	369.3842	
395.32682	$C_{23}H_{43}N_2O_3$	Linolenic- 1 DMAPA- 2 O	7.81	4.02E+04	395.3268	0.05	7.34	2.01E+04	395.326	2.07
397.3425	$C_{23}H_{45}N_2O_3$	Linoleic- 1 DMAPA- 2 O	8.09	1.81E+04	397.34119	3.30	9.16	5.24E+04	397.3421	1.01
399.3581	$C_{23}H_{47}N_2O_3$	Oleic- 1 DMAPA- 2 O	17.88	1.28E+04	399.3578	0.75	11.01	3.08E+04	399.3583	-0.50
401.3738	$C_{23}H_{49}N_2O_3$	Stearic- 1 DMAPA-2 O	10.49	8.06E+03	401.3737	0.25	11.32	9.28E+04	401.3736	0.50
411.32173	$C_{23}H_{43}N_2O_4$	Linolenic- 1 DMAPA- 3 O	4.99	1.01E+04	411.3216	0.33	5.26	1.02E+04	411.3213	1.06
413.33738	$C_{23}H_{45}N_2O_4$	Linoleic- 1 DMAPA- 3 O	4.74	1.98E+03	413.3379	-1.25	8.29	7.51E+03	413.3373	0.20
415.35303	$C_{23}H_{47}N_2O_4$	Oleic- 1 DMAPA- 3 O	5.81	2.39E+03	415.3534	-0.88	5.88	1.82E+04	415.3528	0.56
417.36868	$C_{23}H_{49}N_2O_4$	Stearic- 1 DMAPA- 3 O	20.88	4.15E+03	417.3706	-4.59	21.06	3.69E+04	417.3701	-3.39
477.41630	$C_{28}H_{53}N_4O_2$	Linolenic-2 DMAPA	15.33	8.25E+02	477.4158	1.05	6.83	2.29E+03	477.4167	-0.83
479.43195	$C_{28}H_{55}N_4O_2$	Linoleic- 2 DMAPA	0.00	0.00E+00	0.00	0.00	16.1	2.75E+03	479.4317	0.53
481.44760	$C_{28}H_{57}N_4O_2$	Oleic- 2 DMAPA	4.99	5.50E+02	481.4451	5.20	0.00	0.00E+00	0.00	0.00

Table S 2. MALDI FTICR MS relative intensities for the depolymerized native oils, at 1 mg/1 mL, petroleum ether fractions. The name of the fatty acids refers to the number of unsaturation. One unsaturation may be either a double bond or for oxygenated compound a carbonyl function.

Theoretical *m/z*	**$[M+H]^+$**	**Attribution**	**MALDI FTICR MS relative intensity**						
			Linseed stand oil	**Linseed oil**	**Poppy oil**	**Safflower oil**	**Walnut oil**	**Tung oil**	**Castor oil**
296.2948	$C_{19}H_{38}NO$	Palmitic with $N(CH_3)_2$ of 1 DMAPA	2.50E+06	1.30E+07	6.91E+08	1.70E+08	1.85E+08	4.97E+07	4.48E+06
318.2791	$C_{21}H_{36}NO$	Linolenic with $N(CH_3)_2$ of 1 DMAPA	0.00E+00	5.56E+07	4.62E+08	1.51E+07	1.86E+08	5.52E+08	1.26E+06
320.2947	$C_{21}H_{38}NO$	Linoleic with $N(CH_3)_2$ of 1 DMAPA	1.91E+06	1.61E+07	1.10E+11	1.00E+09	1.03E+09	8.28E+07	2.31E+07
322.3104	$C_{21}H_{40}NO$	Oleic with $N(CH_3)_2$ of 1 DMAPA	3.54E+06	2.99E+07	1.29E+10	2.86E+08	2.53E+08	1.02E+08	1.26E+07
324.3261	$C_{21}H_{42}NO$	Stearic with $N(CH_3)_2$ of 1 DMAPA	5.73E+07	7.89E+06	1.39E+09	6.53E+07	5.82E+07	5.05E+07	6.23E+06
339.33699	$C_{21}H_{43}N_2O$	Palmitoleic- 1 DMAPA	1.33E+08	3.72E+07	4.17E+07	1.69E+06	1.16E+06	7.12E+05	6.06E+06
341.3526	$C_{21}H_{45}N_2O$	Palmitic- 1 DMAPA	8.32E+09	9.05E+08	5.65E+07	6.68E+06	6.70E+06	2.35E+06	6.11E+07
355.3319	$C_{21}H_{43}N_2O_2$	Palmitoleic- 1 DMAPA- 1 O	4.25E+06	1.46E+06	0.00E+00	0.00E+00	0.00E+00	7.38E+05	2.56E+05
357.3476	$C_{21}H_{45}N_2O_2$	Palmitic- 1 DMAPA- 1 O	1.94E+08	5.03E+07	0.00E+00	0.00E+00	0.00E+00	0.00E+00	4.94E+05
363.33699	$C_{23}H_{43}N_2O$	Linolenic- 1 DMAPA	1.37E+10	3.70E+09	4.98E+08	7.25E+06	1.70E+07	2.01E+07	9.18E+07
365.3526	$C_{23}H_{45}N_2O$	Linoleic- 1 DMAPA	7.33E+09	1.09E+09	7.67E+08	4.88E+07	4.46E+07	5.48E+06	1.54E+08
367.3683	$C_{23}H_{47}N_2O$	Oleic- 1 DMAPA	1.37E+10	1.98E+09	3.33E+08	1.61E+07	1.10E+07	7.09E+06	1.27E+08
369.3839	$C_{23}H_{49}N_2O$	Stearic – 1 DMAPA	1.23E+10	6.91E+08	6.50E+07	4.74E+06	3.66E+06	3.38E+06	9.40E+07
379.3319	$C_{23}H_{43}N_2O_2$	Linolenic- 1 DMAPA- 1 O	2.79E+08	3.38E+08	1.26E+07	0.00E+00	1.04E+06	3.21E+06	3.40E+07
381.3476	$C_{23}H_{45}N_2O_2$	Linoleic- 1 DMAPA- 1 O	1.86E+08	1.19E+08	0.00E+00	1.70E+06	1.20E+06	7.63E+05	1.43E+08

383.3632	$C_{23}H_{47}N_2O_2$	Oleic- 1 DMAPA- 1 O	2.63E+08	1.83E+08	0.00E+00	0.00E+00	0.00E+00	1.20E+06	1.80E+08
385.3789	$C_{23}H_{49}N_2O_2$	Stearic- 1 DMAPA- 1 O	2.09E+08	5.05E+07	1.20E+07	2.46E+06	2.47E+06	0.00E+00	2.02E+06
395.3268	$C_{23}H_{43}N_2O_3$	Linolenic- 1 DMAPA- 2 O	8.65E+07	1.12E+08	0.00E+00	0.00E+00	0.00E+00	3.53E+06	1.29E+07
397.3425	$C_{23}H_{45}N_2O_3$	Linoleic- 1 DMAPA- 2 O	7.20E+07	5.42E+07	0.00E+00	1.92E+06	1.66E+06	0.00E+00	5.54E+07
399.3581	$C_{23}H_{47}N_2O_3$	Oleic- 1 DMAPA- 2 O	3.42E+07	2.05E+07	0.00E+00	0.00E+00	0.00E+00	0.00E+00	3.19E+07
401.3738	$C_{23}H_{49}N_2O_3$	Stearic- 1 DMAPA-2 O	2.64E+06	0.00E+00	0.00E+00	8.92E+05	1.18E+06	0.00E+00	1.88E+06
411.3217	$C_{23}H_{43}N_2O_4$	Linolenic- 1 DMAPA- 3 O	1.11E+08	6.21E+07	0.00E+00	0.00E+00	8.89E+05	3.65E+06	8.80E+06
413.3374	$C_{23}H_{45}N_2O_4$	Linoleic- 1 DMAPA- 3 O	3.55E+07	1.61E+07	7.56E+08	5.10E+06	3.59E+06	0.00E+00	4.06E+07
415.3530	$C_{23}H_{47}N_2O_4$	Oleic- 1 DMAPA- 3 O	2.21E+07	2.56E+06	5.17E+07	1.03E+06	0.00E+00	0.00E+00	3.16E+07
425.4465	$C_{27}H_{57}N_2O$	Behenic- 1DMAPA	0.00E+00	0.00E+00	0.00E+00	0.00E+00	0.00E+00	0.00E+00	5.35E+05
427.3167	$C_{23}H_{43}N_2O_5$	-	3.67E+08	4.31E+07	0.00E+00	0.00E+00	0.00E+00	0.00E+00	1.24E+06
417.3687	$C_{23}H_{49}N_2O_4$	Stearic- 1 DMAPA- 3 O	3.32E+07	1.44E+08	0.00E+00	0.00E+00	0.00E+00	0.00E+00	8.75E+06
477.4163	$C_{28}H_{53}N_4O_2$	Linolenic-2 DMAPA	1.09E+07	1.11E+06	0.00E+00	0.00E+00	0.00E+00	8.41E+05	0.00E+00
479.43195	$C_{28}H_{55}N_4O_2$	Linoleic- 2 DMAPA	1.81E+07	0.00E+00	0.00E+00	0.00E+00	0.00E+00	0.00E+00	2.97E+05
481.4476	$C_{28}H_{57}N_4O_2$	Oleic- 2 DMAPA	1.79E+07	0.00E+00	0.00E+00	0.00E+00	0.00E+00	0.00E+00	0.00E+00
641.5616	$C_{41}H_{73}N_2O_3$	C36:6- 1 DMAPA-2 O	6.26E+08	8.32E+06	0.00E+00	0.00E+00	0.00E+00	0.00E+00	0.00E+00
643.5772	$C_{41}H_{75}N_2O_3$	C36:5- 1 DMAPA-2 O	3.37E+08	4.62E+06	0.00E+00	0.00E+00	0.00E+00	0.00E+00	3.05E+05
645.5929	$C_{41}H_{77}N_2O_3$	C36:4- 1 DMAPA-2 O	9.56E+07	3.28E+06	0.00E+00	0.00E+00	0.00E+00	0.00E+00	1.30E+06
671.5721	$C_{42}H_{75}N_2O_4$	C37:6- 1 DMAPA-3 O	0.00E+00	4.94E+07	0.00E+00	0.00E+00	0.00E+00	7.52E+05	0.00E+00
725.6667	$C_{46}H_{85}N_4O_2$	Linolenic, linoleic C-C dimer– 2 DMAPA	9.43E+09	1.28E+07	0.00E+00	0.00E+00	0.00E+00	0.00E+00	0.00E+00
727.6823	$C_{46}H_{87}N_4O_2$	Linoleic C-C dimer– 2 DMAPA	4.48E+09	3.82E+06	0.00E+00	0.00E+00	0.00E+00	0.00E+00	2.41E+05
729.6981	$C_{46}H_{89}N_4O_2$	Linoleic, oleic C-C dimer– 2 DMAPA	9.02E+08	9.88E+05	0.00E+00	0.00E+00	0.00E+00	0.00E+00	2.03E+05
741.6616	$C_{46}H_{85}N_4O_3$	Linolenic, linoleic C-O dimer– 2 DMAPA	3.52E+08	3.01E+07	0.00E+00	0.00E+00	7.84E+05	0.00E+00	0.00E+00
743.6773	$C_{46}H_{87}N_4O_3$	Linoleic C-O dimer– 2 DMAPA	1.71E+08	1.32E+07	0.00E+00	0.00E+00	0.00E+00	0.00E+00	7.39E+05
745.6934	$C_{46}H_{89}N_4O_3$	Linoleic, oleic C-O dimer– 2 DMAPA	4.57E+07	1.64E+07	0.00E+00	0.00E+00	0.00E+00	0.00E+00	1.32E+06
757.6565	$C_{46}H_{85}N_4O_4$	Linolenic, linoleic dimer +2O– 2 DMAPA	6.17E+07	1.23E+07	0.00E+00	0.00E+00	0.00E+00	0.00E+00	3.46E+05
759.6722	$C_{46}H_{87}N_4O_4$	Linoleic dimer +2O– 2 DMAPA	3.29E+07	7.68E+06	0.00E+00	0.00E+00	0.00E+00	8.15E+05	1.27E+06
761.6875	$C_{46}H_{89}N_4O_4$	Linoleic, oleic dimer +2O– 2 DMAPA	9.93E+06	4.97E+06	0.00E+00	0.00E+00	0.00E+00	0.00E+00	3.22E+06
773.6515	$C_{46}H_{85}N_4O_5$	Linolenic, linoleic dimer +3O– 2 DMAPA	4.32E+07	9.91E+06	0.00E+00	0.00E+00	0.00E+00	0.00E+00	7.72E+05
775.6617	$C_{46}H_{87}N_4O_5$	Linoleic dimer +3O– 2 DMAPA	3.92E+06	9.87E+05	1.49E+07	0.00E+00	0.00E+00	0.00E+00	3.19E+06
777.6828	$C_{46}H_{89}N_4O_5$	Linoleic, oleic dimer +3O– 2 DMAPA	4.10E+06	3.94E+06	0.00E+00	0.00E+00	0.00E+00	0.00E+00	2.55E+06

789.6464	$C_{46}H_{85}N_4O_6$	Linolenic, linoleic dimer +4O– 2 DMAPA	7.84E+06	5.02E+06	0.00E+00	0.00E+00	0.00E+00	0.00E+00	9.57E+05
791.6621	$C_{46}H_{87}N_4O_6$	Linoleic dimer +4O– 2 DMAPA	5.27E+06	2.35E+06	0.00E+00	0.00E+00	1.03E+06	0.00E+00	2.86E+06
793.6776	$C_{46}H_{89}N_4O_6$	Linoleic, oleic dimer +4O– 2 DMAPA	0.00E+00	2.03E+06	0.00E+00	0.00E+00	0.00E+00	0.00E+00	3.03E+06
805.6413	$C_{46}H_{85}N_4O_7$	Linolenic, linoleic dimer +5O– 2 DMAPA	2.87E+06	3.18E+06	0.00E+00	0.00E+00	0.00E+00	0.00E+00	9.08E+05
807.65693	$C_{46}H_{87}N_4O_7$	Linoleic dimer +5O– 2 DMAPA	0.00E+00	1.39E+06	0.00E+00	0.00E+00	0.00E+00	0.00E+00	2.49E+06
809.6727	$C_{46}H_{89}N_4O_7$	Linoleic, oleic dimer +5O– 2 DMAPA	0.00E+00	0.00E+00	0.00E+00	0.00E+00	0.00E+00	0.00E+00	2.22E+06
821.6362	$C_{46}H_{85}N_4O_8$	Linolenic, linoleic dimer +6O– 2 DMAPA	1.71E+06	2.49E+06	0.00E+00	0.00E+00	7.95E+05	0.00E+00	5.57E+05
823.6518	$C_{46}H_{87}N_4O_8$	Linoleic dimer +6O– 2 DMAPA	0.00E+00	1.17E+06	0.00E+00	0.00E+00	0.00E+00	0.00E+00	1.32E+06
825.6677	$C_{46}H_{89}N_4O_8$	Linoleic, oleic dimer +6O– 2 DMAPA	0.00E+00	0.00E+00	0.00E+00	0.00E+00	0.00E+00	0.00E+00	4.82E+06
837.6311	$C_{46}H_{85}N_4O_9$	Linolenic, linoleic dimer +7O– 2 DMAPA	0.00E+00	1.82E+06	0.00E+00	0.00E+00	0.00E+00	0.00E+00	0.00E+00
839.6468	$C_{46}H_{87}N_4O_9$	Linoleic dimer +7O– 2 DMAPA	0.00E+00	9.21E+05	0.00E+00	8.59E+05	0.00E+00	0.00E+00	8.67E+05
841.6624	$C_{46}H_{89}N_4O_9$	Linoleic, oleic dimer +7O– 2 DMAPA	0.00E+00	0.00E+00	0.00E+00	0.00E+00	0.00E+00	0.00E+00	0.00E+00

Table S 3. MALDI FTICR MS relative intensities for the depolymerized oil films after ageing, at 1/1000 (mg/µL), petroleum ether fractions. The name of the fatty acid refers to the number of unsaturation. One unsaturation may be either a double bond or for oxygenated compound a carbonyl function.

Theoretical *m/z*	$[M+H]^+$	Attribution	MALDI FTICR MS relative intensity			
			Linseed oil 1week	Linseed oil 1 week + heating 1week at 80 °C	Linseed oil Irradiated at 395 nm for 44 days	Poppy oil 1 week
296.2948	$C_{19}H_{38}NO$	Palmitic with $N(CH_3)_2$ of 1 DMAPA	5.40E+06	8.43E+06	3.39E+07	2.45E+08
318.2791	$C_{21}H_{36}NO$	Linolenic with $N(CH_3)_2$ of 1 DMAPA	1.66E+06	0.00E+00	3.25E+06	2.04E+07
320.2947	$C_{21}H_{38}NO$	Linoleic with $N(CH_3)_2$ of 1 DMAPA	2.95E+06	1.47E+06	2.61E+06	1.45E+09
322.3104	$C_{21}H_{40}NO$	Oleic with $N(CH_3)_2$ of 1 DMAPA	8.03E+06	2.97E+06	1.65E+07	6.03E+08
324.3261	$C_{21}H_{42}NO$	Stearic with $N(CH_3)_2$ of 1 DMAPA	4.46E+06	4.97E+06	2.35E+07	1.23E+08
339.33699	$C_{21}H_{43}N_2O$	Palmitoleic- 1 DMAPA	2.94E+06	5.54E+06	1.41E+08	1.83E+06
341.3526	$C_{21}H_{45}N_2O$	Palmitic- 1 DMAPA	1.72E+08	8.24E+07	2.32E+09	1.35E+06
355.3319	$C_{21}H_{43}N_2O_2$	Palmitoleic- 1 DMAPA- 1 O	2.23E+06	2.15E+07	1.15E+08	0.00E+00
357.3476	$C_{21}H_{45}N_2O_2$	Palmitic- 1 DMAPA- 1 O	6.06E+06	1.19E+07	1.44E+08	0.00E+00
363.33699	$C_{23}H_{43}N_2O$	Linolenic- 1 DMAPA	4.12E+07	1.88E+06	5.35E+07	1.87E+07
365.3526	$C_{23}H_{45}N_2O$	Linoleic- 1 DMAPA	4.88E+07	2.05E+07	1.20E+08	1.62E+07
367.3683	$C_{23}H_{47}N_2O$	Oleic- 1 DMAPA	6.26E+06	3.17E+07	1.24E+09	6.80E+06
369.3839	$C_{23}H_{49}N_2O$	Stearic – 1 DMAPA	7.26E+07	2.77E+07	2.07E+09	1.91E+06
379.3319	$C_{23}H_{43}N_2O_2$	Linolenic- 1 DMAPA- 1 O	1.41E+07	1.22E+07	2.57E+07	0.00E+00
381.3476	$C_{23}H_{45}N_2O_2$	Linoleic- 1 DMAPA- 1 O	3.00E+07	5.65E+07	7.64E+07	0.00E+00
383.3632	$C_{23}H_{47}N_2O_2$	Oleic- 1 DMAPA- 1 O	1.01E+08	6.67E+07	6.52E+08	0.00E+00
385.3789	$C_{23}H_{49}N_2O_2$	Stearic- 1 DMAPA- 1 O	4.38E+06	1.24E+07	6.34E+07	3.14E+06
395.3268	$C_{23}H_{43}N_2O_3$	Linolenic- 1 DMAPA- 2 O	4.41E+06	4.19E+06	1.22E+07	0.00E+00
397.3425	$C_{23}H_{45}N_2O_3$	Linoleic- 1 DMAPA- 2 O	1.08E+07	3.93E+07	9.66E+07	0.00E+00
399.3581	$C_{23}H_{47}N_2O_3$	Oleic- 1 DMAPA- 2 O	1.75E+07	2.82E+07	1.01E+08	0.00E+00
401.3738	$C_{23}H_{49}N_2O_3$	Stearic- 1 DMAPA-2 O	3.78E+06	1.75E+07	2.46E+07	1.08E+06
411.3217	$C_{23}H_{43}N_2O_4$	Linolenic- 1 DMAPA- 3 O	3.22E+06	1.12E+06	2.72E+06	0.00E+00
413.3374	$C_{23}H_{45}N_2O_4$	Linoleic- 1 DMAPA- 3 O	5.35E+06	6.38E+06	1.58E+07	4.02E+06
415.3530	$C_{23}H_{47}N_2O_4$	Oleic- 1 DMAPA- 3 O	3.07E+06	1.72E+06	5.88E+06	0.00E+00
425.4465	$C_{27}H_{57}N_2O$	Behenic-1DMAPA	0.00E+00	1.31E+06	2.71E+06	0.00E+00
427.3167	$C_{23}H_{43}N_2O_5$	-	4.21E+05	1.72E+07	6.16E+07	0.00E+00
417.3689	$C_{23}H_{49}N_2O_4$	Stearic- 1 DMAPA- 3 O	1.98E+06	0.00E+00	1.42E+06	0.00E+00
477.4163	$C_{28}H_{53}N_4O_2$	Linolenic-2 DMAPA	4.51E+06	4.52E+06	1.33E+07	0.00E+00

479.43195	$C_{28}H_{55}N_4O_2$	Linoleic- 2 DMAPA	2.79E+06	6.85E+06	9.07E+06	0.00E+00
481.4476	$C_{28}H_{57}N_4O_2$	Oleic- 2 DMAPA	1.02E+06	2.52E+06	1.04E+07	0.00E+00
641.5616	$C_{41}H_{73}N_2O_3$	C36:6- 1 DMAPA-2 O	0.00E+00	0.00E+00	0.00E+00	0.00E+00
643.5772	$C_{41}H_{75}N_2O_3$	C36:5- 1 DMAPA-2 O	0.00E+00	0.00E+00	0.00E+00	0.00E+00
645.5929	$C_{41}H_{77}N_2O_3$	C36:4- 1 DMAPA-2 O	0.00E+00	0.00E+00	0.00E+00	0.00E+00
671.5721	$C_{42}H_{75}N_2O_4$	C37:6- 1 DMAPA-3 O	0.00E+00	0.00E+00	9.81E+05	9.39E+05
725.6667	$C_{46}H_{85}N_4O_2$	Linolenic, linoleic C-C dimer– 2 DMAPA	3.79E+05	0.00E+00	2.70E+06	9.20E+05
727.6823	$C_{46}H_{87}N_4O_2$	Linoleic C-C dimer– 2 DMAPA	3.90E+05	5.68E+05	2.33E+06	0.00E+00
729.6981	$C_{46}H_{89}N_4O_2$	Linoleic, oleic C-C dimer– 2 DMAPA	0.00E+00	0.00E+00	1.30E+06	0.00E+00
741.6616	$C_{46}H_{85}N_4O_3$	Linolenic, linoleic C-O dimer– 2 DMAPA	0.00E+00	0.00E+00	1.86E+06	0.00E+00
743.6773	$C_{46}H_{87}N_4O_3$	Linoleic C-O dimer– 2 DMAPA	4.02E+05	8.38E+05	1.75E+06	0.00E+00
745.6934	$C_{46}H_{89}N_4O_3$	Linoleic, oleic C-O dimer– 2 DMAPA	5.95E+05	0.00E+00	9.72E+05	0.00E+00
757.6565	$C_{46}H_{85}N_4O_4$	Linolenic, linoleic dimer +2O– 2 DMAPA	4.25E+05	7.42E+05	1.18E+06	0.00E+00
759.6722	$C_{46}H_{87}N_4O_4$	Linoleic dimer +2O– 2 DMAPA	7.53E+05	6.24E+05	1.50E+06	0.00E+00
761.6875	$C_{46}H_{89}N_4O_4$	Linoleic, oleic dimer +2O– 2 DMAPA	5.94E+05	0.00E+00	1.25E+06	0.00E+00
773.6515	$C_{46}H_{85}N_4O_5$	Linolenic, linoleic dimer +3O– 2 DMAPA	4.65E+05	0.00E+00	3.30E+06	0.00E+00
775.6617	$C_{46}H_{87}N_4O_5$	Linoleic dimer +3O– 2 DMAPA	4.72E+05	0.00E+00	1.13E+06	1.47E+06
777.6828	$C_{46}H_{89}N_4O_5$	Linoleic, oleic dimer +3O– 2 DMAPA	9.59E+05	7.09E+05	6.88E+06	0.00E+00
789.6464	$C_{46}H_{85}N_4O_6$	Linolenic, linoleic dimer +4O– 2 DMAPA	0.00E+00	6.20E+05	1.69E+06	0.00E+00
791.6621	$C_{46}H_{87}N_4O_6$	Linoleic dimer +4O– 2 DMAPA	6.21E+05	0.00E+00	3.39E+06	0.00E+00
793.6776	$C_{46}H_{89}N_4O_6$	Linoleic, oleic dimer +4O– 2 DMAPA	5.81E+05	0.00E+00	1.31E+06	0.00E+00
805.6413	$C_{46}H_{85}N_4O_7$	Linolenic, linoleic dimer +5O– 2 DMAPA	0.00E+00	0.00E+00	0.00E+00	0.00E+00
807.65693	$C_{46}H_{87}N_4O_7$	Linoleic dimer +5O– 2 DMAPA	0.00E+00	0.00E+00	8.36E+05	0.00E+00
809.6727	$C_{46}H_{89}N_4O_7$	Linoleic, oleic dimer +5O– 2 DMAPA	5.49E+05	0.00E+00	7.86E+05	0.00E+00
821.6362	$C_{46}H_{85}N_4O_8$	Linolenic, linoleic dimer +6O– 2 DMAPA	0.00E+00	6.01E+05	0.00E+00	0.00E+00
823.6518	$C_{46}H_{87}N_4O_8$	Linoleic dimer +6O– 2 DMAPA	0.00E+00	0.00E+00	0.00E+00	7.81E+05
825.6677	$C_{46}H_{89}N_4O_8$	Linoleic, oleic dimer +6O– 2 DMAPA	0.00E+00	0.00E+00	0.00E+00	0.00E+00
837.6311	$C_{46}H_{85}N_4O_9$	Linolenic, linoleic dimer +7O– 2 DMAPA	0.00E+00	5.58E+05	0.00E+00	0.00E+00
839.6468	$C_{46}H_{87}N_4O_9$	Linoleic dimer +7O– 2 DMAPA	0.00E+00	6.47E+05	0.00E+00	0.00E+00
841.6624	$C_{46}H_{89}N_4O_9$	Linoleic, oleic dimer +7O– 2 DMAPA	0.00E+00	0.00E+00	0.00E+00	0.00E+00

Table S 4. The unique MALDI FTICR MS peaks found after heating of linseed oil at 80 °C with their corresponding relative abundances in petroleum ether and ethyl acetate fractions (additional peaks not found after natural polymerization of 1 week).
%: In comparison to the minor composition presented by the peaks in this table.

Theoretical *m/z* $[M+H]^+$	**Formula $[M+H]^+$**	**Attribution**	**Relative abundance of the heated linseed oil at 80° C (%)**	
			Petroleum ether fraction	**Ethyl acetate fraction**
407.3381	$C_{23}H_{43}N_4O_2$	Trideca-2,4,6-trienoic-2 DMAPA	0.55	3.02
417.3687	$C_{23}H_{49}N_2O_4$	Stearic- 1 DMAPA- 3 O	0.99	0.62
421.3537	$C_{24}H_{45}N_4O_2$	5,8,11-Tetradecatrienoic- 2 DMAPA	1.15	0.38
425.3738	$C_{25}H_{49}N_2O_3$	Eicosadienoic- 1 DMAPA- 2O	1.75	1.47
431.3632	$C_{27}H_{47}N_2O_2$	Docosapentaenoic- 1 DMAPA- 1 O	5.26	1.47
433.3901	$C_{26}H_{49}N_4O$	6,9,12-Hexadecatrienoic aldehyde- 2 DMAPA	2.25	0.75
445.3901	$C_{27}H_{49}N_4O$	Heptadecadien-8-ynoic aldehyde- 2 DMAPA	0.76	0.66
449.3374	$C_{26}H_{45}N_2O_4$	Heneicosapentaenoic- 1 DMAPA- 3 O	0.84	2.31
451.3530	$C_{26}H_{47}N_2O_4$	Methyl arachidonate- 1 DMAPA- 3 O	0.80	0.60
455.3843	$C_{26}H_{51}N_2O_4$	Heneicosadienoic- 1 DMAPA- 3 O	0.60	0.62
463.4007	$C_{27}H_{51}N_4O_2$	$C_{17}H_{28}O_2$- 2 DMAPA	1.13	0.33
463.3530	$C_{27}H_{47}N_2O_4$	Docosapentaenoic- 2 DMAPA- 3 O	1.05	1.18
465.4527	$C_{28}H_{57}N_4O$	Oleic aldehyde- 2 DMAPA	1.21	0.59
467.34795	$C_{26}H_{47}N_2O_5$	Methyl arachidonate- 1 DMAPA- 4 O	1.30	0.52
467.43195	$C_{27}H_{55}N_4O_2$	Heptadecenoic- 2 DMAPA	0.67	0.46
471.3694	$C_{28}H_{47}N_4O_2$	Octadecadiene-9,11-diynoic- 2 DMAPA	0.63	0.55
473.3850	$C_{28}H_{49}N_4O_2$	Isanic- 2 DMAPA	0.92	3.86
475.4370	$C_{29}H_{55}N_4O$	Isanic aldehyde- 2 DMAPA	3.77	0.59
479.3845	$C_{28}H_{51}N_2O_4$	Tricosadiynoic- 1 DMAPA- 3 O	0.41	1.10
481.4476	$C_{28}H_{57}N_4O_2$	Oleic- 2 DMAPA	1.90	0.00
487.4370	$C_{30}H_{55}N_4O$	Arachidonic aldehyde- 2 DMAPA	1.21	0.45
489.4163	$C_{29}H_{53}N_4O_2$	10,13-Nonadecadiynoic-2 DMAPA	0.78	1.61
489.4527	$C_{30}H_{57}N_4O$	Eicosatrienoic aldehyde– 2DMAPA	2.42	4.81
491.3843	$C_{29}H_{51}N_2O_4$	Tetracosapentaenoic-1 DMAPA- 3 O	0.53	0.72
491.43195	$C_{29}H_{55}N_4O_2$	Methyl linolenate- 2 DMAPA	0.94	0.37
497.4061	$C_{27}H_{53}N_4O_4$	Heptadecadienoic-2 DMAPA- 2 O	0.46	0.89

505.4476	$C_{30}H_{57}N_4O_2$	Eicosatrienoic– 2DMAPA	3.52	0.40
507.4269	$C_{29}H_{55}N_4O_3$	Isanic- 2 DMAPA- 1 O	1.08	2.09
507.4633	$C_{30}H_{59}N_4O_2$	Possible dimer with degraded fatty acids chain- 2 DMAPA	11.49	0.48
509.4425	$C_{29}H_{57}N_4O_3$	Methyl linoleate- 2 DMAPA- 1 O	0.78	0.36
511.4582	$C_{29}H_{59}N_4O_3$	Methyl oleate- 2 DMAPA- 1 O	0.68	0.34
513.4163	$C_{31}H_{53}N_4O_2$	Cannabidiol- 2 DMAPA	0.55	0.65
515.43195	$C_{31}H_{55}N_4O_2$	Heneicosapentaenoic- 2 DMAPA	0.65	0.76
515.4683	$C_{32}H_{59}N_4O$	Docosatetraenoic aldehyde- 2 DMAPA	0.78	1.52
517.4476	$C_{31}H_{57}N_4O_2$	Methyl arachidonate- 2 DMAPA	1.32	0.80
519.4269	$C_{30}H_{55}N_4O_3$	Arachidonic- 2 DMAPA- 1 O	0.91	2.05
519.4633	$C_{31}H_{59}N_4O_2$	Methyl 11,14,17-eicosatrienoate- 2 DMAPA	2.61	0.51
521.4789	$C_{31}H_{61}N_4O_2$	Heneicosadienoic- 2 DMAPA	3.33	0.36
523.4218	$C_{29}H_{55}N_4O_4$	Isanic- 2 DMAPA- 2 O	1.12	0.78
523.4582	$C_{30}H_{59}N_4O_3$	Eicosadienoic- 2 DMAPA- 1 O	1.35	0.75
525.4374	$C_{29}H_{57}N_4O_4$	Methyl linoleate- 2 DMAPA- 2 O	0.48	0.37
525.4738	$C_{30}H_{61}N_4O_3$	Paullinic- 2 DMAPA- 1 O	1.66	4.71
529.4687	$C_{29}H_{61}N_4O_4$	Methyl stearate- 2 DMAPA- 2 O	3.93	0.43
531.4633	$C_{32}H_{59}N_4O_2$	Docosatetraenoic- 2 DMAPA	1.33	0.72
533.4789	$C_{32}H_{61}N_4O_2$	Docosatrienoic- 2 DMAPA	2.49	0.43
537.4374	$C_{30}H_{57}N_4O_4$	Eicosatrienoic– 2DMAPA- 2 O	1.07	0.45
545.4789	$C_{33}H_{61}N_4O_2$	Tricosadiynoic– 2DMAPA	1.02	0.75
551.4531	$C_{31}H_{59}N_4O_4$	Methyl 11,14,17-eicosatrienoate- 2 DMAPA- 2 O	1.63	1.02
565.4687	$C_{32}H_{61}N_4O_4$	Docosatrienoic- 2 DMAPA- 2 O	1.02	5.08
567.4844	$C_{32}H_{63}N_4O_4$	Docosadienoic- 2 DMAPA- 2 O	0.87	0.44
579.4844	$C_{33}H_{63}N_4O_4$	C23:3- 2 DMAPA- 2 O	0.57	0.54
595.5157	$C_{34}H_{67}N_4O_4$	5,9-tetracosadienoic- 2 DMAPA- 2 O	0.70	0.91
597.5313	$C_{34}H_{69}N_4O_4$	Nervonic- 2 DMAPA- 2 O	0.70	1.80
611.5469	$C_{35}H_{71}N_4O_4$	Pentacosenoic- 2 DMAPA- 2 O	0.72	3.59
637.5626	$C_{38}H_{73}N_4O_4$	Tetramethyltetracosatrienoic- 2 DMAPA- 2 O	4.98	1.98
639.5783	$C_{37}H_{75}N_4O_4$	Heptacosenoic acid- 2 DMAPA- 2 O	3.32	4.18
653.5576	$C_{37}H_{73}N_4O_5$	Compound-2 DMAPA- 3 O	1.32	14.37
655.5732	$C_{37}H_{75}N_4O_5$	Heptacosenoic acid- 2 DMAPA- 3 O	2.62	1.04

665.5939	$C_{39}H_{77}N_4O_4$	27-Methyl-5,9-octacosadienoic- 2 DMAPA- 2 O	0.84	3.96
671.5681	$C_{37}H_{75}N_4O_6$	Heptacosenoic acid- 2 DMAPA- 4 O	0.49	3.49
691.5732	$C_{40}H_{75}N_4O_5$	Possible dimer- 2 DMAPA- 3 O	0.68	7.22
701.6416	$C_{42}H_{81}N_6O_2$	$C_{22}H_{48}O_2$- 3 DMAPA	2.61	0.79
709.5838	$C_{40}H_{77}N_4O_6$	Lauryl linolenate- 2 DMAPA- 4 O	0.48	0.00

Chapter 9: Driers & pigments effect on siccativation

Introduction

Driers and pigments play crucial roles in the formulation of paints, coatings, and other materials, influencing their aesthetic properties and performance. Driers, also known as drying agents, are compounds that accelerate the curing process of coatings by promoting the oxidation and polymerization of binders, such as oils or resins (alkyd resins).

Common driers include metal salts like cobalt, manganese, and iron. They catalyze the siccativation or chemical drying reaction after the physical drying process done by solvent evaporation. On the other hand, pigments are finely ground substances that impart color, opacity, and additional physical properties to materials.

They can be organic or inorganic in nature. Indeed, inorganic pigments such as titanium dioxide can provide whiteness and opacity, while organic pigments offer a wide range of vibrant colors.

Understanding the chemistry behind these components that may affect siccativation mechanism is essential for developing high-performance coatings and assesing the drying speed of the final 3D-siccativated oil paints' films.

The aim of the work here is to respond to these open questions:

- Can the driers and pigments affect the formation of the 3-D crosslinked oil film?
- If yes, how they can interact with binders and at which step during siccativation mechanism?
- Are there any structural differences after formulating oil binders directly with metal driers in comparison to their formulation with pigments?
- And, do contemporary oil paint tubes present any additional difference?
- What is the signature of oil paint formulations after ageing?
- Can our new methodology be sensitive to analyse museum size oil paintings?

Article 6

Oil artists' paints structural deciphering & study of the parameters affecting oil polymerization mechanisms including transition metal driers and pigments for better conservation of artistic works in museums

ABSTRACT: Oil paintings are invaluable cultural heritage objects which can be preserved for centuries. Oil paints are formed mainly of inorganic transition metal driers as pigments and siccative vegetable siccative oil(s) as binder; the most common historical binders are linseed, poppy and walnut oils. The drying process of these binders in the presence of light and oxygen which called siccativation is a very complex reaction still under investigation. It may depend on many parameters during all the lifetime of the polymeric film such as the drying oil type, the unsaturation ratio, the ageing rate and the metal transitions used as driers or pigments. The aim of this study is to assess the siccativation mechanism of oil films, first by the study of different mock-up samples of linseed oil binder formulated with transition metal driers and artistic pigments, by varying the metal drier ratio and the drier type for short and long-term polymerization. Secondly, oil paint tubes were studied directly and after polymerization for a specific period and finally oil artist's paintings have been analyzed. For this aim, our recently developed innovative methodology was used after certain optimization. Oil paints were transamidated with 3-(dimethylamino)-1-propylamine (DMAPA) then the obtained products were analyzed by the advanced mass spectrometry techniques MALDI FTICR MS and LC-MS. The mass spectrometry spectra showed the traces of the remaining polyunsaturated fatty acids and the presence of dimers linked by C-C or C-O bonds in addition to their oxygenated species. The distribution of these products in the 3D-crosslinked network was found to be very dependent not only on the siccative oil but also on the pigment. This methodology was scaled down to the analysis of tenths of micrograms of samples and applied to museum-size paintings from XXth century.

Keywords: Oil paints, fatty acids, siccativation/polymerization, linseed oil, ageing, metal driers, inorganic pigments, depolymerization, transamidation, MALDI FTICR MS, ESI LC-Orbitrap-MS.

Oil paints are typically composed of two major phases: Organic such as siccative oil binders, adhesives and varnishes, and inorganic such as pigments. Pigments can be also organic such as azo compounds.[1-2]

Metal driers are found in artworks since the Renaissance but they were widely used since the 19th century to accelerate the oil film drying rate.[3] There are different types of driers: Primary, secondary and auxiliary driers.[4] In historical paints, the driers were lead salts or the pigments their selves.[5-7] In addition, cobalt(II) 2-ethylhexanoate (2-ethyl-hexanoic acid, cobalt(2+) salt (2:1)) was the historically well-known powerful drier used in artworks.[8] Other metal driers have been also described such as the cobalt(II) acetylacetonate (2,4-pentanedione cobalt(II) derivative), manganese(II) 2-ethylhexanoate (2-ethyl-hexanoic acid, manganese(2+) salt (2:1)), manganese(III) acetylacetonate (2,4-pentanedione manganese(III) derivative) [$Mn(acac)_3$], manganese(II) carboxylates treated with various *N*,*N*-chelating ligands, iron(III) 2-ethylhexanoate, Iron(II) complexes bearing polydentate ligands of 5 nitrogen donors, benzoylferrocene, oxovanadium(IV) acetylacetonate, and oxovanadium(IV) acetylacetonate modified with ligands.[9]

Transition metals contained in pigments or added driers are catalyzing the formation of the crosslinked oil film during siccativation mechanism that affords in its early stages hydroperoxides.[10] Indeed, metal driers speed up the decomposition of the formed hydroperoxides and initiate autoxidation. They react directly in a Fenton redox reaction with hydroperoxides yielding after hydrogen abstraction carbon and oxygen centered radicals propagating and forming the high molecular weight crosslinked polymeric film.[10-15]

Polymerization extent and rate are affected by the presence of (poly)unsaturated fatty acids, oxygen concentration, light, temperature,[10] humidity, metals (transition metals from pigments), and other additives in paint formulations. Siccativation mechanism depends also on thermal treatment of vegetable oils during their industrial production or through any heating source. Heating-induced reactions, which are anaerobic, involve *cis-trans* isomerization of fatty acids, naturally found in their *cis* configuration, cyclization reactions, affording for example Diels-Alder products, and the hydrolysis of triglyceride molecules.[16]

This siccativation mechanism is a very complex mechanism which is still debated. This study will focus on the effect of metal driers and pigments on the formation of the final oil film by testing several oil paint tubes and mock-up oil paints' samples formulated with various transition metal driers and artistic pigments for different polymerization rate and time. For this aim, the crosslinked films will be studied after depolymerization at room temperature by transamidation with 3-(dimethylamino)-1-propylamine (DMAPA) and the products will be analyzed by ultra-high resolution mass spectrometry.

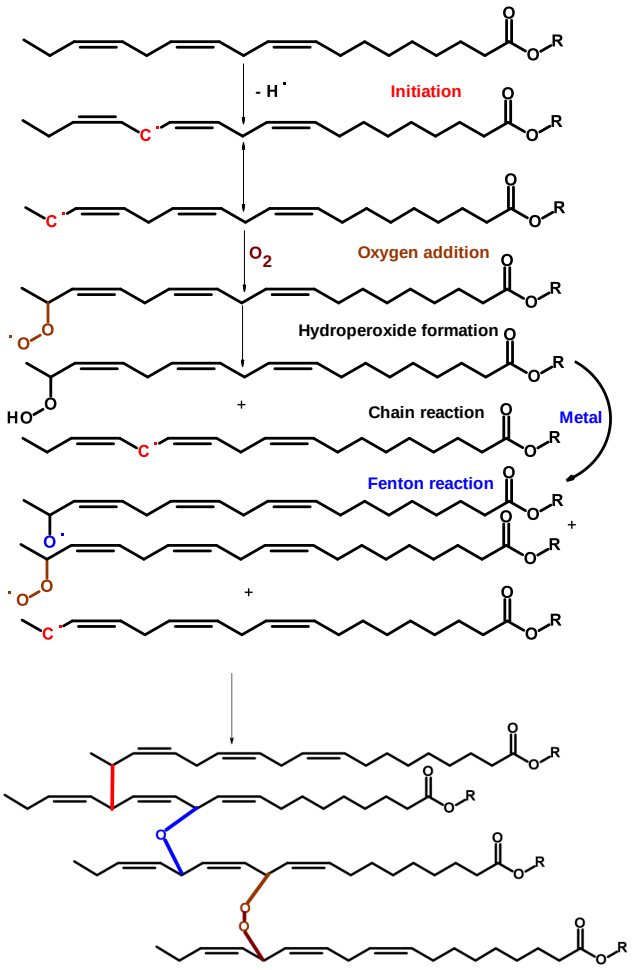


Figure 1. Proposed siccativation mechanism of oil films with driers or pigments.

EXPERIMENTAL SECTION

Chemicals. All aqueous solutions were prepared from ultrapure grade water obtained by water filtration with a two stages Millipore system (Milli-Q® Academic with a cartouches Q-Gard 1 and Progard 2, Merck Millipore, Burlington, MA, United States). All solvents were MS analytical grade. All solvents and chemicals were purchased from Merck (Merck KGaA, Darmstadt, Germany) and used without further purification. 3-(Dimethylamino)-1-propylamine also called *N,N*-dimethyl-1,3-propanediamine (DMAPA) 99% was used as received.

Samples. Linseed oil, cobalt (II) 2-ethylhexanoate 65% in mineral spirits, cobalt (II) acetylacetonate ≥ 99%, iron (III) chloride hexahydrate 97%, copper (II) acetate hydrate, palladium (II) acetate 98% and titanium (IV) oxide nanopowder 99.7%, anatase were purchased from Merck (Merck KGaA, Darmstadt, Germany).

The artistic pigment Cobalt Dark Bleu was purchased from Kremer company (Kremer Pigmente GmbH & Co., Aichstetten, Germany).

The contemporary oil paint tubes: Prussian Bleu (318, série 2) and Titanium White (116, série 1) were purchased from *Sennelier* (Sennelier, Paris, France).

Mock-up samples preparation.

Linseed oil with cobalt (II) 2-ethylhexanoate. Linseed oil was mixed with cobalt (II) 2-ethylhexanoate drier at 4 percentages w/w (0%, 0.1%, 1% and 10%) and spread homogeneously over clean glass slide for a thickness of almost 40 microns. 50 mg of oil was introduced each time. The formulated oil paints were then aged as following:

(i) Ageing at room temperature: The slides were only left under natural conditions until 2 years.

(ii) Ageing accelerated by heating: The slides were left under natural conditions for one week then they were put in GC oven at the temperature of 80 °C for another one week.

(iii) Ageing accelerated by UV-irradiation: The slides were put directly over UV-LED at 395 nm for 44 days then until 2 years. UV LEDs-B (395 nm, irradiance of 14 $W.cm^{-2}$, Omnicure® AC9150 from Excelitas Technologies Corp., Pittsburgh, PA, USA) was used as light source.

Linseed oil with transition metals and artistic pigments. Linseed oil was mixed with different metal driers and a pigment at 100/50 (w/w) on glass slides (approximate thickness = 0.04 mm) and left under natural conditions until 2 years. The driers were cobalt(II) acetylacetonate (bis(2,4-pentanedionato)cobalt), iron(III) chloride hexahydrate (ferric chloride hexahydrate), copper(II) acetate hydrate (cupric acetate hydrate), palladium(II) acetate and titanium(IV) oxide (titanium dioxide). The artistic pigment was the Cobalt Dark Blue.

***Sennelier* oil paints.** 50 mg of Prussian Blue and Titanum White were spread directly on separated glass slides and left for one week without any accelerated ageing.

All studied oil films were collected carefully (after 1 week and/or 2 years of ageing) using clean scalpel blades before depolymerization.

Depolymerization by direct transamidation on 5 mg. In a 2-mL transparent tube, 5 mg of the collected films were transamidated overnight at room temperature with 1 mL (7.93 mmol) of 3-(dimethylamino)-1-propylamine (DMAPA) under stirring. The mixture was quenched with 400 µL of formic acid then transferred to a 5 mL Falcon™ conical tube (Corning, NY, USA), added to 2 mL of ultrapure water and extracted two times with 2 mL of petroleum ether by centrifugation at 10,000 rpm during 5 minutes at room temperature using Beckman-Coulter (Brea, CA, USA) Allegra® X-30R centrifuge with the corresponding C1015 fixed angle conical tube rotor. The remaining aqueous phase was reextracted two times with 2 mL of ethyl acetate under the same centrifugation conditions. After each centrifugation, the organic phase was transferred to a 2-mL clear glass tube using a glass pipette. The obtained organic phases were evaporated under nitrogen at room temperature and stored in 2-mL glass tube.

Miniaturization of analysis. In a 2-mL clear glass tube, 0.5 mg of films were transamidated overnight at room temperature with 500 µL of DMAPA. The mixture was quenched with an excess of formic acid (200 µL) then transferred to a 1.5 mL Eppendorf® tube (Eppendorf, Hamburg, Germany), added to 1 mL of ultrapure water and extracted two times with 1 mL of petroleum ether by centrifugation at 10,000 rpm during 5 minutes at room temperature using Beckman-Coulter (Brea, CA, USA) Allegra® X-30R centrifuge with the corresponding F-34638 fixed angle conical tube rotor. The remaining aqueous phase was reextracted twice with 1 mL of ethyl acetate under the same centrifugation conditions. The next steps were performed as previously.

Analytical method. For MS samples preparation, the petroleum ether fractions were solubilized in dichloromethane at 1 mg/10 µL. However, the ethyl acetate fractions were solubilized in methanol at 1 mg/10 µL.

The solubilized fractions were diluted 1000 times in methanol/water/formic acid 30/70/0.1 (v/v/v) for the LC-MS analysis and 100 times (for the same LC-MS analyzed samples) for the MALDI FTICR MS analysis.

For all other MALDI FTICR MS data, the solubilized fractions were diluted 100 times in acetonitrile/water/formic acid 5/95/0.1 (v/v/v).

MALDI FTICR MS analysis. The analyses were performed on a SolariX XR instrument with a 9.4 Tesla actively shielded superconducting magnet fitted with a dynamically harmonized cell (Bruker Daltonics, Bremen, Germany) and controlled by FTMS Control software. MALDI FTICR mass spectra were acquired in positive ion mode. The matrix used was α-cyano-4-hydroxycinnamic acid. Spectra were acquired using broadband detection, 8 M points, 32 scans accumulation for a better signal-to-noise ratio with a mass range from *m/z* 100 to 1,500 with 2.936 s transient time. Instrument calibration was achieved using red phosphorous as external calibrant and a quadratic calibration. The obtained spectra were processed using Data Analysis software version 5.0 (Bruker Daltonics, Bremen, Germany).[10]

LC-ESI MS analysis. LC-MS analyses were performed on an Orbitrap LTQ XL mass spectrometer hyphenated to a Dionex Ultimate 3000 HPLC System (ThermoFisher Scientific, Bremen, Germany). The analysis was performed using a 40 min gradient at a flow rate of 0.50 mL.min^{-1} on a Hypersil GOLD™ C18 column (2.1 µm i.d. × 150 mm) packed with 3 µm beads from ThermoFisher Scientific; placed in an oven at a temperature of 50 °C. The depolymerized products were separated using a multi-step gradient of 40 minutes with a mobile phase of 30% methanol in acidified water, 0.1% formic acid (solution A) and 50% methanol, 50% 2-propanol in acidified water, 0.1% formic acid (solution B) as described in Almasri et al. pupblication.[10] The MS scans were acquired from *m/z* 200 to 1,000 with a 60,000 resolution at *m/z* 200. Data acquisition and interpretation were performed using FreeStyle™ 1.8 SP2 QF1 software (Thermo Fisher Scientific).

RESULTS AND DISCUSSIONS

First, mock-up samples' serial of linseed oil with cobalt (II) 2-ethylhexanoate was prepared for 0%, 0.1%, 1% and 10% (w/w) of this historically strong drier. Their polymerization was studied over time under natural polymerization, after heating and UV-irradiation. The second serial was prepared by mixing 25 mg of transition metal driers or artistic pigment with 50 mg of linseed oil. Linseed oil having high percentages of linolenic acid (C18:3) has been chosen in this study because of its excellent drying properties.[10] Cobalt, iron, copper, palladium and titanium complexes have been also used for these formulations. The *Sennelier* oil tubes of white and blue coloration: Titanium White and Prussian Blue were studied with and without autoxidation. The coloration blue has been studied in detail using cobalt (II) 2-ethylhexanoate and cobalt (II) acetylacetonate driers, the artistic pigment Cobalt Dark Blue and the previously mentioned blue oil tube.

For this aim, soft chemical depolymerization combined with advanced mass spectrometry was performed. This strategy was recently used to study the effect of oil binders on siccativation.[10] However, here the quantity of the starting oil material was smaller (5 mg instead of 100 mg). Indeed, this small amount of oil paints was transamidated overnight using 3-(*N,N*-dimethylamino)-1-propylamine (DMAPA) at room temperature, quenched with an excess of formic acid followed by liquid-liquid extractions first with petroleum ether then ethyl acetate. The extracted fractions were finally dried, resolubilized in methanol or dichloromethane, diluted and then analyzed by LC-MS and MALDI FTICR-MS.

The extraction yield, measured based on recovered weight, in petroleum ether in all samples was lower than that that in ethyl acetate. It was different according to the percentage of cobalt drier introduced and the mode of ageing. Indeed, after one week of natural polymerization, the total extraction yield including petroleum ether and ethyl acetate extractions was 70% for the linseed oil's polymer without drier and 65%, 62% and 52% for the oil paints with cobalt 0.1%, 1% and 10% respectively. However, after 3 weeks of natural autoxidation the extraction yield decreased by up to 1% in all fractions. After heating at 80 °C, it decreased drastically registering 29%, 28%, 26% and 15% for the polymerized linseed oil films with 0%, 0.1%, 1% and 10% cobalt (II) 2-ethylhexanoate respectively. The 44 days of irradiation diminished even more these extraction yields (Figure 2). This confirms that the extraction yields of oil paints decrease with polymerization rate due to the increase of oxygen diffusion during sicativation. The polymerization rate was in function of the drier starting amount, polymerization time and ageing by heating or irradiation.

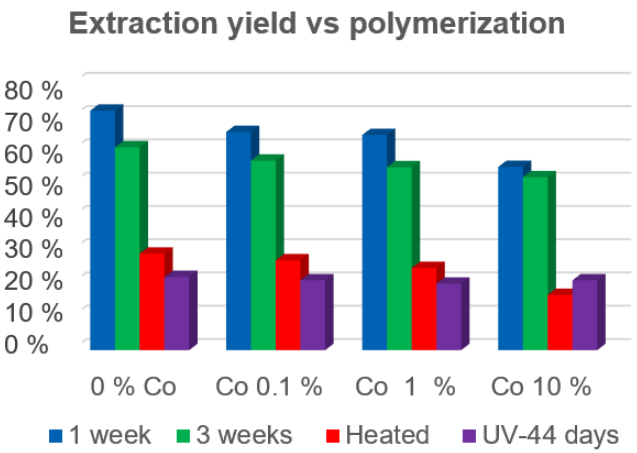


Figure 2. Extraction yield of linseed oil films in the presence of cobalt (II) 2-ethylhexanoate for 4 different ageing modes.

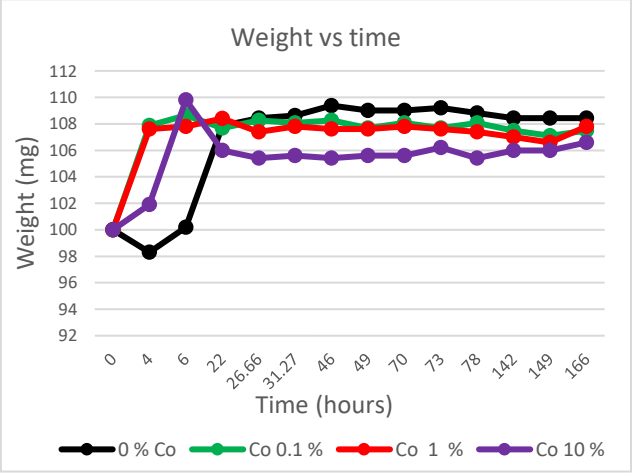
The extraction yields of linseed oil films formulated with metal driers and pigments were compared. Indeed, they registered 91%, 99.6%, 87%, 98% and 73% for linseed oil polymerized for one week with cobalt (II) acetylacetonate, iron (III) chloride hexahydrate, copper(II) acetate hydrate, palladium(II) acetate and titanium(IV) oxide respectively.

For the *Sennelier* oil paint tubes, coming directly from their tubes, they registered after depolymerization extraction yields of 78% and 76% for Prussian Blue and Titanium White respectively. These yields decreased to 56% and 66%

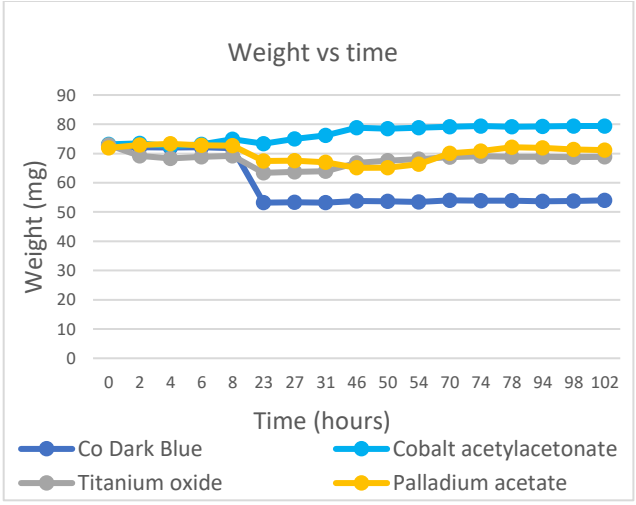
for their corresponding films after one week of polymerization under natural conditions.

Siccativation of linseed oil in the presence of driers. The drying process of oil films has been followed over 5 days on each mock-up oil slide containing initially 50 mg of linseed oil by the measurement of oil weight each 2-4 hours during a week (no measurements have been performed at night).

The polymerized linseed oil films before and after polymerization with Co (II) 2-ethylhexanoate drier showed that the film of oil without driers had an increase of weight up to 7% during the first 22 hours. However, the weight increased up to a maximum of 10% in the presence of Co 10%, and 8-9 % with cobalt 0.1% and 1% after only 6 hours of siccativation under the natural conditions. This confirms that the oxygen uptake is accelerated with the rate of polymerization. Some of this weight gain will be then lost during the drying of films due to decomposition and loss of volatile organic compounds (VOC) as a result of oxidation reactions (Figure 3, (a)). On the other hand, in the presence of the pigment Cobalt Dark Blue introduced in half-weight of oil, it showed a stabilization of weight during the first 8 hours of siccativation followed by a strong decrease of 20% in the next 15 hours then it was stabilized for the remaining days. This shows a rapid drying and loss of VOC in the presence of this pigment. However, in the presence of cobalt acetylacetonate, an oxygen uptake was observed after 8 hours of siccativation followed by an increase of 10% of the weight demonstrating that this film is still in the early stages of its drying (Figure 3, (b)).



(a)



(b)

Figure 3. Evolution of polymerized linseed oil films weight during 5 days of polymerization at room temperature. (a): In the presence of Co (II) 2-ethylhexanoate for 2 slides together; (b): In the presence of some driers and pigments.

In the case of linseed oil with Co (II) 2-ethylhexanoate drier, the oxygen uptake was clearly present after an induction period within the first day resulting in the weight gain of oil films. Furthermore, the loss of volatile compounds (VOC) was clearly present in the fast-drying process with the artistic pigment Cobalt Dark Blue. These observations confirm the siccativation mechanism already proposed in Almasri et al. publication.[10] In fact, the siccativation process proceeds via a radical autoxidation of the double bonds in the carbon chains of the binder's fatty acids, normally composed of initiation, propagation and finally chain termination. The transition metals such as cobalt can decompose easily the hydroperoxide formed after the bis-allylic proton abstraction. A Fenton reaction which is a redox reaction can be done at this step catalyzing the decomposition of hydroperoxides (Figure 4). Then the propagation and termination steps continue providing the 3D-crosslinked film with C-O and C-C links (Figure 1 & SI, Figure S1).

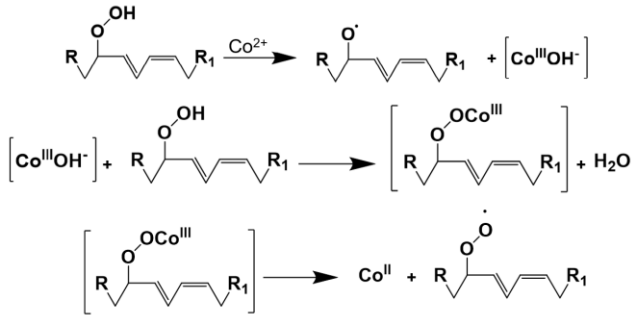


Figure 4. Fenton reaction occurred during oil siccativation.

LC-MS analysis. A multi-step gradient of 40 minutes was set using solvent A formed of 30% of methanol with 0.1% of formic acid and solvent B formed of 50% of isopropanol, 50% methanol and 0.1% formic acid. The products of depolymerization were identified based on the

mass/charge (m/z) ratio after a dilution of 1 mg/mL (the final concentration of the injected samples was 1 mg/10 mL).

LC-MS results of petroleum ether fractions of the polymerized linseed oil for one week under natural conditions in the presence of metal driers and the different percentages of cobalt drier showed the presence of the main unsaturated fatty acids oleic (C18:1), linoleic (C18:2) and linolenic (C18:3) acids detected mono- and di-derivatized with DMAPA molecules. They showed also the presence of the main saturated fatty acids, stearic (C18:0) and palmitic (C16:0) acids found mono-transamidated at m/z 369.384 and m/z 341.353 respectively. The MS spectra were obtained with very high accuracy for an Orbitrap (0-5 ppm).

First, concerning the linseed oil film formulated with cobalt (II) 2-ethylhexanoate drier present at 0%, 0.1%, 1% and 10% which was left for one week under natural conditions, the percentage of the mono-derivatized palmitic acid was 19%, 32%, 34% and 27% respectively; and the percentage of the mono-derivatized stearic acid was 15%, 23%, 23% and 21% respectively. However, the percentage of the unsaturated fatty acids presented by their mono-derivatized forms: Linolenic [$C_{23}H_{42}N_2O + H^+$], linoleic [$C_{23}H_{44}N_2O + H^+$], and oleic [$C_{23}H_{46}N_2O + H^+$] acids were the highest for the films without driers. The linolenic acid percentage decreased from 7% to 1% and 0.3% for polymerized linseed film with Co 0.1% and Co 1% respectively then increased until 3% with Co 10%. This same evolution was observed for linoleic and oleic acids. The linoleic acid percentage was 8%, 2.8%, 0.6% and 3.3% with Co 0%, 0.1%, 1% and 10% respectively. The oleic acid abundance was 31%, 26.5%, 17% and 26.7% respectively with increasing the cobalt percentage. These data showed that the siccativation reaction degrades the unsaturation of fatty acids. For Co 0%, 0.1% and 1%, there was an increasing consumption of these fatty acids. But with cobalt 10%, its fast drying resulted in the loss of some oxygen atoms diffused in its film. Indeed, the oxygenated species abundance was 10.43%, 10.92%, 13.32% and 9.34% respectively with the increasing cobalt drier percentage (SI, Table S1 and Figure S2).

Comparing the sum of abundances of each unsaturated fatty acid under its mono- and di-derivatized forms to the sum of abundances of both main saturated fatty acids, the abundances of each unsaturated fatty acid vs saturated fatty acid was in decrease after one week of polymerization with Co 0%, Co 0.1% and Co 1% as shown in Table 1. (The di-derivatized forms abundance was quite negligible). The corresponding calculation is given by this formula:

$$\text{Ratio of unsaturared fatty acid vs saturated fatty acids} = \frac{\sum unsaturated\ fatty\ acid\ abundances}{\sum C16{:}\,0\ abundances + \sum C18{:}\,0\ abundances}$$

The abundance of each unsaturated fatty acid is calculated in comparison to the major composition, according to the following general formula:

$$\text{Abundance of a fatty acid's peak} = \frac{Relative\ intensity\ of\ this\ \text{fatty acid's peak}}{Relative\ intensity\ of\ the\ major\ composition\ peaks} \times 100$$

Table 1. LC-MS data: Ratio of main unsaturated fatty acids in comparison to saturated fatty acids present in the polymerized linseed oil films at Co 0%, 0.1%, 1% and 10%, petroleum ether fraction.

Ratio	Co 0%	Co 0.1%	Co 1%	Co 10%
C18:1 vs saturated	0.19	0.02	0.00	0.05
C18:2 vs saturated	0.24	0.05	0.01	0.07
C18:3 vs saturated	0.88	0.48	0.29	0.56

Moving to the investigation of dimers in these samples. First, dimers may be differentiated by their M+1 peak at + 0.5 Da.

If M is the monomer, the double charged dimer appears at:

$$\frac{[2\ (M-H)+2\ H]}{2}$$

For instance, the dimers found after LC-MS analysis of the linseed oil film formulated with Co 10% were C-C dimers of linolenic acid appeared at m/z 362.329 and 362.830 (theoretical m/z were 362.329 and 362.831). A mixed dimer of linoleic and linolenic acids appearing at m/z 363.838 was also detected. These dimers were detected in petroleum ether and ethyl acetate fractions (SI, Figure S3).

However, the dimers of linoleic acid appeared at m/z 364.345 and 364.846 (theoretical m/z are 364.345 and 364.846) only in the polymerized linseed oil film without driers.

Moving to linseed oil films formulated with metal driers and the Cobalt Dark Blue pigment polymerized for one week under natural conditions, the linolenic acid was predominant in the presence of the iron drier, iron(III) chloride hexahydrate. In the polymerized linseed oil film using this iron drier, the linoleic and oleic acid relative contents were the highest among the polymerized fractions (35% and 38% respectively). Unlike the iron drier in which the depolymerized fractions were rich in linolenic acid, the polymeric films with all the other driers had high content of oleic, then linoleic and finally linolenic acids. Concerning the oxidized unsaturated C18 fatty acids, the polymerized linseed oil films had traces of oxidized linoleic and oleic acids comparing to the oxidized linolenic acid. The highest relative ratio of oxidized linolenic acid vs saturated fatty acids was observed with the two cobalt driers, cobalt(II) acetylacetonate and the artistic pigment Cobalt Dark Blue registering 24.7 and 17.6 respectively. This content decreased with copper(II) acetate hydrate, titanium(IV) oxide, palladium(II) acetate, and iron(III) chloride hexahydrate driers having relative ratios of 16.5, 14.2, 11.5 and 5.1 respectively (Table 2).

Table 2. LC-MS data: Relative percentages of fatty acids present in the linseed oil films formulated with metal driers, polymerized for one week under natural conditions.

	Cobalt(II) acetylacetonate	Iron(III) chloride hexahydrat	Palladium (II) acetate	Copper (II) acetate hydrate	Titanium(IV) oxide	Cobalt Dark Blue
Relative % C18:1	84%	38%	85%	80%	94%	85%
Relative % C18:2	11%	27%	10%	12%	5%	8%
Relative % C18:3	5%	35%	5%	8%	1%	7%
Relative % C16:0	34%	29%	46%	44%	51%	39%
Relative % C18: 0	62%	66%	49%	50%	43%	55%
Relative % C20:0	5%	5%	6%	6%	6%	5%
Relative ratio C18:1 vs saturated	70	92	81	68	64	55
Relative ratio C18:2 vs saturated	9	67	9	10	3	5
Relative ratio C18:3 vs saturated	4	85	5	6	1	4
Relative % C18:1 - 1 O	1%	3%	2%	2%	2%	1%
Relative % C18:2 - 1 O	1%	5%	4%	4%	10%	4%
Relative % C18:3 - 1 O	99%	92%	94%	94%	88%	95%
Relative ratio C18:1 -1 O vs saturated	0.1	0.2	0.2	0.3	0.3	0.2
Relative ratio C18:2 -1 O vs saturated	0.2	0.3	0.5	0.8	1.5	0.7
Relative ratio C18:3 -1 O vs saturated	24.7	5.1	11.5	16.5	14	17

It is necessary to mention that the calculated percentages in Table 2 are relative, without considering all the major composition peaks. Indeed, the relative percentage of each unsaturated fatty acid is given in comparison to the sum of the three main unsaturated fatty acids C18:1, C18:2 and C18:3; and the relative percentage of each saturated fatty acid is given in comparison to the sum of the three main saturated fatty acids C16:0, C18:0 and C20:0. Same calculations are achieved for the oxygenated unsaturated compounds. In addition, the relative ratios are always calculated in comparison to the sum of the three previously mentioned saturated fatty acids.

These relative calculations are only used in Table 2:

$$\text{Relative percentage of unsaturated fatty acid's peak} = \frac{Relative\ intensity\ of\ this\ \text{fatty acid's peak}}{\sum Relative\ intensities\ of\ C18{:}\,1, C18{:}\,2, C18{:}\,3} \times 100$$

$$\text{Relative percentage of saturated fatty acid's peak} = \frac{Relative\ intensity\ of\ this\ \text{fatty acid's peak}}{\sum Relative\ intensities\ of\ C16{:}\,0, C18{:}\,0, C20{:}\,0} \times 100$$

$$\text{Relative percentage of unsaturated oxygenated peak} = \frac{Relative\ intensity\ of\ this\ \text{peak}}{\sum Relative\ intensities\ of\ oxygenated\ C18{:}\,1, C18{:}\,2, C18{:}\,3} \times 100$$

$$\text{Ratio of a given peak vs saturated fatty acids} = \frac{Relative\ intensity\ of\ this\ \text{fatty acid's peak}}{\sum Relative\ intensities\ of\ C16{:}\,0, C18{:}\,0, C20{:}\,0}$$

The di-derivatized forms were negligible in these calculations.

MALDI FTICR MS analysis. The MALDI FTICR MS analyses have been done on all polymerized films with different formulations and on the oil tubes. All spectra were registered with very high accuracy (0-2 ppm). In petroleum ether fractions, the number of peaks per spectrum was very high, up to 52,000 peaks. The ethyl acetate and petroleum ether fractions showed differences in structural composition and in intensities of the common peaks due to the affinity of depolymerized compounds to be extracted in these both different polar solvents as shown in SI, Figure S4.

After almost 2 years of continuous polymerization under UV-irradiation at 395 nm, the polymerized films with Co 0.1%, 1% and 10% showed the predominance of the mono-derivatized palmitic acid peak appearing at *m/z* 341.3526 in all samples with 26%, 43% and 52% respectively. The mono-derivatized oleic acid [$C_{23}H_{46}N_2O_2$ + H^+] appearing oxygenated at *m/z* 383.3632 was detected with 13%, 12% and 11% respectively (SI, Table S2). These results confirm the high drying ratio obtained of these films in comparison to the one week drying under natural conditions that their drying was still not complete (Figure 5).

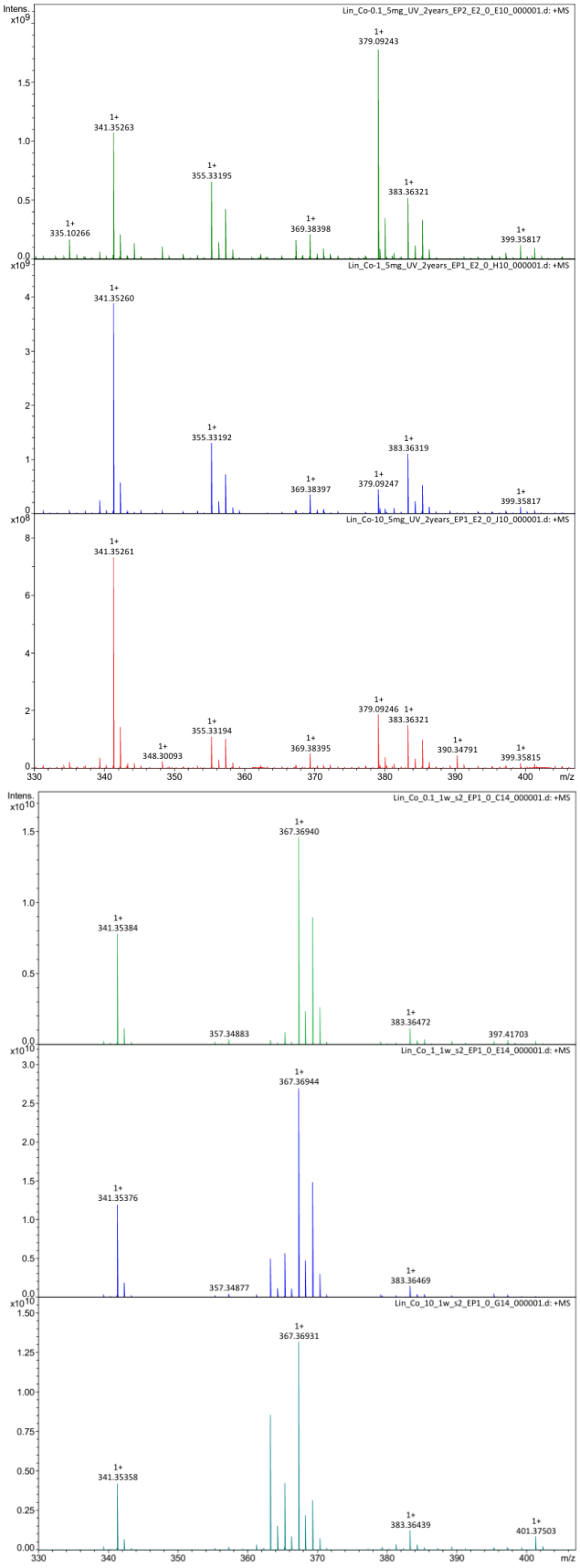


Figure 5. MALDI FTICR MS spectra for the polymerized linseed oil films with Co (II) 2-ethylhexanoate 0.1%, 1% and 10% respectively (*m/z* 330-407). Upper panel: After UV-irradiation of almost 2 years at 395 nm; lower panel: After polymerization for one week under natural conditions. The peak at *m/z* 379.0924 represents HCCA matrix main peak.

Moving to the comparison of the polymerization performances on one week and 2 years under natural conditions concerning the films in the presence of the other cobalt drier cobalt acetylacetonate and the artistic pigment Cobalt Dark Blue.

First, with the metal drier, the mono-derivatized linolenic acid appearing at *m/z* 363.3369 was detected with 29% of the major composition for the short-term polymerization. This percentage decreased strongly to 0.2% after 2 years of siccativation. The same observation was registered for the mono-derivatized oleic acid appearing at *m/z* 367.3683 that was detected with 42% and 0.9% for the short-term and long-term polymerizations respectively. However, this decreasing in the unsaturated fatty acids abundances was replaced by the strong decrease of saturated fatty acids' abundances. Indeed, the abundance of palmitic acid appearing at *m/z* 341.3526 increased drastically from 3% to 63% after 2 years. Same evolution was observed for stearic acid appearing at *m/z* 369.3839 that increased in intensity from 2% to 17% of the major composition. In addition, the oxygenated compounds' abundance increased from 12% to 17% after 2 years of polymerization (SI, Table S3).

Secondly, with the Cobalt Dark Blue artistic pigment, the mono-derivatized linolenic acid appearing at *m/z* 363.3369 was detected with 0.21% for the short-term polymerization then it disappeared totally after 2 years of siccativation. The mono-derivatized oleic acid appearing at *m/z* 367.3683 was detected with 44% and 1% for the short-term and long-term polymerizations respectively. However, the sum of abundances of the main saturated fatty acids went from 32% to 70% of the major composition. Furthermore, the oxygenated compounds' abundance increased from 19% to 27% after 2 years of autoxidation (SI, Table S3).

To compare the efficiency of drying of these cobalt catalysts, the ratios of the unsaturated fatty acids vs saturated fatty acids were calculated confirming that the pigment Cobalt Dark Blue dries faster the linseed oil than the cobalt acetylacetonate (Table 3).

Table 3. MALDI FTICR MS data: Ratios of main unsaturated fatty acids in comparison to saturated fatty acids present in the polymerized linseed oil films formulated with the pigment Cobalt Dark Blue and the drier cobalt acetylacetonate after 1 week and 2 years of polymerization under natural conditions (petroleum ether fraction).

Ratio	Cobalt drier- 1 week	Cobalt drier- 2 years	Cobalt pigment- 1 week	Cobalt pigment- 2 years
C18:1 vs saturated	6.23	0.00	0.01	0.00
C18:2 vs saturated	2.41	0.00	0.12	0.01
C18:3 vs saturated	9.13	0.01	1.39	0.02

After one week of natural drying of linseed oil with cobalt acetylacetonate or Cobalt Dark Blue pigment, many dimers

(C-C, C-O-C) and their oxygenated forms have been detected with two DMAPA molecules constituting almost 0.3% and 0.2% of their major compositions respectively (SI, Table S3).

Indeed, in the presence of the cobalt acetylacetonate drier, C-C dimers of linoleic acid [$C_{46}H_{86}N_4O_2 + H^+$] and linolenic, linolenic [$C_{46}H_{84}N_4O_2 + H^+$] acid have appeared at *m/z* 727.6823 and *m/z* 725.6667 constituting 0.04% of the major composition. The C-O linolenic, linoleic acids' dimer or the dimer with a linoleic acid bearing a hydroxylation [$C_{46}H_{84}N_4O_3 + H^+$] appeared at *m/z* 741.6616 with 0.01% of the major composition. The dimers of linolenic, linoleic [$C_{46}H_{84}N_4O_4 + H^+$], linoleic [$C_{46}H_{86}N_4O_4 + H^+$] and linoleic, oleic [$C_{46}H_{88}N_4O_4 + H^+$] fatty acids with two oxygen atoms appearing at *m/z* 757.6565, *m/z* 759.6722 and *m/z* 761.6875 respectively have been also detected with 0.05% abundance. Their dimers bearing 3 oxygen atoms [$C_{46}H_{84}N_4O_5 + H^+$], [$C_{46}H_{86}N_4O_5 + H^+$] and [$C_{46}H_{88}N_4O_5 + H^+$] were detected at *m/z* 773.6515, *m/z* 775.6617 and *m/z* 777.6828 respectively with 0.05% of the major composition. Even the dimers with 3 oxygen atoms of C18:3-C18:2, C18:2 and C18:2-C18:1 have been detected at *m/z* 789.6464, *m/z* 791.6621 and *m/z* 793.6776 respectively. The dimers with 5 and 6 oxygen atoms have been detected also (SI, Table S3). The total abundance of dimers formed in the presence of the cobalt acetylacetonate drier was diminished from 0.3% to 0.01% after two years of natural polymerization.

In the case of the artistic pigment Cobalt Dark Blue, the abundance of total detected dimers was 0.2% and 0.16% after natural conditions' polymerization of one week and 2 years respectively (SI, Table S3).

Moving to the study of contemporary oil paints' tubes, *Sennelier* Prussian Blue and Titanium White.

First, the Prussian Blue was studied as coming from tubes without polymerization and after polymerization of 1 week under natural conditions. Indeed, for petroleum ether fractions, the main peaks detected in the Prussian Blue sample before polymerization were respectively the mono-derivatized linoleic acid [$C_{23}H_{44}N_2O + H^+$] appearing at *m/z* 365.3526 with 32% and the mono-derivatized oleic acid [$C_{23}H_{46}N_2O + H^+$] appearing at *m/z* 367.3683 with 20% of the major composition. After one week's polymerization, the main peak in petroleum ether fraction was the mono-derivatized palmitic acid [$C_{21}H_{44}N_2O + H^+$] appearing at *m/z* 341.3526 with 39% of the major composition. Its ethyl acetate fraction's main peak was the di-derivatized product [$C_{28}H_{52}N_4O + H^+$] which is a di-derivatized compound appearing at *m/z* 461.4214 with 19% of the major composition (SI, Table S4).

The abundances of the sum of unsaturated fatty acids mono- and di-transamidated will be described in this section. In petroleum ether, the total linolenic acid abundance was consumed from 6.5% before polymerization to 2% after 1 week of polymerization. The abundance of linoleic acid in total decreased from 32% to 6.5% after 1 week. In addition, the oleic acid intensity decreased with the same evolution. However, the palmitic acid abundance has been increased after siccativation from 14% to 39% of the major composition (Table 4 & SI, Table S4).

The dimers detected before polymerization have been increased in intensity from 5% when coming directly from the tube to 8% and 20% in the petroleum ether and ethyl acetate fractions respectively after one week of drying.

Furthermore, the ethyl acetate fraction of the polymerized Prussian Blue showed differences in the intensities of fatty acids and their crosslinks. For example, the oleic acid abundance decreased more in ethyl acetate fraction (15%) in comparison to petroleum ether (25%). More oxygenated species remained in the ethyl acetate fraction: 35% vs 15% in petroleum ether (SI, Table S4 & Figure 6).

The stearic acid for both extracted fractions of the polymerized Prussian Blue and for its fractions without polymerization remained almost constant (around 2% of the major composition).

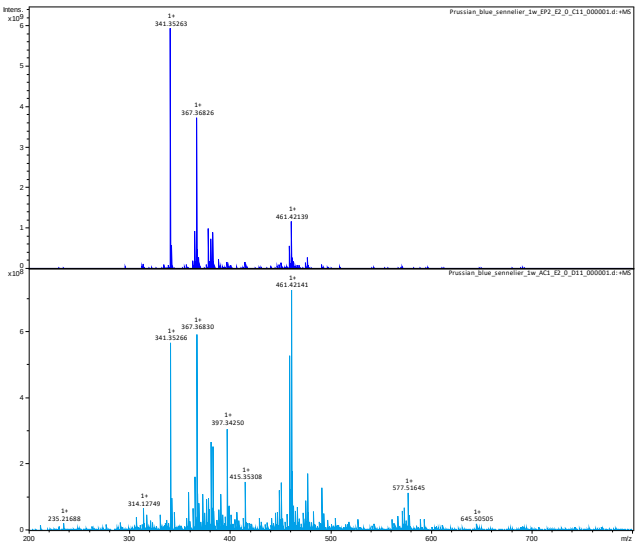


Figure 6. MALDI FTICR MS spectra of the polymerized Prussian Blue for one week under natural conditions (*m/z* 200-800). Upper panel: Petroleum ether fraction, lower panel: Ethyl acetate fraction.

On the other hand, Titanium White was studied after polymerization for one week under natural conditions to compare it with the Prussian Blue samples. Indeed, the Titanium White petroleum ether fraction will be detailed. Its main peaks were the mono-derivatized oxygenated oleic acid [$C_{23}H_{46}N_2O_2 + H^+$] appearing at *m/z* 383.3632 with 24% of the major composition then the mono-derivatized palmitic acid appearing at *m/z* 341.3526 with 23% of the major composition. This fraction contained 19% of dimers and 38% of oxygenated species (SI, Table S4).

All the studied *Sennelier* oil paints' tubes formed initially of safflower oil have contained an un-identified compound appearing at *m/z* 461.4214 tentatively assigned to linoleic acid bearing a carboxyl group and two DMAPA molecules. It has appeared with abundances from 5% in Prussian Blue-

tube to 8% in the Prussian Blue-1week, petroleum ether then 19% in the Prussian Blue-1week, ethyl acetate and Titanium White-one week, petroleum ether (SI, Table S4).

Table 4. Abundances of the main fatty acids and their dimers and oxygenated compounds in *Sennelier* oil paints' tubes before and after polymerization for 1 week under natural conditions (PE: Petroleum ether, EA: Ethyl acetate, and tube: Without polymerization).

	Prussian Blue-Tube	Prussian Blue polymerized for 1 week, EA	Prussian Blue polymerized for 1 week, PE	Titanium White, polymerized for 1 week, PE
% all Dimers	5.39%	19.49%	7.79%	19.42%
% C18:3	6.49%	1.77%	1.32%	0.14%
% C18:2	31.79%	5.01%	6.49%	2.07%
% C18:1	20.36%	16.40%	24.88%	8.83%
% C16:0	13.55%	14.95%	39.29%	22.51%
% C18: 0	2.15%	2.23%	1.83%	2.13%
% Saturated	15.70%	17.19%	41.12%	24.64%
Ratio C18:3 vs saturated	0.41	0.10	0.03	0.01
Ratio C18:2 vs saturated	2.02	0.29	0.16	0.08
Ratio C18:1 vs saturated	1.30	0.95	0.60	0.36
% O	18.08%	34.62%	15.12%	38.55%

All these data confirm that the siccativation mechanism affording the 3D-crosslinked films depends not only on oil type and ageing time but also on type of pigments and metal driers and their formulation recipes in the presence of light and oxygen.

Miniaturization of analysis, application on museum-size samples. The MS analysis was tested on 0.5 mg of polymerized linseed oil film (without drier) left for 2 years under natural conditions. The test was done by varying the DMAPA volume. Indeed, 5 volumes of DMAPA have been tested: 100 µL, 200 µL, 300 µL, 400 µL and 500 µL. The formic acid quenching in excess was performed by adding 40 µL, 80 µL, 120 µL, 160 µL and 200 µL respectively. The quantity of water added to create phases was 500 µL for the first two trials and 1 mL for the remaining trials. This quantity of water was the same for each solvent of extraction (petroleum ether and ethyl acetate). The results of all these trials have been analyzed by MALDI FTICR MS. Indeed, the best result was found to be the depolymerization of 0.5 mg of oil paint using 500 µL of DMAPA as the obtained MS spectrum was excellent having the remaining traces of fatty acids after 2 years of polymerization at high sensitivity. In the other MS spectra, the peak of the matrix HCCA appearing at *m/z* 379.0924 was very high competing with the depolymerized fatty acids' peaks (SI, Figure S5).



Figure 7. Oil painting on canvas dated between the two world wars. Left panel: Full painting; right panel: Close-up of the studied area. The white arrow indicates the position of the analyzed green part.

This miniaturized methodology was applied on oil painting from the 20th century. The pale green area indicated in Figure 7 was studied. Indeed, the depolymerization was successful in which the remaining traces of palmitic and oleic acids of the original oil paint have been detected at *m/z* 341.3526 and *m/z* 367.3683 respectively with high accuracy, resolution and sensitivity as shown in Figure 8.

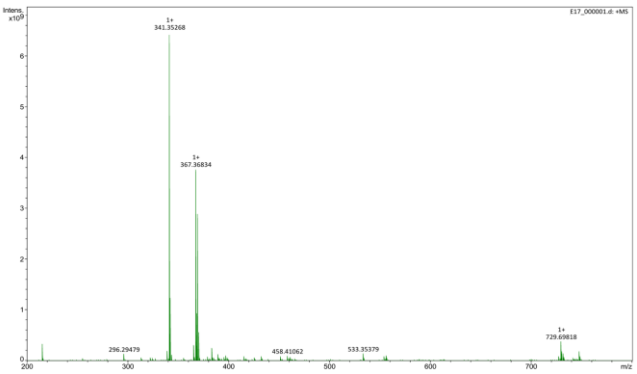


Figure 8. MALDI FTICR MS spectrum of the green part of the old painting from the 20th century.

CONCLUSIONS AND PERSPECTIVES

The innovative methodology of chemical depolymerization by transamidation with DMAPA at room temperature, combined to advanced mass spectrometry (MALDI FTICR MS and LC-MS) was applied on mock-up samples of linseed oil formulated with various percentages and types of metal driers and artistic pigments and aged differently for short-term and long-term. Oil paints' tubes from *Sennelier* have been also studied with and without polymerization. The effect of transition metal present in pigments was discussed for the siccativation mechanism. These driers affected the presence of degraded unsaturated fatty acids and the formed oxygenated species, crosslinks and dimers during the oil film lifetime. The drying rate was followed-up. This methodology has been miniaturized and applied successfully on oil paints from 20th century while preserving the original painting affording detailed results with good sensitivity. This method will be applied on other

types of oil paints such as alkyd paints and industrial polyester's resins.

ASSOCIATED CONTENT

Supporting Information

Additional experimental details and characterization data.

AUTHOR INFORMATION

First author

Bayan Almasri - Univ. Lille, CNRS, UAR 3290, MSAP, Miniaturisation pour la Synthèse l'Analyse et la Protéomique, F-59000 Lille, France ; Laboratoire de Chimie Appliquée, Faculté des Sciences III, Université Libanaise, Ras Maska, Tripoli, Liban ; orcid.org/0009-0001-9467-5716.

Note

The authors declare no competing financial interest.

AKNOWLEDGMENT

Bayan ALMASRI gratefully acknowledges the funding of her joint PhD between University of Lille and Lebanese University by the PAUSE funding program. The mass spectrometer was funded by University of Lille, CNRS, Région Hauts-de-France and the European Regional Development Fund (ERDF). The authors gratefully acknowledge the financial support of the FTICR MS facility from the IR INFRANALYTICS FR2054 CNRS and of the EU_FTICR _MS project Grant Agreement 731077 funded by EU Horizon 2020 Research and Innovation Program.

REFERENCES

1. Blumenroth, D.; Zumbühl, S.; Scherrer, N. C.; Müller, W., Sensitivity of modern oil paints to solvents. Effects on synthetic organic pigments. *Issues in Contemporary Oil Paint* **2014**, 351-362.
2. Lomax, S. Q.; Learner, T., A review of the classes, structures, and methods of analysis of synthetic organic pigments. *Journal of the American Institute for conservation* **2006,** *45* (2), 107-125.
3. Bielman, J. H., Driers. In *Surface Coatings Springer* Dordrecht, 1993.
4. Oil; Association, C. C.; Bielman, J., Driers. *Surface Coatings: Volume 1 Raw Materials and Their Usage* **1993**, 592-610.
5. Tumosa, C. S.; Mecklenburg, M. F., The influence of lead ions on the drying of oils. *Studies in Conservation* **2005,** *50* (sup1), 39-47.
6. Meneghetti, S. M.; de Souza, R. F.; Monteiro, A. L.; de Souza, M. O., Substitution of lead catalysts by zirconium in the oxidative polymerization of linseed oil. *Progress in organic coatings* **1998,** *33* (3-4), 219-224.
7. Mallégol, J.; Lemaire, J.; Gardette, J.-L., Drier influence on the curing of linseed oil. *Progress in organic coatings* **2000,** *39* (2-4), 107-113.
8. Lima, G. E. S.; Nunes, E. V.; Dantas, R. C.; Meneghetti, M. R.; Meneghetti, S. M. P., Systematic investigation of the oxidative polymerization of linseed oil catalyzed by Co (II), Mn (II), and Fe (II) complexes with chelating nitrogen ligands. *European Journal of Lipid Science and Technology* **2015,** *117* (2), 229-234.
9. Honzicek, J., Curing of air-drying paints: a critical review. *Industrial & engineering chemistry research* **2019,** *58* (28), 12485-12505.
10. Almasri, B.; Rolando, C., Siccative vegetable oils and their mock-up for oil-based paints applications: Oil differentiation and ageing for drying process assessment using a new methodology of soft chemical depolymerization with advanced mass spectrometry analysis. To submit.
11. Rasti, F.; Scott, G., The effects of some common pigments on the photo-oxidation of linseed oil-based paint media. *Studies in conservation* **1980,** *25* (4), 145-156.
12. Samain, L.; Grandjean, F.; Long, G. J.; Martinetto, P.; Bordet, P.; Strivay, D., Relationship between the synthesis of Prussian blue pigments, their color, physical properties, and their behavior in paint layers. *The Journal of Physical Chemistry C* **2013,** *117* (19), 9693-9712.
13. Samain, L.; Gilbert, B.; Grandjean, F.; Long, G. J.; Strivay, D., Redox reactions in Prussian blue containing paint layers as a result of light exposure. *Journal of Analytical Atomic Spectrometry* **2013,** *28* (4), 524-535.
14. Osmond, G., Zinc white: a review of zinc oxide pigment properties and implications for stability in oil-based paintings. *AICCM bulletin* **2012,** *33* (1), 20-29.
15. Artesani, A., Zinc oxide instability in drying oil paint. *Materials Chemistry and Physics* **2020,** *255*, 123640.
16. Zovi, O.; Lecamp, L.; Loutelier-Bourhis, C.; Lange, C. M.; Bunel, C., Stand reaction of linseed oil. *European Journal of Lipid Science and Technology* **2011,** *113* (5), 616-626.


Deciphering the secrets of oil paintings
Siccative oils
Metal driers
Artistic pigments
Ageing until 2 years
Ultraviolet
Temperature
Natural conditions
Oil paint tubes
Historical paintings

Supporting information

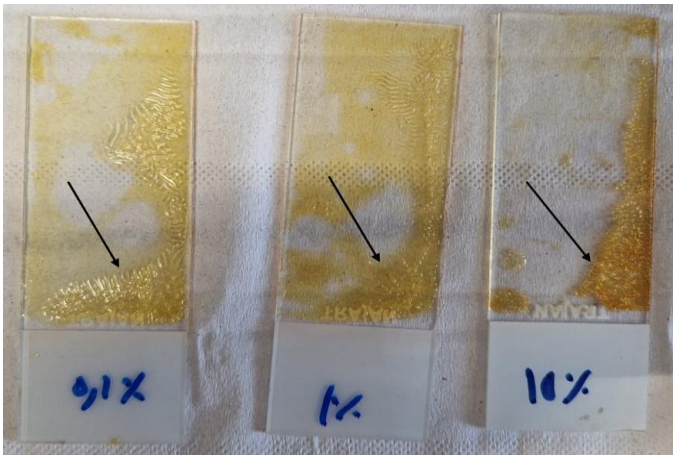


Figure S 1. Linseed oil mock-up samples of 2 years old after natural drying: With cobalt drier Co(II), bis(2-ethylhexanoate) of 0.1%, 1% and 10% respectively.

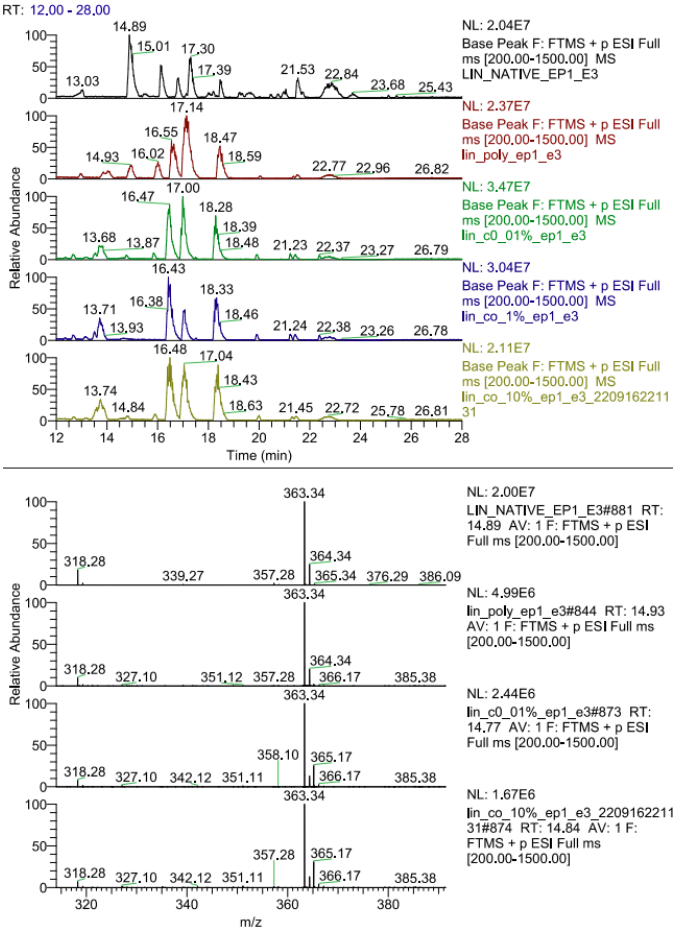


Figure S 2. LC chromatograms and MS associated spectra of native and polymerized linseed oil for one week under natural conditions, petroleum ether fraction: Native, polymerized without and with cobalt (II) 2-ethylhexanoate at cobalt 0.1%, 1% and 10% respectively, with the intensity of linolenic acid in each sample.

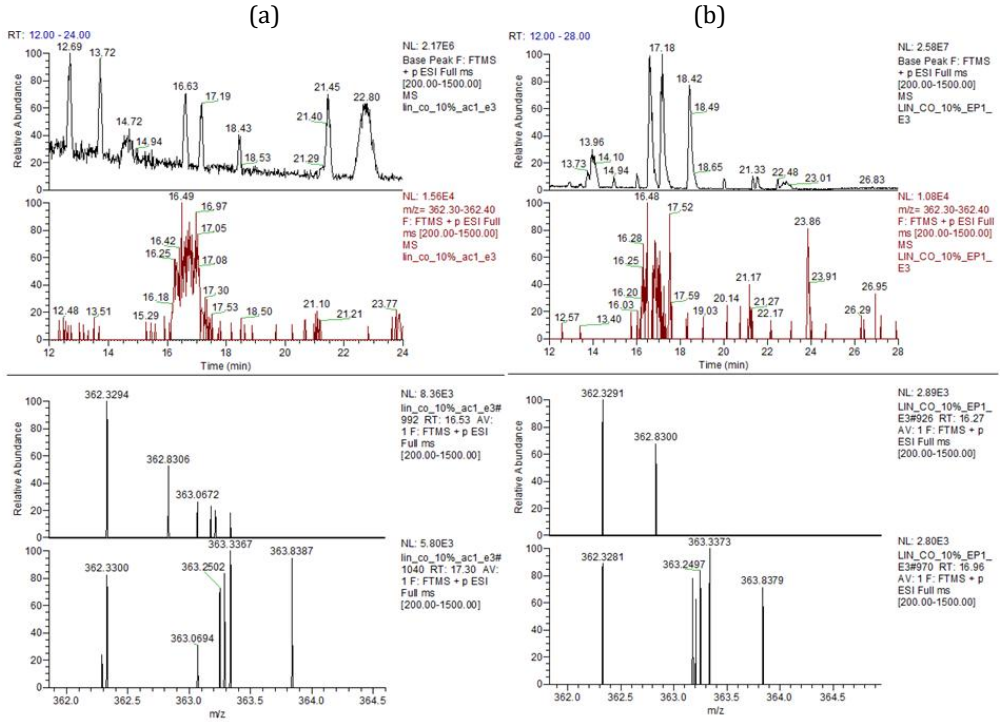


Figure S 3. LC chromatograms and MS associated MS spectra of linseed oil film formulated with Co 10% (Co (II) 2-ethylhexanoate) and polymerized for one week under natural conditions, from 12 min to 24 min. (a): Ethyl acetate fraction; (b): Petroleum ether fraction.

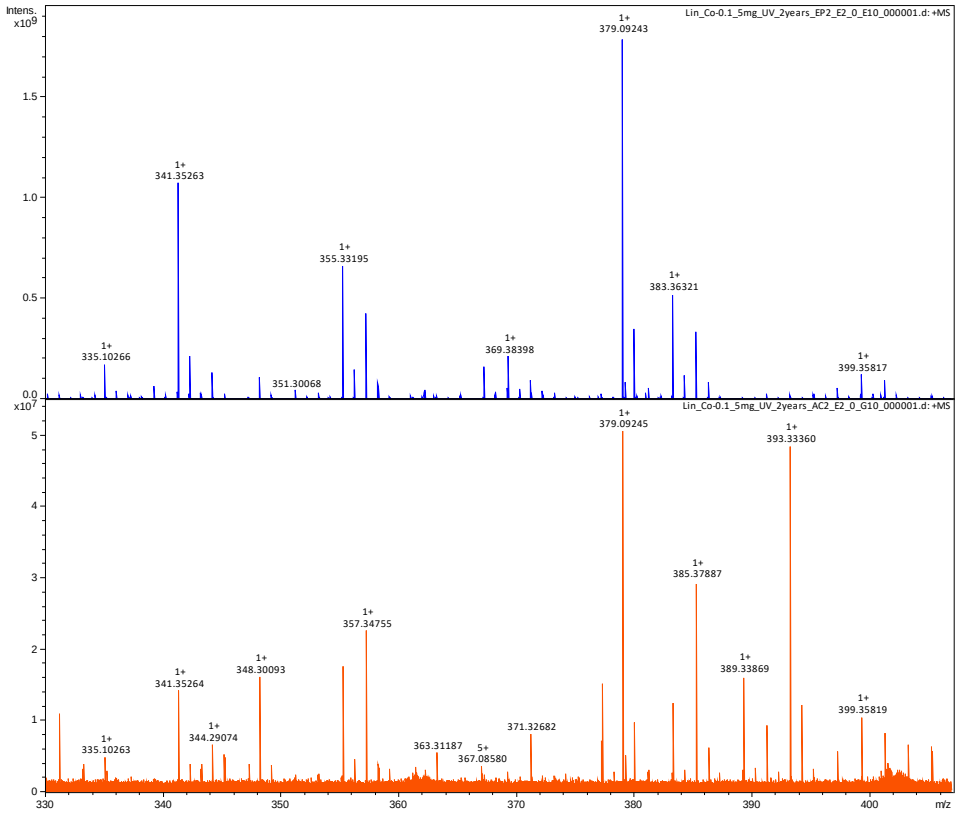


Figure S 4. MALDI FTICR MS spectra (*m/z* 330-407) for the polymerized linseed oil film with Co 0.1% (Co (II) 2-ethylhexanoate) after UV-irradiation of almost 2 years at 395 nm. Upper panel: Petroleum ether fraction; lower panel: Ethyl acetate fraction.

Table S 1. LC-MS relative intensities for the polymerized linseed oil for one week under natural conditions in the presence of cobalt (II) 2-ethylhexanoate at Co 0.1%, 1% and 10% (at 1 mg/10 mL, petroleum ether fractions).

Theoretical *m/z*	**$[M+H]^+$**	**Attribution**	**Polymerized linseed oil for 1 week, Co 0.1%**			**Polymerized linseed oil for 1 week, Co 1%**			**Polymerized linseed oil for 1 week, Co 10%**		
			RT (min)	Intensity	Error (ppm)	RT (min)	Intensity	Error (ppm)	RT (min)	Intensity	Error (ppm)
296.295	$C_{19}H_{38}NO$	Palmitic with $N(CH_3)_2$ of 1 DMAPA	20.55	2.09E+04	-1.38	16.43	4.93E+06	-1.72	16.57	4.09E+06	-2.06
320.295	$C_{21}H_{38}NO$	Linoleic with $N(CH_3)_2$ of 1 DMAPA	19.88	5.17E+03	-12.44	12.68	1.39E+05	0.05	16.01	2.06E+05	-0.89
322.310	$C_{21}H_{40}NO$	Oleic with $N(CH_3)_2$ of 1 DMAPA	21.03	1.61E+04	-0.49	17.03	1.93E+06	-1.73	17.15	3.39E+06	-1.73
324.326	$C_{21}H_{42}NO$	Stearic with $N(CH_3)_2$ of 1 DMAPA	22.22	1.35E+04	-1.57	18.27	2.85E+06	-1.57	18.43	2.33E+06	-2.49
339.337	$C_{21}H_{43}N_2O$	Palmitoleic- 1 DMAPA	19.11	1.45E+03	-0.03	15.09	3.39E+02	-0.62	15.23	9.11E+04	-0.62
341.353	$C_{21}H_{45}N_2O$	Palmitic- 1 DMAPA	20.53	5.88E+05	-1.17	16.43	3.01E+07	-1.76	16.59	2.55E+07	-2.05
355.332	$C_{21}H_{43}N_2O_2$	Palmitoleic- 1 DMAPA- 1 O	14.78	1.15E+03	-1.69	9.86	2.34E+05	-0.28	10.01	1.92E+05	-0.28
357.348	$C_{21}H_{45}N_2O_2$	Palmitic- 1 DMAPA- 1 O	20.62	1.43E+03	-0.84	16.68	2.13E+05	-0.28	16.83	1.31E+05	-0.28
363.337	$C_{23}H_{43}N_2O$	Linolenic- 1 DMAPA	18.73	1.88E+04	-0.58	14.81	2.26E+05	-0.58	14.94	2.42E+06	-0.58
365.353	$C_{23}H_{45}N_2O$	Linoleic- 1 DMAPA	19.88	5.23E+04	-0.82	15.89	4.88E+05	-1.09	16	3.10E+06	-1.09
367.368	$C_{23}H_{47}N_2O$	Oleic- 1 DMAPA	21.03	4.87E+05	-1.63	17.08	1.47E+07	-1.36	17.18	2.55E+07	-1.63
369.384	$C_{23}H_{49}N_2O$	Stearic – 1 DMAPA	22.22	4.32E+05	-2.44	18.33	2.04E+07	-1.90	18.42	1.99E+07	-1.90
379.332	$C_{23}H_{43}N_2O_2$	Linolenic- 1 DMAPA- 1 O	16.52	4.22E+03	-0.25	11.1	3.79E+04	-27.1	11.25	1.57E+05	0.28
381.348	$C_{23}H_{45}N_2O_2$	Linoleic- 1 DMAPA- 1 O	16.79	8.25E+03	0.26	12.46	1.60E+05	0.79	12.26	1.65E+05	0.52
383.363	$C_{23}H_{47}N_2O_2$	Oleic- 1 DMAPA- 1 O	18.19	1.25E+05	-1.83	13.71	9.83E+06	-1.04	13.96	7.68E+06	-1.04
385.379	$C_{23}H_{49}N_2O_2$	Stearic- 1 DMAPA- 1 O	18.02	3.95E+04	-0.38	18.46	1.95E+05	0.40	18.6	1.26E+05	-0.12
395.327	$C_{23}H_{43}N_2O_3$	Linolenic- 1 DMAPA- 2 O	16.6	1.43E+03	-2.48	7.68	1.10E+04	0.56	8.01	1.04E+04	1.32
397.343	$C_{23}H_{45}N_2O_3$	Linoleic- 1 DMAPA- 2 O	13.97	1.95E+03	2.01	10.9	9.28E+04	0.76	9.14	1.21E+05	0.76
399.358	$C_{23}H_{47}N_2O_3$	Oleic- 1 DMAPA- 2 O	22.43	6.32E+03	-1.75	13.93	1.43E+05	0.50	10.48	9.48E+04	1.00
401.374	$C_{23}H_{49}N_2O_3$	Stearic- 1 DMAPA-2 O	15.41	2.55E+03	-1.74	11.15	6.41E+05	-0.75	11.32	1.79E+05	0.25
411.322	$C_{23}H_{43}N_2O_4$	Linolenic- 1 DMAPA- 3 O	0.45	5.55E+02	1.06	5.07	2.66E+03	-2.59	5.25	2.78E+03	-0.65
413.338	$C_{23}H_{45}N_2O_4$	Linoleic- 1 DMAPA- 3 O	0.45	6.21E+02	-1.73	9.27	1.43E+04	-2.22	8.29	6.94E+03	0.45
415.353	$C_{23}H_{47}N_2O_4$	Oleic- 1 DMAPA- 3 O	0.43	6.22E+03	-0.16	11	5.93E+03	-0.40	6.14	6.05E+03	-1.12
417.369	$C_{23}H_{49}N_2O_4$	Stearic- 1 DMAPA- 3 O	25.42	1.59E+03	-3.39	20.97	6.66E+04	-3.39	21.03	4.69E+04	-3.87
477.416	$C_{28}H_{53}N_4O_2$	Linolenic-2 DMAPA	25.42	1.88E+03	2.73	21.11	2.28E+03	0.43	21.09	3.09E+03	3.78
479.432	$C_{28}H_{55}N_4O_2$	Linoleic- 2 DMAPA	10.92	4.00E+02	0.53	6.85	1.67E+03	-0.72	0.00	0.00E+00	0.00
481.448	$C_{28}H_{57}N_4O_2$	Oleic- 2 DMAPA	35.49	5.78E+02	0.22	10.02	1.85E+03	2.50	9.15	9.88E+02	2.09

Table S 2. MALDI FTICR MS relative intensities for the depolymerized linseed oil film after irradiation at 395 nm for 2 years, at 1/1000 (mg/μL), petroleum ether fractions.

Theoretical *m/z*	**$[M+H]^+$**	**Attribution**	**Irradiated linseed oil for 2 years, Co 0.1%**		**Irradiated linseed oil for 2 years, Co 1%**		**Irradiated linseed oil for 2 years, Co 10%**	
			Intensity	Error (ppm)	Intensity	Error (ppm)	Intensity	Error (ppm)
296.2948	$C_{19}H_{38}NO$	Palmitic with $N(CH_3)_2$ of 1 DMAPA	5.92E+06	-0.27	2.13E+07	-0.20	4.59E+06	0.10
320.2947	$C_{21}H_{38}NO$	Linoleic with $N(CH_3)_2$ of 1 DMAPA	0.00E+00	0.00	0.00E+00	0.00	0.00E+00	0.00
322.3104	$C_{21}H_{40}NO$	Oleic with $N(CH_3)_2$ of 1 DMAPA	2.20E+06	0.19	3.51E+06	0.22	0.00E+00	0.00
324.3261	$C_{21}H_{42}NO$	Stearic with $N(CH_3)_2$ of 1 DMAPA	1.82E+06	0.93	6.18E+06	-0.03	1.44E+06	-0.83
339.33699	$C_{21}H_{43}N_2O$	Palmitoleic- 1 DMAPA	6.57E+07	-0.15	2.56E+08	-0.15	3.73E+07	-0.06
341.3526	$C_{21}H_{45}N_2O$	Palmitic- 1 DMAPA	1.07E+09	-0.09	3.85E+09	0.00	7.33E+08	-0.03
355.3319	$C_{21}H_{43}N_2O_2$	Palmitoleic- 1 DMAPA- 1 O	6.64E+08	-0.14	1.30E+09	-0.06	1.10E+08	-0.11
357.3476	$C_{21}H_{45}N_2O_2$	Palmitic- 1 DMAPA- 1 O	4.24E+08	0.11	7.29E+08	0.14	1.01E+08	0.11
363.33699	$C_{23}H_{43}N_2O$	Linolenic- 1 DMAPA	1.30E+07	-0.06	1.07E+07	-0.08	0.00E+00	0.00
365.3526	$C_{23}H_{45}N_2O$	Linoleic- 1 DMAPA	1.97E+07	-0.22	2.12E+07	-0.22	3.75E+06	0.05
367.3683	$C_{23}H_{47}N_2O$	Oleic- 1 DMAPA	1.61E+08	0.03	6.56E+07	-0.03	1.31E+07	0.03
369.3839	$C_{23}H_{49}N_2O$	Stearic – 1 DMAPA	2.10E+08	-0.22	3.46E+08	-0.19	5.09E+07	-0.14
379.3319	$C_{23}H_{43}N_2O_2$	Linolenic- 1 DMAPA- 1 O	8.67E+07	-0.14	1.09E+08	-0.17	1.39E+07	-0.12
381.3476	$C_{23}H_{45}N_2O_2$	Linoleic- 1 DMAPA- 1 O	5.42E+07	-0.03	1.05E+08	-0.05	1.62E+07	-0.03
383.3632	$C_{23}H_{47}N_2O_2$	Oleic- 1 DMAPA- 1 O	5.25E+08	-0.03	1.10E+09	0.03	1.49E+08	-0.03
385.3789	$C_{23}H_{49}N_2O_2$	Stearic- 1 DMAPA- 1 O	3.33E+08	-0.09	5.35E+08	-0.06	9.96E+07	-0.04
395.3268	$C_{23}H_{43}N_2O_3$	Linolenic- 1 DMAPA- 2 O	2.14E+07	-0.20	2.14E+07	-0.20	4.45E+06	-0.03
397.3425	$C_{23}H_{45}N_2O_3$	Linoleic- 1 DMAPA- 2 O	5.31E+07	0.10	5.70E+07	0.05	1.08E+07	0.25
399.3581	$C_{23}H_{47}N_2O_3$	Oleic- 1 DMAPA- 2 O	1.21E+08	-0.18	1.29E+08	-0.18	1.87E+07	-0.13
401.3738	$C_{23}H_{49}N_2O_3$	Stearic- 1 DMAPA-2 O	9.49E+07	0.05	7.03E+07	0.02	1.71E+07	0.15
411.3217	$C_{23}H_{43}N_2O_4$	Linolenic- 1 DMAPA- 3 O	4.69E+06	0.06	4.93E+06	-0.09	0.00E+00	0.00
413.3373	$C_{23}H_{45}N_2O_4$	Linoleic- 1 DMAPA- 3 O	1.46E+07	-0.06	9.94E+06	-0.16	2.39E+06	-3.40
415.3530	$C_{23}H_{47}N_2O_4$	Oleic- 1 DMAPA- 3 O	2.20E+07	-0.01	1.68E+07	-0.01	2.37E+06	0.06
417.3687	$C_{23}H_{49}N_2O_4$	Stearic- 1 DMAPA- 3 O	6.97E+06	-0.09	2.15E+06	-0.13	0.00E+00	0.00
477.4163	$C_{28}H_{53}N_4O_2$	Linolenic-2 DMAPA	2.43E+07	-0.25	3.61E+07	-0.22	5.85E+06	-0.25

479.43195	$C_{28}H_{55}N_4O_2$	Linoleic- 2 DMAPA	4.19E+07	-0.16	3.83E+07	-0.18	9.46E+06	-0.10
481.4476	$C_{28}H_{57}N_4O_2$	Oleic- 2 DMAPA	6.35E+07	-0.14	6.52E+07	-0.16	1.73E+07	-0.03

Table S 3. MALDI FTICR MS relative intensities for the polymerized linseed oil films in the presence of the cobalt drier cobalt acetylacetonate and the industrial pigment Cobalt Dark Blue after one week and 2 years of polymerization under natural conditions, at 1/1000 (mg/μL), petroleum ether fractions.

Theoretical *m/z*	**$[M+H]^+$**	**Attribution**	**Relative intensity**			
			Polymerized linseed oil for 1 week, Co (II) acetyl acetonate	**Polymerized linseed oil for 2 years, Co (II) acetyl acetonate**	**Polymerized linseed oil for 1 week, Cobalt dark blue**	**Polymerized linseed oil for 2 years, Cobalt dark blue**
296.2948	$C_{19}H_{38}NO$	Palmitic with $N(CH_3)_2$ of 1 DMAPA	1.61E+07	1.87E+07	2.76E+07	4.82E+07
320.2947	$C_{21}H_{38}NO$	Linoleic with $N(CH_3)_2$ of 1 DMAPA	1.05E+07	0.00E+00	2.95E+06	1.86E+06
322.3104	$C_{21}H_{40}NO$	Oleic with $N(CH_3)_2$ of 1 DMAPA	2.48E+07	2.35E+06	2.45E+07	0.00E+00
324.3261	$C_{21}H_{42}NO$	Stearic with $N(CH_3)_2$ of 1 DMAPA	7.89E+06	6.69E+06	3.04E+07	1.78E+07
339.33699	$C_{21}H_{43}N_2O$	Palmitoleic- 1 DMAPA	3.02E+07	1.36E+08	1.48E+08	1.62E+08
341.3526	$C_{21}H_{45}N_2O$	Palmitic- 1 DMAPA	5.51E+08	8.02E+09	4.23E+09	2.79E+09
355.3319	$C_{21}H_{43}N_2O_2$	Palmitoleic- 1 DMAPA- 1 O	3.06E+07	2.92E+08	1.41E+07	1.53E+08
357.3476	$C_{21}H_{45}N_2O_2$	Palmitic- 1 DMAPA- 1 O	1.35E+08	3.89E+08	3.01E+08	3.44E+08
363.33699	$C_{23}H_{43}N_2O$	Linolenic- 1 DMAPA	5.26E+09	2.88E+06	5.21E+07	0.00E+00
365.3526	$C_{23}H_{45}N_2O$	Linoleic- 1 DMAPA	2.03E+09	1.81E+07	9.60E+08	2.89E+07
367.3683	$C_{23}H_{47}N_2O$	Oleic- 1 DMAPA	7.71E+09	1.11E+08	1.10E+10	5.89E+07
369.3839	$C_{23}H_{49}N_2O$	Stearic – 1 DMAPA	2.94E+08	2.12E+09	3.69E+09	1.21E+09
379.3319	$C_{23}H_{43}N_2O_2$	Linolenic- 1 DMAPA- 1 O	2.17E+07	1.80E+07	2.04E+07	1.68E+07
381.3476	$C_{23}H_{45}N_2O_2$	Linoleic- 1 DMAPA- 1 O	4.11E+07	3.50E+07	8.21E+07	2.67E+07
383.3632	$C_{23}H_{47}N_2O_2$	Oleic- 1 DMAPA- 1 O	1.03E+09	6.25E+08	2.83E+09	3.18E+08
385.3789	$C_{23}H_{49}N_2O_2$	Stearic- 1 DMAPA- 1 O	1.18E+08	4.43E+08	3.29E+08	4.75E+08
395.3268	$C_{23}H_{43}N_2O_3$	Linolenic- 1 DMAPA- 2 O	7.80E+06	4.45E+06	5.35E+06	5.72E+06
397.3425	$C_{23}H_{45}N_2O_3$	Linoleic- 1 DMAPA- 2 O	1.80E+07	2.86E+07	7.97E+07	4.61E+07
399.3581	$C_{23}H_{47}N_2O_3$	Oleic- 1 DMAPA- 2 O	1.81E+07	5.25E+07	6.23E+07	3.42E+07
401.3738	$C_{23}H_{49}N_2O_3$	Stearic- 1 DMAPA- 2 O	7.08E+08	2.97E+08	1.11E+09	9.40E+07
411.3217	$C_{23}H_{43}N_2O_4$	Linolenic- 1 DMAPA- 3 O	6.54E+06	1.47E+06	2.89E+06	0.00E+00
413.3374	$C_{23}H_{45}N_2O_4$	Linoleic- 1 DMAPA- 3 O	5.19E+06	3.62E+06	3.19E+06	3.66E+06
415.3530	$C_{23}H_{47}N_2O_4$	Oleic- 1 DMAPA- 3 O	1.69E+07	4.75E+06	2.20E+07	2.93E+06
417.3687	$C_{27}H_{57}N_2O$	Stearic- 1 DMAPA- 3 O	3.08E+06	1.13E+07	1.04E+07	3.92E+06
425.4465	$C_{23}H_{43}N_2O_5$	Behenic-1DMAPA	3.36E+07	1.13E+07	4.53E+07	5.30E+06

427.3167	$C_{23}H_{49}N_2O_4$	-	4.93E+06	0.00E+00	1.79E+06	0.00E+00
477.4163	$C_{28}H_{53}N_4O_2$	Linolenic-2 DMAPA	5.99E+06	1.69E+07	2.74E+07	1.84E+07
479.43195	$C_{28}H_{55}N_4O_2$	Linoleic- 2 DMAPA	1.75E+06	5.58E+06	0.00E+00	4.54E+06
481.4476	$C_{28}H_{57}N_4O_2$	Oleic- 2 DMAPA	2.20E+06	1.27E+07	3.06E+06	8.42E+06
641.5616	$C_{41}H_{73}N_2O_3$	C36:6- 1 DMAPA-2 O	0.00E+00	0.00E+00	0.00E+00	0.00E+00
643.5772	$C_{41}H_{75}N_2O_3$	C36:5- 1 DMAPA-2 O	0.00E+00	0.00E+00	0.00E+00	0.00E+00
645.5929	$C_{41}H_{77}N_2O_3$	C36:4- 1 DMAPA-2 O	0.00E+00	0.00E+00	0.00E+00	0.00E+00
671.5721	$C_{42}H_{75}N_2O_4$	C37:6- 1 DMAPA-3 O	0.00E+00	0.00E+00	0.00E+00	0.00E+00
725.6667	$C_{46}H_{85}N_4O_2$	Linolenic, linoleic C-C dimer– 2 DMAPA	3.86E+06	0.00E+00	0.00E+00	0.00E+00
727.6823	$C_{46}H_{87}N_4O_2$	Linoleic C-C dimer– 2 DMAPA	4.01E+06	0.00E+00	0.00E+00	0.00E+00
729.6981	$C_{46}H_{89}N_4O_2$	Linoleic, oleic C-C dimer– 2 DMAPA	0.00E+00	0.00E+00	0.00E+00	0.00E+00
741.6616	$C_{46}H_{85}N_4O_3$	Linolenic, linoleic C-O dimer– 2 DMAPA	1.79E+06	0.00E+00	0.00E+00	0.00E+00
743.6773	$C_{46}H_{87}N_4O_3$	Linoleic C-O dimer– 2 DMAPA	0.00E+00	0.00E+00	0.00E+00	0.00E+00
745.6934	$C_{46}H_{89}N_4O_3$	Linoleic, oleic C-O dimer– 2 DMAPA	0.00E+00	0.00E+00	0.00E+00	0.00E+00
757.6565	$C_{46}H_{85}N_4O_4$	Linolenic, linoleic dimer +2O– 2 DMAPA	5.84E+06	0.00E+00	1.83E+06	0.00E+00
759.6722	$C_{46}H_{87}N_4O_4$	Linoleic dimer +2O– 2 DMAPA	4.44E+06	0.00E+00	1.96E+06	0.00E+00
761.6875	$C_{46}H_{89}N_4O_4$	Linoleic, oleic dimer +2O– 2 DMAPA	0.00E+00	0.00E+00	0.00E+00	0.00E+00
773.6515	$C_{46}H_{85}N_4O_5$	Linolenic, linoleic dimer +3O– 2 DMAPA	2.13E+06	1.76E+06	7.97E+06	0.00E+00
775.6617	$C_{46}H_{87}N_4O_5$	Linoleic dimer +3O– 2 DMAPA	2.39E+06	0.00E+00	3.56E+06	0.00E+00
777.6828	$C_{46}H_{89}N_4O_5$	Linoleic, oleic dimer +3O– 2 DMAPA	4.78E+06	0.00E+00	7.99E+06	3.44E+06
789.6464	$C_{46}H_{85}N_4O_6$	Linolenic, linoleic dimer +4O– 2 DMAPA	3.88E+06	0.00E+00	6.04E+06	0.00E+00
791.6621	$C_{46}H_{87}N_4O_6$	Linoleic dimer +4O– 2 DMAPA	4.85E+06	0.00E+00	4.26E+06	0.00E+00
793.6776	$C_{46}H_{89}N_4O_6$	Linoleic, oleic dimer +4O– 2 DMAPA	5.26E+06	0.00E+00	0.00E+00	1.68E+06
805.6413	$C_{46}H_{85}N_4O_7$	Linolenic, linoleic dimer +5O– 2 DMAPA	1.96E+06	0.00E+00	3.01E+06	1.95E+06
807.65693	$C_{46}H_{87}N_4O_7$	Linoleic dimer +5O– 2 DMAPA	2.16E+06	0.00E+00	2.78E+06	0.00E+00
809.6727	$C_{46}H_{89}N_4O_7$	Linoleic, oleic dimer +5O– 2 DMAPA	2.52E+06	0.00E+00	3.25E+06	1.98E+06
821.6362	$C_{46}H_{85}N_4O_8$	Linolenic, linoleic dimer +6O– 2 DMAPA	2.01E+06	0.00E+00	1.93E+06	0.00E+00

823.6518	$C_{46}H_{87}N_4O_8$	Linoleic dimer +6O– 2 DMAPA	2.27E+06	0.00E+00	2.27E+06	0.00E+00
825.6677	$C_{46}H_{89}N_4O_8$	Linoleic, oleic dimer +6O– 2 DMAPA	0.00E+00	0.00E+00	0.00E+00	0.00E+00
837.6311	$C_{46}H_{85}N_4O_9$	Linolenic, linoleic dimer +7O– 2 DMAPA	0.00E+00	0.00E+00	0.00E+00	0.00E+00
839.6468	$C_{46}H_{87}N_4O_9$	Linoleic dimer +7O– 2 DMAPA	0.00E+00	0.00E+00	0.00E+00	0.00E+00
841.6624	$C_{46}H_{89}N_4O_9$	Linoleic, oleic dimer +7O– 2 DMAPA	0.00E+00	0.00E+00	0.00E+00	0.00E+00

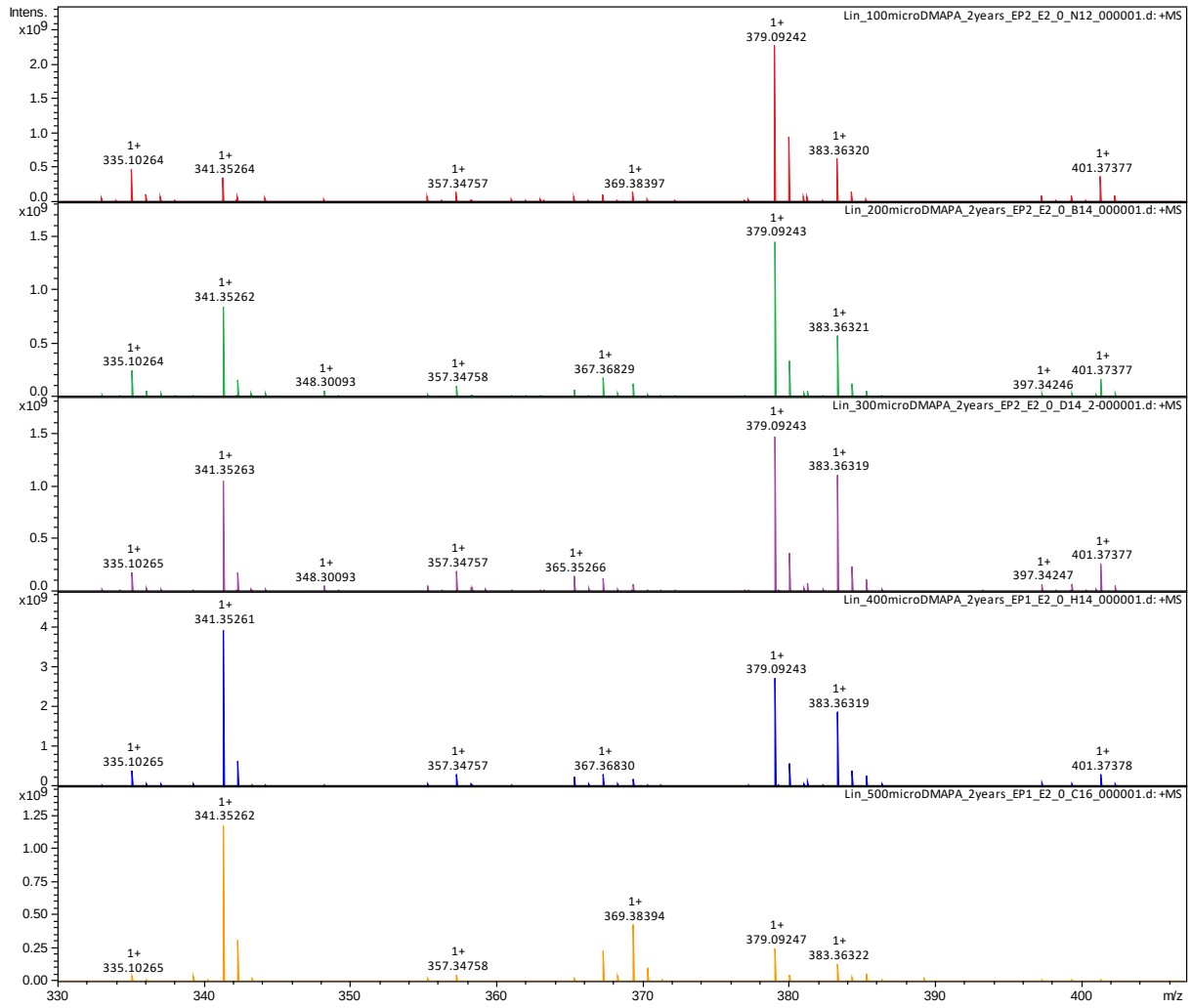


Figure S 5. MALDI FTICR MS spectra of the depolymerized oil paint of 0.5 mg starting quantity treated with 100 µL, 200 µL, 300 µL, 400 µL and 500 µL of DMAPA respectively (*m/z* 330-407), dilution 1mg/1000 µL, petroleum ether fractions.

Table S 4. MALDI FTICR MS relative intensities for the polymerized *Sennelier* oil paint Prussian Blue after one week of autoxidation under natural conditions (petroleum ether (PE) and ethyl acetate (EA) fractions) and their corresponding data without polymerization (tube, PE fraction), in addition to Titanium White after polymerization (PE fraction) at 1/1000 (mg/μL).

Theoretical *m/z*	$[M+H]^+$	Attribution	Relative intensity			
			Prussian Blue-Tube	Prussian Blue polymerized for 1 week, EA	Prussian Blue polymerized for 1 week, PE	Titanium White, polymerized for 1 week, PE
296.2948	$C_{19}H_{38}NO$	Palmitic with $N(CH_3)_2$ of 1 DMAPA	3.42E+06	3.88E+06	5.03E+07	4.01E+07
320.2947	$C_{21}H_{38}NO$	Linoleic with $N(CH_3)_2$ of 1 DMAPA	1.39E+07	2.18E+06	2.02E+07	3.74E+06
322.3104	$C_{21}H_{40}NO$	Oleic with $N(CH_3)_2$ of 1 DMAPA	2.93E+06	3.64E+06	4.71E+07	1.89E+07
324.3261	$C_{21}H_{42}NO$	Stearic with $N(CH_3)_2$ of 1 DMAPA	0.00E+00	0.00E+00	9.99E+06	6.12E+06
339.33699	$C_{21}H_{43}N_2O$	Palmitoleic- 1 DMAPA	1.25E+07	2.20E+07	8.76E+07	2.05E+07
341.3526	$C_{21}H_{45}N_2O$	Palmitic- 1 DMAPA	3.24E+08	5.61E+08	5.90E+09	6.02E+08
355.3319	$C_{21}H_{43}N_2O_2$	Palmitoleic- 1 DMAPA- 1 O	4.76E+06	1.32E+07	4.79E+07	1.74E+07
357.3476	$C_{21}H_{45}N_2O_2$	Palmitic- 1 DMAPA- 1 O	3.94E+06	3.85E+07	9.77E+07	6.41E+07
363.33699	$C_{23}H_{43}N_2O$	Linolenic- 1 DMAPA	1.55E+08	6.63E+07	1.98E+08	3.75E+06
365.3526	$C_{23}H_{45}N_2O$	Linoleic- 1 DMAPA	7.56E+08	1.61E+08	9.60E+08	5.09E+07
367.3683	$C_{23}H_{47}N_2O$	Oleic- 1 DMAPA	4.81E+08	5.98E+08	3.73E+09	2.33E+08
369.3839	$C_{23}H_{49}N_2O$	Stearic – 1 DMAPA	5.13E+07	8.38E+07	2.75E+08	5.70E+07
379.3319	$C_{23}H_{43}N_2O_2$	Linolenic- 1 DMAPA- 1 O	5.48E+07	4.47E+07	6.28E+07	1.06E+07
381.3476	$C_{23}H_{45}N_2O_2$	Linoleic- 1 DMAPA- 1 O	9.30E+07	2.62E+08	7.30E+08	1.04E+08
383.3632	$C_{23}H_{47}N_2O_2$	Oleic- 1 DMAPA- 1 O	1.19E+07	2.51E+08	8.75E+08	6.35E+08
385.3789	$C_{23}H_{49}N_2O_2$	Stearic- 1 DMAPA- 1 O	1.80E+06	1.54E+07	6.40E+07	3.37E+07
395.3268	$C_{23}H_{43}N_2O_3$	Linolenic- 1 DMAPA- 2 O	2.87E+07	4.25E+07	3.96E+07	9.44E+06
397.3425	$C_{23}H_{45}N_2O_3$	Linoleic- 1 DMAPA- 2 O	1.33E+08	3.11E+08	1.68E+08	4.08E+07
399.3581	$C_{23}H_{47}N_2O_3$	Oleic- 1 DMAPA- 2 O	2.95E+07	7.37E+07	7.66E+07	4.57E+07
401.3738	$C_{23}H_{49}N_2O_3$	Stearic- 1 DMAPA-2 O	4.42E+06	4.86E+07	8.33E+07	5.91E+07
411.3217	$C_{23}H_{43}N_2O_4$	Linolenic- 1 DMAPA- 3 O	1.03E+07	8.96E+06	4.14E+06	1.67E+06
413.3374	$C_{23}H_{45}N_2O_4$	Linoleic- 1 DMAPA- 3 O	3.88E+07	3.87E+07	7.26E+06	2.24E+06
415.3530	$C_{23}H_{47}N_2O_4$	Oleic- 1 DMAPA- 3 O	1.68E+07	1.47E+08	1.19E+07	3.83E+06
417.3687	$C_{27}H_{57}N_2O$	Stearic- 1 DMAPA- 3 O	0.00E+00	3.81E+06	1.45E+06	2.80E+06
425.4465	$C_{23}H_{43}N_2O_5$	Behenic-1DMAPA	1.83E+06	2.12E+06	0.00E+00	0.00E+00
427.3167	$C_{23}H_{49}N_2O_4$	-	4.17E+06	3.50E+06	2.09E+06	0.00E+00
461.4214	$C_{28}H_{53}N_4O$	Linolenic aldehyde- 2 DMAPA	1.09E+08	7.17E+08	1.16E+09	5.14E+08
477.4163	$C_{28}H_{53}N_4O_2$	Linolenic-2 DMAPA	1.34E+07	1.68E+08	2.74E+08	7.72E+07

479.43195	$C_{28}H_{55}N_4O_2$	Linoleic- 2 DMAPA	3.34E+06	2.65E+07	1.38E+07	4.53E+06
481.4476	$C_{28}H_{57}N_4O_2$	Oleic- 2 DMAPA	4.74E+06	1.77E+07	8.78E+06	3.13E+06
671.5721	$C_{41}H_{73}N_2O_3$	C37:6- 1 DMAPA-3 O	0.00E+00	1.53E+06	0.00E+00	1.59E+06
725.6667	$C_{41}H_{75}N_2O_3$	Linolenic, linoleic C-C dimer– 2 DMAPA	0.00E+00	0.00E+00	0.00E+00	1.53E+06
727.6823	$C_{41}H_{77}N_2O_3$	Linoleic C-C dimer– 2 DMAPA	0.00E+00	0.00E+00	0.00E+00	0.00E+00
729.6981	$C_{42}H_{75}N_2O_4$	Linoleic, oleic C-C dimer– 2 DMAPA	0.00E+00	0.00E+00	0.00E+00	0.00E+00
741.6616	$C_{46}H_{85}N_4O_2$	Linolenic, linoleic C-O dimer– 2 DMAPA	0.00E+00	0.00E+00	0.00E+00	0.00E+00
743.6773	$C_{46}H_{87}N_4O_2$	Linoleic C-O dimer– 2 DMAPA	2.35E+06	0.00E+00	0.00E+00	0.00E+00
745.6934	$C_{46}H_{89}N_4O_2$	Linoleic, oleic C-O dimer– 2 DMAPA	0.00E+00	0.00E+00	0.00E+00	1.79E+06
757.6565	$C_{46}H_{85}N_4O_3$	Linolenic, linoleic dimer +2O– 2 DMAPA	0.00E+00	0.00E+00	0.00E+00	0.00E+00
759.6722	$C_{46}H_{87}N_4O_3$	Linoleic dimer +2O– 2 DMAPA	2.03E+06	0.00E+00	0.00E+00	0.00E+00
761.6875	$C_{46}H_{89}N_4O_3$	Linoleic, oleic dimer +2O– 2 DMAPA	2.87E+06	0.00E+00	0.00E+00	0.00E+00
773.6515	$C_{46}H_{85}N_4O_4$	Linolenic, linoleic dimer +3O– 2 DMAPA	1.66E+06	0.00E+00	0.00E+00	0.00E+00
775.6617	$C_{46}H_{87}N_4O_4$	Linoleic dimer +3O– 2 DMAPA	2.48E+06	1.68E+06	3.18E+06	0.00E+00
777.6828	$C_{46}H_{89}N_4O_4$	Linoleic, oleic dimer +3O– 2 DMAPA	2.78E+06	2.56E+06	2.14E+06	0.00E+00
789.6464	$C_{46}H_{85}N_4O_5$	Linolenic, linoleic dimer +4O– 2 DMAPA	0.00E+00	2.82E+06	0.00E+00	0.00E+00
791.6621	$C_{46}H_{87}N_4O_5$	Linoleic dimer +4O– 2 DMAPA	1.69E+06	0.00E+00	2.49E+06	0.00E+00
793.6776	$C_{46}H_{89}N_4O_5$	Linoleic, oleic dimer +4O– 2 DMAPA	0.00E+00	2.28E+06	0.00E+00	0.00E+00
805.6413	$C_{46}H_{85}N_4O_6$	Linolenic, linoleic dimer +5O– 2 DMAPA	0.00E+00	1.60E+06	0.00E+00	0.00E+00
807.65693	$C_{46}H_{87}N_4O_6$	Linoleic dimer +5O– 2 DMAPA	1.61E+06	1.67E+06	0.00E+00	0.00E+00
809.6727	$C_{46}H_{89}N_4O_6$	Linoleic, oleic dimer +5O– 2 DMAPA	2.17E+06	1.81E+06	0.00E+00	0.00E+00
821.6362	$C_{46}H_{85}N_4O_7$	Linolenic, linoleic dimer +6O– 2 DMAPA	0.00E+00	0.00E+00	0.00E+00	0.00E+00
823.6518	$C_{46}H_{87}N_4O_7$	Linoleic dimer +6O– 2 DMAPA	0.00E+00	0.00E+00	0.00E+00	2.10E+06
825.6677	$C_{46}H_{89}N_4O_7$	Linoleic, oleic dimer +6O– 2 DMAPA	0.00E+00	0.00E+00	0.00E+00	1.71E+06
837.6311	$C_{46}H_{85}N_4O_8$	Linolenic, linoleic dimer +7O– 2 DMAPA	0.00E+00	0.00E+00	1.74E+06	0.00E+00
839.6468	$C_{46}H_{87}N_4O_8$	Linoleic dimer +7O– 2 DMAPA	0.00E+00	0.00E+00	0.00E+00	0.00E+00
841.6624	$C_{46}H_{89}N_4O_8$	Linoleic, oleic dimer +7O– 2 DMAPA	0.00E+00	0.00E+00	0.00E+00	0.00E+00

Annex: First trials before finding the best methodology

1. Experimental work

1.1. Adjusting formic acid ratio in transamidation methodology

Siccative oils from different suppliers: *Sennelier* (Paris, France), *Le Franc Bourgeois* (Paris, France), *Gamblin* (Portland, OR, USA), *Michael Harding* (London, UK) and *Winsor & Newton* (London, UK) were studied starting from 100 mg of sample followed by 1 mL addition of DMAPA then the transamidation reaction was quenched with 100 µL of formic acid. After extraction with petroleum ether and ethyl acetate solvents, the extraction yield was higher than 100%.

So, this method was modified only at the step of neutralization. A neutralization with an excess of formic acid was achieved using 400 µL of formic acid instead of 100 µL. This improvement allowed to avoid the spurious extraction of DMAPA.

1.2. HFIP introduction

Another approach incorporating HFIP before transamidation (as in the case of PET) was tested. Indeed, an optimization of quantities and protocol steps have been made: In a glass tube, 5 mg of oil paint was put with 400 mg of HFIP for 1 day under stirring at room temperature but the oil paints were not soluble in HFIP even after 6 days. Heating at the reflux temperature of HFIP was also tested as shown in the following section.

The obtained mixture was transamidated with 1 mL of DMAPA at room temperature for 1 day, so the paint was perfectly soluble. The reaction was stopped by 400 µL of formic acid and the products put in 2 mL of ultrapure water were extracted first with petroleum ether then with ethyl acetate by centrifugation at 10,000 rpm for 5 minutes, two times for each organic solvent. The organic phases were collected, dried and analyzed by LC-MS and MALDI FTICR MS as previously.

Using this approach with HFIP, many samples have been studied from canvases of 3 years old and 30 years old (Annex 1 & 2).



Annex 1. Oil paints' mock-up canvas of 3 years old; and their analyzed green and brown samples respectively.



Annex 2. Oil paint on canvas of 30 years old; and close-up of the studied area respectively. The white arrow indicates the position of the analyzed green sample.

1.3. Comparison of methods with and without HFIP

Both methods with and without HFIP were compared using the mock-up samples of 1 year of linseed and poppy oils without drier or artificial ageing. Here, to improve the solubilization in HFIP, the sample was put in glass centrifugation tube of 15 mL and put directly in oil bath preheated at 58 °C for 1 day before doing the transamidation at room temperature.

The 1 year's polymerized linseed oil film was not very well solubilized in HFIP. But, the 1 year's polymerized poppy oil film was perfectly soluble in HFIP. These two samples were soluble after addition of DMAPA (Annex 3). Meanwhile, the direct addition of DMAPA without HFIP to both oil films' samples allowed a perfect solubility after 1 day of stirring at room temperature without heating (Annex 4).

(a) (b) (c)



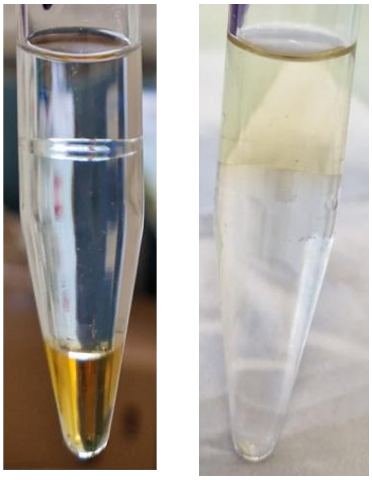
Annex 3. Solubility aspects in HFIP of linseed oil and poppy oil mock-up samples of 1 year old. (a), (b): Before and (c): After DMAPA addition.



Annex 4. Solubility aspects in DMAPA (without HFIP addition) of linseed oil (left panel) and poppy oil (right panel) mock-up samples of 1 year old.

For both methods, the extraction with petroleum ether formed three distinct phases instead of two phases but the extraction with ethyl acetate formed two phases (Annex 5).

(a) (b)



Annex 5. Solubility aspects of linseed oil films of 1 year old after centrifugation with (a): Petroleum ether and (b): Ethyl acetate solvents.

Extraction yields were also compared for the used two methods as shown in Table 1.

Table 1. Recovered weight (mg) of linseed and poppy oils polymerized for 1 year under natural conditions, after depolymerization with and without HFIP (PE: Petroleum ether and EA: Ethyl acetate).

	Linseed oil without HFIP	**Linseed oil with HFIP**	**Poppy oil without HFIP**	**Poppy oil with HFIP**
PE1	0.8	1.2	1.2	1.3
PE2	0.3	0.4	0.5	0.2
EA1	1.4	4.5	1.5	5.5
EA2	6.5	0.2	0.9	0.4

A solubility test has been performed with the different used solvents and reagents in order to adjust and validate the place of each product. Indeed, HFIP, solvent, water, DMAPA and formic acid were added in precise volumes to mimic our present conditions.

10 tests were performed as shown in Table 2.

Table 2. Solubility tests ingredients (PE: Petroleum ether and EA: Ethyl acetate).

Test N°	**HFIP weight (mg)**	**Solvent type + volume (µL)**	**Water volume (µL)**	**DMAPA volume (µL)**	**Formic acid volume (µL)**
N° 1-1	800 = 0.5 mL	PE, 500	-	-	-
N° 1-2	800 = 0.5 mL	EA, 500	-	-	-
N° 2-1	800 = 0.5 mL	PE, 500	500	-	-
N° 2-2	800 = 0.5 mL	EA, 500	500	-	-
N° 3-1	200	PE, 1000	1000	500	-
N° 3-2	200	EA, 1000	1000	500	-
N° 4-1	200	PE, 1000	1000	500	200
N° 4-2	200	EA, 1000	1000	500	200
N° 5	400	-	1000	1000	-
N° 6	400	-	1000	1000	400

At first general test, HFIP and water were miscible forming only one transparent phase (Annex 6 (a)). HFIP, water and DMAPA were also miscible (test N° 5, Annex 6 (b)). However, HFIP, water, DMAPA and formic acid constituted two phases (test N° 6, Annex 6 (c)).

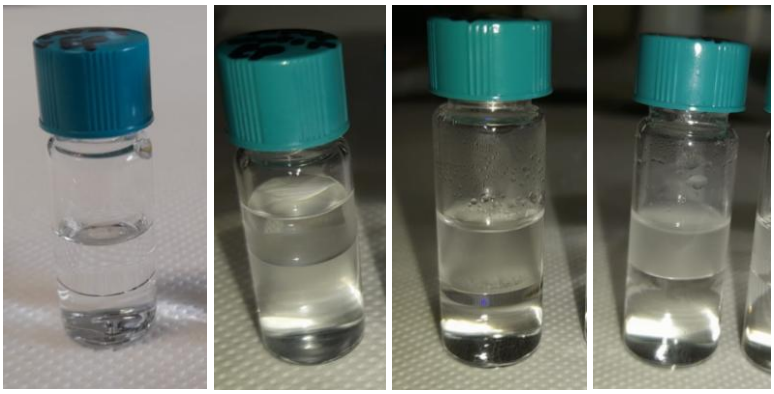
(a) (b) (c)



Annex 6. Solubility tests mixtures. (a): HFIP and water; (b): HFIP, water and DMAPA; (c): HFIP, water, DMAPA and formic acid.

The tests with petroleum ether solvent gives the following phases: Two with HFIP alone; two with HFIP and water in which the upper phase is petroleum ether; 3 phases with HFIP, water and DMAPA and also 3 phases with HFIP, water, DMAPA and formic acid (Annex 7).

(a) (b) (c) (d)



Annex 7. Solubility tests mixtures in the presence of petroleum ether with: (a): HFIP; (b): HFIP and water; (c): HFIP, water and DMAPA; and (d): HFIP, water, DMAPA and formic acid.

However, the tests with ethyl acetate solvent gives the following phases: Two with HFIP alone; two with HFIP and water in which the upper phase is ethyl acetate; 3 phases with HFIP, water and DMAPA in which HFIP is at the bottom and 3 phases with HFIP, water, DMAPA and formic acid (Annex 8).

(a) (b) (c) (d)



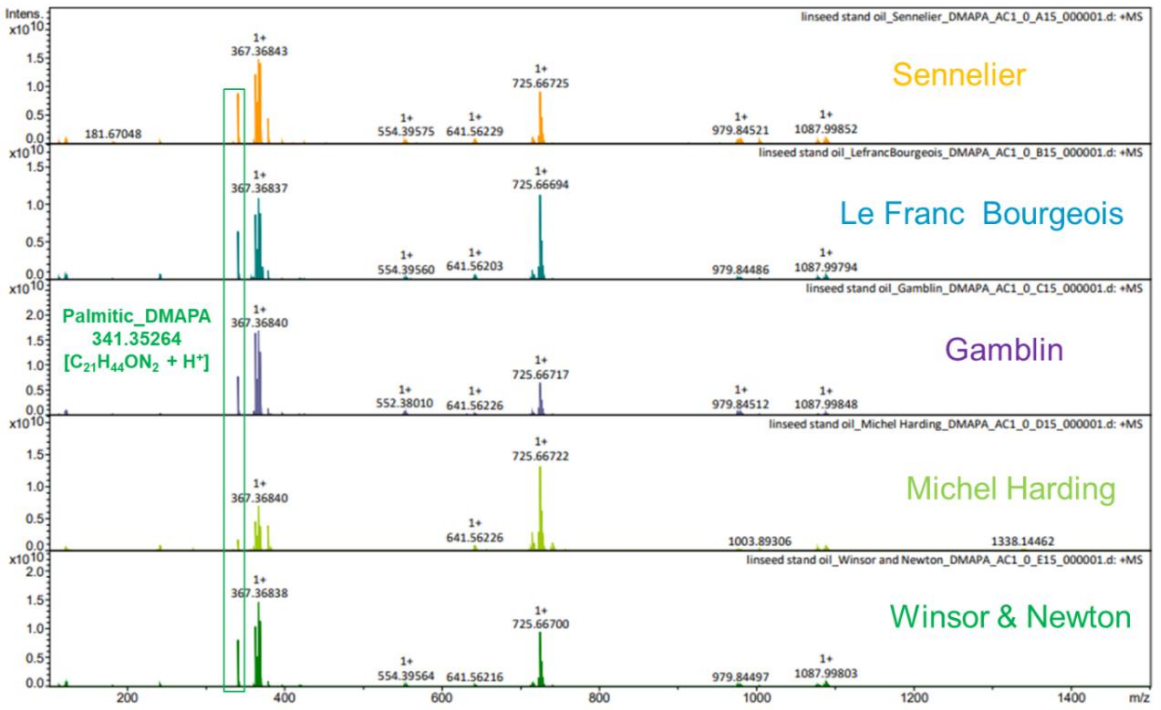
Annex 8. Solubility tests mixtures in the presence of ethyl acetate with: (a): HFIP; (b): HFIP and water; (c): HFIP, water and DMAPA; and (d): HFIP, water, DMAPA and formic acid.

2. Results and discussions

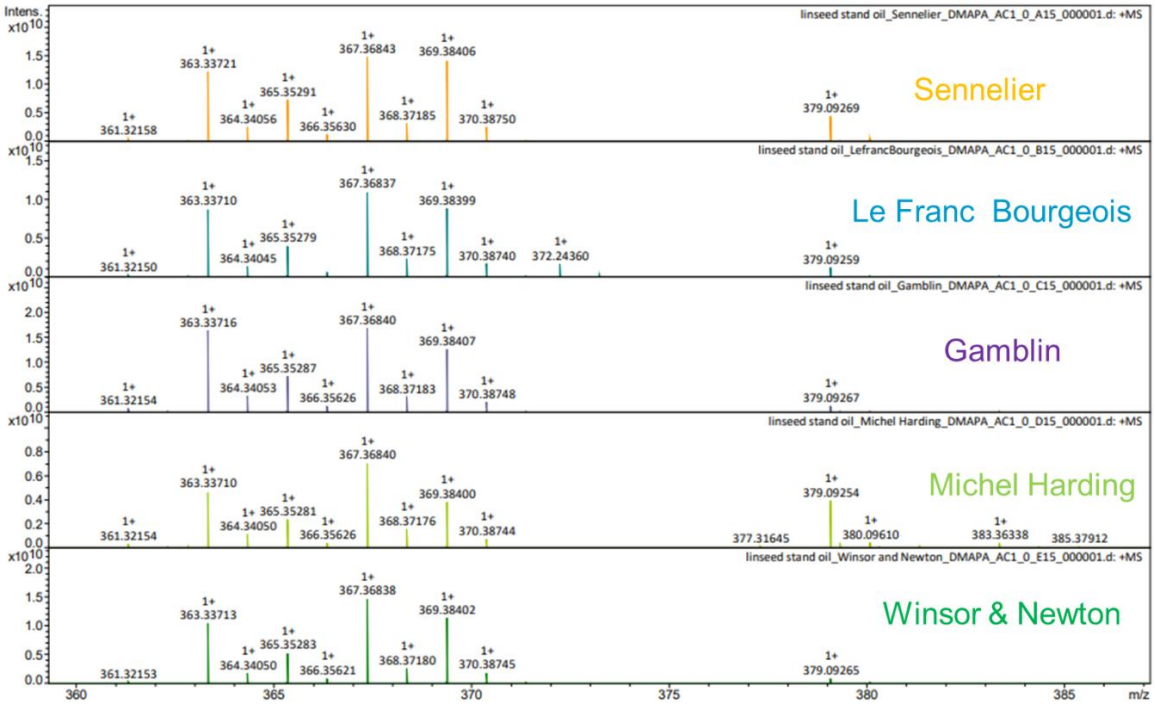
2.1. Siccative native oils: Effect of oils' suppliers/manufacturers

Siccative native linseed oils from different suppliers were studied: *Sennelier* (France), *Le Franc Bourgeois* (France), *Gamblin* (US), *Michael Harding* (UK) and *Winsor & Newton* (UK). MALDI FTICR MS analysis of the ethyl acetate fractions of these oils showed the presence of the saturated palmitic acid (C16:0) appearing at *m/z* 341.3526 in all blends with different intensity (Annex 9 (a)). Stearic (C18:0), linoleic (C18:2) and oleic (C18:1) acids have appeared at *m/z* 369.3839, 365.3526 and 367.3683 respectively with different intensities depending on the oil's supplier. The linolenic acid (C18:3) appeared also in all analyzed oils at *m/z* 363.3369. The British *Michel Harding* siccative oil had a peak at *m/z* 383.3632 that corresponds to the oxygenated oleic acid (Annex 9 (b)).

All the mentioned fatty acids have been appeared mono-derivatized.



(a)



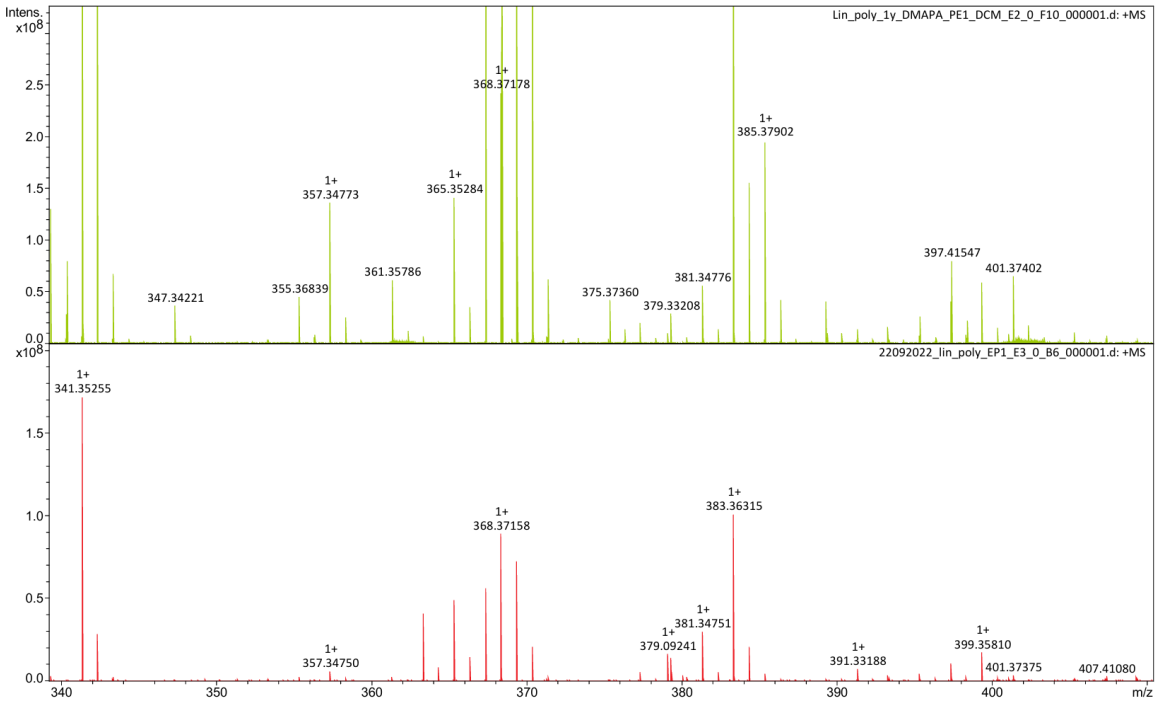
(b)

Annex 9. MALDI FTICR MS spectra of native linseed oil from 5 different suppliers from France and UK. (a): Full spectra *m/z* 100-1,500, (b): Spectra *m/z* 358-387.

2.2. Oil mock up samples: Effect of oil type, polymerization time and drier

First, linseed oil mock-up samples polymerized for one week and one year under natural conditions were compared.

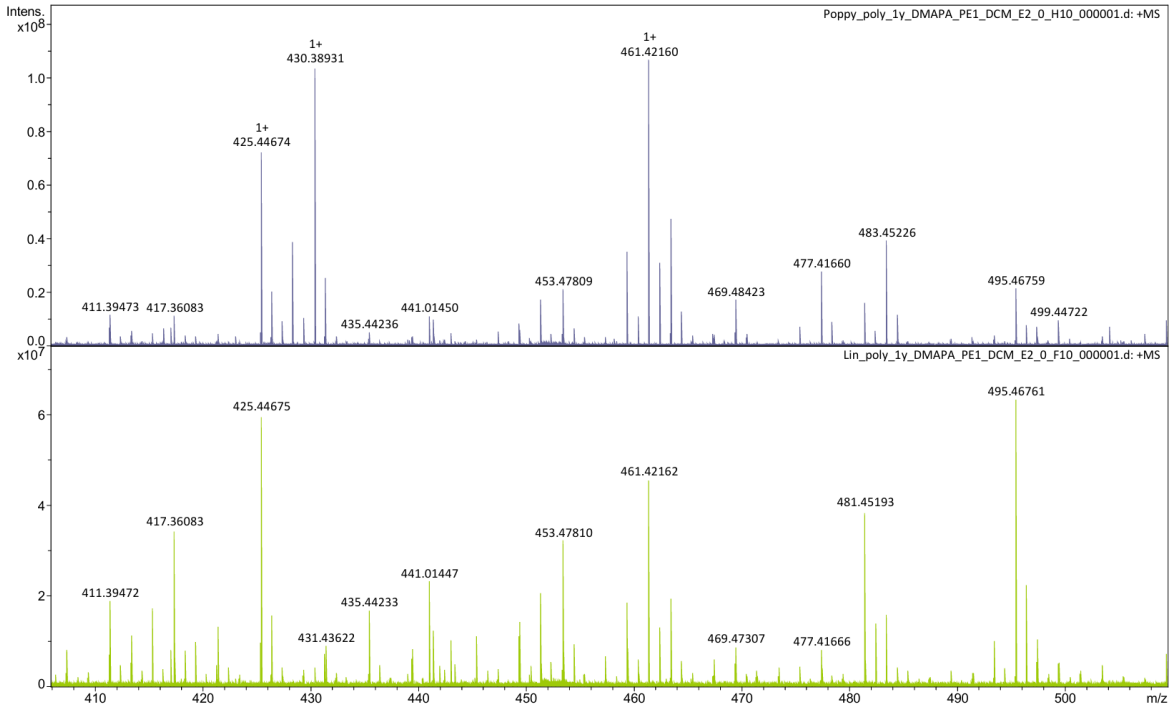
The linseed oil polymeric film without drier and polymerized for one week were analyzed by MALDI FTICR MS. The more aged film of 1 year showed higher intensities in general especially for the oxygenated products. Some compounds have disappeared partially or totally after one year such as the peak appearing at *m/z* 631.5521 of chemical formula $C_{38}H_{71}N_4O_3$ corresponding to octacosatetraenoic acid with two DMAPA molecules and one oxygen (Annex 10).



Annex 10. MALDI FTICR MS spectra of depolymerized linseed oil mock up samples naturally dried *m/z* 339-409. Upper panel: After 1 year of polymerization; lower panel: After 1 week of polymerization.

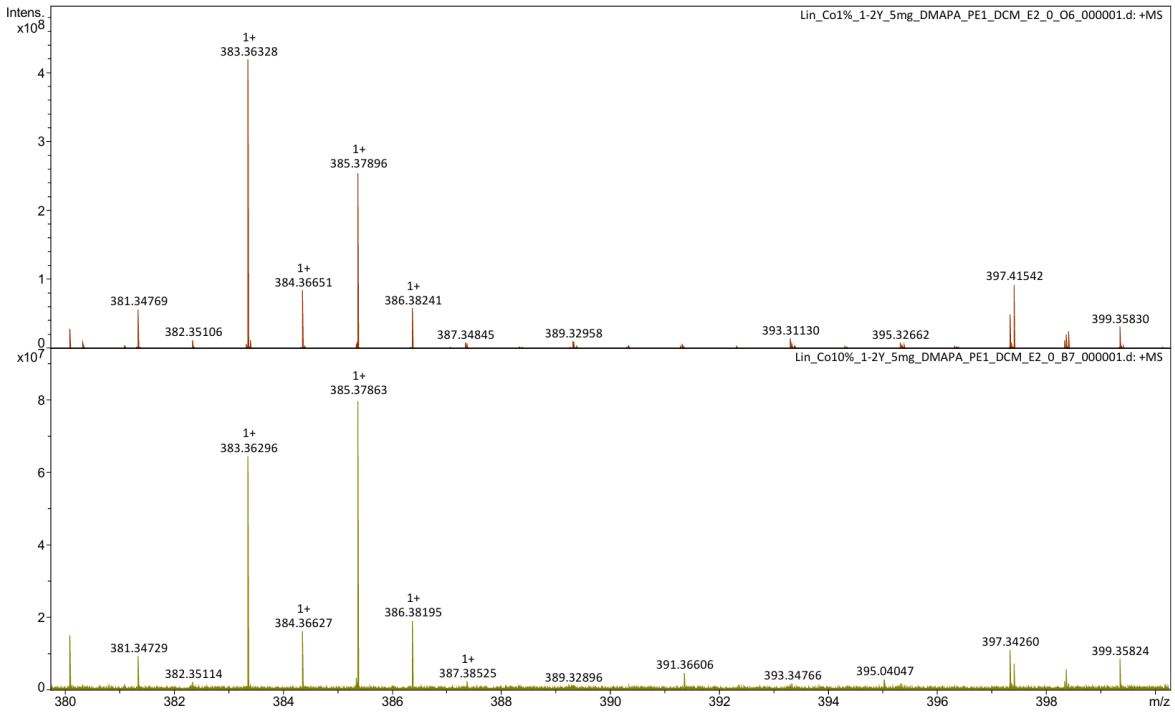
Then, MALDI FTICR MS analysis of poppy and linseed oils polymerized for almost 1 year under natural conditions showed also the presence of the common main fatty acids' peaks with different intensities.

Many peaks between *m/z* 405 and *m/z* 500 were detected as shown in Annex 11. This confirms the effect of the type of oil on its siccativation mechanism.



Annex 11. MALDI FTICR MS spectra of poppy and linseed oil polymerized naturally for 1 year respectively.

In addition, the comparison between linseed oil film polymerized naturally for 1 year with different percentages of cobalt drier showed differences in the intensity of common peaks. More oxidation occurred with more drier percentages as indicating in Annex 12 comparing the two films of linseed oil with Co 1% and Co 10% (Co(II), bis(2-ethylhexanoate)). This confirmed the previous data mentioned in my articles: the ageing depends on the percentage of drier added to the oil.

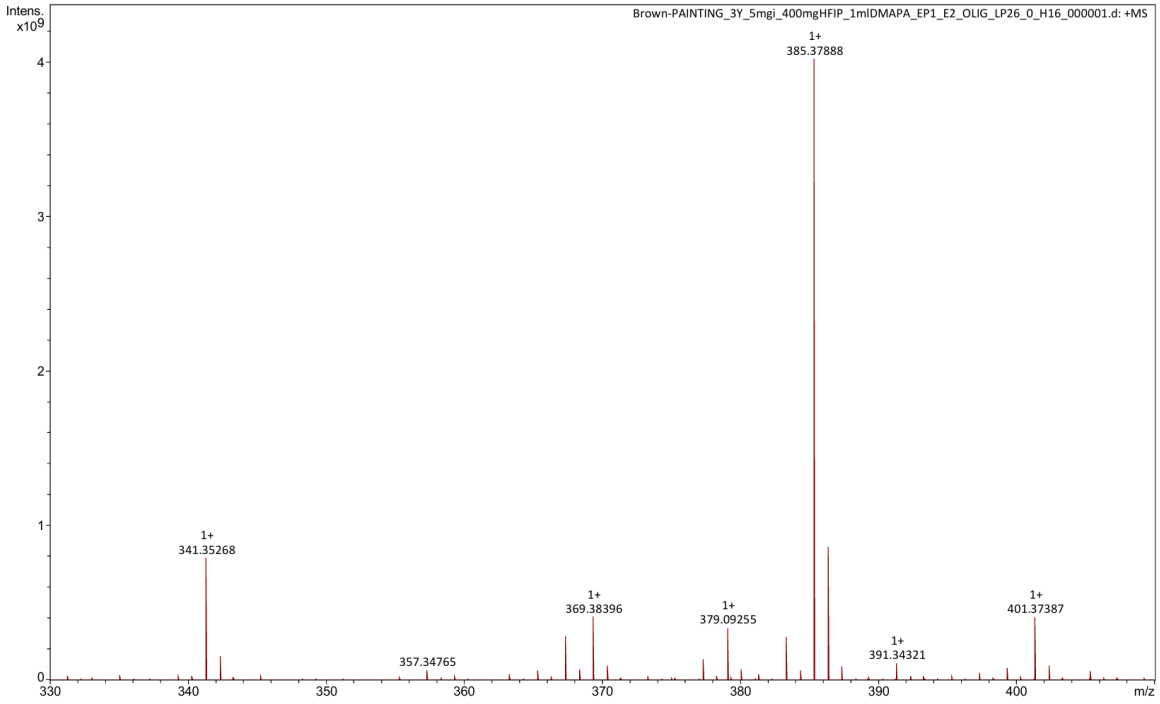


Annex 12. MALDI FTICR MS spectra of linseed oil polymerized naturally for 1 year: With Co 1% and Co 10% respectively.

2.3. Application on canvas and oil paintings

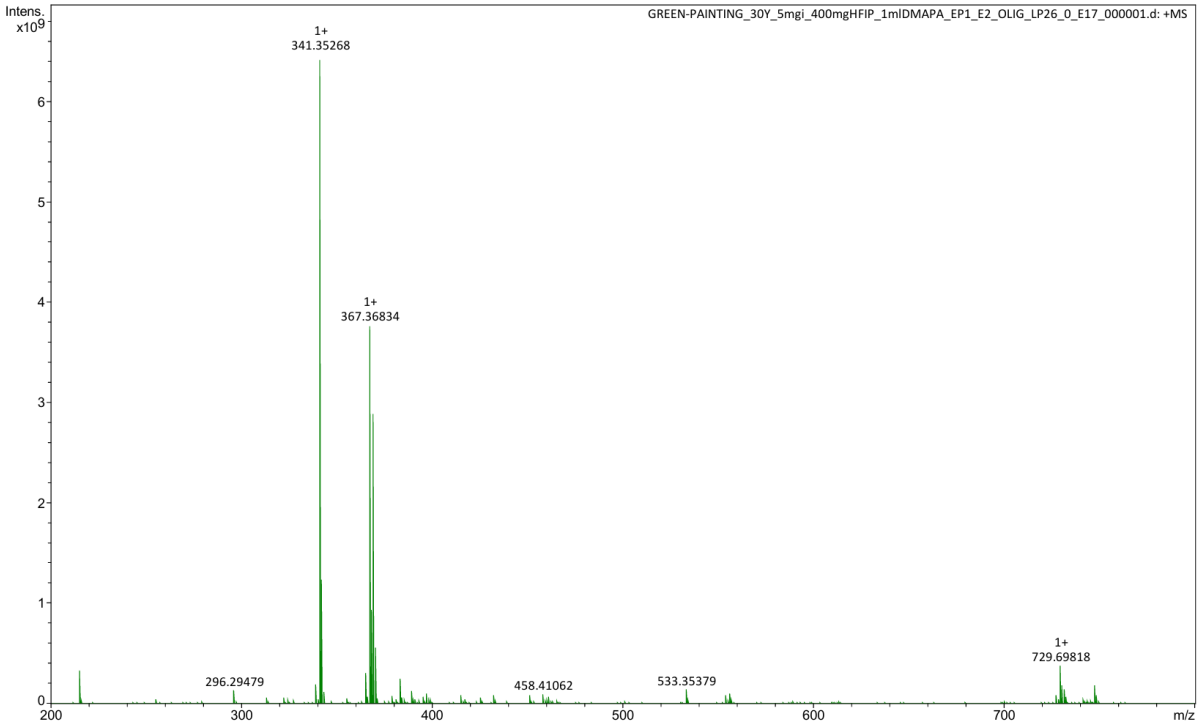
The first canvas of 3 years old constituting of brown pigment (Annex 1) was analyzed by MALDI FTICR MS between *m/z* 100 and *m/z* 1,500. The petroleum ether fraction of this oil paint showed, after depolymerization, the presence of the main derivatized fatty acids with one DMAPA molecule mentioned here in descending order in term of relative abundances: Stearic (C18:0), palmitic (C16:0), oleic (C18:1) and linoleic (C18:2) acids appearing at *m/z* 369.3839, 341.3526, 367.3683 and 365.3526 respectively. Linolenic acid (C18:3) has appeared as traces at *m/z* 363.3369. The main peak appearing at *m/z* 385.3789 corresponds to the mono-derivatized stearic acid with 1 oxygen. This saturated fatty acid was also present with 3 oxygen atoms at *m/z* 401.3738 (Annex 13).

These results shows the effect of 3 years' natural ageing on the depolymerization products where more oxygenated species were detected.



Annex 13. MALDI FTICR MS spectrum of the brown oil paint on canvas polymerized naturally for 3 years.

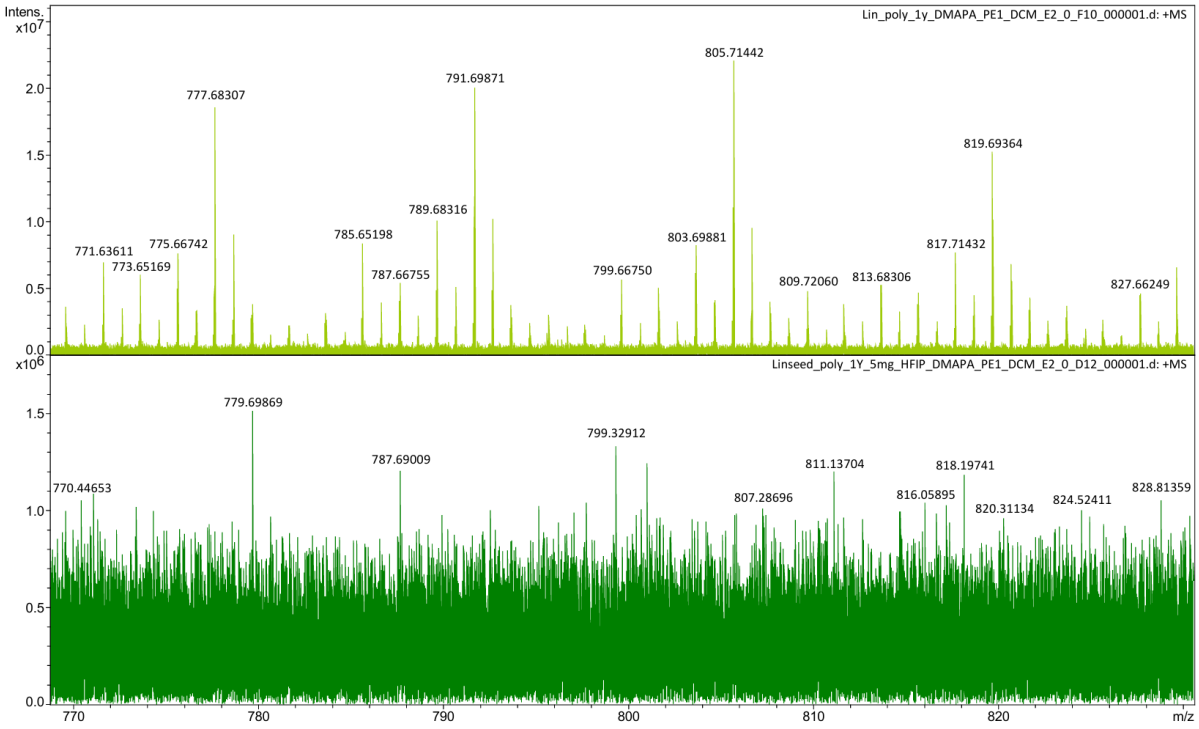
The green painting of 30 years old showed the high abundance of palmitic acid followed by oleic then stearic acids. The oxygenated species were present here but in lower intensity than the brown canvas of 3 years old (Annex 14). This shows the effect of other parameters on ageing which is the pigment and its type in addition to the period of ageing. The green painting was better preserved.



Annex 14. MALDI FTICR MS spectrum of the green oil paint from an oil painting of 30 years old.

2.4. Comparison of depolymerization methods

The depolymerization protocol using DMAPA with an excess of formic acid proved its efficiency and has been used. The comparison between the two methodologies with and without HFIP showed that at high masses, the signal to noise ratio is high for the transamidated products without HFIP. More noise was detected at high masses in the presence of HFIP, this may affect the identification by loss of some peaks (Annex 15). The direct transamidation without HFIP was better in term of MS ionization, facility of the methodology and solubility of oil; it is also time economizing. No additional benefits were found using HFIP for siccative oils and oil paints.

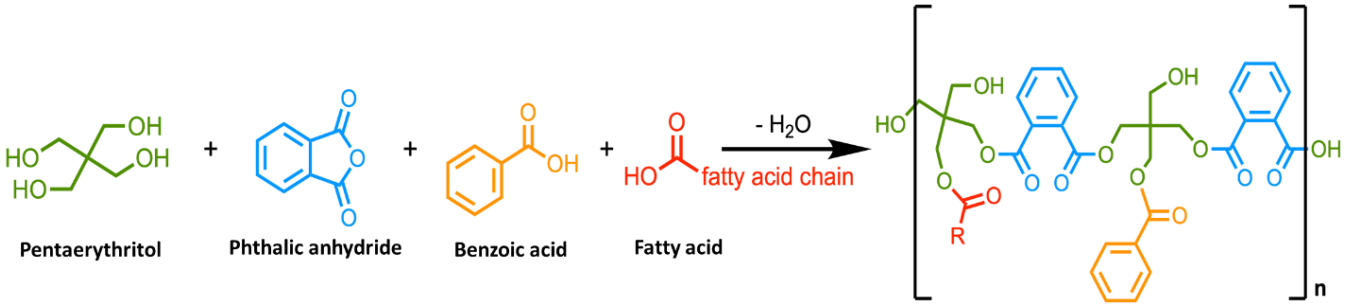


Annex 15. MALDI FTICR MS spectra of linseed oil polymerized naturally for 1 year (*m/z* 769- *m/z* 829). Upper panel: Depolymerization without HFIP; lower panel: Depolymerization with HFIP.

Chapter 10: Alkyd paints and industrial resins

Introduction

Alkyds are organic polyesters synthesized for the first time in 1927 by R. H. Kienle. They are used in artists' paints, industrial paints and thermosetting plastics.The following figure shows an example of alkyd resin synthesis method in which fatty acid chains and pentaerythritol polyols are present in addition to phthalic anhydride. Benzoic acid is an additive used to control the viscosity of the resin.[1] After formulating alkyd resins with pigments and driers, they provide the alkyd paints.



As for oil paints, the drying in alkyd paints depends on two different mechanisms: Physical drying, happening through solvent evaporation and chemical drying, involving autoxidative drying mechanisms leading to crosslinking via free radical mechanism which is still debated. An over oxidation or an over crosslinking may favor the competing β-scission phenomena leading to the formation of both radical compounds and low molecular weight species, which can either remain in the paint film or be either volatilized or solubilized through some specific solvents. The presence of azelaic acid in the aged polymeric films is a clear marker of β-scission phenomenon.[2,3,4]

The aim of this work is to develop analytical methods for the full structural analysis of alkyd paints and resins to better understand their degradation mechanisms. Many alkyd paints' tubes have been studied from *Winsor and Newton* and *Gamblin* brands. Some are shown in details in article 7.

References

1. Swann, M. H., Adams, M. L., & Weil, D. J. (1956). Determination of Benzoic Acid in Alkyd Resins. *Analytical Chemistry*, *28*(1), 72-73.
2. Lorenzo, V.; Pizzimenti, S.; Caroti, G.; LA NASA, J.; Duce, C.; Bonaduce, I., Disclosing the chemistry of oil curing by mass spectrometry using methyl linoleate as a model binder. *Microchemical journal* **2021,** *173*.
3. Honzicek, J., Curing of air-drying paints: a critical review. *Industrial & engineering chemistry research* **2019,** *58* (28), 12485-12505.
4. Bootsma, J.; Browne, W. R.; Flapper, J.; de Bruin, B., Photoactive Fe Catalyst for Light-Triggered Alkyd Paint Curing. *JACS Au* **2022,** *2* (2), 531-540.

Article 7

Structural deciphering of alkyd paints and industrial resins

ABSTRACT: Alkyd paints are a specific variety of oil paints' formulations constituted of esters of phthalic or isophthalic acids and polyols in addition to the unsaturated fatty acids part normally present in oil paints. Like classical oil paints, alkyd paints contain binders and pigments or metal driers. Despite their wide use in artist art paintings and in house and industrial paints, little is known about the structure of the 3D-polymer formed after their siccativation after oxygen and light interactions. To assess their structural modifications at molecular level, their insoluble films were depolymerized under mild conditions before their analysis. Indeed, two derivatization methods have been used to identify the carboxylic acid part including fatty acids and phthalic acids and the alcoholic part including diols and/or polyols. Practically, the fatty acid chains of alkyd paints were transamidated at room temperature with 3-(dimethylamino)-1-propylamine (DMAPA) while their diols and/or polyols were derivatized by a free-water methanolysis reaction followed by a specific benzoylation using 4-(dimethylamino)benzoyl chloride. All the derivatized products were finally analyzed using ultra-high resolution mass spectrometry techniques, MALDI FTICR MS and LC-Orbitrap ESI MS. Alkyd paints from a popular brand have been studied with and without autoxidation of one week under natural conditions. These methods allowed the successful deciphering of both parts, carboxylic acids and alcohols, providing data about the traces of the remaining polyunsaturated fatty acids and the formed dimers linked by C-C or C-O bonds as well as the oxygenated species. The identified compounds granted more comprehension of the siccativation process of alkyd paints. The described strategies have been applied on alkyd industrial resins allowing their full characterization.

Keywords: Alkyd paints, fatty acids, polyols, siccativation/polymerization, ageing, polyester resins, inorganic pigments, structural modifications, depolymerization, transamidation, methanolysis, benzoylation, MALDI FTICR MS, LC-Orbitrap-MS

At the end of 19th century, classical paints have been made from natural compounds such as oils and gums. The introduction of synthetic resins has changed the market of artistic binding media.

Alkyds are organic polyesters synthesized at early 20th century. They are formed of polyunsaturated fatty acids, polyols, and polyacids usually phthalic or isophthalic acids. The alkyd resins were originally developed for both house paint and industrial purposes because resins improve mechanical properties. However, the oil-modified paints named alkyd paints started to appear in artistic work since 1920s due to their remarkable excellent properties in comparison to the classical oils, such as their high gloss and fast-drying time, up to only two days. Pablo Picasso appreciated these new formulations that have been commercialized since 1960s. The oil over resin ratio was used to determine the possible application of alkyds. Indeed, a ratio less than 40 was intended for automotive and industrial formulations. However, a ratio higher than 60 was determined for decorative coatings.[1-6]

Alkyd resins may be synthesized by two methods. Indeed, in the monoglyceride method, oil and polyol are introduced in excess in the presence of catalyst and heating in order to afford monoglyceride. This last compound reacts with phthalic anhydride to form the final alkyd resin. The fabrication of resins can be started from oil with isophthalic acid by acidolysis method.[3]

For the colour of alkyd paints, pigments based on transition metals such as Cobalt (II) and manganese (II) were used traditionally. As classical oil paints, the drying after solvent evaporation which is called siccativation is still debated. The formation of crosslinking alkyd films is not a very clear subject. Many researches assumed a similar mechanism to oil paints by free radical chain mechanism in the presence of light and oxygen; and others confirmed the necessity of the presence of apolar environment.[7-8]

The aim of this study is to assess the siccativation mechanism of alkyd paints through mock-up samples of alkyd paints' tubes polymerized under natural conditions for one week. The results will be compared to alkyd paints' tubes without autoxidation. Then an industrial alkyd resin will be fully characterized.

The analysis of all parts of alkyds necessitates derivatization of all their constituting parts. For this reason, a transamidation at room temperature was performed on fatty acid chains using 3-(dimethylamino)-1-propylamine (DMAPA). However, the free polyols were derivatized by benzoylation using 4-(dimethylamino)benzoyl chloride (DMABC) after a free-water transesterification with methanol under specific conditions (Figure 1).

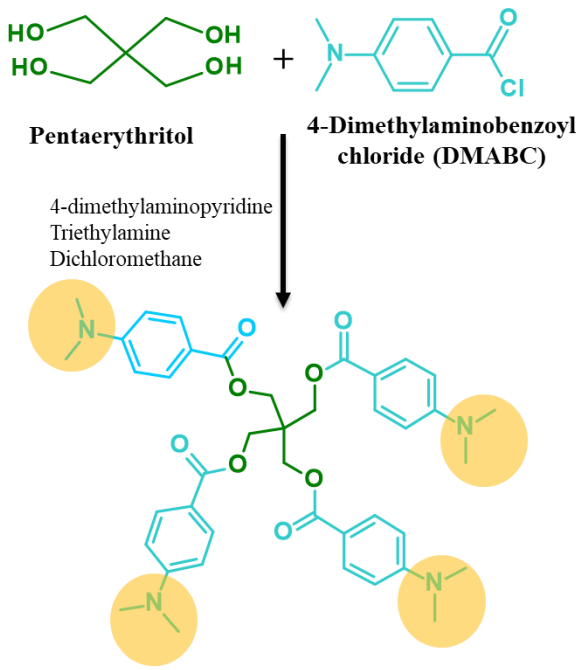


Figure 1. Benzoylation reaction of polyols in alkyds.

EXPERIMENTAL SECTION

Chemicals. All aqueous solutions were prepared from ultrapure grade water obtained by water filtration with a two stages Millipore system (Milli-Q® Academic with a cartouches Q-Gard 1 and Progard 2, Merck Millipore, Burlington, MA, United States). All solvents were purchased from Merck (Merck KGaA, Darmstadt, Germany); they were MS analytical grade and were used as received.

All chemicals were MS analytical grade: 4-Dimethylaminobenzoyl chloride (DMABC) 97%, 4-dimethylaminopyridine 99%, triethylamine ≥ 99.5% and 3-(dimethylamino)-1-propylamine also called *N,N*-dimethyl-1,3-propanediamine (DMAPA) 99%. All these chemicals were purchased from Merck (Merck KGaA, Darmstadt, Germany) and used without further purification. Additional chemical was purchased from Merck also: Sodium hydride (NaH) 60% dispersion in mineral oil but was washed in pentane under N_2 inert atmosphere before utilization.

Other chemicals were used for post-reactional treatment of benzoylation: Sodium bicarbonate ($NaHCO_3$) ≥ 99.7%, hydrochloric acid (HCl) 37%, magnesium sulfate $MgSO_4$ anhydrous, Reagent Plus® ≥ 99.5%; they were purchased from Merck (Merck KGaA, Darmstadt, Germany). Only sodium chloride NaCl ≥ 99.5% was purchased from Fischer Scientific (Fischer Scientific, Loughborough, UK).

Samples. Contemporary alkyd paints' tubes from *Winsor & Newton* (*W&N*, London, UK) brand were the blue paints: Griffin alkyd "Prussian Blue" and Griffin alkyd "French Ultramarine". An industrial alkyd resin of unknown composition was purchased from a coating company in France.

Mock-up samples preparation.

50 mg of alkyd paints was spread homogeneously directly on clean microscopic glass slides for a thickness of almost 40 microns. The slides were left under natural conditions for 1 week. The solid films were eliminated carefully by scalpel blades before depolymerization.

Derivatization of carboxylic acids by direct transamidation.

In a 2-mL transparent tube, 5 mg of the collected films were transamidated overnight at room temperature with 1 mL (7.93 mmol) of 3-(dimethylamino)-1-propylamine (DMAPA) under stirring. The mixture was quenched with 400 µL of formic acid then transferred to a 5 mL Falcon™ conical tube (Corning, NY, USA), added to 2 mL of ultrapure water and extracted twice with 2 mL of petroleum ether by centrifugation at 10,000 rpm during 5 minutes at room temperature using Beckman-Coulter (Brea, CA, USA) Allegra® X-30R centrifuge with the corresponding C1015 fixed angle conical tube rotor. The remaining aqueous phase was reextracted twice with 2 mL of ethyl acetate under the same centrifugation conditions. After each centrifugation, the organic phase was transferred to a 2-mL clear glass tube using a glass pipette. The obtained organic phases were evaporated under nitrogen at room temperature and stored in 2-mL glass tube.

Derivatization of polyols by a combined methanolysis-benzoylation strategy.

In a flask of 25 mL, 60 mg of NaH was washed five times with 5 mL of *n*-pentane, then 2.5 ml of methanol (in ice bath) was added and stirred for 1 minute. After that, 250 mg (0.25 mmol) of alkyd resins were added to the mixture. They were left under magnetic stirring and N_2 atmosphere for 24 hours. The mixture was neutralized with formic acid (41 µL, 50 mg), then evaporated until dryness. The remaining residues were extracted with petroleum ether. The flask was vortexed (after friction by spatula if necessary to solubilize the soluble part in petroleum ether), and left for 5 minutes. Using glass pipette, the soluble phase was taken and put in another flask which was evaporated and then transamidated by 1 mL of 3-(dimethylamino)-1propylamine (DMAPA) at room temperature.

However, the solid residue remaining in the initial flask was evaporated until full dryness then benzoylated. Indeed, to 2 mmol of the solid residue cooled with an ice bath, almost 0.1 mg of the catalyst 4-dimethylaminopyridine in 5 mL of dichloromethane and 8 mmol of triethylamine were added. The mixture was stirred under N_2 during 10 minutes. Then 8 mmol of 4-(dimethylamino)benzoyl chloride (DMABC) dissolved in 2 mL of dichloromethane were added to the mixture cooled with an ice bath. After stirring for 30 minutes with an ice bath cooling, the mixture was heated at solvent reflux by an oil bath set at 45 °C for 24 h under N_2 inert atmosphere. For post-benzoylation treatment, the obtained mixture was cooled at room temperature then by an ice bath. To this mixture, almost 1 mL of 10% of HCl aqueous solution was added to neutralize the excess of triethylamine. After that, it was washed successively with saturated $NaHCO_3$ solution to neutralize the excess of hydrochloric acid, then with Brine solution of aqueous sodium chloride NaCl, and three times by ultrapure water. The obtained solution was then dried over $MgSO_4$, filtrated and

evaporated using rotary evaporation. The recovered solid was resolubilized and analyzed by LC-MS.

Analytical method. For MS samples' preparation, the petroleum ether fractions were solubilized in dichloromethane at 1 mg/10 µL. However, the ethyl acetate fractions were solubilized in methanol at 1 mg/10 µL.
The solubilized fractions were diluted in methanol/water/formic acid 30/70/0.1 (v/v/v), 1000 times for LC-MS analysis and 100 times for MALDI FTICR MS analysis.

MALDI FTICR MS analysis. The analyses were performed on a SolariX XR instrument with a 9.4 Tesla actively shielded superconducting magnet fitted with a dynamically harmonized cell (Bruker Daltonics, Bremen, Germany) and controlled by FTMS Control software. MALDI FTICR mass spectra were acquired in positive ion mode. The matrix used was α-cyano-4-hydroxycinnamic acid. MS spectra were acquired using broadband detection, 8 M points; 32 scans accumulation for a better signal-to-noise ratio with a mass range from *m/z* 100 to 1,500 with 2.936 s transient time. Instrument calibration was achieved using red phosphorous as external calibrant and a quadratic calibration. The obtained spectra were processed using Data Analysis software version 5.0 (Bruker Daltonics, Bremen, Germany).[9-10]

LC-ESI MS analysis. LC-MS analyses were performed on an Orbitrap LTQ XL mass spectrometer hyphenated to a Dionex Ultimate 3000 HPLC System (ThermoFisher Scientific, Bremen, Germany). The analysis was performed using a 40 min gradient at a flow rate of 0.50 mL.min^{-1} on a Hypersil GOLD™ C18 column (2.1 µm i.d. × 150 mm) packed with 3 µm beads from ThermoFisher Scientific; placed in an oven at a temperature of 50 °C. The depolymerized products were separated using a multi-step gradient of 40 minutes with a mobile phase of 30% methanol in acidified water, 0.1% formic acid (solution A) and 50% methanol, 50% 2-propanol in acidified water, 0.1% formic acid (solution B) as described in Almasri et al. publication.[10] The MS scans were acquired from *m/z* 200 to 1,000 with a 60,000 resolution at *m/z* 200.
Data acquisition and interpretation were performed using Xcalibur™ 4.21 SP1 software (Thermo Fisher Scientific).

RESULTS AND DISCUSSIONS

As oil paints, a transamidation at room temperature for alkyd paints was performed using 3-(dimethylamino)-1-propylamine (DMAPA) followed by liquid-liquid extractions.[9-10] The fatty acids were successfully analyzed by mass spectrometry. However, free polyols of alkyds are soluble in water and may be lost during the liquid-liquid extractions. So, two strategies have been used to determine the full composition of these polyesters. First, a transamidation for the acidic parts was used and then a benzoylation of polyols after separation of phases by methanolysis was performed. Indeed, polyols had to be derivatized before MS analysis to increase their mass and so to can possibly analyze them by mass spectrometry. The benzoylated fractions were analyzed by LC-MS and the transamidated fractions by both MALDI FTICR MS and LC-MS.

Alkyd paints. For transamidation of alkyd paints, the extraction yield in petroleum ether in all samples was lower than that in ethyl acetate fraction. And the polymerized alkyd paints after one week of polymerization had lower extraction yield than those not polymerized. For instance, the *W&N* alkyd paint tube Prussian Blue had an extraction yield of 90% and 22% before and after polymerization of one week respectively (Table 1). However, the extraction yield of the French Ultramarine registered 46% after one week of polymerization. The extraction yields were calculated based on the recovered weight after depolymerization.

Table 1. Recovered weight (in mg) in *W&N* Griffin Alkyd Prussian Blue samples before and after polymerization of one week under natural conditions. PE: Petroleum ether fraction; EA: Ethyl acetate fraction, Tube: Without polymerization.

	Prussian Blue-Tube	**Prussian Blue-1 week**
PE1	1.5	0.1
PE2	0.4	0.3
EA1	1.9	0.1
EA2	0.7	0.6
All fractions	4.5	1.1

The drying process of alkyd paints' films has been followed over 5 days on each mock-up slide containing initially 50 mg of paint by the measurement of weight evolution each 2 hours in the first day then 4 hours during the remaining days (no measurements have been performed at night).
Unlike oils and classical oil paints, no increasing of weight was observed. The oxygen uptake was not demonstrated by the follow-up of films' weights. Indeed, both alkyd paints' slides had the same evolution of weight. It decreased 10% in the first 4 hours then was stabilized very fast. The French Ultramarine film had a little increase of less than 1% in comparison to the Prussian Blue film (Figure 2).

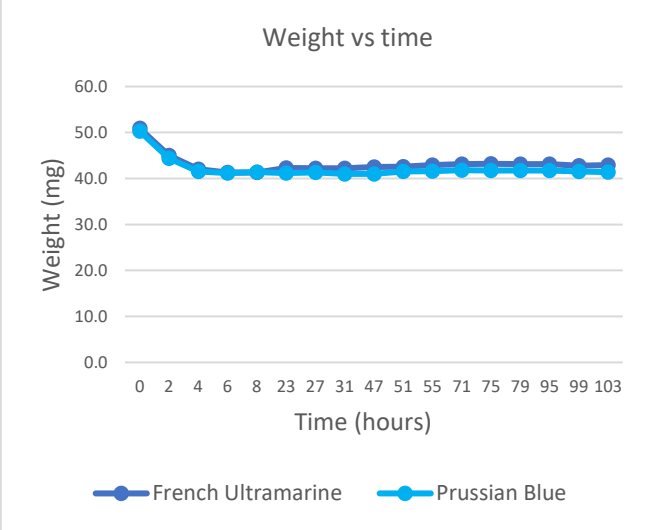


Figure 2. Evolution of polymerized *W&N* alkyd paint films' weight during 5 days of polymerization at room temperature. In clear blue: Griffin Alkyd Prussian Blue and in dark blue: Griffin Alkyd French Ultramarine.

The MALDI FTICR MS analyses of alkyd paints were registered before and after polymerization. All MS spectra were registered with very high accuracy, almost 0-0.5 ppm. In petroleum ether fractions, the number of peaks per spectrum was very high up to 51,500 peaks.

The ethyl acetate and petroleum ether fractions showed differences in structural composition and in intensities of the common peaks due to the affinity of depolymerized compound to be extracted in these both different polar solvents as shown in Figure 3.

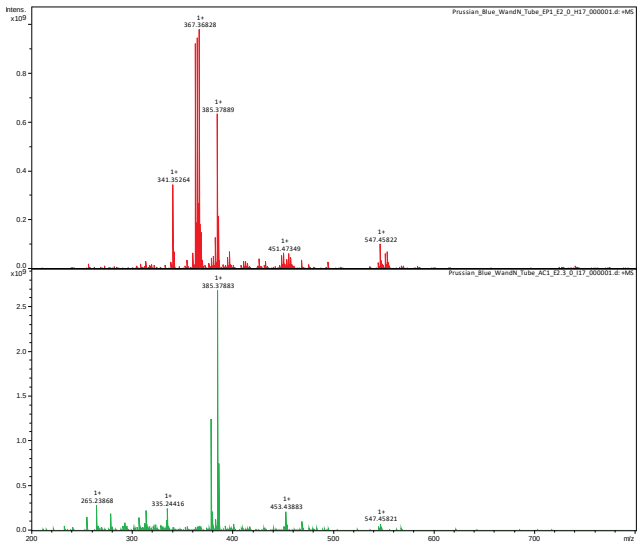


Figure 3. MALDI FTICR MS spectra for the *W&N* Griffin Alkyd Prussian Blue film without polymerization. Upper panel: Petroleum ether fraction; lower panel: Ethyl acetate fraction.

For instance, both fractions in the extraction solvents of the French Ultramarine alkyd paint were compared. Indeed, the mono-derivatized oleic acid [$C_{23}H_{46}N_2O$ + H^+] appearing at *m/z* 367.3683 was the main peak in petroleum ether fraction with 36% of the major composition. It constituted only 12% of the major composition in the ethyl acetate fraction. However, the main peak in ethyl acetate fraction was the oxidized stearic acid [$C_{23}H_{48}N_2O_2$ + H^+] appearing at *m/z* 385.3789 with 44% (vs 19% in petroleum ether fraction). The saturated fatty acid C16:0 has appeared mono-derivatized at *m/z* 341.3526 with 9% and 5% in petroleum ether and ethyl acetate fractions respectively. In general, the ethyl acetate fraction contained more oxygenated species than the petroleum ether one with 69% and 42% of their major composition respectively (SI, Table S1).

Moving to the Prussian Blue alkyd paint before and after polymerization of 1 week under natural conditions; considering only the petroleum ether fraction for its peaks' following abundances. The main peaks found before polymerization were the mono-transamidated oleic [$C_{23}H_{46}N_2O$ + H^+], linoleic [$C_{23}H_{44}N_2O$ + H^+] and linolenic [$C_{23}H_{44}N_2O$ + H^+] acids appearing at *m/z* 367.3683, *m/z* 365.3526 and *m/z* 363.33699 respectively. They constituted 21%, 20.5% and 20% respectively of the petroleum ether major composition. These C18 unsaturated fatty acids constituted only 14%, 3% and 2% of the major composition respectively after polymerization (Table 2) showing a strong consumption of double bonds due to siccativation. This consumption was compensated by the formation of the oxygenated compounds oleic and stearic acids appearing at *m/z* 383.3632 and *m/z* 385.3789 respectively with 31% and 19% of the major composition (SI, Table S1). The abundance of oxygenated species was multiplied almost by 3 after polymerization (65% of the major composition).

Prussian Blue before polymerization showed the presence of many dimers and crosslinked products (C-C, C-O, and with one or multiple oxygen atoms addition) that were detected with two DMAPA molecules constituting almost 1% of its petroleum ether major composition (SI, Table S1 and Table 2). The C-C dimers of linolenic, linoleic acids [$C_{46}H_{84}N_4O_2$ + H^+], linoleic acid [$C_{46}H_{86}N_4O_2$ + H^+] and linoleic, oleic [$C_{46}H_{88}N_4O_2$ + H^+] acids appeared at *m/z* 725.6667, *m/z* 727.6823 and 729.69797 constituting 0.37% of the major composition. The C-O dimer or C-C dimer with a hydroxylated fatty acid of linolenic, linoleic acids [$C_{46}H_{84}N_4O_3$ + H^+], linoleic acid [$C_{46}H_{86}N_4O_3$ + H^+] and linoleic, oleic acids [$C_{46}H_{88}N_4O_3$ + H^+] were appeared at *m/z* 741.6616, *m/z* 743.6773 and *m/z* 745.6934 respectively with 0.14% of the major composition. Similarly, dimers with 2 oxygen atoms of linolenic, linoleic [$C_{46}H_{84}N_4O_4$ + H^+], linoleic [$C_{46}H_{86}N_4O_4$ + H^+] and linoleic, oleic [$C_{46}H_{88}N_4O_4$ + H^+] fatty acids appearing at *m/z* 757.6565, *m/z* 759.6722 and *m/z* 761.6875 respectively have been also detected with 0.3% abundance in petroleum ether fraction. The corresponding linolenic, linoleic acids' dimer with 3 oxygen atoms [$C_{46}H_{84}N_4O_5$ + H^+] was detected at *m/z* 773.6515. Even the dimers with 4 oxygen atoms of C18:3-C18:2, C18:2 and C18:2-C18:1 have been detected at *m/z* 789.6464, *m/z* 791.6621 and *m/z* 793.6776 respectively. The dimers with

5 and 6 oxygen atoms have been identified also for the linolenic acid only (SI, Table S1).

The abundance of these dimers was higher in ethyl acetate fraction. As in French Ultramarine, dimers abundance increased from 0.03% to 1.6% of the major composition. This alkyd paint had higher dimers abundance than Prussian Blue (Table 2).

All abundances are calculated in comparison to the major composition formed by the 56 detected peaks put in SI, Table S1 and given by the following formula:

$$\text{Abundance of a given peak} = \frac{\textit{Relative intensity of this peak}}{\textit{Relative intensity of the major composition's peaks}} \times 100$$

Table 2. Abundances of the main fatty acids and their dimers and oxygenated compounds in *W&N* Griffin Alkyd oil paints' tubes (PE: Petroleum ether, EA: Ethyl acetate and Tube: Without polymerization).

	Prussian Blue-Tube PE	**Prussian Blue polymerized for 1 week, PE**	**French Ultramarine polymerized for 1 week, PE**	**French Ultramarine polymerized for 1 week, EA**
% All dimers	0.88%	0.00	0.03%	1.59%
% C18:3	20.05%	1.63%	1.44%	0.61%
% C18:2	20.52%	2.69%	2.87%	1.65%
% C18:1	21.36%	14.91%	35.68%	12.37%
% C16:0	7.60%	5.22%	9.18%	5.23%
% C18: 0	3.34%	2.72%	3.11%	3.33%
% Saturated	10.94%	7.94%	12.29%	8.56%
Ratio C18:3 vs saturated (C16:0, C18:0)	1.83	0.20	0.12	0.07
Ratio C18:2 vs Saturated (C16:0, C18:0)	1.88	0.34	0.23	0.19
Ratio C18:1 vs saturated (C16:0, C18:0)	1.95	1.88	2.90	1.44
% O	23.43%	65.17%	41.61%	68.66%

The di-derivatized phthalic acid [$C_{18}H_{30}N_4O_2 + H^+$] appearing at *m/z* 335.2442 was detected in all analyzed samples either in their petroleum ether fraction or ethyl acetate fraction or both (Figure 4).

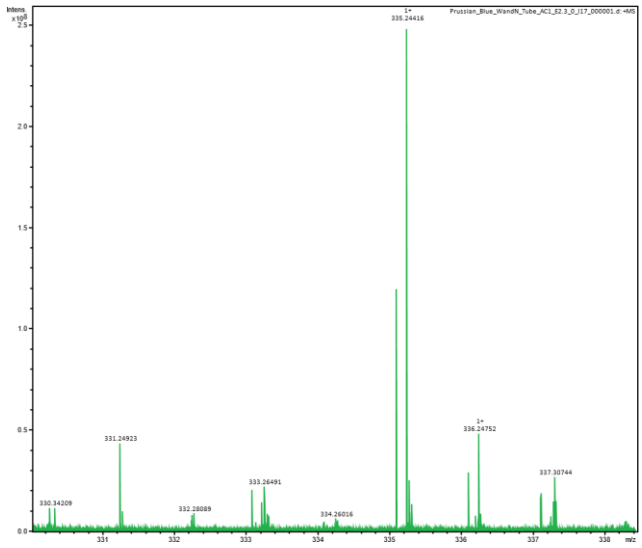


Figure 4. MALDI FTICR MS spectrum for the *W&N* Griffin Alkyd Prussian Blue without polymerization, ethyl acetate fraction (*m/z* 300-340).

The LC-MS analysis confirmed the presence of this peak which appeared at 0.63 min as shown in Figure 5.

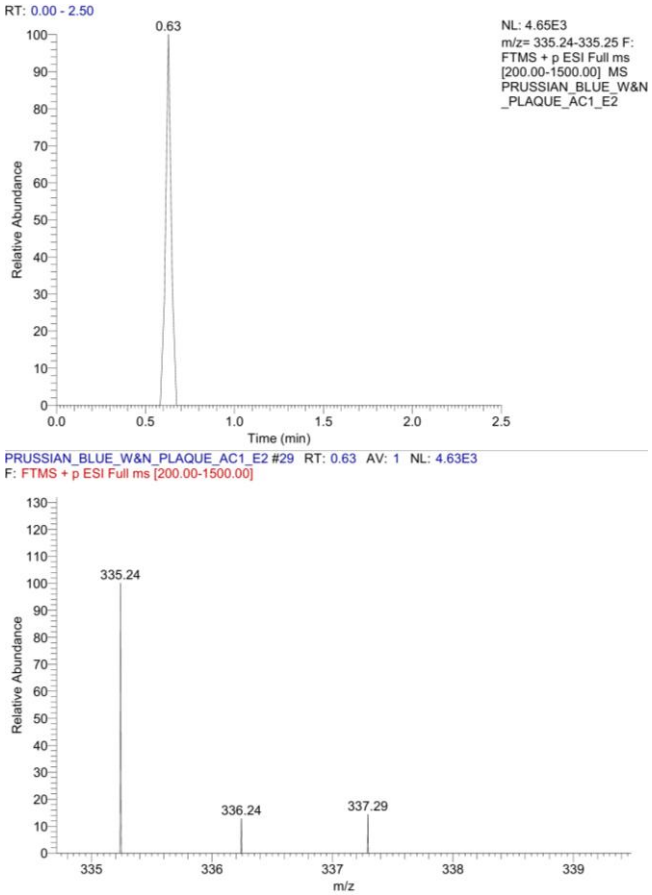


Figure 5. LC chromatogram and MS associated spectrum for the phthalic acid appearing at *m/z* 335.244 in the *W&N* Griffin Alkyd Prussian Blue polymerized for 1 week, ethyl acetate fraction (0 min-2.5 min).

Industrial alkyd resin analysis. The alkyd resin purchased from a French coatings company was first transamidated with DMAPA amine and extracted with petroleum ether and ethyl acetate solvents in order to decipher its fatty acids and aromatic diacids.

The transamidated products were analyzed by MALDI FTICR MS and LC-MS. The main peak found was the mono-transamidated linoleic acid (C18:2) appearing at *m/z* 365.3526 followed by the oleic acid (C18:1) appearing at *m/z* 367.3683 in the petroleum ether fraction. In addition, palmitic (C16:0), linolenic (C18:3), and stearic (C18:0) fatty acids have been detected with high accuracy (Figure 6, (a)).

The phthalic part [$C_{18}H_{30}N_4O_2$ + H^+] was identified in trace after verifying its isotopic ratio. It appeared at *m/z* 335.2442 (Figure 6, (b)).

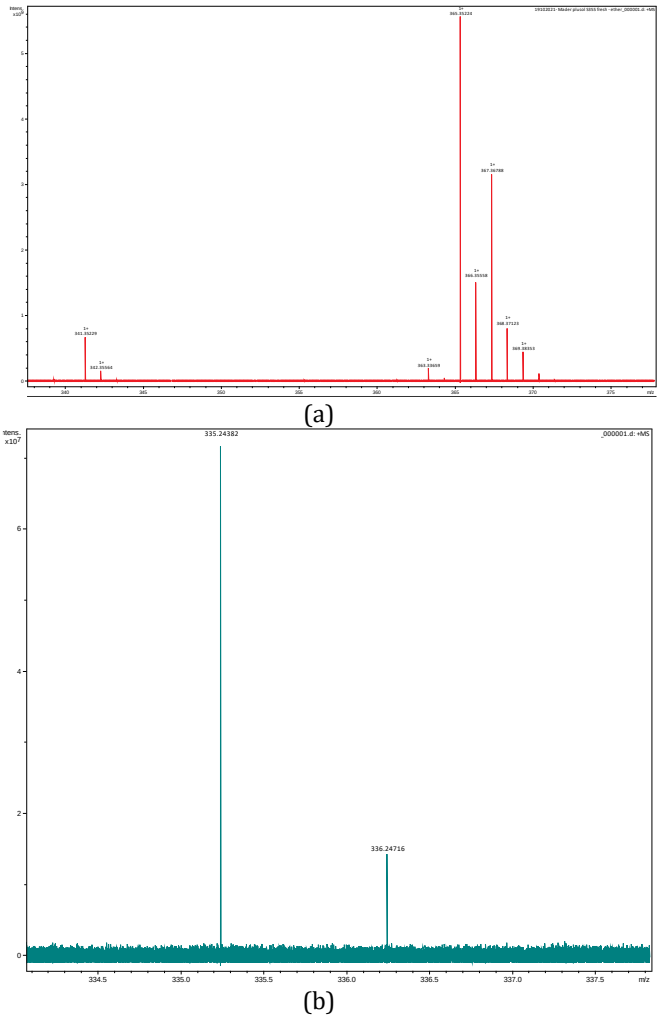


Figure 6. MALDI FTICR MS spectrum for the industrial alkyd resin after transamidation, petroleum ether fraction. (a): Fatty acids area (*m/z* 338-377); (b): Amplified phthalic acid area (*m/z* 334-338).

This same fraction was analyzed by LC-MS. A multi-step gradient of 40 minutes was set using solvent A formed of 30% of methanol with 0.1% of formic acid and solvent B formed of 50% isopropanol, 50% methanol and 0.1% formic acid. The products of depolymerization were identified based also on the mass/charge (*m/z*) ratio after a dilution of 1 mg/mL; the final concentration injected in LC was 1 mg/10 mL.

LC-MS results of petroleum ether fraction of the transamidated industrial alkyd resin showed similarly the presence of the main unsaturated fatty acids: Oleic (C18:1), linoleic (C18:2) and linolenic (C18:3) acids detected mono-derivatized with DMAPA. They showed also the presence of the main saturated fatty acids: Stearic (C18:0) and palmitic (C16:0) acids found mono-transamidated at *m/z* 369.384 and *m/z* 341.353 respectively. The MS spectra were obtained with very high accuracy for an Orbitrap (0-5 ppm). Indeed, the mono-derivatized linolenic, linoleic and oleic acids were detected around 19 min, 20 min and 21 min respectively.as shown in Figure 7.

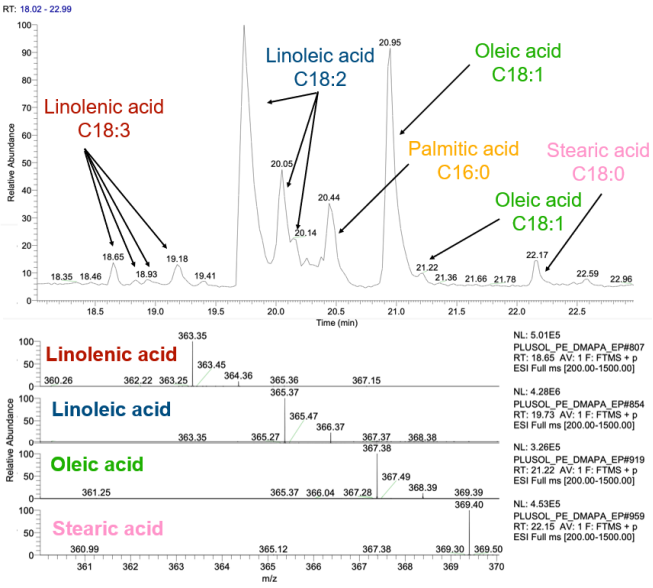


Figure 7. LC chromatogram and MS associated spectra for lipids present in the industrial oil-modified resin (18 min-23 min).

After the characterization of the lipidic part of the alkyd resin, the methanolysis followed by benzoylation strategy has been applied to determine its polyol's nature. Indeed, two main compounds have been detected. The tri-benzoylated pentaerythritol [$C_{32}H_{37}N_3O_7$ + H^+] was detected at *m/z* 560.276 and the tetra-benzoylated pentaerythritol [$C_{41}H_{49}N_4O_8$ + H^+] was detected at *m/z* 726.362 in LC-MS (Figure 8).

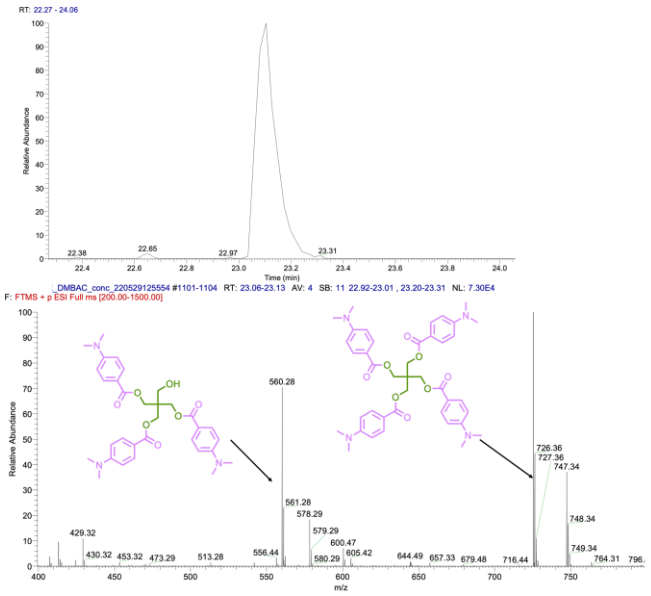


Figure 8. LC chromatogram and MS associated spectrum for the pentaerythritol polyol present in the industrial oil-modified resin (RT: 22.3 min-24 min).

These data allowed the deciphering of the polyol present during the manufacturing of this resin.

CONCLUSIONS AND PERSPESCTIVES

Two analytical strategies were developed for the analysis of alkyd paints that contain two main parts. Fatty acids and aromatic di-acids were transamidated by 3-(dimethylamino)-1propylamine (DMAPA) at room temperature. However, polyols were transesterified then benzoylated by 4-(dimethylamino)benzoyl chloride (DMABC). All the derivatized products were analyzed by LC-MS and MALDI FTICR MS. The promising results of analysis allowed the structural deciphering of alkyd paints' tubes from *Winsor and Newton* brand and the determination of their structural modifications induced by siccativation. The traces of the remaining polyunsaturated fatty acids and the formed dimers and oxygenated species were identified. Combining the two strategies allowed the full characterization of alkyd paints. These strategies have been applied to an alkyd industrial resin allowing the full deciphering of its composition. The analysis results showed that it was initially manufactured with pentaerythritol as polyol. These methods will be used on other brands and colors of alkyd paints to study their effect on oil siccativation reaction.

ASSOCIATED CONTENT

Supporting Information

Additional experimental details and characterization data.

AUTHOR INFORMATION

First author

Bayan Almasri - Univ. Lille, CNRS, UAR 3290, MSAP, Miniaturisation pour la Synthèse l'Analyse et la Protéomique, F-59000 Lille, France ; Laboratoire de Chimie Appliquée, Faculté des Sciences III, Université Libanaise, Ras Maska, Tripoli, Liban ; orcid.org/0009-0001-9467-5716.

Note

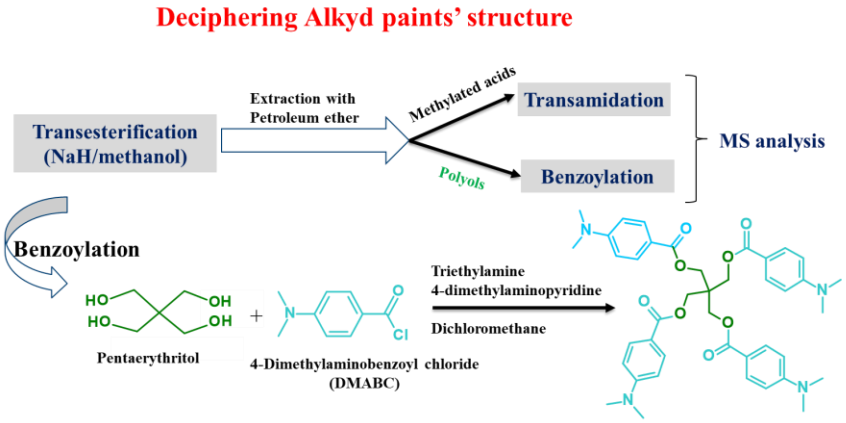
The authors declare no competing financial interest.

AKNOWLEDGMENT

Bayan ALMASRI gratefully acknowledges the funding of her joint PhD between University of Lille and Lebanese University by the PAUSE funding program. The mass spectrometer was funded by University of Lille, CNRS, Région Hauts-de-France and the European Regional Development Fund (ERDF). The authors gratefully acknowledge the financial support of the FTICR MS facility from the IR INFRANALYTICS FR2054 CNRS and of the EU_FTICR _MS project Grant Agreement 731077 funded by EU Horizon 2020 Research and Innovation Program.

REFERENCES

1. Learner, T., A review of synthetic binding media in twentieth-century paints. *The conservator* **2000,** *24* (1), 96103.
2. Fuster-López, L.; Izzo, F. C.; Piovesan, M.; Yusá-Marco, D. J.; Sperni, L.; Zendri, E., Study of the chemical composition and the mechanical behaviour of 20th century commercial artists' oil paints containing manganese-based pigments. *Microchemical Journal* **2016,** *124*, 962-973.
3. Kroschwitz, J. I., Mark, H.F. (Eds.), . E, Hoboken, NJ., Hoboken, NJ., 2003.
4. Dredge, P., A history of Australian housepaint technology from the 1920s to the 1950s, with reference to its use by Australian artists, particularly Sidney Nolan. *AICCM Bulletin* **2012,** *33* (1), 53-61.
5. Dredge, P., Sidney Nolan's adventures in paint—An analytical study of the artist's use of commercial paints in the 1940s and'50s. *AICCM Bulletin* **2013,** *34* (1), 15-23.
6. Ploeger, R.; Scalarone, D.; Chiantore, O., The characterization of commercial artists' alkyd paints. *Journal of Cultural Heritage* **2008,** *9* (4), 412-419.
7. Muizebelt, W.; Hubert, J.; Nielen, M.; Klaasen, R.; Zabel, K., Crosslink mechanisms of high-solids alkyd resins in the presence of reactive diluents. *Progress in Organic Coatings* **2000,** *40* (1-4), 121-130.
8. Van Gorkum, R.; Bouwman, E., The oxidative drying of alkyd paint catalysed by metal complexes. *Coordination chemistry reviews* **2005,** *249* (17-18), 1709-1728.
9. Almasri, B.; Rolando, C., Oil artists' paints structural deciphering & study of the parameters affecting oil polymerization mechanisms including transition metal driers and pigments for better conservation of artistic works in museums. To submit.
10. Almasri, B.; Rolando, C., Siccative vegetable oils and their mock-up for oil-based paints applications: Oil differentiation and ageing for drying process assessment using a new methodology of soft chemical depolymerization with advanced mass spectrometry analysis. To submit.


Deciphering Alkyd paints' structure
Transesterification (NaH/methanol)
Extraction with Petroleum ether
Methylated acids
Polyols
Transamidation
Benzoylation
MS analysis
Benzoylation
HO
HO
OH
OH
Pentaerythritol
4-Dimethylaminobenzoyl chloride (DMABC)
Triethylamine
4-dimethylaminopyridine
Dichloromethane

Supporting information

Table S 1. MALDI FTICR MS relative intensities for the *W&N* Griffin Alkyd oil paints' tubes (PE: Petroleum ether, EA: Ethyl acetate, Tube: Without polymerization), at 1/1000 (mg/µL).

Theoretical *m/z*	**$[M+H]^+$**	**Attribution**	**MALDI FTICR MS relative intensity**			
			Prussian Blue-Tube, PE	**Prussian Blue polymerized naturally for 1 week, PE**	**French Ultramarine polymerized naturally for 1 week, PE**	**French Ultramarine polymerized naturally for 1 week, EA**
296.2948	$C_{19}H_{38}NO$	Palmitic with $N(CH_3)_2$ of 1 DMAPA	5.25E+06	1.98E+06	2.20E+07	0.00E+00
320.2947	$C_{21}H_{38}NO$	Linoleic with $N(CH_3)_2$ of 1 DMAPA	1.86E+07	3.85E+06	4.78E+06	0.00E+00
322.3104	$C_{21}H_{40}NO$	Oleic with $N(CH_3)_2$ of 1 DMAPA	1.40E+07	4.62E+06	5.09E+07	2.19E+06
324.3261	$C_{21}H_{42}NO$	Stearic with $N(CH_3)_2$ of 1 DMAPA	2.38E+06	2.25E+06	6.37E+06	0.00E+00
335.2442	$C_{18}H_{31}N_4O_2$	Phthalic acid- 2 DMAPA	0.00E+00	7.69E+06	0.00E+00	1.50E+06
339.33699	$C_{21}H_{43}N_2O$	Palmitoleic- 1 DMAPA	2.71E+07	8.18E+06	2.38E+07	2.88E+06
341.3526	$C_{21}H_{45}N_2O$	Palmitic- 1 DMAPA	3.47E+08	1.43E+08	7.07E+08	3.82E+07
355.3319	$C_{21}H_{43}N_2O_2$	Palmitoleic- 1 DMAPA- 1 O	1.79E+06	7.17E+06	1.68E+07	2.41E+06
357.3476	$C_{21}H_{45}N_2O_2$	Palmitic- 1 DMAPA- 1 O	2.75E+06	1.18E+07	4.19E+07	4.50E+06
363.33699	$C_{23}H_{43}N_2O$	Linolenic- 1 DMAPA	9.15E+08	4.47E+07	1.11E+08	4.42E+06
365.3526	$C_{23}H_{45}N_2O$	Linoleic- 1 DMAPA	9.34E+08	6.59E+07	2.14E+08	1.20E+07
367.3683	$C_{23}H_{47}N_2O$	Oleic- 1 DMAPA	9.72E+08	4.03E+08	2.74E+09	8.88E+07
369.3839	$C_{23}H_{49}N_2O$	Stearic – 1 DMAPA	1.52E+08	7.49E+07	2.39E+08	2.43E+07
379.3319	$C_{23}H_{43}N_2O_2$	Linolenic- 1 DMAPA- 1 O	4.39E+07	2.75E+07	3.03E+07	4.26E+06
381.3476	$C_{23}H_{45}N_2O_2$	Linoleic- 1 DMAPA- 1 O	5.14E+07	8.98E+07	1.41E+08	1.14E+07
383.3632	$C_{23}H_{47}N_2O_2$	Oleic- 1 DMAPA- 1 O	1.27E+08	5.27E+08	1.06E+09	8.62E+07
385.3789	$C_{23}H_{49}N_2O_2$	Stearic- 1 DMAPA- 1 O	6.28E+08	8.47E+08	1.49E+09	3.21E+08
395.3268	$C_{23}H_{43}N_2O_3$	Linolenic- 1 DMAPA- 2 O	4.50E+07	1.59E+07	1.43E+07	2.48E+06
397.3425	$C_{23}H_{45}N_2O_3$	Linoleic- 1 DMAPA- 2 O	7.10E+07	4.85E+07	4.24E+07	1.42E+07
399.3581	$C_{23}H_{47}N_2O_3$	Oleic- 1 DMAPA- 2 O	1.39E+07	5.00E+07	7.93E+07	1.40E+07
401.3738	$C_{23}H_{49}N_2O_3$	Stearic- 1 DMAPA- 2 O	1.58E+07	1.33E+08	2.66E+08	3.13E+07

411.3217	$C_{23}H_{43}N_2O_4$	Linolenic- 1 DMAPA- 3 O	3.02E+07	3.97E+06	2.74E+06	2.26E+06
413.3374	$C_{23}H_{45}N_2O_4$	Linoleic- 1 DMAPA- 3 O	3.12E+07	5.38E+06	7.89E+06	2.24E+06
415.3530	$C_{23}H_{47}N_2O_4$	Oleic- 1 DMAPA- 3 O	5.86E+06	2.10E+07	1.33E+07	3.82E+06
417.3687	$C_{27}H_{57}N_2O$	Stearic- 1 DMAPA- 3 O	1.47E+06	2.60E+06	5.48E+06	0.00E+00
425.4465	$C_{23}H_{43}N_2O_5$	Behenic-1DMAPA	1.75E+06	0.00E+00	1.88E+06	0.00E+00
427.3167	$C_{23}H_{49}N_2O_4$	-	4.05E+07	2.83E+06	2.19E+06	0.00E+00
461.4214	$C_{28}H_{53}N_4O$	Linolenic aldehyde- 2 DMAPA	0.00E+00	1.07E+08	2.38E+08	3.42E+07
477.4163	$C_{28}H_{53}N_4O_2$	Linolenic-2 DMAPA	2.33E+06	7.17E+07	1.16E+08	7.05E+06
479.43195	$C_{28}H_{55}N_4O_2$	Linoleic- 2 DMAPA	2.27E+06	7.95E+06	7.16E+06	0.00E+00
481.4476	$C_{28}H_{57}N_4O_2$	Oleic- 2 DMAPA	2.84E+06	6.49E+06	6.84E+06	1.40E+06
671.5721	$C_{41}H_{73}N_2O_3$	C37:6- 1 DMAPA-3 O	0.00E+00	0.00E+00	0.00E+00	0.00E+00
725.6667	$C_{41}H_{75}N_2O_3$	Linolenic, linoleic C-C dimer– 2 DMAPA	5.38E+06	0.00E+00	0.00E+00	0.00E+00
727.6823	$C_{41}H_{77}N_2O_3$	Linoleic C-C dimer– 2 DMAPA	5.99E+06	0.00E+00	1.86E+06	0.00E+00
729.6981	$C_{42}H_{75}N_2O_4$	Linoleic, oleic C-C dimer– 2 DMAPA	5.48E+06	0.00E+00	0.00E+00	0.00E+00
741.6616	$C_{46}H_{85}N_4O_2$	Linolenic, linoleic C-O dimer– 2 DMAPA	2.47E+06	0.00E+00	0.00E+00	0.00E+00
743.6773	$C_{46}H_{87}N_4O_2$	Linoleic C-O dimer– 2 DMAPA	2.53E+06	0.00E+00	0.00E+00	0.00E+00
745.6934	$C_{46}H_{89}N_4O_2$	Linoleic, oleic C-O dimer– 2 DMAPA	1.57E+06	0.00E+00	0.00E+00	0.00E+00
757.6565	$C_{46}H_{85}N_4O_3$	Linolenic, linoleic dimer +2O– 2 DMAPA	3.15E+06	0.00E+00	0.00E+00	1.71E+06
759.6722	$C_{46}H_{87}N_4O_3$	Linoleic dimer +2O– 2 DMAPA	3.12E+06	0.00E+00	0.00E+00	0.00E+00
761.6875	$C_{46}H_{89}N_4O_3$	Linoleic, oleic dimer +2O– 2 DMAPA	2.83E+06	0.00E+00	0.00E+00	0.00E+00
773.6515	$C_{46}H_{85}N_4O_4$	Linolenic, linoleic dimer +3O– 2 DMAPA	3.38E+06	0.00E+00	0.00E+00	0.00E+00
775.66174	$C_{46}H_{87}N_4O_4$	Linoleic dimer +3O– 2 DMAPA	0.00E+00	0.00E+00	0.00E+00	0.00E+00
777.6828	$C_{46}H_{89}N_4O_4$	Linoleic, oleic dimer +3O– 2 DMAPA	0.00E+00	0.00E+00	0.00E+00	0.00E+00
789.6464	$C_{46}H_{85}N_4O_5$	Linolenic, linoleic dimer +4O– 2 DMAPA	3.49E+06	0.00E+00	2.16E+06	2.61E+06
791.6621	$C_{46}H_{87}N_4O_5$	Linoleic dimer +4O– 2 DMAPA	4.28E+06	0.00E+00	0.00E+00	3.61E+06

793.6776	$C_{46}H_{89}N_4O_5$	Linoleic, oleic dimer +4O– 2 DMAPA	2.77E+06	0.00E+00	0.00E+00	0.00E+00
805.6413	$C_{46}H_{85}N_4O_6$	Linolenic, linoleic dimer +5O– 2 DMAPA	2.43E+06	0.00E+00	0.00E+00	1.88E+06
807.6569	$C_{46}H_{87}N_4O_6$	Linoleic dimer +5O– 2 DMAPA	1.80E+06	0.00E+00	0.00E+00	1.76E+06
809.6727	$C_{46}H_{89}N_4O_6$	Linoleic, oleic dimer +5O– 2 DMAPA	1.59E+06	0.00E+00	0.00E+00	0.00E+00
821.6362	$C_{46}H_{85}N_4O_7$	Linolenic, linoleic dimer +6O– 2 DMAPA	3.07E+06	0.00E+00	0.00E+00	0.00E+00
823.6518	$C_{46}H_{87}N_4O_7$	Linoleic dimer +6O– 2 DMAPA	0.00E+00	0.00E+00	0.00E+00	0.00E+00
825.6677	$C_{46}H_{89}N_4O_7$	Linoleic, oleic dimer +6O– 2 DMAPA	0.00E+00	0.00E+00	0.00E+00	0.00E+00
837.6311	$C_{46}H_{85}N_4O_8$	Linolenic, linoleic dimer +7O– 2 DMAPA	1.86E+06	0.00E+00	0.00E+00	0.00E+00
839.6468	$C_{46}H_{87}N_4O_8$	Linoleic dimer +7O– 2 DMAPA	0.00E+00	0.00E+00	0.00E+00	0.00E+00
841.6624	$C_{46}H_{89}N_4O_8$	Linoleic, oleic dimer +7O– 2 DMAPA	0.00E+00	0.00E+00	0.00E+00	0.00E+00

Chapter 11: Related works

Oil pastel analysis

Few researchers studied oil pastels. The binder for these oil crayons is basically a mixture of a drying oil (safflower or linseed oil), palm oil or Japan wax and beeswax.[1] Beeswax is a natural wax, a lipid containing different classes of components (hydrocarbons, mono-, di-& tri-esters, hydroxy polyesters, free acids and polyols with other compounds).[2] A recent study showed the analysis of some oil pastels from materials collection of the MUNCH museum in Oslo; using Py-GC-MS and μ-FTIR for the binder.[1,3] Very few data are known for this type of oil paints.

Experimental work

1. First innovative approach: With and without HFIP

In a glass tube, 5 mg of oil pastel fragments were added to 400 mg of HFIP. The tube was left in an oil bath preheated at 58 °C overnight. First, I tried the Blue Delfi oil pastel from the *Sennelier*'s Set. It was not soluble in HFIP so we decided to study the HFIP extract. A centrifugation at 2800 g for 20 minutes then MALDI FTICR MS analysis were performed on 3 trials for the direct HFIP extract as it is and diluted 100 times in addition to the extract after evaporation and solubilization in dichloromethane.

Then grinding of this oil pastel was done using Agate mortar and pestle. The solubility of the grinded pastel was better than that without grinding (Figure 1).

After separation of pigment by centrifugation at 2800 g for 20 minutes, 1 mL of DMAPA was added and stirred overnight. 400 μL of formic acid were added and centrifuged after addition of 2 mL of ulrapure water with 2 mL of petroleum ether (two times) and with ethyl acetate (two times). Both organic phases were collected, dried then analyzed by mass spectrometry.

(a) (b) (c) (d)

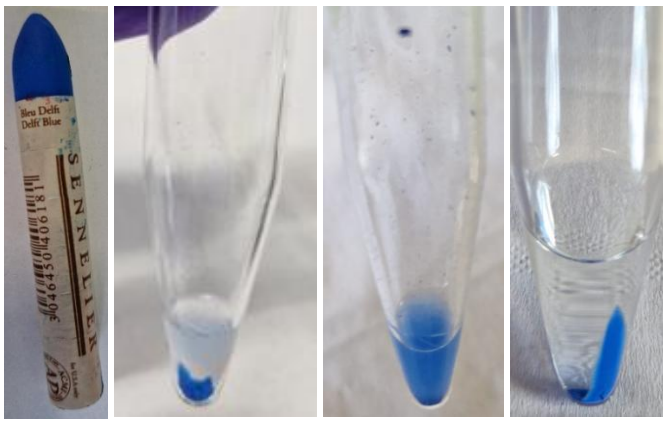


Figure 1. Blue Delfi oil pastel (a) and its aspects in HFIP after heating. (b): Before grinding; (c): After grinding and (d): After centrifugation.

After the success of this method by grinding, three different blue colors from three different brands and three green colors from two different brands were studied skipping the HFIP addition; a direct addition at room temperature of 1 mL of DMAPA was performed with stirring overnight then the post-transamidation was done as before. The details are shown in Table 1 and Figure 2.

Table 1. List of studied oil pastels by direct transamidation, with their brands.

Oil pastel name	**Brand**
Blue Delfi	*Sennelier*
Azure Blue	*Sennelier*
Phthalo Blue	*Faber Castell*
Prussian Blue	*JmPaillard*
Green Medium	*Sennelier*
Pine Green	*Sennelier*
English Green	*JmPaillard*



Figure 2. Studied oil pastels with their brands.

The recovered weights of the studied oil pastels reflecting their extraction yields are shown in Table 2. The starting oil pastels' weight was 5 mg.

Table 2. Recovered weights (in mg) of the studied oil pastels.

	Blue Delfi *Sennelier*	**Azure Blue - *Sennelier***	**Phthalo Blue - *Faber - Castell***	**Prussian Blue - *Jm Paillard***	**Green Medium - *Sennelier***	**Pine Green - *Sennelier***	**English Green - *Jm Paillard***
PE1	0.8	4.3	2.2	3.0	3.3	5.1	1.9
PE2	0.3	1.2	1.1	1.9	3.3	3.0	1.8
EA1	1.4	0.6	0.6	0.8	0.6	0.8	0.7
EA2	6.5	0.1	0.3	0.4	0.3	0.6	0.3

2. Second innovative approach: With TFA

In 15-mL glass centrifugation tube, 100 mg of grinded oil pastel was added with 1 mL of pure TFA 100%. This approach was applied on the four samples from the set *Sennelier*:

- Blue Delfi
- Azure Blue
- Green Medium
- Yellow Ochre

Many observations at this step were investigated. Indeed, after the addition of 1 mL of 100% of TFA, the Blue Delfi sample was soluble and the solution became kind of blue. However, for the

Azure Blue sample the solution became green with small grey aggregates. For the Green Medium sample, the solution became yellowish instantaneously but turned into green after stirring. For the Yellow Ochre, the sample was highly insoluble in TFA and it was necessary to push the sample directly in the TFA solution to make the solution turning to yellow.

After 1 day of stirring at room temperature, a centrifugation at 2800 g for 20 minutes was performed to separate pigments but a dispersion was formed making the separation very difficult (Figure 3). So, the soluble phase (supernatant) was added to 1 mL of ultrapure water and $NaHCO_3$ (weight according to the volume of remaining soluble recovered phase, almost 1 g). Then an additional 1 mL of ultrapure water was added, and the liquid-liquid extraction by centrifugation was performed after adding 2 mL of ethyl acetate (Figure 4). After taking the organic upper phase using glass pipette, the drying of this fraction was performed under N_2. Finally, MALDI FTICR MS analysis was performed.

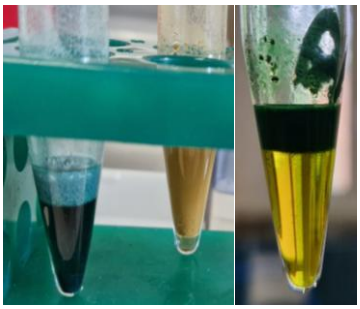


Figure 3. The dispersion problem after the first centrifugation of oil pastels in the presence of 100% of TFA.

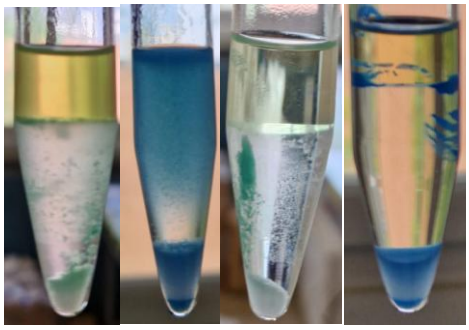


Figure 4. Aspects of Green Medium and Blue Delfi oil pastels before (2 first photos) and after (2 remaining photos) liquid-liquid extraction in the presence of ethyl acetate; second approach with TFA.

Results and discussions

All methods used for oil pastels' depolymerization were successful. This is an interesting preliminary study affording good data about the structure of oil pastel and the new methodologies used for their depolymerization. It is a big advantage as only very few researchers have already worked on oil pastels.

As in the case of oil paints, no additional benefits were found using HFIP before transamidation. The main methods used for depolymerizing oil pastels, the direct transamidation method and the TFA method, were investigated on the same oil pastels (such as Azure Blue, shown in Figure 5). Both petroleum ether and ethyl acetate fractions of the transamidated products were compared to the ethyl acetate fraction of the TFA-acidic compounds. In all methods, palmitic C16:0 and stearic C18:0 fatty acids in addition to traces of the 3 unsaturated C18 fatty acids were identified.

An extra peak of chemical formula $C_{22}H_{45}N_2O$ corresponding to methyl palmitoleate has been appeared at *m/z* 353.3526 in the presence of TFA.

For the direct transamidation methodology: At high masses, the ethyl acetate fraction was better in term of signal to noise ratio and in term of abundance of products than the petroleum ether fraction. All these methodologies found to be complementary to decipher the full structure of oil pastels.

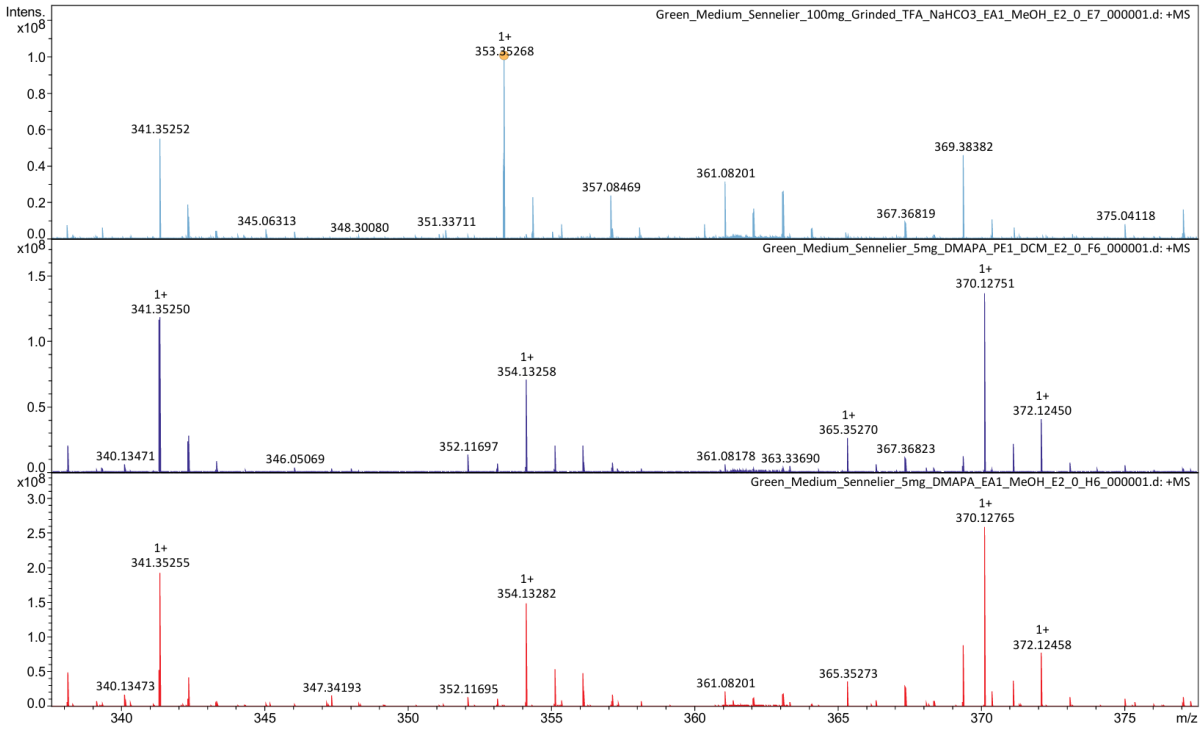


Figure 5. MALDI FTICR MS spectra of Green Medium oil pastel from *Sennelier* color set depolymerized with 3 different methods: Using TFA 100%, by direct transamidation and by transamidation after HFIP solubilization respectively.

The comparison of oil pastels of two different colors from the same supplier (*JmPaillard*) was performed using English Green and Prussian Blue oil pastels. MALDI FTICR MS spectra confirmed their successful depolymerization which is indicated by the presence of derivatized fatty acids and their oxygenated compounds. Indeed, the saturated fatty acids palmitic, oxygenated palmitic and stearic acids were the most abundant in both pastels and appeared mono-derivatized at *m/z* 341.3526, 357.3476 and 369.3839 respectively. Oleic, linoleic and linolenic acids appeared in traces but they were present in both oil pastels. These two oil pastels were differentiated. For example, a peak at *m/z* 425.2297 (structure under investigation) was highly intense in the green pigmented oil pastel while it was present only in traces in the blue one (Figure 6).

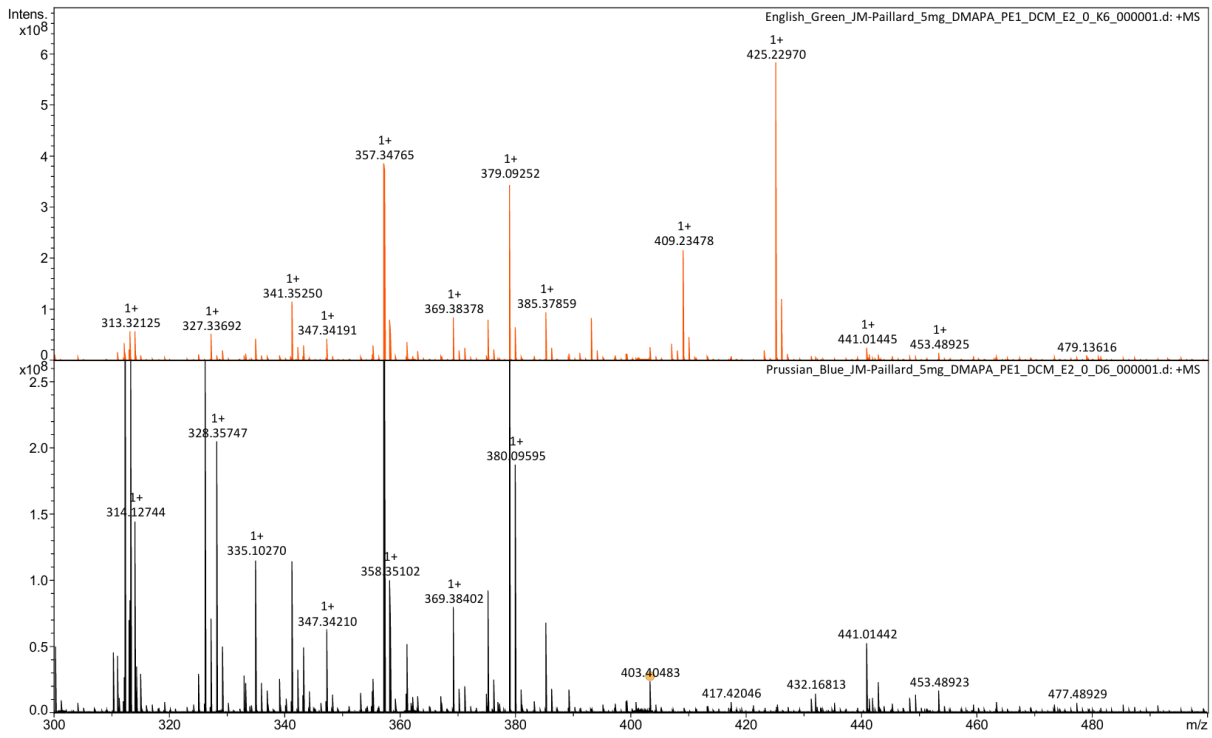


Figure 6. MALDI FTICR MS spectra of oil pastels from *JmPaillard* Color set. Upper panel: English Green; lower panel: Prussian Blue.

Three suppliers of blue oil pastels were compared: *Sennelier*, *Faber Castell*, and *JmPaillard*. Their corresponding oil pastels were Azure Blue, Phthalo Blue and Prussian Blue respectively. The blue color was difficult to depolymerize for obtaining good spectra especially that for *Sennelier* brand. For *Sennelier*, the main peaks were palmitic C16:0 and linoleic C18:2 fatty acids. For *Faber Castell* which afforded the best MS spectrum, the main peaks were the saturated fatty acids C16:0 and C18:0. However, *JmPaillard* was the most oxygenated color set with the presence of the oxygenated palmitic acid as main peak as well as the oxygenated stearic acid (Figure 7).

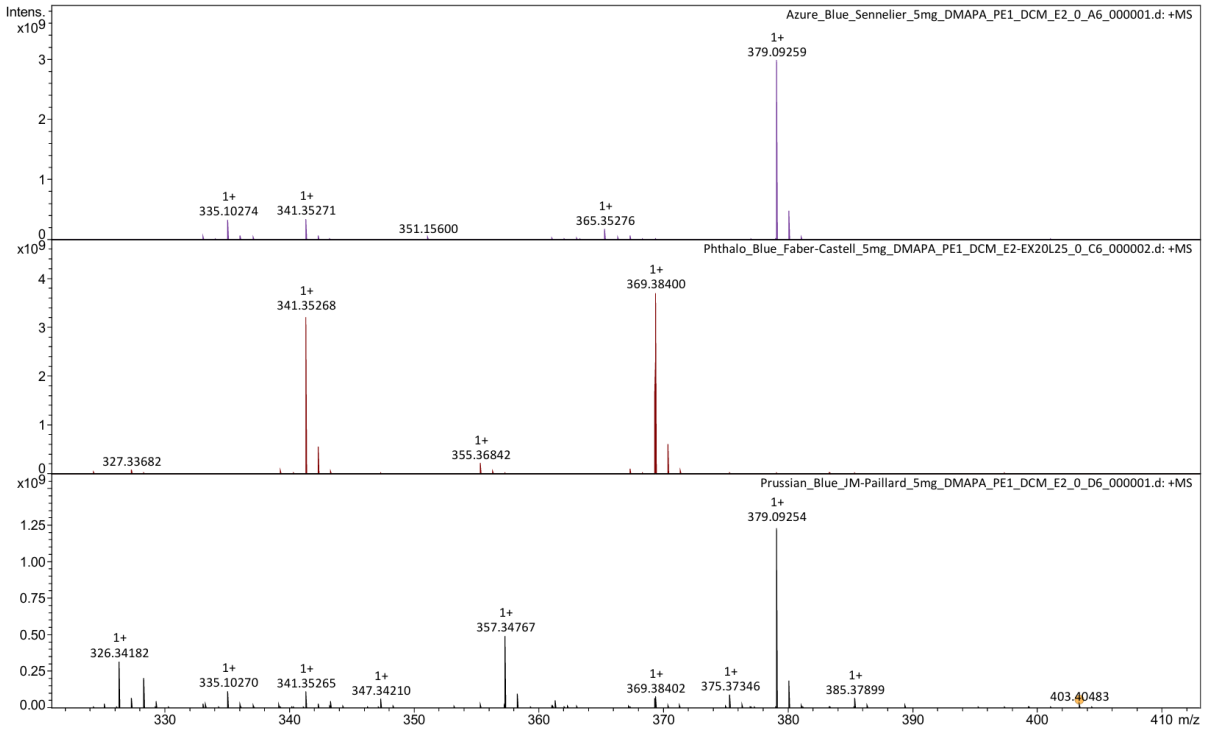


Figure 7. MALDI FTICR MS spectra of blue oil pastels: Azur Blue from *Sennelier*; Phthalo Blue from *Faber Castell* and Prussian Blue from *JmPaillard* respectively.

Sennelier color set was not very well detected in comparison to the other sets for other colors also. More problems of dispersion were found for *Sennelier*. This may due to the very small pores of the powder constituting their oil pastels. Further investigation and methodological improvements are still needed.

References

1- La Nasa, J.; Doherty, B.; Rosi, F.; Braccini, C.; Broers, F. T.; Degano, I.; Matinero, J. M.; Miliani, C.; Modugno, F.; Sabatini, F., An integrated analytical study of crayons from the original art materials collection of the MUNCH museum in Oslo. *Scientific Reports* **2021,** *11* (1), 7152.

2- Tulloch, A. P., Beeswax—composition and analysis. *Bee world* **1980,** *61* (2), 47-62.

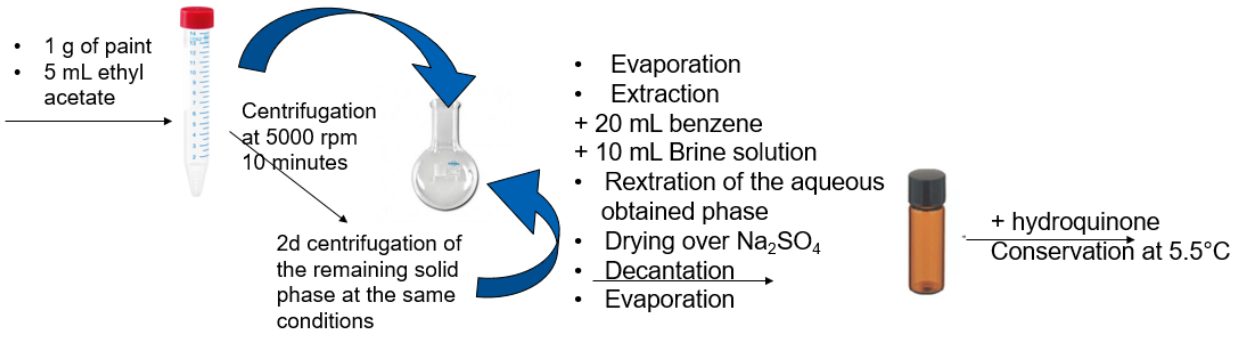
3- Cardoso, A. M.; Sandu, I. C. A.; Sandbakken, E.; Manhita, A.; Valadas, S.; Barrocas Dias, C.; Candeias, A., Edvard Munch's Collection of Drawing Materials: Crayon Characterization. **2022**.

Annex

1. Extraction of vintage oil paints' pots

Some types of vintage oil paints' pots from the sixties were extracted and the protocol of their extraction was optimized. The results were analyzed by ^{1}H NMR spectroscopy 300 MHz, FST ULille, Lille.

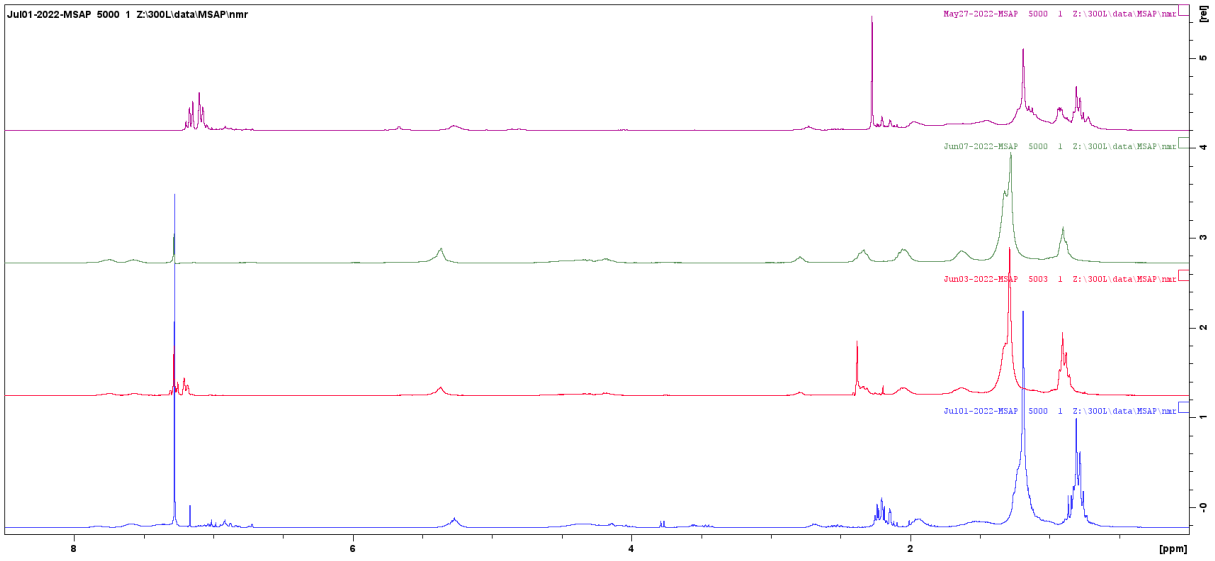
Annex 1 shows in detail the protocol of this extraction.



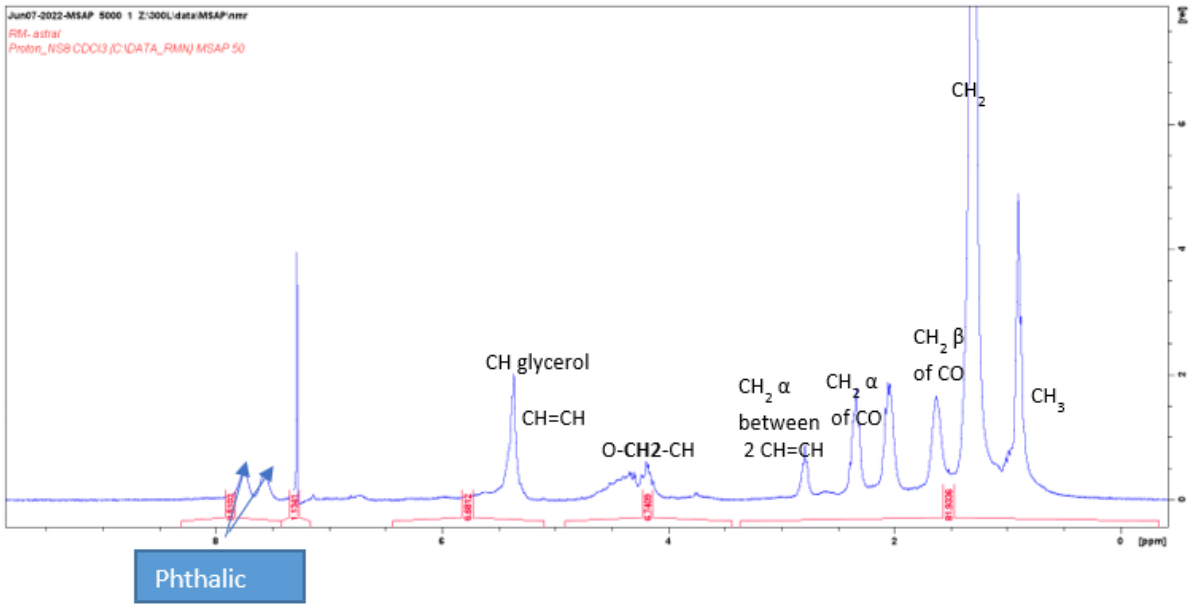
Annex 1. Protocol of extraction of binder from paint.

The extracted vintage oil paints' pots which were "Ripolin rouge", "Astral", "Val irisé", and "Dulox" were analyzed by ^{1}H NMR spectroscopy 300 MHz.

The ^{1}H NMR spectra of these paints are present below. These results were compared to native linseed oil peaks. Indeed, comparable peaks were found common and additional peaks of phthalic acid appearing around 7.6 and 7.7 ppm were observed. For instance, the amplified spectrum of "Astral" paint had the signals corresponding to the terminal methyl group, the CH_2 groups constituting the fatty acid chain backbone, the β-CH_2 group next to COO, the CH_2 in α position of CH=CH, the α-hydrogens of COO group, the CH_2 between two unsaturations, the CH_2 protons of the glycerol, the CH proton of the glycerol, the olefinic protons of unsaturation in fatty acid chains and the phthalic peaks respectively from the lower chemical shift to the deshielded zone as shown in Annex 2.



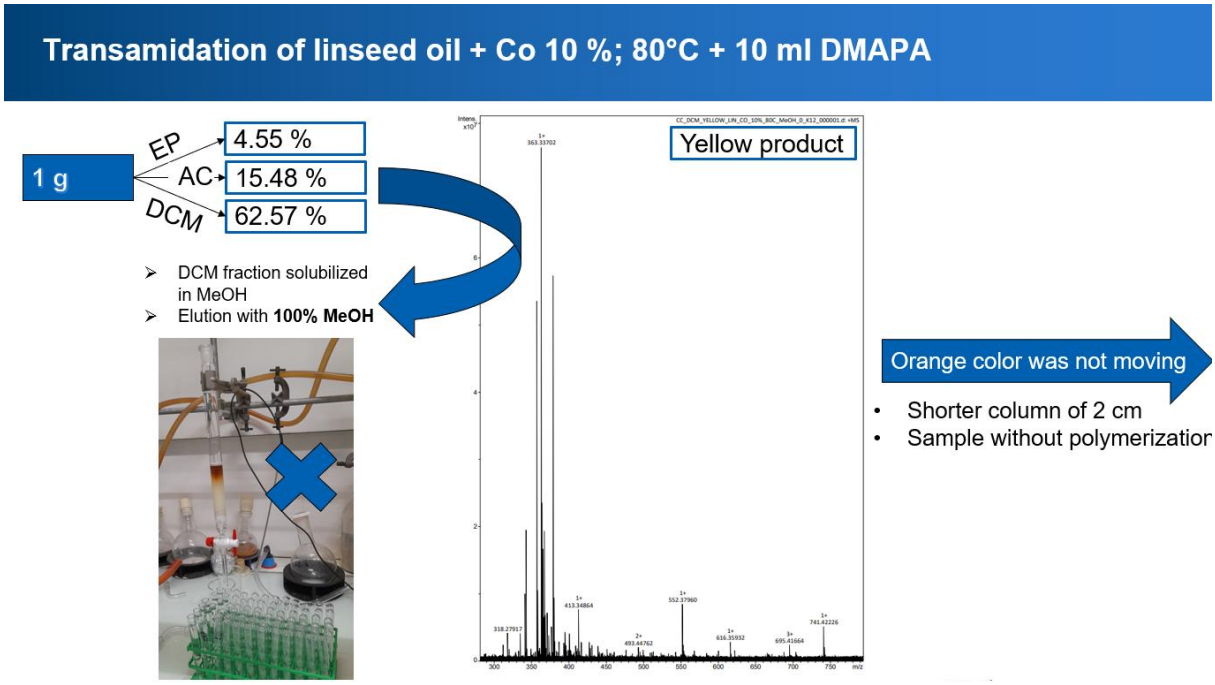
(a)



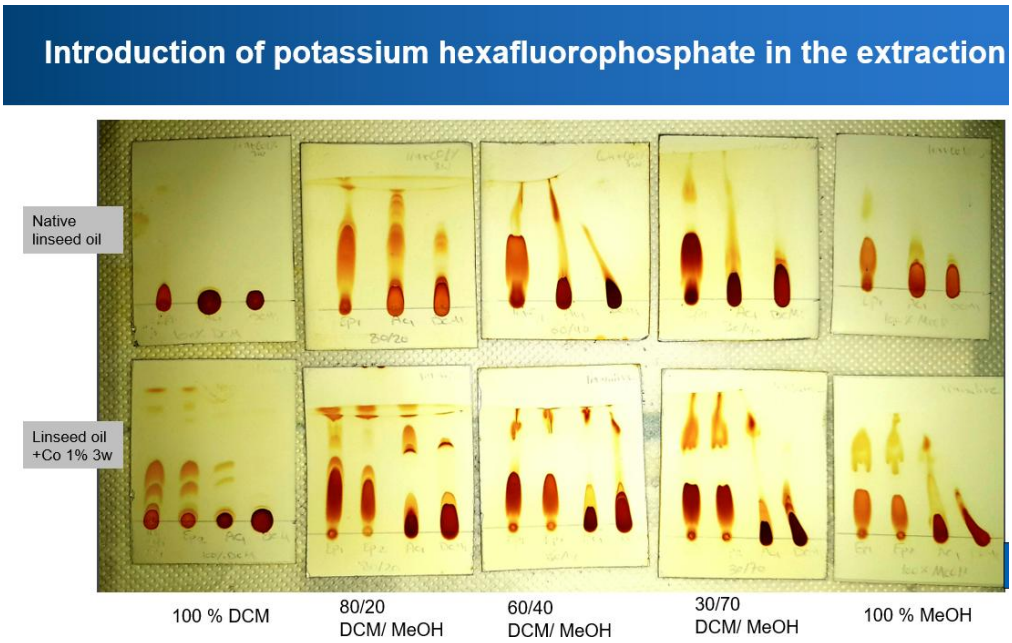
(b)

Annex 2. (a) ^{1}H NMR spectroscopy of oil paints: Ripolin rouge; Astral, Val irisé and Dulox respectively; (b) Amplified ^{1}H NMR spectroscopy peaks of Astral paint.

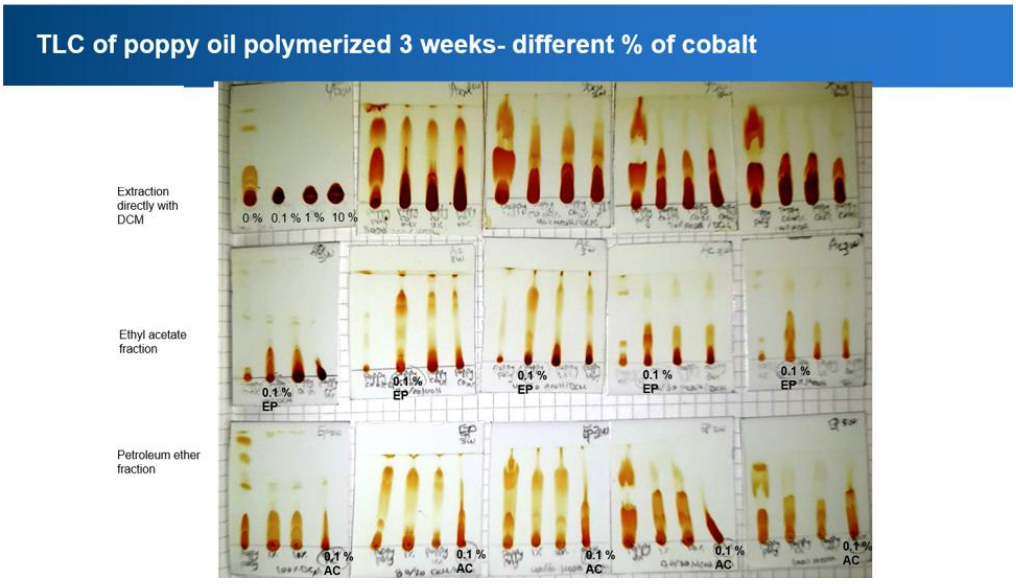
2. Column chromatography of polymerized binders



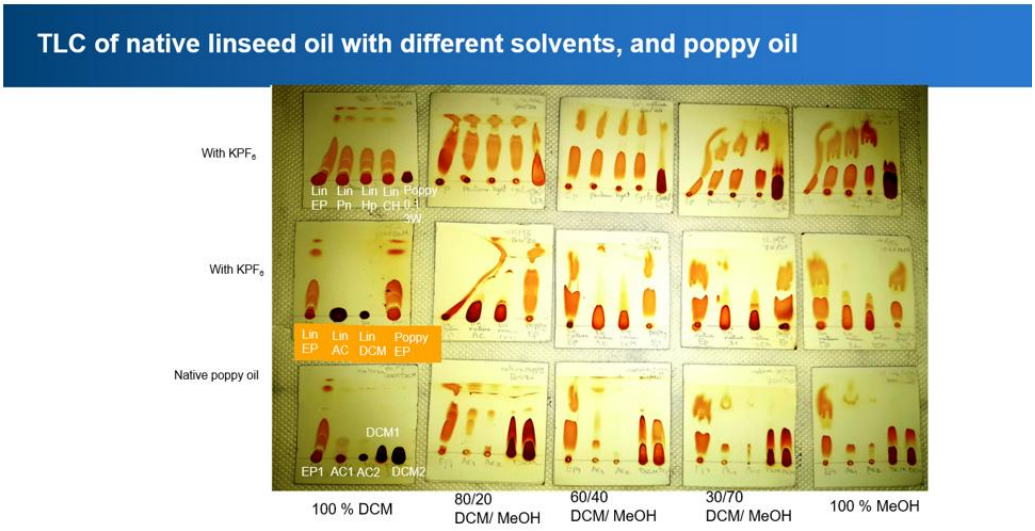
Annex 3. Transamidation of linseed oil film formulated with cobalt drier Co(II), bis(2-ethylhexanoate) 10% after heating, necessity to use shorter column chromatography for less polymerized paints.



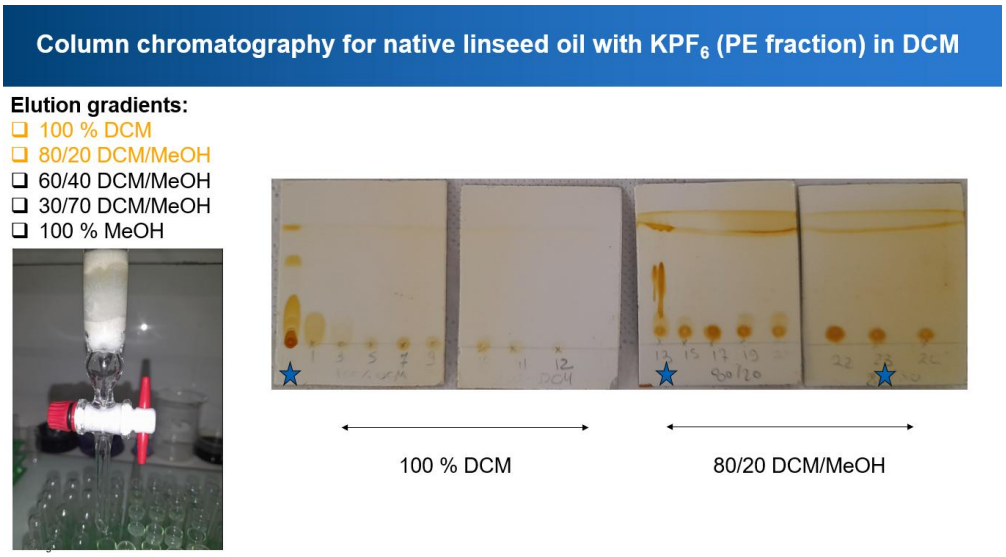
Annex 4. TLC of native and polymerized linseed oil for three weeks under natural conditions in the presence of Co(II), bis(2-ethylhexanoate); introduction of KPF_6 in the extraction protocol.



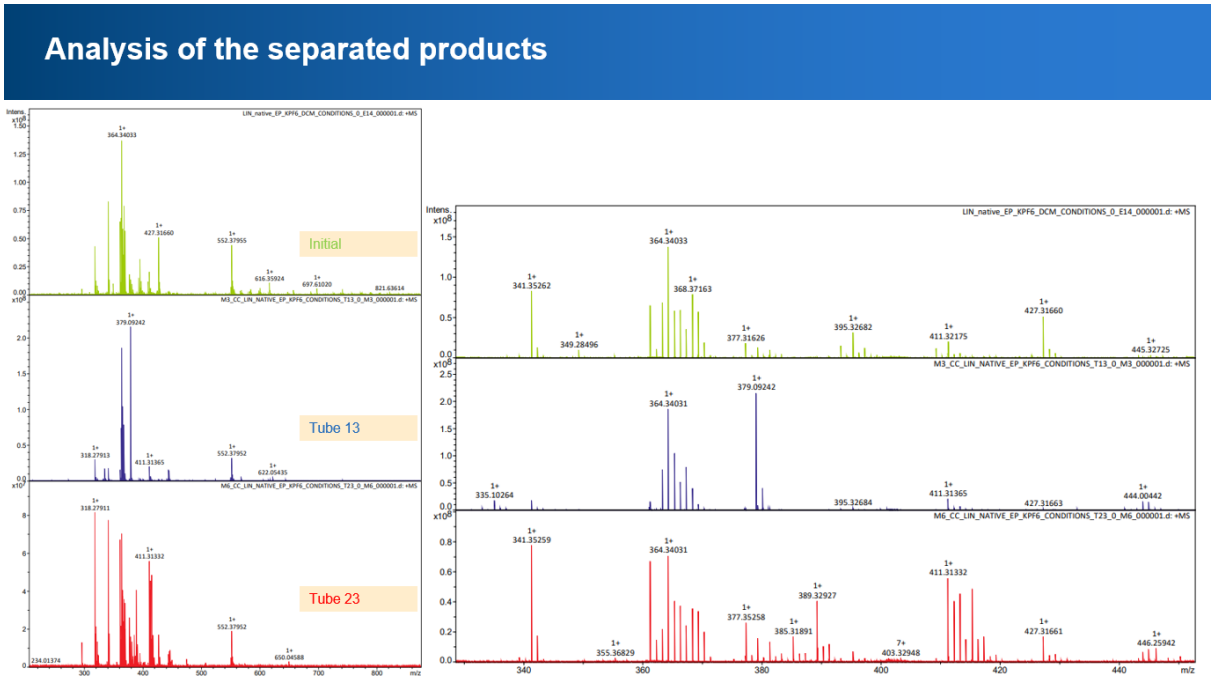
Annex 5. TLC of poppy oil polymerized naturally for 3 weeks in the presence of different percentages of the cobalt drier: Co(II), bis(2-ethylhexanoate).



Annex 6. TLC of native linseed oil with different solvents and of poppy oil.

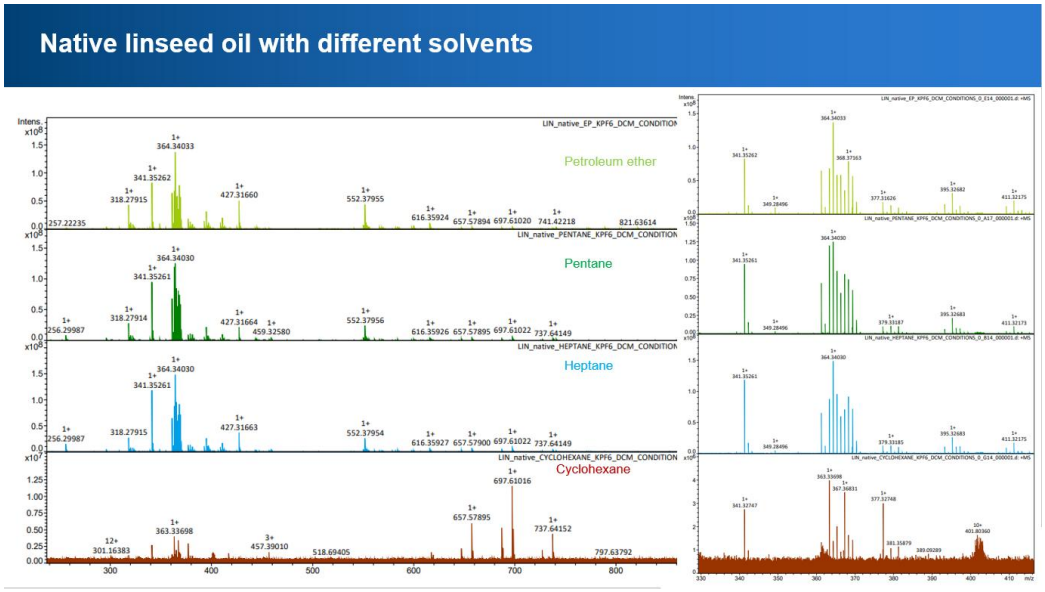


Annex 7. Column chromatography for native linseed oil (petroleum ether fraction) in dichloromethane.

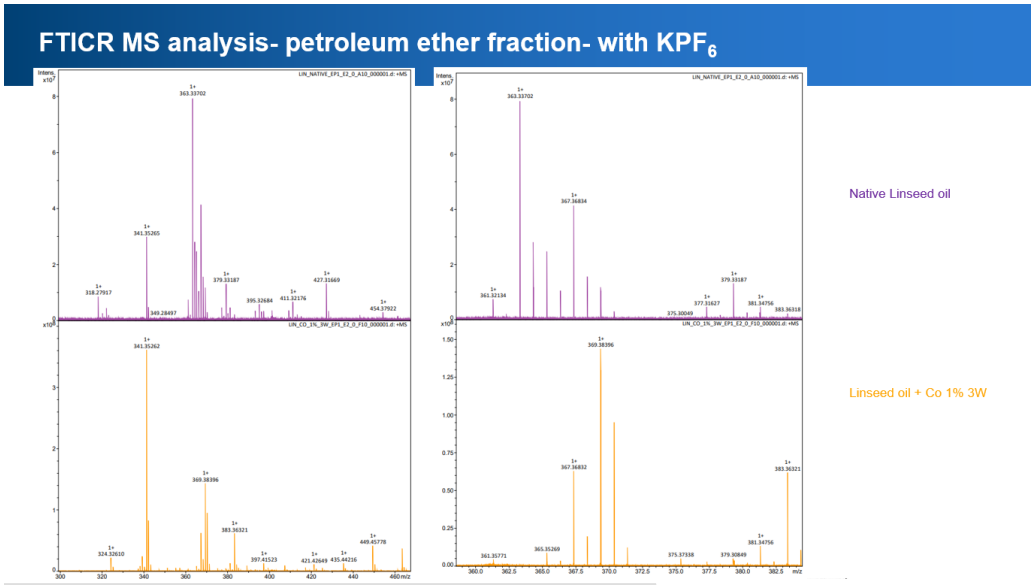


Annex 8. MALDI FTICR MS spectra of the separated products of native linseed oil by column chromatography.

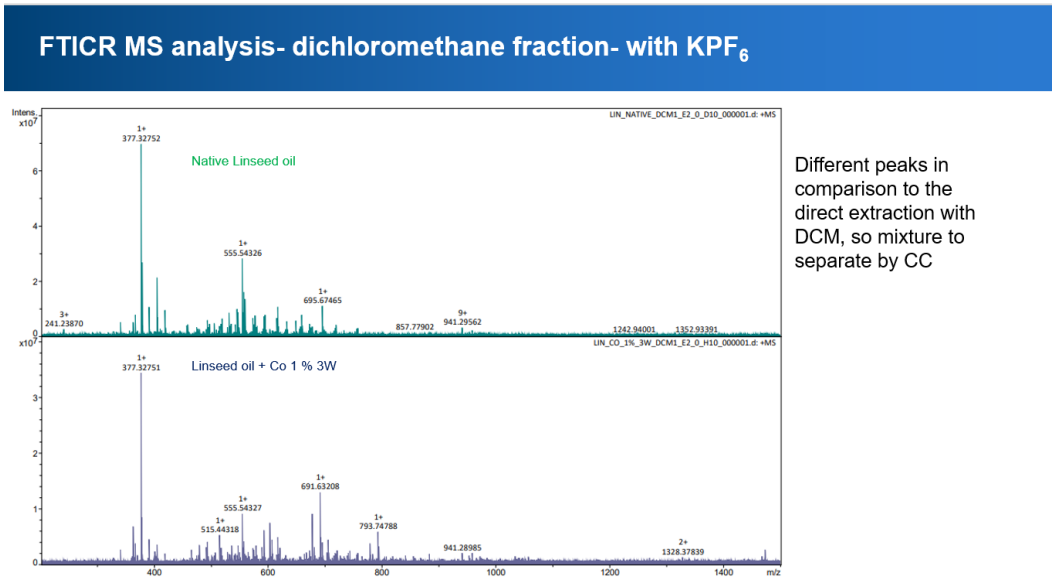
3. Adjusting solvents for the liquid-liquid extractions



Annex 9. MALDI FTICR MS spectra of depolymerized native linseed oil extracted with different extraction solvents.

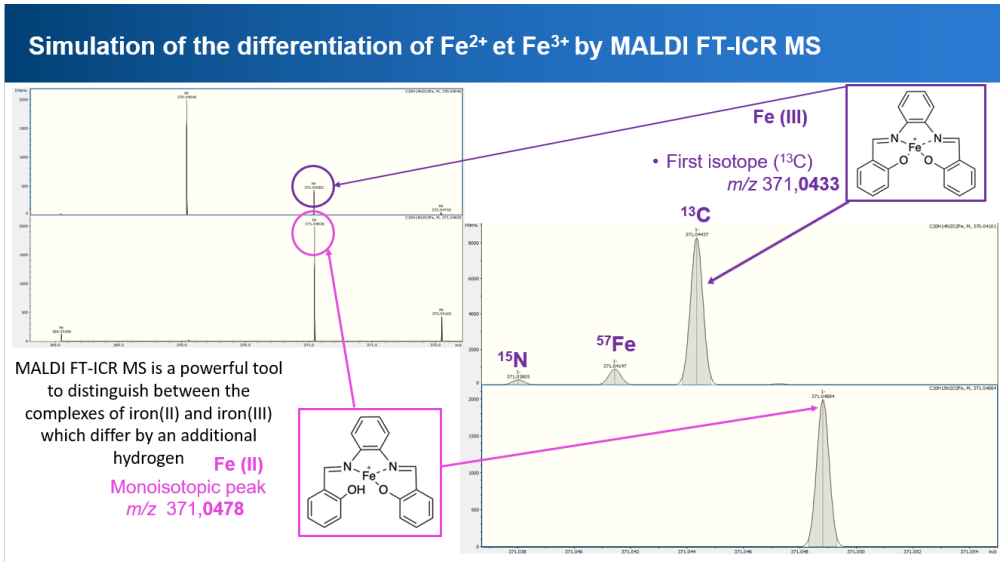


Annex 10. MALDI FTICR MS spectra of native and polymerized linseed oil for three weeks under natural conditions in the presence of Co(II), bis(2-ethylhexanoate) using KPF_6 during the extraction (petroleum ether fraction).

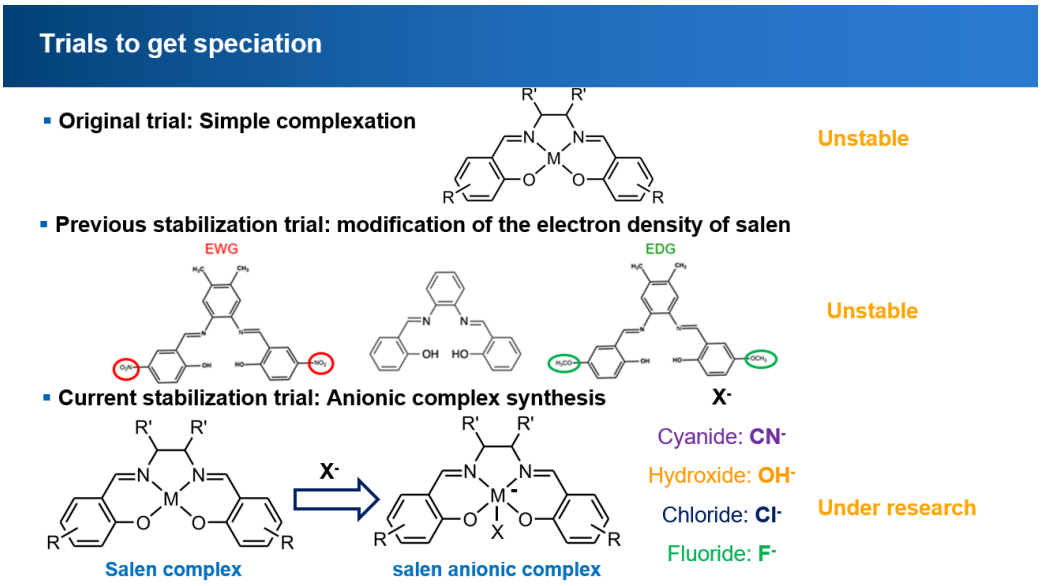


Annex 11. MALDI FTICR MS spectra of native and polymerized linseed oil for three weeks under natural conditions in the presence of cobalt drier using KPF_6 during the extraction (dichloromethane fraction).

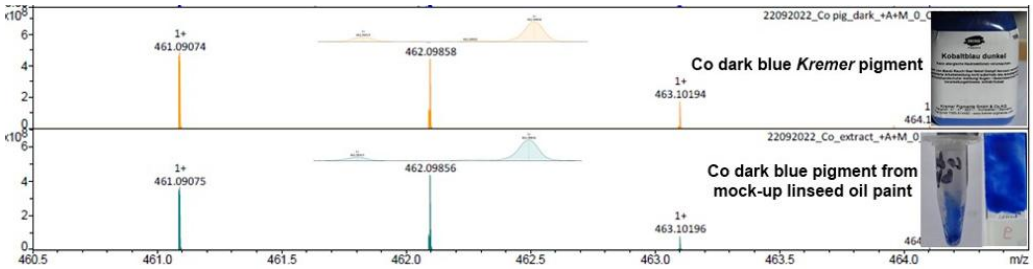
4. Metal driers complexation



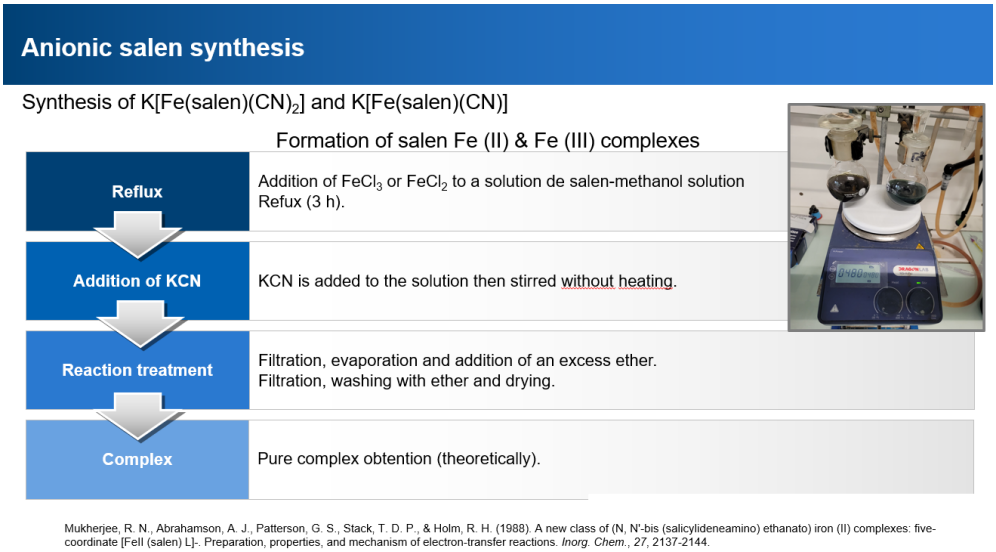
Annex 12. Complexation, simulation of differentiation of iron ions by MALDI FTICR MS.



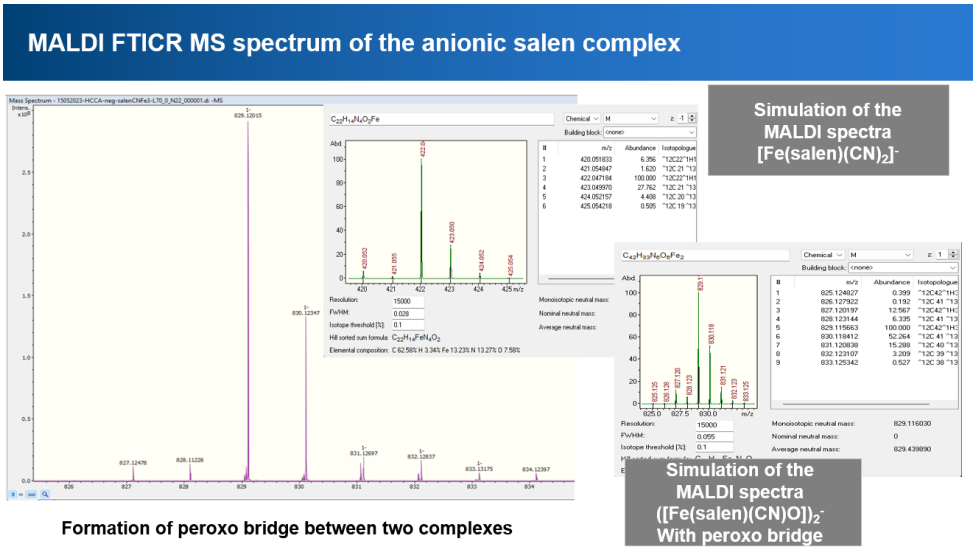
Annex 13. Trials to get speciation in our laboratory.



Annex 14. Results on linseed oil paints and driers (extraction of pigment: After depolymerization by DMAPA then centrifugation, solubilization of pigment in acidic medium) with the cationic Salen complex.



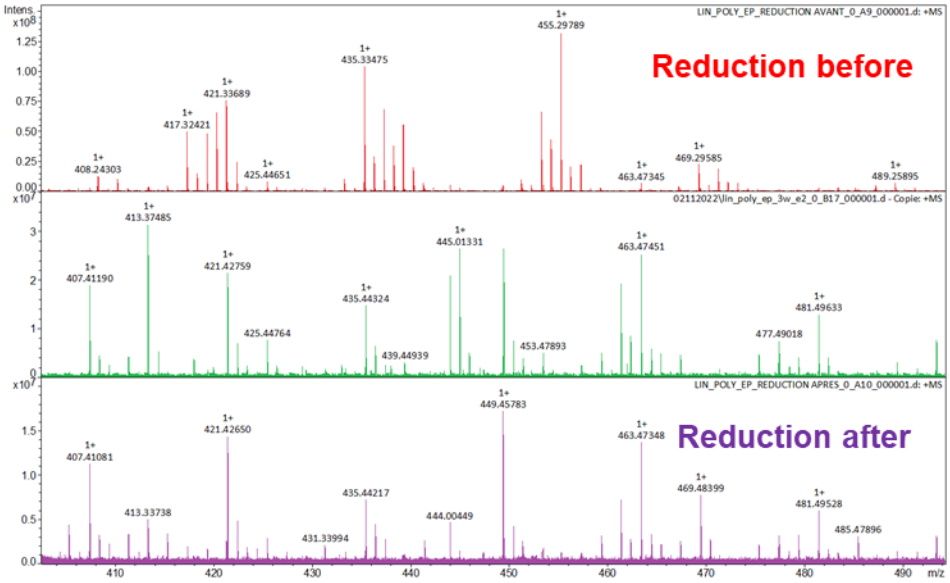
Annex 15. Anionic Salen complex synthesis.



Annex 16. MALDI FTICR MS results for the anionic Salen complex.

5. Reduction conditions: Aldehydes?

To identify exactly some structures of the polymeric linseed oil films that contain aldehyde, a reduction of the polymeric film before and after transamidation using sodium cyanoborohydride was performed. Some peaks disappeared or decreased in intensity and the others increased in intensity according to the reduction either before or after depolymerization (Annex 17).



Annex 17. MALDI FTICR MS of the reduced linseed oil films polymerized 3 weeks under natural conditions without drier before and after depolymerization in comparison to the transamidated product.

6. Analysis by ^{1}H NMR spectroscopy

The ^{1}H NMR spectroscopy 500 MHz (1D and DOSY (Diffusion-Ordered NMR Spectroscopy)), done at the Faculty of pharmacy of the University of Lille, was performed for the native linseed oil, native safflower oil, and for the industrial alkyd resin in $CDCl_3$.

In DOSY, molecules diffuse for a delay Δ between two magnetic field pulse gradients, the signal intensity changes with:

$$I = I_0 e^{-D\gamma^2 g^2 \delta^2 (\Delta - \delta/3)}$$

I: The observed intensity,

I_0: The reference intensity,

γ: Gyromagnetic ratio,

g: The gradient intensity,

δ: Delay of gradient,

Δ: The time of diffusion,

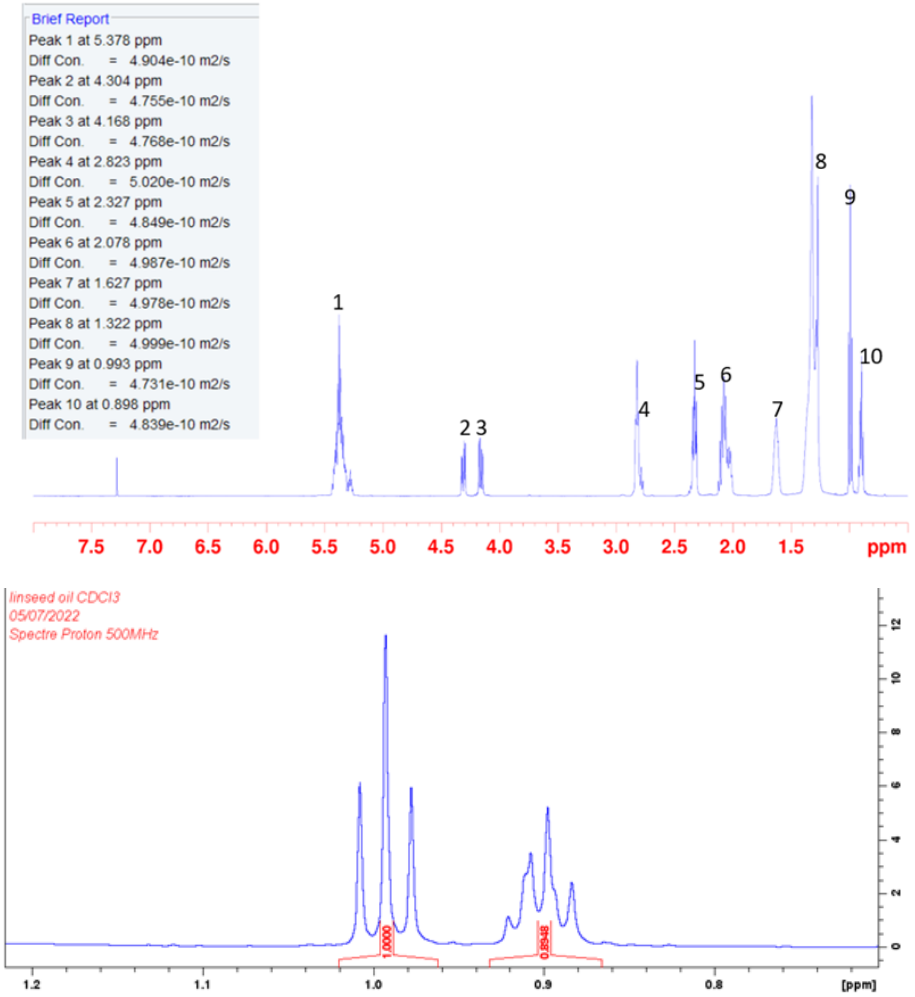
D: Coefficient of diffusion.

δ = 2 xP30

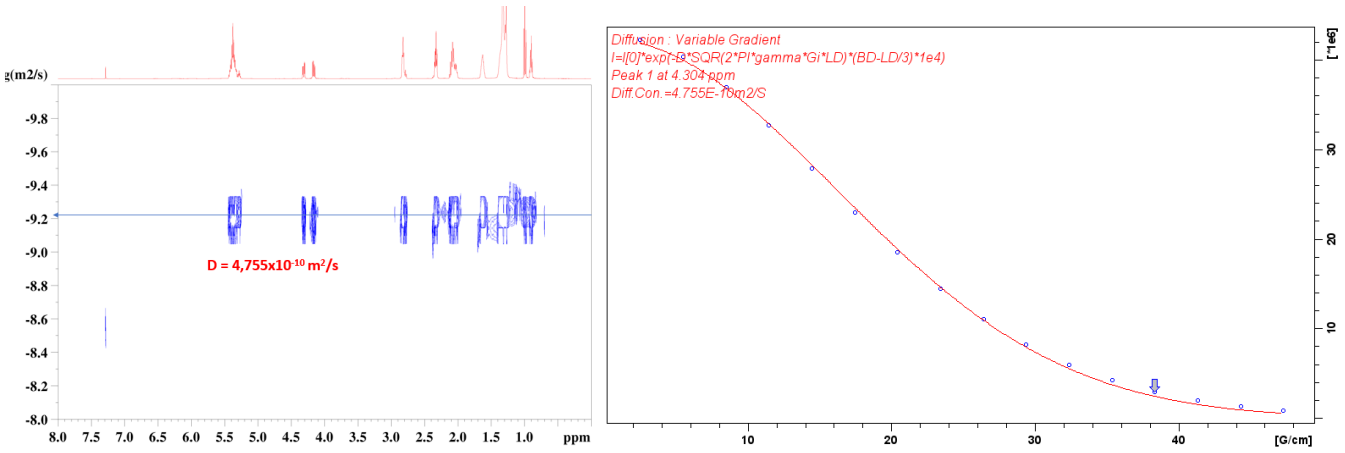
D = D20

^{1}H NMR analysis of native oils

1. Linseed oil



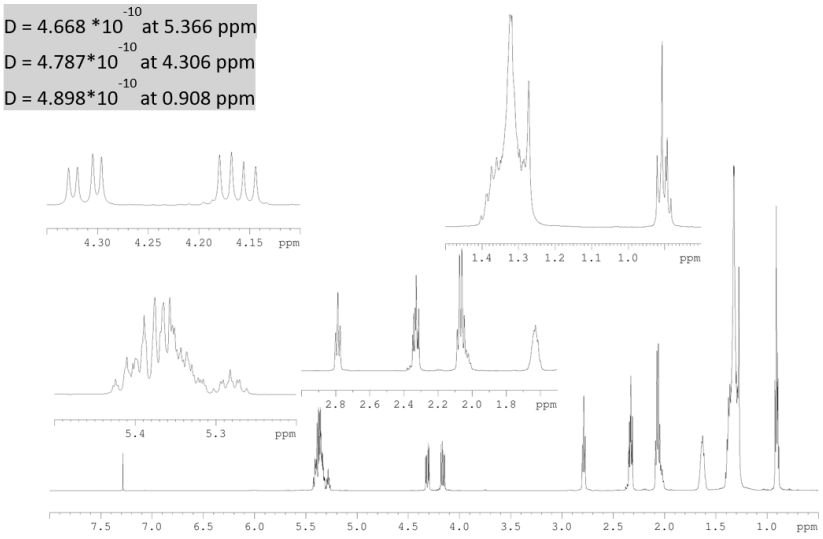
Annex 18. Linseed oil ^{1}H NMR 500 MHz spectrum.



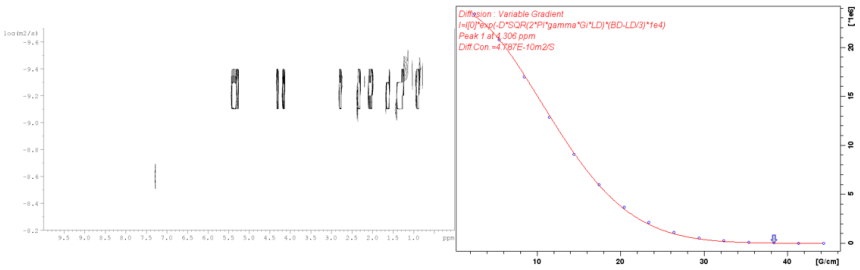
Annex 19. DOSY 2D NMR spectroscopy of linseed oil in $CDCl_3$, P30 = 1.2 ms, D20= 100 ms.

The analysis of ^{1}H NMR spectra of native linseed oil showed that the signal at 0.898 ppm corresponds to the terminal methyl group in the fatty acid chains without unsaturation at their end. The proton at 0.993 ppm which is a triplet corresponds to the terminal methyl of linolenic acid. The signal around 1.3 ppm represents CH_2 groups constituting the fatty acid chain backbone and at 1.627 ppm, it is the β-CH_2 group next to COO. The signal around 2 ppm corresponds to CH_2 in α position of CH=CH. The triplet appearing at 2.327 ppm corresponds to α-hydrogens of COO group. The signal at 2.823 ppm corresponds to CH_2 between two groups of CH=CH; and the signal constituted of two doublets of doublets at around 4.14 and 4.3 ppm, corresponds to the CH_2 protons of the glycerol. Finally, the signal at around 5.26 ppm can be attributed to the CH proton of glycerol and at 5.378 ppm to the olefinic protons of unsaturation in the fatty acid chains.

2. Safflower oil

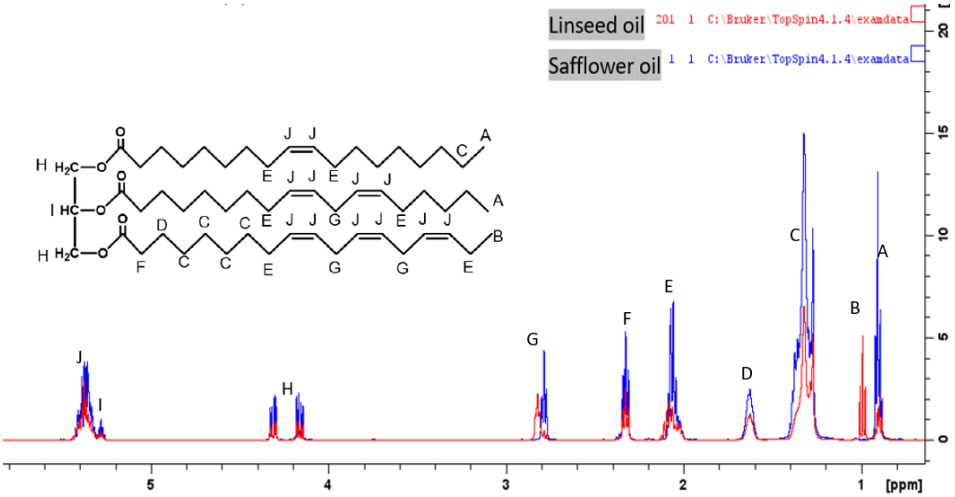


Annex 20: Safflower oil ^{1}H NMR 500 MHz spectrum.



Annex 21. DOSY 2D NMR spectroscopy of safflower oil in $CDCl_3$.

Attribution of peaks of linseed oil and safflower oil



Annex 22. Comparison between linseed and safflower oils spectra, ^{1}H NMR 500 MHz, $CDCl_3$.

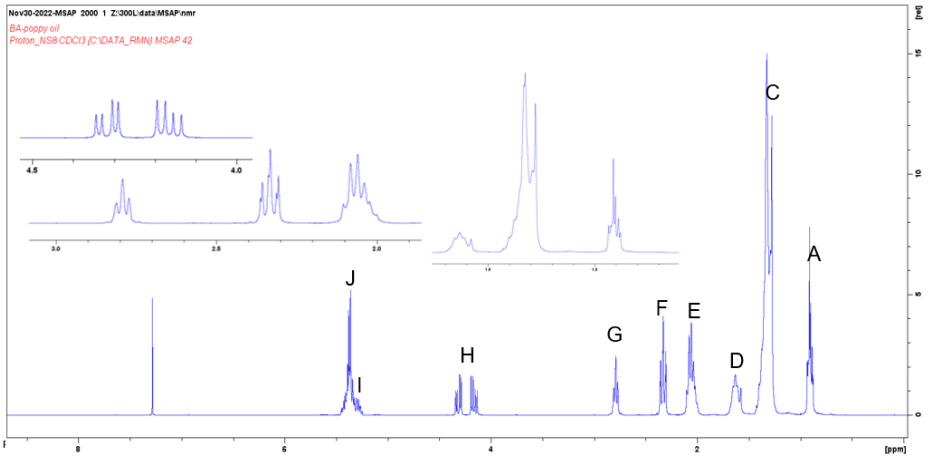
The attribution of peaks in linseed oil and safflower oil with exact chemical shift will appear in Table annex 1. Safflower oil contained all the peaks of linseed oil except the peak "B", this indicates that safflower oil does not contain linolenic fatty acid.

Table annex 1. Attribution of peaks for linseed oil.

Proton	Attribution	Chemical shift (ppm)
A	CH_3 of the chain	0.898
B	CH_3 of linolenic acid	0.993
C	CH_2 in the chain	1.332
D	CH_2 in β of CO	1.627
E	CH_2 in α of CH=CH	2.078
F	CH_2 in α of CO	2.327
G	CH_2 between CH=CH	2.823
H	O-**CH_2**-CH	4.168
I	CH of glycerol	5.261
J	CH=CH	5.378

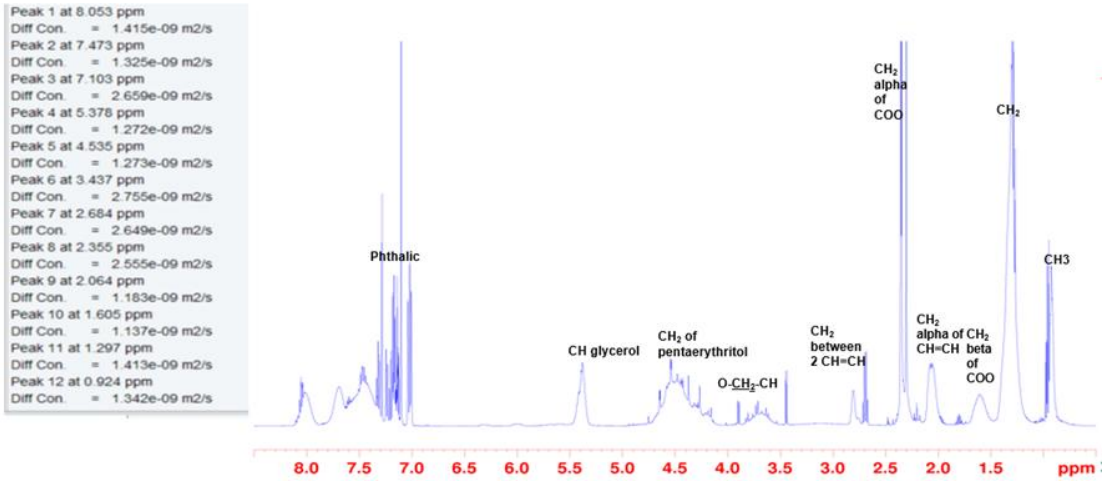
3. Poppy oil (*Gamblin*)

The native poppy oil was analyzed by ^{1}H NMR spectroscopy 1D (300 MHz), FST, MSAP, ULille. Poppy oil does not contain linolenic acid chains as safflower oil. The analysis of ^{1}H NMR spectrum of poppy oil shows that the signal at 0.88 ppm corresponds to the terminal methyl group in the fatty acid chains without unsaturation at their end. The signal "C" represents CH_2 groups constituting the fatty acid chain backbone and the signal "D" around 1.6 ppm represents the β-CH_2 group next to COO. The signal around 2 ppm corresponds to CH_2 in α position of CH=CH. The next triplet "F" corresponds to α-hydrogens of COO group. The signal at 2.76 ppm corresponds to CH_2 of =CH-CH_2-CH= group; and the signal constituted of two doublets of doublets at around 4.15 and 4.3 ppm, corresponds to the CH_2 protons of the glycerol. Finally, the signal at around 5.26 ppm can be attributed to the CH proton of glycerol and the signal "J" to the olefinic protons of unsaturation in the fatty acid chains.

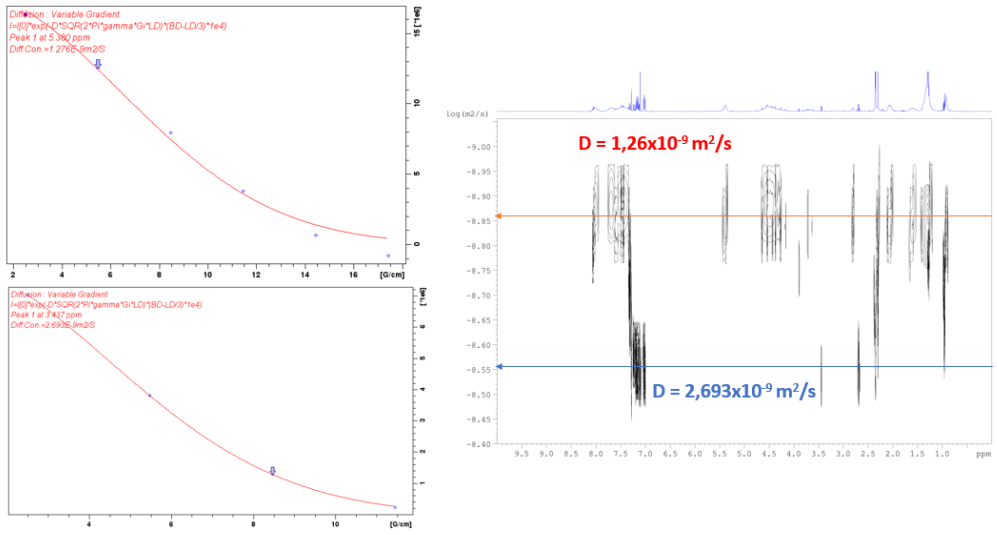


Annex 23. Poppy oil ^{1}H NMR 300 MHz spectrum in $CDCl_3$.

4- ^{1}H NMR analysis of alkyd resin



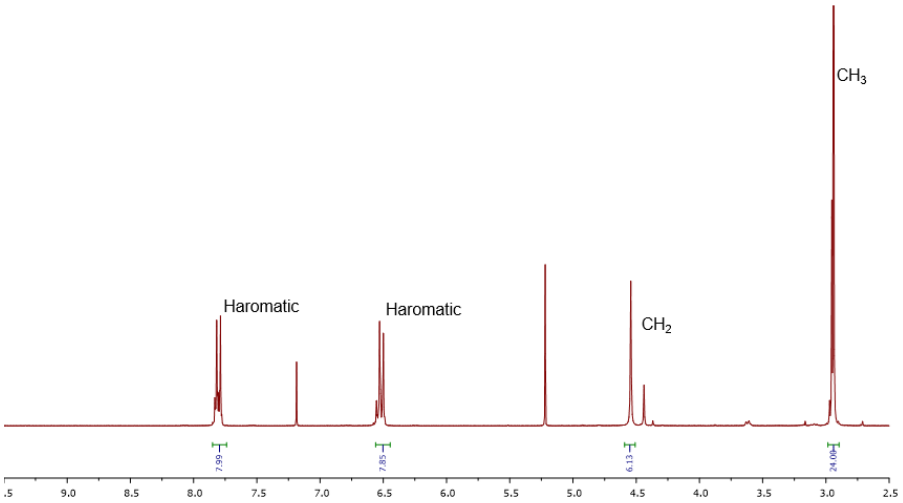
Annex 24. ^{1}H NMR (500 MHz) spectrum of the industrial alkyd resin.



Annex 25. DOSY 2D spectroscopy of the industrial alkyd resin, D20= 150 ms, P30 = 1.5 ms.

By this spectroscopy, the peaks of fatty acid chain, of phthalic protons which appear around 7.3 ppm, and the peaks of the polyol pentaerythritol appearing at around 4 ppm were identified.

The other peaks on the same line (blue line in DOSY) are the peaks of the solvent present in this alkyd resin, because the solvent diffuse faster.



Annex 26. ^{1}H NMR spectrum of the benzoylated alkyd industrial resin derivatized with 4-(dimethylamino)benzoyl chloride (DMABC).

7. ESI analysis on Orbitrap

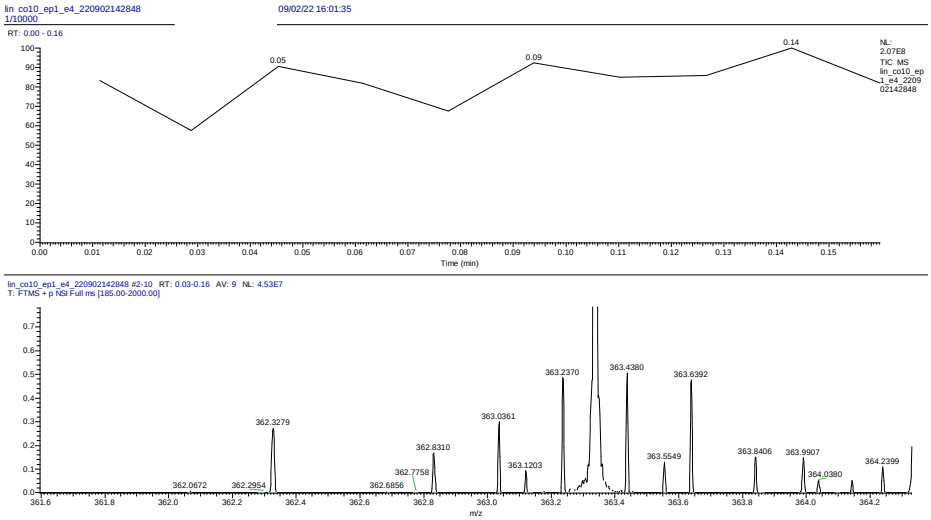
The difference of *m/z* of $N(CH_3)_2$ from the amine DMAPA/fatty acid which is 45.057301 was identified.

Table annex 2. The difference of *m/z* of $N(CH_3)_2$ from the amine DMAPA with the identified fatty acids.

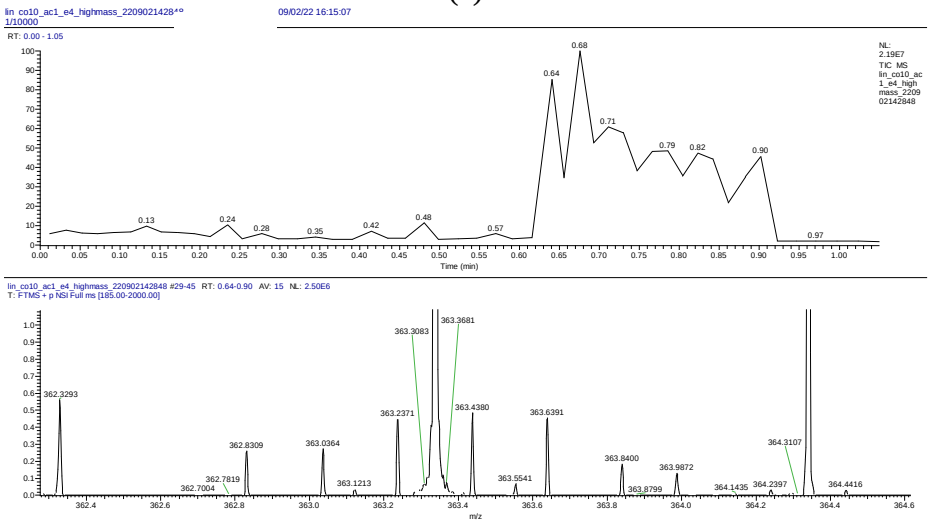
Fatty acid	**Fatty acid *m/z***	**The associated $N(CH_3)_2$ *m/z***
Oleic- DMAPA - 1O	383.3636	338.3057
Linolenic	363.3372	318.2791
Linoleic	365.3530	320.2949
Palmitic	341.3533	296.2953
Oleic	367.3689	322.3110
Stearic	369.3846	324.3268
Arachidic	397.4155	352.3575

I performed ESI in infusion for linseed oil with cobalt 10% (Co(II), bis(2-ethylhexanoate)drier), polymerized under natural conditions. For the ethyl acetate fraction, I performed one acquisition at ca *m/z* 400 so that the fatty acid did not blur the high masses to have the possibility to see also trimers and may be tetramers. In the two extracted fractions, we can find the mixed dimer, the

linolenic acid dimer. In petroleum ether fraction, we have a peak at *m/z* 362.6856 which may be a trimer (theoretical *m/z* is 362.6620).



(a)



(b)

Annex 27. ESI in infusion of linseed oil film formulated with cobalt 10% (Co(II), bis(2-ethylhexanoate)drier) polymerized under natural conditions, 2 fractions. (a): Petroleum ether fraction; (b): Ethyl acetate fraction.

Conclusions and perspectives: Part II

Conclusions

- Many methodologies of depolymerization of oil paints, alkyd paints and oil pastels at mild conditions were developed and compared in order to afford their full structural characterization with high sensitivity and accuracy.
- A new, innovative and sensitive methodology of depolymerization at room temperature by direct transamidation combined with advanced mass spectrometry (MALDI FTICR MS and LC-MS) has proved its success on oil paints and alkyd paints.
- Another new methodology was developed for detecting polyols of alkyd paints.
- An industrial resin was fully characterized.
- Different oil mock-up samples were studied.
- The ageing was studied after short and long-term polymerization under natural conditions or after accelerated ageing by temperature and UV-irradiation.
- The parameters affecting oil paint's siccativation mechanism were studied: Type of siccative oil, its supplier, polymerization duration, presence of drier, percentage of drier, etc.
- Historical oil paintings of museum-size samples were studied after analysis miniaturization.
- Innovative methodologies were developed for oil pastels allowing the preliminary comparison of the structure of different oil pastels' pigments and suppliers.

Perspectives

- Data treatment of the remaining depolymerized products.
- Quantification of oil paints by synthesizing an internal standard based on fatty esters such as methyl stearate.
- More investigations on oil pastels structures.

GENERAL CONCLUSIONS & PERSPECTIVES

In this PhD dissertation, new, original and sensitive methodologies have been developed for polyesters and co-polyesters' structural identification allowing their analysis at molecular level and the follow-up of their degradation by weathering (UV, temperature, etc.). Synthetic and natural polymers have been studied in details: Polyethylene terephthalate (PET) polyesters and microplastics, plastics' co-polyesters (PETG, PBAT, mussel nets…), vegetable siccative oils, oil paints, alkyd paints, alkyd resins, etc.

Indeed, an efficient soft chemical depolymerization by transamidation using 3-(dimethylamino)-1-propylamine (DMAPA) was developed to cleave ester bonds. In parallel, free diols and polyols of polyesters were derivatized for better identification using a new combined strategy of free-water methanolysis followed by benzoylation using 4-(dimethylamino)benzoyl chloride. The derivatized samples were analyzed by ultra-high resolution mass spectrometry techniques FTICR MS and LC Orbitrap MS. The utilization of both ionization mode MALDI and ESI on these two different analytical devices enhanced reliability of the complementary data on the full composition of samples. These methodologies allowed the identification and quantification of depolymerized samples with very high accuracy and resolution. New databases of the derivatized natural and synthetic polymers have been created.

First concerning synthetic polyesters and co-polyesters, 1,1,1,3,3,3-hexafluoro-2-propanol (HFIP) solvent was used. It allowed a transamidation of microplastics at room temperature and a higher extraction yield. PET packaging objects showed specific chemical signature according to their content, brand and manufacturing countries. PET dimers, oligomers, degradation products and oxygenated species were identified. For example, soft drinks' bottles showed the presence of derivatized compounds having cyclohexanemethanol, the main diol in PETG (poly(ethyleneglycol-co-1,4-cyclohexanedimethanol terephthalate)) co-polyester. This compound is used to rigidify the final material of PET.

Many additives including plasticizers, antioxidants, flame retardant and crosslinking agents were identified. They can be used for the prediction of additives migration from food packaging objects into beverages to study their toxicity. In addition, enchased products remaining in the polymeric pores were detected; this last information is important and can be used to determine packaging objects' content.

Accelerated ageing by heating and UV-irradiation was studied and the difference of these ageing parameters on PET degradation products was described. Natural experiments in Liane river and semi-natural experiments in seawater have been performed on water and cola bottles indicating the effect of salinity and type of bottle on the degradation products. It was found that the accelerated and natural weathering enhances the formation of phthalates NIAS, favorizes the C-C coupling of degradation products, forms more oxidized species and diminishes or even disappears some additives especially antioxidants and plasticizers. Environmental marine samples from the English Channel have been analyzed showing biological signature in addition to their chemical fingerprinting.

Furthermore, the methodology of benzoylation after transesterification with methanol revealed more data about PET diols (and their modifications) including ethylene glycol, diethylene glycol, triethylene glycol, propanol, butanediol, hexanol, ...

These strategies allowed the depolymerization of other co-polyesters and marine objects. Indeed, the co-polymer polybutylene adipate terephthalate (PBAT) was successfully depolymerized and the biodegradable mussel nets, which are still in the early stages of market introduction, were deciphered showing PBAT as their main constitutive polymer.

All these data will help to determine the pollution source by PET waste in the polluted ecosystems especially sea and oceans in order to predict their lifetime and fate in the environment.

Finally, for health concerns, a new protocol for the synthesis of not denatured PET nanoparticles was developed in which nano-PETs were soluble in water with BSA for further biological assays. The size of the generated nano-PETs is still to adjust and another protocol by grinding will be developed.

Secondly concerning siccative oils & oil and alkyd paints, the direct transamidation using DMAPA was sufficient for their depolymerization at room temperature, without adding HFIP. Indeed, historical siccative oils including linseed, walnut and poppy oils were studied before and after ageing under natural conditions. Fatty acids, their oxygenated species and crosslinked dimers were determined with very high accuracy. The differentiation of oils in function of their structural composition and polymerization rate was achieved. The siccativation mechanism of oils in the presence of light and oxygen yielding the 3D-crosslinked films has been approved according to the identified compounds and the follow-up of oil’s drying.

This method was used also to assess the effect of driers and pigments on the formation of the final polymeric film of oils. Indeed, mock-up samples of linseed oil formulated with various percentages and

types of metal driers and artistic pigments were studied after different ageing modes for short-term and long-term. Oil paint tubes from *Sennelier* have been also studied with and without polymerization. The effect of transition metal present in pigments was discussed for the siccativation mechanism. These driers affected the presence of the degraded unsaturated fatty acids and the formed oxygenated species, crosslinks and dimers during the oil film lifetime.

This methodology has been miniaturized and applied successfully on oil paints from 20th century while preserving the original painting affording high quality analytical results with good sensitivity.

On the other hand, oil-modified paints known as alkyd paints were also studied and their polyols content was determined. They showed the presence of phthalic parts in their constitutive resins. Alkyd paints' tubes from *Winsor and Newton* brand were studied and their structural modifications induced by siccativation was determined. The traces of the remaining polyunsaturated fatty acids and the formed dimers and oxygenated species were identified as previously.

These strategies have been applied to an alkyd industrial resin allowing its full characterization; it was initially manufactured of pentaerythritol as polyol.

The previous results will allow the determination of the type of binder used in the museum oil paintings in order to conserve these artworks for long-term. These methods will be used on other brands and colors of oil and alkyd paints.

Finally, innovative methodologies were developed for oil pastels allowing the preliminary comparison of the structure of different oil pastels' pigments and suppliers. More investigations on oil pastels structures are still needed.

As conclusion, many polyesters and co-polyesters from cultural heritage and plastics' Worlds were identified at molecular level using our new innovative methodologies.

Thèse de Doctorat

Par

Bayan ALMASRI



La Chimie parle!

PhD Dissertation

By

Bayan ALMASRI



Chemistry talks!